ISSN 2636-8498

Environmental Research & Technology

Year 2025
Volume 8
Number 2

https://dergipark.org.tr/en/pub/ert

ISSN 2636-8498

Environmental Research & Technology

Volume 8 Number 2 Year 2025

EDITOR-IN-CHIEF

Prof. Dr. Ahmet Demir, *Yıldız Technical University, İstanbul, Türkiye*
Prof. Dr. Mehmet Sinan Bilgili, *Yıldız Technical University, İstanbul, Türkiye*

ACADEMIC ADVISORY BOARD

Prof. Dr. Adem Baştürk, *Yıldız Technical University, İstanbul, Türkiye*
Prof. Dr. Mustafa Öztürk, *Yıldız Technical University, İstanbul, Türkiye*
Prof. Dr. Lütfi Akça, *İstanbul Technical University, İstanbul, Türkiye*
Prof. Dr. Oktay Tabasaran, *University of Stuttgart, Germany*

SCIENTIFIC DIRECTOR

Prof. Dr. Ahmet Demir, *Yıldız Technical University, İstanbul, Türkiye*

ASSISTANT EDITOR

Dr. Hanife Sarı Erkan, *Yıldız Technical University, İstanbul, Türkiye*

LANGUAGE EDITOR

Prof. Dr. Güleda Engin, *Yıldız Technical University, İstanbul, Türkiye*

Abstracting and Indexing

The following is a list of the Abstracting and Indexing databases that cover
TUBITAK TR Index, Scopus, EBSCO, ROAD, SJIFactor, EurAsianScientific Journal Index (ESJI), Research Bib(Academic Resource Index), ScientificIndexing Services, ASOS Index, MIAR, IndexCopernicus, Open Ukranian Citation Index (OUCI), Scilit, Ideal Online, Google Scholar, Directory of Research Journals Indexing.

Publisher (Owner)

Mehmet Sinan Bilgili
E-mail: mbilgili@yildiz.edu.tr

ISSN 2636-8498

Environmental Research & Technology

Volume 8 Number 2 Year 2025

CO-EDITORS (AIR POLLUTION)

Prof. Dr. Mohd Talib Latif, *Department of National University of Malaysia/Universiti Kebangsaan Malaysia, Malaysia*

Prof. Dr. Nedim Vardar, *Inter American University, Puerto Rico*

Prof. Dr. Sait Cemil Sofuoğlu, *İzmir Institute of Technology, İzmir, Türkiye*

Prof. Dr. Wina Graus, *Copernicus Institute of Sustainable Development, Utrecht University, Netherlands*

CO-EDITORS (ENVIRONMENTAL ENGINEERING AND SUSTAINABLE SOLUTIONS)

Prof. Dr. Bülent İnanç, *İstanbul Technical University, İstanbul, Türkiye*

Prof. Dr. Güleda Engin, *Yıldız Technical University, İstanbul, Türkiye*

Prof. Dr. Hossein Kazemian, *University of Northern British Columbia, Canada*

Prof. Dr. Raffaella Pomi, *La Sapienza, Italy*

Prof. Dr. Yılmaz Yıldırım, *Zonguldak Bülent Ecevit University, Zonguldak, Türkiye*

CO-EDITORS (WASTE MANAGEMENT)

Prof. Dr. Bestami Özkaya, *Yıldız Technical University, İstanbul, Türkiye*

Prof. Dr. Bülent Topkaya, *Akdeniz University Faculty of Engineering, Antalya, Türkiye*

Prof. Dr. Kahraman Unlu, *Department of Environmental Engineering, Middle East Technical University, Ankara, Türkiye*

Prof. Dr. Mohamed Osmani, *Loughborough University, School of Architecture, Building and Civil Engineering, United Kingdom*

Prof. Dr. Pin Jing He, *Tongji University, China*

CO-EDITORS (WATER AND WASTEWATER MANAGEMENT)

Prof. Dr. Ayşe Filibeli, *Dokuz Eylül University, İzmir, Türkiye*

Prof. Dr. Barış Çallı, *Marmara University, İstanbul, Türkiye*

Prof. Dr. Marina Prisciandaro, *University Of L'aquila, Italy*

Prof. Dr. Md. Ahmaruzzaman, *National Institute of Technology Silchar, India*

Prof. Dr. Selvam Kaliyamoorthy, *Mie University, Japan*

Prof. Dr. Subramanyan Vasudevan, *Academy For Scientific and Innovative Research, New Delhi, India*

ISSN 2636-8498

Environmental Research & Technology

Volume 8 Number 2 Year 2025

EDITORIAL BOARD

Prof. Dr. Andjelka Mihajlo, *Department of Environmental Engineering and Occupational Safety and Health, Faculty of Technical Sciences, University of Novi Sad, Serbia*
Prof. Dr. Artur J. Badyda, *Warsaw University of Technology, Poland*
Prof. Dr. Azize Ayol, *Dokuz Eylül University, İzmir, Türkiye*
Prof. Dr. Didem Balkanlı, *Yıldız Technical University, İstanbul, Türkiye*
Prof. Dr. Erwin Binner, *University of Natural Resources and Life Science Vienna, Austria*
Prof. Dr. Eyüp Debik, *Yıldız Technical University, İstanbul, Türkiye*
Prof. Dr. Dilek Sanin, *Middle East Technical University, Ankara, Türkiye*
Prof. Dr. Gülsüm Yılmaz, *İstanbul University-Cerrahpaşa, İstanbul, Türkiye*
Prof. Dr. Hamdy Seif, *Beirut Arab University, Beirut, Lebanon*
Prof. Dr. Hanife Büyükgüngör, *Ondokuz Mayıs Universıty, Samsun, Türkiye*
Prof. Dr. Ilırjan Malollari, *University of Tirana, Albania, Albanian Academy of Sciences, Albania*
Prof. Dr. İsmail Koyuncu, *İstanbul Technical University, İstanbul, Türkiye*
Prof. Dr. Jaakko Puhakka, *Tampere University of Applied Sciences, Tampere, Finland*
Prof. Dr. Lucas Alados Arboledas, *University of Granada, Granada, Spain*
Prof. Dr. Mahmoud A. Alawi, *University of Jordan, Amman, Jordan*
Prof. Dr. Marcelo Antunes Nolasco, *University of São Paulo, São Paulo, Brasil*
Prof. Dr. Martin Kranert, *University of Stuttgart, Stuttgart, German*
Prof. Dr. Mesut Akgün, *Yıldız Technical University, İstanbul, Türkiye*
Prof. Dr. Mukand S. Babel, *Asian Institute of Technology, Pathum Thani, Thailand*
Prof. Dr. Mustafa Odabaşı, *Dokuz Eylül University, İzmir, Türkiye*
Prof. Dr. Müfide Banar, *Eskişehir Technical University, Eskişehir, Türkiye*
Prof. Dr. Mufit Bahadır, *Technische Universität Braunschweig, German*
Prof. Dr. Neslihan Doğan Sağlamtimur, *Niğde Ömer Halisdemir University, Niğde, Türkiye*
Prof. Dr. Nihal Bektaş, *Gebze Technical University, Gebze, Türkiye*
Prof. Dr. Osman Arıkan, *İstanbul Technical University, İstanbul, Türkiye*
Prof. Dr. Osman Nuri Ağdağ, *Pamukkale University, Denizli, Türkiye*
Prof. Dr. Pier Paolo Manca, *University of Cagliari, Italy*
Prof. Dr. Saim Özdemir, *Sakarya University, Sakarya, Türkiye*
Prof. Dr. Serdar Aydın, *İstanbul University-Cerrahpaşa, İstanbul, Türkiye*
Prof. Dr. Timothy O. Randhir, *University of Massachusetts Amherst, USA*
Prof. Dr. Ülkü Yetis, *Middle East Technical University, Ankara, Türkiye*
Prof. Dr. Victor Alcaraz Gonzalez, *University of Guadalajara, Mexico*
Prof. Dr. Ejaz Khan, *Health Services Academy, Pakistan*

ISSN 2636-8498

Environmental Research & Technology

Volume 8 Number 2 Year 2025

CONTENTS

Research Articles

234 **Water quality and spatial distribution of wells in the Eastern Side of Nineveh Governorate – Iraq**
Kotayba T. AL-YOUZBAKEY , Ali M. SULAIMAN

245 **Sulfonated plastic waste: A solution for water hardness reduction**
Minjal PATEL, Bina Birenkumar PATEL, Isha LAD

255 **Heavy metal contamination in the groundwater of the southern expanse of the Northwestern Himalayan region: An evaluation of pollution indices and health risks utilizing Mathematical Modelling**
Uzma IMTIYAZ, Mushtaq Ahmad RATHER

281 **Assessment of drainage capacity of a surface drain in Rajshahi, Bangladesh**
Sribash DAS, Meher Nigar JERIN

288 **Evaluation of adsorption isotherms and kinetics of chloride ion in water using biochar derived from locally available agro-waste**
Mohd ISHAQ, RC CHHIPA, Anupama SHARMA, Gh ALİ

297 **Bibliometric analysis of environmental, social and corporate governance (ESG) articles published in the Scopus database**
Ümran BULUT SU, Yasemin ERTAN

315 **A Comprehensive study on adsorption kinetics and equilibrium: Utilizing olive mill by-products as a sustainable biosorbent for cobalt (II) Removal**
Khaled Muftah ELSHERIF, Abdunaser Mabrok EWLAD-AHMED, Abdelmeneim EL-DALI, Rima Abdessalam SAAD, Abdullah A. TREBAN

328 **Optimization of biodiesel production from jatropha oil and its impact on engine performance and emissions using response surface methodology**
Sangeetha KRISHNAMOORTHI, L.PRABHU, M.PRABHAHAR, Adil ABDULLA , Adil MEHABOOB

345 **From self-care to earth care: Uncovering the role of self-compassion in the link between environmental identity and pro-environmental behaviors in young men**
Adem KANTAR, Begum YILMAZCAN

354 **Spatio-temporal patterns of air quality on commuter lane of the sub-urban area of Yogyakarta, Indonesia**
Arif Ashari, Rizqya P.S. Nurussolikhin, Audyana Putri, Muhamad Ervin, Muhammad A.I. Wardoyo

ISSN 2636-8498

Environmental Research & Technology

Volume 8 Number 2 Year 2025

CONTENTS

Research Articles

372 **Impact of additives on combustion behaviour and performance of a diesel engine powered by diesel-CIME blend: A comparative analysis**
Anant G. NAGPURE, Walmik S. RATHOD, Supriya B. CHAVAN

382 **Central composite experimental design for Indigo Carmine dye removal from solutions by applying electrocoagulation and electrooxidation processes**
Mustafa KORKMAZ

399 **Assessing the carbon footprint of Gaziantep University's sporium building: A step towards environmental awareness and climate action in Türkiye**
Serap ULUSAM SEÇKINER, Belkıs Şevval ŞAHINALP

410 **Can renewable energy sources alleviate the pressure of military expenditures on the environment? Empirical evidence from Turkiye**
Emre AKUSTA

425 **Carica papaya L. Latex mediated green synthesis of ZnO nanoparticles for its antimicrobial activity**
Ananya MISHARA, Sagarika PARIDA

429 **Predictive analysis of urban wastewater capacity using ANN and ODE model: A case study**
Recep Sinan ARSLAN, Murat TAŞYÜREK, Bahatdin DAŞBAŞI, Teslima DAŞBAŞI

447 **Exploring the relationship between rainfall and crop yield and best practices adoption using participatory approach**
Arunya KALAIYARASI GANESAPANDIAN, Krishnaveni MUTHIAH

Review Articles

456 **A decade of eco-friendly active and intelligent food packaging research: A quantitative review**
Supratim SUIN

471 **Examining the use of marble waste as a substitute of conventional materials in concrete: A brief review**
Mustapha Nuhu GARKO, Shashivendra DULAWAT, Esar AHMAD, Salihu Sarki UBAYI, Ibrahim Abdullahi IBRAHIM

487 **Enhancement of biogas production by means of ultrasonic pre-treatment: State of art and review**
Rana KIDAK

499 **Study of microplastic accumulation in halophyte plants and macroalgae: A critical review**
Meita Eka FARA, Muslim MUSLIM, Miftakul MUNIR

Environ Res Tec, Vol. 8, Issue. 2, pp. 234–244, June 2025

Environmental Research and Technology
https://dergipark.org.tr/en/pub/ert
DOI: https://10.35208/ert.1484374

Environmental Research & Technology

Research Article

Water quality and spatial distribution of wells in the Eastern Side of Nineveh Governorate – Iraq

Kotayba T. AL-YOUZBAKEY*[1], Ali M. SULAIMAN[1]

[1]*Dams and Water Resources Research Center, University of Mosul, Mosul , Iraq*

ARTICLE INFO

Article history
Received: 16 May 2024
Revised: 26 Jul 2024
Accepted: 04 Aug 2024

Key words:
WQI, water assessment, water quality, groundwater, nineveh.

ABSTRACT

The quality of groundwater in the studied area are related to the reservoir rock types, which are mainly represented by the dolomitic limestone of Pila Spi Formation, the limestone and gypsum of Fat'ha Formation, the sandstone of Injana Formation, the sandstone of Muqdadiya Formation. These rocks exposed at the feet of Bashiqa and Ain Al-Safra mountains. The ability of minerals in these rocks to dissolve under weathering conditions also affects water quality.
The water quality index (WQI) was calculated to determine its suitability for domestic uses based on the physical (pH, E.C, T.D.S and T.H) and chemical (Ca^{2+}, Mg^{2+}, N^{a+}, K^{+}, HCO_{3}^{-}, SO_{4}^{2-}, Cl^{-} and NO_{3}^{-}) specifications of forty-one wells. The distribution of wells was determined according to their specifications. In general, the study area was divided from north to south into six regions with QWI; excellent water, good water, unsuitable water, poor water quality, while the area adjacent to Ain Al-Sufra Mountain has a good water, and the area located to the southwest towards the Tigris River is very poor water.
The SAR ratio (< 10) and the sodium percentage (SSP% < 75%) indicated a low soda content, the amount of RSBC < 1.25 meq L-, the Kelly ratio (KR < 1) and permeability index (PI < 75%) have no effect on the soil properties and no negative impacts on the quality of irrigation water, thus the well water source is suitable for irrigating most crops and all types of soil.

Cite this article as: Al-Youzbakey KT, Sulaiman AM. Water quality and spatial distribution of wells in the Eastern Side of Nineveh Governorate – Iraq. Environ Res Tec 2025;8(2)234-244.

INTRODUCTION

Groundwater is an important resource, especially in areas where water resources do not meet the requirements of life. Therefore, population centers in areas far from rivers are linked to the quantity and quality of groundwater available. The study area represents a large part of the eastern part of Nineveh Governorate, which is dotted with small cities and villages with population and agricultural activity.

Study area

Nineveh Governorate is located in the northern part of Iraq, and the study area is located east of the Tigris River within the eastern side of Nineveh Governorate between (36°00'00' - 36°45'00") to the north and (42°45'00" - 43°45'00" to the east, The area of the study area is 4,110 km2, bordered to the north by Mount Al-Qosh, Mount Dehqan, Mount Qand, and Mount Bashiqa to the northeast, Mount Ain Al-Safra to the east, the Khazar River and the Great Zab River to the south-east, and the Tigris River to the southwest and west, (Fig. 1).

***Corresponding author.**
*E-mail address: kotaybatawfiq@gmail.com

This is an open access article under the CC BY-NC license (http://creativecommons.org/licenses/by-nc/4.0/).

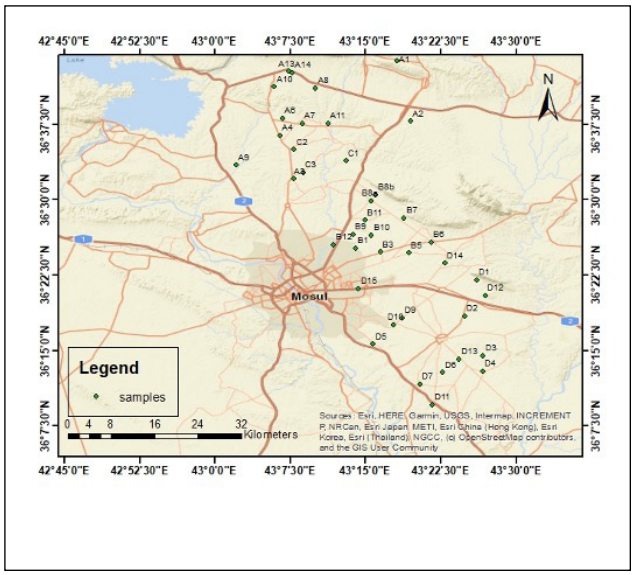


Figure 1. The distribution of the wells in the studied area.

The most important structural features in the region are the presence of mountains surrounding the region from the eastern side, represented by the Qand Mountain (about 450 m.a.s.l.), which represents the Qand anticline, which is located in the northeastern side and its axis is northwest-southeast. Its length is 22.5 km and its width ranges from (2.5-4.5) km. Then Mount Bashiqa (657 m.a.s.l.), which represents the Fadhiliyah and Bashiqa anticlines, which follow in the same direction northwest - southwest, with a length of 15 km and 10 km, respectively, with a width of 2 km. And Ain Al-Safra Mountain (68 m.a.s.l.) represents Ain Al-Safra Anticline, which is located to the southeast of Mount Bashiqa and its axis is northwest-southeast, with a length of 8 km and a width of 3.5 km.

Geological setting

Rocks belong to several formations are exposed in the region, the oldest of which is the Pila Spi Formation (Middle-Upper Eocene), which composed of hard, stratified dolomitized limestone, represent the Bashiqa and Ain Al-Safra Mountains, and occupy the core of these folds [1]. The Fatha Formation (Middle Miocene) finds appear at the feet of the Bashiqa and Ain Al-Safra mountains in the form of a belt surrounding them [2]. The Fatha Formation includes several depositional cycles consisting of successions of green marl, limestone, clay and gypsum-anhydrite rocks [3, 4]. The Ingana Formation (Upper Miocene) follows the Fatha Formation and appears as discontinuous ridges around the Bashiqa-Fadhiliya anticlines and the Ain Al-Safra anticline [5], while its rocks represent Mount Qand [6]. The Injana Formation consists of sedimentary cycles of sandstone, siltstone, and mudstone [1]. It is followed by the Muqdadiya Formation (Pliocene), consisting of a succession of sandstone, shale, and siltstone, with layers of sandstone containing gravel [1, 2]. Bai Hassan Formation (Pliocene – Pleistocene), it is considered the newest formation in the region, consists of alternation of thick conglomerate and reddish-brown claystone, with thin gray sandstone [1, 5].

The above formations are covered by Quaternary deposits (Pleistocene), and are represented by river terrace deposits consisting of conglomerates containing sand and alluvial lenses, slope deposits, floodplain deposits, [5, 7], and alluvial fans containing rock fragment components. Some of them are bound with calcareous cement [1]. These sediments generally represent the products of weathering of the above formations that are exposed to weathering and erosion activities [2]. As for the upper layer of soil, it is of the type of aerated and riverine transported soil. It has a fine texture, a brown color, and contains a high percentage of sulphates and carbonates, resulting from the weathering of evaporite rocks and limestone belonging to the Fatha Formation mainly [8, 9].

The region is generally characterized by its varying terrain, ranging from flat to slightly sloping and undulating towards the southwest, and its average elevation ranges between 300-400 m.a.s.l. The region generally descends from mountainous areas towards the south and southwest towards the Tigris River, and the region is interspersed with a group of main and subsidiary valleys towards the south and southwest towards the Tigris River and the Greater Zab River, [2, 8, 9, 10]. The region also slopes topographically from the city of Mosul in a northeasterly direction, and thus the study area forms a wide, low-lying depression represented midway between the city of Mosul and the mountains of Bashiqa and Qand, [11]. This depression represents the area where rainfall in the region reaches 375-425 mm on average for the period 2010-2020, according to data from the Iraqi General Authority for Meteorology, [12], that feeds it with groundwater, through the many parallel valleys extending from the mountainous areas towards the region, [13]. The valleys also transport the products of weathering and erosion from the high areas, which often represent outcrops of geological formations in the region, and these sediments are spread to cover the region [1].

Al-Youzbakey and Eclimes, [14] pointed out that the topography of the region has contributed to influencing the hydrochemical characteristics of the water. Shallow wells in the Al-Hamdaniya area, as the phenomena of seepage and rainwater infiltration reflected the activity of dissolution processes for the rock components present in the resent sediments derived from the rocks of the region and in the soil, which are mainly composed of evaporites and marl, in addition to the carbonate components.

Al-Youzbakey and Sulaiman [13] showed that the study area is generally characterized by two types of underground wells. The first type is characterized by being shallow, shallow wells that represent underground reservoirs within the sandstone layer belonging to the Injana Formation, with a low content of salts. The other type is with deep wells that reach underground reservoirs within the Fatha Formation, which is a network of dissolution channels within the gypsum rocks, and therefore its sulfate content is high, which makes the use of water limited for irrigation purposes and

for specific types of crops that tolerate high sulfur concentrations.

The results of Al-Saffawi et al [15] study indicated that the water quality index values in the wells of the Hamdaniya region ranged between (33.0 to 282) due to the different geological formations through which the water passes, as 45% of the water samples were of the invalid category, and 25% from the category of poor-quality water. The remaining 30% is water suitable for watering livestock and poultry.

Al-Sayegh and Khaled [9] explain that most of the soils of the study area are calcareous soils, as the highest value was recorded in the fifth horizon of the Tal Kayf soil in the Al-Qosh Plain (450.8 g.kg-1), while the lowest values were recorded in the Bashiqa soil (268.4 gm.kg-1). As for the distribution of calcium carbonate in the soil, the results showed some increases in the calcium carbonate content with depth.

Najeeb and Saeed [16] calculated the water quality factor for selected wells in the Al-Hamdaniya District and found that the water quality is not suitable for drinking. They pointed out that the phenomenon of drought and declining rainfall are among the most prominent factors affecting water quality in the region.

The study aims to determine the distribution of wells according to their quality for the purpose of determining the different areas of their use or non-use due to their quality.

METHODOLOGY

Forty-one wells were selected to cover the study area: A1 (Taq Harb), A2 (Mahad complex), A3 (Batnay), A4 (Telskuf), A6 (Dughat), A7 (Sershka), A8 (Shekhka), A9 (Gara Eshaq), A10 (Sharafya), A11 (Alqosh), A12 (Dahqan sagheer), A13 (Zaytoon farm1), A14 (Zaytoon farm2), B1 (Orta Kharab), B3 (Dar Smagh), B5 (Abu Jarbuaa), B6 (Bashiqa cross), B7 (Al-Benit farm), B8a (Al-Fadhelya1), B8b (Al-Fadhelya2), B9 (Bibukhet), B1 (Telyara), B11 (Semaqya), B12 (Abasya), C1 (Rakaba), C2 (Bakufa), C3 (Mar Oraha), D1 (Basakhra), D2 (Karamleas), D3 (kabarly), D4 (Khraba Sultan), D5 (Yarghanty), D6 (Kahreez), D7 (Omar Khan), D9 (Manara Shabak), D10 (Ali Rash), D11 (Tel Aakub), D12 (Bazkertan), D13 (Plawat), D14 (Teas Kharab), D15 (Kogjaly), (Fig. 1).

The temperature, acid function, and electrical conductivity were measured in the field, using a portable Ec type (hold / 3meter), and laboratory analyzes were conducted according to standard methods [17]. Total hardness, calcium and magnesium were measured by elution with EDTA, and chloride by elution with HCl. The flame spectrophotometer method was used with a JENWAY PEP7 type flame spectrophotometer to measure sodium and potassium. Colorimetric methods were used to measure sulphates and nitrates using a device (UV- Spectrophoto-meter type - OGAWA, OSK 7724). Total soluble salts were measured laboratory by the traditional method [18].

The ionic balance was used between the concentrations of cations and anions in (meq L-1) to achieve analytical accuracy according to equation (1), [19].

$$\text{Ionic balance (\%)} = (\Sigma cat. - \Sigma ani.) / (\Sigma cat. + \Sigma ani.) \times 100 \quad \ldots\ldots (1)$$

The Water Quality Index (WQI) represents the conversion of all data related to water quality into a mathematical number that expresses the level of water quality [20, 21, 22] to determine the suitability of well water in the two study areas. For drinking and civilian uses, the water quality index (WQI) was calculated using all of the above parameters and based on World Health Organization standards (Table 1) [23], and according to equation (2) and table (2). [24]:

$$IWQI=\sum Qi*Wi/\sum Wi \quad \ldots\ldots (2)$$

$$Qi=100\times(Vm-Vi)/(Vs-Vi)$$

$$Wi=K/Vs$$

whereas:

Qi = is a measure of the total element quality in the water.

Vm = measured value of water samples (measured analytes)

Vi = the ideal value is zero for most parameters, except pH =7 according to [24].

Vs = standard values of the water quality parameters given by WHO..... [23]

Wi = is the relative unit weight of the element n.

K = is a constant of proportionality, and its value = 1.

The following equations were used to calculate the sodium adsorption rate (SAR), the percentage of sodium (SSP), the amount of carbon remaining in the soil (Residual sodium carbonate, RSBC), the permeability index (PI), the percentage of magnesium (MAR), and the Kelley ratio (KR). All the concentrations are in meq L-:

$$SAR=Na^{+}/(\sqrt{(Ca^{2}+Mg^{2+}/2} \quad \ldots\ldots (3)$$

$$SSP(Na\%) = (Na^{+} + K^{+} X 100) / (Ca^{2+} + Mg^{2+} + Na^{+} + K^{+}) \quad \ldots\ldots (4)$$

$$RSBC=(CO_3^{2-}+HCO_3^{-})-(Ca^{2+}+Mg^{2+}) \quad \ldots\ldots (5)$$

$$PI=(Na^{+}+\sqrt{HCO_3^{-}}X100)/Ca^{2+}+Mg^{2+}+Na^{+}) \quad \ldots\ldots (6)$$

$$KR=Na+/(Ca^{2+}+Mg^{2+}) \quad \ldots\ldots (7)$$

$$MAR=Mg^{2+}X100/(Ca^{2+}+Mg^{2+}) \quad \ldots\ldots (8)$$

RESULTS AND DISCUSSION

Table (3) shows the physical (pH, E.C., TDS, TH) and chemical (Ca^{2+}, Mg^{2+}, Na^{+}, K^{+}, HCO_3^{-}, SO_4^{2-}, Cl^{-} and NO_3^{-}) specifications that control the water quality of the wells of the study area. The pH values (Minimum-Maximum and Average) for the four groups A, B, C and D were (7.1-8.13, 7.42), (6.94-7.94, 7.34), (7.50-8.00, 7.77) and (7.00-8.10, 7.53). respectively. The TDS values for the four groups were (279-1758, 834), (1060-3440, 1882), (943-1185, 1097) and (255-3316, 1374) mg L-, respectively, and lower values are noted in group A compared to the other groups. This is also reflected in the electrical conductivity values of the four groups (350-

Table 1. The chemical standard specifications (Vs) for drinking water according [23].

pH	EC	TDS	TH	HCO_3^-	SO_4^{2-}	Cl^-	NO_3^-	Ca^{2+}	Mg^{2+}	Na^+	K^+
8.5	1400	1000	500	400	400	250	50	75	50	200	55

1685, 733), (1183-3528, 2068), (2010-2521, 2340) and (340-4443, 1976) µs.cm-, respectively. It is noted that the electrical conductivity values in the group are lower. A compared to other groups, despite the presence of wells with high concentrations of total dissolved salts, either due to a local change in the location of the well, such as a topographical change, an increase in human activity (agricultural and domestic), or a change in the characteristics of the host rocks. The total hardness values reached TH for the four groups (74-2100, 702), (780-2320, 1273), (965-1537, 1221) and (114-1817, 787) mg L-, respectively. Low values are generally observed in groups A and D compared to groups B and C.

The concentrations of calcium for the four groups were (16-661, 167), (168-559, 314), (198-322, 256) and (26-395, 168) mg L-, respectively, and for magnesium in the four groups (11-126, 56), (41-164, 86), (80-178, 116) and (12-208, 86) mg L-, respectively.

Table 2. Water quality scale, according to [24]

WQI values	0-25	26-50	51-75	76-100	>100
Water class	Excellent	Good	Poor	Very poor	Unsuitable

Table 3. The physical and chemical properties of well's water in the studied area.

W. S.	PH	E.C µs.cm-	T.D.S mg L-	T.H mg L-	Ca^{2+} mg L-	Mg2+ mg L-	Na^+ mg L-	K^+ mg L-	HCO_3^- mg L-	SO_4^{2-} mg L-	Cl^- mg L-	NO_3^- mg L-
A1	7.20	510	381	94	19	11	100	4	290	24	35	1
A2	7.40	350	279	98	24	20	28	10	105	83	13	12
A3	7.84	542	524	740	97	86	10	2	438	179	15	1
A4	7.34	579	548	380	54	37	20	2	140	187	10	2
A6	7.40	536	493	520	85	51	15	2	305	141	10	2
A7	7.22	631	605	580	120	24	18	3	249	187	13	6
A8	7.20	490	388	74	16	35	42	9	207	32	19	14
A9	7.30	570	1758	878	144	126	192	11	536	692	97	8
A10	7.10	550	557	195	56	41	27	3	256	91	32	2
A11	7.40	450	1396	980	262	80	41	5	334	744	23	4
A12	7.10	1000	929	487	91	70	125	2	73	530	89	6
A13	7.77	1638	1480	2000	661	68	12	3	134	1835	8	1
A14	8.13	1685	1510	2100	537	78	16	5	312	1321	24	1
Min.	7.1	350	279	74	16	11	10	2	73	24	8	1
Max.	8.13	1685	1758	2100	661	126	192	11	536	1835	97	14
Aver.	7.42	733	834	702	167	56	50	5	260	465	30	5
B1	7.24	3528	3440	1760	490	119	217	3	448	1397	219	41
B3	7.01	2898	2660	1480	492	74	203	2	392	1362	167	28
B5	7.55	3500	3129	2320	559	164	130	2	344	1759	115	28
B6	7.94	1183	1060	780	231	41	9	2	268	384	33	13
B7	6.94	1376	1360	1200	232	70	37	1	376	499	27	3
B8a	7.24	1271	1060	920	252	50	20	1	392	498	31	11
B8b	7.26	1500	1449	1080	277	72	20	2	388	556	23	10
B9	7.31	2048	1860	1380	252	114	10	2	428	623	74	47
B10	7.33	2268	2048	1160	266	87	62	2	412	480	186	47
B11	7.37	1649	1460	1020	240	81	30	1	528	509	74	7
B12	7.50	1523	1180	900	168	74	69	1	512	362	68	8
Min.	6.94	1183	1060	780	168	41	9	1	268	362	23	3

W. S.	PH	E.C µs.cm-	T.D.S mg L-	T.H mg L-	Ca^{2+} mg L-	Mg2+ mg L-	Na^{+} mg L-	K^{+} mg L-	HCO_3^- mg L-	SO_4^{2-} mg L-	Cl^- mg L-	NO_3^- mg L-
Max.	7.94	3528	3440	2320	559	164	217	3	528	1759	219	47
Aver.	7.34	2068	1882	1273	314	86	73	2	408	766	92	22
C1	7.50	2521	1185	965	198	90	210	1	420	162	296	582
C2	7.80	2489	1164	1161	249	80	154	1	473	450	248	144
C3	8.00	2010	943	1537	322	178	94	16	298	1400	50	24
Min.	7.5	2010	943	965	198	80	94	1	298	162	50	24
Max.	8	2521	1185	1537	322	178	210	16	473	1400	296	582
Aver.	7.77	2340	1097	1221	256	116	153	6	397	671	198	250
D1	7.20	1260	716	560	156	41	16	2	207	312	71	1
D2	7.00	4109	2476	1567	285	208	164	3	360	1201	248	1
D3	7.90	810	499	114	26	12	131	2	174	120	71	1
D4	7.70	935	787	786	158	95	382	2	305	936	281	9
D5	7.80	3780	2270	1161	212	153	230	2	332	1105	106	46
D6	7.80	940	3316	971	244	88	674	2	98	1268	738	15
D7	7.50	1390	786	451	90	55	96	2	238	264	71	56
D9	7.30	4042	2350	1331	317	146	64	146	455	768	355	116
D10	7.70	1224	720	414	94	50	6	70	270	192	80	67
D11	7.20	4443	2726	1817	395	171	9	142	220	1297	248	130
D12	7.20	1527	888	679	158	44	4	67	217	336	124	1
D13	7.70	970	562	247	56	26	102	2	216	138	71	25
D14	8.10	340	255	263	67	23	48	1	312	30	27	24
D15	7.30	1895	891	653	100	98	160	1	586	240	125	109
Min.	7	340	255	114	26	12	4	1	98	30	27	1
Max.	8.1	4443	3316	1817	395	208	674	146	586	1297	738	130
Aver.	7.53	1976	1374	787	168	86	149	32	285	586	187	43

Table (3) indicates that the calcium values in the well water of groups A and D are low compared to the rest of the groups, while magnesium is low in group A relative to the rest of the groups. The table also indicates that calcium concentrations are higher than magnesium concentrations, and this is due to the widespread presence of calcium sulphate phases such as gypsum, anhydrite, and calcite, more than the dolomite phase in the soil of the region derived from the erosion of exposed rocks belonging to the Pila Spi and Fat'ha formations.

Sodium and potassium are among the most important ions that make up the group of halides minerals, the most important of which is halite, which consists of sodium chloride and a small percentage of potassium substitution. The mineral halite is found within the group of evaporite rocks in the form of lenses of limited extent and small size, especially in the rocks of the Fatha Formation. It is also found in the form of secondary minerals in the upper part of the soil and on its surface as a result of the continuous dissolution, transport, and sedimentation factors to which the soil is exposed due to rainwater and surface water, especially during rainfall. The sodium concentration for the four groups ranged from (10-192, 50), (9-217, 73), (94-210, 153) and (4-674, 149) mg L-, respectively, and the potassium concentration for the four groups (2-11, 5), (1-3, 2), (1-16, 6) and (1-146, 32) mg L-, respectively. It is noted from Table (3) that the variations in sodium concentrations are due to the varying influence of climate factors, the most important of which are rainfall and a successive increase in temperature. The topography of the region directs surface water towards low-lying locations, which helps water accumulate and then precipitate halite in the event of interruption of rainfall and an increase in temperature. Potassium concentrations reflect agricultural activity that depends on the use of chemical fertilizers, and therefore its concentrations vary according to the soil content of these fertilizers, in addition to the fact that it is an ion with a high ability to dissolve and move from the surrounding areas. Low concentrations of potassium may represent the effect of clay minerals that absorb potassium and lose potassium during the washing and dissolution processes [10].

Bicarbonate is produced from many sources; The most important of which is the dissolution of carbonate minerals in the limestone rocks exposed in the region and belonging to the Pila Spi and Fatha formations, or as a result of the exposure of the carbonate clastic components in the upper part of

the soil to the influence of weathering factors, rain, and surface water resulting from them. Carbonate cement materials also contribute to marl rocks and marly limestones that are subject to chemical weathering. The bicarbonate levels for the four groups ranged from (73-536, 260), (268-528, 408), (298-473, 397) and (98-586, 285) mg L-, respectively. The bicarbonate concentrations do not vary significantly due to the similar influence of the rocky outcrops in the studied area, especially along the northeastern and northern parts of the study area, mainly represented by the Ain Safra and Bashiqa mountains, as well as the Alqosh and Dahqan Mountains in the northern and northwestern part of the study area.

Sulphates represent the most concentrated ion in well water in general. This is due to the prevalence of evaporite rocks in the Fatha Formation, which contains partial water in the form of dissolution channels and cavitations due to dissolution. This water is usually in hydraulic contact with groundwater stored in sandstones to form Injana, and therefore the water, with its sulphate content, mixes with underground reservoirs in Injana Formation. On the other hand, the soils derived from the erosion and weathering of exposed rocks of the Pila Spi and Fat'ha formations contain clastic components consisting of carbonate and gypsum minerals. These components are a source of supplying sulphates to rainwater and surface water seeping through the soil. In light of this, the region's well water varies greatly in its sulfate content depending on the effect of the above factors on water quality, as sulfate concentrations range for the four groups (24-1835, 465), (23-219, 766), (162-1400, 671) and (30-1297, 586) mg L-, respectively. It is noted from Table (1) that the sulphate concentration is very high in Group C due to the presence of water within the rocks of the Fatha Formation, and the sulphate concentrations are also high in Group D due to the influence of soil rich in carbonate and gypsum clastic components. Compared to well water in other groups.

The chloride concentration is usually associated with the sodium concentration in the well water of the study area [10] due to their presence mostly in the halite phase, and therefore its source is either from the halite lenses present within the gypsum rocks to form the hole or/and the presence of halite in the form of secondary salts in the upper part of the soil. The chloride concentration for the four groups ranges from (8-97, 30), (23-219, 92), (50-298, 198) and (27-738, 187) mg L-, respectively. These ranges reflect the effect of surface water and rainfall activities on the soil surface that contain different amount of secondary halite [25].

There are many sources of nitrates in well water. Some nitrates come from the atmosphere as a result of dissolution in rainwater and then being fixed in the soil by bacteria, or as a result of agricultural activities such as the use of complex chemical fertilizers or organic fertilizers by farmers or animal husbandry. Therefore, the concentration of nitrates in general is low except for well water located within fields with Agricultural activity and animal husbandry, so nitrate concentrations for the four groups range (1-14, 5), (3-47, 22), (24-582, 250) and (1-130, 43) mg L-, respectively.

It appears from Table (4) that the quality of water in the region's wells varies from excellent to unsuitable. Figure (2) shows the distribution of wells according to their quality. It appears that there are several areas in the north of the study area, where the wells located in the first sector near Mount Qand (in the area located on the northern flank of the Qand anticline) are distinguished by being of the excellent type. This is due to the fact that the groundwater in this

area is found within the sandy sedimentary forms belonging to the Injana Formation with There is little effect of the soil components that contain the products of sandstone erosion, and therefore the well water is of excellent quality. While the wells located to the south of Mount Qand and adjacent to the area representing the southern flank of the Qand anticline and extending south, the wells' water is of good quality and suitable for drinking. As for the wells located to the south of the previous area, their water is characterized by being unsuitable for drinking, and they are wells (C1 - C3). This is due to the fact that the water of these wells is found in reservoir rocks of the evaporite type represented by gypsum-anhydrite rocks belonging to the Fat'ha Formation. The well water in the area between Mount Bashiqa and the city of Mosul, which is located geographically to the south of the previous area, is characterized by the fact that the well water is of poor quality and is not suitable for drinking. The reason is that the water of these wells is found within the rocks of the Muqdadiya Formation and is greatly affected by the seepage of water through the containing soil. On rock pieces of carbonate and gypsum coming from the erosion of the rocks of the Pila Spi Formation and the exposed opening in the southwestern flank of the Bashiqa anticline.

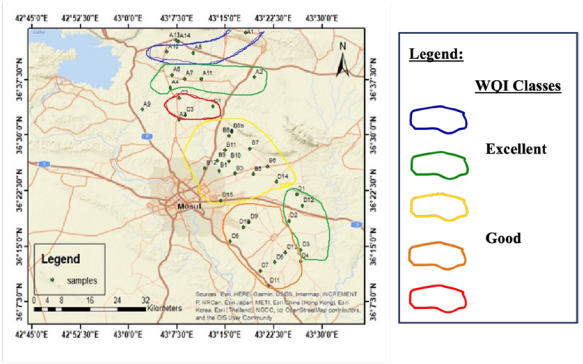


Figure 2. The general spatial distribution map of wells according to WQI.

As for the wells located within the area adjacent to the southwestern wing of the Ain Al-Safra anticline, their water is characterized by being of good quality and suitable for drinking due to the lack of influence of the soil on water quality, while the group of wells located to the southwest of the previous group is distinguished by the fact that the well water is of very poor quality. This is due to the effect of soil derived and transported from the erosion of rocks exposed within the southwestern flank of the Ain Sufra anticline, which contains clastic components of sulphate and carbonate. Therefore, the water seeping through this soil will be rich in sulfate and carbonate ions, which will lead to a significant deterioration in water quality.

Table (5) displays the ionic balance between cations and anions, which reflects the accuracy of the analysis results because the difference between the total cations and anions is generally less than 5% [19]. These values are used to calculate well water parameters for irrigation purposes.

Water quality parameters for irrigation

Nineveh Governorate is characterized by agricultural activity, especially the cultivation of wheat and barley, which depend mainly on rain. Well water, especially with low salinity, can be used for irrigation during periods of declining rainfall or for supplementary irrigation, in addition to being used to irrigate farms that grow trees and other crops.

Well water can be classified according to irrigation parameters [26]. Sodium is one of the most prominent main elements responsible for evaluating well water for irrigation purposes, because it affects soil properties more than other cations. Several parameters are used to evaluate the sodium content of well water and its effect on soil properties, such as the sodium adsorption ratio (SAR). Table (6) shows that the ratio (SAR < 10) indicates a low soda content, and thus the well water source is suitable for irrigating most crops and all types of soil. The percentage of sodium (SSP%) does not exceed 75%, which also indicates the suitability of well water for irrigation. As for the amount of residual sodium bicarbonate, it has no effect on the soil properties because all wells have RSBC values < 1.25. The Kelly ratio and permeability index (KR < 1) and (PI < 75%), respectively, indicate that well water don't have a negative impact on the quality of irrigation water and that they are good - suitable for irrigation.

It should be noted that the waters of some wells located in the northwestern part of the Nineveh plain were classified as a high content of magnesium (MAR > 50%) (Table 6), because the soil prevailing in this part is transport and derived from the dolomitic limestone and dolostone of Pila Spi Formation, and contains fragments of dolomite and dolomitic limestone.

On the other hand, sulfates do not negatively affect plants and soil, but it was noted through field observations and inquiries from farmers that high concentrations of sulfates lead to damage the plant parts, especially in the early stages of growth, in addition to the use of well water with high sulfates leads to salinization of the soil, during several years of irrigation. Therefore, well water with concentrations exceeding 20 epm (960 mg/L) is not suitable for use for irrigation purposes [27], such as wells (A13, A14, B1, B3, B5, C3, D2, D5, D6 and D11).

Table 4. Water quality index (WQI) values and classification for the well's water, according to [24].

Well Symb.	Well name	WQI	Class	Well Symb.	Well name	WQI	Class
A1	Taq Harb	15.09		A9	Gara Eshaq	60.88	
A8	Shekhka	21.70	Excellent	A11	Alqosh	61.33	
A10	Sharafyia	19.80		D4	Khraba sultan	73.21	
B7	Al-benit farm	38.55		D7	Omar kan	53.20	Poor
B8a	Al-Fadhelyia1	48.48		D10	Ali rash	71.96	
A2	Mahad complex	26.43		D14	Teas Kharab	59.20	
A4	Telskuf	27.84		D15	Kogjaly	67.77	
A6	Dughat	36.02		B1	OrtaKharab	98.45	
A7	Sershka	28.14	Good	B3	Dar Smagh	76.61	
A12	Dahqan sagheer	32.28		D2	Karamleas	79.15	Very poor
D1	Basakhra	33.55		D5	Yarghanty	99.54	
D3	kabarly	42.86		D6	Kahreez	93.22	
D12	Bazkertan	45.36		B5	Abu Jarbuaa	122.01	Unsuitable
D13	Plawat	45.40		A13	Zaytoon farm1	110.96	
B6	Bashiqa cross	70.89		A14	Zaytoon farm2	115.58	
B8b	Al-Fadhelyia2	56.27		C1	Rakaba	175.71	
B9	Bibukhet	72.80		C2	Bakufa	105.19	
B10	Telyara	70.27	Poor	C3	Mar Oraha	117.77	
B11	Semaqya	58.98		D9	Manara Shabak	124.52	
B12	Abasyia	56.09		D11	Tel Aakub	134.95	
A3	Batnay	61.24					

Table 5. The ionic balance for the water of the studied wells (meq L-).

	Ca^{2+}	Mg^{2+}	Na^{+}	K^{+}	Total	HCO_3^-	SO_4^{2-}	Cl^-	NO_3^-	Total	Δ
A1	0.95	0.90	4.35	0.10	6.30	4.75	0.50	0.99	0.02	6.26	0.04
A2	1.20	1.64	1.22	0.26	4.32	1.72	1.73	0.37	0.19	4.01	0.31
A3	4.84	7.07	0.43	0.05	12.40	7.18	3.73	0.42	0.02	11.34	1.06
A4	2.69	3.04	0.87	0.05	6.66	2.29	3.89	0.28	0.03	6.50	0.16
A6	4.24	4.19	0.65	0.05	9.14	5.00	2.94	0.28	0.03	8.25	0.89
A7	5.99	1.97	0.78	0.08	8.82	4.08	3.89	0.37	0.10	8.44	0.38
A8	0.80	2.88	1.83	0.23	5.73	3.39	0.67	0.54	0.23	4.82	0.91
A9	7.19	10.36	8.35	0.28	26.18	8.79	14.40	2.74	0.13	26.05	0.13
A10	2.79	3.37	1.17	0.08	7.42	4.20	1.89	0.90	0.03	7.02	0.4
A11	13.07	6.58	1.78	0.13	21.56	5.47	15.49	0.65	0.06	21.67	0.11
A12	4.54	5.76	5.43	0.05	15.78	1.20	11.03	2.51	0.10	14.84	0.94
A13	32.98	5.59	0.52	0.08	39.17	2.20	38.20	0.23	0.02	40.64	1.47
A14	26.80	6.41	0.70	0.13	34.03	5.11	27.50	0.68	0.02	33.30	0.73
B1	24.45	9.79	9.43	0.08	43.75	7.34	29.08	6.18	0.66	43.26	0.49
B3	24.55	6.09	8.83	0.05	39.51	6.43	28.35	4.71	0.45	39.94	0.43
B5	27.89	13.49	5.65	0.05	47.08	5.64	36.62	3.24	0.45	45.95	1.13
B6	11.53	3.37	0.39	0.05	15.34	4.39	7.99	0.93	0.21	13.53	1.81
B7	11.58	5.76	1.61	0.03	18.97	6.16	10.39	0.76	0.05	17.36	1.61
B8a	12.57	4.11	0.87	0.03	17.58	6.43	10.37	0.87	0.18	17.84	0.26
B8b	13.82	5.92	0.87	0.05	20.66	6.36	11.57	0.65	0.16	18.74	1.92
B9	12.57	9.38	0.43	0.05	22.44	7.02	12.97	2.09	0.76	22.83	0.39
B10	13.27	7.15	2.70	0.05	23.17	6.75	9.99	5.25	0.76	22.75	0.42
B11	11.98	6.66	1.30	0.03	19.97	8.65	10.60	2.09	0.11	21.45	1.48
B12	8.38	6.09	3.00	0.03	17.49	8.39	7.54	1.92	0.13	17.97	0.48
C1	9.88	7.40	9.13	0.03	26.44	6.88	3.37	8.35	9.39	27.99	1.55
C2	12.43	6.58	6.70	0.03	25.73	7.75	9.37	6.99	2.32	26.44	0.71
C3	16.07	14.64	4.09	0.41	35.20	4.88	29.14	1.41	0.39	35.82	0.62
D1	7.79	3.41	0.69	0.05	11.94	3.39	6.50	2.00	0.02	11.91	0.03
D2	14.20	17.12	7.12	0.06	38.50	5.90	24.99	7.00	0.02	37.91	0.59
D3	1.30	0.98	5.71	0.05	8.04	2.86	2.50	2.00	0.02	7.37	0.67
D4	7.88	7.81	16.61	0.05	32.36	5.00	19.48	7.92	0.15	32.55	0.19
D5	10.60	12.60	9.98	0.04	33.22	5.44	23.00	3.00	0.74	32.17	1.05
D6	12.18	7.24	29.30	0.05	48.77	1.61	26.39	20.81	0.24	49.06	0.29
D7	4.50	4.52	4.19	0.04	13.25	3.90	5.50	2.00	0.90	12.30	0.95
D9	15.82	12.01	2.78	3.73	34.34	7.46	15.99	10.01	1.87	35.33	0.99
D10	4.69	4.11	0.26	1.79	10.85	4.43	4.00	2.26	1.08	11.76	0.91
D11	19.71	14.06	0.39	3.63	37.80	3.61	27.00	6.99	2.10	39.69	1.89
D12	7.88	3.62	0.17	1.71	13.39	3.56	6.99	3.50	0.02	14.06	0.67
D13	2.80	2.14	4.44	0.04	9.42	3.54	2.87	2.00	0.41	8.82	0.6
D14	3.36	1.89	2.09	0.03	7.36	5.12	0.62	0.76	0.38	6.89	0.47
D15	4.99	8.06	6.96	0.04	20.04	9.60	5.00	3.52	1.76	19.88	0.16

Table 6. The water parameters for Irrigation.

	SAR	SSP (%)	RSBC (meq L^-)	PI (%)	KR	MAR (%)
A2	1.02	28.21	-1.12	32.61	0.43	57.87
A3	0.18	3.51	-4.73	21.74	0.04	59.37
A4	0.51	13.06	-3.44	23.06	0.15	53.03
A6	0.32	7.14	-3.44	24.67	0.08	49.72
A7	0.39	8.87	-3.88	23.19	0.10	24.79
A8	1.35	31.85	-0.28	33.81	0.50	78.28
A9	2.82	31.89	-8.76	11.77	0.48	59.05
A10	0.67	15.83	-1.97	28.07	0.19	54.68
A11	0.57	8.27	-14.18	11.00	0.09	33.48
A12	2.40	34.43	-9.10	7.30	0.53	55.90
A13	0.12	1.33	-36.38	3.80	0.01	14.50
A14	0.17	2.04	-28.10	6.69	0.02	19.31
B1	2.28	21.57	-26.89	6.42	0.28	28.58
B3	2.26	22.34	-24.21	6.65	0.29	19.86
B5	1.24	12.00	-35.74	5.17	0.14	32.59
B6	0.14	2.55	-10.51	13.73	0.03	22.63
B7	0.55	8.48	-11.17	13.19	0.09	33.21
B8a	0.30	4.95	-10.26	14.49	0.05	24.64
B8b	0.28	4.21	-13.38	12.28	0.04	29.99
B9	0.13	1.94	-14.93	11.85	0.02	42.71
B10	0.84	11.63	-13.68	11.35	0.13	35.02
B11	0.43	6.53	-9.98	14.82	0.07	35.74
B12	1.12	17.15	-6.08	16.76	0.21	42.06
C1	3.11	34.54	-10.40	10.28	0.53	42.83
C2	2.17	26.03	-11.25	11.09	0.35	34.62
C3	1.04	11.61	-25.82	6.47	0.13	47.67
D1	0.29	5.78	-7.81	15.54	0.06	30.43
D2	1.80	18.49	-25.42	6.50	0.23	54.66
D3	5.35	71.02	0.58	21.88	2.50	42.99
D4	5.93	51.33	-10.70	7.44	1.06	49.77
D5	2.93	30.04	-17.76	7.33	0.43	54.31
D6	9.41	60.09	-17.81	3.20	1.51	37.28
D7	1.97	31.62	-5.12	15.27	0.46	50.11
D9	0.75	8.10	-20.37	9.01	0.10	43.15
D10	0.12	2.40	-4.38	23.24	0.03	46.71
D11	0.10	1.04	-30.17	5.57	0.01	41.64
D12	0.07	1.30	-7.95	16.17	0.02	31.46
D13	2.83	47.14	-1.40	20.53	0.90	43.32
D14	1.29	28.34	-0.13	31.12	0.40	36.02
D15	**2.72**	**34.71**	**-3.45**	**15.83**	**0.53**	**61.76**

CONCLUSION

The study area includes several types of rocks that store groundwater, dating back to the geological formations that spread in the region. They are represented by marl, limestone, and gypsum rocks belonging to the Fatha Formation, and sand rocks belonging to the Injana and Muqdadiya Formations. The quality of water is affected by the quality of reservoir rocks and exposed rocks, especially in topographically rugged areas such as the feet of the Ain Safra and Bashiqa mountains, as well as the soil covering the area containing clastic components of carbonate and gypsum, which represent the products of weathering and erosion of the rocks from which the soil is derived. Therefore, a large number of wells had a high TDS content as a result of high concentrations of sulfate and bicarbonate, in addition to calcium and magnesium. The chemical specifications were reflected the quality of water (WQI), from excellent to unsuitable water. The percentage of wells was 7% excellent water, 27% good water, 34% poor water, 12% very poor water, and 20% unsuitable water for domestic use. These categories were generally divided the studied area into six regions, interspersed with some locations that were affected by the type and intensity of activity there.

The ratio (SAR < 10) and the percentage of sodium (SSP%) does not exceed 75% indicates a low soda content, and thus the well water source is suitable for irrigating most crops and all types of soil, the amount of RSBC values < 1.25, the Kelly ratio (KR < 1) and permeability index (PI < 75%) have no effect on the soil properties and negative impact on the quality of irrigation water.

DATA AVAILABILITY STATEMENT

The author confirm that the data that supports the findings of this study are available within the article. Raw data that support the finding of this study are available from the corresponding author, upon reasonable request.

CONFLICT OF INTEREST

The author declared no potential conflicts of interest with respect to the research, authorship, and/or publication of this article.

USE OF AI FOR WRITING ASSISTANCE

Not declared.

ETHICS

There are no ethical issues with the publication of this manuscript.

REFERENCES

[1] V. K. Sissakian, "Geomorphology and Morphometry of the Greater Zab River Basin, North of Iraq". Iraqi Bulletin of Geology and Mining, 9 (3), p 21 - 49. 2013.

[2] K. T. Al-Youzbakey, and Y. F. Eclimes, "Hydrological and Hydrogeochemical Study of Al-Qush Plain, Northern Iraq" The proceeding of the 9th Periodical Scientific Conference of Dams and Water Resources Research Center, 28-29 Nov. 2018, 165-176. 2018.

[3] M. A. R. Al-Mubarak and R.Y. Youkhanna, "Report on the regional geological mapping of AL-Fat'ha-Mosul area." Unpublished report, Directorate General of Geological. Survey, and Mineral Investigation, Baghdad, 753A, 95P. 1976.

[4] A. I. Al-Juboury, and T. McCann, "The Middle Miocene Fatha (Lower Fars) Formation, Iraq." GeoArabia, 13 (3), Gulf PetroLink, Bahrain. pp141-174. 2008.

[5] M. M. Alsalmany, R. Gh. Thannoun, and A. T. Shehab, "Determining the impact of climatic elements on vegetation cover based on remote sensing data - (Al-Hamdaniya district as a case study)." Iraqi National Journal of Earth Science, Vol. 23, No. 1, 2023 (13-25), DOI: 10.33899/earth.2022.134400.1017. 2003.

[6] M. A. M. Al-Rashidi, "Sedimentary study of the Injana Formation in the Qand anticline / northern Iraq." Unpublished MSc Thesis, College of Science, University of Mosul. 135P. 2005.

[7] R. G. Th., Al-Banna, "Geomorphology of the Qand Structure in Northern Iraq Using Remote Sensing Techniques," Unpublished MSc Thesis, College of Science, University of Mosul, 119P. 2002.

[8] K. T. Al-Youzbakey, and Y. F. Eclimes, "Hydrogeochemical and Geophysical Study of Selected Deep Boreholes in Al-Hamdanyia Area, North Iraq." Al-Rafidain Journal of Sciences, 16(1), 136-151. 2005.

[9] N. N. Al-Sayegh, and K. A. Khaled, "Using the Standard Multiplication and Addition Methods in Evaluating the Agricultural Lands for a Selected Areas at Northeastern Nineveh Governorate." Mesopotamia Journal of Agriculture, 49 (2), 1-8. 2021.

[10] K. T. Al-Youzbakey, and A. M. Sulaiman, "Ground Water Quality of Selected Areas in the Northeastern Mosul City and their Assessments for Domestic and Agricultural Usage." Iraqi National Journal of Earth science, 20(1), 107-126. 2020.

[11] K. T. Al-Youzbakey, A. M. Sulaiman, and D. A. Ismaeel, "The Evaluation of Chemical Characterization for Selected Wells Water in Mosul – Bahshiqa – Shalalat Area, Ninivah Governorate, Northern Iraq." The proceeding of the 9th Periodical Scientific Conference of Dams and Water Resources Research Center, 28-29 Nov. 2018, 201-216. 2018.

[12] A. S. Kateb and K. T. Al-Youzbakey, "Development and Evaluation of the Drinking Water Quality Index in the Eastern Bank of Nineveh Governorate." Italian Journal of Engineering Geology and Environ-

ment, 2, 17-30. DOI: 10.4408/IJEGE.2022-02.O-02. 2023.

[13] K. T. Al-Youzbakey, and A. M. Sulaiman, "Evaluation of Ground Water Quality in Al-Qush – Tel Kafe Area, North Mosul City." The proceeding of the 8th Periodical Scientific Conference of Dams and Water Resources Research Center, 28-29 Nov. 2012, 155-164. 2012.

[14] K. T. Al-Youzbakey and Y. F. M. Eclimes, "Hydrogeochemical Evaluation of Selected Shallow Boreholes in Al-Hamdanyia Area, North Iraq." Proceeding of the 1st Conference of The Environment and Controlling of Pollution Research Center, 5-6 June, 78-88. 2007.

[15] A. Y. T. Al-Saffawi, N. D. S. Al-Taay, and A. Y. H. Kaplan, "Qualitative assessment of groundwater for livestock and poultry watering: A case study of water wells in Hamdaniya district, Nineveh governorate, Iraq." IOP Conf. Series: Earth and Environmental Science 735, 012018 .IOP Publishing. doi:10.1088/1755-1315/735/1/012018. 2021.

[16] R. R. Najeeb and I. O. Saeed, (2022) "Evaluating Groundwater Quality in Al-Hamdaniya District For Drinking Purpose Using the Canadian Water Quality Index Model (CCME WQI)." Egyptian Journal of Aquatic Biology & Fisheries, Vol. 26(6): 243 – 255. 2022.

[17] W. E. Federation, APHA, AWWA, W.E.F. "Standard Methods for examination of water and wastewater." In Anales de Hidrología Médica, 5(2): 185-186. 2012.

[18] Abbawi, S. A. and M. S. Hassan, The Practice Engineering for Environment. Water Analysis. Dar Al-Hekma for Publishing, University of Mosul. Engineering for Environment. 296P. 1990.

[19] R. B. Baird, A. D. Eaton and E. W. Rice, APHA, Standard Methods for the Examination of Water and Wastewater. 23rd.American Public Health Association. American Water Works Association and Water Environment Federation, 1504P. 2017.

[20] S. K. Kumar, A. Logeshkumaran, N. S. Magesh, P. S. Godson and N. Chandrasekar, "Hydro-geochemistry and application of water quality index (WQI) for groundwater quality assessment, Anna Nagar, part of Chennai City, Tamil Nadu, India." Applied Water Science 5: 4, 335–343. https://doi.org/10.1007/s13201-014-0196-4. 2015.

[21] G. J. Udom, H.O. Nwankwoala, and T. E. Daniel, "Determination of Water Quality Index of Shallow Quaternary Aquifer Systems in Ogbia, Bayelsa State, Nigeria." British Journal of Earth Sciences Research 4: 1, 23–37. 2016.

[22] K. E. Leizou, J. O. Nduka and A. W. Verla, "Evaluation of Water Quality Index of the Brass River, Bayelsa State, South-South, Nigeria." International Journal of Research - Granthaalayah 5: 8, 277–287. https://doi.org/10.5281/zenodo.894650. 2017.

[23] WHO (World Health Organization), Guidelines for Drinking-Water Quality. 4th Edition, World Health Organization, Geneva. 564P. 2017.

[24] R. Gupta and A. K. Misra, "Groundwater quality analysis of quaternary aquifers in Jhajjar District, Haryana, India: Focus on groundwater fluoride and health implications." Alexandria Engineering Journal 57 (1): 375–381. https://doi.org/10.1016/j.aej.2016.08.031. 2016.

[25] F. R. Najeeb, S. A. Saleh and M. F. Abed, "Hydrogeology of Al-Hamdaniya, Northern Iraq." Iraqi Geological Journal, 54 (2B), 112-121. 2021.

[26] C. H. Yilmaz, H. Aytop and M. R. Sünbül, "Evaluation of Quality of Some Well Waters Used in Agricultural Irrigation in terms of Plant Nutrition". Toprak Su Dergisi, 10 (2), 94-103. 2021.

[27] N. Adimalla, Li. Peiyue and S. Venkatayogi, "Hydrogeochemical evaluation of groundwater quality for drinking and irrigation purposes and integrated interpretation with water quality index studies." Environmental Processes, 5(2), 363–383. 2018.

Environ Res Tec, Vol. 8, Issue. 2, pp. 245-254, June 2025

Environmental Research and Technology
https://dergipark.org.tr/en/pub/ert
DOI: https://10.35208/ert.1498026

Research Article

Sulfonated plastic waste: A solution for water hardness reduction

Minjal PATEL[1], Bina Birenkumar PATEL[2*], Isha LAD[3]

[1]Assistant Environment Engineer Gujarat Pollution Control Board, Gandhinagar, India
[2] Assistant Professor Environmental Engineering Department, L. D. College of Engineering, Ahmedabad, India
[3]Assistant Professor, Civil Engineering Department, Parul University, Vadodara, India

ARTICLE INFO

Article history
Received: 09 Jun 2024
Revised: 24 Jul 2024
Accepted:20 Aug 2024

Key words:
Air bubble plastic resin, ground water, hardness, styrofoam resin, waste plastic

ABSTRACT

This study focused on the utilisation of waste plastic as an ion exchanger to reduce water hardness. The three identical glass columns R1, R2, and R3 were used, each containing different types of waste plastic resin, such as styrofoam resin (SR), air bubble plastic resin (AR), or a mixture of both resins (MR), respectively. The plastics underwent a sulfonation process after crushing and sieving; their sulfonation was confirmed using FTIR analysis. For lab-scale experiments, each glass column was filled with sand, gravel, and coconut fiber as supporting media and equipped with a pump and flow-control valves. Groundwater collected from an urban area was passed through the columns at different flow rates and contact times. The process takes place by exchanging the Na+ ions of resins with polluting ions present in hard water. The treatment parameters involved are total hardness, calcium hardness, magnesium hardness, chloride, TDS, and pH. During the treatment process, pH was maintained between 7 and 8.5. All the parameters were tested twice, and the average of the observations was noted. The results showed that the maximum total hardness reduction achieved in reactors R1, R2, and R3 was 63%, 52%, and 58.6%, respectively, at a contact time of 24 h.

Cite this article as: Patel M, Patel BB, Lad I. Sulfonated plastic waste: A solution for water hardness reduction. Environ Res Tec 2025;8(2) 245-254.

Nomenclature

AR- Air bubble plastic resin

Ca-Calcium

$CaCO_3$- Calcium carbonate

FTIR- Fourier transform infrared spectroscopy

H_2SO_4 - Sulfuric acid

LDPE-Low-density polyethylene

Mg-Magnesium

MR-Mixture of styrofoam and air bubble plastic resin

NaCl- Sodium chloride

SO_3 – Sulfur trioxide

SR-Styrofoam resin

TDS- Total dissolved solids

TH-Total hardness

***Corresponding author.**
*E-mail address: bina.patel@ldce.ac.in

This is an open access article under the CC BY-NC license (http://creativecommons.org/licenses/by-nc/4.0/).

INTRODUCTION

Plastic waste has become a major environmental concern in recent years due to its non-biodegradable nature and the enormous amount of waste produced globally. Due to the fact that millions of tons of plastic garbage are produced each year, waste plastic has recently grown to be a significant environmental problem. A lot of the plastic waste still ends up in landfills or pollutes the environment, despite some nation's efforts to limit it by outlawing specific single-use plastics or putting recycling programs in place. Because plastic waste takes hundreds of years to disintegrate and releases hazardous chemicals that can pollute soil and water, it poses a serious risk to both the environment and human health when it is disposed of [1]–[3].

Despite efforts to mitigate its impact through legislation and recycling initiatives, the sheer volume of plastic produced annually continues to pose significant challenges. Of particular concern is polystyrene plastic, widely utilized in various industries for its versatile properties, including hardness reduction capabilities. An evaluation conducted by a previous study shows that the relative importance of reduce, reuse, repair, recycle, recover, and dispose of in a waste management strategy is shown by a six-level pyramid. Among all these factors, the most crucial one is lowering our own desire to purchase ostentatious plastic items [1], [4].

Ion exchange technology actually refers to the fact that when water passes through the ion exchange column, cations and anions in the water are exchanged with H+ ion of the positive resin and OH- ion of the negative resin ion, which is widely used for various purposes, especially pollutant reduction in water and wastewater treatment [5]–[10]. Table 1 highlights some of the previous studies using the ion exchange method, which have attempted to reduce the water hardness using different kinds of waste plastics.

Table 1. Types of waste plastic utilized by different studies with their summary results

Types of hard water sample	Column study or other	Type of waste plastic used	Procedure To check Sulfonation	Achieved hardness reduction	References
Synthetic hard water	Other	On-spec Polystyrene Sample, Waste Polystyrene Off-spec sample and waste plastic	FTIR	Ca: 47- 51% Mg: 68 - 74%	[11]
Synthetic hard water	Other	White coffee cup	FTIR	Ca: 60% Mg: 60%	[12]
Actual ground water	Column	Polystyrene foam	-	Total hardness: 42%	[10]
Synthetic hard water	Other	Virgin Polystyrene and Off spec Polystyrene	FTIR	Ca: 47 - 49%. Mg: 68 - 74%	[13]
Actual ground water	Column	Zeolite	FTIR for aluminium silicate and hydrogen bond	Total :81% Ca: 82% Mg: 84%	[14]
Wastewater	Other	Waste polystyrene	FTIR	Effective Lead and cadmium removal	[15]
Synthetic Hard water	Other	Rice straw	FTIR	Ca: 98%	[16]
Synthetic hard water	Other	LDPE	FTIR	Effective Lead and cadmium removal	[17]

MATERIALS AND METHODS

The study's methodology comprises seven steps. Initially, the reduction of groundwater hardness involved selecting appropriate plastic materials capable of effectively exchanging ions post-treatment. This was achieved by reacting various plastic forms with concentrated H2SO4 to produce resin. Subsequently, FTIR testing was conducted to assess the extent of sulfonation. The ion exchange capacity of the prepared resins was then determined. Following this, lab-scale reactors were set up, and their performance was evaluated with varying contact times. All the parameters were tested twice, and the average of the observations was noted. Experimental work was undertaken to test parameters such as hardness, chloride, pH, and Total Dissolved Solids (TDS) removal.

Groundwater collection and characteristic

Groundwater is pivotal in tackling water scarcity in many developing nations due to its widespread availability, reliability, and cost-effectiveness, making it the preferred choice for

various water needs. It is vital for drinking water, particularly in India, where it fulfils a significant portion of both rural and urban water demands. However, the increasing dependence on groundwater has led to its extensive and sometimes unregulated exploitation across the country, posing challenges [18]. Hardness concentrations in natural water vary, with levels ranging from 10 to 500 mg/L as $CaCO_3$ in drinking water [19].

The entire study was conducted using groundwater obtained from the western part of Ahmedabad, an urban area in Gujarat, India. Table 2 shows the characteristics of the collected groundwater.

Table 2. Characteristics of the collected groundwater

Characteristics	Noted Value
pH	7.8
Total dissolved solids (TDS)	1718 mg/L
Total hardness (as CaCO3)	650.3 mg/L
Chloride	653.4 mg/L

Selection of waste plastic and its characteristics

Low-density polyethylene (LDPE) is a lightweight and flexible variant of polyethylene commonly used in plastic bags, packaging films, and flexible bottles, offering moisture resistance. Air bubble plastic, or bubble wrap, contains tiny air pockets and is primarily used for cushioning items during packaging. It can sometimes be recyclable. Styrofoam, or polystyrene resin, provides excellent thermal insulation and chemical resistance but is non-biodegradable and has adverse environmental effects.

Styrofoam and air bubble plastic, both commonly employed in packaging, were sourced from domestic suppliers. They subsequently underwent a thorough cleaning process which aimed to remove impurities such as dust and discoloration.

Resin preparation methods

The preparation of all the three types of resins, i.e., styrofoam resins (SR) (Fig 1a), Air bubble plastic resin (AR) (Fig 1b), and a mixed resin (MR) of styrofoam and Air bubble plastic (Fig 1c), involved the following detailed steps:

1. The styrofoam and air bubble plastic were crushed to produce particles ranging between 0.2 and 0.3 mm in size, each weighing 20-30 grams. This crushing process increased the surface area of the waste plastic, facilitating better interaction with H_2SO_4 during the subsequent reaction.
2. A flask was charged with 100 ml of concentrated H_2SO_4 (98%) and 5 grams of dry crushed plastic. The crushed plastic was mixed with a sulfonating compound, concentrated H2SO4, to undergo sulfonation, which involves adding sulfonic acid groups to the resin [10], [17], [20]. The reaction mixture was agitated, and the duration of agitation was adjusted to optimize reaction conditions. Proper agitation ensured thorough mixing and distribution of the acid throughout the resin.
3. The reaction proceeded until a light brown colour was obtained in the resin, indicating the completion of the sulfonation process.
4. The resulting slurry was filtered using a funnel and washed with 250 ml of distilled water. Filtration separated the sulfonated resin from the reaction mixture, removing solid contaminants and undissolved particles. Subsequently, the sulfonated resin underwent rinsing with 250 ml of distilled water, which helped eliminate any residual H_2SO_4 and other contaminants. pH paper was used to test a portion of the filtrate to ensure complete removal of leftover H_2SO_4 after seven to eight washes.
5. The sulfonated resin was then dried at 40°C for 30 minutes to remove any remaining water content, ensuring that the resin was dry and ready for further processing or analysis.

After the resin, preparation, to check the resin properties and their ion exchange capacity, the degree of sulfonation in SR, MR, and AR was identified using FTIR analysis. As per the research study, the particle size has decreased and the degree of sulfonation has increased. Also, the sulfonation is increased, and the ion exchange capacity of resins is increased [4], [21].

FTIR analysis of AR non-sulfonated (Fig 2a) and sulfonated (Fig 2b) revealed peaks to the polystyrene backbone, SO_3 present at 1190.18 cm-1 also the C-H stretching vibration at around 3032.04 cm-1 and the C=C stretching vibration at around 1465.22 cm-1.

FTIR analysis of SR non-sulfonated (Fig 2c) and sulfonated (Fig 2d) revealed peaks linked to the polyethylene backbone, SO_3 present at 1180.18 cm-1, also the C-H stretching vibration at around 3332.04 cm-1 and the C=C stretching vibration at around 1492.22 cm-1.

After preparing the resin, check the sulfonation of resin which is identified in the FTIR spectra analysis. The sulfonation reaction of SR and AR with sulfuric acid can be represented by the following chemical Eq (1).

After preparing the resin, check the sulfonation of resin which is identified in the FTIR spectra analysis. The sulfonation reaction of SR and AR with sulfuric acid can be represented by the following chemical Eq (1).

$$\underset{\text{Styrofoam}}{C_6H_5\text{-}CH(CH_3)\text{-}[CH_2]n\text{-}CH_2} + \underset{\text{Sulfuric acid}}{H_2SO_4} \rightarrow \underset{\text{Sulfonated styrofoam}}{C_6H_5\text{-}CH(CH_3)\text{-}[CH_2]n\text{-}SO_3H} + \underset{\text{water}}{H_2O} \quad \text{Eq (1)}$$

Sulfonic acid groups are found along the polymer chain of the resultant sulfonated styrofoam Resin (SSR). These sulfonic acid groups improve the ion-exchange characteristics of SSR, making it helpful in applications such as ion-exchange resins and catalyst supports. The sulfonation reaction facilitates the addition of sulfonic groups to polymer chains. The reaction mechanism involves the initial gener-

ation of sulfur trioxide (SO_3) from sulfuric acid. This process occurs at the interface between the organic solvent and sulfuric acid. Due to steric considerations, sulfonation of the phenyl rings predominantly occurs at the para position [22]. The LDPE structure is mostly intact during the sulfonation process, with sulfonic acid groups. ($-SO_3H$) added as attached groups along the polymer chain. These sulfonic acid groups are denoted as follows Eq (2).

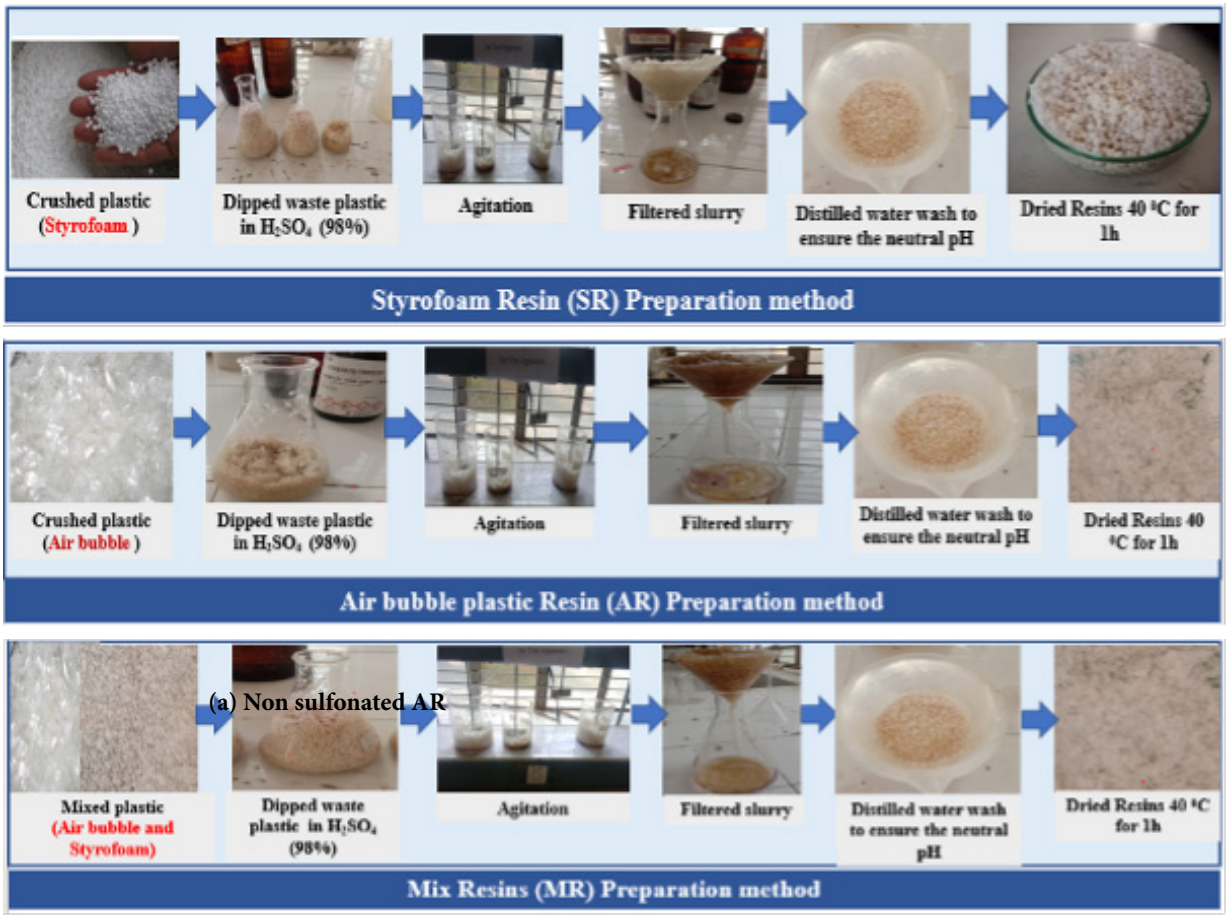
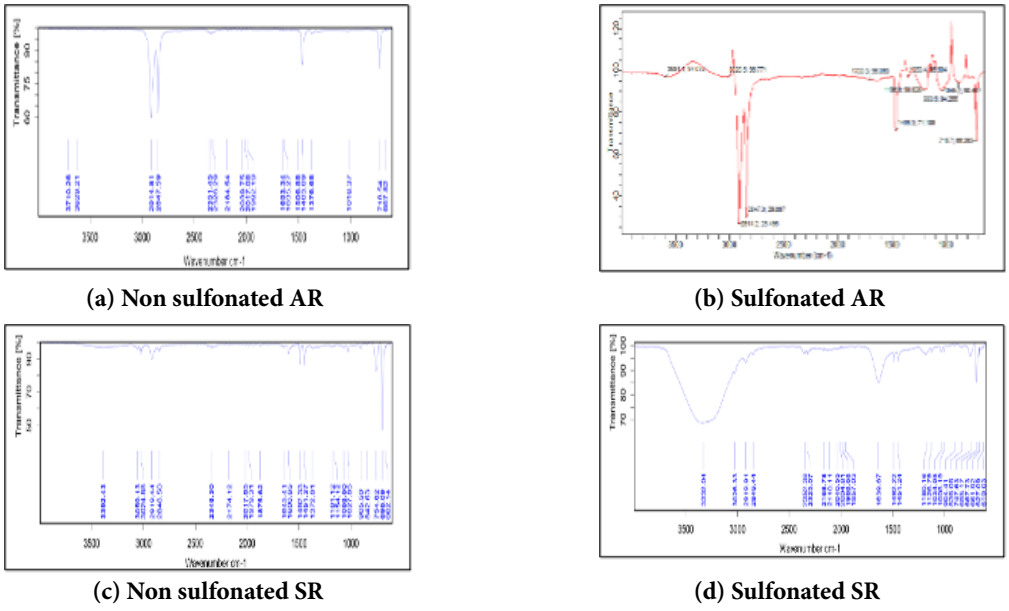


Figure 1. Waste plastic resin preparation method for (a) SR (b) AR and (c) MR



(a) Non sulfonated AR **(b) Sulfonated AR**

(c) Non sulfonated SR **(d) Sulfonated SR**

Figure 2. (a to d). FTIR Graphs showing comparison of non-sulfonated and sulfonated AR & SR

$$(C_2H_4)_n + H_2SO_4 \rightarrow (C_2H_3\text{-}SO_3H)_n \quad \text{Eq (2)}$$

Air bubble plastic — Sulfuric acid — Sulfonated air bubble plastic

Ground water passing from sulfonated and non-sulfonated resins

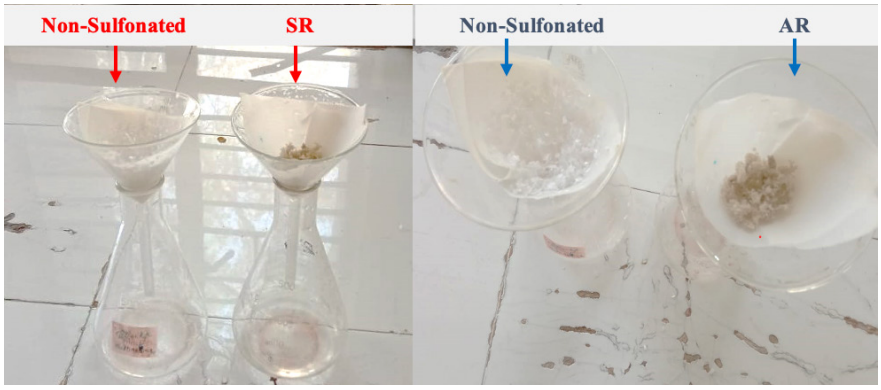


Figure 3. Groundwater pass through the sulfonated and non-sulfonated resins

To verify the efficiency of sulfonated resins, 10 ml of ground water has passed through the sulfonated and non-sulfonated resins (Fig 3). In non-sulfonated resins, only 2% total hardness reduction efficiency was noted, whereas in sulfonated resins, 7%, 9%, and 8% were noted in AR, SR, and MR, respectively, which is due to the sulfonation process of the resins.

Neutralization of the resins

The process of neutralizing sulfonated polystyrene resin involved treating it with a 1 M sodium chloride (NaCl) solution. During this process, sodium ions replace the sulfonic acid groups, resulting in the resin being converted into its sodium form. Neutralization was done by stirring the dried resin in a 500 mL 1 M NaCl solution for 2 h for to provide contact between the resins, and solution for neutralization to occur similarly to the previous studies [11], [16], [23]. Sulfonated Styrofoam Resin is then neutralised after sulfonation by treating it with sodium chloride (NaCl), which is a commonly used base for neutralisation in Eq (3).

$$C_6H_5\text{-}CH(CH_3)\text{-}[CH_2]n\text{-}SO_3H + NaCl \rightarrow C_6H_5\text{-}CH(CH_3)\text{-}[CH_2]n\text{-}SO_3Na + H_2O \quad \text{Eq (3)}$$

Sulfonated Styrofoam — Sodium Chloride — Neutralized Styrofoam — water

The sulfonic acid group (-SO3H) is transformed into a sulfonate ion (-SO3Na) in this reaction by accepting a sodium ion (Na+) from the base Eq (4). As a by-product, water (H2O) is generated.

$$(C_2H_3\text{-}SO_3H)_n + NaCl \rightarrow (C_2H_3\text{-}SO_3Na)_n + HCl \quad \text{Eq (4)}$$

Sulfonated AR — Sodium Chloride — Neutralized AR

The earlier study also attempted the sulfonation of crushed waste polystyrene, which attaches the sulfonic groups to polymer chains. The noted degree of sulfonation was 16%, and the cation exchange capacity was 0.8 meq/100 g of clay. The adsorption isotherms of resin indicated that the cation exchange capacity of polymers was 50 and 130 meq/100 g for lead and cadmium, respectively, with simulated wastewater. Observed greater than 70% lead and cadmium removal [24].

Fabrication of the three glass reactors

The experimental investigation utilised a lab-scale arrangement comprising three identical glass reactors or columns labelled R1, R2, and R3, interconnected in parallel. The columns, with a height of 50 cm and a diameter of 3 cm, were partitioned into inlet storage, media storage, and outlet storage sections. Various resins, namely SR, AR, and MR, were employed within the media compartments to address water hardness via ion exchange. Specifically, R1 was packed with SR, R2 with AR, and R3 with MR.

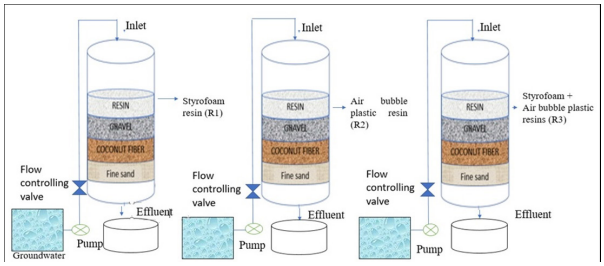


Figure 4. Experimental Set up for the study

Fig 4 is the drawing of reactor where the inlet is provided through the pump and the flow control valve (nob) is provided. Where the 5 cm of each media is filled with resin. The outlet is also provided, which is collected in a container.

Types of media used for resin support

The support media in the experiment included sand (Fig 5a), gravel (Fig 5b), coconut (Fig 5c), and cotton. These materials were chosen because of their substantial surface area, adsorption capacity, ion exchange capability, and chemical inertness.



(a) Gravel (8.25 mm) (b) Sand (1.25 mm) (c) Coconut Fiber

Figure 5. Types of support media used in the reactors to fill the prepared resin

Experimental run hardness reduction

In this study, three identical columns were used: R1 with SR, R2 with AR and R3 with MR to simulate the treatment of groundwater. As support, cotton was placed at the bottom and then layers of sand, coconut husk, and gravel were put in equal column heights of 5 cm each, as shown in Fig 6. To maintain a consistent flow of ground water through the resin column, a pump (DC 6-12V) was employed. Plastic containers were placed at the inlet and outlet. A flow monitoring valve was used to regulate the groundwater's flow rate, and a pump was utilized to move the water through the tank's intake. The experimental work was done in the batch process considering different time intervals of 2, 3, 5, 6, 8, 10, 12, 14, 18 and 24 h. Parameters like total hardness, calcium (Ca) hardness, magnesium (Mg) hardness, chloride, pH, and TDS were measured from the inlet and outlet. All the parameters were tested twice, and the average of the observations was noted.

Table 3 shows the different parameters and media used in this study, as well as the different contact times for the experimental runs.

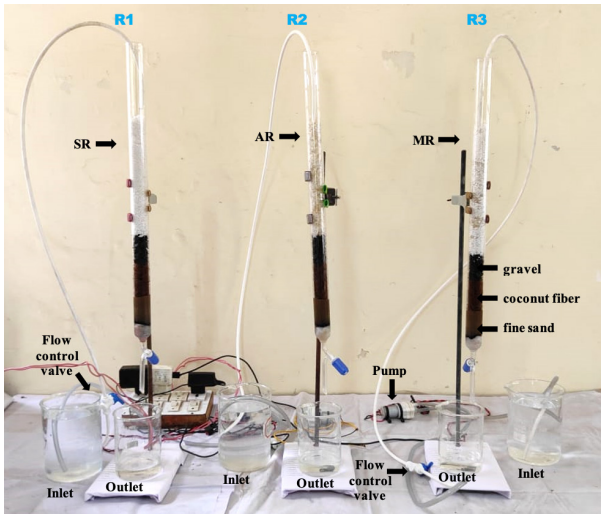


Figure 6. Working reactor during experimental work

Table 3. Experimental work details

Sr. no.	Parameters	Value
1	Flow rate (ml/h)	50-709
2	Contact time (h)	24,18,14,12,10,8,6,5,3,2
3	Reactor depth (cm)	50
4	Reactor diameter (cm)	3
5	Volume of reactor	1413 cm^3
6	Filter media (as per length)	5 cm
	Sand	5 cm
	Coconut Husk	5 cm
	Gravel	
	Resin	5 cm

RESULTS AND DISCUSSIONS

Experimental runs for hardness reduction

The experiments for hardness reduction involved varying contact times and flow rates. The study began with a 24 h contact time and progressively reduced it to 2 h. Flow rates ranged from 59 to 709 ml/h, managed through flow control valves and pumps. The experimental run has been done in two trials, in the first trial (T1), which was started with 24 h and reduced to 10 h. At the 10 h contact time, the resin capacity is exhausted, as the observed water quality of the inlet and outlet was similar. Therefore, after 5 experimental runs, fresh resins were placed, and a further second trial (T2) from 8 h to 2 h contact time has been taken.

In trial T1, with contact times ranging from 24 h to 10 h, Reactor R1 (filled with SR resin) achieved the highest hardness reduction, starting at 63% at 24 h and decreasing to 5% at 2 h. Reactor R3 (MR resin) followed with 58.6% at 24 h, dropping to 3.9% at 2 h, and Reactor R2 (SR resin) reduced total hardness by 52% at 24 h, falling to 2.5% at 2 h. Trial 2, with shorter contact times of 8 h to 2 h, mirrored these results: R1 showed a 50.71% reduction at 8 h, decreasing to 5.9% at 2 h; R3 achieved a 50.6% reduction at 8 h, dropping to 3.9% at 2 h; and R2 recorded a 42.5% reduction at 8 h, falling to 2.5% at 2 h. These findings highlight the significant impact of contact time on the effectiveness of the resins, with SR resin consistently outperforming the others across both trials. In the past column study, wastes of polystyrene were prepared from the foam of food packaging, and air bubble plastic also showed a 40–45% reduction in the hardness of ground water [19].

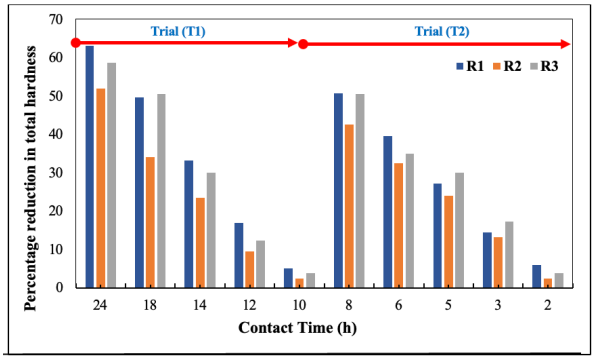


Figure 7. Effect of various contact time with percentage total hardness reduction

During the entire experiment, pH observed into the neutral range. Fig 8(a) represents the capacity of calcium hardness reduction in R1, R2, and R3. In the first trial (T1), the maximum calcium hardness reduction observed in R1, R2, and R3 was 58.6%, 49%, and 36.45%, respectively, at 24 h of contact time. In the second trial (T2), started with a contact time of 8 h. In trial 2 (T2), with an 8 h contact time, reactor R1 reduced calcium hardness by 36.16%, R2 by 33.47%, and R3 by 33.58%.

In trial 1 (T1), after 5 runs, reactor R1, filled with SR, showed the highest magnesium hardness removal capacity at a 24 h contact time, achieving a 54% reduction. In contrast, R2 with AR achieved a 45% reduction, and R3 with MR achieved a 49% reduction under the same conditions. In trial 2 (T2), with an 8 h contact time, R1 achieved a 36.13% reduction, R2 a 30.13% reduction, and R3 a 34.26% reduction in magnesium hardness removal capacity (Fig 8(b)).

Fig 9(a) illustrates chloride reduction in reactors R1, R2, and R3 with varying contact times. In trial 1 (T1), after 5 runs, the highest chloride removal capacity was observed in R1 filled with SR, achieving a 39.38% reduction at a 24 h contact time. In comparison, R2 with AR achieved a 24.6% reduction, and R3 with MR achieved a 22.77% reduction under the same conditions. In trial 2 (T2), with an 8 h contact time, R1 achieved a 14.08% reduction, R2 a 12.20% reduction, and R3 a 12.60% reduction in chloride reduction. These results suggest that longer contact times lead to more effective removal, as observed in the experiments.

Fig 9(b) displays TDS reduction in three reactors with varying contact times. In trial 1 (T1), after taking 5 experiment runs, the highest TDS removal capacity was observed in R1 filled with SR, achieving a 20.52% reduction at a 24 h contact time. In comparison, R2 achieved a 16% reduction, and R3 attained a 14.02% reduction under the same conditions. In trial 2 (T2), with an 8 h contact time, R1 achieved a 23.52% reduction, R2 a 14% reduction, and R3 a 15.02% reduction in TDS removal. These results indicate that the second trial yielded the best results in TDS reduction.

Breakthrough point of resin

At the experiment's outset, the outlet hardness level was lower than the inlet due to the initial high efficiency in the three columns. However, over time, the outlet hardness increased, likely due to the decreasing ion exchange capacity. Eventually, the outlet hardness equaled the inlet, indicating that the ion exchange capacity was depleted, with the resins fully saturated with Ca+2 and Mg+2 ions. The breakthrough point, when the outlet concentration reaches 650 mg/L (groundwater hardness), signifies the need for resin replacement. In this study, the second trial with different or reduced contact times aimed to assess the resin's removal capacity.

Table 4 demonstrates that this study surpasses previous research because, typically, ion exchange resin exhaustion occurs after 2 to 3 cycles. However, in the present study, it's evident that the resin loses its ion exchange capacity after completing five cycles or experimental runs.

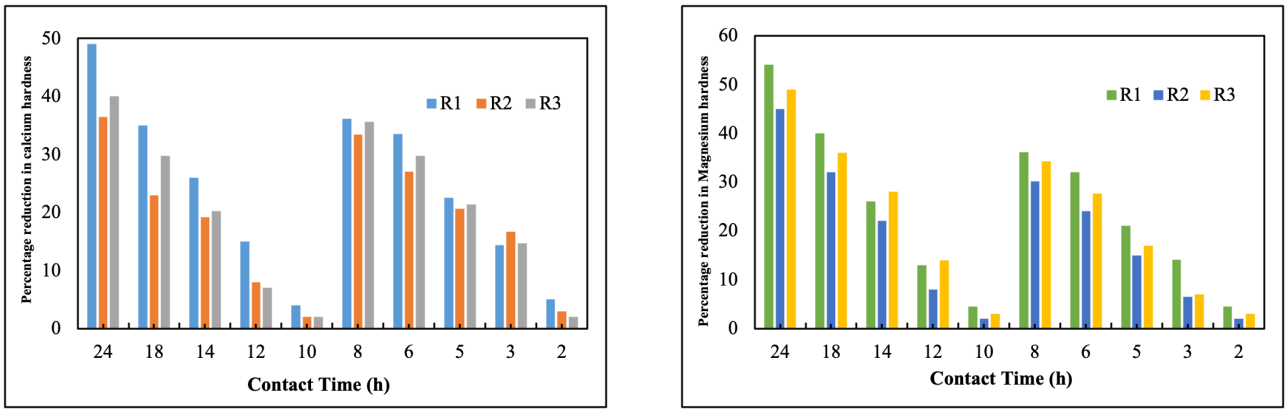


Fig 8. Percentage reduction at varied contact time (a) Calcium hardness (b) Magnesium hardness

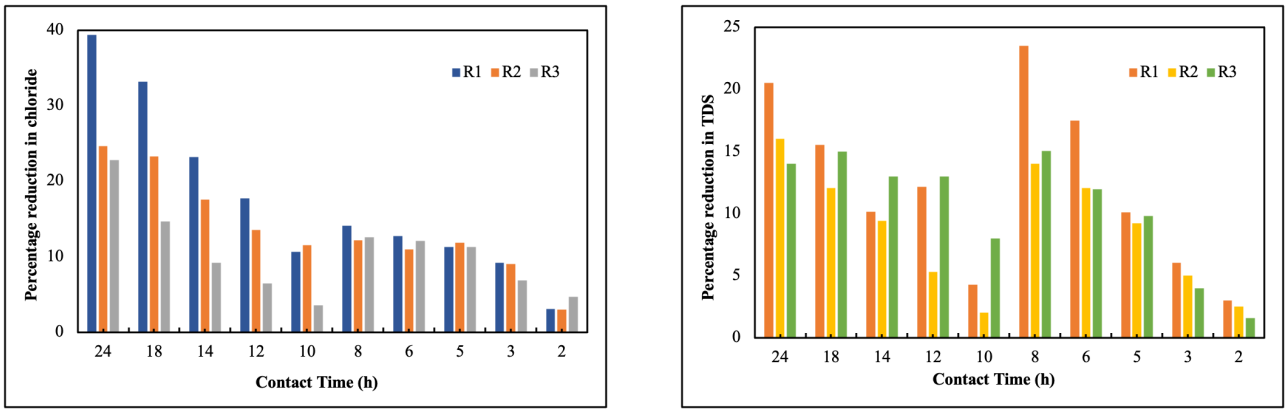


Fig 9. Percentage reduction at varied contact time (a) Chloride (b) TDS

Table 4. Comparison of resin exhausted their ion exchange capacity

Sr. No.	Resin	Flow	Exhausted resin	References
1	Food packaging	1 l/min	After 1 cycle 42.5% reduction in TH	[10]
2	White coffee cup	2.5 l/h	After 3 cycles	[15], [25]
3	Polystyrene	51 and 34 ml/min	After 2 cycles 42.5% reduction in TH	[26]
4	Air buble and styrofoam	50-140 ml/h	After 5 cycles	This study

The study concluded that reactor R1, filled with SR resin, was the most efficient in reducing groundwater hardness, followed by R2 and R3. These results suggest that using waste plastic for hardness reduction is a promising approach, offering a sustainable solution for both plastic waste management and water quality improvement.

CONCLUSIONS

The experimentation involved activating three types of resins (SR, AR, and MR) using styrofoam and air bubble plastic waste through sulfonation, as confirmed by FTIR analysis. The sulfonated compounds were neutralized by sodium salt structures. Three reactors (R1 with AR, R2 with SR, and R3 with MR) were analyzed at various contact times, i.e. starting at 24 h and being reduced to 2 h to determine hardness reduction efficiencies. After five experimental runs, resin replacement was necessary due to hardness reduction capacity exhaustion.

Results showed maximum total hardness reduction efficiencies at 24 h contact time (63% in R1, 42% in R2, and 58.6% in R3). Subsequent runs with an 8 h contact time revealed total hardness efficiencies of 50.71% in R1, 42.5% in R2, and 50.6% in R3. Initial calcium hardness reduction capacities were 49% in R1, 36% in R2, and 40% in R3, with subsequent runs yielding 36.16%, 33.47%, and 35.58%, respectively. Magnesium hardness removal capacities were highest in the first trial (54% in R1, 45% in R2, 49% in R3) and lower in the second trial (36.13%, 30.13%, and 34.26%, respectively).

A neutral pH range was noted throughout the entire experiment run. The most significant chloride reduction was achieved in R1, which was filled with SR, showing a 39.38% reduction at 24 h of contact time. In comparison, R2 with AR achieved a 24.6% reduction, and R3 with MR achieved a 22.77% reduction under identical conditions. These findings indicate that longer contact times enhance chloride reduction efficiency in all three reactors. Regarding TDS reduction, R1 with SR demonstrated the highest, achieving a 23.52% reduction at 8 h contact time. R2 showed a 14% reduction, and R3 exhibited a 15.02% reduction in TDS.

The results suggest that waste plastic can serve as a viable solution for hardness reduction while concurrently addressing the challenge of plastic waste management.

DATA AVAILABILITY STATEMENT

The author confirm that the data that supports the findings of this study are available within the article. Raw data that support the finding of this study are available from the corresponding author, upon reasonable request.

CONFLICT OF INTEREST

The author declared no potential conflicts of interest with

respect to the research, authorship, and/or publication of this article.

USE OF AI FOR WRITING ASSISTANCE

Not declared.

ETHICS

There are no ethical issues with the publication of this manuscript.

REFERENCES

[1] M. G. Kibria, N. I. Masuk, R. Safayet, H. Q. Nguyen, and M. Mourshed, "Plastic Waste: Challenges and Opportunities to Mitigate Pollution and Effective Management," Int. J. Environ. Res., vol. 17(1), p. 20, 2023.

[2] J. Simitzis and D. Fountas, "Utilization of wastes of foam polystyrene as sorbents," J. Appl. Polym. Sci., vol. 55 (6), pp. 879–887, 1995.

[3] J. Bartram, L. Fewtrell, and T.-A. Stenstrom, "Harmonised assessment of risk and risk management for water-related infectious disease: an overview. In Water Quality: Guidelines, Standards and Health – Assessment of risk and risk management for water-related infectious disease. (eds L. Fewtrell and J.," Water Qual. Guidel. Stand. Heal., pp. 1–16, 2001.

[4] T. A. Moghny, "Preparation of sorbent materials for the removal of hardness and organic pollutants from water and wastewater," vol. 11(5), pp. 461–468, 2017.

[5] Z. Zhao and X. Wang, "Application of AnMBR Ion Exchange Technology in Water Treatment," IOP Conf. Ser. Earth Environ. Sci., vol. 791(1), 2021.

[6] J. N. Apell and T. H. Boyer, "Combined ion exchange treatment for removal of dissolved organic matter and hardness," Water Res., vol. 44(8), pp. 2419–2430, 2010.

[7] S. Rengaraj, K.-H. Yeon, and S.-H. Moon, "Removal of chromium from water and wastewater by ion exchange resins," J. Hazard. Mater., vol. 87 (1), pp. 273–287, 2001.

[8] A. Dabrowski, Z. Hubicki, P. Podkościelny, and E. Robens, "Selective removal of the heavy metal ions from waters and industrial wastewaters by ion-exchange method," Chemosphere, vol. 56(2), pp. 91–106, 2004.

[9] S. M. Moosavirad, R. Sarikhani, E. Shahsavani, and S. Z. Mohammadi, "Removal of some heavy metals from inorganic industrial wastewaters by ion exchange method," J. Water Chem. Technol., vol. 37(4), pp. 191–199, 2015.

[10] P. Pentamwa, W. Thipthara, and S. Nuangon, "Removal of Hardness from Groundwater by Synthetic Resin from Waste Plastics," Int. J. Environ. Sci. Dev., vol. 19, pp. 479–482, 2011.

[11] E. Nassef, M. Mousa, D. Elgayar, and M. Hussein, "A Novel Technique for Water Hardness Removal by Using Polystyrene," Aust. J. Basic Appl. Sci., vol. 12(7), pp. 126–138, 2018.

[12] I. Bekri-Abbes, S. Bayoudh, and M. Baklouti, "A technique for purifying wastewater with polymeric flocculantproduced from waste plastic," Desalination, vol. 204, pp. 198–203, 2007.

[13] D. M. Hussein, D. E. Nassef, and M. A. Ibrahim, "Water Hardness Removal by Using Waste Polystyrene," SDRP J. Nano Technol. Mater. Sci., vol. 1(1), pp. 40–44, 2016.

[14] Y. Hailu, E. Tilahun, A. Brhane, H. Resky, and O. Sahu, "Ion exchanges process for calcium, magnesium and total hardness from ground water with natural zeolite," Groundw. Sustain. Dev., vol. 8, pp. 457–467, 2019.

[15] I. Bekri-Abbes, S. Bayoudh, and M. Baklouti, "Converting waste polystyrene into adsorbent: Potential use in the removal of lead and cadmium ions from aqueous solution," J. Polym. Environ., vol. 14(3), pp. 249–256, 2006.

[16] M. Moubark, T. A. Moghny, M. A. Mousa, A.-H. A.-A. El-Bellihi, and A. E. Awadallah, "Sulfonated Ion Exchange Polystyrene Composite Resin for Calcium Hardness Removal," Int. J. Emerg. Technol. Adv. Eng., vol. 5, pp. 20–29, 2015.

[17] M. R. Kazimi, T. Shah, S. Shima Binti Jamari, I. Ahmed, and C. Ku Mohammad Faizal, "Sulfonation of low-density polyethylene and its impact on polymer properties," Polym. Eng. Sci., vol. 54(11), pp. 2522–2530, 2014.

[18] M. Madhukar, S. P. Manjunath, and R. V. Gopal, "Preliminary studies on removal of nitrate and hardness from ground water using polystyrene beads," Water Supply, vol. 14(2), pp. 299–303, 2014.

[19] W. Bajdur, J. Pajączkowska, B. Makarucha, A. Sułkowska, and W. W. Sułkowski, "Effective polyelectrolytes synthesised from expanded polystyrene wastes," Eur. Polym. J., vol. 38(2), pp. 299–304, 2002.

[20] H. Tabekh, M. H. Al Kurdi, and Z. Ajji, "Sulphonation of expanded polystyrene waste with commercial sulphuric acid for potential use in removal of heavy metals from contaminated waters," Polimeri, vol. 36(1), pp. 11–14, 2015.

[21] Y. Inagaki, M. Kuromiya, T. Noguchi, and H. Watanabe, "Reclamation of waste polystyrene by sulfonation," Langmuir, vol. 15(2), pp. 4171–4175, 1999.

[22] L. B. Tran, T. T. Nguyen, S. Padungthon, T. T. Le, Q. A. Nguyen Thi, and N. H. Nguyen, "Advanced natural hydrated iron-alum oxides cation exchange resin for simultaneous phosphate and hardness removal," npj Clean Water, vol. 5(1), p. 43, 2022.

[23] S. Farmanbordar, D. Kahforoushan, and E. Fatehifar, "A new method in the removal of Ca and Mg ions

from industrial wastewater," Desalin. Water Treat., vol. 57(19), pp. 8904–8910, 2016.

[24] N. Nori Ismail, "Experimental study on Ion Exchange Rate of Calcium Hardness in Water softening process Using Strong Acid Resin DOWEX HCR S/S," Coll. Eng. J., vol. 91(1), pp. 107–114, 2016.

[25] I. Bekri-Abbes, S. Bayoudh, and M. Baklouti, "The removal of hardness of water using sulfonated waste plastic," Desalination, vol. 222, pp. 81–86, 2008.

[26] D. Ruziwa, N. Chaukura, W. Gwenzi, and I. Pumure, "Removal of Zn2+ and Pb2+ ions from aqueous solution using sulphonated waste polystyrene," J. Environ. Chem. Eng., vol. 3(4), pp. 2528–2537, 2015.

Environ Res Tec, Vol. 8, Issue. 2, pp. 255-280, June 2025

Environmental Research and Technology
https://dergipark.org.tr/en/pub/ert
DOI: https://10.35208/ert.1499961

Research Article

Heavy metal contamination in the groundwater of the southern expanse of the Northwestern Himalayan region: An evaluation of pollution indices and health risks utilizing Mathematical Modelling

Uzma IMTIYAZ*[,1], Mushtaq Ahmad RATHER[1]

[1] *Department of Chemical Engineering, National Institute of Technology, Srinagar, India*

ARTICLE INFO

Article history
Received: 12 Jun 2024
Revised: 06 Aug 2024
Accepted: 22 Aug 2024

Key words:
Groundwater quality assessment, nemerow pollution index, carcinogenic risk, non-carcinogenic risk, human health risk.

ABSTRACT

Water quality has a direct impact on both human health and the socioeconomic system's viability. Pollutants, especially heavy metals, seep into water systems and deteriorate water quality as human activity increases. The purpose of this study was to evaluate the heavy metal contamination in groundwater and its potential health risk posed to humans in the southern part of the Northwestern Himalayan region, encompassing four Kashmir districts (Anantnag, Pulwama, Shopian, and Kulgam), during both pre- and post-monsoon, using atomic absorption spectroscopy. The research scrutinized heavy metal levels in 25 borewell water samples. The Nemerow pollution index was employed to assess water quality, revealing varying degrees: Dooru Shahabad exhibited excellent quality (NPI < 0.5), Hillar and Kakapura were classified as good (NPI 0.5–0.75), while Wanpoh and Zeewan displayed moderate quality (NPI 0.75–1). The remaining 20 samples showed consistently poor quality (NPI > 1). Spatial distribution of heavy metals (Pb, Ni, Mn, Cd, Cu, Fe, Zn) was mapped using contour maps, revealing concentrations ranging from 0.01 mg/L to 0.15 mg/L for Pb, 0.05 mg/L to 0.2 mg/L for Ni, and 0.1 mg/L to 0.5 mg/L for Mn. Statistical analysis, including ANOVA, showed no significant variations in mean concentrations of Pb (0.05 ± 0.01 mg/L), Ni (0.1 ± 0.02 mg/L), Cd (0.01 ± 0.005 mg/L), Cu (0.03 ± 0.01 mg/L), Fe (0.4 ± 0.1 mg/L), and Zn (0.2 ± 0.05 mg/L) ($p > 0.05$), Principal component analysis and cluster analysis showed that the main source of heavy metal pollution in the groundwater of study area is anthropogenic. The contamination extent underscores the necessity to evaluate its human health impact. The carcinogenic and noncarcinogenic hazards were calculated using the measured concentration of heavy metals and the average daily water intake. The calculated carcinogenic risk values for Pb is 2.31x 10-3, Cd is 6.51x10-5, and Ni is 3.94 x 10-5 exceeds the acceptable limit of 1.0 x 10-6 as per different agencies. Non-carcinogenic risk rankings across districts were Pb>Ni>Mn>Cd>Cu>Fe>Zn, with Pb posing the highest carcinogenic risk. Subsequently, total health risk, incorporating non-carcinogenic risks for seven heavy metals and carcinogenic risks for three, was mathematically computed. Lead was found to contribute 72% to the total health risk. This research illuminates the degree of pollution caused by heavy metals in a region of paramount importance, urging further investigation into its health implications that can support the decision-making of local government organisations regarding the sustainable use of groundwater resources and the efficient protection of the groundwater environment.

Cite this article as: Imtiyaz U, Rather MA. Heavy metal contamination in the groundwater of the southern expanse of the Northwestern Himalayan region: An evaluation of pollution indices and health risks utilizing mathematical modelling. Environ Res Tec 2025;8(2) 255-280.

***Corresponding author.**
*E-mail address: uzma6phd19@nitsri.ac.in

This is an open access article under the CC BY-NC license (http://creativecommons.org/licenses/by-nc/4.0/).

INTRODUCTION

The impending climate crisis has put the whole human existence on our planet in jeopardy. At present, the world's depleting resources, the energy crisis, and environmental issues have become increasingly prominent. Water being one of the utmost fundamental requirements of life acts as a universal solvent thereby providing ionic balance and nutrient aid to all forms of life. It dissolves various toxic organic and inorganic substances that are detrimental to its quality and affects individuals' health. Increasing and unregulated industrial and agricultural activities, including, pharmaceuticals, pesticides, garments, and technocratic civilization, are responsible for the contamination of water. With a mere 2.5% of the world's water being non saline, the imbalance between the freshwater availability and the ever-growing population is intensifying with time [1].

Groundwater in its essence is one of the key natural resources, used for both drinking and agricultural purposes. It is important not only for the survival of mankind but also for the social and economic development of any nation. Groundwater contamination is one of the prime environmental issues that the world is facing [2]. Groundwater contamination is susceptible in the areas where population density is high and human land use is exhaustive [3]. Furthermore, groundwater pollution is caused by the disposal of domestic, agricultural, industrial and commercial waste, and constituents (trace metals) of soil, rocks and plateaus because of their direct contact. Heavy metals are one of the major contaminants consistently found in groundwater which prove hazardous and toxic [4,5].

Sixty -three point five to two hundred point six (63.5 to 200.6) being the range of atomic weights, heavy metals have a relatively high density when compared to water. Among these the harmful heavy metals are lead, uranium, selenium, chromium, mercury, zinc, arsenic, nickel [6]. Heavy metals occurring naturally in the environment have no harmful effect and are rather beneficial when present in low concentrations. However, their presence in higher concentrations can have an adverse effect on mankind [4].The heavy metal contamination in groundwater is both natural and man-made. Natural sources include disintegration of rocks, degradation of organic matter, and volcanic eruptions [7,8], while human activities that could potentially contribute to environmental pollution include mining and extraction, agricultural practices, industrial waste, solid waste management, and medical waste disposal [9]. Infiltration of heavy metals into the groundwater occurs by surface runoff from contaminated water source, leaching of landfill sites [10,11].

India's 90% of rural population and 30% urban pollution are dependent on groundwater as their primary source of drinking water and for their domestic needs [12]. Most of the water used is untreated and not fit for drinking. Therefore, the vulnerability towards toxic pollutants prevailing in groundwater is rising significantly [13]. The presence of heavy metals beyond permissible limits in water is causing abnormal functioning of human body despite being essential at the lower concentrations. Illness and fatality rates are increasing due to constant and prolonged exposure [11,14]. Exposure to heavy metal contamination can result in both short-term and long-term health effects, ranging from mild symptoms like food poisoning and headaches to severe conditions such as liver cirrhosis, kidney dysfunction, permanent harm to the neuron system, cardiovascular disease, infertility, cancer [15, 16, 17].

Taking into consideration the vast impact of heavy metals pollution on human health it is imperative to assess and estimate the contamination level of heavy metals in the water and the potential risk imposed by them on human health [13,18]. Studies have been conducted in countries across the globe employing different pollution indices to assess the degree of heavy metal contamination such as India, Syria, Thailand, Bangladesh, China, Mexico, North America, and Turkey. Bangladesh's industrial discharges, agricultural practices, and insufficient waste management systems have resulted in worrying levels of groundwater pollution. In South Fukra, Kashiani, Gopalganj, Bangladesh, Shaibur conducted research on the distribution of heavy metals and arsenic in groundwater. Significant relationships between these pollutants were found in the study, highlighting the interconnectedness of groundwater pollution. These kinds of studies yield important information about the dynamics of groundwater contamination and its possible effects on human health. High concentrations heavy metals have also been reported in China's cities, especially in heavily industrialised and populated areas. Mexico, which is well-known for its quick urbanisation, has serious groundwater contamination from home and industrial wastewater discharge as well as fertiliser and pesticide-filled agricultural runoff. Additionally, research has shown that heavy metals can be found in a variety of metropolitan contexts, indicating that groundwater contamination is a problem in North America. Research conducted in India has revealed the existence of heavy metals in urban groundwater, which is mostly related to industrial operations and urban growth [19-25].

Even though the Kashmir Valley's groundwater is crucial, there are not many thorough research on heavy metal pollution in the area. Prior studies have focused on groundwater salinity and have not thoroughly examined heavy metal contaminants and their seasonal fluctuations. In order to fill in these gaps, this study performs a thorough examination of water samples collected during the pre- and post-monsoon seasons from 25 borewells spread over four districts (Anantnag, Pulwama, Shopian, and Kulgam). It uses atomic absorption spectroscopy to investigate a wide range of heavy metals (lead, nickel, manganese, cadmium, copper, iron, and zinc) and utilises the Nemerow Pollution Index to provide a detailed evaluation of the water quality. The main advantage of Nemerow pollution index is that it is way more accurate and simpler as compared to any other pollution indexes. This study is new since it uses contour maps to visualise geographical distribution using IDW (inverse distance weightage). The underlying presumption of inverse distance weighted (IDW) interpolation is that objects closer together are more similar than those located further apart. To predict a value for any unmeasured site, IDW uses the measured values surrounding the expected location. The findings of measurements taken closest to the prediction site have a greater

influence on the expected value than do measurements taken farther away. IDW operates under the presumption that each measured location has a local influence that gets smaller in distance. "Inverse distance weighted" is a method whereby sites closest to the projected place are given higher weights, and these weights decrease with distance. Study also covers a wide variety of heavy metals, employs a dual-season methodology, and sophisticated pollution index. It also includes a thorough health risk assessment that computes the risks of cancer and non-cancerous diseases. To better understand the links between various metals, it combines sophisticated statistical studies such as ANOVA, Cluster analysis, Principal component analysis and Pearson correlation coefficients. These comprehensive methods considerably advance the understanding of groundwater contamination in the Kashmir Valley by offering critical insights into the health and environmental effects of heavy metal pollution.

MATERIALS AND METHODS

Research Area Description

Kashmir is one of the most fascinating, mesmerising and picturesque place lying in the northwest Himalaya. Situated between 33° 30′ and 34° 45′ N latitudes and 74° and 75° 30′ E longitudes it covers an area of 5200 sq. km. Present study of heavy metal pollution in ground water includes four districts of Southern part of Kashmir namely, Anantnag, Pulwama, Shopian and Kulgam. District Anantnag is southern-most district of Kashmir province, Pir Panjal range separates it from the Jammu province.it is located between 33017'20" and 34015'30" latitude and 740 30'15" and 740 35'00" East longitude. Discharge of ground water in these areas occurs both by natural and artificial ways. Spring flow adequate to the natural discharge and heavy with drawls are made from tube wells and dug wells for household and agricultural purposes. Figure 1(a) shows the map of the study area with the sampling locations demarcated on it.

Hydrogeology

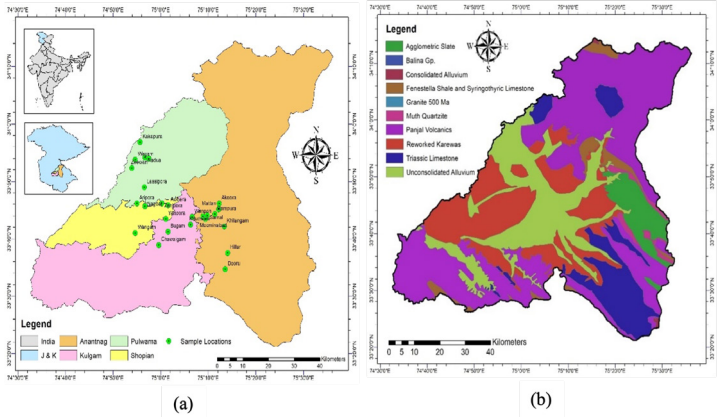
Groundwater in the study area exists in both the unconfined water table and confined conditions within soft rock aquifers. The presence of groundwater is influenced by various hydrogeological factors, including lithology, structure, and geomorphic configuration (CGWB, 2017). The hydrogeological composition of Pulwama district can be delineated into two distinct aquifer systems: a hard rock system, comprising semi-consolidated to consolidated rock units, and a soft sedimentary aquifer primarily composed of unconsolidated sediment (CGWB, 2016-17). The geological map of the study area is presented in figure 1(b). The depth of groundwater within the study area plays a pivotal role in determining water availability and long-term sustainability. The distance to the water table within the study area's aquifers spans from 10 to 390 feet. Groundwater sources in the region exhibit a spectrum of depths, ranging from shallow to deep aquifers. Shallow groundwater reservoirs, situated in proximity to the surface, typically offer greater accessibility and ease of utilization. The depth of groundwater also has implications for water quality; shallow sources are more vulnerable to contamination, whereas deeper sources tend to be more shielded. Monitoring and comprehending groundwater depth are vital for sustainable management.

Groundwater recharge and discharge

In Kashmir rivers, lakes, wetlands, snowfall, irrigation return flow, precipitation, and manmade techniques such recharge wells are the main sources of groundwater replenishment. Heavy monsoon rains and the melting of the Himalayan glaciers are the main causes, with rivers like the Jhelum infiltrating deeply and contributing significantly. Surface water features like Dal Lake and agricultural irrigation contribute to recharging. Natural springs, rivers, streams, lakes, wetlands, and extraction for home and industrial usage are some of the ways that groundwater is released into the environment [14].

Sampling and Analysis

A total of 25 water samples were collected randomly from different National Hydrograph stations installed by Central Ground Water Board in four districts of South Kashmir to assess the heavy metals concentration in the ground water. The water samples were collected in one Litre polyethylene bottles which were rinsed properly with distilled water before using. Water from the bore well was flushed for 10 minutes before collecting the sample for analysis. The samples collected were filtered through Whatman filter Paper and preserved with Nitric acid. Sample collection was done following the procedures cited by APHA -2005 [26]. The analysis of these preserved samples was carried out in triplicates and the average of three



(a) (b)

Figure 1. (a) Sampling locations (b) Geological maps of heavy metals in the study area

was taken, using Perkin Elmer Atomic Absorption Spectrophotometer Analyst 400 at Sher Kashmir University of Agriculture Science and Technology -Kashmir in the Division of Research Centre for Residue and Quality Analysis. A series of known concentrations solutions were prepared and calibration curve was plotted based on the absorbance of the said element including the blank sample and the unknown concentrations were found on the basis of absorbance [27]. AAS works based on the principle of absorption of light by atoms. The sample is atomized, usually by heating, and then exposed to a specific wavelength of light. The atoms in the sample absorb the light, and the amount of absorption is in direct proportions to the concentration of the element being measured. By measuring the intensity of the absorbed light, the concentration of the element can be determined. AAS is preferred for heavy metal analysis due to its accuracy, sensitivity, and selectivity. It allows for the quantification of individual metals and can detect low concentrations, making it suitable for assessing heavy metal contamination in environmental samples like groundwater. Table 1 and Figure 2 shows the Concentrations of various Heavy metals in Groundwater (µg/l) found in the study area.

Table 1. Concentration of various heavy metals in groundwater (µg/l)

S no.	District	Location	Latitude	Longitude	Well Depth (ft)	Pre-Monsoon (µg/l)							Post Monsoon (µg/l)						
						Ci (Fe)	Ci (Mn)	Ci (Ni)	Ci (Pb)	Ci (Zn)	Ci (Cd)	Ci (Cu)	Ci (Fe)	Ci (Mn)	Ci (Ni)	Ci (Pb)	Ci (Zn)	Ci (Cd)	Ci (Cu)
1	**Shopian**	**Nagbal**	**33° 76' 10"**	**74° 94' 50"**	**100**	**ND**	**26.9**	**87.8**	**550.0**	**39.2**	**ND**	**16.3**	**ND**	**28.2**	**90.4**	**561.0**	**42.3**	**ND**	**ND**
2		**Wangam**	**34° 27' 50"**	**74° 30' 71"**	**100**	**224.6**	**43.8**	**39.2**	**370.0**	**5.4**	**ND**	**ND**	**235.8**	**46.0**	**40.4**	**377.4**	**5.8**	**ND**	**ND**
3		**Awnera**	**33° 76' 41"**	**75° 02' 61"**	**120**	**160.0**	**50.0**	**20.0**	**460.0**	**20.0**	**ND**	**ND**	**168.0**	**52.5**	**20.6**	**469.2**	**21.6**	**ND**	**ND**
4		**Zanipora**	**33° 77' 60"**	**75° 00' 41"**	**80**	**50.0**	**20.0**	**60.0**	**320.0**	**40.0**	**20.0**	**ND**	**52.5**	**21.0**	**61.8**	**326.4**	**43.2**	**20.4**	**ND**
5		**Aripora**	**33° 71' 70 "**	**74° 83'61"**	**100**	**33.0**	**604.8**	**0.9**	**2.3**	**10.0**	**ND**	**1.0**	**34.7**	**635.0**	**0.9**	**2.3**	**10.8**	**ND**	**ND**
6	**Pulwama**	**Lassipora**	**33° 81' 62"**	**74° 94' 31"**	**120**	**ND**	**9.0**	**38.1**	**450.0**	**47.6**	**6.0**	**10.0**	**ND**	**9.5**	**39.2**	**459.0**	**51.4**	**6.1**	**ND**
7		**Nadua**	**33° 81' 35"**	**74° 76' 31"**	**100**	**420.0**	**30.0**	**10.0**	**220.0**	**130**	**ND**	**10.0**	**441.0**	**31.5**	**10.3**	**224.4**	**140.4**	**ND**	**ND**
8		**Wagam**	**33° 89' 61"**	**74° 91' 10"**	**75**	**240.0**	**40.0**	**57.0**	**150.0**	**70.0**	**ND**	**20.0**	**252.0**	**42.0**	**58.7**	**153.0**	**75.6**	**ND**	**ND**
9		**Lajoora**	**33° 89' 93"**	**74° 95' 92"**	**120**	**350.0**	**30.0**	**44.0**	**390.0**	**20.0**	**ND**	**ND**	**367.5**	**31.5**	**45.3**	**397.8**	**21.6**	**ND**	**ND**
10		**Kakapura**	**33 °55' 35"**	**74° 53 '54"**	**100**	**29.6**	**20.0**	**20.0**	**4.5**	**5.4**	**ND**	**ND**	**31.1**	**21.0**	**20.6**	**4.6**	**5.8**	**ND**	**ND**
11		**Zeewan**	**33° 87' 18"**	**74 °89' 93"**	**90**	**214.5**	**10.0**	**34.0**	**3.9**	**103**	**ND**	**ND**	**225.2**	**10.5**	**35.0**	**4.0**	**111.2**	**ND**	**ND**

Table 1. Concentration of various heavy metals in groundwater (µg/l)

12	Anantnag	Sarnal	33° 73' 28"	75° 16' 00"	100	ND	133.6	43.4	530.0	88.3	6.0	ND	ND	140.3	44.7	540.6	95.4	6.1	ND
13		Malaknag	33° 43' 25"	75° 90' 12"	80	ND	16.8	30.7	440.0	6.1	ND	ND	ND	17.6	31.6	448.8	6.6	ND	ND
14		Mattan	33° 45' 80"	75° 12'11"	75	ND	ND	41.3	380.0	6.0	ND	ND	ND	ND	42.5	387.6	6.5	ND	ND
15		Akoora	33° 76' 89"	75° 20' 51"	80	ND	42.7	64.5	330.0	8.9	ND	ND	ND	44.8	66.4	336.6	9.6	ND	ND
16		Khilangam	33° 70' 21"	75° 22' 31"	65	ND	ND	55.0	440.0	17.7	ND	ND	ND	ND	56.7	448.8	19.1	ND	ND
17	Pulwama	Moominabad	33° 72' 41"	75° 15'70"	100	632.9	6.7	58.2	310.0	69.0	ND	ND	664.5	7.0	59.9	316.2	74.5	ND	ND
18		Rampura	33° 73' 81"	75° 19' 12"	80	ND	23.6	50.8	530.0	110.4	0.0	0.0	0.0	24.8	52.3	540.6	119.2	ND	ND
19		Dooru	33° 57 '79"	75 °22' 60"	100	40.8	23.0	14.5	5.2	3.7	ND	20.0	42.8	24.2	14.9	5.3	4.0	ND	ND
20		Wanpoh	33 °72' 96"	75 °10' 86"	80	27.2	330.0	31.3	2.7	24.8	ND	ND	28.6	346.5	32.2	2.8	26.8	ND	ND
21		Hillar	33 °62' 54"	75° 23' 48"	120	43.1	350.0	14.6	ND	47.6	ND	ND	45.3	367.5	15.0	ND	51.4	ND	ND
22	Kulgam	Khudwani	33° 72' 32"	75° 02' 63"	100	29.5	1721	36.0	440.0	207.8	ND	ND	31.0	1807	37.1	448.8	224.4	ND	ND
23		Chawalgam	33° 64' 81"	74° 99' 34"	100	454.8	299.8	52.9	290.0	96.4	ND	ND	477.5	314.8	54.5	295.8	104.1	ND	ND
24		Yaripora	33° 72' 40"	75° 01' 81"	70	20.0	210.0	30.0	250.0	10.0	ND	ND	21.0	220.5	30.9	255.0	10.8	ND	ND
25		Bugam	33° 68' 72"	75° 02' 60"	100	ND	959.0	41.3	480.0	17.1	ND	ND	ND	1007	42.5	489.6	18.5	ND	ND

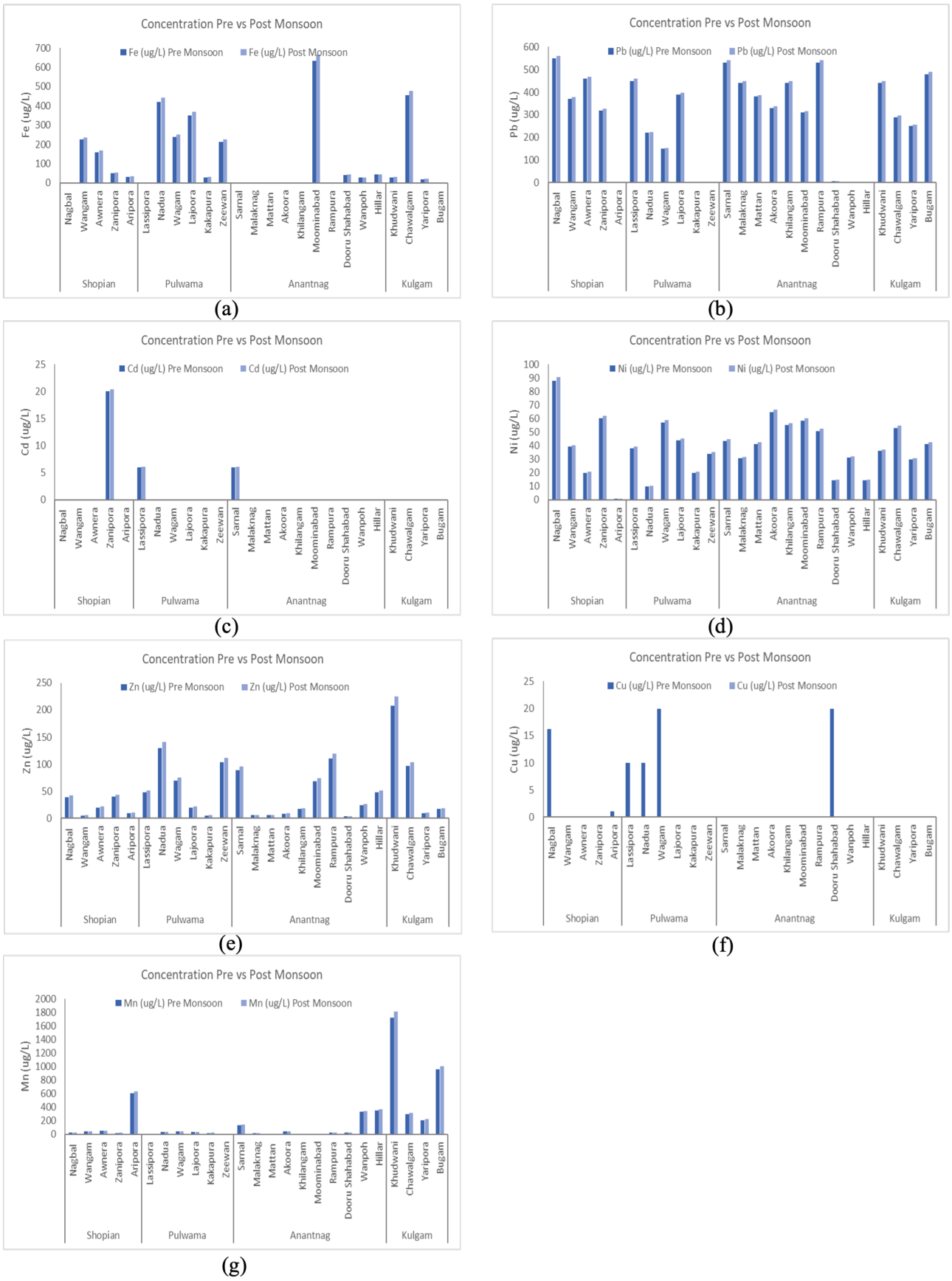


Fig 2. Graphical representation concentrations of various heavy metals in groundwater (µg/l) in Pre and Post Monsoon (a) Iron (b) Lead (c) Cadmium (d) Nickle (e) Zinc (f) Copper (g)

Heavy Metal Pollution Index

The groundwater standard in the study area has been analysed using both a complete index factor and a single factor index. The BIS 2012 acceptable limits and the concentration of heavy metal at each sampling point are related by the single factor index. The single factor index (Fi) is calculated using the following formula:

$F_i=C_i/C_0$

Ci is the measured concentration of heavy metal in Groundwater, and C0 is the permissible limit of the heavy metal concentration recommended by Bureau of Indian Standard for drinking water. Table 2 Shows the BIS 10500, 2012 limits of different heavy metals in drinking water.

Water quality does not meet the criteria if the value of Fi is more than 1, and it does if the value of Fi is less than 1 [28].

The comprehensive index was calculated by Nemerow Index method, this particular method was designed by two scientists named as Nemerow and Sumitomo in the year 1971, it is the most simplified pollution index and can be determined using following formula [29,30].

$$F = \sqrt{\frac{(F_{max}^2 + \bar{F}^2)}{2}}$$

In above equation the Nemerow pollution index is designated by F, Fi is a single evaluation index, and Fmax is the highest value that can be found in Fi's score value.F_{max} was calculated using following Equation (3)

$$F = \sqrt{\frac{(F_{max}^2 + \bar{F}^2)}{2}}$$

n denotes the number of sampling points assessed. Table 3 shows the water quality classification as per USEPA.

Human Health Risk

The Carcinogenic impact of presence of heavy metals present in drinking water was calculated utilising following equation:

$$R_i^c = \frac{1 - exp^{(-D_i q_i)}}{L}$$

In the equation above, RCi stands for the average annual risk of carcinogenesis which a carcinogen i in drinking water poses to one person. Equation (6) was used to compute Di, which stands for the average exposure dosage of carcinogen i per person daily in drinking water, and qi, which stands for the cancer slope factor of carcinogen (i) in water used for drinking purpose, mg/(kg d). The cancer slope factor (CSF) represents the increase in cancer risk per unit of exposure to the substance over a lifetime. It is a measure used in toxicology and risk assessment to estimate the potential carcinogenic risk associated with exposure to a specific chemical or substance. In the current study, a value of 15 for Cd, 8.5 for pb, and 0.84 for Ni [IRIS, WHO, CALEPA] was utilised, and L is the average life expectancy, which is believed to be 65 years in India [31].

The non- Carcinogenic health risk is calculated using the following equation:

$$R_i^n = \frac{D_i \times 10^{-6}}{RfD_i \times L}$$

In the above equation Rni denotes average annual risk caused by non-carcinogens i present in drinking water (a−1), RfDi denotes reference dose of the non-carcinogen i present in drinking water, mg/(kg·d). The RfDi values are shown in table 4.

Table 2. BIS 10500:2012 Indian standard drinking water specifications in µg/l.

Heavy Metal	Fe	Pb	Zn	Cd	Ni	Cu	Mn
Permissible Limit	300	10	15000	3	20	1500	300
Acceptable limit	300	10	5000	3	20	50	100

Table 3. Groundwater quality classification standard as per USEPA.

S No.	Nemerow Pollution Index (F)	Water Quality Classification
1	< 0.5	Excellent
2	0.5 to 0.75	Good
3	0.75 to 1.0	Moderate
4	> 1.0	Poor

Table 4. Reference dose of heavy metals of carcinogens and cancer slope factor

S No.	Heavy Metal	RfDi Value	Source	CSF	Source
1	Fe	0.3	USEPA 2001	-	-
2	Pb	1.4×10-3	WHO	8.5	[33]
3	Zn	3.0×10-1	IRIS	-	-
4	Cd	1×10-3	IRIS 2011	6.1	CALEPA
5	Ni	2×10-2	IRIS 2011	0.84	CALEPA
6	Cu	5×10-3	IRIS	--	-
7	Mn	1.4×10-1	IRIS 2011		-

The Di is calculated by the following equation:

$Di = (CW \times IR \times EF \times ED)/ (BW \times AT)$

where body weight is denoted by BW in kg (65 kg was selected for the adults in the study area), the period of exposure is denoted by ED (70 years for the carcinogen, and 30 years for the non-carcinogen), the intake of drinking water on a daily basis is indicated by IR (a value of 2.26 L/d was used), exposure frequency is indicated by EF (365 days/ year), and average exposure time is calculated as 365 × ED. (AS per USPA 2015).

Equation (7) was used to calculate the total health risk brought on by both carcinogens and non-carcinogens in groundwater. The reference values for each risk level are shown in Table 5 according to the international standards of various authorities.

$$R = \sum_{i=1}^{n} R_i^c + \sum_{i=1}^{n} R_i^n$$

Table 5. Reference values of the risk level (a-1) set by different agencies.

Agency Name	Maximum Acceptable Limit	Negligible Limit	Comment
The Swedish Environmental Protection Agency	1.0×10^{-6}	-	Chemical toxins
The Dutch Ministry of Construction and the Environment	1.0×10^{-6}	1.0×10^{-8}	Chemical toxins
Royal Society of UK	1.0×10^{-6}	1.0×10^{-7}	-
International Commission on Radiological Protection	5.0×10^{-5}	-	Radiation
Environmental Protection Agency of US	1.0×10^{-4}	-	-

Multivariate Statistical Analysis

For the analytical data interpretation, descriptive statistical analysis (Box and Whisker plot), Pearson's correlation analysis, Cluster Analysis and Analysis of variance and principal component analysis were performed.

Pearson Correlation Analysis:

To examine the connections between the quantities of heavy metals (such as Pb, Ni, Fe, Mn, Cu and Cd) in contaminated water samples, the Pearson correlation coefficients were computed. These coefficients help to understand the co-occurrence and possible causes of pollution of the heavy metals by revealing the degree of linear correlations among them [20].

Cluster Analysis

By dividing similar data points into clusters using cluster analysis, a statistical technique, which helps evaluate how similar the structures and patterns of dataset are. Cluster analysis is a crucial tool for identifying areas with similar contamination profiles and likely pollution sources when assessing heavy metal contamination in groundwater. In this study, cluster analysis was used with Origin Pro 2018 software to determine the same source of contaminants, which are heavy metals [32].

Analysis of Variance

Analysis of variance (ANOVA) was used to look for any notable differences in the mean amounts of heavy metals in

groundwater across four districts. The Origin programme 2018 was utilised to do the statistical analysis [8,13].

Principal component analysis

Using Origin Pro 2018 software, PCA has been carried out on groundwater for quantitative analysis of complex data. Four regulating factors with eigenvalues greater than one were found in this study using principal component analysis (PCA) to look into the likely source of the water quality [33]. The varimax normalised rotation is used to calculate the loading values for each parameter under the primary PCs [8]. For every PC, a collection of related metrics with both positive and negative loading values are used to understand the fundamental procedures involved in analysing and evaluating the water quality.

For every principal component, the variance and cumulative variance (%) were obtained (PC). The variance in statistics is used to calculate dispersion, which shows how far apart data points are from their average values [8,33]. Three groups were created based on the loading values of PCs: strong > 0.75, 0.75 > moderate > 0.5, and 0.5 > weak > 0.4. Less important parameter loading values (less than 0.4) were disregarded. These PCs were used to assess anthropogenic and natural processes that have an impact on water systems. By dividing the values of the laboratory-analysed data by their corresponding maximum values, the data were normalised [33]. These normalised value sets were used for PCA.

RESULTS

Box and Whisker Plots for Concentration of Heavy Metals

A boxplot, often named as "box-and-whisker" plot, usually consists of a oblong box containing three lines that denote the bottom, central, and top quartiles of the data. In addition to this, above and below the box are positioned two points and parallel lines. The middle line within the oblong signifies the intermediate value of the dataset, while the bottom and top lines indicate the values at the first and third quartiles, respectively. The elevated and lower values in the dataset are illustrated by the points positioned above and below the box and whiskers. The vertical lines elongated from the box's edges, referred to as whiskers, generally correlate with the values at the 5% and 95% percentiles of the dataset. Figure 3 demonstrates the various variables associated with the quality of groundwater like Pb, Ni, Mn, Cd, Cu, Fe and Zn. The assessment of the heavy metal data using box whisker plot depicted their variance accurately. The mean concentrations of Mn showed a statistically notable variations as indicated by ANOVA analysis ($p<0.05$). This could be the association linked to the presence of manganese and marshy gases in the deep aquifers of Kashmir valley. Locations like khudwani, bugam and aripora has significant variation probably due to consistency of a same origin of geological crust [28]. The introduction of manganese into the groundwater occurs as a result of leaching from minerals containing iron, facilitated by the existence of manganiferous phases [34,35]. However heavy metals Pb, Ni, Cd, Cu, Fe and Zn showed insignificant variation in the mean as $p>0.05$, that attributes to having contrasting hydro geochemical setup.

Pearson Correlation Analysis

One approach for determining potential pollution sources is Pearson's correlation coefficient (r). The correlation between the variables is strong if the value of r varies between 0.9 and 1, moderate if the value is between 0.9 and 0.5, and bad if the value is less than 0.5 [36]. The current investigation found that Pb and Ni (r = 0.5629) and Mn and Zn (r = 0.469) had moderately positive correlations (0.5), indicating that these metals originated from the same source. This interaction between water and rocks is caused by the decomposition of pyrite and aluminosilicates. Table 6 displays the several heavy metals' Pearson's correlation coefficients.

Table 6. Pearson Correlation coefficient of seven heavy metals.

Heavy Metal	Fe	Mn	Ni	Pb	Zn	Cd	Cu
(Fe)	1	-0.1819	0.05951	-0.1084	0.28499	-0.1565	0.02409
(Mn)	-0.1819	1	-0.1806	0.04739	0.46901	-0.1298	-0.2087
(Ni)	0.05951	-0.1806	1	0.56292	0.06736	0.22038	0.10592
(Pb)	-0.1084	0.04739	0.56292	1	0.14043	0.1469	-0.1308
(Zn)	0.28499	0.46901	0.06736	0.14043	1	0.0143	0.02197
(Cd)	-0.1565	-0.1298	0.22038	0.1469	0.0143	1	-0.0585
(Cu)	0.02409	-0.2087	0.10592	-0.1308	0.02197	-0.0585	1

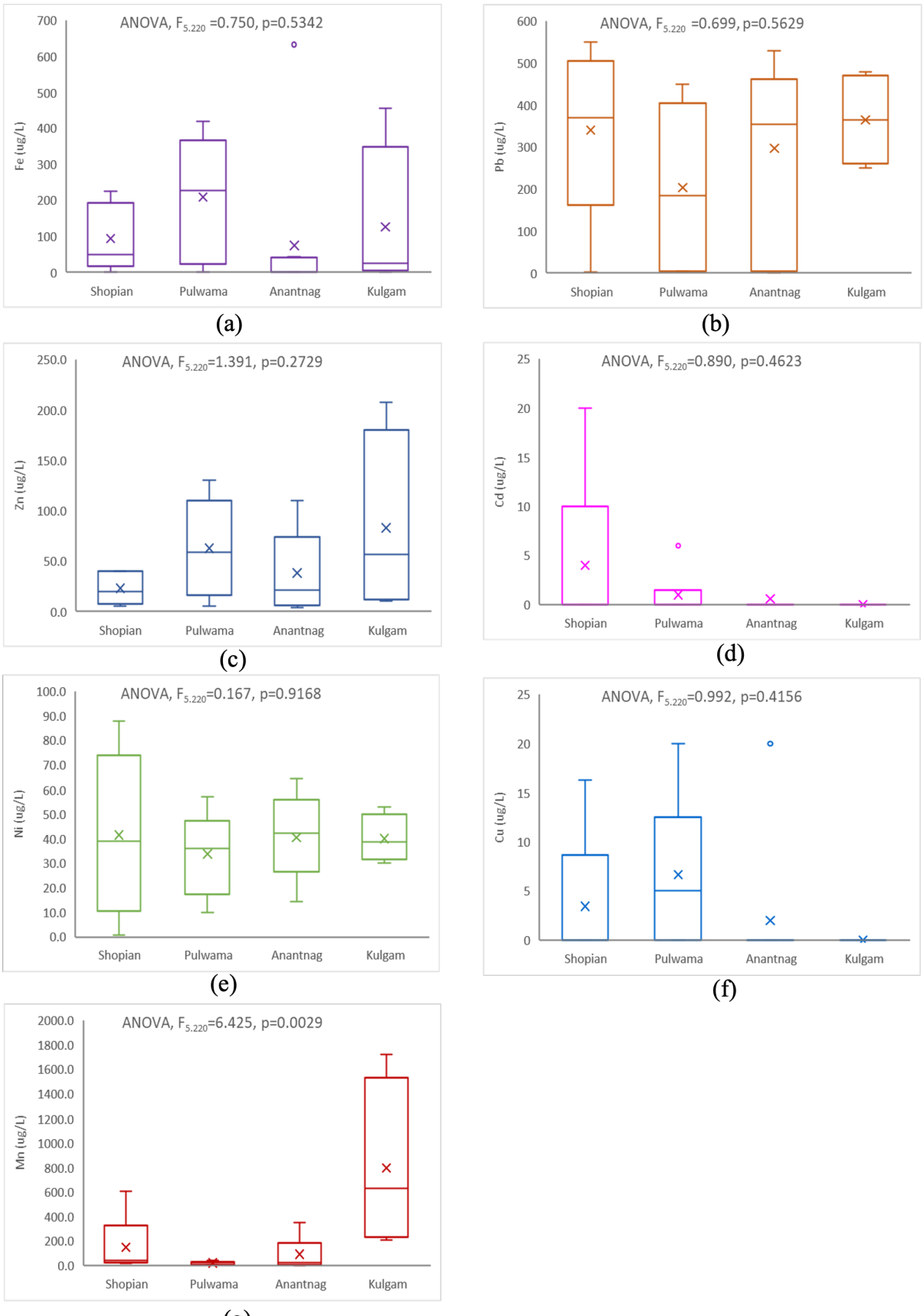


Fig 3. Boxplot illustrating the distribution of heavy metals in groundwater across various watersheds, accompanied by an analysis of variance (ANOVA) with a significance level of $p < 0.05$ (a) Iron (b) Lead (c) Zinc (d) Cadmium (e) Nickle (f) Copper (g) Manganese

Cluster Analysis

Cluster analysis (CA) is a statistical technique that has been used to analyse the relationship between metals and establish their nature, i.e., whether they come from natural or anthropogenic sources [28]. Hierarchical cluster analysis is used to classify the heavy metals in the research area into two main clusters, C1 and C2, as illustrated in Fig. 4 Fe, Mn, and Zn were found together in the first component, based on the initial component matrix indicators. Because it predominates throughout the entire study area, this component (C1) was designated as the "anthropogenic factor." Together, these metals account for 18% of the contamination in the research region. Auto shops, home wastewater, tyre wear and petrol combustion are probably the main sources of these metals. Pb, Ni, Cd, and Cu all showed total similarity in the second component (C2), which can be attributed to both the "natural factor" and anthropogenic factor because the composition of parent rocks and different anthropogenic activities in the study area seem to control the concentrations of these heavy metals. Based on the data, these metals account for about 41 percent of the total contamination in the area under study.

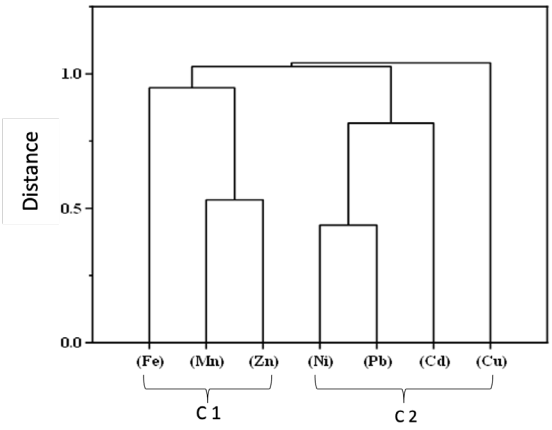


Figure 4. Dendrogram illustrating cluster analysis for seven heavy metals.

Principal component analysis

To find the group of metals with the same origin, elemental data was analysed using the PCA approach. It reduces the dataset's dimensionality and shows the relationship between the variables. All elements must be measured in the same units in order to execute PCA with the covariance function [33]. Seven measurable variables and a total of 25 monitoring points from the data matrix were used in this study to determine the categorization. The dataset's key gradients are used to calculate PC and its eigenvalues. The first four PCs had the most significant components, accounting for 78.32% of the variance in water quality overall. As shown in Table 7, the PC1, PC2, PC3, and PC4 explained 24.29%, 22.19%, 18.41%, and 13.43% of the variation, respectively. The three factors with eigenvalues > 1 (1.70, 1.55, 1.28, 0.94), after varimax rotation, were extracted from the major factor matrix. The first component (PC1), which accounts for the largest variance of 24.29%, has significant positive loadings of Ni (0.657), Pb (0.632), and Cd (0.376), making it useful in recognising changes in water quality. Because of human and environmental influences, the PC1 factors had the biggest impact on the chemistry of the groundwater. Significant indications can leak into groundwater as a result of mineral weathering that contains silicate and salt as well as interactions between water, soils, and rocks [37]. PC2 showed significant positive loadings of Zn (0.642) and Mn (0.679), which together accounted for 22.19% of the variance and indicated the relationship with adjacent human activity. Additionally, PC3 explained 18.41% of the variance, indicating a significant positive loading of Zn (0.335), Cu (0.429), and Fe (0.730). It seems that PC3 comes from various human sources, such as car and industrial pollution (47,48). PC4 demonstrates that a large positive loading of Cu (0.81) accounts for 13.43% of the variance. The scree plot is a method for identifying multiple significant components by seeing a large split in the size of the eigen values, which causes the plot's slope to change from steep to shallow, as seen in Fig. 5(b) [8,33]. When the first three parameters are taken into account, the plot's slope changes from steep to shallow. The eigenvalues drop below one as component 3 and factor 5 are farther moved. This suggests that the best option for this investigation would be a four-component solution, which explains the overall variance of 78.32%. Most of the variables in the loadings plot of the first two PCs (PC1 and PC2) are distributed in the first and fourth quadrants depicted in Fig. 5(a). The contributions of each variable to the samples are shown by the lines passing through the origin and linking the variables. The degree of reciprocal relationship between two variable lines is indicated by their proximity [33]. The loading plot's grouping of variables (Pb, Fe, and Zn; Mn; Cu, Cd, and Ni) shows a strong positive association with one another. PCs score plots show sample attributes and offer details on how they are distributed geographically. The PCs scores plot (Fig.5(a)), which was produced with the assistance of the PC1 and PC2 components, confirms the spatial distribution and clustering of site-specific samples. Figures 5(a) and 5(b)show that samples arranged in the top quadrants have higher concentrations of maximum elements like Pb, Fe, Mn, and Zn, whereas samples in the lower quadrants have higher concentrations of Cu, Cd, and Ni. According to the groundwater scores plot shown in Fig 5 (a), the sample distributions is scattered. Moreover, the two main components, PC1 and PC2, which account for 24.29% and 24.29% of the total variance and have large loadings of (≥0.40), were also found to be primarily in charge of controlling the amounts of metals in the groundwater in the study area [33]. This is due to the fact that only 40% of the elements examined in the research region come under these two components with a substantial loading (0.40). In contrast, PC3 and PC4 showed substantial positive loadings of 13.43% and 18.41%, respectively, together with low variance characteristics. Because of their smaller variance, they were consequently assigned the lowest priority when it came to controlling the metal concentrations in ground water.

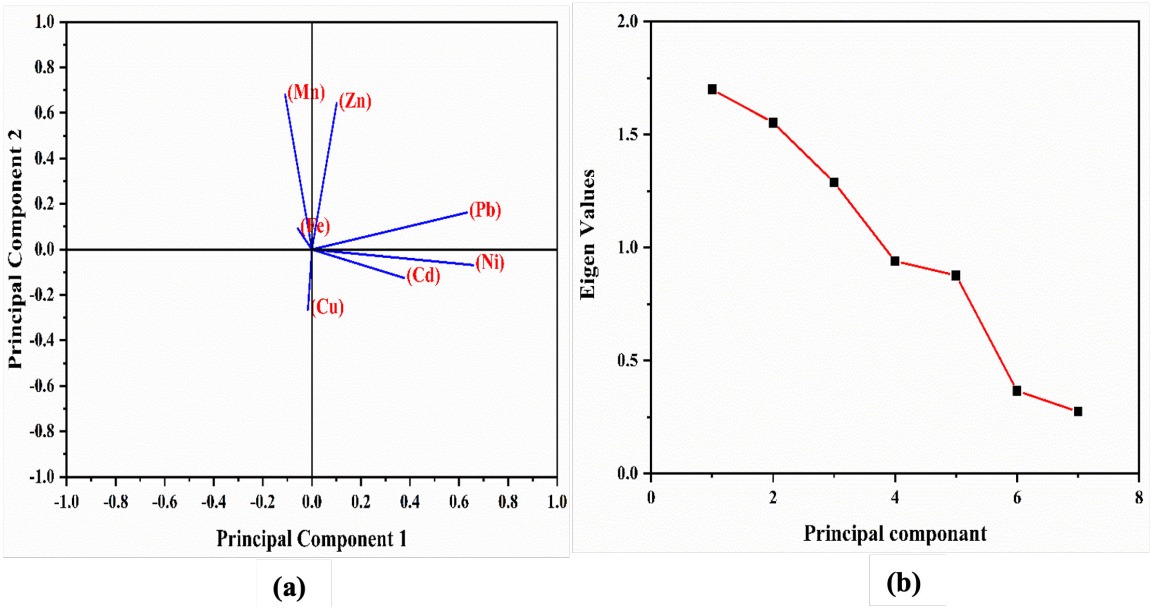


Figure 5. (a) Plot of PCA loadings scores for data set and (b)PCA scree plot of the eigen value.

Table 7. Principal component loadings for metals in groundwater.

Heavy Metal	Coefficients of PC1	Coefficients of PC2	Coefficients of PC3	Coefficient Of PC4
(Fe)	-0.0573	0.09196	0.73042	-0.4863
(Mn)	-0.1094	0.67964	-0.2536	0.24547
(Ni)	0.65771	-0.0688	0.1988	0.03786
(Pb)	0.63258	0.16258	-0.0826	-0.0512
(Zn)	0.10079	0.6423	0.33586	0.16664
(Cd)	0.37631	-0.1251	-0.2425	0.00809
(Cu)	-0.0163	-0.2651	0.4292	0.81938

Single-Factor Evaluation

Groundwater samples totalling 25 were examined in pre and post monsoon season for the presence of heavy metals, and the results showed that the concentrations of these metals can be categorised as follows: Pb > Mn > Fe > Zn > Ni > Cu > Cd. Furthermore, coefficient of variation was greater than 1 at majority of the sampling points, hydro-chemical properties of the groundwater showed inconsistency in both the seasons. Locations like Hillar and Chawalgam has insignificant variation in pre and post monsoon season probably due to consistency of a similar source of origin (geological crustal) during both seasonal periods [28].Comparison of seven heavy metals when done with the BIS for ground water quality (Table 8), it was observed that the quality of 19 water samples did not comply the Pb and Ni concentration requirement as per BIS, accounting to 76% for each element in pre monsoon seasons and in post monsoon season 19 and 21 water samples did not comply the Pb and Ni concentration requirement as per BIS, accounting to 76% and 84% for each element respectively . Additionally, the concentration of manganese was greater than permissible limits at 5 and 6 locations in pre and post monsoon seasons respectively accounting to 20% and 24%. The findings indicated that Pb, Ni, Fe, and Mn contamination existed in the local groundwater. Figure 6 depicts the spatial distribution map of Iron, Lead, Copper, Cadmium, Nickle, Manganese, Zinc concentrations.

Table 8. Statistical characteristics of heavy metals in ground water (µg/l)

Index	Pre-Monsoon (µg/l)							Post Monsoon (µg/l)						
	Ci (Fe)	Ci (Mn)	Ci (Ni)	Ci (Pb)	Ci (Zn)	Ci (Cd)	Ci (Cu)	Ci (Fe)	Ci (Mn)	Ci (Ni)	Ci (Pb)	Ci (Zn)	Ci (Cd)	Ci (Cu)
Max (conc.)	**632.9**	**550.0**	**207.8**	**20.0**	**87.8**	**20.0**	**1721.4**	**664.5**	**561.0**	**224.4**	**20.4**	**90.4**	**0.0**	**1807.5**
Min (conc.)	**0.0**	**0.0**	**3.7**	**0.0**	**0.9**	**0.0**	**0.0**	**0.0**	**0.0**	**4.0**	**0.0**	**0.9**	**0.0**	**0.0**
Sampling points exceeding	**4.0**	**19.0**	**0.0**	**3.0**	**19.0**	**0.0**	**5.0**	**4.0**	**19.0**	**0.0**	**3.0**	**21.0**	**0.0**	**6.0**
BIS limit (Each)	**16%**	**76%**	**0%**	**12%**	**76%**	**0%**	**20%**	**16%**	**76%**	**0%**	**12%**	**84%**	**0%**	**24%**
Exceeding the standard (%)	**118.8**	**293.9**	**48.2**	**1.3**	**39.0**	**3.1**	**200.0**	**124.7**	**299.8**	**52.0**	**1.3**	**40.2**	**0.0**	**210.0**
Mean	**176.0**	**192.3**	**50.7**	**4.2**	**19.6**	**6.5**	**389.7**	**184.8**	**196.2**	**54.8**	**4.3**	**20.2**	**0.0**	**409.2**
Standard Deviation	**1.48**	**0.65**	**1.05**	**3.31**	**0.50**	**2.12**	**1.95**	**1.48**	**0.65**	**1.05**	**3.31**	**0.50**	**2.04**	**1.95**
Coefficient of variation (100%)	**240.0**	**40.0**	**57.0**	**150.0**	**70.0**	**ND**	**20.0**	**252.0**	**42.0**	**58.7**	**153.0**	**75.6**	**ND**	**ND**

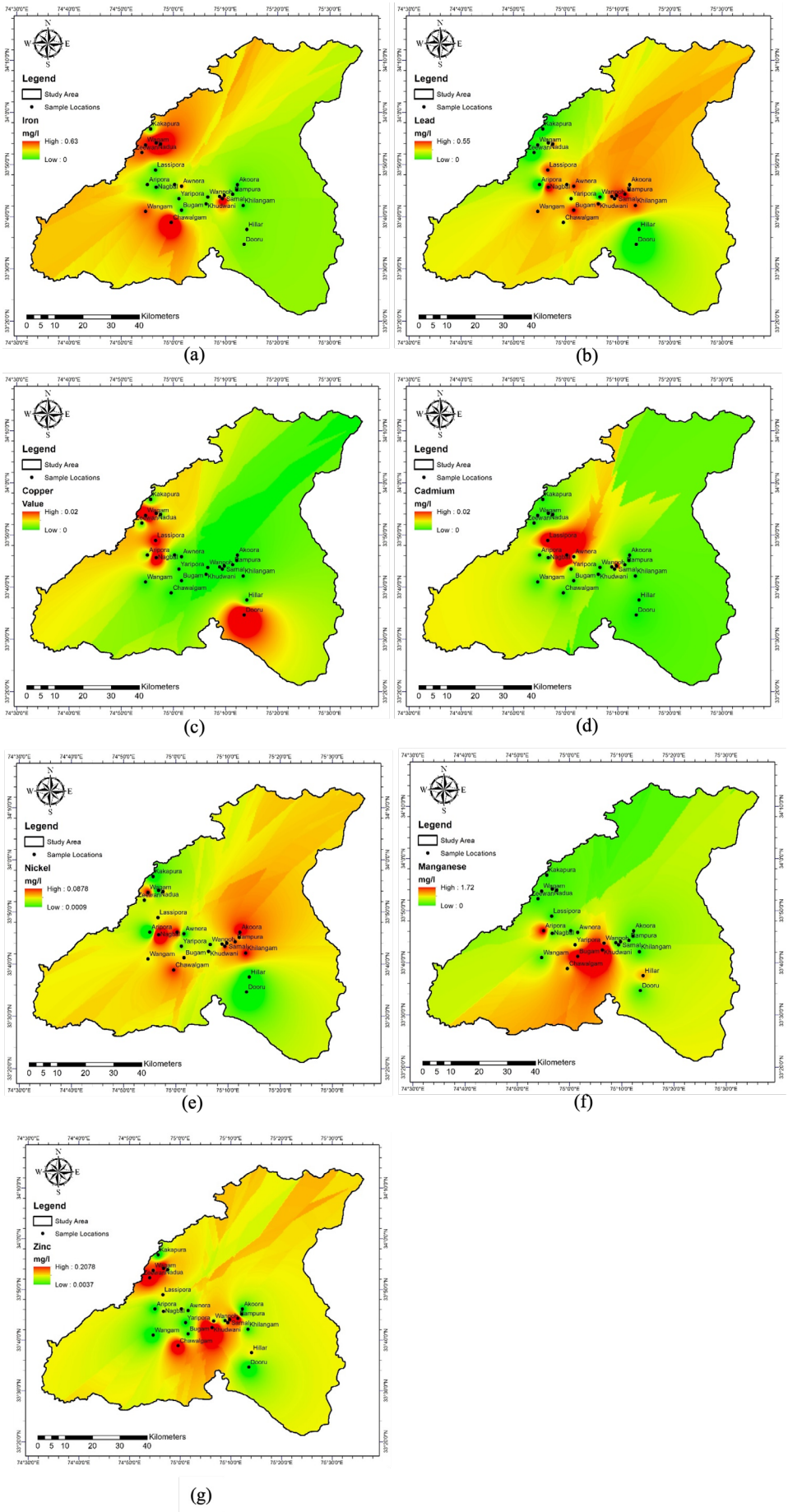


Figure 6. Spatial distribution of heavy metals: (a) Iron (b) Lead (c) Copper (d) Cadmium (e) Nickle (f) Manganese (g) Zinc in the research area.

Comprehensive Evaluation

The score of water quality of individual sample point is demonstrated in Table 9. In both the seasons Out of 25 samples, the quality of one sample was excellent, the quality of 2 samples were good, the quality of 2 samples were moderate and 20 water samples had a very poor-quality accounting to 4%,8%, 8% and 80% respectively. The Excellent and good quality water accounted 12%, suggesting that the quality of water in the research area was very poor and majority of the sampling sites were contaminated. The results found in comprehensive evaluation validated the results of single factor evaluation.

Human Health Risk Assessment

Non-Carcinogenic Risk Assessment

The recommended values for risk limit suggested by some institutions are presented in Table 5. The derived non-cancerous health risk value of following heavy metals viz, lead, nickel, iron, manganese, zinc, copper and cadmium are depicted in the table 10 and 11 for pre monsoon season and post monsoon season, showing maximum value at 8.88 × 10-4 and 9.06 × 10-4 in pre and post monsoon season respectively. The results indicate that the level of non- cancerous health risk induced by zinc, nickel, lead and manganese in the groundwater of said area is very high and can cause serious harm to human health. It has been revealed after the calculation of non -carcinogenic health risk the following seven heavy metals can be graded as Pb>Ni>Mn>Cd>Cu>Fe>Zn. Among these lead and manganese are contributing the most, accounting 96%, 92% respectively, of the total health risk values.

Carcinogenic Health Risk Assessment

Table 10 and 11 show the carcinogenic health risk assessment for pre and post monsoon season respectively. The carcinogenic risk value for lead was found between 0 and 2.31 × 10-3 and 0 and 2.35 × 10-3 in pre and post monsoon season respectively .24 samples exceeded the maximum acceptable Pb level recommended by The Dutch Ministry of construction and Environment, The Royal society and The Swedish Environmental Protection Agency. Nineteen samples (76%) exceeded the permissible limit recommended by US environmental Protection Agency and International Commission on Radiological Protection for lead in both the seasons. The carcinogenic risk value for Cadmium was found between 0 and 6.51×10-5in pre monsoon and 0 and 6.64 10-5 in post monsoon season. Three samples accounting 12% exceeding the maximum acceptable limits recommended for cadmium by The Dutch Ministry of construction and Environment, The Royal society, and The Swedish Environmental Protection Agency. One sample accounting 4 % exceeds the maximum acceptable limits recommended for cadmium by International Commission on Radiological Protection in both the seasons. The carcinogenic risk value for Nickle was found between 0 and 3.9 × 10-5in pre monsoon season and 0 and 4.06×10-5 in post monsoon season. 24 samples exceeded the maximum acceptable Ni level recommended by The Dutch Ministry of construction and Environment, The Royal society and The Swedish Environmental Protection Agency accounting 96% in both the seasons. The results show a clear picture of carcinogenic health risk in the groundwater of the study area and the relevant authorities should seriously take the health risk into consideration.

Overall Health Risk Assessment

Tables 10 and 11 demonstrate that the carcinogenic risk assessment value is the main cause of the overall health risk. The average carcinogenic risk in pre monsoon season throughout the 25 sampling points was 4.27 ×10-4, or 72.41% of the total health risk, while the average non-carcinogenic risk was 27.59%. and for post monsoon season the average carcinogenic risk throughout the 25 sampling points was 4.35 ×10-4, or 72.38% of the total health risk, while the average non-carcinogenic risk was 27.62%. The findings demonstrated that both carcinogenic risk and non-carcinogenic risk contribute to the overall health risk of the study area's ground water. However, the risk of cancer is slightly higher than the risk of other diseases. Lead requires particular attention in the aforementioned study region as it accounts for 71% of the carcinogenic health risk.

Table 9. The calculation of Nemerow pollution index (F)

S No.	Location	Pre-Monsoon										Post Monsoon									
		Fi (Fe)	Fi (Pb)	Fi (Zn)	Fi (Cd)	Fi (Ni)	Fi (Cu)	Fi (Mn)	F_{max}	F	F	F_i (Fe)	F_i (Pb)	F_i (Zn)	F_i (Cd)	F_i (Ni)	F_i (Cu)	F_i (Mn)	F_{max}	F	F
1	Nagbal	0	55	0	0	4.39	0.01	0.09	55	8.5	27.83	0	56.1	0	0	4.52	0.01	0.09	56.1	8.68	28.38
2	Wangam	0.75	37	0	0	1.96	0	0.15	37	5.69	18.72	0.79	37.74	0	0	2.02	0	0.15	37.74	5.81	19.09
3	Awnera	0.53	46	0	0	1	0	0.17	46	6.81	23.25	0.56	46.92	0	0	1.03	0	0.18	46.92	6.96	23.72
4	Zanipora	0.17	32	0	6.67	3	0	0.07	32	5.99	16.28	0.18	32.64	0	6.8	3.09	0	0.07	32.64	6.11	16.6
5	Shopian	0.11	0.23	0	0	0.05	0	2.02	2.02	0.34	1.02	0.12	0.23	0	0	0.05	0	2.12	2.12	0.36	1.07
6	Lassipora	0	45	0	2	1.9	0.01	0.03	45	6.99	22.77	0	45.9	0	2.04	1.96	0.01	0.03	45.9	7.13	23.23
7	Nadua	1.4	22	0.01	0	0.5	0.01	0.1	22	3.43	11.13	1.47	22.44	0.01	0	0.52	0.01	0.11	22.44	3.51	11.36
8	Wagam	0.8	15	0	0	2.85	0.01	0.13	15	2.69	7.62	0.84	15.3	0.01	0	2.94	0.01	0.14	15.3	2.75	7.77
9	Lajoora	1.17	39	0	0	2.2	0	0.1	39	6.07	19.73	1.23	39.78	0	0	2.27	0	0.11	39.78	6.2	20.13
10	Kakapura	0.1	0.45	0	0	1	0	0.07	1	0.23	0.51	0.1	0.46	0	0	1.03	0	0.07	1.03	0.24	0.53
11	Zeewan	0.72	0.39	0.01	0	1.7	0	0.03	1.7	0.41	0.87	0.75	0.4	0.01	0	1.75	0	0.04	1.75	0.42	0.9
12	Sarnal	0	53	0.01	2	2.17	0	0.45	53	8.23	26.82	0	54.06	0.01	2.04	2.24	0	0.47	54.06	8.4	27.35
13	Malaknag	0	44	0	0	1.53	0	0.06	44	6.51	22.24	0	44.88	0	0	1.58	0	0.06	44.88	6.65	22.68
14	Mattan	0	38	0	0	2.06	0	0	38	5.72	19.21	0	38.76	0	0	2.13	0	0	38.76	5.84	19.6
15	Akoora	0	33	0	0	3.23	0	0.14	33	5.2	16.7	0	33.66	0	0	3.32	0	0.15	33.66	5.3	17.04
16	Khilangam	0	44	0	0	2.75	0	0	44	6.68	22.25	0	44.88	0	0	2.83	0	0	44.88	6.82	22.7
17	Moominabad	2.11	31	0	0	2.91	0	0.02	31	5.15	15.71	2.22	31.62	0	0	3	0	0.02	31.62	5.27	16.03
18	Rampura	0	53	0.01	0	2.54	0	0.08	53	7.95	26.8	0	54.06	0.01	0	2.62	0	0.08	54.06	8.11	27.33
19	Dooru	0.14	0.52	0	0	0.73	0.01	0.08	0.73	0.21	0.38	0.14	0.53	0	0	0.75	0.01	0.08	0.75	0.22	0.39
20	Wanpoh	0.09	0.27	0	0	1.57	0	1.1	1.57	0.43	0.81	0.1	0.28	0	0	1.61	0	1.16	1.61	0.45	0.84
21	Hillar	0.14	0	0	0	0.73	0	1.17	1.17	0.29	0.6	0.15	0	0	0	0.75	0	1.23	1.23	0.3	0.63
22	Khudwani	0.1	44	0.01	0	1.8	0	5.74	44	7.38	22.31	0.1	44.88	0.01	0	1.85	0	6.02	44.88	7.55	22.76
23	Chawalgam	1.52	29	0.01	0	2.65	0	1	29	4.88	14.7	1.59	29.58	0.01	0	2.72	0	1.05	29.58	4.99	15
24	Yaripora	0.07	25	0	0	1.5	0	0.7	25	3.9	12.65	0.07	25.5	0	0	1.55	0	0.74	25.5	3.98	12.9
25	Bugam	0	48	0	0	2.06	0	3.2	48	7.61	24.3	0	48.96	0	0	2.13	0	3.36	48.96	7.78	24.79

Table 10. Health risk assessment (a-1), pre-monsoon

S No.	Location	Health Risk Assessment, Pre-Monsoon										
		Non-Carcinogenic Risk							Carcinogenic Risk			Total Health Risk
		Fe	Pb	Zn	Cd	Ni	Cu	Mn	Pb	Cd	Ni	
1	**Nagbal**	**0**	**8.8x10-4**	**2.9x10-7**	**0**	**9.9x10-6**	**7.3x10-6**	**4.3x10-7**	**2.3x10-3**	**0**	**3.9x10-5**	**3.2x10-3**
2	**Wangam**	**1.6x10-6**	**5.9x10-4**	**4.0x10-8**	**0**	**4.4x10-6**	**0**	**7.0x10-7**	**1.5x10-3**	**0**	**1.7x10-5**	**2.2x10-3**
3	**Awnera**	**1.2x10-6**	**7.4x10-4**	**1.5x10-7**	**0**	**2.2x10-6**	**0**	**8.0x10-7**	**1.9x10-3**	**0**	**8.9x10-6**	**2.7x10-3**
4	**Zanipora**	**3.7x10-7**	**5.1x10-4**	**3.0x10-7**	**4.5x10-5**	**6.7x10-6**	**0**	**3.2x10-7**	**1.3x10-3**	**6.5x10-5**	**2.6x10-5**	**2.0x10-3**
5	**Shopian**	**2.49x10-7**	**3.7x10-6**	**7.5x10-8**	**0**	**1.0x10-7**	**4.5x10-7**	**9.7x10-6**	**1.0x10-5**	**0**	**4.0x10-7**	**2.5x10-5**
6	**Lassipora**	**0**	**7.2x10-4**	**3.5x10-7**	**1.3x10-5**	**4.3x10-6**	**4.5x10-6**	**1.4x10-7**	**1.9x10-3**	**1.9x10-5**	**1.7x10-5**	**2.7x10-3**
7	**Nadua**	**3.16x10-6**	**3.5x10-4**	**9.7x10-7**	**0**	**1.1x10-6**	**4.5x10-6**	**4.8x10-7**	**9.6x10-4**	**0**	**4.4x10-6**	**1.3x10-3**
8	**Wagam**	**1.8x10-6**	**2.4x10-4**	**5.2x10-7**	**0**	**6.4x10-6**	**9.0x10-6**	**6.4x10-7**	**6.6x10-4**	**0**	**2.56x10-5**	**9.5x10-4**
9	**Lajoora**	**2.6x10-6**	**6.3x10-4**	**1.5x10-7**	**0**	**4.9x10-6**	**0**	**4.8x10-7**	**1.6x10-3**	**0**	**1.9x10-5**	**2.3x10-3**
10	**Kakapura**	**2.2x10-7**	**7.2x10-6**	**4.0x10-8**	**0**	**2.2x10-6**	**0**	**3.2x10-7**	**2.0x10-5**	**0**	**8.9x10-6**	**3.9x10-5**
11	**Zeewan**	**1.6x10-6**	**6.3x10-6**	**7.7x10-7**	**0**	**3.8x10-6**	**0**	**1.6x10-7**	**1.7x10-5**	**0**	**1.5x10-5**	**4.5x10-5**

Table 10. Health risk assessment (a-1), pre-monsoon

S No.	Location	Health Risk Assessment, Pre-Monsoon										
		Non-Carcinogenic Risk							Carcinogenic Risk			Total Health Risk
		Fe	Pb	Zn	Cd	Ni	Cu	Mn	Pb	Cd	Ni	
12	**Sarnal**	**0**	**8.5x10-4**	**6.6x10-7**	**1.3x10-5**	**4.9x10-6**	**0**	**2.1x10-6**	**2.2x10-3**	**1.9x10-5**	**1.9x10-5**	**3.1x10-3**
13	**Malaknag**	**0**	**7.1x10-4**	**4.6x10-8**	**0**	**3.4x10-6**	**0**	**2.7x10-7**	**1.8x10-3**	**0**	**1.3x10-5**	**2.6x10-3**
14	**Mattan**	**0**	**6.1x10-4**	**4.5x10-8**	**0**	**4.6x10-6**	**0**	**0**	**1.6x10-3**	**0**	**1.8x10-5**	**2.2x10-3**
15	**Akoora**	**0**	**5.3x10-4**	**6.7x10-8**	**0**	**7.2x10-6**	**0**	**6.8x10-7**	**1.4x10-3**	**0**	**2.9x10-5**	**2.0x10-3**
16	**Khilangam**	**0**	**7.1x10-4**	**1.3x10-7**	**0**	**6.2x10-6**	**0**	**0**	**1.8x10-3**	**0**	**2.4x10-5**	**2.6x10-3**
17	**Moominabad**	**4.7x10-6**	**5.0x10-4**	**5.2x10-7**	**0**	**6.5x10-6**	**0**	**1.0x10-7**	**1.3x10-3**	**0**	**2.6x10-5**	**1.8x10-3**
18	**Rampura**	**0**	**8.5x10-4**	**8.3x10-7**	**0**	**5.7x10-6**	**0**	**3.8x10-7**	**2.2x10-3**	**0**	**2.2x10-5**	**3.1x10-3**
19	**Dooru**	**3.0x10-7**	**8.3x10-6**	**2.7x10-8**	**0**	**1.6x10-6**	**9.0x10-6**	**3.7x10-7**	**2.3x10-5**	**0**	**6.5x10-6**	**4.9x10-5**
20	**Wanpoh**	**2.0x10-7**	**4.3x10-6**	**1.8x10-7**	**0**	**3.5x10-6**	**0**	**5.3x10-6**	**1.2x10-5**	**0**	**1.4x10-5**	**3.9x10-5**
21	**Hillar**	**3.2x10-7**	**0**	**3.5x10-7**	**0**	**1.6x10-6**	**0**	**5.6x10-6**	**0**	**0**	**6.5x10-6**	**1.4x10-5**
22	**Khudwani**	**2.2x10-7**	**7.1x10-4**	**1.5x10-6**	**0**	**4.0x10-6**	**0**	**2.7x10-5**	**1.8x10-3**	**0**	**1.6x10-5**	**2.6x10-3**

Table 10. Health risk assessment (a-1), pre-monsoon

S No.	Location	Health Risk Assessment, Pre-Monsoon										
		Non-Carcinogenic Risk							Carcinogenic Risk			Total Health Risk
		Fe	Pb	Zn	Cd	Ni	Cu	Mn	Pb	Cd	Ni	
23	**Chawalgam**	**3.4x10-6**	**4.6x10-4**	**7.2x10-7**	**0**	**5.9x10-6**	**0**	**4.8x10-6**	**1.2x10-3**	**0**	**2.3x10-5**	**1.7x10-3**
24	**Yaripora**	**1.5x10-7**	**4.0x10-4**	**7.5x10-8**	**0**	**3.3x10-6**	**0**	**3.3x10-6**	**1.1x10-3**	**0**	**1.3x10-5**	**1.5x10-3**
25	**Bugam**	**0**	**7.7x10-4**	**1.2x10-7**	**0**	**4.6x10-6**	**0**	**1.5x10-5**	**2.0x10-3**	**0**	**1.8x10-5**	**2.8x10-3**
	Total	**2.4x10-5**	**1.1x10-2**	**9.0x10-6**	**7.2x10-5**	**1.1x10-4**	**3.4x10-5**	**8.0x10-5**	**3.1x10-2**	**1.0x10-4**	**4.3x10-4**	**4.4x10-2**
	Khilangam	**0**	**7.1x10-4**	**1.3x10-7**	**0**	**6.2x10-6**	**0**	**0**	**1.8x10-3**	**0**	**2.4x10-5**	**2.6x10-3**
	Mean	**1.7x10-6**	**9.1x10-4**	**6.9x10-7**	**5.5x10-6**	**8.4x10-6**	**2.6x10-6**	**6.2x10-6**	**2.4x10-3**	**8.0x10-6**	**3.3x10-5**	**3.4x10-3**

Table 11. Health risk assessment (a-1), post-monsoon

S No.	Location	Health Risk Assessment, Pre-Monsoon										
		Non-Carcinogenic Risk							Carcinogenic Risk			Total Health Risk
		Fe	Pb	Zn	Cd	Ni	Cu	Mn	Pb	Cd	Ni	
1	**Nagbal**	**0**	**9.0x10-4**	**3.1x10-7**	**0**	**1.0x10-5**	**7.3x10-6**	**4.5x10-7**	**2.3x10-3**	**0**	**4.0x10-5**	**3.3x10-3**
2	**Wangam**	**1.7x10-6**	**6.0x10-4**	**4.3x10-8**	**0**	**4.5x10-6**	**0**	**7.4x10-7**	**1.6x10-3**	**0**	**1.8x10-5**	**2.2x10-3**
3	**Awnera**	**1.2x10-6**	**7.5x10-4**	**1.6x10-7**	**0**	**2.3x10-6**	**0**	**8.4x10-7**	**1.9x10-3**	**0**	**9.2x10-6**	**2.7x10-3**
4	**Zanipora**	**3.9x10-7**	**5.2x10-4**	**3.2x10-7**	**4.6x10-5**	**6.9x10-6**	**0**	**3.3x10-7**	**1.4x10-3**	**6.6x10-5**	**2.7x10-5**	**2.0x10-3**
5	**Shopian**	**2.6x10-7**	**3.7x10-6**	**8.1x10-8**	**0**	**1.0x10-7**	**4.5x10-7**	**1.0x10-5**	**1.0x10-5**	**0**	**4.1x10-7**	**2.6x10-5**
6	**Lassipora**	**0**	**7.4x10-4**	**3.8x10-7**	**1.3x10-5**	**4.4x10-6**	**4.5x10-6**	**1.5x10-7**	**1.9x10-3**	**2.0x10-5**	**1.7x10-5**	**2.7x10-3**
7	**Nadua**	**3.3x10-6**	**3.6x10-4**	**1.0x10-6**	**0**	**1.1x10-6**	**4.5x10-6**	**5.0x10-7**	**9.8x10-4**	**0**	**4.6x10-6**	**1.3x10-3**
8	**Wagam**	**1.9x10-6**	**2.4x10-4**	**5.7x10-7**	**0**	**6.6x10-6**	**9.0x10-6**	**6.7x10-7**	**6.8x10-4**	**0**	**2.6x10-5**	**9.7x10-4**
9	**Lajoora**	**2.7x10-6**	**6.4x10-4**	**1.6x10-7**	**0**	**5.1x10-6**	**0**	**5.0x10-7**	**1.7x10-3**	**0**	**2.0x10-5**	**2.3x10-3**
10	**Kakapura**	**2.3x10-7**	**7.4x10-6**	**4.3x10-8**	**0**	**2.3x10-6**	**0**	**3.3x10-7**	**2.0x10-5**	**0**	**9.2x10-6**	**4.0x10-5**
11	**Zeewan**	**1.7x10-6**	**6.4x10-6**	**8.3x10-7**	**0**	**3.9x10-6**	**0**	**1.7x10-7**	**1.8x10-5**	**0**	**1.5x10-5**	**4.6x10-5**

Table 11. Health risk assessment (a-1), post-monsoon

S No.	Location	Health Risk Assessment, Pre-Monsoon										
		Non-Carcinogenic Risk							Carcinogenic Risk			Total Health Risk
		Fe	Pb	Zn	Cd	Ni	Cu	Mn	Pb	Cd	Ni	
12	**Sarnal**	**0**	**8.7x10-4**	**7.1x10-7**	**1.3x10-5**	**5.0x10-6**	**0**	**2.2x10-6**	**2.2x10-3**	**2.0x10-5**	**2.0x10-5**	**3.2x10-3**
13	**Malaknag**	**0**	**7.2x10-4**	**4.9x10-8**	**0**	**3.5x10-6**	**0**	**2.8x10-7**	**1.9x10-3**	**0**	**1.4x10-5**	**2.6x10-3**
14	**Mattan**	**0**	**6.2x10-4**	**4.8x10-8**	**0**	**4.8x10-6**	**0**	**0**	**1.6x10-3**	**0**	**1.9x10-5**	**2.3x10-3**
15	**Akoora**	**0**	**5.4x10-4**	**7.2x10-8**	**0**	**7.5x10-6**	**0**	**7.2x10-7**	**1.4x10-3**	**0**	**2.9x10-5**	**2.0x10-3**
16	**Khilangam**	**0**	**7.2x10-4**	**1.4x10-7**	**0**	**6.4x10-6**	**0**	**0**	**1.9x10-3**	**0**	**2.5x10-5**	**2.6x10-3**
17	**Moominabad**	**5.0x10-6**	**5.1x10-4**	**5.6x10-7**	**0**	**6.7x10-6**	**0**	**1.1x10-7**	**1.3x10-3**	**0**	**2.6x10-5**	**1.9x10-3**
18	**Rampura**	**0**	**8.7x10-4**	**8.9x10-7**	**0**	**5.9x10-6**	**0**	**4.0x10-7**	**2.2x10-3**	**0**	**2.3x10-5**	**3.1x10-3**
19	**Dooru**	**3.2x10-7**	**8.5x10-6**	**3.0x10-8**	**0**	**1.6x10-6**	**9.0x10-6**	**3.9x10-7**	**2.4x10-5**	**0**	**6.7x10-6**	**5.0x10-5**
20	**Wanpoh**	**2.1x10-7**	**4.4x10-6**	**2.0x10-7**	**0**	**3.6x10-6**	**0**	**5.5x10-6**	**1.2x10-5**	**0**	**1.4x10-5**	**4.1x10-5**
21	**Hillar**	**3.4x10-7**	**0**	**3.8x10-7**	**0**	**1.7x10-6**	**0**	**5.9x10-6**	**0**	**0**	**6.7x10-6**	**1.5x10-5**
22	**Khudwani**	**2.3x10-7**	**7.2x10-4**	**1.6x10-6**	**0**	**4.1x10-6**	**0**	**2.9x10-5**	**1.9x10-3**	**0**	**1.6x10-5**	**2.6x10-3**

Table 11. Health risk assessment (a-1), post-monsoon

S No.	Location	Health Risk Assessment, Pre-Monsoon										
		Non-Carcinogenic Risk							Carcinogenic Risk			Total Health Risk
		Fe	Pb	Zn	Cd	Ni	Cu	Mn	Pb	Cd	Ni	
23	**Chawalgam**	**3.6x10-6**	**4.7x10-4**	**7.8x10-7**	**0**	**6.1x10-6**	**0**	**5.0x10-6**	**1.2x10-3**	**0**	**2.4x10-5**	**1.8x10-3**
24	**Yaripora**	**1.5x10-7**	**4.1x10-4**	**8.1x10-8**	**0**	**3.4x10-6**	**0**	**3.5x10-6**	**1.1x10-3**	**0**	**1.3x10-5**	**1.5x10-3**
25	**Bugam**	**0**	**7.9x10-4**	**1.3x10-7**	**0**	**4.8x10-6**	**0**	**1.6x10-5**	**2.0x10-3**	**0**	**1.9x10-5**	**2.9x10-3**
	Total	**2.3x10-5**	**1.2x10-2**	**9.8x10-6**	**7.3x10-5**	**1.1x10-4**	**3.4x10-5**	**8.4x10-5**	**3.2x10-2**	**1.0x10-4**	**4.5x10-4**	**4.5x10-2**
	Mean	**3.1x10-7**	**9.1x10-4**	**6.9x10-7**	**5.5x10-6**	**8.4x10-6**	**2.6x10-6**	**6.2x10-6**	**2.4x10-3**	**8.0x10-6**	**3.3x10-4**	**3.7x10-3**

DISCUSSION

Human activities and Environmental negligence:
The ignorant behaviour of people towards the environment, haphazard disposal of anthropogenic wastes, use of excess agricultural chemicals, untreated sewage discharges and clay and silty lithology has caused the deterioration of groundwater in Kashmir valley [38,39].

Sources and health impacts of iron and manganese:
Based on previous research it is found that salinity of groundwater is not an issue in the UT of Jammu and Kashmir, however the problem of iron, manganese contamination prevails. Deep aquifers in Kashmir valley have iron and marshy gases contributing to the contamination. Manganese leaches into the groundwater from iron bearing minerals due to presence of manganiferous phases [34,35]. Alluvium based aquifer, limestone and shales contribute to the iron and manganese contamination in the groundwater of Kashmir valley [40].

Manganese and iron are important heavy metals for human body, if consumed in the right or prescribed proportions. However, a slight increase in the consumption of the following elements can cause damage to the human health. According to WHO and EPA, the standard concentration of iron in drinking water is 0.1mg/l. Elevated levels of iron is associated with increasing heart disease, Hyperkeratosis, altered pigmentation and other illnesses like arthritis, endocrine problems, diabetes and also liver disease. Likewise, WHO and EPA, prescribe the standard concentration of manganese in drinking water is 0.05mg/l. Manganese if present excess in water imparts color, odor, or taste to the drinking water [19]. Exceeded values of manganese can cause Alzheimer's disease and various respiratory disorders. High exposure of manganese is also associated neurological problems in children including difficulty in speech, loss of memory and retard behaviour [41].

Lead contamination, causes and health impacts:
Lead is a hazardous component; it is injurious even in minor quantities. WHO and BIS has set the permissible limit of lead as 0.001mg/l in drinking water. Lead is both carcinogenic and non- carcinogenic depending upon the concentration consumption. Exceeded limit of lead consumption causes brain damage, anxiety, central nervous system damage and kidney failure[42]. Lead contamination can occur due to excavation, industrial and recycling activities. Delivery of drinking water through lead pipes can also cause lead contamination. Long term effects to human health like high blood pressure and kidney damage. In addition, it causes miscarriage, premature birth in pregnant ladies. Lead toxicity is more prominent in children causing irreversible health impacts mainly related to brain and nervous system development. The Public health impact of chemicals: knowns and unknowns nearly 50% of 2 million fatality is caused due to known exposure was due to lead in 2019 as is presented in a report furnished by world health organisation in 2021. [19].

Sources and health effects of nickel and cadmium:
Nickle and cadmium are some of the heavy metals that are cancerous to humans and their chronic exposure increases the possibility of cancer [36,43]. The exposure to Nickle contamination causes allergies to skin, Lung Fibrosis and lung cancer and other cancers related to respiratory system. Mechanism behind cancers caused by Nickle is unknown however few research show that the mechanism might be genetic or epigenetic. Ni-enriched insecticides/fertilizers used in the agricultural activities could be the primary cause of contamination in groundwater samples [44,45].

According to WHO and EPA, the standard concentration of Cd in potable water is 0.005 mg/l. Cd is one of the most poisonous metals which is produced as a byproduct of zinc manufacturing. This metal if ingested by humans can lead to a very serious impact to human body.it causes a liver disease known as hepatotoxicity. It also causes various kidney related infections leading to kidney failures [46]. Considering the presence of the above toxic elements in the groundwater of our study area it is necessary for the relevant Government authorities to take effective measures to strengthen the protection from these elements.

CONCLUSION

The findings of the present study have shed light on the distressing reality of heavy metal contamination in the aquifers of four districts in South Kashmir. Both natural and human-induced activities were found to play a significant role in compromising the water quality of the study area. Notably, Pb emerged as the most predominant contaminant, with contamination levels ranking in the order of Pb > Mn > Fe > Zn > Ni > Cu > Cd. The highest health risks were associated with lead and nickel, with lead accounting for 72% of the carcinogenic health risk. It is, therefore, imperative to accord special attention to mitigating the levels of lead, manganese, iron, and nickel in the area's groundwater. The results of this study provide a valuable insight into the extent of heavy metal contamination in groundwater and its adverse impact on human health, thereby enabling researchers to build on this foundation. Furthermore, the transformation of paddy agricultural lands to orchards in Kashmir has augmented the risk of groundwater contamination due to the excessive use of chemicals. It is, therefore, recommended to establish a dedicated groundwater department in Kashmir to analyse and monitor the quality of groundwater and curb its deterioration. It is incumbent on the authorities to prioritize these four elements, raise awareness, and implement measures to mitigate their deleterious impact on health.

Notations

Abbreviation

AAS: Atomic Absorption Spectroscopy

APHA: American Public Health Association

BIS: Bureau of Indian Standards

CALEPA: California Environmental Protection Agency

Cd: Degree of Contamination

EPA: Environment Protection Act

PCA: Principal Component Analysis

CA: Cluster Analysis

IRIS: Integrated Risk Information System

ND: Not Detected

NPI: Nemerow Pollution Index

WHO: World Health Organisation

CGWB: Central Groundwater Board

ACKNOWLEDGEMENTS

The authors extend their appreciation to the Division of Research Centre for Residue and Quality Analysis at Sher-e-Kashmir University of Agriculture Science and Technology, Kashmir, for providing access to the Atomic absorption spectrophotometer and facilitating its use in this study.

DATA AVAILABILITY STATEMENT

The author confirm that the data that supports the findings of this study are available within the article. Raw data that support the finding of this study are available from the corresponding author, upon reasonable request.

CONFLICT OF INTEREST

The author declared no potential conflicts of interest with respect to the research, authorship, and/or publication of this article.

USE OF AI FOR WRITING ASSISTANCE

Not declared.

ETHICS

There are no ethical issues with the publication of this manuscript.

REFERENCES

[1] C. Okello, B. Tomasello, N. Greggio, N. Wambiji, and M. Antonellini, "Impact of population growth and climate change on the freshwater resources of Lamu Island, Kenya," Water (Switzerland), vol. 7, no. 3, pp. 1264–1290, 2015, doi: 10.3390/w7031264.

[2] P. Li, D. Karunanidhi, T. Subramani, and K. Srinivasamoorthy, "Sources and Consequences of Groundwater Contamination," Archives of Environmental Contamination and Toxicology, vol. 80, no. 1, pp. 1–10, 2021, doi: 10.1007/s00244-020-00805-z.

[3] M. Rodell, I. Velicogna, and J. S. Famiglietti, "Satellite-based estimates of groundwater depletion in India," Nature, vol. 460, no. 7258, pp. 999–1002, 2009, doi: 10.1038/nature08238.

[4] A. Rezaei, H. Hassani, S. Hassani, N. Jabbari, S. B. Fard Mousavi, and S. Rezaei, "Evaluation of groundwater quality and heavy metal pollution indices in Bazman basin, southeastern Iran," Groundwater for Sustainable Development, vol. 9, p. 100245, 2019, doi: 10.1016/j.gsd.2019.100245.

[5] F. Alshehri, S. Almadani, A. S. El-Sorogy, E. Alwaqdani, H. J. Alfaifi, and T. Alharbi, "Influence of seawater intrusion and heavy metals contamination on groundwater quality, Red Sea coast, Saudi Arabia," Marine Pollution Bulletin, vol. 165, p. 112094, 2021, doi: 10.1016/j.marpolbul.2021.112094.

[6] G. Dodbiba, J. Ponou, and T. Fujita, "Biosorption of heavy metals," Microbiology for Minerals, Metals, Materials and the Environment, vol. 7, no. 4, pp. 409–426, 2015, doi: 10.4018/978-1-5225-8903-7.ch077.

[7] K. Kumar Yadav et al., "Mechanistic understanding and holistic approach of phytoremediation: A review on application and future prospects," Ecological Engineering, vol. 120, pp. 274–298, 2018, doi: 10.1016/j.ecoleng.2018.05.039.

[8] M. Hasan, M. A. Islam, M. J. Alam, M. Rahman, and M. A. Hasan, "Hydrogeochemical characterization and quality assessment of groundwater resource in Savar — an industrialized zone of Bangladesh," Environmental Monitoring and Assessment, vol. 194, no. 8, 2022, doi: 10.1007/s10661-022-10137-1.

[9] N. J. Pawar and J. B. Pawar, "Intra-annual variability in the heavy metal geochemistry of ground waters from the Deccan basaltic aquifers of India," Environmental Earth Sciences, vol. 75, no. 8, pp. 1–24, 2016, doi: 10.1007/s12665-016-5450-7.

[10] P. Patel, N. J. Raju, B. C. S. R. Reddy, U. Suresh, D. B. Sankar, and T. V. K. Reddy, "Heavy metal contamination in river water and sediments of the Swarnamukhi River Basin, India: risk assessment and environmental implications," Environmental Geochemistry and Health, vol. 40, no. 2, pp. 609–623, 2018, doi: 10.1007/s10653-017-0006-7.

[11] S. I. Abba et al., "Trace element pollution tracking in the complex multi-aquifer groundwater system of Al-Hassa oasis (Saudi Arabia) using spatial, chemometric and index-based techniques," Environmental Research, vol. 249, p. 118320, 2024, doi: 10.1016/j.envres.2024.118320.

[12] P. Sharma, A. Dubey, S. K. C.-I. J. S. E. Res, and U. 2013, "Determination of heavy metals in surface and ground water in an around (Agrang Block) Raipur District, Chhattisgarh, India," International Journal of Scientific and Engineering Research, vol. 4, no. 9, pp. 722–724, 2013, [Online]. Available: https://www.researchgate.net/profile/Amit-Dubey-5/publication/337622173_Determination_of_heavy_metals_in_surface_and_ground_water_in_

an_around_Agrang_block_Raipur_district_Chhattisgarh_India/links/5de5f32f299bf10bc33a8919/Determination-of-heavy-metals-in-

[13] D. A. Ayejoto, J. C. Agbasi, J. C. Egbueri, and S. I. Abba, "Evaluation of oral and dermal health risk exposures of contaminants in groundwater resources for nine age groups in two densely populated districts, Nigeria," Heliyon, vol. 9, no. 4, p. e15483, Apr. 2023, doi: 10.1016/j.heliyon.2023.e15483.

[14] C. C. Aralu, P. A. C. Okoye, H. O. Abugu, K. E. Ochiagha, and J. C. Egbueri, "Evaluating the seasonal variations of risks associated with potentially toxic elements in underground water sources near a dumpsite in Awka, Nigeria," Journal of Hazardous Materials Advances, vol. 15, p. 100440, 2024, doi: 10.1016/j.hazadv.2024.100440.

[15] G. Katalakute, V. Wagh, D. Panaskar, and S. Mukate, "Impact of Drought on Environmental, Agricultural and Socio-economic Status in Maharashtra State, India," Natural Resources and Conservation, vol. 4, no. 3, pp. 35–41, 2016, doi: 10.13189/nrc.2016.040301.

[16] A. Jamal, M. A. Delavar, A. Naderi, N. Nourieh, B. Medi, and A. H. Mahvi, "Distribution and health risk assessment of heavy metals in soil surrounding a lead and zinc smelting plant in Zanjan, Iran," Human and Ecological Risk Assessment, vol. 25, no. 4, pp. 1018–1033, 2019, doi: 10.1080/10807039.2018.1460191.

[17] M. Kaur, A. Kumar, R. Mehra, and I. Kaur, "Quantitative assessment of exposure of heavy metals in groundwater and soil on human health in Reasi district, Jammu and Kashmir," Environmental Geochemistry and Health, vol. 42, no. 1, pp. 77–94, 2020, doi: 10.1007/s10653-019-00294-7.

[18] P. K. Rai, S. S. Lee, M. Zhang, Y. F. Tsang, and K. H. Kim, "Heavy metals in food crops: Health risks, fate, mechanisms, and management," Environment International, vol. 125, pp. 365–385, 2019, doi: 10.1016/j.envint.2019.01.067.

[19] D. A. Ayejoto and J. C. Egbueri, "Human health risk assessment of nitrate and heavy metals in urban groundwater in Southeast Nigeria," Acta Ecologica Sinica, vol. 44, no. 1, pp. 60–72, 2023, doi: 10.1016/j.chnaes.2023.06.008.

[20] K. Sharma, N. Janardhana Raju, N. Singh, and S. Sreekesh, "Heavy metal pollution in groundwater of urban Delhi environs: Pollution indices and health risk assessment," Urban Climate, vol. 45, p. 101233, 2022, doi: 10.1016/j.uclim.2022.101233.

[21] B. Abou Zakhem and R. Hafez, "Heavy metal pollution index for groundwater quality assessment in Damascus Oasis, Syria," Environmental Earth Sciences, vol. 73, no. 10, pp. 6591–6600, 2015, doi: 10.1007/s12665-014-3882-5.

[22] D. Attarde, M. Jain, P. K. Singh, and S. K. Gupta, "Energy-efficient seawater desalination and wastewater treatment using osmotically driven membrane processes," Desalination, vol. 413, pp. 86–100, 2017, doi: 10.1016/j.desal.2017.03.010.

[23] I. Doyi, D. Essumang, G. Gbeddy, S. Dampare, E. Kumassah, and D. Saka, "Spatial distribution, accumulation and human health risk assessment of heavy metals in soil and groundwater of the Tano Basin, Ghana," Ecotoxicology and Environmental Safety, vol. 165, pp. 540–546, 2018, doi: 10.1016/j.ecoenv.2018.09.015.

[24] V. M. Wagh, D. B. Panaskar, S. V. Mukate, S. K. Gaikwad, A. A. Muley, and A. M. Varade, "Health risk assessment of heavy metal contamination in groundwater of Kadava River Basin, Nashik, India," Modeling Earth Systems and Environment, vol. 4, no. 3, pp. 969–980, 2018, doi: 10.1007/s40808-018-0496-z.

[25] S. Nazneen, S. Singh, and N. J. Raju, "Heavy metal fractionation in core sediments and potential biological risk assessment from Chilika lagoon, Odisha state, India," Quaternary International, vol. 507, pp. 370–388, 2019, doi: 10.1016/j.quaint.2018.05.011.

[26] D. Huang, H. Gui, M. Lin, and W. Peng, "Accumulation characteristics and health risk of heavy metals in soil and plant: A case study from huaibei coalfield, China," Fresenius Environmental Bulletin, vol. 25, no. 12, pp. 8246–8254, 2017.

[27] K. Ravindra and S. Mor, "Distribution and health risk assessment of arsenic and selected heavy metals in Groundwater of Chandigarh, India," Environmental Pollution, vol. 250, pp. 820–830, 2019, doi: 10.1016/j.envpol.2019.03.080.

[28] Z. Zhaoyong, J. Abuduwaili, and J. Fengqing, "Heavy metal contamination, sources, and pollution assessment of surface water in the Tianshan Mountains of China," Environmental Monitoring and Assessment, vol. 187, no. 2, pp. 1–13, 2015, doi: 10.1007/s10661-014-4191-x.

[29] Ammar Salman Dawood, "Using of Nemerow's Pollution Index (NPI) for Water Quality Assessment of Some Basrah Marshes, South of Iraq," Journal of University of Babylon, vol. 25, no. 5, pp. 1708–1720, 2017.

[30] Y. Jiang et al., "Source apportionment and health risk assessment of heavy metals in soil for a township in Jiangsu Province, China," Chemosphere, vol. 168, pp. 1658–1668, 2017, doi: 10.1016/j.chemosphere.2016.11.088.

[31] S. Pervez et al., "Sources and health risk assessment of potentially toxic elements in groundwater in the mineral-rich tribal belt of Bastar, Central India," Groundwater for Sustainable Development, vol. 14, p. 100628, 2021, doi: 10.1016/j.gsd.2021.100628.

[32] V. P. Dheeraj, C. S. Singh, A. K. Sonkar, and N. Kishore, "Heavy metal pollution indices estimation and principal component analysis to evaluate the groundwater quality for drinking purposes in coalfield region, India," Sustainable Water Resources Management, vol. 10, no. 1, pp. 1–16, 2024, doi: 10.1007/s40899-023-01013-y.

[33] P. Ravikumar and R. K. Somashekar, "Principal

component analysis and hydrochemical facies characterization to evaluate groundwater quality in Varahi river basin, Karnataka state, India," Applied Water Science, vol. 7, no. 2, pp. 745–755, 2017, doi: 10.1007/s13201-015-0287-x.

[34] R. A. Mir and K. A. Lone, "A Recent Scenario of Groundwater Quality in Kashmir, Northwest Himalaya, India," in Bioremediation and Biotechnology, Vol 4, vol. 4, Cham: Springer, 2020, pp. 39–63. doi: 10.1007/978-3-030-48690-7_3.

[35] W. Xie et al., "Shale gas wastewater characterization: Comprehensive detection, evaluation of valuable metals, and environmental risks of heavy metals and radionuclides," Water Research, vol. 220, p. 118703, 2022, doi: 10.1016/j.watres.2022.118703.

[36] S. Cao et al., "Health risks from the exposure of children to As, Se, Pb and other heavy metals near the largest coking plant in China," Science of the Total Environment, vol. 472, pp. 1001–1009, 2014, doi: 10.1016/j.scitotenv.2013.11.124.

[37] H. K. Alluri, S. R. Ronda, V. S. Settalluri, B. Jayakumar Singh, V. Suryanarayana, and P. Venkateshwar, "Biosorption: An eco-friendly alternative for heavy metal removal," African Journal of Biotechnology, vol. 6, no. 25, pp. 2924–2931, 2007, doi: 10.5897/ajb2007.000-2461.

[38] Y. Wang, C. Xin, S. Yu, Y. Xie, W. Zhang, and R. Fu, "Health Risk Assessment Based on Source Identification of Heavy Metal(loid)s: A Case Study of Surface Water in the Lijiang River, China," Toxics, vol. 10, no. 12, p. 726, 2022, doi: 10.3390/toxics10120726.

[39] G. H. Jeelani, R. A. Shah, and A. Hussain, "Hydrogeochemical assessment of groundwater in Kashmir Valley, India," Journal of Earth System Science, vol. 123, no. 5, pp. 1031–1043, 2014, doi: 10.1007/s12040-014-0446-8.

[40] S. C. Homoncik, A. M. MacDonald, K. V. Heal, B. É. Ó Dochartaigh, and B. T. Ngwenya, "Manganese concentrations in Scottish groundwater," Science of the Total Environment, vol. 408, no. 12, pp. 2467–2473, 2010, doi: 10.1016/j.scitotenv.2010.02.017.

[41] C. Anastassiadis, "Effects of a high-fat diet and an exercise-based rescue on neuroanatomy in the triple-transgenic mouse model of Alzheimer's disease," no. July. 2020. [Online]. Available: https://escholarship.mcgill.ca/concern/theses/ww72bh10r

[42] D. Khan, S. Qayyum, S. Saleem, and F. Khan, "Lead-induced oxidative stress adversely affects health of the occupational workers," Toxicology and Industrial Health, vol. 24, no. 9, pp. 611–618, 2008, doi: 10.1177/0748233708098127.

[43] H. N. Saleh et al., "Carcinogenic and Non-carcinogenic Risk Assessment of Heavy Metals in Groundwater Wells in Neyshabur Plain, Iran," Biological Trace Element Research, vol. 190, no. 1, pp. 251–261, 2019, doi: 10.1007/s12011-018-1516-6.

[44] V. Andreu and E. Gimeno-García, "Total content and extractable fraction of cadmium, cobalt, copper, nickel, lead, and zinc in calcareous orchard soils," Communications in Soil Science and Plant Analysis, vol. 27, no. 13–14, pp. 2633–2648, 1996, doi: 10.1080/00103629609369728.

[45] N. Defarge, J. Spiroux de Vendômois, and G. E. Séralini, "Toxicity of formulants and heavy metals in glyphosate-based herbicides and other pesticides," Toxicology Reports, vol. 5, pp. 156–163, 2018, doi: 10.1016/j.toxrep.2017.12.025.

[46] S. Punitha and G. Selvarajan, "Analysis of Heavy Metals Concentration in Ground Water From Kilvelur Taluk, Nagapattinam District, Tamil Nadu, India," Journal of Chemistry and Chemical Sciences, vol. 8, no. 3, pp. 538–547, 2018, doi: 10.29055/jccs/608.

Environmental Research and Technology
https://dergipark.org.tr/en/pub/ert
DOI: https://10.35208/ert.1469199

Environmental Research & Technology

Research Article

Assessment of drainage capacity of a surface drain in Rajshahi, Bangladesh

Sribash DAS*[1], Meher Nigar JERIN[1]

[1] *Rajshahi University of Engineering & Technology, Department of Civil Engineering, Rajshahi, Bangladesh*

ARTICLE INFO

Article history
Received: 29 Apr 2024
Revised: 08 Aug 2024
Accepted: 28 Aug 2024

Key words:
Surface drains; drainage capacity; sludge depth; clear space

ABSTRACT

The drainage capacity of a community is essential for promoting environmental resilience, effective water management, and fostering a healthy urban lifestyle. The surface drains in Rajshahi City receive a mix of waste, including sanitary wastewater, stormwater runoff, and solid waste from roadsides and households. To improve the drainage facilities of Rajshahi, some new drains have been constructed. This study considered a recently constructed drain in the Rajshahi City Corporation (RCC), running from Talaimari to Chowddopai. The primary objective of this study is to assess the drainage capacity of this drain during both dry and monsoon seasons, ensuring its capability to contain the generated waste. Additionally, the investigation encompasses observing the sludge depth, and clear space of the drain. A field survey was conducted, employing a measuring rod and scale to precisely measure the depth, width, and sludge accumulation. The results show that the total volume of the drainage system is 117670 ft^3, while the total volume of solid deposition is 6287.60 ft^3. Solid deposition occupies 95% of the entire drainage path, leaving 5% as clear space. The total solid deposition volume represents approximately 5.34% of the total volume of the drainage system (6287.60 ft^3 of 117670 ft^3). This study revealed that during typical rainfall intensity in Rajshahi City, the portions of drains from Talaimari to Octroimor and from Rajshahi University main gate to Chowddopai have sufficient open space to prevent water overflow, but the capacity of the drains in the portion between Kajla and Rajshahi University main gate is inadequate.

Cite this article as: Das S, Jerin MN. Assessment of drainage capacity of a surface drain in Rajshahi, Bangladesh. Environ Res Tec 2025;8(2) 281-287.

INTRODUCTION

Efficient drainage infrastructure is pivotal for mitigating the adverse impacts of heavy rainfall and preventing flooding, which can endanger lives, disrupt livelihoods, and cause extensive damage to property and infrastructure. Water, in any form – groundwater, surface water, or rain runoff – is a major contributor to road failure and damage [1]. So, a drainage system that includes the pavement and the water handling system must be properly designed, built, and maintained [2]. The purpose of drainage facilities is to ensure the timely removal of surface water runoff and sewage from large, impermeable areas [3]. Different drainage systems have varying effects on drainage capacity. Sustainable drainage systems (SuDS) improve retention and management of runoff quantities and flow rates by concentrating on slower processes like evapotranspiration and infiltration [4]. Runoff rates are impacted differentially by different types of SuDS; vertical construction in apartments results in reduced peak runoff. Runoff rates are reduced more by SuDS on existing infrastructure than on undeveloped land [5]. In comparison to soak ways and infiltration trenches, the capacity down pipe SuDS tech-

***Corresponding author.**
*E-mail address: sribash275@gmail.com

This is an open access article under the CC BY-NC license (http://creativecommons.org/licenses/by-nc/4.0/).

nique—which includes ponds and filter strips—can greatly increase drainage capacity in metropolitan settings, fostering effective water management and cost-effectiveness [6]. With a high starting velocity and minimal energy consumption, the vertical drainage capacity of an advanced electro-osmotic drainage board may effectively enhance drainage in extremely soft clayey ground [7]. The availability of SuDS and surface cover types can have an impact on peak runoff rates and total runoff volumes, which in turn can affect a landscape's overall drainage capacity [8]. In low-gradient landscapes, different drainage systems, such as seepage erosion and overland flow, affect drainage capacity by causing different channel development processes depending on substrate, rainfall, and relief conditions [9]. The drainage density and shape of hillslopes are influenced by several processes, including diffusive-advective transition, erosion thresholds, and land sliding. These factors affect the landscape drainage capacity, which is contingent upon environmental parameters such as rainfall and relief [10]. various drainage methods affect drainage capacity by improving soil protection, generating a groundwater reservoir, and reducing the consequences of climate change like floods and droughts [11]. The frequency and amount of stormwater flows will grow in the future, posing challenges for drainage systems [12]. Therefore, it is now urgently needed in the industry to accurately measure the drainage system's service performance and simulate its operational status [13].

Using the best drainage engineering principles, an effective drainage plan must be established to understand the drainage issues that Bangladeshi cities face [14]. Rajshahi, a prominent northern Bangladeshi city, established in 1876 as one of the first Municipalities, transitioned to Rajshahi Pourashava and finally to RCC in 1987 [15]. According to the Drainage Master Plan, Rajshahi City features primary, secondary, and tertiary drains, with 65% of tertiary, 14% of secondary, and 19% of primary drains in good structural condition. The city's management is organized into 30 wards, overseeing 132.27 km of various drain categories, originally designed to cater to the core area between the Railway line and the river Padma embankment, where the countryside elevations range from 16.75 to 18.25m[16]. The drainage pattern of Rajshahi City is still filthy despite significant yearly budgets for development and reform; this is because insufficient planning led to a failure to meet demand [17].Rajshahi City Corporation has recently taken some projects to increase surface drainage facilities in the city. Such a new drainage network has been constructed recently, in 2023, from Talaimari to Chowddopai.

A recent work on the characteristics of drainage liquid wastes and deposited drainage solids of the old drains of Rajshahi City has been conducted [18]. Now, our research focus is on these newly constructed drains, finding the physical properties of the drains and their capacity along with some other factors about this drain.

MATERIALS AND METHODS

Study Area

The study area Rajshahi, as shown in Fig.1, is situated between latitudes 24°21' and 24°25' N and longitudes 88°32' and 88°40' E. The Rajshahi City Corporation, the location of study, has given careful consideration to the city's drainage system to maintain a clean city. There are a lot of outdated drains, a lot of recently constructed new drains, and additional drain construction is ongoing. Among them, a new drainage network that begins from Talaimari and finishes at the Chowddopai primary drain has been built in front of the Rajshahi University of Engineering & Technology (RUET). In Fig. 2, the red, pink, and blue color is the path of drainage line and sky color border is the border of RUET.

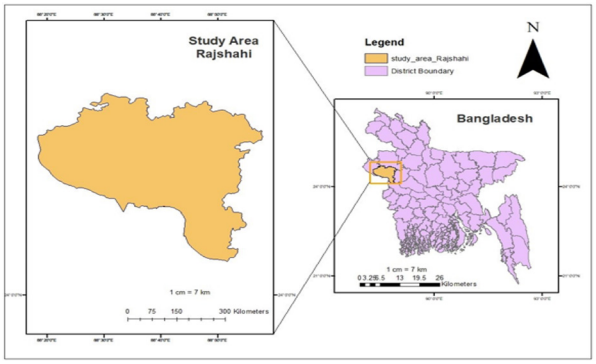




Figure 2. Drainage Network from Talaimari to Chowddopai in Google

Fig.2 shows the drain's path. We sought to determine its dimensions and capacity—that is, the amount of solid material that has already been deposited and the amount of space that may be used to convey trash to the principal drain. The image of the study area from Google Earth.

Materials

A measuring tape with a steel rod and a bamboo were used for measuring the dimension of drain shown in Fig 3 at different sections and thickness of deposited sludge at the bottom of the drain as well as the depth of flowing wastewater. The software Google Earth Pro and ArcGIS were used for preparing the route of drain and locations of data collection. The acquired data was analyzed by Microsoft Excel.



Figure 3. Materials for measuring dimension

Method

After selecting the study area and collecting materials, some points were selected for conducting a field survey. From the starting point Talaimari, points were selected at intervals of 100 meters to the endpoint Chowddopai. In Fig 4, the pins were placed in Google Earth Pro which indicates the points that were selected to conduct the field survey. The distance was approximately 2.8 km, so 28 points were selected.



Figure 4. Picture of the study area (from Google Earth Pro)

For a better understanding of the work, a drainage map was made in ArcGIS software shown in Fig 5.

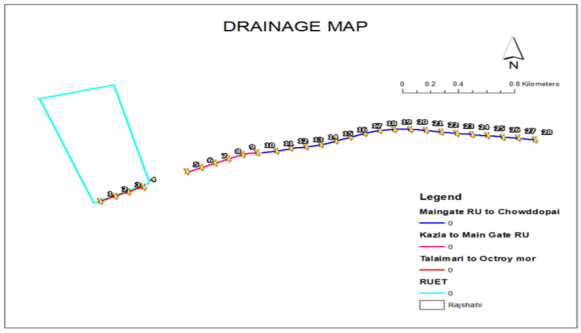


Figure 5. Data collection points

During the field survey, A rod was inserted into the bottom of the drain. After that, the rod was leveled at the opening point of the drain, and took measurements. Thus, the total depth of the drain was ascertained. Proceed in the same manner, but this time, the rod was inserted into the drain at a depth where the solid deposit's surface was still visible. Then, the rod was pointed again and the measurement was taken. Thus, the clear space of the drain was measured. After that, with the measuring tape, the width of the drain was determined. After completion of the data collection, the data was plotted in Excel and the physical characteristics of the drain has been determined.

The capacity of the drain is determined based on rainfall data of the Rajshahi City. If the clear space of the drain is available enough to hold the rainfall water, then it is considered as "Adequate" to hold rain water. In either way, the drain is termed as "Inadequate".

Equations

The actual cross-sectional area using the actual depth of the drain using the equation

A1 =b*D.....(i); here, b=Width of the drain, and D= depth of the drain

The clear cross-section of the drain,

A2 = b*d.....(ii); here, d=depth of clear space.

The Solid Deposition area,

A= A1-A2.....(iii)

Solid Deposition depth, d= A/b

The total capacity of the drain,

V1= A1*L.....(iv); here, L= Total length of drain =2.8km (approx.)

The available capacity of the drain V2= A2*L.....(v)

Rainfall Calculation:

Total Rainfall volume,

V = h * La * ba.....(vi); where, h = Rainfall depth, La = Length of catchment area and, ba= Average width of the catchment area

If, Clear space volume > Total Rainfall volume: Adequate

If, Clear space volume < total Rainfall volume: Inadequate

FINDINGS AND DISCUSSIONS

Data Collection

A total of 28 points were selected as data points from the Talaimari to the Chowddopai. Four points were selected from the Talaimari to the Octroimor. No drain was found from the Octroimor to the Kajla. From the Kazla gate to the Rajshahi University (RU) main gate, five points were selected while from the RU main gate to the Chowddopai total of 19 points were selected. All the collected data are presented in Table 1.

Table 1. Drain data

Location	Actual width	Actual Depth	Actual cross-sectional area (ft2)	Depth above solid	Area above Solid Waste (ft2)	Solid Deposition (ft2)
Talaimari to Octroimor	4'-0"	4'-7"	18.33	4'-5"	17.67	0.66
				4'-6"	18	0.33
				4'-7"	18.33	0
				4'-5"	17.67	0.66
Kazla Gate to RU Main Gate	1'-9"	2'-3"	3.94	2'-2.5"	3.86	0.08
				2'-0"	3.5	0.44
				2'-2.7"	3.89	0.05
				2'-2.9"	3.92	0.02
				2'-3"	3.94	0
RU Main Gate to Chowd-dopai	4'-0"	4'-0"	16	4'-0"	16	0
				3'-9"	15	1
				3'-9"	15	1
				3'-9"	15	1
				3'-8"	14.67	1.33
				3'-11"	15.67	0.33
				3'-10"	15.33	0.67
				3'-7"	14.33	1.67
				3'-10"	15.33	0.67
				3'-10"	15.33	0.67
				3'-9"	15	1
				3'-11.5"	15.83	0.17
				3'-7"	14.33	1.67
				3'-8"	14.67	1.33
				3'-9.5"	15.17	1.17
				3'-8.75"	14.92	1.08
				3'-7"	14.33	1.67
				3'-8"	14.67	1.33
				3'-10"	15.33	0.67
Chowddopai Primary drain	17'-0"	Actual Depth 10'-0"				

Capacity of the Drain during Dry Season

Analysis of the capacity of the drain during the dry season is presented in Table 2.

Table 2. Analysis of the capacity of drain during dry season

Zone	Total length (ft)	Total volume (ft3)	Solid deposition (sq ft)	The volume of deposition in this zone (ft3)	Volume of clear space (ft3)
Talaimari to Octroimor	984	18036.76	0.4125	405.9	17630.86
Kazla gate to RU main gate	1312	5169.28	0.118	154.82	5014.46
RU Main gate to Chowddopai	5904	94464	0.97	5726.88	88737.12
Overall Analysis	8200	117670	1.5	6287.60	111382.44

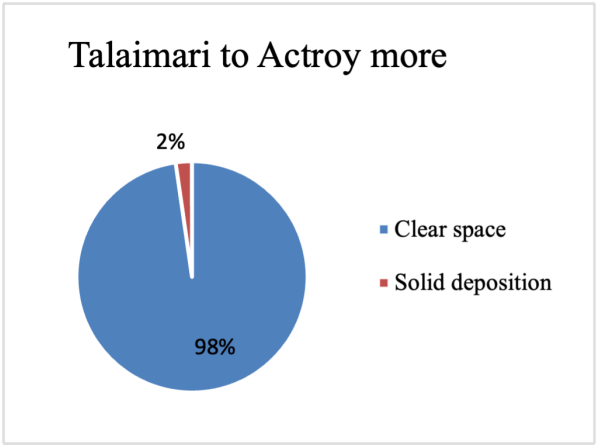


Figure 6. Clear space and solid deposition in Talaimari to Octroimor

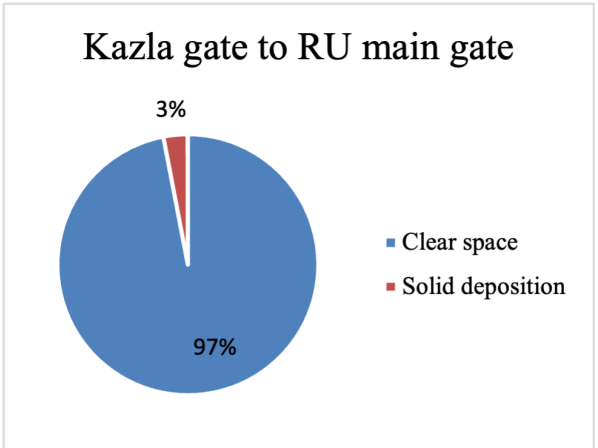


Figure 7. Clear space and solid deposition in Kazla gate to RU main gate

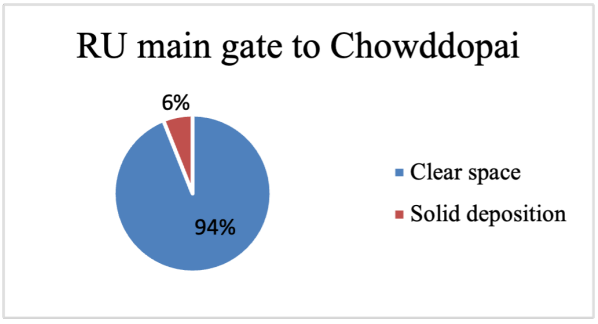


Figure 8. Clear space and solid deposition in RU main gate to Chowddopai.

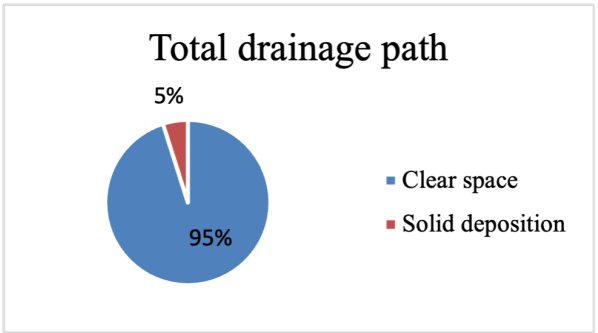


Figure 9. Clear space and solid deposition of the entire drainage path

A comparison between the volume of the clear space and the volume of the solid deposition in Talaimari to Octroimor is shown in Fig 6. A comparison between the volume of the clear space and the volume of the solid deposition in Kazla gate to RU main gate is shown in Fig 7. A comparison between the volume of the clear space and the volume of the solid deposition in RU main gate to Chowddopai is shown in Fig 8. A comparison between the total volume of the clear space and the total volume of the solid deposition in the entire drainage system is shown in Fig 9.

Capacity of the Drain during Monsoon

Rainfall intensity According the to Bangladesh Metrological Department, the average rainfall of Rajshahi is 3.74 inches (0.31 ft). The drain passes along the road. So, for the calculation of rainwater volume, the length and width of the road have been taken using Google Earth Pro. Analysis of the capacity of the drain during the monsoon season is presented in Table 3.

Table 3. Analysis of the capacity of drain during monsoon season

Zone	Total length (ft)	Average width	Solid deposition (sq ft)	The volume of deposition in this zone (ft3)	Volume of clear space (ft3)	Adequate/ Inadequate
Talaimari to Octroimor	984			984*33.3*0.31 =10157	17630.86	Total rainfall volume < volume of clear space of drain; Adequate
Kazla gate to RU main gate	1312	66.2/2 =33.3	0.31	1312*33.3*0.31 = 13543.77	5014.46	Total rainfall volume > volume of clear space of drain; Inadequate
RU Main gate to Chowddopai	5904			5904*33.1*0.31 = 60947	88737.12	Total rainfall volume < volume of clear space of drain; Adequate

DISCUSSION

The area of solid deposition in the drain varies from 0 to 1.67 square feet. Maximum solid deposition was found between the RU main gate and Chowddopai while minimum solid deposition was found in the Kazla gate to the RU main gate. In Chowddopai, the primary drain is rooted in which has a 10 ft actual depth and 17 ft actual width. The drain portion from Talaimari to Octroy mor and the RU main gate to Chowddopai is adequate for the average rainfall of Rajshahi but From Kazla to RU main gate portion of the drain is inadequate. So, this portion of the drain should be reconstructed. A map was created in ArcGIS providing all the data collected from field surveys.

This drainage path is very promising as it has adequate width and depth as well as solid deposition is also acceptable. It is capable enough to handle rainwater runoff, road safety, property protection, and urban planning. For typical rainfall intensity in Rajshahi City, the drain between Talaimari and Octroi more and between RU main gate and Chowddopai has enough open space to prevent the spilling of water, however, the drain between Kazla and Ru Main Gate does not.

CONCLUSIONS

In this paper, one of the newly constructed surface drains has been considered. The depth of sludge deposition, clear space, and drainage capacity of the Talaimari to Chowddopai drainage network in RCC is calculated by conducting a field survey. As it is a new drain, the capacity of the drain is in satisfactory condition. The sludge accumulation is quite low as it has a low amount of solid deposition. To keep good performance of the drain, sludge should be kept minimum. For this reason, the drain should be cleaned at regular intervals, so sludge accumulation can be under control. Solid deposition is comparatively more in RU's main gate to the Chowddopai area. Still, it is capable of flowing rainwater. But the dimension of the drain from Kazla to RU main gate is less. So, it is inadequate for the average rainfall of Rajshahi.

ACKNOWLEDGEMENTS

The authors thank the Department of Civil Engineering's academic staff for their efforts in contributing to the research.

DATA AVAILABILITY STATEMENT

The author confirm that the data that supports the findings of this study are available within the article. Raw data that support the finding of this study are available from the corresponding author, upon reasonable request.

CONFLICT OF INTEREST

The author declared no potential conflicts of interest with respect to the research, authorship, and/or publication of this article.

USE OF AI FOR WRITING ASSISTANCE

Not declared.

ETHICS

There are no ethical issues with the publication of this manuscript.

REFERENCES

[1] M. M. E. Zumrawi, 'International Journal of Multidisciplinary and Scientific Emerging Research The Impacts of Poor Drainage on Road Performance in Khartoum', 2014. [Online]. Available: http://www.ijmser.com/

[2] G. Kebede Warati, 'Assessment of the Effect of Urban Road Surface Drainage: A Case Study at Ginjo Guduru Kebele of Jimma Town', International Journal of Science, Technology and Society, vol. 3, no. 4, p. 194, 2015, doi: 10.11648/j.ijsts.20150304.20.

[3] C. O. Owuama, 'Sustainable Drainage System for Road Networking', International Journal of Innovation, Management and Technology, vol. 5, no. 2, 2014, doi: 10.7763/ijimt.2014.v5.491.

[4] V. Stovin, R. Quinn, and C. Rouge, 'Study of Continuous Simulation Supporting Multiple Design Criteria for Sustainable Drainage Systems', Journal of Sustainable Water in the Built Environment, vol. 9, no. 3, Aug. 2023, doi: 10.1061/jswbay.sweng-495.

[5] C. Chapman and J. W. Hall, 'The influence of built form and area on the performance of sustainable drainage systems (Suds)', Future Cities and Environment, vol. 7, 2021, doi: 10.5334/fce.112.

[6] K. Frost and M. Scholz, 'Capacity Down Pipe: Comparisons with Other Sustainable Drainage Systems', Science Discovery, vol. 3, no. 1, pp. 7–17, 2015, doi: 10.11648/j.sd.s.2015030201.

[7] Y. Shen, Y. de Li, W. jun Huang, H. dong Xu, and P. fei Hu, 'Vertical drainage capacity of new electrical drainage board on improvement of super soft clayey ground', Journal of Central South University, vol. 22, no. 10, pp. 4027–4034, Oct. 2015, doi: 10.1007/s11771-015-2946-3.

[8] J. Pablo, R. Sánchez, J. Hathaway, E. A. Barragán, C. Chapman, and J. W. Hall, 'The potential for sustainable drainage systems (SuDS) in a regional urbanization project', 2030.

[9] B. G. Sockness and K. B. Gran, 'An experimental study of drainage network development by surface and subsurface flow in low-gradient landscapes', Earth Surface Dynamics, vol. 10, no. 3, pp. 581–603, Jun. 2022, doi: 10.5194/esurf-10-581-2022.

[10] G. E. Tucker and R. L. Bras, 'Hillslope processes, drainage density, and landscape morphology', Water Resources Research, vol. 34, no. 10, pp. 2751–2764, 1998, doi: 10.1029/98WR01474.

[11] J. Pešková and J. Štibinger, 'Computation method of the drainage retention capacity of soil layers with a subsurface pipe drainage system', Soil and Water Research, vol. 10, no. 1, pp. 24–31, 2015, doi: 10.17221/119/2013-SWR.

[12] Q. Zhou, T. E. Panduro, B. J. Thorsen, and K. Arnbjerg-Nielsen, 'Adaption to extreme rainfall with open urban drainage system: An integrated hydrological cost-benefit analysis', Environmental Management, vol. 51, no. 3, pp. 586–601, Mar. 2013, doi: 10.1007/s00267-012-0010-8.

[13] H. Q. Peng, Y. Liu, H. W. Wang, and L. M. Ma, 'Assessment of the service performance of drainage system and transformation of pipeline network based on urban combined sewer system model', Environmental Science and Pollution Research, vol. 22, no. 20, pp. 15712–15721, Oct. 2015, doi: 10.1007/s11356-015-4707-0.

[14] M. A. Ashraf and M. S. A. Chowdhury, 'Drainage Planning in the Cities of Bangladesh: Case Study of Drainage and Water Logging in Chaktai Commercial area, Chittagong', Journal of Bangladesh Institute of Planners, vol. 2, pp. 49–60, Jan. 1970, doi: 10.3329/jbip.v2i0.9556.

[15] I. Faridatul and S. Jahan, 'People's Perception Regarding the Development of Community Facilities: A Case Study of Rajshahi City Corporation', 2014.

[16] M. S. Islam, S. M. Islam, and A. M. Islam, 'Assessment of efficacy of drainage system in Rajshahi City Corporation, Bangladesh', Advances in Environmental Research, vol. 10, no. 2, pp. 105–116, 2021, doi: 10.12989/aer.2021.10.2.105.

[17] M.M.M.N. Ullah, M.S. Hossain, M. Shahiduzaman, M.S. Islam, M.Z. Islam, M.S.R. Choudhary, "A study on some aspects of drainage system in Rajshahi city, Bangladesh', Scientific Journal of Environmental Sciences, no. 2, pp. 118–124, 2013, doi: 10.14196/sjes.v2i6.1005.

[18] N. Md. Bari, A. Chowdhury, J. Islam, M.M. Alam, M. Munni, S. Hasan, M. Shahorian, M.K.A. Limon, 'Study on the characteristics of drainage liquid wastes and diposited drainage solids of Rajshahi City', 2024.

Environmental Research and Technology
https://dergipark.org.tr/en/pub/ert
DOI: https://10.35208/ert.1491915

Research Article

Evaluation of adsorption isotherms and kinetics of chloride ion in water using biochar derived from locally available agro-waste

Mohd ISHAQ[1],*, RC CHHIPA[1], Anupama SHARMA[1], Gh ALİ[2]

[1]*Department of Chemistry, Suresh Gyan Vihar University Jaipur, 302017, Rajasthan, India*
[2]*Department of Chemistry, Campus Kargil, University of Ladakh, 194103, India*

ARTICLE INFO

Article history
Received: 29 May 2024
Revised: 25 Aug 2024
Accepted: 28 Aug 2024

Key words:
Adsorption; chloride; isotherm; kinetics; modified biochar

ABSTRACT

The uses of agricultural byproduct solid wastes to develop low cost sorbents are advantageous and promising for the removal of water contaminants. It serves the purposes of both environmental remediation and appropriate management of agricultural waste generated during agricultural processing. In this study, locally available apricot seed shell and Salix Alba leaves were utilized as agro-waste for the preparation of adsorbents. The biochar was prepared at 300-400°C via pyrolysis and 80 mesh particle sizes were modified by 1N HCl. The unmodified and acid modified local Salix Alba leaves and Apricot seed shell biochar were used to study the adsorption of chloride ion in water, which can damage appliances of industries and also poses health issues at elevated concentration. Adsorption kinetics including pseudo 1st and 2nd order and equilibrium studies including Langmuir and Freundlich isotherm were conducted at pH 7. The adsorption efficiency of modified biochar was much higher than the unmodified biochar due to induce surface positive charge. The Langmuir maximum adsorption of modified Salix Alba leaves sorbent was found to 22.98 mg/g, while modified Apricot seed shell biochar was found to 25.83 mg/g. The experimental data were simulated and applied to fit adsorption isotherm and kinetics models and found a better compliance with Langmuir isotherm model and pseudo 2nd order kinetics model. The RL value and KL value indicated favorable sorption and enhanced sorption affinity. The kinetics also indicated that there is interaction between adsorbate and adsorbent active sites and the result indicated a significant potential of both adsorbents for the removal of chloride ion.

Cite this article as: Ishaq M, Chhipa RC, Sharma A, Ali G. Evaluation of adsorption isotherms and kinetics of chloride ion in water using biochar derived from locally available agro-waste. Environ Res Tec 2025;8(2) 288-296.

INTRODUCTION

Adsorption is the most common and effective separation technique used in the water and wastewater treatment [1-3]. The commercially available activated carbon (AC) is commonly uses in the water and wastewater treatment methods due to its large porous structure, huge surface area, high capacity, and hydrophobic properties, however, commercially activated carbon is expensive and has major regeneration concerns [1, 2, 4]. Therefore there are a significant number of reports are available on the development and uses of organic, inorganic, nanomaterial adsorbents and ion exchange resins for wastewater treatment. One of the known materials is biochar has regarded six times less expensive than commercially available activated carbon [5]. However, modern research has concentrated on using materials of biological origin, particularly agricultural waste, to remove contaminants due to many beneficial reasons. Agricultural byprod-

***Corresponding author.**
*E-mail address: isackar440@gmail.com

This is an open access article under the CC BY-NC license (http://creativecommons.org/licenses/by-nc/4.0/).

uct solid wastes, such as fruit and vegetable wastes, leaves, seeds, tree waste, fibers, fruit peels, dates, sawdust, bark, etc., are being utilizing for the development of an effective adsorbent alternative to costly activated carbon and other inorganic and organic materials [6, 7]. The use of agricultural wastes in water and wastewater treatment serves the purpose of both environmental remediation and suitable management of agricultural waste generated during processing [8, 9]. However a large number of studies have reported that the adsorption capacity of raw agricultural waste materials for pollutants is rather lower, due to their inherent chemical composition and structure [9, 10]. As a result, chemical and physical surface changes are done to improve their adsorption properties. Chemical surface modification approaches include protonation, amine grafting, metals or metal oxides impregnation and surfactants, whereas physical modification involves heating materials to remove impurities and volatile matter [9-13].

Biochar, an inexpensive carbonaceous porous material obtained by heating agricultural wastes without oxygen, is an effective sorbent for the removal of a variety of pollutants, due to its improved adsorbing properties [4, 5, 7, 12]. However, commercial anionic ion exchange resins such as Indion NSSR, Amberlite IRN-78, Amberlite IRA 400, Imac HP555, and Purolite A100 are available but are more expensive [14]. A significant number of studies available on the use of biochar and activated biochar for the treatment of cations, metals and dyes. Rice husk activated biochar was used to remove ranitidine [2]. The biochar of rice husks treated with HCl and NaOH increases the surface area and used to remove Mn (II), Se (II), and Fe (II) [5]. Banana pith, an agricultural waste, was utilized to make biochar, which was used to remove As (V) [6]. The biochar of bagasse, bamboo, poplar wood and wheat bran impregnated with Fe and Ca have 12-70 times higher adsorption efficiency for phosphate ion than unmodified biochar [11]. Similarly, biochar from pecan shells, pistachio shells and wood sawdust treated with KOH and FeCl3 were used to remove phenol [12]. The biochar of Conocarpus green waste removed 90% of NO3- ion on impregnation with magnesium and iron oxides [13]. Apricot shell biochar has high adsorption capacity for atrazine [15]. Similarly biochar obtained from reed have enhanced adsorption capacity toward pentachlorophenol by six-fold on treatment with 1 M HCl [16]. Similarly, NaOH impregnation of wheat straw biochar enhances adsorption capacity of toluene by three-fold [17]. The biochar derived from various agricultural wastes have been employed for adsorption of chloride ions from aqueous solution by many researchers. The non- modified biochar and chemically modified biochar derived from date palms were utilized to removal free residual chlorine from aqueous solution [18]. Similarly biochar derived from malt spent rootlets, walnut shells, and kernels of apricot, olive, carob and grape were also utilized for the removal of free and total chlorine from water [19]. Though the presence of chloride ions in water has no significant health issues, but an excess of chloride ions enhances the hardness, conductivity and saltiness of the water, which can damages appliances. The present study work employed biochar and acid activated biochar derived from locally available agricultural wastes including Salix alba leaves and apricot seed shell for the removal of chloride ions from aqueous solution using batch adsorption model.

Availability of Chloride in Water

Chloride in water increases electrical conductivity and corrosivity of water and can damage water pipelines, industrial appliances and would raise metal ions level in water. Chloride ions in water are associated with sodium, potassium, and calcium. The presence of chloride in groundwater can be caused through weathering of rock, salt spray deposition, wastewater, inorganic fertilizer, septic tanks, and intrusion of ocean water into the groundwater sources in coastal areas [8, 20]. The usage of salt for de-icing the roads is one of the most common anthropogenic sources of chloride ions in water [20]. Chloride levels in drinking water greater than 250 mg/l are considered undesirable according to regulation [20].

Local agricultural Waste

Many species of Salix grows naturally in the cold, arid region of Ladakh in the Trans-Himalaya. Salix Alba (SA), often known as white willow, is a deciduous tree whose leaves are utilized mainly as cattle feed in the region. Similarly, Ladakh is the largest Apricot producing state in India, producing 15,789 tonnes of Apricot annually [21]. A significant volume of seed shell is producing during the processing. The Apricot shell shells (ASS) are hard material not been use in any form, other than being burned in the local heating system to warm rooms during winter. Figure 1 depicts the Salix leaves and see shell.



Figure 1. a) Salix Alba leaves b) Apricot seed shell

The main purposes of this study were to: i) evaluate the adsorption removal of anion (Cl^- ion) from synthetic water using raw Salix alba leaves biochar (SALB) and acid activated Salix Alba leaves biochar (ASALB), (ii) evaluate the adsorption removal of anion (Cl^- ion) using Apricot seed shell biochar (ASSB) and acid activated Apricot seed shell biochar (AASSB), (iii) study the adsorption kinetics and isotherms.

MATERIALS AND METHODS

All the chemicals and reagents of analytical grade were purchased from Biological museum , Agra, India and were used. Synthetic water was prepared by dissolving Potassium Chloride (KCl) in distil water to obtain 100 mg/l concentration. 0.05N KCrO4 and 0.01N AgNO3 solution were used in

the analysis. Fresh Salix Alba leaves and Apricot seed shell were were collected from Kargil, UT Ladakh. Muffle furnace (model- MSW 25) and Bruker Alpha II- FTIR spectrometer were used as instrumentation.

Preparation of biochar

The fresh leaves were washed with tape water and then with deionized water to remove dirt. The leaves were cut in to small pieces and then dried in an oven at 100 oC for 24 hour. Similarly Apricot seed shells were collected from the oil processing unit at Hardas, Kargil of UT Ladakh and were washed with water and deionized water to remove dirt. 300g of leaves and seed shells were placed in the reactor of muffle furnace (model- MSW 251). The biochar of the materials were prepared by subjecting the material to pyrolysis at a temperature of 300°C, 330°C, 350°C, 370°C and 400°C with a continuous flow of nitrogen gas at the flow rate of 100-200 ml/min. The gases formed during pyrolysis were bubbled in water. The temperature of the reactor was adjusted by using the temperature knob. After 5 hour the material were allowed to cool down and then powdered the materials to get a mesh size of 80. The yield of biochar was found higher at 370°C and get decreased with the temperature rise. A systematic representation for processing of biochar is depicted in figure 2 and 3.



Figure 2. Apricot seed shell biochar



Figure 3. Salix Alba leaves biochar

10g of Salix Alba leaves biochar (SALB) and Apricot seed shell biochar (ASSB) were soaked in 1N HCl solution for 3hr and separated. The adsorbents were washed with deionized water till pH become neutral and then dried in oven at 60 0C.

Characterization with Zero point of charge (ZPC)

A base electrolyte of 0.01 M NaCl was taken in a series of volumetric flasks and adjusted the pH of solution with pH range (2-10) by using 0.1N HCl and 0.1N NaOH solution. 1g of adsorbents were added in 50 ml of each flask and kept at the shaker for 8h and recorded the pH using pH meter as pHf. A plot of pH (pHf- pHi) against pHi was plotted and at zero ΔpH, the ZPC of the adsorbents were recorded.

Fourier transform infrared spectrometry (FTIR)

The surface functional groups and the effect of chloride on the surface functional groups of the adsorbents were characterized by using Bruker Alpha II- FTIR spectrometer in the wavelength of 4000-500 cm^{-1}.

Chloride analysis

Mohr's method of chloride determination was used [22, 23]. The volumetric method involves the titration of chloride solution against standard solution of silver nitrate (AgNO3) in the presence of potassium chromate as indicator. During the titration a white precipitate of silver chloride (AgCl) was formed and at the equivalence point a red brown color of silver chromate appeared.

$$Cl^- + Ag^+ \rightleftharpoons AgCl\ (s)$$

$$2Ag^+ + CrO_4^{2-} \rightleftharpoons Ag_2CrO_4(s)$$

The analysis were carried at neutral pH, as below pH 6 chromate get converted to dichromate and above pH 8 silver get converted to silver hydroxide.

Adsorption kinetics

The adsorption kinetics of unmodified and acid modified biochar were conducted by adding 1.0 g adsorbent in to 100 ml of 100 mg/l chloride solution at neutral pH and shaked at different time intervals of 10, 30, 50, 70, 90, 110, 130, 150, 170, 190 minutes. At each time intervals the biochar was separated and amount of chloride ion in the filtrate was determined as per the procedure described in chloride analysis section. The amount of chloride adsorbed per gram of adsorbent (mg/g) and removal percentage were calculated using the following formula.

$$Q_t = \frac{(C_i - C_t) * V}{m}$$

$$\text{Removal (\%)} = \frac{(C_i - C_t)}{C_i} * 100$$

Qe: amount of chloride adsorbed per gram of adsorbent at equilibrium (mg/g).

Ce: equilibrium concentration of chloride ion (mg/l).

Ci: initial Concentration of Chloride ion (mg/l).

The adsorptions of nitrate were fitted to Langmuir isotherm and Freundlich isotherm models using the equations.

Langmuir model: $$\frac{C_e}{Q_e} = \frac{1}{Q_{max}\, K_L} + \frac{1}{Q_{max}} * C_e$$

Qmax: maximum amount of chloride ion adsorbed (mg/g).

KL: Langmuir constant (L/mg).

RL: is a dimensionless quantity calculated from KL by the equation, Rl = 1/1+Kl Ci) . The parameters of the Langmuir isotherm with RL values 0< RL <1, favours and improved adsorption [30].

Freundlich model: LogQe = log Kf + 1/nlogCe

Kf and n are Freundlich constants (mg/g) (L/mg) 1/n).

RESULT AND DISCUSSION

Characterization with Zero point of Charge (ZPC)

The adsorption of charged ions depends on the zero point of charge of the adsorbent. When pH of the solution is greater than zero point of charge (ZPC), the surface of the adsorbent becomes negatively charged and favors the adsorption of cations, and vice versa [24]. Therefore pH of the solution plays an important role in the adsorption. The zero point charge of unmodified and acid modified Salix alba leaves biochar were recorded to 4.6 and 8.4, indicating modified sorbent could better adsorb negatively charged species up to pH 8.4. Similarly the ZPC of pure and acid modified apricot seed shell biochar were shown to shift from 5.8 to 8.9. Therefore the acid modified biochar shows better adsorption efficiency for negatively charged ions than unmodified biochar at neutral pH.

Fourier transform infrared spectrometry (FTIR)

The IR spectra of Apricot seed shell biochar (ASSB), acid treated, and chloride loaded are shown in figure 4. A prominent peak around 1580-1700 cm-1 indicated the presence of many functonal groups. The peak around 1636 cm−1 is ascribed to (C=O) stretching vibration of aromatic carbonyl group [2]. The peaks around 1690-1700 cm^{-1} indicates stretching vibration of amide group and 1540–1640 cm^{-1} corresponds the existence of carbonyl groups (C=O) and carboxylic acid, while as the absorption peak of methylene in long-chain saturated alkanes (-CH2-) appears at 2838–2843cm^{-1} [15]. The peak around 1600 cm^{-1} also ascribed to C=C stretching of aromatic component and the peak at 1457 cm^{-1} and 1376 cm^{-1} are assigned to –CH2 and –CH3 bending vibrations, respectively [27]. The IR bands in 1300-1000 cm^{-1} are observed and are assigned to C–O or C–O–C stretching in acids, alcohols, phenols, ethers or esters groups [29] There are no prominent changes observed in the spectra on treatment with acid, however loaded with chloride changes the peak pattern in the regions 2400 cm^{-1} and 800-600 cm^{-1}. The various groups on the surface of biochar served for the adsorption of solute.

The FTIR spectra of salix alba biochar is illustrate in figure 5. The peak around 3400-3200 cm^{-1} correspomd to stretching vibration of O-H group could have originated from the alcohols, phenols, and carboxylic acid content, while the absorption peak of methylene in long-chain saturated alkanes appears at 2838–2843cm-1 [15]. The characteristic methyl (C–H) stretching vibration can be seen at 2927 cm^{-1} [28]. The peak around 2346 cm^{-1} correspond to stretching vibration of to C –N triple bond. The band in 1690–1700 cm^{-1} is the stretching vibration band of –CO-N amide groups and 1540–1640 cm−1 corresponds the existence of carbonyl groups (C=O) and carboxylic acid [15]. The peak around 1636 cm^{-1} is ascribed to (C=O) stretching vibration of aromatic carbonyl group [2]. The peak around 1600 cm^{-1} is also ascribed to C=C stretching of aromatic component [27]. The peaks at 1457 cm^{-1}1 and 1376 cm^{-1} are assigned to –CH2 and –CH3 bending vibrations, respectively [27]. The temperature does not cause any appreciable impact on the spectra.

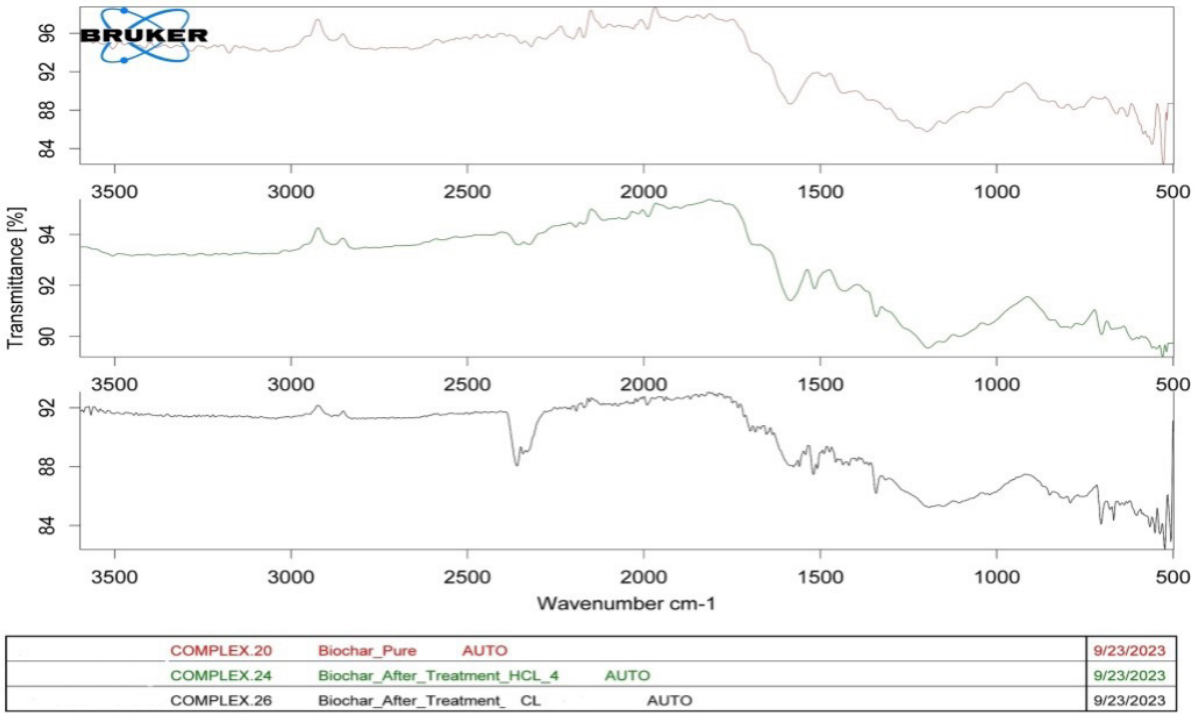


Figure 4. FTIR Spectra of apricot seed shell biochar

Adsorption Kinetics

The rate of adsorption of chloride ion on to the pure and acid modified Salix Alba leaves and Apricot seed shell adsorbent at neutral pH were analyzed for contact time period of 10-190 minute. The pure biochar sorbents have very less adsorption as the surface have negatively charged functional groups which caused repulsion. However acid modified biochar exhibited an enhanced adsorption at neutral pH due to protonation of the surface functional groups and induced surface positive charge. The adsorption slightly faster at the beginning and increases with increasing contact time and attained equilibrium around 150 min. The % removal of chloride ion by the adsorbents are illustrated in figure 6.

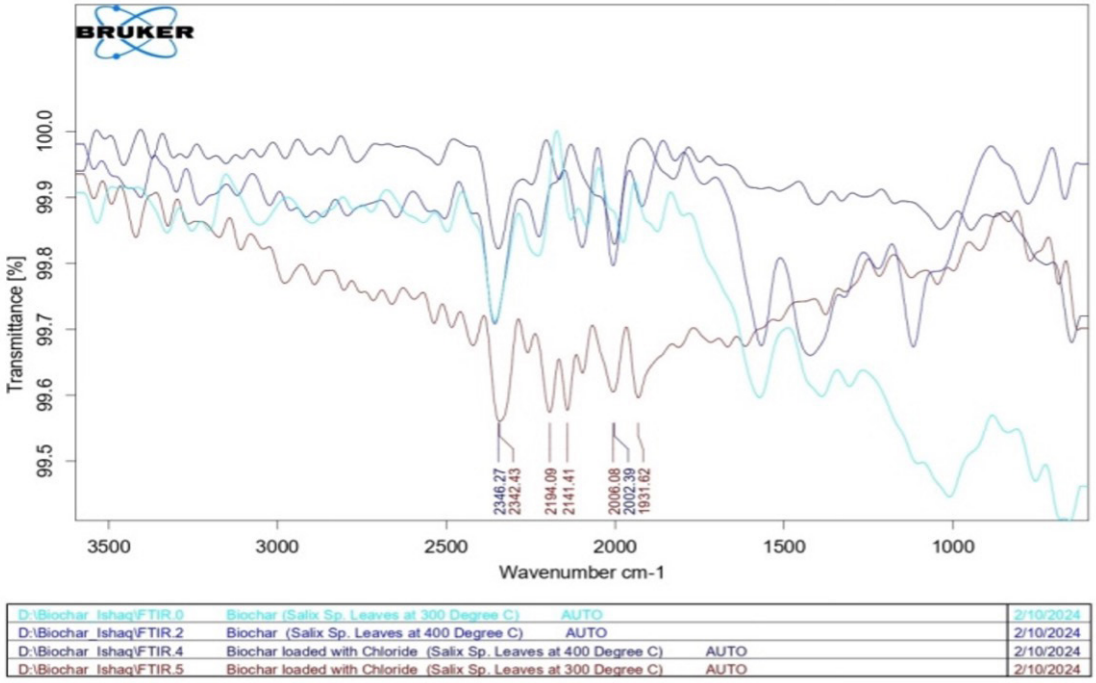


Figure 5. FTIR Spectra of Salix Alba leaves biochar

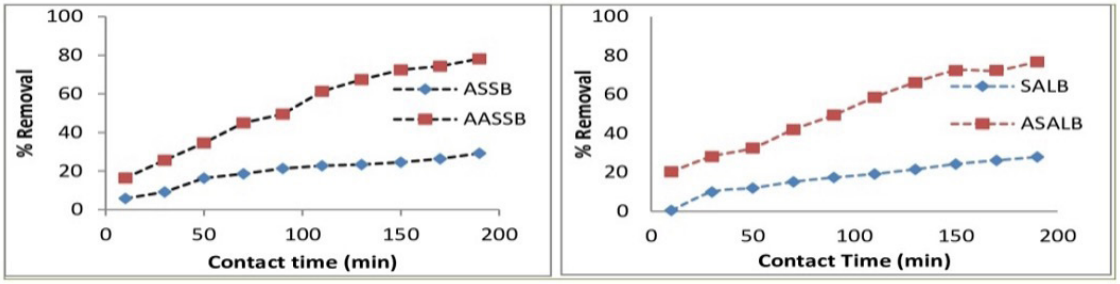


Figure 6. Effect of Contact time.

Table 1. Relevant parameters of adsorption kinetics

Adsorbents	Pseudo 1st order kinetic				Pseudo 2nd order kinetic		
	Qecal (mg/g)	K1	R2	Qe exp(mg/g) (at contact time of 150 min)	Qecal(mg/g)	K2	R2
SALB	2.948	0.0236	0.9191	2.62	3.637	0.003	0.9548
ASALB	8.800	0.0217	0.8352	6.88	10.822	0.001	0.8915
ASSB	2.856	0.017	0.9605	2.74	3.898	0.003	0.9704
AASSB	7.446	0.0185	0.9006	6.82	9.813	0.0013	0.9495

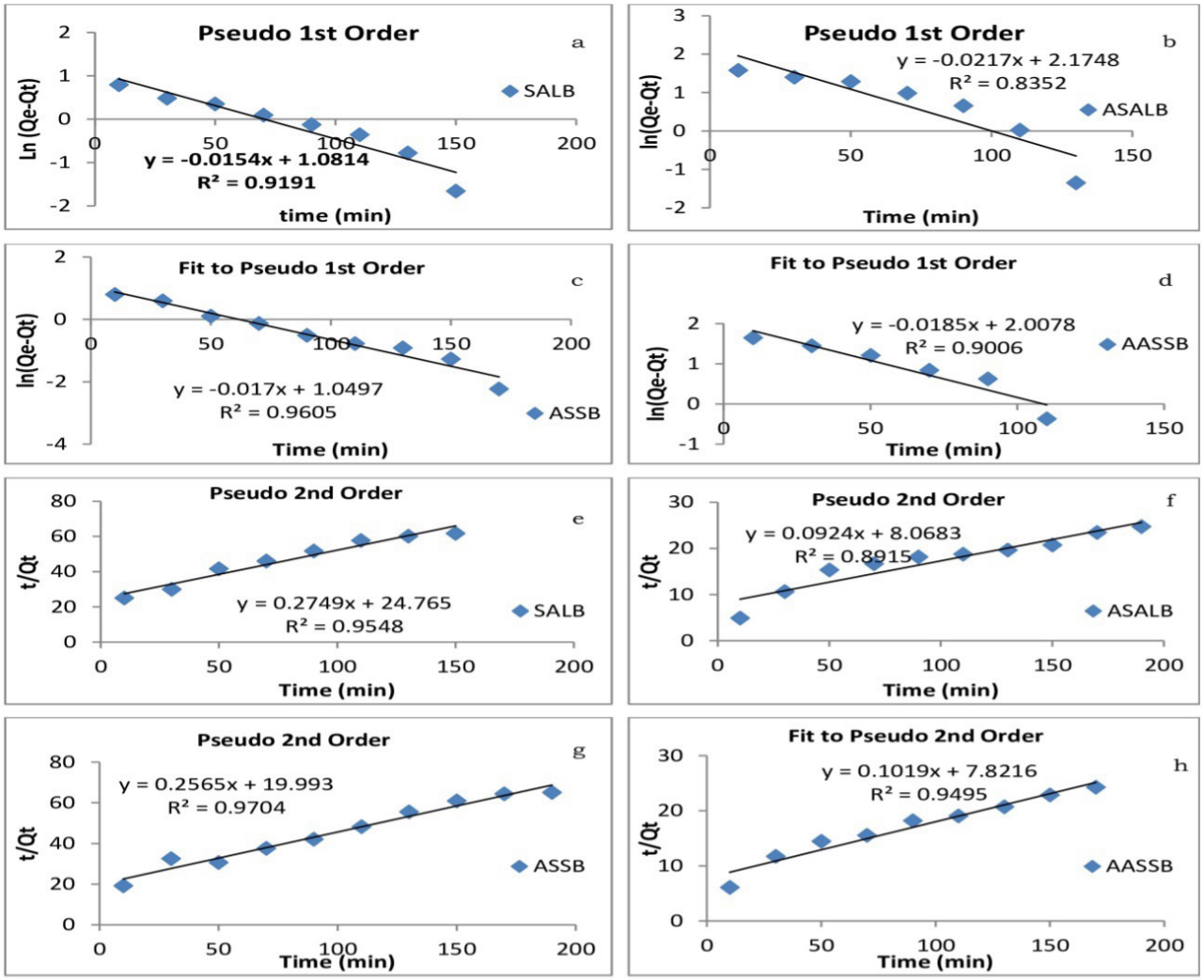


Figure 7. Fit to adsorption kinetics- Pure (a,c,e,g) and activated (b,d,f,h) adsorbents.

Adsorption equilibrium

The % removals of chloride ion by the pure and acid activated biochar were analyzed at different dosage of adsorbents (0.5-2 g), using 100mg/L of chloride solution at neutral pH and the result is depicted in figure 8. The adsorption increases with dosage at neutral pH due to increasing available surface sites of adsorbent and more and more adsorbate get adsorbed.

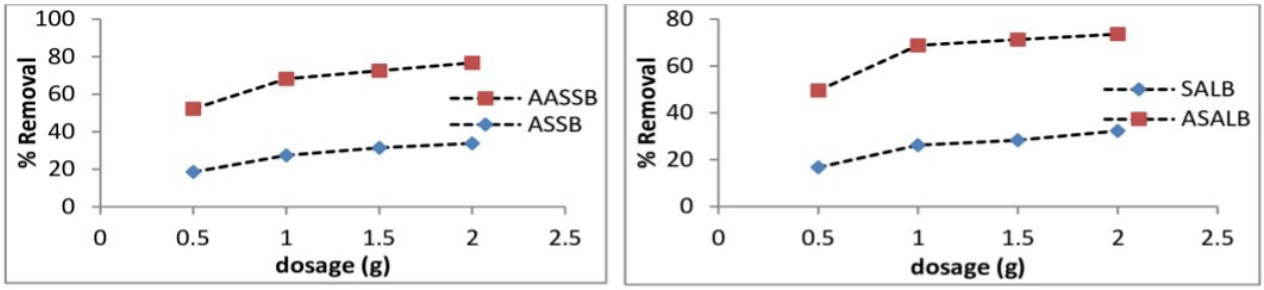


Figure 8. Effect of dosage on % removal of ion

The experimental data obtained by using 100 mg/l at different adsorbent dosage of 0.5,1,1.5 and 2g and contact time period of 150 min at neutral pHwere simulated by using ms excel and fitted to Langmuir and Freundlich isotherm models (figure 9). The Langmuir maximum adsorption capacities (Qmax) of pure and acid activated Salix Alba leaves biochar were found to be 5.537 mg/g and 22.988 mg/g while that of pure and acid activated Apricot seed shell were found to be 6.373 mg/g and 25.839 mg/g respectively.

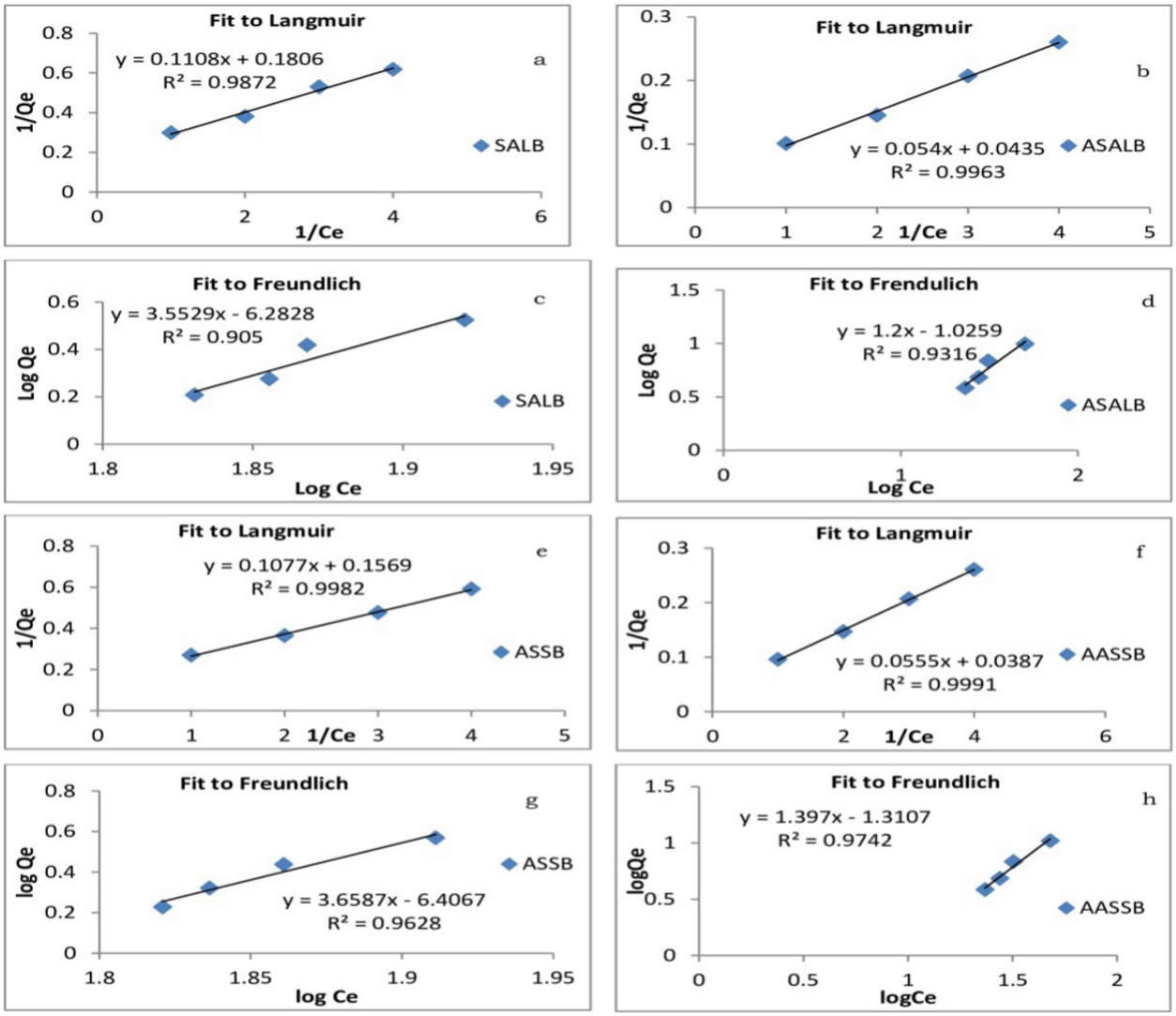


Figure 9. Fit to isotherm models- Pure biochar (a,c,e,g), Activated biochar (b,d,f,h)

The relevant parameters of Langmuir and Freundlich isotherm models are shown in table 2. The coefficient of determination (R2) for Langmuir and Freundlich isotherm model for SALB and ASALB were 0.9872, 0.9050, 0.9963 and 0.9316 respectively, while as for ASSB and AASSB were 0.9982, 0.9628, 0.9991 and 0.9742 respectively. The Langmuir model has two dimensionless constants- RL and KL values. The RL values indicate the favorability, if (0 < RL< 1), unfavorable, if (RL > 1), linearity, if (RL = 1), or irreversibility, if (RL = 0) of a given system [24, 30]. The RL was found to be less than 1 indicated a favourable sorption and relatively showed a better compliance with Langmuir isotherm model.

Table 2. Relevant parameters of adsorption isotherms

Adsorbents	Langmuir isotherm				Freundlich isotherm		
	Qmax (mg/g)	K_L	R_L	R^2	n	K_f	R^2
SALB	5.537	1.563	0.012	0.9872	0.281	533.78	0.9050
ASALB	22.98	0.805	0.024	0.9963	0.833	2.789	0.9316
ASSB	6.373	1.456	0.013	0.9982	0.273	605.89	0.9628
AASSB	25.84	0.697	0.278	0.9991	0.715	0.269	0.9742

CONCLUSION

In light of the global water pollution crisis, scientists/researchers are focusing on developing strategies and technology for preventing and reducing contaminants in water ecosystems. In this study, biochar produced from locally available agricultural wastes (Apricot seed shell and Salix Alba leaves) were used to investigate sorption capacities towards anionic contaminant (chloride ions) using a batch adsorption model. The experimental results showed that acid activated biochar are more effective for removing anion (chloride ion) from water than pure biochar at neutral pH. The Langmuir maximum adsorption capacity (Qmax) of activated Salix Alba leaves biochar recorded to 22.98 mg/g, which is significantly greater than the 5.537 mg/g of the unmodified biochar of Salix Alba leaves. Similarly the Langmuir maximum adsorption capacity (Qmax) of activated Apricot seed shell biochar becomes 25.84 mg/g, which is much greater than the unmodified Apricot seed shell biochar's value of 6.373 mg/g. The experimental data were simulated and fitted to the Langmuir and Freundlich isotherms, and the results were in a close consistent with the Langmuir isotherm. The adsorption kinetics experimental data were also simulated using MS Excel and fitted to pseudo first and second order kinetics and the results exhibited a close agreement with pseudo 2nd order kinetic, showing the involvement of surface contact diffusion, electrostatic interaction, and ion exchange in the adsorption process. Both agricultural wastes have little utility in the region, and their conversion to potential sorbents incurs a minimal capital cost. As a result, these agricultural wastes might be utilized into an effective and sustainable sorbents for the removal of anionic pollutants from water and wastewater.

ACKNOWLEDGEMENT

We are indebted and grateful to Department of Chemistry, University of Ladakh for providing facilities in conducting some portion of experimental work.

DATA AVAILABILITY STATEMENT

The data that support the findings of this study are available within the article and more raw data are available on request from the corresponding author.

AUTHORS CONTRIBUTION

Mohd Ishaq conceived and designed the study. He conducted the experimental work, simulated data, compiled and drafted the manuscript. RC Chippa provided critical feedback, participated in interpretation of data and drafting the manuscript. Anupama Sharma reviewed selected literature. Gh. Ali supported in experimental works.

CONFLICT OF INTEREST

The authors have no conflict of interest to declare in respect of content and publication of this article. Also there is no financial interest to report.

USE OF AI FOR WRITING ASSISTANCE

Not declared.

ETHICS

The authors declare that there is no ethical issue with the publication of this article.

REFERENCES

[1]. T. K. Sen, "Agricultural solid wastes based adsorbent materials in the remediation of heavy metal ions from water and wastewater by adsorption: a review," Molecules, Vol. 28(14), pp.5575, 2023.

[2]. S. Das, and V. V. Goud, "Characterization of a low-cost adsorbent derived from agro-waste for ranitidine removal," Materials science for energy technologies, Vol. 3, pp.879-888, 2020.

[3]. M. Kalaruban, P. Loganathan, W. G. Shim, J. Kandasamy, H. H. Ngo, and S. Vigneswaran, "Enhanced removal of nitrate from water using amine-grafted agricultural wastes," Science of the Total Environment, Vol. 565, pp. 503-510, 2016.

[4]. S. Ghosh, M. Nandasana, T. J. Webster, and S. Thongmee, "Agrowaste-generated biochar for the sustainable remediation of refractory pollutants," Frontiers in Chemistry, Vol. 11: 1266556, 2023.

[5]. M. C. Collivignarelli, W. A.M. A. N. Illankoon, C. Milanese, S. Calatroni, F. M. Caccamo, M. Medina-Llamas, A. Girella, and S. Sorlini, "Preparation and Modification of Biochar Derived from Agricultural Waste for Metal Adsorption from Urban Wastewater," Water, Vol. 16(5), pp. 698, 2024.

[6]. S. Lata, R. Prabhakar, A. Adak, and S. R. Samadder, "As (V) removal using biochar produced from an agricultural waste and prediction of removal efficiency using multiple regression analysis," Environmental Science and Pollution Research, Vol. 26, pp. 32175-32188, 2019.

[7]. T. G. Ambaye, M. Vaccari, E. D. Van Hullebusch, A. Amrane, and S. J. I. J. O.E.S Rtimi, "Mechanisms and adsorption capacities of biochar for the removal of organic and inorganic pollutants from industrial wastewater," International Journal of Environmental Science and Technology, Vol. 18(10), pp. 3273-3294, 2021.

[8]. S. Dey, G. T. N. Veerendra, A. V. P. Manoj, and S. S. A. B. Padavala, "Removal of chlorides and hardness from contaminated water by using various biosorbents: A comprehensive review," Water-Energy Nexus, Vol. 7, pp. 39-76, 2024.

[9]. M. Ishaq, R. C. Chippa, A. Sharma, and G. Ali, "Agro-Waste as a Potential Source for the Development of Adsorbents in Water and Wastewater Treat-

ment," International Journal of Agriculture & Environmental Science, Vol. 10(06), pp. 10-18, 2023.

[10]. G. Liu, Z.Dai, X. Liu, R. A. Dahlgren,and J. Xu, "Modification of agricultural wastes to improve sorption capacities for pollutant removal from water–a review," Carbon Research, Vol. 1(1), pp. 1-24, 2022.

[11]. W. Ou, X. Lan, J. Guo, A. Cai, P. Liu, N. Liu, Y. Liu, and Y. Lei, "Preparation of iron/calcium-modified biochar for phosphate removal from industrial wastewater," Journal of Cleaner Production, Vol. 383, pp. 135468, 2023.

[12]. K. A. Komnitsas, and D. Zaharaki, "Morphology of modified biochar and its potential for phenol removal from aqueous solutions," Frontiers in Environmental Science, Vol. 4, pp. 26, 2016.

[13]. A. R. Usman, M. Ahmad, M. El-Mahrouky, A. Al-Omran, Y. S. Ok, A. S. Sallam, and M. I. Al-Wabel, "Chemically modified biochar produced from conocarpus waste increases NO 3 removal from aqueous solutions," Environmental geochemistry and health, Vol. 38, pp. 511-521, 2016.

[14]. M. Kalaruban, P. Loganathan, W. Shim, J. Kandasamy, G. Naidu, T. V. Nguyen, and S. Vigneswaran, "Removing nitrate from water using iron-modified Dowex 21K XLT ion exchange resin: Batch and fluidised-bed adsorption studies," Separation and Purification Technology, Vol. 158, pp. 62-70, 2016.

[15]. Z. Zhang, C. Zhou, J. Yang, B. Yan, J. Liu, S. Wang, Q. Li and M. Zhou, "Preparation and characterization of apricot kernel shell biochar and its adsorption mechanism for atrazine," Sustainability, Vol. 14(7), pp. 4082, 2022.

[16]. P. Peng, Y. H. Lang, and X. M. Wang, "Adsorption behavior and mechanism of pentachlorophenol on reed biochars: pH effect, pyrolysis temperature, hydrochloric acid treatment and isotherms," Ecological Engineering, Vol. 90, pp.225-233, 2016.

[17]. M. H. Mosleh, and H. Rajabi, "NaOH-benzoic acid modified biochar for enhanced removal of aromatic VOCs," Separation and Purification Technology, Vol. 330, pp. 125453, 2024.

[18]. S.K. Alfaiz, D. A. Yaseen, and W. A. Alawadi, "Water De-Chlorination by Non-Modified and Modified Biochar Derived from Date Palm," Journal of Ecological Engineering, 24(12), 2023.

[19]. L.N. Sklivaniotis, P. Economou, H. K. Karapanagioti, and I. D. Manariotis, "Chlorine removal from water by biochar derived from various food waste natural materials," Environmental Processes, 10(1), pp.4, 2023.

[20]. World Health Organization, Geneva. (1996). Chloride in Drinking-water: Guidelines for drinking-water quality, Health criteria and other supporting information, 2nd ed. Vol. 2. https://www.who.int/publications/i/item/9241544805.

[21]. T. Stobdan, D. Namgial, O.P. Chaurasia, M. Wani, T. Phunchok, and M. Zaffar, "Apricot (Prunus armeniaca L.) in trans-Himalayan Ladakh, India: Current status and future directions," Journal of Food Agricultural Research, Vol. 1, pp. 86-105, 2021.

[22]. D. Blagojević, A. Polovina, D. Lazić, and D. Jelić, "DETERMINATION OF CHLORIDE CONTENT IN BOTTLED MINERAL WATER," Acta Scientifica Balcanica, Vol. 3(1), pp. 13-21, 2022.

[23]. S. Apte, S. S. Apte, V. S. Kore, and S. V. Kore, "Chloride removal from wastewater by biosorption with the plant biomass," Universal Journal of Environmental Research & Technology, Vol. 1(4), pp. 416, 2011.

[24]. A. Hashem, C. O. Aniagor, O. M. Morsy, A. Abou-Okeil, and A. A. Aly, "Apricot seed shell: an agro-waste biosorbent for acid blue193 dye adsorption," Biomass Conversion and Biorefinery, 1-14, 2022.

[25]. S.K. Alfaiz, D. A. Yaseen, and W. A. Alawadi, "Water De-Chlorination by Non-Modified and Modified Biochar Derived from Date Palm," Journal of Ecological Engineering, 24(12), 2023.

[26]. L.N. Sklivaniotis, P. Economou, H. K. Karapanagioti, and I. D. Manariotis, "Chlorine removal from water by biochar derived from various food waste natural materials," Environmental Processes, 10(1), pp.4, 2023.

[27]. R. Janu, V. Mrlik, D. Ribitsch, J. Hofman, P. Sedláček, L. Bielská, and G. Soja, "Biochar surface functional groups as affected by biomass feedstock, biochar composition and pyrolysis temperature," Carbon Resources Conversion, 4, 36-46, 2021.

[28]. A. Y. Elnour, A. A. Alghyamah, H. M. Shaikh, A. M Poulose, S. M. Al-Zahrani, A. Anis and M. I. Al-Wabel, "Effect of pyrolysis temperature on biochar microstructural evolution, physicochemical characteristics, and its influence on biochar/polypropylene composites", Applied sciences, 9(6), 1149, 2019.

[29]. A. L. I. Jawad, D. T. Al-Heetim, and R. Abd Rashid, "Biochar from orange (Citrus sinensis) peels by acid activation for methylene blue adsorption," Iranian Journal of Chemistry and Chemical Engineering, 38(2), 91-105, 2019.

[30]. B. S. Stromer, B. Woodbury, & C. F. Williams, "Tylosin sorption to diatomaceous earth described by Langmuir isotherm and Freundlich isotherm models," Chemosphere, 193, 912-920, 2018.

Environ Res Tec, Vol. 8, Issue. 2, pp. 297-314, June 2025

Environmental Research and Technology
https://dergipark.org.tr/en/pub/ert
DOI: https://10.35208/ert.1504755

Research Article

Bibliometric analysis of environmental, social and corporate governance (ESG) articles published in the Scopus database

Ümran BULUT SU *[1], Yasemin ERTAN[1]

[1] *Uludag University, Business Management. Dept., Özlüce Görükle Kampüsü, 16059 Bursa, Türkiye*

ARTICLE INFO

Article history
Received: 25 Jun 2024
Revised: 06 Aug 2024
Accepted: 28 Aug 2024

Key words:
Bibliometric analysis, ESG, sustainability

ABSTRACT

The aim of this study is to examine the literature on environmental, social and governance (ESG) studies using bibliometric analysis methods, to analyze authors, documents, sources and country performance, and to reveal the conceptual structure of the field. For this purpose, 2,055 articles published in the Scopus database between 2007 and 2024 were analyzed. As a result of the study, it was revealed that Khaled Hussainey is the most productive and influential author in the field. The article, entitled "Firms and Social Responsibility: A Review of ESG and CSR Research in Corporate Finance", published by S. Gillan et al. in 2021, is the most influential document, the journal with the highest number of publications is Sustainability (Switzerland), and the country where the most recent studies are conducted is China. In addition, the study found that the articles published in this field were grouped into 6 clusters and the most recent keywords were "green innovation" and digital transformation.

Cite this article as: Bulut Su U, Ertan Y. Bibliometric analysis of environmental, social and corporate governance (ESG) articles published in the Scopus database. Environ Res Tec 2025;8(2) 297-314.

INTRODUCTION

Human society will continue to search for progress as long as there is life. Today, with the advancement of economy, technology and society, the world faces a variety of opportunities and challenges. In 2020, there have been many "black swan" events, the global spread of COVID-19, the US stock market crash four times in two weeks, the locust epidemic in Africa, the delisting of Luckin Coffee due to fraud, environmental (E), social (S) and governance (G) issues have raised global concerns. As a result, the issue of "sustainable and inclusive development" has become a global agenda. International organizations and countries around the world have proposed sustainable development action plans, such as ESG, to establish a framework for sustainable and inclusive development in response to the growing challenges of sustainable development in the environment, society and the financial market [1]. Over the past two decades, there has been a significant increase in interest in socially responsible investing (SRI), also known as ethical investing or sustainable investing, around the world as awareness of the importance of sustainable activities has grown. SRI is defined as the integration of non-financial issues such as environmental, social and corporate governance (ESG) into the investment decision-making process [2].

As a result of pressure from regulators, NGOs and stakeholders, and in the wake of financial scandals, more and more companies are seeking to incorporate environmental, social and other local regulations into their strategies. Companies aim to give stakeholders a clear picture of their corporate re-

***Corresponding author.**
*E-mail address: umran.su@mudanya.edu.tr - 712114005@ogr.uludag.edu.tr

This is an open access article under the CC BY-NC license (http://creativecommons.org/licenses/by-nc/4.0/).

sponsibility practices and efforts. As a result, corporate disclosure of ESG issues has been developing in various dimensions for more than two decades, and an increasing number of companies have started to engage in ESG disclosure activities [3]. These activities have led to the emergence of ESG rating agencies. ESG rating agencies screen companies using proprietary research methodologies, assess companies" sustainability performance and provide ESG ratings. Thomson Reuters" ASSET4, the Ethical Investment Research Service (EIRIS), MSCI"s Kinder Lydenberg Domini & Co. (KLD) and the Sustainable Asset Management Group (SAM) are among the most prominent ESG rating agencies. Other rating agencies, such as Bloomberg Sustainability, also calculate and publish ESG disclosure scores [2]. Socially responsible managers and investors take ESG ratings into account in their decision-making, and they have become an important resource for conscientious consumers [4].

The rapid development of ESG ratings in the recent period has led the academic world to address the issue. According to proponents of ESG ratings, these ratings objectively and effectively measure a company's ESG efforts while correcting information asymmetries for stakeholders [5], providing access to resources, improving corporate competitiveness, social reputation and performance [6]. In contrast, some scholars argue that ESG ratings are not effective. They believe that ESG ratings symbolically force companies to comply with external requirements in order to gain various benefits, which does not contribute meaningfully to corporate sustainability behavior [7] but rather represents corporate decline and may mislead stakeholders [8]. As a result of these divergent views, numerous studies have been conducted on the effectiveness of environmental, social and governance (ESG) ratings [9]. ESG ratings and corporate financial performance or capital market reactions have generally been the focus of these studies [10], [11].

This study analyses studies in the field of ESG using a bibliometric analysis method. The aim of the study is to identify the leading authors, articles, sources and countries in the field by analyzing the literature and to reveal the conceptual structure of the field. It is expected that the study will inform researchers wishing to work in the field about the structure of the field and the issues can focuses on, provide guidance by highlighting the gaps in the field, and thus contribute to sustainability in ESG dimensions. In the following sections of the study, the literature on bibliometric studies in the field of ESG will be mentioned. The methodology of the study will then be explained and the findings and results will be presented. Finally, the limitations of the study are mentioned and suggestions for future studies are provided.

LITERATURE REVIEW

In recent years, the number of ESG studies has increased in parallel with the importance and awareness of ESG activities. Some of the studies in this field have focused on the financial implications of ESG performance. For example, [12] find that companies with high CSR performance face lower capital constraints, which is supported by stakeholder engagement and transparency. [13] reveal that there is a generally positive relationship between ESG and firm financial performance and that this effect is stable over time. In addition, [14] find a moderate positive relationship between ESG disclosure and corporate efficiency, with the strongest effect coming from governance information. In this field, there are also studies that examine the relationship between ESG performance and firms" strategic decisions. [15] stated that companies respond positively to the issuance of green bonds, which increases the liquidity of their shares. [16] conducted a study for multinational logistics companies and found that "greenhouse gas emissions" is the most important criterion and "eco-efficiency" is the best environmental competitive strategy. These results show that ESG performance is closely linked not only to financial results but also to strategic decisions. Some studies have also examined how ESG activities are perceived under political and economic conditions. [17] reported that investors pay a premium for environmental and social investments during periods of high political uncertainty. This shows that social and environmental investments have a significant impact on investors" decisions. In addition, [18] show that companies increase their ESG activities during periods of high economic policy uncertainty, and that these activities are perceived as risk-reducing and value-enhancing.

There are also studies in the literature that have been analyzed using bibliometric methods. These are summarized in Table 1.

Table 1. Studies conducted using the bibliometric analysis method in the field of ESG

No	Author(s)	Title	Publication year	Period covered	Database covered	Number of analysed publication	Aim of the study
1	T. S. Legendre A. Ding Ki-Joon Back [19]	A bibliometric analysis of the hospitality and tourism environmental, social, and governance (ESG) literature	2024	1978 -2021	WoS	704	To carry out a bibliometric analysis of the studies carried out in the field of ESG
2	M.S. Khamisu A.R. Paluri [20]	What's past is prologue: reminiscing research on environment social governance (ESG) disclosures	2024	2006-2022	Scopus WoS	794	To analyse the literature on ESG disclosure
3	X. Zhao D. Nan C. Chen S. Zhang S. Che J.H.Kim [21]	Bibliometric study on environmental, social, and governance research using CiteSpace	2023	2007–2021	WoS	849	To provide an overview of the state of the art of ESG research and the emerging trends
4	J. Karishma P.S. Tripathi [22]	Mapping the environmental, social and governance literature: a bibliometric and content analysis	2023	2018-2023	Scopus WoS	190	To quantify and map the academic literature on ESG from a bibliometric perspective and provide a
5	G. Wan A.Y.Dawod S. Chanaim S.S.Ramasamy [23]	Hotspots and trends of environmental, social and governance (ESG) research: a bibliometric analysis	2023	2004-2021	WoS	755	To analyse the literature on ESG-related topics
6	G. Wan A. Y. Dawod C. Nopasit [24]	A bibliometric and visual analysis in the field of environment, social and governance (ESG) between 2004 and 2021	2023	2004-2021	WoS	1735	To examine the performance and structure of the ESG literature and identify future areas of research
7	S.Senadheera R.Gregory J.Rinklebe M.Farrukh J.Rhee Y.Tamam [25]	The development of research on environmental, social, and governance (ESG): a bibliometric analysis	2022	2001 - 2021	Scopus	981	To explore current and future research directions in ESG

8	S.Galletta S. Mazzù V. Naciti[26]	A bibliometric analysis of ESG performance in the banking industry: from the current status to future directions	2022	1986–2021	Wos	271	To assess the development of the literature on ESG in the banking sector, the characteristics of authors and articles, and to examine research trends.
9	N.O.D. Ellili [27]	Bibliometric analysis and systematic review of environmental, social, and governance disclosure papers: current topics and recommendations for future research	2022	2010-2021	Scopus	161	To provide an analysis of the literature on ESG disclosure
10	H.-j. Siao S.-H. Gau J.-H. Kuo M.-G. Li C.-J. Sun[28]	Bibliometric analysis of environmental, social, and governance management	2022	2002-2021	WoS	3599	To examine the trend and evolution of published research from 2002 to 2021
11	S. Gao F. Meng Z. Gu Z. Liu M.Farrukh [29]	Mapping and clustering analysis on environmental, social and governance field a bibliometric analysis using Scopus	2021	1990- 2020	Scopus	690	To conduct a bibliometric and visualisation study of the ESG literature.

As can be seen in Table 1, there are bibliometric analysis studies in the literature that have been conducted to examine studies in the field of ESG based on specific sectors [19], [26]. There are also studies that focus on specific areas related to ESG, such as ESG disclosure [20], [27]. In some bibliometric analysis studies, all studies in the field of ESG have been reviewed. Some of these studies cover both the WoS and Scopus databases [22], some only the WoS database [21], [23], [23] and some only the Scopus database [25], [29]. As can be seen in Table 1, the data of bibliometric studies based on Scopus are older than those based on other databases. Documents published in 2023 and 2024 are not included in bibliometric studies based on Scopus. However, as mentioned in the publication trends section of this study, a significant number of documents in this field were published in 2023 and 2024. In addition, when examining studies conducted using the Scopus database, it is noted that [29] focused on studies in the "Business, Management and Accounting" and "Economics, Econometrics and Finance" categories, and [25] included terms such as index, rating and score along with ESG in their search terms to avoid including publications unrelated to business, such as those in medicine and engineering, and manually excluded irrelevant publications from the dataset. The authors noted that manual cleaning was a limitation of their study.

The importance of ESG is increasingly recognized and is the subject of more and more academic studies. The aim of this study is to conduct a bibliometric analysis of ESG studies in the "Business, Management and Accounting" category of the Scopus database. It covers all sectors, including the most recent studies up to 27 May 2024. Therefore, in contrast to the literature, this study also includes studies from 2023 and 2024 in the analysis. In addition, the data included in the study belong in a different way to the studies in the category "Business, management and accounting" than other studies in the literature. The study was conducted on 2,055 documents published in the Scopus database in the field of ESG between 2006 and 2024 and aims to identify the main themes in the field, recent focuses, leading authors, documents, sources and countries.

METHOD

In this study, the literature on ESG studies was analyzed us-

ing bibliometric analysis method. Bibliometric analysis is a quantitative technique used to assess and monitor the current state of research in a particular area of scientific interest [30]. Unravelling and mapping the evolutionary nuances of scientific fields and cumulative scientific knowledge can be done using the bibliometric analysis method, which allows the analysis of large amounts of unstructured data [31] and involves the use of quantitative techniques [32].

Performance analysis and science mapping are two types of bibliometric analysis techniques that consider the contributions of research components. Performance analysis assesses the performance of the components of the field (e.g. authors, documents, sources, countries), while science mapping focuses on the relationships between research components. Performance analysis is carried out using different metrics. One of the issues to be taken into account when analyzing performance is that articles with an earlier publication date tend to receive more citations. This creates a problem when comparing the effectiveness of recently published articles with the effectiveness of earlier published articles in the field. In order to reduce this negative effect, the study used the average normalized (norm.) citation count metric [33]. Citation analysis, co-citation analysis, bibliographic matching, co-occurrence of keywords as part of the performance analysis, the h-indexes of the authors working in the field and of the sources published in the field were also analyzed. The h-index is a metric that measures the scientific output of a research component in terms of both productivity and quality [34]. The main theme of the field is usually revealed by the co-occurrence of keywords [35]. In this study, the co-occurrence of keywords analysis, one of the scientific mapping methods, was used to determine the conceptual structure of the field.

Bibliometric analysis has gained popularity in recent years, thanks to software such as Gephi, Leximancer and VOSviewer, and the increasing availability and accessibility of scientific databases such as Scopus and Web of Science [36]. In this study, VosViewer version 1.6.20 was used to perform performance analysis and scientific mapping. This program is particularly useful for visualizing bibliometric analyses involving large amounts of data using distance-based maps. The purpose of visualizing data using VOSviewer is to facilitate the understanding and interpretation of complex data [37]. Visual maps consist of nodes and links. Nodes can represent elements such as countries, institutions and keywords. The size of nodes is a measure of the quantity or frequency of publications; as node size increases, so does the quantity or frequency of publications [38]. Co-operation, co-occurrence or co-citation relationships are represented by the links between nodes [39]. Different clusters or years can be represented by the color of the nodes and lines [38].

Data and Analysis

The most commonly used databases for bibliometric analysis are Scopus and WoS. Both databases contain high quality publications and allow data to be exported without manual processes. However, the Scopus database contains more documents in the fields of economics, finance and management than WoS [25]. In other words, the Scopus database is the largest research repository containing publications of acceptable quality [27]. The purpose of this study is to analyze studies related to ESG in the category "Business, management and accounting". One of the reasons for focusing on documents in the Scopus database in this study is that it contains a higher number of publications in the "business, management and accounting" category. Another reason for focusing on the Scopus database, as mentioned in the literature section, is that no bibliometric analysis study has been found that examines documents on ESG published in this database in 2023-2024.

The data analyzed in the study were obtained from the Scopus database on 27/05/2024. In the Scopus database, the words “ESG” and “Environmental, Social and Governance” were searched using the Boolean operator “or” between “article title, abstract, keywords” and it was found that 11,249 documents were available. 2,874 of these documents were written in the field of business, management and accounting. 2,055 of the documents written in the field of business, management and accounting are articles. The analysis of the study was carried out by considering 2,055 articles. The process of determining which documents to include in the analysis is illustrated in the PRISMA flowchart in Figure 1.

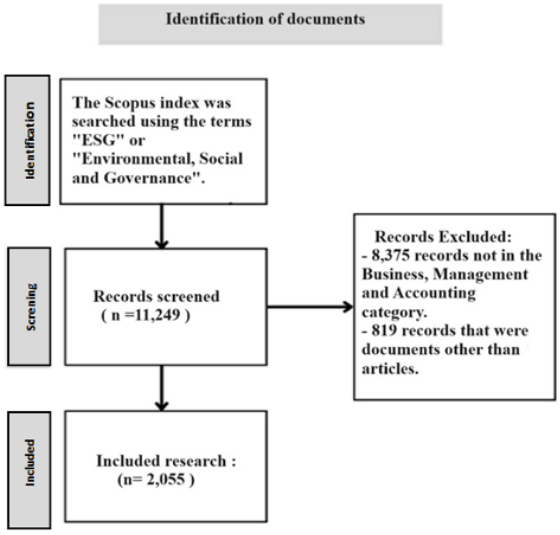


Figure 1. Prisma flow diagram demonstrating the identification of documents

FINDINGS

Publication Trend

This study analyses 2,055 articles written in the field of ESG and published in the Scopus database. The distribution of these articles by year is shown in Figure 2.

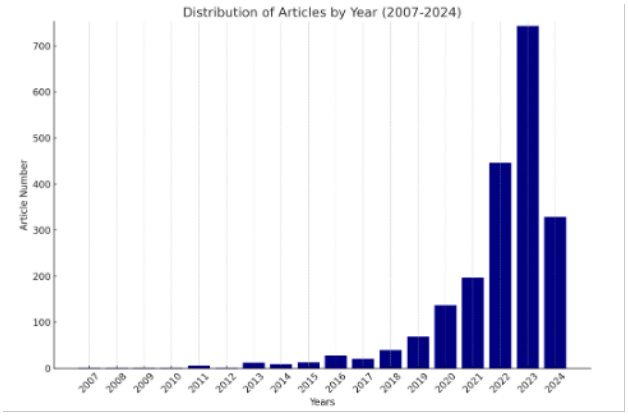


Figure 2. Distribution of publications by years

The first article (published between 2007 and 2024) in this field was written by M.J. Kiernan in 2007, entitled "Universal owners and ESG: Leaving money on the table?" The article emphasized the need for universal owners to recognize their power and responsibility to shape their investment strategies to improve the ESG practices of the companies in which they invest. In 2007, 2008, 2009 and 2010, 1 article was published in this field.

Looking at the change in the number of articles per year, we can see that the number of articles has been increasing since 2018, and that the increase has gained momentum since 2020. The data of the study were determined on 27/05/2024. Therefore, in the evaluation of the number of articles in 2024 (n=329), it should be taken into account that 5 months of the year are still behind and the number of publications will probably increase in the following months of 2024.

PERFORMANCE ANALYSIS

Performance of Authors

The performance of authors is measured by their productivity and impact. The number of publications by authors is an indicator of their productivity, and the average number of citations is an indicator of their impact.

However, publications with earlier publication dates are likely to receive more citations. When the number of citations is examined by removing the effect of time, the average normalized number of citations becomes a parameter of impact.

The articles analyzed in the study were written by a total of 4,978 authors. Table 2 provides quantitative information on the 10 authors with the highest number of publications.

Table 2. Quantitative information on the authors with the 10 highest number of publications

No	Author(s)	Document number	Citation number	Average citation	Norm. citation	Average norm. citation	Averagepublication year	H- index
1	K.Hussainey	9	265	29.44	38.83	4.31	2023.11	45
2	A. Buallay	8	589	73.62	12.18	1.52	2020.62	21
3	H.A.Amosh	8	118	14.75	28.11	3.51	2023.12	13
4	I.Makarenko	8	40	5.00	1.81	0.23	2021.38	39
5	F. Paolone	7	105	15	8.80	1.26	2022.86	15
6	R. Rajesh	6	301	50.17	11.35	1.89	2021.67	24
7	K. Singh	6	7	1.17	2.37	0.39	2023.33	5
8	R. Lueg	6	114	19	3.43	0.57	2020.83	17
9	V. Barros	6	95	15.83	6.67	1.11	2022.50	11
10	E.E Olmedo	5	479	95.80	8.99	1.80	2021.67	10

[1] There are a total of 21 authors with 5 publications. The author with 5 publications in Table 2 is the author with the highest number of citations among the authors with 5 publications.

[2] The average number of citations is calculated by dividing the number of citations by the number of publications.

Table 3 provides quantitative information on the 10 authors whose publications are most cited. As can be seen in Table 3, George Serafeim (n=1,821) is the most cited author in this field and he has 3 articles. The average year of publication of his articles is 2019.67.

Among the most cited authors, Stuart L. Gillan and Andrew Koch have the highest average number of normalised citations (n=17.86). The authors co-authored a paper entitled 'Firms and social responsibility: A review of ESG and CSR research in corporate finance', published in 2021, in which they examine environmental, social and governance (ESG) and corporate social responsibility (CSR) research from a corporate finance perspective (Gillan, Koch & Starks, 2021). The norma. average number of citations was calculated by dividing the norm. number of citations by the number of publications.

As can be seen in Table 2, "Khaled Hussainey" has the highest number of publications and normalized citations. This indicates that this author is the most productive and influential author in the field of ESG. In addition, Khaled Hussainey has the highest h-index. The author is the most influential author when all his publications are taken into account. Also, the average publication year (2023.11) of this author is the most recent among his publications. When analyzing the authors in terms of average citation, Elena Escrig- Olmedo, who has 5 publications, is the author with the highest average number of citations (n= 95.80). The average publication year of Elena Escrig- Olmedo is 2021.67. The average norm. citation of the author (1.80) is not very high. This is an indication that the author's publications are cited more because they are older, rather than because they are more influential.

On the other hand, Table 3 presents quantitative information about the 10 authors whose publications are cited the most. As seen in Table 3, George Serafeim (n=1.821), the most cited author in this field and he has 3 articles. The average publication year of the author's articles is 2019.67. Among the most cited authors, Stuart L. Gillan and Andrew Koch have the highest average number of norm. citations (n=17.86). The authors have a co-authored paper in this field titled "Firms and social responsibility: A review of ESG and CSR research in corporate finance," published in 2021, in which they examine ESG and corporate social responsibility research from a corporate finance perspective [40].

Table 3. Quantitative information on the 10 most cited authors

No	Author(s)	Document number	Citation number	Average citation	Norm. citation	Average norm. citation	Average publication year	H-indeks
1	G. Serafeim	3	1,821	607.00	19.37	6.46	2019.67	29
2	B. Cheng	1	1,736	1736.00	7.30	7.30	2014.00	1
3	I. Ioannou	1	1,736	1736.00	7.30	7.30	2014.00	13
4	T. Busch	2	1,316	658.00	11.76	5.88	2015.50	26
5	G. Friede	2	1,156	576.00	9.73	4.87	2017.00	3
6	A. Bassen	2	1,125	562.50	9.17	4.59	2015.50	11
7	L.T.Starks	2	626	313.00	20.17	10.58	2022.50	37
8	S.L.Gillan	1	624	624.00	17.86	17.86	2021.00	15
9	A. Koch	1	624	624.00	17.86	17.86	2021.00	7
10	A. Bually	8	589	73.62	12.18	1.52	2020.62	21

Source: Data obtained from citation analysis in Vosviewer

Among the most cited authors in this field, Laura T. Starks has the highest h-index of 37. Laura Starks has the second highest average norm. citation. This indicates that the author is the most influential in the ESG field and she is the most influential author among the authors in Table 3 considering all publications (in all fields) of authors. The top three authors with the most recent ESG research are Laura T. Starks, Stuart L. Gillan and Andrew Koch in terms of average publication years.

Performance of Documents

A total of 2,055 articles were analyzed in the study. As a result of the document citation analysis conducted to determine the performance of the articles, information on the quantitative characteristics of the articles identified as the 10 most cited articles is presented in Table 4.

Table 4. Findings of the most cited articles

No	Author	Article title	Journal title	Citation number	Norm. citation	Publication year
1	G.Serafeim I. Ioannou B.Cheng[12]	Corporate Social Responsibility and Access to Finance	Strategic Management Journal,35,1-23	1736	7.30	2014
2	G. Friede T.Busch A.Bassen[13]	ESG and Financial Performance: Aggregated Evidence from more than 2000 Empirical Studies	Journal of Sustainable Finance and Investment,5, 210-233	1114	9.02	2015
3	S.Gillan A.Koch T.Starks[40]	Firms and Social Responsibility: A Review of ESG and CSR Research in Corporate Finance	Journal of Corporate Finance,66	624	17.86	2021
4	J.Xie W.Nozawa M.Yagi H.Fujii S.Managi[14]	Do Environmental,Social and Governance Activities İmprove Corporate Financial Performance?	Business Strategy and The Environment,28,286-300	375	7.00	2018
5	D.Y.Tang Y.Zhang[15]	Do Shareholders Benefit from Green Bonds?	Journal of Corporate Finance,61	367	8.07	2020
6	S. Drempetic C.Klein B.Zwergel[41]	The İnfluence of Firm Size on The ESG Score:Corporate Sustainability Ratings Under Review	Journal of Business Ethics,167,333-360	365	8.03	2020
7	L.H.Pedersen S.Fitzgibbons L.Pomorski[42]	Responsible İnvesting: The ESG-Efficient Frontier	Journal of Financial Economics,142,572-597	364	10.42	2021
8	L. Pastor R.F. Stambaugh L.A.Taylor[43]	Sustainable Investing in Equilibrium	Journal of Financial Economics,142,550-571	344	9.85	2021
9	A.S Garcia W.Silva da Mendes R. Orsato[44]	Sensitive Industries Produce Better ESG Performance: Evidence from Emerging Markets	Journal of Cleaner Production,150,135-147	340	2.95	2017
10	N.Cucari S. Esposito de Falco B.Orlando[45]	Diversity of Board of Directors and Environmental Social Governance:Evidence from İtalian listed Companies	Corporate Social Responsibility and Environmental Management, 25,250-266	340	3.97	2018

Source: Data obtained from citation analysis in Vosviewer

As seen in Table 4, the most cited article (n=1,736) is "Corporate Social Responsibility and Access to Finance" written by "G.Serafeim, I Ioannou; B.Cheng" in 2014. The article, which examines the impact of corporate social responsibility practices on companies" access to finance, shows that companies with high corporate social responsibility performance have easier access to finance due to increased stakeholder engagement and reduced information asymmetry [12]. The second most cited article (n=1,114) is "ESG and Financial Performance: Aggregated Evidence from more than 2000 Empirical Studies", written by G. Friede et al. in 2015. The article examines the results of academic studies in the field of ESG and financial performance and finds that 90% of the studies show a positive or neutral relationship between ESG and financial performance. It emphasizes that incorporating ESG criteria into investments brings environmental, social and financial benefits to companies [13].

When the norm. citation numbers of the articles are examined, it is seen that the articles titled "Firms and Social Responsibility: A Review of ESG and CSR Research in Corporate Finance" published by "S.Gillan et al." in 2021 and "Responsible Investing: The ESG-Efficient Frontier" by "Pedersen et al." in 2021 are the articles with the highest normalized citation numbers.

Performance of Journals

A total of 2,055 articles analyzed in this study were published in 469 different journals. Journal citation analysis was used to determine the performance of the journals. Information on the quantitative characteristics of the 10 most cited journals is shown in Table 5.

Table 5. Findings of the most cited sources

No	Journal name	Number of publications	Number of citations	Average citation	Number of norm. citation	Average norm. citation	Average publication Year	H- index
1	Sustainability (Switzerland)	308	4886	15.86	210.59	0.68	2022.55	169
2	Business Strategy and Environment	89	3921	44,06	207.09	2.33	2021.78	147
3	Journal of Business Ethics	29	2769	95.48	75.41	2.60	2019.31	253
4	Journal of Sustainable Finance and	74	2245	30.34	104.41	1.41	2020.22	35
5	Corporate Social Responsibility and Environmental Management	104	2114	20.33	132.40	1.27	2022.55	113
6	Journal of Cleaner Production	60	1624	27.07	79.82	1.33	2022.33	309
7	Journal of Corporate Finance	13	1482	114	39.04	3.00	2021.69	131
8	Journal of Business Research	14	779	55.64	44.92	3.21	2021.86	265
9	Research in International Business and Finance	44	702	15.95	65.46	1.49	2023.07	73
10	Journal of Asset Management	23	687	29.87	11.65	0.51	2020.52	23

As can be seen in Table 5, the journal with the highest number of publications in this field is "Sustainability (Switzerland)", which shows that this journal is the most productive journal in this field. When journals are ranked according to the average number of citations to publications in this field, Journal of Business Ethics has the highest average number of citations. However, the average publication year of "Journal of Business Ethics" is 2019.31 and the average normalized citation (2.60) is the third highest. The fact that this is the journal with the highest average number of citations, but not the journal with the highest average normalized citation, is explained by the fact that the publications are relatively old and therefore high cited. The journal with the highest normalized citation count (3.21) is the "Journal of Business Ethics". This is the most influential journal in the field. If the journals are compared by h-index, the "Journal of Cleaner Production" comes first. This journal does not stand out in terms of productivity or effectiveness in the field of ESG. However, it is the most influential of the journals in Table 4, taking into account all the articles published in the journal. The top three journals with the most recent ESG studies are "Research in International Business and Finance", "Corporate Social Responsibility and Environmental Management" and "Sustainability (Switzerland)".

Performance of Countries

The articles analyzed in this study were written by academics from 100 different countries. A country citation analysis was carried out to determine the productivity and impact of the countries from which ESG studies originate. Table 6 provides information on the 10 countries with the highest number of publications.

Table 6. Quantitative data of the countries with the highest number of publications

No	Country	Publication number	Citation number	Average citation number	Norm. citation	Average norm. citaion	Average publication year
1	China	360	3387	9.41	427.69	1.19	2022.84
2	U.S.A.	259	7643	29.51	344.60	1.33	2021.98
3	United Kingdom	213	7494	35.18	325	1.53	2021.94
4	Italy	211	5047	23.92	255.86	1.21	2022.13
5	India	142	1446	10.18	118.67	0.84	2022.35
6	Australia	111	2664	24	127.70	1.15	2021.49
7	Spain	103	2523	24.50	108.53	1.05	2021.23
8	South Korea	102	1161	11.38	66.71	0.65	2022.13
9	Germany	93	4482	48.19	117.06	1.26	2021.05
10	Malaysia	459	1361	15.12	86.07	0.96	2021.77

Source: Data obtained from citation analysis in Vosviewer

As seen in Table 6, the country with the highest number of publications in this field is China (n=360). However, when the countries are ranked according to the impact of the publications in this field, China, with an average norm. citation of 1.19, ranks 5th among the countries with the highest number of publications. The country with the highest impact of publications in this field is the United Kingdom with 213 publications and 1.53 average norm. citations. The top three countries with the most up-to-date studies in the field of ESG are China, Italy and the USA, respectively.

Moreover, this table 6 is very useful for comparing the scientific publication performance and impact of different countries. Metrics such as number of publications, number of citations, normalized citations and average publication year can be used to understand the scientific impact and relevance of each country. The United Kingdom and the United States, in particular, stand out with their high citation counts and normalized citation values, while China and India stand out with their more recent publications. These data provide important clues for evaluating and improving scientific research and publication strategies.

Keyword Analysis

A keyword analysis was carried out in order to identify the main themes that ESG publications focus on, in other words, to identify the conceptual structure of the field. There are 4,886 keywords in the articles analyzed in the study. Keywords are words that indicate the main points on which the articles focus. The keyword analysis was carried out to determine the conceptual structure of the literature in the field of ESG and to find the most emphasized themes, concepts and keywords. Table 7 shows the 10 keywords with the highest frequency and information about these keywords.

Table 7. Quantitative data on the most frequent keywords

No	Keywords	Occurrence	Average publication year
1	ESG	906	2022.20
2	Sustainability	239	2022.16
3	Esg Performance	187	2022.20
4	Corporate Social Responsibility	152	2021.30
5	Environmental	130	2021.23
6	Sustainable Development	128	2021.80
7	Esg Disclosure	115	2021.95
8	Corporate Governance	114	2021.39
9	Financial Performance	98	2021.80

As shown in Table 7, the most frequently used keywords in the literature are "ESG" (n=906), "Sustainability" (n=239) and "ESG Performance" (n=187). When analyzing the average year of publication of the most frequent keywords, "ESG", "ESG Performance" and "Sustainability" are the words with the latest average year of publication.

The network visualization of the keyword analysis, which was carried out by considering 53 keywords with a frequency of at least 20 in order to determine the areas on which the studies in this field focus, is shown in Figure 1.

As a result of the keyword co-occurrence analysis, the keywords were grouped into 6 clusters as shown in Figure 3. This indicates that studies in the field of ESG focus on 6 main topics. Each cluster in Figure 3 is shown in a different color. The size of the circles in the figure corresponds to the frequency of occurrence of the keywords. In Table 8, quantitative information about the 3 most common keywords in each cluster is given.

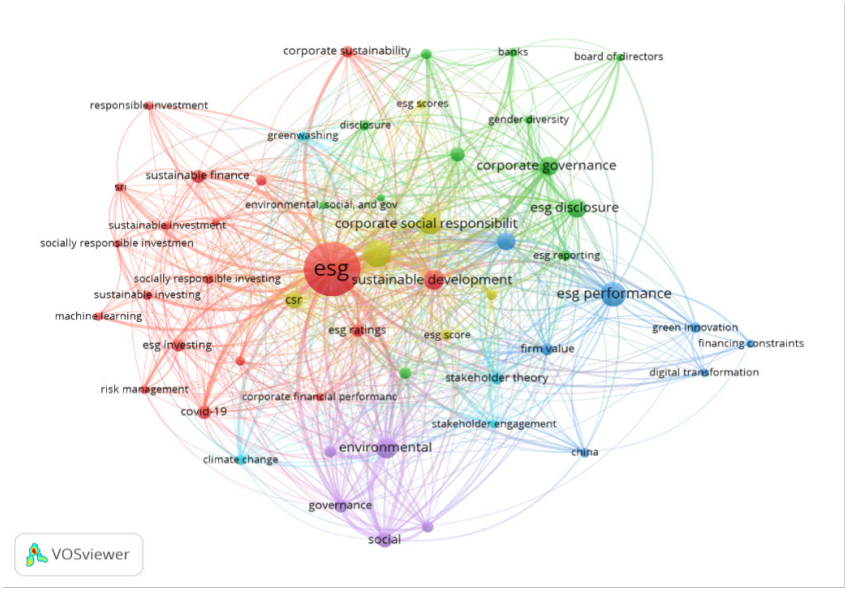


Figure 3. Network visualization for keyword analysis based on occurrence

Table 8. Quantitative data on the 3 most frequent keywords of the clusters

No	Cluster color	Most viewed 3 keywords	Frequency	Average number of citations	Average normalized number of citations	Average year of publication
1	Red	ESG	906	14.98	1	2022.20
		Sustainable Development	128	30.95	1.31	2021.80
		Sustainable Finance	57	9.68	0.80	2022.32
		Corporate Governance	114	33.18	1.24	2021.39
2	Green	ESG Disclosure	115	31.32	1.40	2021.95
		Sustainability Reporting	62	31.45	1.24	2021.37
3	Blue	ESG Performance	187	20.96	1.12	2022.20
		Financial Performance	98	37.12	1.42	2021.80
		Firm Value	52	30.79	1.08	2021.69
		Sustainability	239	22.06	0.94	2022.16
4	Yellow	Corporate Social Responsibility	152	50.82	1.40	2021.30
		Firm Performance	38	22.13	1.30	2021.89
		Environmental	130	31.55	1.08	2021.23
5	Purple	Social	73	38.77	1.32	2021.21
		Governance	57	39.26	1.34	2021.79
		Stakeholder Theory	45	24.40	0.82	2021.42
6	Light Blue	Climate Change	38	13.37	1.10	2022.42
		Green Washing	28	25.57	1.63	2022.54

The keywords in Cluster 1 are shown in red in Figure 3. As can be seen in Table 8, the most repeated keywords in this cluster are "ESG", "sustainable development" and "sustainable finance". The articles in Cluster 1 emphasize the importance of taking ESG factors into account when making investment decisions in the financial sector. The integration of ESG criteria is seen as a fundamental component of sustainable finance [46]. The literature also explores the intersection of ESG (environmental, social and governance) criteria, sustainable finance and sustainable development [47], [48].

In Figure 3, the keywords in Cluster 2 are shown in green. As can be seen in Table 8, the most repeated keywords in this cluster are “corporate governance”, “ESG disclosures” and “sustainability reporting”. The articles using the keywords in cluster 2 focus on the relationship between corporate dynamics, ESG disclosures and sustainability reporting [49], [50], [51] and the current state and shortcomings of ESG disclosures and sustainability reporting in different sectors [52].

The keywords in Cluster 3 are shown in blue in Figure 3. As shown in Table 8, the most recurring keywords in this cluster are “ESG performance”, “financial performance” and “firm value”. The articles using the keywords in this cluster generally focus on the impact of ESG performance on company value and financial performance; [53]; [54]; [55]; [56] and the impact of ESG on company financial performance [57].

The keyword group in Cluster 4 is shown in yellow in Figure 3. As can be seen in Table 8, the most repeated keywords in this cluster are “sustainability”, “corporate social responsibility” and “firm performance”. The articles in this cluster focus on the relationship between corporate social responsibility and firm performance [58], [59], [60] and the relationship between firm dynamics and corporate social responsibility [61].

In Figure 3, the keywords in Cluster 5 are coloured purple. As can be seen in Table 8, the most recurring keywords in this cluster are “environmental”, “governance” and “social”. Articles in this cluster generally examine whether ESG metrics are similar at the country level and the factors that cause ESG metrics to differ across countries [62], [63].

In Figure 3, the keywords in cluster 6 shown in light blue.

The most occurring keywords of cluster 6 are “stakeholder theory”, “climate change” and “green washing”. The articles in this cluster examine the link between stakeholder theory, climate change, and green washing and how companies shape their sustainability strategies [64], how investors react to the COP26 news [65] and how companies can take climate-friendly steps, encourage stakeholder participation and collaboration, and avoid green washing [66].

Looking at the keywords in Table 8 in terms of their average publication time, the keywords with the most recent average publication year are "green washing" (2022.54) and "climate change" (2022.42), which are in Cluster 6. Other keywords with an average publication date within 2022 are "sustainable finance" (2022.32) and "ESG" (2022.20) in Cluster 1 and "ESG performance" in Cluster 2. The overlay visualizations created by considering the average publication years of all keywords included in the keyword analysis can be seen in Figure 4. The keywords in the circles shown in purple in the figure are the keywords with the oldest average publication date. The keywords with an average publication date closer to 2024 are shown in green and the keywords closest to 2024 are shown in yellow.

As seen in Figure 4, "climate change", "green washing", "sustainable finance", "ESG", "ESG performance", "ESG rating", "sustainability performance", "funding constraints", "machine learning", "covid 19", "digital transformation", and "green innovation" are the keywords used recently. We mentioned above the average publication years and clusters of “climate change”, “green washing”, “sustainable finance”, “ESG” and “ESG performance”. As shown in Figures 3 and 4, the keywords with the most recent average publication years include machine learning (2022.77), Covid-19 (2022.49), and ESG rating (2022.29) in cluster 1; sustainability performance (2022.45) in cluster 2; and green innovation (2023.17), digital transformation (2023.13), and financing constraints (2022.82) in cluster 3.

CONCLUSION

In this study, 2,055 articles published in Scopus in the field of Business, Management and Accounting on the concepts of “ESG” and “Environmental Social and Governance” were examined and the publication trend by years; the performance of authors, articles, journals, countries and the conceptual structure of the literature were investigated.

As a result of the research, it was observed that studies on ESG have increased over the years and this increase has gained momentum since 2018. According to the 2017 US Global Change Research Program Climate Science 4th Special Report, the global warming observed in recent years and the impact of the human factor on this warming are increasing [67]. The increase in global warming and society’s growing awareness of its role in this increase can explain the increase in the number of studies written in the field of ESG. As noted in the work of [68], another important reason for the increase in the number of publications is the Covid-19 pandemic. The pandemic has highlighted the importance of ESG and led investors to focus more on non-financial factors that can affect the sustainability of companies.

According to the results of the analysis, the most productive and influential author in the field of ESG is Khaled Hussainey. The author also has the highest H-index. [24], in their study analyzing ESG documents published in the WoS database between 2004-2021, also found that Khaled Hussainey is one of the authors with the highest H-index. When analyzing the performance based on the citations received

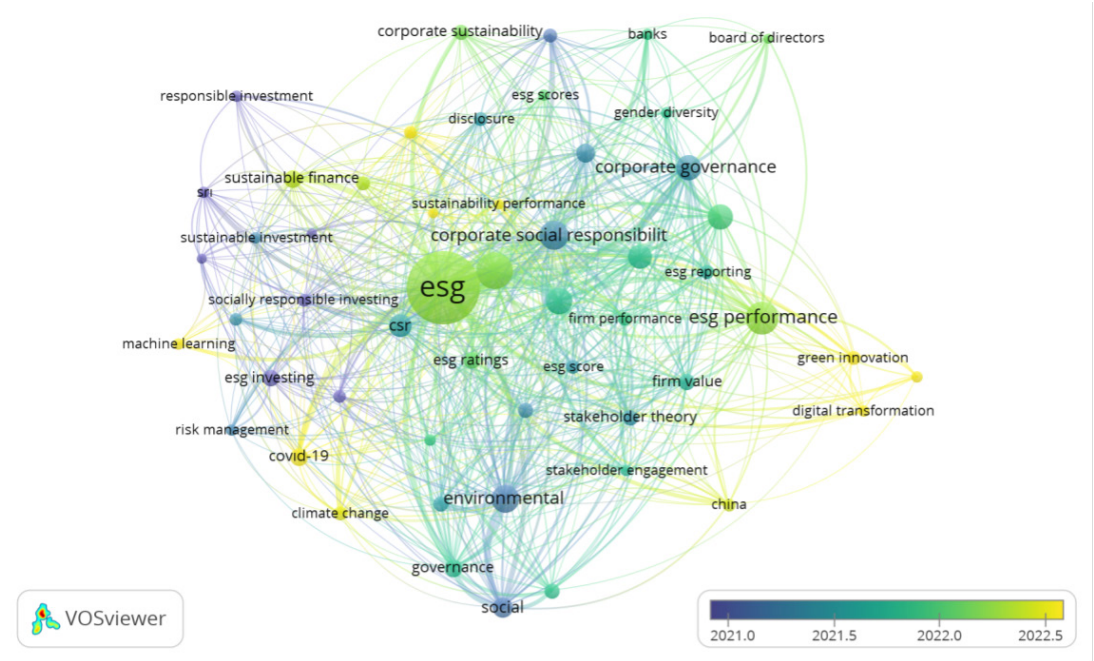


Figure 4. Overlay visualization of keyword analysis based on occurrence

for publications in this area, the most cited author is found to be George Serafeim, who has published 3 articles in this field. Among the most cited authors, the authors with the highest average normalized number of citations are Stuart L. Gillan and Andrew Koch. Laura Starks is a high-impact author, ranking 1st in h-index. Examining the publications of these authors would be beneficial to researchers conducting research in this field.

As a result of the document performance analysis, it is found that the most cited article in this field is "Corporate Social Responsibility and Access to Finance" written by "G. Serafeim, I. Ioannou; B. Cheng" in 2014. Looking at the norm. citation numbers of the articles, it can be seen that the articles titled "Firms and Social Responsibility: A Review of ESG and CSR Research in Corporate Finance" published by "S. Gillan et al." in 2021 and "Responsible Investing: The ESG-Efficient Frontier" by "Pedersen et al." in 2021 have the highest number of citations. It would be beneficial to read these articles as a priority when conducting research in this field.

When analyzing the performance of journals publishing in this field, the most productive journal (the one with the highest number of articles published in this field) is "Sustainability (Switzerland)".The journal with the highest average number of citations is the "Journal of Business Ethics". The most influential journal in this field (the one with the highest normalized number of citations) is "Journal of Business Research". "Journal of Business Research" is the most influential journal in this field. If we look at the h-index of the journals, we see that "the Journal of Business Ethics" is in first place. These journals can be the main targets for researchers in this field to publish their studies.

The country performance analysis shows that four of the countries with the highest number of ESG publications are G10 countries [68]. Looking at the number of publications, these countries are the US, the UK, Italy and Germany, and looking at the countries in terms of the average citations received by publications and normalized citations, the G10 countries are at the top. In other words, these countries are highly productive and effective in terms of publications in this field. China is the country with the highest number of publications in this field and, as we know, it does not belong to the G10. Although China ranks first in terms of productivity, its average number of citations is not very high, but it is the country with the highest number of normalized citations, as the average publication year of its publications is more recent than that of other countries. It can therefore be said that publications from China are just beginning to appear in the literature, but are influential in the field. [20], [22] found similar results in their bibliometric study of ESG documents published in WoS and Scopus. They emphasized that most ESG research is conducted in developed countries and that there is great potential for future research in developing countries.

As a result of the keyword analysis carried out to determine the conceptual structure of the field, it was found that the publications in this field are grouped into six clusters, i.e. six main themes. The focus of the articles using the keywords in these clusters can be summarized as follows:

Cluster 1: The importance of considering ESG factors when making investment decisions in the financial sector and the integration of ESG criteria as a fundamental component of sustainable finance.

Cluster 2: The relationship between corporate dynamics, ESG disclosure and sustainability reporting.

Cluster 3: The impact of ESG performance on shareholder value and financial performance.

Cluster 4: The relationship between corporate social responsibility, corporate dynamics and corporate performance.

Cluster 5: The study of ESG metrics at the country level.

Cluster 6: The link between stakeholder theory, climate change and green washing and the impact of these concepts on corporate sustainability strategies.

When examining the keywords in terms of their average publication years, the keywords with the most recent average publication years are "Sustainable finance" and "ESG" in Cluster 1, "Machine learning", "Covid-19" and "ESG rating", "ESG performance" and "Sustainability performance" in Cluster 2, "Green innovation", "Digital transformation" and "Financing constraints" in Cluster 3, "Green washing" and "Climate change" in Cluster 6. Clusters 4 and 5 have no keywords with a recent average publication year. In future studies, prioritizing topics related to the above keywords and clusters will enable the current literature to be captured and contribute to the accumulation of scientific knowledge. In addition, this study, which conducted a bibliometric analysis of articles published on ESG in the Scopus database, found that studies related to "ESG assurance" are still underrepresented in the literature. In today's world, where the importance of ESG factors for stakeholders continues to grow, providing assurance on ESG reports will reduce information asymmetry between stakeholders and companies and prevent green washing practices [69]. Future research in this area will be a contribution to the development of the literature.

It is hoped that this study will contribute to the enrichment of ESG theory and the discovery of new research areas related to ESG. As with any bibliometric study, this study has some limitations. This study has several limitations. The most critical limitation is that the analysis is carried out through the Scopus database and other databases, especially other sources that are not circulated online, are not included in the study. Another limitation of the study is the use of "titles, abstracts or keywords" as search parameters. The results of similar analyses using different search parameters may differ. Another limitation of the study is that it only includes articles. Different results may be obtained in studies using different types of documents such as books, book chapters, conference proceedings. It would be useful to extend this study to include other databases and document types in subsequent periods. In addition, future studies that examine the thematic development of the field and the structure of collaboration in the field can contribute to the literature.

DATA AVAILABILITY STATEMENT

The author confirm that the data that supports the findings of this study are available within the article. Raw data that support the finding of this study are available from the corresponding author, upon reasonable request.

CONFLICT OF INTEREST

The author declared no potential conflicts of interest with respect to the research, authorship, and/or publication of this article.

USE OF AI FOR WRITING ASSISTANCE

Not declared.

ETHICS

There are no ethical issues with the publication of this manuscript.

REFERENCES

[1] T.-T. Li, K. Wang, T. Sueyoshi, and D. D. Wang, "ESG: Research Progress and Future Prospects," Sustainability, vol. 13, no. 21, p. 11663, Oct. 2021, doi: 10.3390/su132111663.

[2] G. Dorfleitner, G. Halbritter, and M. Nguyen, "Measuring the level and risk of corporate responsibility – An empirical comparison of different ESG rating approaches," Journal of Asset Management, vol. 16, no. 7, pp. 450–466, Dec. 2015, doi: 10.1057/jam.2015.31.

[3] B. A. Alareeni and A. Hamdan, "ESG impact on performance of US S&P 500-listed firms," Corporate Governance: The International Journal of Business in Society, vol. 20, no. 7, pp. 1409–1428, Nov. 2020, doi: 10.1108/CG-06-2020-0258.

[4] T. Elbasha and E. Avetisyan, "A framework to study strategizing activities at the field level: The example of CSR rating agencies," European Management Journal, vol. 36, no. 1, pp. 38–46, Feb. 2018, doi: 10.1016/j.emj.2017.02.001.

[5] M. Cappucci, "The ESG Integration Paradox," Journal of Applied Corporate Finance, vol. 30, no. 2, pp. 22–28, Spring/Summer 2018, doi: 10.1111/jacf.12296.

[6] A. Buallay, "Is sustainability reporting (ESG) associated with performance? Evidence from the European banking sector," Management of Environmental Quality: An International Journal, vol. 30, no. 1, pp. 98–115, Jan. 2019, doi: 10.1108/MEQ-12-2017-0149.

[7] G. T. Garvey, J. Kazdin, R. LaFond, J. Nash, and H. Safa, "A Pitfall in Ethical Investing: ESG Disclosures Reflect Vulnerabilities, Not Virtues," Journal of Investment Management, vol. 15, no. 2, pp. 51–64, 2017.

[8] E. Avetisyan and K. Hockerts, "The Consolidation of the ESG Rating Industry as an Enactment of Institutional Retrogression," Business Strategy and the Environment, vol. 26, no. 3, pp. 316–330, Mar. 2017, doi: 10.1002/bse.1919.

[9] Y. Tan and Z. Zhu, "The effect of ESG rating events on corporate green innovation in China: The mediating role of financial constraints and managers' environmental awareness," Technology in Society, vol. 68, p. 101906, Feb. 2022, doi: 10.1016/j.techsoc.2022.101906.

[10] R. Atan, F. A. Razali, J. Said, and S. Zainun, "Environmental, Social and Governance (ESG) Disclosure and Its Effect on Firm's Performance: A Comparative Study," International Journal of Economics and Management, vol. 10, no. S2, pp. 355–375, 2016.

[11] J. Feng, J. W. Goodell, and D. Shen, "ESG rating and stock price crash risk: Evidence from China," Finance Research Letters, vol. 46, p. 102476, May 2022, doi: 10.1016/j.frl.2021.102476.

[12] B. Cheng, I. Ioannou, and G. Serafeim, "Corporate social responsibility and access to finance," Strategic Management Journal, vol. 35, no. 1, pp. 1–23, Jan. 2014, doi: 10.1002/smj.2131.

[13] G. Friede, T. Busch, and A. Bassen, "ESG and financial performance: aggregated evidence from more than 2000 empirical studies," Journal of Sustainable Finance and Investment, vol. 5, no. 4, pp. 210–233, Oct. 2015, doi: 10.1080/20430795.2015.1118917.

[14] J. Xie, W. Nozawa, M. Yagi, H. Fujii, and S. Managi, "Do environmental, social, and governance activities improve corporate financial performance?," Business Strategy and the Environment, vol. 28, no. 2, pp. 286–300, Feb. 2019, doi: 10.1002/bse.2224.

[15] D. Y. Tang and Y. Zhang, "Do shareholders benefit from green bonds?," Journal of Corporate Finance, vol. 61, p. 101427, Apr. 2020, doi: 10.1016/j.jcorpfin.2018.12.001.

[16] H. G. Gündoğdu, A. Aytekin, Ş. Toptancı, S. Korucuk, and Ç. Karamaşa, "Environmental, social, and governance risks and environmentally sensitive competitive strategies: A case study of a multinational logistics company," Business Strategy and the Environment, vol. 32, no. 7, pp. 4874–4906, Nov. 2023, doi: 10.1002/bse.3398.

[17] A. Azimli and K. Cek, "Can sustainability performance mitigate the negative effect of policy uncertainty on the firm valuation?," Sustainability Accounting, Management and Policy Journal, vol. 15, no. 3, pp. 752–775, Apr. 2024, doi: 10.1108/SAMPJ-09-2022-0464.

[18] Ç. Vural-Yavaş, "Economic policy uncertainty, stakeholder engagement, and environmental, social, and governance practices: The moderating effect of competition," Corporate Social Responsibility and Environmental Management, vol. 28, no. 1, pp. 82–102, Jan. 2021, doi: 10.1002/csr.2034.

[19] T. S. Legendre, A. Ding, and K.-J. Back, "A bibliometric analysis of the hospitality and tourism environmental, social, and governance (ESG) literature," Journal of Hospitality and Tourism Management, vol. 58, pp. 309–321, Mar. 2024, doi: 10.1016/j.jhtm.2024.01.003.

[20] M. S. Khamisu and A. R. Paluri, "What's past is prologue: reminiscing research on environment social governance (ESG) disclosures," International Journal of Disclosure and [21] X. Zhao, D. Nan, C. Chen, S. Zhang, S. Che, and J. H. Kim, "Bibliometric study on environmental, social, and governance research using CiteSpace," Frontiers in Environmental Science, vol. 10, p. 1087493, Jan. 2023, doi: 10.3389/fenvs.2022.1087493.

[22] K. Jain and P. S. Tripathi, "Mapping the environmental, social and governance literature: a bibliometric and content analysis," Journal of Strategy and Management, vol. 16, no. 3, pp. 397–428, Aug. 2023, doi: 10.1108/JSMA-05-2022-0092.

[23] G. Wan, A. Y. Dawod, S. Chanaim, and S. S. Ramasamy, "Hotspots and trends of environmental, social and governance (ESG) research: a bibliometric analysis," Data Science and Management, vol. 6, no. 2, pp. 65–75, Jun. 2023, doi: 10.1016/j.dsm.2023.03.001.

[24] G. Wan, Y. D. Ahmad, and C. Nopasit, "A Bibliometric and Visual Analysis in the Field of Environment Social and Governance (ESG) Between 2004 and 2021," International Journal of Information Science and Management, vol. 21, no. 2, Apr. 2023, doi: 10.22034/ijism.2023.1977765.0.

[25] S. S. Senadheera, R. Gregory, J. Rinklebe, M. Farrukh, J. H. Rhee, and Y. S. Ok, "The development of research on environmental, social, and governance (ESG): A bibliometric analysis," Sustainable Environment, vol. 8, no. 1, p. 2125869, Dec. 2022, doi: 10.1080/27658511.2022.2125869.

[26] S. Galletta, S. Mazzù, and V. Naciti, "A bibliometric analysis of ESG performance in the banking industry: From the current status to future directions," Research in International Business and Finance, vol. 62, p. 101684, Dec. 2022, doi: 10.1016/j.ribaf.2022.101684.

[27] N. O. D. Ellili, "Bibliometric analysis and systematic review of environmental, social, and governance disclosure papers: current topics and recommendations for future research," Environmental Research Communications, vol. 4, no. 9, p. 092001, Sep. 2022, doi: 10.1088/2515-7620/ac8b67.

[28] H.-J. Siao, S.-H. Gau, J.-H. Kuo, M.-G. Li, and C.-J. Sun, "Bibliometric Analysis of Environmental, Social, and Governance Management Research from 2002 to 2021," Sustainability, vol. 14, no. 23, p. 16121, Dec. 2022, doi: 10.3390/su142316121.

[29] S. Gao, F. Meng, Z. Gu, Z. Liu, and M. Farrukh, "Mapping and Clustering Analysis on Environmental, Social and Governance Field: A Bibliometric Analysis Using Scopus," Sustainability, vol. 13, no. 13, p. 7304, Jun. 2021, doi: 10.3390/su13137304.

[30] P. Dzikowski, "A bibliometric analysis of born global firms," Journal of Business Research, vol. 85, pp. 281–294, Apr. 2018, doi: 10.1016/j.jbusres.2017.12.054. Governance, Mar. 2024, doi: 10.1057/s41310-024-00231-w.

[31] N. Donthu, S. Kumar, D. Mukherjee, N. Pandey, and W. M. Lim, "How to conduct a bibliometric analysis: An overview and guidelines," Journal of Business Research, vol. 133, pp. 285–296, Sep. 2021, doi: 10.1016/j.jbusres.2021.04.070.

[32] R. N. Broadus, "Toward a definition of 'bibliometrics'," Scientometrics, vol. 12, no. 5–6, pp. 373–379, Nov. 1987, doi: 10.1007/BF02016680.

[33] M. Visser, N. J. Van Eck, and L. Waltman, "Large-scale comparison of bibliographic data sources: Scopus, Web of Science, Dimensions, Crossref, and Microsoft Academic," Quantitative Science Studies, vol. 2, no. 1, pp. 20–41, Apr. 2021, doi: 10.1162/qss_a_00112.

[34] J. E. Hirsch, "An index to quantify an individual's scientific research output," Proceedings of the National Academy of Sciences, vol. 102, no. 46, pp. 16569–16572, Nov. 2005, doi: 10.1073/pnas.0507655102.

[35] H. K. Baker, S. Kumar, and N. Pandey, "Forty years of the Journal of Futures Markets: A bibliometric overview," Journal of Futures Markets, vol. 41, no. 7, pp. 1027–1054, Jul. 2021, doi: 10.1002/fut.22211.

[36] M. A. Khan, D. Pattnaik, R. Ashraf, I. Ali, S. Kumar, and N. Donthu, "Value of special issues in the journal of business research: A bibliometric analysis," Journal of Business Research, vol. 125, pp. 295–313, Mar. 2021, doi: 10.1016/j.jbusres.2020.12.015.

[37] N. J. Van Eck and L. Waltman, "Software survey: VOSviewer, a computer program for bibliometric mapping," Scientometrics, vol. 84, no. 2, pp. 523–538, Aug. 2010, doi: 10.1007/s11192-009-0146-3.

[38] Y.-D. Liang, Y. Li, J. Zhao, X.-Y. Wang, H.-Z. Zhu, and X.-H. Chen, "Study of acupuncture for low back pain in recent 20 years: a bibliometric analysis via CiteSpace," Journal of Pain Research, vol. 10, pp. 951–964, Apr. 2017, doi: 10.2147/JPR.S132808.

[39] D. Chen, Z. Liu, Z. Luo, M. Webber, and J. Chen, "Bibliometric and visualized analysis of emergy research," Ecological Engineering, vol. 90, pp. 285–293, May 2016, doi: 10.1016/j.ecoleng.2016.01.026.

[40] S. L. Gillan, A. Koch, and L. T. Starks, "Firms and social responsibility: A review of ESG and CSR research in corporate finance," Journal of Corporate Finance, vol. 66, p. 101889, Feb. 2021, doi: 10.1016/j.jcorpfin.2021.101889.

[41] S. Drempetic, C. Klein, and B. Zwergel, "The Influence of Firm Size on the ESG Score: Corporate Sustainability Ratings Under Review," Journal of Business Ethics, vol. 167, no. 2, pp. 333–360, Nov. 2020, doi: 10.1007/s10551-019-04164-1.

[42] L. H. Pedersen, S. Fitzgibbons, and L. Pomorski, "Responsible investing: The ESG-efficient fron-

tier," Journal of Financial Economics, vol. 142, no. 2, pp. 572–597, Nov. 2021, doi: 10.1016/j.jfineco.2020.11.001.

[43] L. Pastor, R. F. Stambaugh, and L. A. Taylor, "Sustainable Investing in Equilibrium," unpublished manuscript. [Publication details needed – please verify journal or source].

[44] A. S. Garcia, W. Mendes-Da-Silva, and R. J. Orsato, "Sensitive industries produce better ESG performance: Evidence from emerging markets," Journal of Cleaner Production, vol. 150, pp. 135–147, May 2017, doi: 10.1016/j.jclepro.2017.02.180.

[45] N. Cucari, S. Esposito De Falco, and B. Orlando, "Diversity of Board of Directors and Environmental Social Governance: Evidence from Italian Listed Companies," Corporate Social Responsibility and Environmental Management, vol. 25, no. 3, pp. 250–266, May 2018, doi: 10.1002/csr.1452.

[46] A. K. Singh, Y. Zhang, and Anu, "Understanding the Evolution of Environment, Social and Governance Research: Novel Implications From Bibliometric and Network Analysis," Evaluation Review, vol. 47, no. 2, pp. 350–386, Apr. 2023, doi: 10.1177/0193841X221121244.

[47] M. J. Muñoz-Torres, M. Á. Fernández-Izquierdo, J. M. Rivera-Lirio, and E. Escrig-Olmedo, "Can environmental, social, and governance rating agencies favor business models that promote a more sustainable development?," Corporate Social Responsibility and Environmental Management, vol. 26, no. 2, pp. 439–452, Mar. 2019, doi: 10.1002/csr.1695.

[48] L. Huang, "Green bonds and ESG investments: Catalysts for sustainable finance and green economic growth in resource-abundant economies," Resources Policy, vol. 91, p. 104806, Apr. 2024, doi: 10.1016/j.resourpol.2024.104806.

[49] M. Arayssi, M. Dah, and M. Jizi, "Women on boards, sustainability reporting and firm performance," Sustainability Accounting, Management and Policy Journal, vol. 7, no. 3, pp. 376–401, Sep. 2016, doi: 10.1108/SAMPJ-07-2015-0055.

[50] F. Bravo and N. Reguera-Alvarado, "Sustainable development disclosure: Environmental, social, and governance reporting and gender diversity in the audit committee," Business Strategy and the Environment, vol. 28, no. 2, pp. 418–429, Feb. 2019, doi: 10.1002/bse.2258.

[51] I. Zumente and N. Lāce, "Understanding Corporate Sustainability Drivers Across Corporate Life Cycle," presented at the 14th International Multi-Conference on Complexity, Informatics and Cybernetics (IMCIC), Virtual Conference, Mar. 2023, pp. 168–175, doi: 10.54808/IMCIC2023.01.168.

[52] R. Y. J. Siew, "Critical Evaluation of Environmental, Social and Governance Disclosures of Malaysian Property and Construction Companies," Construction Economics and Building, vol. 17, no. 2, pp. 81–91, Jun. 2017, doi: 10.5130/AJCEB.v17i2.5328.

[53] Y.-M. Tan, K. Szulczyk, and Y.-H. Sii, "Performance of ESG-integrated smart beta strategies in Asia-Pacific stock markets," Research in International Business and Finance, vol. 66, p. 102008, Oct. 2023, doi: 10.1016/j.ribaf.2023.102008.

[54] A. M. Habib, "Does real earnings management affect a firm's environmental, social, and governance (ESG), financial performance, and total value? A moderated mediation analysis," Environment, Development and Sustainability, Aug. 2023, doi: 10.1007/s10668-023-03809-6.

[55] W. Cho, J. Lee, and J. Park, "Higher highs and lower lows: investor valuation of ESG and financial performance," Applied Economics Letters, pp. 1–6, Mar. 2023, doi: 10.1080/13504851.2023.2193720.

[56] A. Srivastava and A. Anand, "ESG performance and firm value: The moderating role of ownership concentration," Corporate Ownership and Control, vol. 20, no. 3, pp. 169–179, 2023, doi: 10.22495/cocv20i3art11.

[57] S. Chen, Y. Song, and P. Gao, "Environmental, social, and governance (ESG) performance and financial outcomes: Analyzing the impact of ESG on financial performance," Journal of Environmental Management, vol. 345, p. 118829, Nov. 2023, doi: 10.1016/j.jenvman.2023.118829.

[58] L. Kong, M. Akbar, and P. Poulova, "The Role of Environment, Social, and Governance Performance in Shaping Corporate Current and Future Value: The Case of Global Tech Leaders," Sustainability, vol. 15, no. 17, p. 13114, Aug. 2023, doi: 10.3390/su151713114.

[59] A. K. Widagdo, S. Murni, S. Nurlaela, and Rahmawati, "Corporate social responsibility, earnings management, and firm performance: Are the companies really ethical?," IOP Conference Series: Earth and Environmental Science, vol. 824, no. 1, p. 012118, Jul. 2021, doi: 10.1088/1755-1315/824/1/012118.

[60] P. Choongo, "A Longitudinal Study of the Impact of Corporate Social Responsibility on Firm Performance in SMEs in Zambia," Sustainability, vol. 9, no. 8, p. 1300, Jul. 2017, doi: 10.3390/su9081300.

[61] M. S. Sial, F. Chunmei, M. H. Khan, H. K. Nguyen, and F. Z. Comite, "Does Corporate Social Responsibility Mediate the Relation between Boardroom Gender Diversity and Firm Performance of Chinese Listed Companies?," Sustainability, vol. 10, no. 10, p. 3591, Oct. 2018, doi: 10.3390/su10103591.

[62] H. R. Mian, K. Hewage, and R. Sadiq, "Responsible financing and investment: identification, development, and assessment of Environmental, Social, and Governance (ESG) metrics," Sustainable Futures, vol. 8, p. 100246, Dec. 2024, doi: 10.1016/j.sftr.2024.100246.

[63] P. Patsoulis and D. Demetriou, "Assessing the convergence process of ESG metrics: a research note on the role of economic freedom," Letters in Spatial and Resource Sciences, vol. 17, no. 1, p. 18, Dec. 2024, doi: 10.1007/s12076-024-00383-x.

[64] S. L. Bager and E. F. Lambin, "Sustainability strategies by companies in the global coffee sector," Business Strategy and the Environment, vol. 29, no. 8, pp. 3555–3570, Dec. 2020, doi: 10.1002/bse.2596.

[65] X. Ge, M. Xue, and R. Cao, "Do Chinese carbon-intensive stocks overreact to climate transition risk? Evidence from the COP26 news," International Review of Financial Analysis, vol. 94, p. 103334, Jul. 2024, doi: 10.1016/j.irfa.2024.103334.

[66] A.-S. Gay, J. M. Warden, and H. Lane, "Climate labels and the restaurant industry: a qualitative study," Environmental Systems and Decisions, vol. 44, no. 2, pp. 369–379, Jun. 2024, doi: 10.1007/s10669-023-09919-w.

[67] U.S. Global Change Research Program et al., Climate Science Special Report: Fourth National Climate Assessment, Volume I, U.S. Global Change Research Program, 2017, doi: 10.7930/J0J964J6.

[68] World Population Review, "G10 Countries 2024," Accessed: Aug. 2, 2024. [Online]. Available: https://worldpopulationreview.com/country-rankings/g10-countries

[69] B. Gipper, S. Ross, and S. Shi, "ESG Assurance in the United States," SSRN Electronic Journal, 2022, doi: 10.2139/ssrn.4263085.

Environ Res Tec, Vol. 8, Issue. 2, pp. 315-327, June 2025

Environmental Research and Technology
https://dergipark.org.tr/en/pub/ert
DOI: https://10.35208/ert.1510237

Research Article

A Comprehensive study on adsorption kinetics and equilibrium: Utilizing olive mill by-products as a sustainable biosorbent for cobalt (II) removal

Khaled Muftah ELSHERIF*[1,2], Abdunaser Mabrok EWLAD-AHMED[3], Abdelmeneim EL-DALI[1,2], Rima Abdessalam SAAD[3], Abdullah A. TREBAN[3]

[1]Libyan authority for scientific research, Tripoli, Libya,
[2]Chemistry Department, Faculty of Science, University of Benghazi, Benghazi, Libya
[3]Chemistry Department, Faculty of Arts and Science Msallata, Elmergib University, Al-Khoms, Libya

ARTICLE INFO

Article history
Received: 12 Jul 2024
Revised: 27 Aug 2024
Accepted: 30 Aug 2024

Key words:
Biosorbent, co(II), adsorption, isotherms, kinetic

ABSTRACT

Aiming to remove cobalt from wastewater in a sustainable manner, this work marks a major advancement in industrial and technological advancements. We study if dried olive mill solid residues (DOMSR), a byproduct of the olive oil business, may effectively remove Co(II) ions from aqueous solutions by acting as a biosorbent. We have been able to offer useful insights by carefully analyzing the adsorption process and optimizing crucial variables such contact time, pH levels, initial metal concentration, and adsorbent dosage. Our experimental results demonstrate that higher initial cobalt concentrations increased the adsorption capacity, reaching a maximum of 120 mg/L. At pH 6.0, the maximum removal percentage was 82%, and the optimum adsorption achieved after 40 min of contact time. The adsorption process was best described by the pseudo-second-order model, according to kinetic studies, suggesting that chemisorption is the rate-limiting stage. The best fit was given by the Langmuir isotherm model (R^2=0.9948), which indicated homogenous active sites and a maximal sorption capacity (Q_m) of 41.84 mg/g. This research underscores the potential of agricultural waste-based biosorbents like OMSR for efficient cobalt removal, thereby offering a valuable contribution to sustainable wastewater treatment practices and environmental conservation.

Cite this article as: Elsherif KM, Ewlad-Ahmed AM, El-Dali A, Saad RA, Treban AA. A comprehensive study on adsorption kinetics and equilibrium: Utilizing olive mill by-products as a sustainable biosorbent for cobalt (II) removal. Environ Res Tec 2025;8(2) 315-327.

INTRODUCTION

The industrial and digital revolutions have marked significant milestones in human history, leading to an increasing demand for specialty elements like cobalt across various industries. This demand has been particularly driven by the growth of electronic devices, electric vehicles, and renewable energy technologies, all of which rely heavily on cobalt for the production of lithium-ion batteries and other essential components. As a result, heavy metal ions such as cobalt, copper, nickel, and zinc are frequently detected in the waste streams from industries such as electronics manufacturing, electroplating, petrochemicals, mining operations, tanneries, and textile production. The widespread use of these metals in modern industrial processes underscores the importance of developing efficient methods for their removal from wastewater to mitigate environmental impact [1].

***Corresponding author.**
*E-mail address: elsherif27@yahoo.com

This is an open access article under the CC BY-NC license (http://creativecommons.org/licenses/by-nc/4.0/).

It was predicted that the price of cobalt would rise around five times between 2015 and 2018 due to the high demand, particularly from the automotive and technology sectors [2]. Because of increasing demand and value for cobalt, the mining sector has grown to be extremely profitable for governments and investors around the world [3]. According to projections, the world's cobalt demand is predicted to rise dramatically from 50 kT yearly in 2007 to 110 kT annually by 2030[4]. However, research has revealed that the present supply chains and mining practices for cobalt are not only unsustainable but also seriously dangerous for the environment because of uncontrolled industrial processes, depleted reserves, and unequal resource distribution [5]. These methods have resulted in the depletion of limited raw resources and water contamination, exceeding the permissible cobalt thresholds for both human (above 0.05 mg/L) and livestock (above 1 mg/L) consumption in irrigation water [6,7]. The World Health Organisation (WHO) has established that 2 µg/L is the highest level of cobalt ions that can be present in drinking water [3]. The development of workable and effective methods for removing cobalt (II) ions from water sources that are contaminated and cleaning and sanitising industrial effluent requires quick action [8].

To remove heavy metals, a variety of technologies are frequently used, including coagulation, chemical precipitation, adsorption, nanofiltration, ion exchange with resins, and other methods [9–20]. Among these, adsorption is considered the most effective method. Adsorption is a physicochemical process where mass transfers between a solid surface and a fluid phase, effectively removing metals at low concentrations. This technique is particularly suitable for extracting and recovering metal ions from wastewater, as it is user-friendly, cost-effective, and allows for the regeneration of the adsorbent through various methods [21]. Extensive research has been conducted on various adsorbents for wastewater purification, including carbonaceous, cellulose, biochar materials, and different agricultural wastes [22-30]. Because of its pore structure, which offers a lot of surface area for physical adsorption, and its innate functional groups, which may allow for chemical adsorption of heavy metal ions, biochar in particular has grown in popularity [31]. Additionally, there is a rising trend in using biosorbent materials for metal recovery due to their natural abundance, cost-effectiveness, and sustainability. This could reduce the overall cost of the adsorption process and enhance its overall value [32].

The effective use of waste products from both the agricultural and industrial industries has had a significant impact on the development of efficient and sustainable adsorption treatment methods. As a result, numerous adsorbents have been developed [33]. Waste from agriculture that are widely accessible and can be sourced responsibly have shown promise as viable and affordable substitutes for removing cobalt ion contaminants [34]. These agricultural waste materials have not only demonstrated their efficacy in effectively eliminating cobalt ions but also provided an environmentally friendly solution, thereby significantly contributing to the use of sustainable practices.

Numerous studies have focused on the removal of Co(II) ions from aqueous solutions using a variety of adsorbent materials, each offering unique benefits and mechanisms. Amoo et al. [3] explored the use of cow bone (CB), cow bone char (CBC), and activated cow bone carbon (ACBC) as adsorbents, finding that these materials, characterized by mesoporosity and hydroxyapatite properties, effectively removed Co^{2+} ions. The adsorption process for ACBC was driven by strong electrostatic attraction, with a pseudo second-order kinetic model indicating chemisorption. Thermodynamic analysis revealed different behaviors, with ACBC showing endothermic and non-spontaneous adsorption, while CB and CBC exhibited exothermic and physisorptive properties. Similarly, Demirbas [7] studied the adsorption of Co(II) using activated carbon derived from hazelnut shells. The process followed a pseudo-second-order kinetic model and was pH-dependent, with optimal adsorption capacity observed at 13.88 mg Co(II)/g. The thermodynamic analysis also indicated an endothermic nature of adsorption. Elsherif et al. [13] investigated tea and coffee powders as low-cost and environmentally friendly adsorbents, with adsorption influenced by various factors such as contact time and pH. The Langmuir isotherm model best described the equilibrium data, showing high maximum adsorption capacities of 244 mg/g for both adsorbents. Conte et al. [21] optimized the synthesis of mesoporous activated carbon using a factorial design, identifying conditions that enhanced cobalt removal through the formation of surface oxygenated groups. The rapid adsorption process reached equilibrium in just 15 minutes, and desorption studies highlighted the potential for effective cobalt recovery using sulfuric acid. Ghanavati et al. [22] explored the potential of MgO nanoparticles deposited on chitosan for Co(II) ion removal. Their study, involving a batch adsorption test system, showed that the adsorption process followed both first and second-order kinetic models and was effectively described by Freundlich and Langmuir isotherms. Thermodynamic analysis further demonstrated the suitability of this adsorbent for heavy metal remediation. Together, these studies underscore the diverse approaches and materials available for efficient Co(II) ion removal from aqueous environments.

This study sought to assess the efficacy of Dried Olive Mill Solid Residues (DOMSR), a by-product of the olive oil industry, as a novel and sustainable adsorbent for cobalt removal from aqueous solutions. Unlike conventional adsorbents, DOMSR offers an environmentally friendly and cost-effective alternative by utilizing waste material, thereby contributing to waste valorization and sustainable water treatment practices. The research effort focused on optimizing key parameters that govern the cobalt adsorption process, including contact time, pH, initial metal concentration, and adsorbent dosage. In addition, this study provides a comprehensive evaluation of the adsorption behavior by employing various adsorption isotherms and kinetic models, which were rigorously applied to accurately depict the equilibrium and kinetic data obtained from experimental trials. This in-

novative approach not only addresses the pressing issue of industrial wastewater management but also demonstrates the potential of DOMSR as a highly effective adsorbent for heavy metal removal, setting the stage for future applications in environmental remediation

MATERIALS AND METHODS

Chemicals and Regents

The chemicals used in this experiment were carefully provided by Sigma-Aldrich Co. (Merck, Darmstadt, Germany). These chemicals, including sodium hydroxide pellets (≥98.0-100.5%), hydrochloric acid (37%), nitric acid (70%), and potassium thiocyanate (99%), were of the highest quality. Deionized water, crucial for maintaining the purity of the solutions, was obtained from a Labtech Ultra-Pure Water Deionizer. The stock solution of Cobalt (II) ions, a key component of our study, was prepared with utmost care using Cobalt(II) chloride hexahydrate (98%), also purchased from Sigma-Aldrich Co. (Merck, Darmstadt, Germany). All compounds used in the study were of analytical grade, ensuring the accuracy and reliability of our results. The solutions were freshly prepared and stored at room temperature (25°C).

Preparation of adsorbents

For this study, we collected olive mill solid residue from local mills in Msallata, Libya. This solid residue was then processed into a powder called DOMSR (Dried Olive Mill Solid Residue), which served as our adsorbent material. There were multiple phases required in getting DOSR ready. To get rid of any contaminants, we first rinsed the solid olive residue with distilled water. After that, we dried it for a full day at 70°C in an electric oven. Following the drying process, the residues were ground and sieved to create a fine powder with an average particle size of less than 125 µm. After that, the powder was carefully kept in glass vials that were sealed until it was time to employ it as an adsorbent to extract cobalt ions. A digital photograph, shown in Fig. 1, provides a visual depiction of the sieved biosorbent. The photograph includes (a) the Olive Mill Solid Residues (OMSR) after cleaning, and (b) the prepared powder (DOMSR), which serves as the biosorbent.

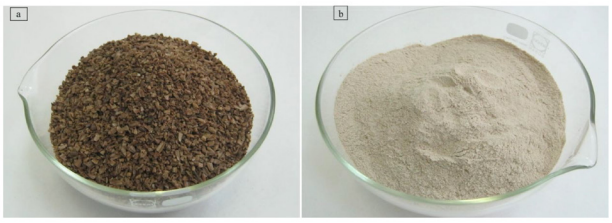


Figure 1. a) Olive mill solid residues (OMSR) and b) the prepared powder (DOMSR)

Metal ion determination

The concentrations of metal ions in the solutions and their levels in the aqueous solutions before and after adsorption were measured using the state-of-the-art JENWAY Molecular Absorption Spectrophotometer 6305. Another cutting-edge instrument used to regulate the pH of the solution—a crucial component of our experiment—was the JENWAY pH Metre 3505. The method described in an earlier publication [13] was used to determine cobalt (II) as a thiocyanate complex, guaranteeing the accuracy and repeatability of our findings. A blue colored complex was formed by adding 2.0 mL of (4M) concentrated potassium thiocyanate solution to a 5.0 mL Co(II) solution. To ensure the stability of the cobalt-thiocyanate complex, the solution was prepared in a 1:1 mixture of water and acetone since the complex is not stable in pure water. Additionally, the solution was acidified with 10% nitric acid (1 mL) to maintain the required acidic environment for optimal complex formation. The resulting solution's absorbance was measured at 620 nm using a spectrophotometer [13]. To enhance the accuracy of our measurements, calibration curves for metal ions were developed using stock solutions with concentrations ranging from 5 to 40 mg/L.

Adsorption procedure

The batch adsorption technique was used to adsorb cobalt(II) ions from an aqueous solution. Here's a detailed explanation of the process: A known initial concentration of Co(II) in a 50-mL solution was combined with a preset amount of DOMSR in 150-mL Erlenmeyer flasks. A blank solution devoid of Co ions was also added to account for adsorption by the adsorbent. Each flask was then covered with parafilm to prevent any external contamination. The mixture was then shaken at 175 rpm for a specific amount of time in a temperature-controlled incubator set at 25°C with a shaking platform. The supernatant and adsorbent were separated via filtration. The Co(II)-SCN complex was measured with a UV-VIS spectrophotometer to ascertain the beginning and ultimate concentrations of cobalt(II). Finally, the adsorption efficiency (%R) and capacity (Qe) were calculated. as follows:

$$\%R = \frac{C_0 - C_e}{C_0} \times 100 \quad (1)$$

$$Q_e = \frac{(C_0 - C_e) \times V}{M} \quad (2)$$

In the equations, Co and Ce (in mg/L) stand for the initial and ultimate equilibrium concentrations of Co(II). The mass of the biosorbent is specified as M (in g), and the volume of the solution is stated as V (in L). Three runs of the experiments were made, and the average values are shown here with the matching standard deviations.

The investigation examined the effects of adsorbent dose, starting concentration, pH, and contact time on the extraction of CO_2+ ions from aqueous solutions. Ideal numbers were found and applied to the kinetics and equilibrium investigations. The adsorbate suspension was supplemented with 0.1 M HCl or 0.1 M NaOH as needed to adjust values within the pH range of 2 to 9. On the other hand, solution samples were obtained for the kinetics analyses at regular intervals (0–60 min), and the cobalt (II) ion concentration was tracked throughout time. To optimise the design of an

adsorption system for the removal of adsorbate, equilibrium adsorption data must be recorded. 50 mL of Co(II) solutions were mixed with the same amount of DOMSR to get the equilibrium adsorption isotherm data. Co(II) ions concentrations in the tests ranged from 10 mg/L to 120 mg/L, and 150 mL Erlenmeyer flasks with the proper pH were used for the studies. It was also looked at how different adsorbent doses, from 0.05 g to 1.00 g, affected the removal of Co(II) ions through adsorption.

RESULTS AND DİSCUSSİON

Influence of pH on adsorption

The rate at which surface reactions occur is largely dependent on the pH level of the solution. The primary reason for the variations in adsorption capacity within a designated pH range is the impact of pH on the surface adsorption characteristics of DOMSR. The change in Co(II) ion removal effectiveness from 2 to 9 pH values is shown in Fig. 2. At pH 2.0, the observed elimination percentage was just 71%. On the other hand, elimination efficiency increased significantly from pH 2.0 to 6.0 (82%). Because the binding locations were positively charged by H+ ions, the adsorption of Co(II) ions was restricted at low pH values, such as 2.0. Electrostatic repulsion prevented the Co(II) ions from attaching to the adsorbent surface as a result of the positive charge on the binding sites. Furthermore, Co(II) species are exclusively found in the divalent ionic form within this pH range. reduced pH values resulted in reduced Co(II) absorption because H+ ions and CO_2+ ions competed for the negatively charged adsorption sites [35, 36].

The concentration of H+ ions in the solution dropped as the pH rose to 5–6. As a result, there were more negatively charged binding sites available for adsorption, and because of their electrostatic attractions, the absorption of CO_2+ increased significantly [37]. This explains why elimination increased steadily beginning at pH 3.0. The maximum clearance percentage of 82% was noted at pH 6.0, suggesting that pH 6.0 is the ideal value for the elimination of Co(II).

However, the overall efficacy of Co(II) ion removal is decreased in the high pH zone (7-9) when several ionic forms of Co(II) are present, such as Co(OH)3, Co(OH)2, and Co(OH)+[7,38]. The adsorption effectiveness keeps rising as the pH rises above this threshold, continuing until the metal ions precipitate (pH > 8) as a result of the precipitate of cobalt hydroxide forming.

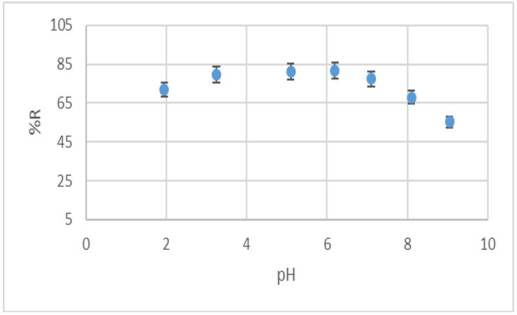


Figure 2. Impact of pH on Co(II) adsorption

Influence of adsorbent dosage

The dose of the adsorbent is important in the field of adsorption research. It establishes the highest amount of metal ions that the adsorbent is capable of removing for a specific solution concentration. Fig. 3 illustrates how increasing the adsorbent dosage from 0.05 to 1 g/50 mL results in an increase in the percentage of Co(II) removal from 66.20% to 84.80%. But from 26.50 mg/g to 1.70 mg/g, the adsorption capability drops. The greater surface area of the adsorbent and the existence of more binding sites are responsible for the higher percentage removal. On the other hand, the adsorbent particles' tendency to aggregate may be the cause of the decline in adsorption capacity, which leads to the overlapping of adsorption sites and a decrease in the surface area that is available for Co(II). Co(II) has a longer diffusion path to the adsorption sites as a result [13, 14]. It is noteworthy that despite a nearly twofold increase in DOMSR dosage (0.6 to 1 g/50 mL), there was no discernible increase in the elimination %. It barely went up to 84.80% from 82.20%. As a result, 0.5 g/50 mL is the most economical adsorbent dosage.

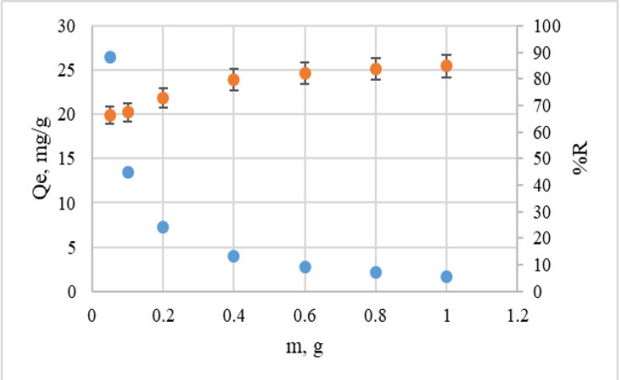


Figure 3. Impact of adsorbent dosage on Co(II) adsorption

Influence of contact time

Determining the equilibrium time is crucial in adsorption studies as it defines the point at which the adsorbent reaches its maximum sorption capacity. This information is essential for designing adsorption systems with appropriate residence times and making informed decisions about time-dependent variables related to the adsorption process [39, 40]. Fig. 4 illustrates the effect of contact duration on the removal efficiency of Co^{2+} ions by the adsorbents. The results indicate a rapid increase in Co^{2+} ion removal during the first 30 minutes, which is attributed to the high concentration gradient between the Co^{2+} ions in the solution and the available sorption sites on the adsorbent [41, 42]. After this initial period, the removal rate begins to decline and eventually levels off. This plateau is primarily due to the gradual saturation of the adsorbent's active sites, leading to a reduced removal rate as the system approaches equilibrium. Fig. 4 confirms that after 40 minutes, the adsorbents achieve saturation, and the percentage of Co^{2+} ions removed stabilizes [43]. This equilibrium is largely a result of the diminishing van der Waals forces between the Co^{2+} ions and the adsorbent's active sites as the adsorption sites become increasingly occupied [44].

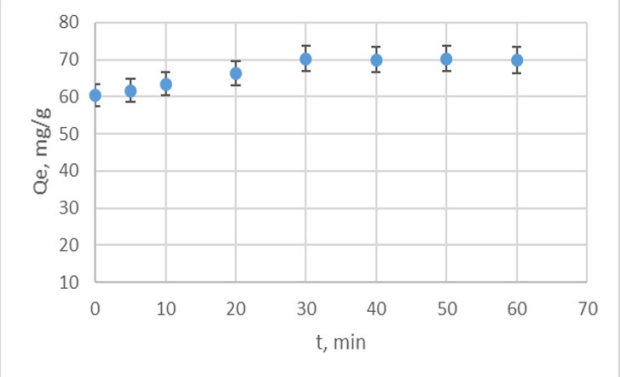


Figure 4. Impact of contact time on Co(II) adsorption

Influence of initial concentration

This study aimed to investigate cobalt's adsorption on the DOMSR adsorbent to determine the equilibration time for maximum uptake and understand the kinetics of the adsorption process. Fig. 5 illustrates the relationship between cobalt concentration and adsorption. Since it provides the required driving power to overcome mass-transfer barrier between the aqueous and solid phases, the initial concentration of cobalt is an important consideration. Consequently, a greater starting metal concentration raises DOMSR's sorption capacity. Fig. 5 shows that when the initial metal concentration rises, the equilibrium adsorption capacity increases linearly and reaches a maximum of 120 mg/L for cobalt ions. The graph indicates that as the initial cobalt concentration rises from 10 to 120 mg/L, the amount absorbed varies from 2.80 to 39.00 mg/g. As the initial concentration rises, the available adsorption sites become limited, leading to a decrease in adsorption percentage. This is because, at a fixed adsorbent dose, the total available adsorption sites are constrained, resulting in similar amounts of the adsorbate being adsorbed. Consequently, the adsorption percentage decreases as the initial adsorbate concentration increases [45,46]. The higher initial concentrations increase the adsorption capacity due to the stronger concentration gradient that drives greater interaction between the Co(II) ions and the binding sites of the adsorbent [47].

Experimental parameters overview

Table 1 provides a comprehensive comparison between the findings of our current study and previous research outcomes.

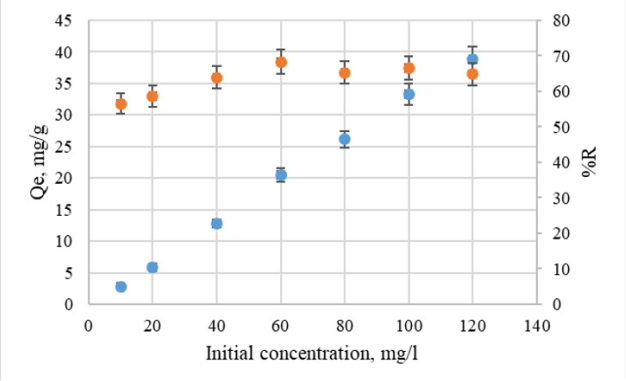


Figure 5. Impact of initial concentration on Co(II) adsorption

The table encompasses crucial information related to the adsorbent material, contact time, pH levels, adsorbent dosage, and initial concentration.

In terms of contact time, the present study found that the optimal adsorption of cobalt ions on olive mill solid residues occurred after 40 min of contact time. This falls within the range reported in previous studies (15-200 min). However, it suggests that our process may yield comparable results in a shorter period of time. The results of our investigation regarding pH indicate that a pH of 6 is the most suitable for the adsorption of cobalt ions onto the powder derived from olive mill solid residues. This discovery is consistent with several previous studies that identified optimal pH ranges of 5-5.5, 5.5-6, and 6. However, it differs from other studies that identified broader pH ranges of 4-5 and 4-9 as optimal. Additionally, the current study used a dosage of 0.5 g/50 ml of solution for the olive mill solid residues powder. While this dosage is similar to some previous studies (0.14g/50mL, 0.22g/50mL), it differs from others that employed different concentrations (0.5g/100mL, 2.0mg/L, 0.1g/50mL, 0.2g/50mL, 1.0g/L, 200mg/L). The optimal dosage can be influenced by various factors, such as the specific surface area of the adsorbent and the initial concentration of the contaminant[17]. Finally, the examination of cobalt ions' initial concentration indicates the highest adsorption capacity at 120mg/L. It is worth noting that this falls within the concentration range (30-600 mg/L) that has been previously studied, indicating that our chosen concentration is representative. Nonetheless, future studies may want to consider examining a wider range of initial concentrations in order to determine the maximum adsorption capacity of the olive mill solid residues powder.

The findings of the present study are consistent with certain prior investigations; however, notable discrepancies do exist. These discrepancies could potentially be attributed to several factors, including the type of surface. The surface characteristics of the adsorbent may vary based on the source material and the activation process employed [37,7]. Furthermore, the specific experimental conditions employed in each study may exert an influence on the observed outcomes.

Table 1. Comparison of the current study with some previous studies

The study	Adsorbent	Contact time (min)	pH	Dosage	Initial concentration (mg/l)
Present study	**Olive mill solid residues powdered**	**40**	**6**	**0.5 g/ 50 ml**	**120**
Amoo et al. [3]	Cow bone (CB), cow bone char (CBC), and activated cow bone carbon (ACBC)	150 for CB, 180 for CBC, 200 for ACBC	4, 5, and 5 for the ACBC, CBC, CB	0.14 g/50 ml, 0.22 g/50 ml, 0.26 g/50 ml for the CB, CBC, ACBC	250
Elsherif et al. [13]	Coffee and tea powder	40	5.5-6.0	1.0 g/l	240
Elsherif et al. [14]	Orange peels powder	30	4.0-5.0	0.1 g/50 ml	600
Ghanavati et al. [22]	MgO nanoparticles deposited on chitosan	50	5.0	0.1 g/50 ml	50
Swelam et al. [35]	Magnetic nano-hydroxyapatite	180	4.0-9.0	0.2 g/50 ml	30
Kolvankar [36]	Activated carbon prepared from coconut tree roots	60	7	0.5 g/100 l	240
Elsherif et al. [39]	Olive leaves powder	30	5.0-5.5	0.1 g/50 ml	150
Nadaroglu and Kalkan [45]	Red mud	15	5.5	2.0 mg/l	50
Narwade and Khairnar [48]	Nano-hydroxyapatite matrix	30	6	200 mg/l	2000

Isotherms models

In order to understand the relationship between the adsorbate and the adsorbent surface, adsorption isotherms are essential. The four most often used models for adsorption isotherm data analysis were Freundlich, Langmuir, Temkin, and Dubinin-Radushkevich (D-R) [13]. By utilising these models on the data, parameters were obtained that provide important information about the sorption mechanism, the adsorbent's surface characteristics, and its affinity. Figs. 6a, 6b, 6c, and 6d show these models' linear graphs. Table 2 contains comprehensive details on the linear equations and parameters for every model.

Table 2. Isotherms models equations and parameters [13,16]

Eq. No.	Isotherms model	Linear equation	Parameters
1	Langmuir	$\frac{1}{Q_e} = \frac{1}{Q_m} + \frac{1}{b\,Q_m\,C_e}$	Qe (mg/g): adsorption capacity Ce (mg/L): equilibrium concentration Qm (mg/g): maximal adsorption capacity b (L/mg): Langmuir constant
2	Freundlich	$\log Q_e = \log K_F + \frac{1}{n} \log C_e$	KF (mg/g (L/mg)1/n): Freundlich adsorption constants n: Empirical constant characterizing the heterogeneity of the adsorbent surface
3	Temkin	$Q_e = B_T \ln K_T + B_T \ln C_e$	BT (J/mol): Temkin adsorption constant KT (L/mg): Temkin isotherm constant
4&5	D-R	**log Qe = log Qm – β ε2** $\varepsilon = RT\,Log\,(1+\frac{1}{C_e})$	β (mol²/J²): Dubinin-Radushkevich constant ε (J/mol): Polanyi potential R (kJ/mol K): The gas constant T (K): The absolute temperature

Using four isotherm models, the adsorption of Co+2 ions onto the DOMSR adsorbent was investigated. Of these models, the Freundlich model came in second (R2=0.9896), while the Langmuir model showed the best fitting (R2=0.9948). Table 3 shows that the Temkin model had the lowest fitting value (R2=0.9294) and the D-R model had the lowest fitting value (R2=0.8052).

This result implies that the adsorbent's active sites are uniform. It was found that the maximal sorption capacity (Qm) was 41.84 mg/g. The equilibrium parameter, RL, is a dimensionless constant that describes the fundamental properties of the Langmuir isotherm:

$$R_L = \frac{1}{1+b\,C_o} \qquad (6)$$

The isotherm's shape is evaluated using RL; values larger than 1 signify an unfavourable shape, RL=1 a linear shape, values between 0 and 1 a favourable shape, and RL=0 an irreversible shape [6]. Table 3 displays RL values that are less than 1 and larger than 0 (0.87-0.36), suggesting that CO_2+ has a favourable adsorption onto the DOMSR adsorbent.

The parameter that characterises the heterogeneity of the adsorbent surface is represented by the constant (n) in the empirical Freundlich model. Favourable adsorption is indicated by a value of $0 < n < 1$, whereas unfavourable adsorption is indicated by a value of $n > 1$. Linear adsorption is represented by a value of $n = 1$. The adsorption process is irreversible if $n = 0$ [49]. The present investigation revealed that the Freundlich constant (n) was not equal to unity (0.52), suggesting that the adsorption process escalated with an increase in ion concentration. This is explained by the DOMSR adsorbent's increasing surface coverage [50].

The following formula can be used to find the adsorption energy values in the Dubinin-Radushkevich (D-R) model, denoted as E:

$$E = \frac{1}{\sqrt{2\beta}} \qquad (7)$$

E is the equivalent of the reaction mechanism. The sorption process is controlled by ion exchange if E is between 8 and 16 kJ/mol. The sorption mechanism may be influenced by physical forces when E is less than 8.0 kJ/mol. The computed E value for CO_2+ adsorption was 0.224 kJ/mol (Table 3). This suggests that physical sorption is the primary mode of sorption.

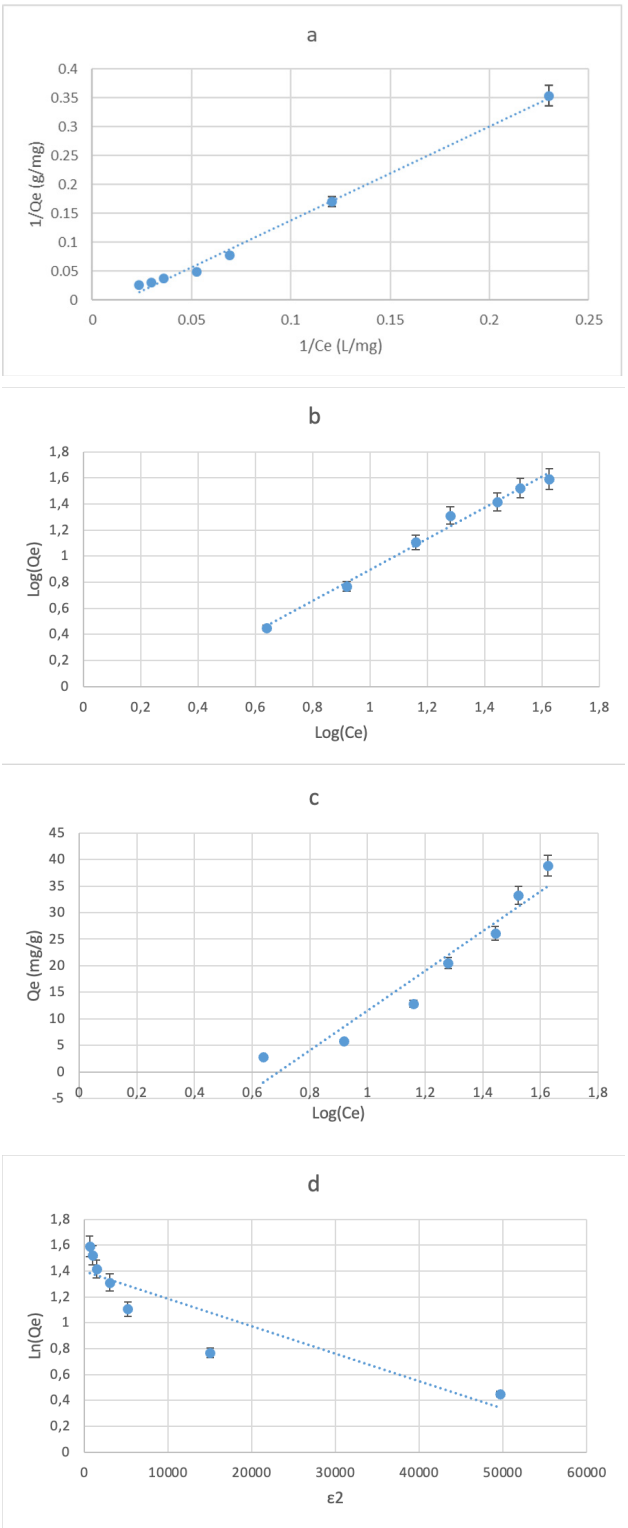


Figure 6. Linear graphs for a) Langmuir model, b) Freundlich model, c) Temkin model, d) D-R model plot of Co(II) adsorption

Table 3. Parameters of Langmuir, Freundlich, Temkin, and Dubinin-Radushkevich isotherm models for the adsorption of Co(II) on DOMSR

Model	Parameter	Value
Langmuir	b (L/mg)	0.015
	Qm (mg/g)	41.84
	R2	0.9948
Freundlich	KF (mg/g (L/mg)1/n)	1.970
	n	2.039
	R2	0.9896
Temkin	BT (J/mol)	37.404
	KT (L/mg)	1.996
	R2	0.9294
Dubinin-Radushkevich	Qm (mg/g)	24.93
	β (mol^2/J^2)	2x10-5
	E (kJ/mol)	0.224
	R2	0.8052

Kinetic models

The concentration of the adsorbate is known to fluctuate over time, as observed in the kinetic process [3]. By studying the kinetics of adsorption, we can understand how the adsorption process evolves from its initial state to equilibrium. This understanding allows us to create predictive models that determine the status of the process at different points in time [51]. Adsorption is the physical process in which ions or atoms of the sorbate move from a less stable region in an aqueous solution to a more stable one. This movement is influenced by Van der Waals forces and/or electrostatic physical forces [40]. In our study, we investigated the kinetics of the produced adsorbent (DOMSR) and compared the results with three kinetic models: Elovich, pseudo-first-order, and pseudo-second-order [3,13,19]. These models were then used to analyze the adsorption data we collected. Understanding the kinetics involved in the adsorption process enables us to design adsorption systems that can effectively remove a targeted percentage of the adsorbate (R%) or optimize the adsorption capacity of the derived adsorbent (Qe). For more detailed information, please refer to Table 4, which provides the linear equations and associated parameters for each model.

Table 4. Kinetic models equations and parameters [13,16]

Eq. No.	Kinetic model	Linear equation	Parameters
8	Pseudo-first-order	$\ln(Q_e - Q_t) = \ln(Q_e) - \frac{k_1}{2.303} \times t$	Qt (mg/g): Adsorbed quantities at t time Qe (mg/g): Adsorbed quantities at equilibrium k1 (min-1): The adsorption rate constant
9	Pseudo-second-order	$\frac{t}{Q_t} = \frac{1}{k_2 \times Q_e^2} + \frac{t}{Q_e}$	k2 (g/mg.min): The adsorption rate constant
10	Elovich	$Q_t = \frac{1}{\beta}\ln(\alpha\beta) + \frac{1}{\beta}\ln(t)$	α (mg/g.min): The initial adsorption rate β (g/mg): The desorption constant

Several kinetic models were used in the analysis of adsorption investigations on the removal of CO_2+ metal ions from an aqueous solution, as shown in Table 4. As shown in Figs. 7a, 7b, and 7c, the goodness of fit of each model was assessed by comparing its correlation coefficient (R2) to unity (1). Table 5 presents the computed kinetic parameters and their accompanying coefficients of determination (R2 values).

As shown in Fig. 7a, the pseudo-first-order kinetic model did not provide a satisfactory fit for the adsorption data, with a coefficient of determination (R^2) of 0.822. The estimated adsorption capacity (Qe(calc)) was 2.67 mg/g, while the experimentally observed adsorption capacity (Qe(exp)) was 70.32 mg/g. Despite the R^2 value being relatively close to 1, this substantial discrepancy between the calculated and experimental capacities indicates a poor fit between the pseudo-first-order model and the experimental data. This sug-

gests that the pseudo-first-order model does not accurately represent the adsorption kinetics in this system.

The pseudo-second-order kinetic model demonstrates an outstanding correlation coefficient of 0.9995, indicating the best fit for the adsorption kinetics of Co^{2+} ions onto the DOMSR adsorbent, as shown in Fig. 7b. This high correlation coefficient, which is close to 1, reflects a strong agreement between the model and the experimental data. Further support for this model's accuracy is provided in Table 5, which compares the calculated adsorption capacity (Qe(calc)) of 14.18 mg/g with the experimental adsorption capacity (Qe(exp)) of 14.10 mg/g. The close match between these values confirms that the pseudo-second-order model is the most suitable for describing the adsorption process. This indicates that chemisorption is the rate-limiting step in the adsorption of Co^{2+} ions onto the prepared adsorbents [3].

The kinetic parameters for the Elovich model are detailed in Table 5, and the corresponding data are illustrated in Fig. 7c. The Elovich model achieves a respectable correlation coefficient (R^2) of 0.8806, with a model constant (α) of 12.34 mg/g·min. Despite these relatively high correlation values, the Elovich model does not adequately fit the experimental data for Co^{2+} ion adsorption onto the DOMSR adsorbent. This suggests that, although the Elovich model shows some correlation, it is not the most suitable model for describing the kinetics of Co^{2+} ion adsorption in this case.

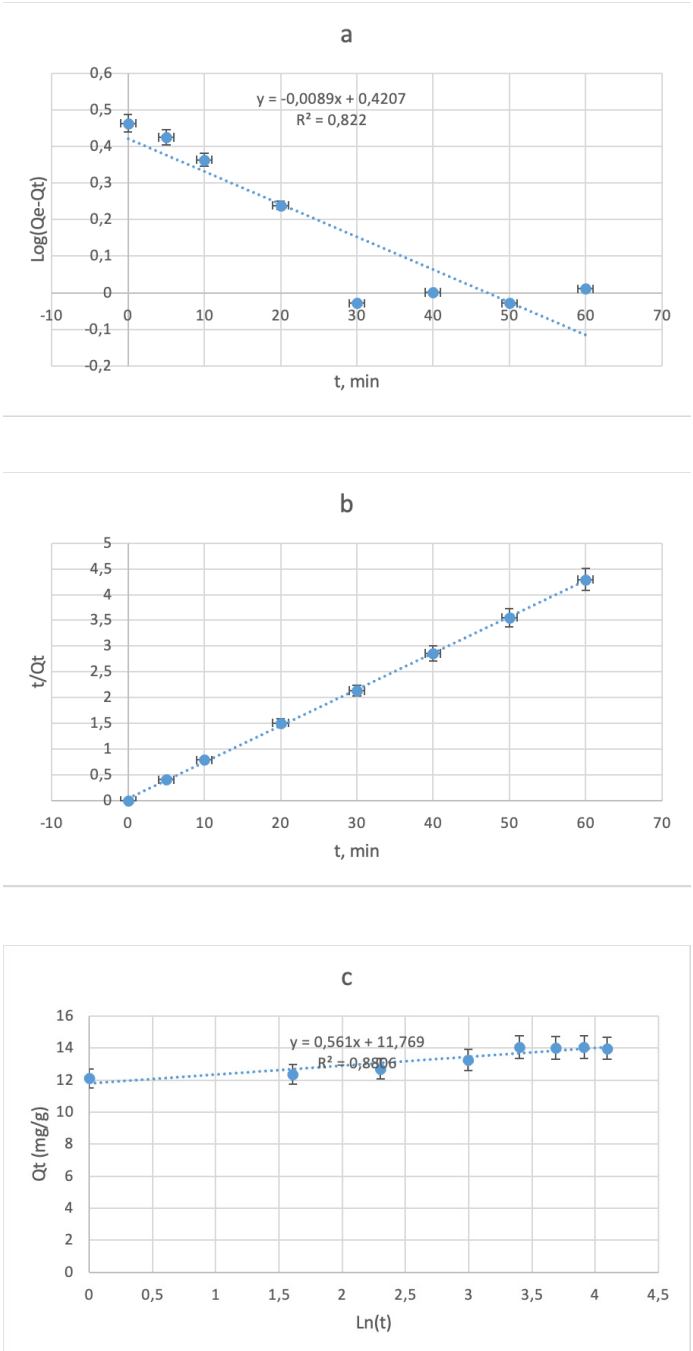


Figure 7. Kinetic model plots of Co(II) adsorption onto DOMSR: a) Pseudo-First-Order model, b) Pseudo-Second-Order model, c) Elovich model

Table 5. Kinetic parameters for Co(II) adsorption onto DSOR

Pseudo-First-Order			
k_1	Q_e (Cal.)	R^2	Q_e (Exp.)
(min^{-1})	(mg/g)		(mg/g)
0.020	2.67	0.8220	14.10
Pseudo-Second-Order			
k_2	Q_e (Cal.)	R^2	Q_e (Exp.)
(g/mg.min)	(mg/g)		(mg/g)
0.106	14.18	0.9995	14.10
Elovich			
β	α	R^2	Q_e (Exp.)
(g/mg)	(mg/g.min)		(mg/g)
0.085	12.34	0.8806	14.10

CONCLUSIONS

In summary, the increasing demand for cobalt due to advancements in industry and technology demands long-term strategies for removing the metal from aqueous solutions. This study examined the possibility of using olive mill solid waste (DOMSR) as a cost-effective and environmentally friendly adsorbent to remove Co(II). In order to improve the cobalt absorption efficiency, tests with adsorbent dose, pH levels, and elemental metal concentrations are conducted. According to the data obtained under these particular conditions, DOMSR is a promising biosorbent for applications involving water purification since it shows a high adsorption capacity for cobalt ions. Kinetic investigations indicate that the pseudo-second-order model best describes adsorption., suggesting that chemisorption is the rate-limiting process. The equilibrium data demonstrated monolayer adsorption at the homogenous adsorbate sites by following the Langmuir isotherm. The Elovitch model fit better than the pseudo-second-order model, although exhibiting a respectable connection. This study emphasises the potential of biosorbents derived from agricultural waste, such DOMSR, for the remediation of heavy metal pollution. The outcomes also showed how successful OMSR is as a long-term cobalt removal method. These critically important breakthroughs have the potential to greatly improve water treatment and save the environment.

ACKNOWLEDGEMENT

We sincerely thank the Chemistry Department of Elmergib University's Faculty of Arts and Science in Msallata for their significant support and contributions to this study. Their commitment and resources were crucial to this study's effective outcome.

DATA AVAILABILITY STATEMENT

The author confirm that the data that supports the findings of this study are available within the article. Raw data that support the finding of this study are available from the corresponding author, upon reasonable request.

CONFLICT OF INTEREST

The author declared no potential conflicts of interest with respect to the research, authorship, and/or publication of this article.

USE OF AI FOR WRITING ASSISTANCE

Not declared.

ETHICS

There are no ethical issues with the publication of this manuscript.

REFERENCES

[1] K. O. Amoo, E. N. Onyeozili, E. E. Kalu, J. A. Omoleye, and V. E. Efeovbokhan, "Activity of varying compositions of Co–Ni–P catalysts for the methanolysis of ammonia borane," International Journal of Hydrogen Energy, vol. 41, no. 46, pp. 21221–21235, 2016. https://doi.org/10.1016/j.ijhydene.2016.08.164.

[2] R. T. Jones and C. Pawlik, "Cobalt recovery from southern African copper smelters," in Proceedings of the 58th Annual Conference of Metallurgists (COM) Hosting the 10th International Copper Conference, vol. 2019, pp. 1–8, 2019.

[3] K. O. Amoo, T. E. Amoo, O. A. Olafadehan, E. E. Alagbe, A. J. Adesina, M. O. Bamigboye, B. D. Olowookere, and K. D. Ajayi, "Adsorption of cobalt (II) ions from aqueous solution using cow bone and its derivatives: Kinetics, equilibrium and thermodynamic comparative studies," Results in Engineering,

vol. 20, p. 101635, 2023. https://doi.org/10.1016/j.rineng.2023.101635.

[4] A. Tisserant and S. Pauliuk, "Matching global cobalt demand under different scenarios of co-production and mining attractiveness," Journal of Economic Structures, vol. 5, no. 4, pp. 1–19, 2016. https://doi.org/10.1186/s40008-016-0035-x.

[5] C. Banza Lubaba Nkulu et al., "Sustainability of artisanal mining of cobalt in DR Congo," Nature Sustainability, vol. 1, no. 9, pp. 495–504, 2018. https://doi.org/10.1038/s41893-018-0139-4.

[6] M. Araissi and E. Elaloui, "The removal of cadmium, cobalt, and nickel by adsorption with Na-Y zeolite," Iranian Journal of Chemical Engineering, vol. 39, no. 5, pp. 169-179, 2020. https://doi.org/1021-9986/2020/5/169-179.

[7] E. Demirbas, "Adsorption of cobalt (II) ions from aqueous solution onto activated carbon prepared from hazelnut shells," Adsorption Science & Technology, vol. 21, pp. 951-963, 2003. https://doi.org/10.1260/026361703607443 80

[8] R. C. Ferreira, D. Dias, I. Fonseca, M. Bernardo, J. L. C. Willimann Pimenta, N. Lapa, and M. A. S. D. de Barros, "Multi-component adsorption study by using bone char: modelling and removal mechanisms," Environmental Technology, vol. 43, no. 6, 2022. https://doi.org/10.1080/09593330.2020.1805026

[9] K. M. Elsherif, A. El-Hashani, and A. El-Dali, "Potentiometric Determination of Fixed Charge Density and Permselectivity for Silver Thiosulphate Membrane," Journal of Applicable Chemistry, vol. 2, no. 6, pp. 1543-1551, 2013.

[10] K. M. Elsherif, A. El-Dali, A. M. Ewlad-Ahmed, A. Treban, and I. Alttayib, "Removal of Safranin Dye from Aqueous Solution by Adsorption onto Olive Leaves Powder," Journal of Material and Environmental Sciences, vol. 12, no. 3, pp. 418-430, 2021.

[11] T. M. Budnyak, J. Piątek, I. V. Pylypchuk, M. Klimpel, O. Sevastyanova, M. E. Lindström, V. M. Gun'ko, and A. Slabon, "Membrane-Filtered Kraft Lignin–Silica Hybrids as Bio-Based Sorbents for Cobalt(II) Ion Recycling," ACS Omega, vol. 5, no. 19, pp. 10847–10856, 2020. https://doi.org/10.1021/acsomega.0c00492

[12] E. Díez, J. M. Gómez, A. Rodríguez, I. Bernabé, P. Sáez, and J. Galán, "A new mesoporous activated carbon as potential adsorbent for effective indium removal from aqueous solutions," Microporous and Mesoporous Materials, vol. 295, p. 109984, 2020. https://doi.org/10.1016/j.micromeso.2019.109984

[13] K. M. Elsherif, I. Haider, and A. El-Hashani, "Adsorption of Co (II) Ions from Aqueous Solution onto Tea and Coffee Powder: Equilibrium and Kinetic Studies," Journal of Fundamental and Applied Sciences, vol. 11, no. 1, pp. 65-81, 2019. https://doi.org/10.4314/jfas.v11i1.5

[14] K. M. Elsherif, A. M. Ewlad-Ahmed, and A. Treban, "Removal of Fe (III), Cu (II), and Co (II) from Aqueous Solutions by Orange Peels Powder: Equilibrium Study," World Journal of Biochemistry and Molecular Biology, vol. 2, no. 6, pp. 46-51, 2017.

[15] A. El Hashani, N. Ben Khayal, and K. M. Elsherif, "Selective Transport of Aromatic Compounds across Parchment Supported Prussian blue Membrane," Chemical Methodologies, vol. 2, no. 3, pp. 194-203, 2018. https://doi.org/10.22034/chemm.2018.60860

[16] K. M. Elsherif, A. El-Dali, A. A. Alkarewi, A. M. Ewlad-Ahmed, and A. Treban, "Adsorption of crystal violet dye onto olive leaves powder: Equilibrium and kinetic studies," Chemistry International, vol. 7, no. 2, pp. 79-89, 2021. https://doi.org/10.5281/zenodo.4441851

[17] M. N. Siddiqui, B. Chanbasha, A. A. Al-Arfaj, T. Kon'kova, and I. Ali, "Superfast removal of cobalt metal ions in water using inexpensive mesoporous carbon obtained from industrial waste material," Environmental Technology & Innovation, vol. 21, p. 101257, 2021. https://doi.org/10.1016/j.eti.2020.101257

[18] K. M. Elsherif, A. El-Hashani, A. El-Dali, and M. Saad, "Ion-Permeation Rate of (1:1) Electrolytes across Parchment-Supported Silver Chloride Membrane," International Journal of Chemistry and Pharmaceutical Sciences, vol. 2, no. 6, pp. 890-897, 2014.

[19] A. M. Alkherraz, K. M. Elsherif, and N. A. Blaybllo, "Safranin adsorption onto Acasia plant derived activated carbon: Isotherms, thermodynamics and kinetic studies," Chemistry International, vol. 9, no. 4, pp. 134-145, 2023. https://doi.org/10.5281/zenodo.8127687

[20] K. M. Elsherif, A. El-Hashani, A. El-Dali, and M. Musa, "Ion selectivity across parchment-supported silver chloride membrane in contact with multi-valent electrolytes," International Journal of Analytical and Bioanalytical Chemistry, vol. 4, no. 2, pp. 58-62, 2014.

[21] N. Conte, E. Díez, B. Almendras, J. M. Gómez, and A. Rodríguez, "Sustainable Recovery of Cobalt from Aqueous Solutions Using an Optimized Mesoporous Carbon," Journal of Sustainable Metallurgy, vol. 9, pp. 266–279, 2023. https://doi.org/10.1007/s40831-022-00644-3

[22] B. Ghanavati, A. Bozorgian, and H. Kazemi Esfeh, "Thermodynamic and kinetic study of adsorption of cobalt II using adsorbent of magnesium oxide nano-particles deposited on chitosan," Progress in Chemical and Biochemical Research, vol. 5, no. 2, pp. 165-181, 2022. Available: https://doi.org/10.22034/pcbr.2022.335475.1219

[23] A. M. Alkherraz, A. K. Ali, and K. M. Elsherif, "Removal of Pb(II), Zn(II), Cu(II) and Cd(II) from aqueous solutions by adsorption onto olive branches activated carbon: Equilibrium and thermodynamic studies," Chemistry International, vol. 6, no.

1, pp. 11-20, 2020. https://doi.org/10.5281/zenodo.2579465

[24] A. M. Alkherraz, A. K. Ali, and K. M. Elsherif, "Equilibrium and thermodynamic studies of Pb(II), Zn(II), Cu(II) and Cd(II) adsorption onto mesembryanthemum activated carbon," Journal of Medicinal and Chemical Sciences, vol. 3, no. 1, pp. 1-10, 2020. https://doi.org/10.33945/SAMI/JMCS.2020.1.1

[25] K. M. Elsherif, A. El-Hashani, and I. Haider, "Biosorption of Fe (III) onto coffee and tea powder: Equilibrium and kinetic study," Asian Journal of Green Chemistry, vol. 2, no. 4, pp. 380-394, 2018. https://doi.org/10.22034/ajgc.2018.65163

[26] K. M. Elsherif, R. A. A. Saad, A. M. Ewlad-Ahmed, A. A. Treban, and A. M. Iqneebir, "Adsorption of Cd(II) onto Olive Stones Powder Biosorbent: Isotherms and Kinetic Studies," Advanced Journal of Chemistry, Section A, vol. 7, no. 1, pp. 59-74, 2024. Available: https://doi.org/10.48309/ajca.2024.415865.1415

[27] A. M. Alkherraz, A. K. Ali, A. El-Dali, and K. M. Elsherif, "Biosorption Study of Zn(II), Cu(II), Pb(II) And Cd(II) Ions by Palm Leaves Activated Carbon," To Chemistry, vol. 4, 2019, pp. 8-17.

[28] K. M. Elsherif, A. El-Dali, A. M. Ewlad-Ahmed, A. A. Treban, H. Alqadhi, and S. Alkarewi, "Kinetics and Isotherms Studies of Safranin Adsorption onto Two Surfaces Prepared from Orange Peels," Moroccan Journal of Chemistry, vol. 10, no. 4, pp. 639-651, 2022. https://doi.org/10.48317/IMIST.PRSM/morjchem-v11i1.32137

[29] K. M. Elsherif, A. El-Hashani, and I. Haider, "Equilibrium and Kinetic Studies of Cu (II) Biosorption Onto Waste Tea and Coffee Powder (WTCP)," Iranian Journal of Analytical Chemistry, vol. 5, no. 2, pp. 31-38, 2018. https://doi.org/20.1001.1.23832207.2018.5.2.5.4

[30] A. M. Alkherraz, K. M. Elsherif, A. El-Dali, N. A. Blayblo, and M. Sasi, "Thermodynamic, equilibrium, and kinetic studies of safranin adsorption onto carpobrotus edulis," Asian Journal of Nanoscience and Materials, vol. 5, no. 2, pp. 118-131, 2022. https://doi.org/10.26655/ajnanomat.2022.2.4

[31] C. Hu, W. Zhang, Y. Chen, N. Ye, D. YangJi, H. Jia, Y. Shen, and M. Song, "Adsorption of Co(II) from aqueous solution using municipal sludge biochar modified by HNO3," Water Science & Technology, vol. 84, no. 1, p. 251, 2021. https://doi.org/10.2166/wst.2021.199

[32] P. B. Cusack, M. G. Healy, P. C. Ryan, I. T. Burke, L. M. T. O'Donoghue, É. Ujaczki, and R. Courtney, "Enhancement of bauxite residue as a low-cost adsorbent for phosphorus in aqueous solution using seawater and gypsum treatments," Journal of Cleaner Production, vol. 179, pp. 217-224, 2018. https://doi.org/10.1016/j.jclepro.2018.01.092

[33] M. A. Grace, E. Clifford, and M. G. Healy, "The potential for the use of waste products from a variety of sectors in water treatment processes," Journal of Cleaner Production, vol. 137, pp. 788-802, 2016. https://doi.org/10.1016/j.jclepro.2016.07.113

[34] E. M. Nigri, M. A. P. Cechinel, D. A. Mayer, L. P. Mazur, J. M. Loureiro, S. D. F. Rocha, and V. J. P. Vilar, "Cow bones char as a green sorbent for fluorides removal from aqueous solutions: batch and fixed-bed studies," Environmental Science and Pollution Research, vol. 24, no. 3, pp. 2364-2380, 2017. https://doi.org/10.1007/s11356-016-7816-5

[35] A. A. Swelam, M. B. Awad, A. M. A. Salem, A. S. El-Feky, "An Economically Viable Method for the Removal of Cobalt Ions from Aqueous Solution Using Raw and Modified Rice Straw," HBRC Journal, vol. 14, no. 3, pp. 255-263, Oct. 2016. https://doi.org/10.1016/j.hbrcj.2016.10.001

[36] A. A. Kolvankar, "Adsorption studies of cobalt (II) by activated carbon prepared from coconut tree root," EPRA International Journal of Research and Development, vol. 4, no. 9, pp. 1-10, 2019.

[37] M. Stevens and B. Batlokwa, "Removal of Nickel(II) and Cobalt (II) from Wastewater Using Vinegar-Treated Eggshell Waste Biomass," Journal of Water Resource and Protection, vol. 9, no. 8, pp. 931-944, 2017. https://doi.org/10.4236/jwarp.2017.98062

[38] S. Rengaraj and S. H. Moon, "Kinetics of adsorption of Co(II) removal from water and wastewater by ion exchange resins," Water Research, vol. 36, no. 7, pp. 1783-1793, 2002. https://doi.org/10.1016/S0043-1354(01)00380-3

[39] K. M. Elsherif, A. M. S. Ewlad-Ahmed, A. A. S. Treban, "Biosorption Studies of Fe (III), Cu (II), and Co (II) from Aqueous Solutions by Olive Leaves Powder," Applied Journal of Environmental Engineering Science, vol. 4, no. 3, pp. 341-352, 2017. https://doi.org/10.48422/IMIST.PRSM/ajees-v3i4.9806

[40] O. A. Olafadehan, K. O. Amoo, K. F. K. Oyedeko, A. M. Bello, V. E. Bello, S. G. Akinfolarin, "Binary adsorption of phenol and 2-chlorophenol on chitosan derived from pink shrimp shell," Petroleum & Petrochemical Engineering Journal, vol. 6, no. 1, pp. 1-18, 2022. https://doi.org/10.23880/ppej-16000292.

[41] A. El-Hashani, K. M. Elsherif, K. Edbey, F. Alfaqih, M. Alomammy, S. Alomammy, "Biosorption of Eriochrome Black T (EBT) onto Waste Tea Powder: Equilibrium and Kinetic Studies," To Chemistry, vol. 1, no. 3, pp. 263-275, 2018.

[42] B. H. Hameed, I. A. W. Tan, A. L. Ahmad, "Adsorption isotherm, kinetic modelling and mechanism of 2,4,6-trichlorophenol on coconut husk-based activated carbon," Chem. Eng. J., vol. 144, no. 2, pp. 235-244, 2008. https://doi.org/10.1016/j.cej.2008.01.028

[43] E. S. Z. El-Ashtoukhy, N. K. Amin, O. Abdelwahab, "Removal of lead (II) and copper (II) from aqueous solution using pomegranate peel as a new adsorbent," Desalination, vol. 223, no. 1-3, pp. 162-173, 2008. https://doi.org/10.1016/j.desal.2007.01.206

[44] J. Villarroel-Rocha, D. Barrera, J. J. Arroyo-Gomez,

K. Sapag, "Insights of adsorption isotherms with different gases at 77 K and their use to assess the BET area of nanoporous silica materials," Adsorption, vol. 27, no. 7, pp. 1081-1093, 2021. https://doi.org/10.1007/s10450-021-00339-3

[45] H. Nadaroglu and E. Kalkan, "Removal of cobalt (II) ions from aqueous solution by using alternative adsorbent industrial red mud waste material," International Journal of Physical Sciences, vol. 7, no. 9, pp. 1386-1394, 2012. https://doi.org/10.5897/IJPS11.1748

[46] A. M. Alkherraz, K. M. Elsherif, A. H. Madiry, and M. S. Sasi, "Evaluating the efficiency of red tea leaves residues in adsorption of methylene blue dye from liquid wastes: isotherms, kinetics, and thermodynamics studies," Arabian Journal of Scientific Research, vol. 5, no. 1, pp. 1-9, 2024. https://doi.org/10.5339/ajsr.2024.2

[47] E. Ajenifuja, J. A. Ajao, and E. O. B. Ajayi, "Adsorption isotherm studies of Cu (II) and Co (II) in high concentration aqueous solutions on photocatalytically modified diatomaceous ceramic adsorbents," Appl Water Sci, vol. 7, pp. 3793–3801, 2017. https://doi.org/10.1007/s13201-017-0527-3

[48] V. N. Narwade and R. S. Khairnar, "Cobalt adsorption on the nano-hydroxyapatite matrix: isotherm and kinetic studies," Bulletin of the Polish Academy of Sciences Technical Sciences, vol. 65, no. 2, pp. 131-137, 2017. https://doi.org/10.1515/bpasts-2017-0016

[49] M. Ghasemi, H. Javadian, N. Ghasemi, S. Agarwal, and V. K. Gupta, "Microporous Nanocrystalline Naa Zeolite Prepared by Microwave-Assisted Hydrothermal Method and Determination of Kinetic, Isotherm and Thermodynamic Parameters of the Batch Sorption of Ni (II)," Journal of Molecular Liquids, vol. 215, pp. 161–169, 2016. https://doi.org/10.1016/j.molliq.2015.12.038

[50] M. Araissi, I. Ayed, E. Elaloui, and Y. Moussaoui, "Removal of barium and strontium from aqueous solution using zeolite 4A," Water Science and Technology, vol. 73, no. 7, pp. 1628–1636, 2016. https://doi.org/10.2166/wst.2015.640

[51] M. Kebir et al., "Water Cleaning by a Continuous Fixed-Bed Column for Cr(VI) Eco-Adsorption with Green Adsorbent-Based Biomass: An Experimental Modeling Study," Processes, vol. 11, no. 2, p. 363, 2023. https://doi.org/10.3390/pr11020363

Environmental Research and Technology
https://dergipark.org.tr/en/pub/ert
DOI: https://10.35208/ert.1485673

Research Article

Optimization of biodiesel production from jatropha oil and its impact on engine performance and emissions using response surface methodology

Sangeetha KRISHNAMOORTHI*[1], L.PRABHU[1], M.PRABHAHAR[1]
Adil ABDULLA[1], Adil MEHABOOB[1]

[1]Department of Mechanical Engineering, Aarupadai Veedu Institute of Technology, Vinayaka Mission's Research Foundation, Deemed to be University, Tamil Nadu, India

ARTICLE INFO

Article history
Received: 18 May 2024
Revised: 03 Aug 2024
Accepted: 03 Sep 2024

Key words:
Emissions; biodiesel; optimization; box–behnken design, RSM.

ABSTRACT

This study aims to improve biodiesel production by assessing the effects of biodiesel-diesel fuel blends on engine performance and emissions using response surface methodology (RSM). The biodiesel was produced by the transesterification process. Here we see how the molar ratio (A), catalyst quantity (B), reaction temperature (C), and reaction time (D) affect the biodiesel conversion rate. During optimization, a Box-Behnken design (BBD) based on RSM was employed. Ideal conditions for achieving a biodiesel yield of 98.2069% were a B of 0.811601 wt%, a C of 75.8837°C, a D of 98.2069 min, and A of 7:1. Adjusting parameters like engine speed and biodiesel fuel mix ratio enhanced engine behavior and condensed exhaust emissions. The trials were structured utilizing the central composite design (CCD) technique grounded on RSM. The optimum operating criteria for the engine were evaluated to be a biodiesel ratio of 12.5845% and speed of engine is 2011.24 rpm. Under these conditions, the power output was 50.0817kW, torque was 254.757 Nm, smoke opacity was 6.48966%, CO emissions were 270.009 ppm, and NOx emissions were 819.573 ppm. These findings indicate that appropriate adjustments in biodiesel-diesel blends and engine parameters can significantly enhance engine performance and reduce exhaust emissions, providing insights into more efficient and environmentally friendly fuel utilization.

Cite this article as: Krishnamoorthi S, Prabhu L, Prabhahar M, Abdulla A, Mehaboob A. Optimization of biodiesel production from jatropha oil and its impact on engine performance and emissions using response surface methodology. Environ Res Tec 2025;8(2) 328-344.

INTRODUCTION

Energy consumption on a worldwide scale is mostly supported by petroleum fuels. Researchers are investigating renewable energy options because of the exhaustion of fossil fuel reserves [1]. A renewable alternative fuel, biodiesel is made from used cooking oils, plant oils, and animal fats [2]. This fuel has more cetane numbers and is renewable, biodegradable, and non-toxic than diesel fuel, and it burns more efficiently and with less pollution in the exhaust [3, 4]. Diesel engines can run on it alone or mix it with diesel fuel for added efficiency [5]. Jatropha oils are edible and environmentally beneficial as they are recyclable and more cost-effective than vegetable-based oils. Utilizing waste oil has benefits in terms of economics, environmental impact, and waste management [6, 7]. Various methods are utilized in biodiesel generation. The transesterification method is the more cost-effective production approach [8, 9]. The effect of process factors on biodiesel conversion rate has been the subject of sev-

***Corresponding author.**
*E-mail address: geetha30981@gmail.com

This is an open access article under the CC BY-NC license (http://creativecommons.org/licenses/by-nc/4.0/).

eral studies [10]. Jatropha typically results in lower emissions of particulate matter and sulfur dioxide, which contribute to improved air quality and reduced acid rain. It can be cultivated on marginal lands, potentially reducing competition with food crops. Assessing the biodiesel production is crucial for determining the fuel quantity. Several factors influence the biodiesel productivity, including speed, molar ratio of alcohol, time, temperature for reaction, and catalyst quantity [11]. Currently, the manufacture of biodiesel has gotten more expensive due to the existing technology. Various mathematical tools are receiving increased attention to address this issue. Mathematical models provide valuable insights for analyzing and predicting processes. They are utilized to optimize input parameters in order to improve process outputs [12, 13]. The response surface methodology is an effective statistical tool for optimizing biodiesel production process factors [14]. Statistically correct results can be obtained with less experimental runs using RSM, which is its main advantage [15]. With RSM, the best possible value for the response variable can be determined. The use of RSM has allowed several studies to fine-tune process factors in biodiesel manufacture. Experts have studied the effect of process factors on low-temperature algal oil biodiesel conversion [16]. RSM and ANN was used to examine the transesterification of algae oil. Relative Standard Deviation (RSD) values for ANN and RSM models were 0.999651 and0.9657, correspondingly. Researchers [17, 18] identified the ideal conditions for the transesterification process of sandbox seed oil. The production of biodiesel required the use of two catalysts: potassium hydroxide and calcined snail shell. Optimization was carried out using the RSM approach. The selected input parameters included time, temperature, and catalyst quantity. Many experts have studied biodiesel's impact on diesel engine efficiency and pollution levels in great detail. Several authors used the RSM to look at how different fuel mixtures and biodiesel affected performance and emissions [19]. The ideal operating parameters for a single-cylinder diesel engine that runs on a mixture of diesel and grape seed biodiesel at various volume ratios (5, 10, and 15%) were determined by researchers [20] using RSM. Exhaust gas temperature (EGT), smoke, NOx, CO, and HC were defined as responses, whereas injection pressure, engine load, biodiesel blend ratio, and brake-specific fuel consumption (BSFC) were chosen as independent factors. Through the application of response surface approaches, an engine that utilized a diesel fuel mixture with mahua oil methyl ester was fine-tuned in terms of both efficiency and emission levels [21]. The effects of various blend-to-torque load ratios on brake thermal efficiency (BTE), smoke opacity, brake specific fuel consumption (BSFC), hydrocarbon (HC), carbon monoxide (CO), and nitrogen oxide (NOx) emissions were studied. Using the BBD technique in RSM, this study seeks to determine the best process parameters for biodiesel production from Jatropha Oil. By optimizing engine variables such as blend ratio and engine speed, CCD based on RSM can increase engine power and torque values while reducing exhaust pollutants. The objective of this study is to evaluate the factors influencing biodiesel productivity and optimize the production process using mathematical models and response surface methodology (RSM). By assessing the impact of variables such as speed, molar ratio of alcohol, reaction time, temperature, and catalyst quantity, the study aims to enhance the efficiency and reduce the costs associated with biodiesel manufacturing. The novelty of this study lies in its application of response surface methodology (RSM) to optimize biodiesel production by systematically evaluating key influencing factors such as speed, molar ratio of alcohol, reaction time, temperature, and catalyst quantity. By leveraging advanced mathematical models, this approach aims to reduce production costs and improve efficiency, providing statistically accurate results with fewer experimental runs. This innovative use of RSM offers a comprehensive and cost-effective solution to enhance biodiesel manufacturing processes.Table1 gives the comparison between the current study with different literatures.

EXPERIMENTAL METHODOLOGY

Process of producing biodiesel

This analysis used Jatropha Oil obtained from households to produce biodiesel. This study used Jatropha Oil obtained from local households to produce biodiesel. Potassium hydroxide (KOH) was chosen as the catalyst and methanol (CH3OH) as the alcohol. Figure 1 displays the biodiesel manufacturing diagram.

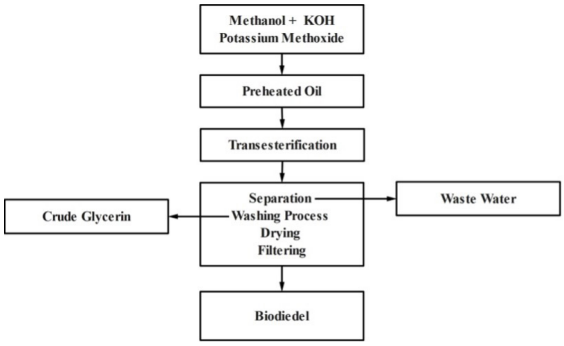


Figure 1. Schematic diagram illustrating the biodiesel production method

Preparing fuel blends for engine testing

Biodiesel produced from Jatropha Oil under ideal conditions was blended with pure diesel at varying volume ratio (0, 30, and 60%). Table 2 displays the apparatus utilized for assessing the fuel characteristics. The transesterification process of Jatropha biodiesel involves converting Jatropha oil into biodiesel by reacting it with methanol in the presence of a catalyst, typically sodium hydroxide or potassium hydroxide.

Engine testing unit

This engine delivers a power output of 89 kW at 3200 rpm and generates a torque of 295 Nm at 1800 rpm. Weighing 325 kg, the engine is equipped with a water-cooled oil cooler, enhancing its performance and durability.

Fuel blends were experimentally tested on a Mitsubishi Canter 4D34-2A type diesel engine with a hydraulic dynamometer to study their effects. Table 3 provides details on the engine unit utilized in studies, whereas Figure 2 shows a schematic representation of the experimental testing unit. While the MRU OpTrans 1600 uses absorption photometry to evaluate smoke opacity levels, the TESTO 350-S flue gas analyzer analyzes NOx and CO emissions. The results and their associated uncertainty are shown in Table 4.

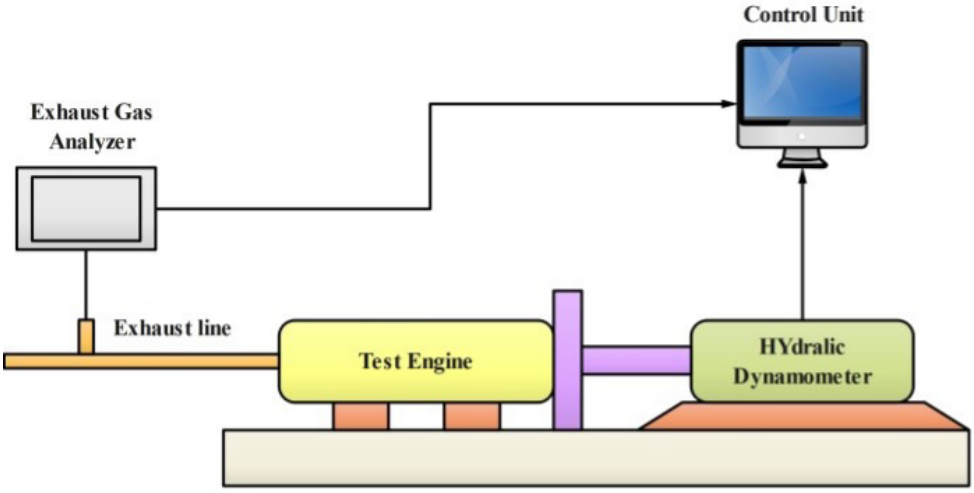


Figure 2. Diagram illustrating the experimental testing unit

Table 1. Comparison of comparison between the current study with recent literature

Authors	Title	Comments
H. Farouk, S. M. Zahraee, A. E. Atabani, M. N. Mohd Jaafar, F. H. Alhassan	Optimization of the esterification process of crude jatropha oil (CJO) containing high levels of free fatty acids: a Malaysian case study	Focuses on optimizing the esterification process for crude jatropha oil with high FFA using RSM in a Malaysian context.
K.-T. Liu, S. Gao, T.-W. Chung, C.-M. Huang, Y.-S. Lin	Effect of process conditions on the removal of phospholipids from Jatropha curcas oil during the degumming process	Investigates the impact of process conditions on phospholipid removal from Jatropha curcas oil during degumming, utilizing RSM.
A. Singh, S. Sinha, A. K. Choudhary	Optimization of Operating Parameters of Diesel Engine Powered with Jatropha Oil Diesel Blend by Employing Response Surface Methodology	Employs RSM to optimize operating parameters of a diesel engine powered by Jatropha oil-diesel blend.
M. Athar et al.	Biodiesel production by single-step acid-catalysed transesterification of Jatropha oil under microwave heating with modelling and optimisation using response surface methodology	Models and optimizes biodiesel production from Jatropha oil via single-step acid-catalyzed transesterification under microwave heating using RSM.
A. Ashok, S. K. Gugulothu, R. V Reddy, H. Ravi	Box-Behnken Response Surface Methodology Based Multi-Objective Optimization on Reactivity Controlled Compression Ignition Engine Characteristics Powered With Ternary Fuel	Uses Box-Behnken RSM for multi-objective optimization of a Reactivity Controlled Compression Ignition engine using ternary fuel.

Table 2. Fuel characteristics measuring devices

S. No	Properties	Units	Range	Accuracy
1	Viscosity@45°C	cSt	4.96	±0.01
2	Density @15°C	g/cm3	895.2	±0.001
3	Higher heating value	kJ/kg	39.871	0.001K
4	Cloud point	°C	0	±1
5	Pour point	°C	+5	±1
6	Cold filter plugging point	°C	+2	–

Table 3. Characteristics of the experimental engine unit

Manufacturer/series type	Mitsubishi canter 4D3A-2A
Engine type	Diesel engine with direct fuel injection and glow plug
Stroke	115 mm
Power	89 kW@3200 rpm
Bore	104 mm
Displacement	3907 cc
Torque	295 Nm at 1800 rpm
Weight	325 kg
Oil cooler	Water cooled

Table 4. Measurement accuracy and result uncertainty

Parameter	Units	Accuracy
Speed	rpm	±2
NOx	ppm	±1
CO	ppm	±10
Brake power	%	±2
Torque	%	±2
Smoke	%	±1
Calculated result		Uncertainty

RSM

In order to maximize the results, the RSM is a mathematical technique that is used to simulate and analyze scenarios impacted by various variables. RSM is a powerful tool for optimizing processes, understanding variable interactions, reducing experimentation efforts, and improving process efficiency and robustness. Equation (1) shows that the RSM model predicts the response surface using a quadratic polynomial equation [22], [23].

$$Y = \beta_0 + \sum_{i=1}^{n}\beta_i x_i + \sum_{i=1}^{n}\beta_{ii} x_i^2 + \sum_{i>j}^{n}\sum_{j}^{n}\beta_{ij} x_i x_j + e \quad (1)$$

Y projected output result

n number of components

b0 constant

bi linear

bii quadratic

bij interaction coefficients

xj are xi independent parameters

e error.

EXPERIMENTAL DESIGN

A Box Benchmen Design in RSM was used to simulate biodiesel synthesis using four variables. Using different values for the following four input parameters. The 29 experiments were carried out to predict biodiesel yield. The trial input factors are listed in Table 5.

Table 5. Input factors and its levels

Factors Code	Units	Levels		
		+1	0	+2
A	**molar ratio**	**4**	**6**	**8**
B	**wt%**	**0.6**	**0.8**	**1.0**
C	**°C**	**50**	**60**	**70**
D	**min**	**60**	**80**	**100**

The engine trials were planned and improved with the help of a CCD. In order to predict and optimize engine outputs at three levels (1, 0, 1), we used two independent factors: blending ratio and speed of the engine.

Table 6. Parameters and levels in engine experimentation

Parameters	Symbol	Units	Levels		
			+1	0	1
Blend	**X**	**%**	**0**	**30**	**60**
Engine speed	**Y**	**rpm**	**1450**	**1850**	**2250**

Table 6 shows the levels of the input parameters. There are a total of 13 experimental runs in the CCD. The number of experimented trials were determined using Equation (2).

$$N = 2^k + 2 * k + NC$$

The number of centre points is indicated by NC, while the no of independent factors is represented by the variable k [24].

RESULTS AND DISCUSSIONS

Optimizing using RSM

The BBD experimental design utilized four independent variables (process parameters) to determine the highest biodiesel yield, as displayed in Table 7. Equation (3) illustrates the coded-component numerical model that links the results to the in depending factors [25], [26].

Biodiesel Yield (Y) = +97.76 +0.3258 A +0.2325 B +1.40 C -0.4025 D +0.3125AB +0.4275 AC +0.1125 AD +0.3425 BC -0.2975 BD -0.1975 CD -3.95 A2 -2.64 B2 -1.31 C2 -1.68 (3)

Table 7. Experimental input and its results of Jatropha Oil biodiesel by BBD

S. No	A	B	C	D	Experimented yield	Theoretical yield	Error
	molar ratio	wt%	°C	min	wt%	wt%	%
1	6	0.8	60	80	98.15	97.76	0.4
2	6	0.6	70	80	94.49	94.64	0.16
3	6	0.8	60	80	98.2	97.76	0.45
4	6	0.8	60	80	98.16	97.76	0.41
5	4	0.8	60	100	92.03	91.29	0.81
6	4	1	60	80	92.16	90.76	1.53
7	6	0.8	50	60	94.05	93.59	0.49
8	4	0.8	70	80	92.53	93.15	0.67
9	8	0.8	60	100	92.8	92.17	0.68
10	6	0.8	50	100	93.27	93.18	0.1
11	8	0.6	60	80	90.97	90.95	0.02
12	8	0.8	50	80	91.62	91.01	0.67
13	8	0.8	70	80	94.5	94.66	0.17
14	6	1	60	100	92.36	92.97	0.66
15	6	0.6	50	80	92.77	92.53	0.26
16	4	0.8	60	60	92.28	92.32	0.04
17	6	0.8	70	60	97.9	96.78	1.15
18	4	0.8	50	80	91.26	91.21	0.05

19	6	1	60	60	94.17	94.37	0.21
20	6	1	70	80	95.83	95.79	0.04
21	8	0.8	60	60	92.5	92.75	0.27
22	6	0.6	60	100	93.1	93.10	0
23	8	1	60	80	92.18	92.04	0.15
24	6	0.8	60	80	98.16	97.76	0.41
25	6	0.8	70	100	96.38	95.58	0.83
26	6	0.6	60	60	93.77	93.31	0.49
27	6	0.8	60	80	97.14	97.76	0.64
28	4	0.6	60	80	91.7	90.92	0.85
29	6	1	50	80	92.64	92.31	0.36

Table 8. Design of CCD and engine response experiments

Run	Input Factors		Power(kW)		Torque (Nm)	
	X (%)	Y (rpm)	Experiment	Predicted	Experiment	Predicted
1	0	2250	55	54.68	259.78	260.15
2	30	2250	52.43	52.82	241.68	241.11
3	30	1850	46.6	46.72	247.71	246.8
4	60	1450	40.14	40.29	240.34	239.59
5	60	1850	43.39	43.3	235.01	235.56
6	30	1850	47.34	46.72	247.04	246.8
7	60	2250	49.52	49.46	229.19	229.39
8	30	1450	43.8	43.76	249.02	250.34
Run	**Input Factors**		**Power(kW)**		**Torque (Nm)**	
	X (%)	**Y (rpm)**	**Experiment**	**Predicted**	**Experiment**	**Predicted**
9	30	1850	47.02	46.72	247.07	246.8
10	30	1850	46.64	46.72	245.81	246.8
11	0	1450	45.83	45.72	268.99	268.41
12	30	1850	46.35	46.72	247.11	246.8
13	0	1850	48.2	48.63	265.15	265.35

Run	Smoke Opacity (%)		CO (ppm)		NOx (ppm)	
	Experimented	Theoretical	Experimented	Theoretical	Experimented	Theoretical
1	7.5	7.56	301	295.64	673	665.24
2	7.3	7.23	266	262.81	790	788.41
3	6.5	6.57	236	244.31	960	960.08
4	10.2	10.16	196	192.97	1263	1254.91
5	6.2	6.23	214	211.47	1086	1083.24
6	6.3	6.57	244	244.31	956	960.08
7	7	7.01	228	229.97	907	911.58
8	10.6	10.63	226	225.81	1127	1131.74
9	6.5	6.57	241	244.31	955	960.08
10	6.7	6.57	244	244.31	956	960.08
11	11.2	11.21	262	258.64	1010	1008.58
12	6.8	6.57	246	244.31	964	960.08
13	7.1	7.03	272	277.14	834	836.91

The engine behaviour and emission testing as well as reaction condition optimization were designed using the Design Expert 13 tool. Engine experimental matrix with both theoretical and experimented data is indicates in Table 8 using the CCD model. Real engine performance parameters are computed using equations (4) and (5). Eqs. (6 - 8) are utilized to calculate real engine exhaust emission parameters.

$$\text{Power} = +46.720 - 2.66\,X + 4.53\,Y + 0.0525\,XY - 0.7524\,X^2 + 1.57\,Y^2 \quad (4)$$

$$\text{Torque} = +246.80 - 14.90\,X - 4.62\,Y - 0.4850\,XY + 3.66\,X^2 - 1.07\,Y^2 \quad (5)$$

$$\text{Smoke OpXcity} = +6.57 - 0.4000\,X - 1.70\,Y + 0.1250\,XY + 0.0586\,X^2 + 2.36\,Y^2 \quad (6)$$

$$\text{CO} = +242.21 - 32.83\,X + 18.50\,Y - 1.75\,XY + 0.7759\,X^2 + 3.78\,Y^2 \quad (7)$$

$$\text{NOx} = +957.79 + 123.17\,X - 171.67\,Y - 4.75\,XY + 3.22\,X^2 + 1.72\,Y^2 \quad (8)$$

The significance of the experiments and the model can be evaluated using ANOVA. Table 9 displays the ANOVA results for biodiesel production. The table displays that the F-value for biodiesel production was 27.22, indicating the model's relevance. P-values below 0.0500 indicate that the model terms are statistically significant. C, A2, B2, C2, and D2 are important model terms in this criterion. A lack of fit value of 1.64 indicates that the lack of fit is not serious. A lack of fit that is not considerable is beneficial for the model's fit. An R2 value of 0.9646 was found by analyzing the regression equation using ANOVA. Predictions for R2 and adjusted R2 were 0.8250 and 0.9291. The anticipated R2 and adjusted R2 values show a close agreement since the difference between them is less than 0.2.

Table 9. ANOVA for biodiesel production

Source	SS	df	MS	F-value	p-value	
Model	157.80	14	11.27	27.22	< 0.0001	significance
A-A	1.27	1	1.27	3.08	0.1013	
B-B	0.6487	1	0.6487	1.57	0.2313	
C-C	23.44	1	23.44	56.59	< 0.0001	
D-D	1.94	1	1.94	4.69	0.0480	
AB	0.3906	1	0.3906	0.9432	0.3479	
AC	0.7310	1	0.7310	1.77	0.2052	
AD	0.0506	1	0.0506	0.1222	0.7318	
BC	0.4692	1	0.4692	1.13	0.3051	
BD	0.3540	1	0.3540	0.8548	0.3708	
CD	0.1560	1	0.1560	0.3767	0.5492	
A^2	101.24	1	101.24	244.45	< 0.0001	
B^2	45.31	1	45.31	109.42	< 0.0001	
C^2	11.06	1	11.06	26.70	0.0001	
D^2	18.27	1	18.27	44.11	< 0.0001	
Residual	5.80	14	0.4141			
Lack of Fit	4.66	10	0.4663	1.64	0.3342	Non- significance
Pure Error	1.14	4	0.2838			
Cor Total	163.60	28				

Table 10. Results on ANOVA on torque and power

Source	Power			Torque		
	SS	F-value	P-value	SS	F-value	P-value
Model	172.56	215.58	< 0.0001	1497.62	379.29	< 0.0001
A-X	42.56	265.85	< 0.0001	1331.46	1686.06	< 0.0001
B-Y	123.13	769.10	< 0.0001	127.88	161.94	< 0.0001
XY	0.0110	0.0689	0.8005	0.9409	1.19	0.3112
X^2	1.56	9.77	0.0167	36.99	46.84	0.0002
Y^2	6.79	42.39	0.0003	3.16	4.01	0.0854
Residual	1.12			5.53		
LOF	0.5130	1.13	0.4383	3.60	2.49	0.1990
Pure Error	0.6076			1.93		
Cor Total	173.68			1503.14		

Table 11. ANOVA for nitrogen oxides, carbon monoxide and smoke opacity

Source	Smoke opacity			CO			NOx		
	SS	F-value	P-value	SS	F-value	P-value	SS	F-value	P-value
Model	**36.69**	**302.28**	**< 0.0001**	**8589.13**	**107.72**	**< 0.0001**	**2.680E+05**	**3207.51**	**< 0.0001**
A-X	**0.9600**	**39.55**	**0.0004**	**6468.17**	**405.58**	**< 0.0001**	**91020.17**	**5447.12**	**< 0.0001**
B-Y	**17.34**	**714.36**	**< 0.0001**	**2053.50**	**128.76**	**< 0.0001**	**1.768E+05**	**10581.63**	**< 0.0001**
XY	**0.0625**	**2.57**	**0.1526**	**12.25**	**0.7681**	**0.4099**	**90.25**	**5.40**	**0.0531**
X^2	**0.0095**	**0.3910**	**0.5516**	**1.66**	**0.1042**	**0.7562**	**28.71**	**1.72**	**0.2313**
Y^2	**15.36**	**632.99**	**< 0.0001**	**39.38**	**2.47**	**0.1601**	**8.21**	**0.4913**	**0.5060**
Residual	**0.1699**			**111.64**			**116.97**		
Lack of Fit	**0.0179**	**0.1571**	**0.9198**	**50.84**	**1.11**	**0.4417**	**60.17**	**1.41**	**0.3623**
Pure Error	**0.1520**			**60.80**			**56.80**		
Cor Total	**36.86**			**8700.77**			**2.681E+05**		

Tables 10 and 11 display the results of the analysis of variance (ANOVA) for the torque, power, smoke, CO, and NOx regression models. With p-values less than 0.05, the model terms are considered statistically significant according to the ANOVA analysis. Results showed that the R2 values for CO, power, smoke, NOx, and torque were 0.9872, 0.9935, 0.9954, 0.9996, and0.9963, respectively. There was an evaluation of adjusted R2 values of 0.9889 for power, 0.9937 for torque, 0.9780 for smoke, 0.9826 for CO, and 0.9993 for NOx. The planned and actual values of biodiesel production are strongly correlated, as seen in Figure 3. An accurate depiction of the biodiesel production experimental data is given by the model.

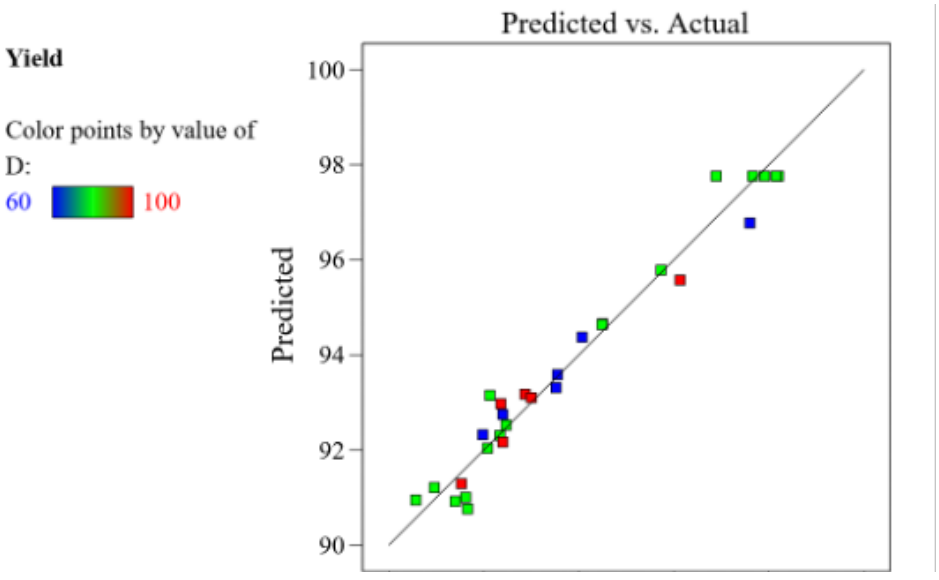


Figure 3. Predicted data and actual yield of Regression plot using RSM

Effects of reaction factors on the production of biodiesel

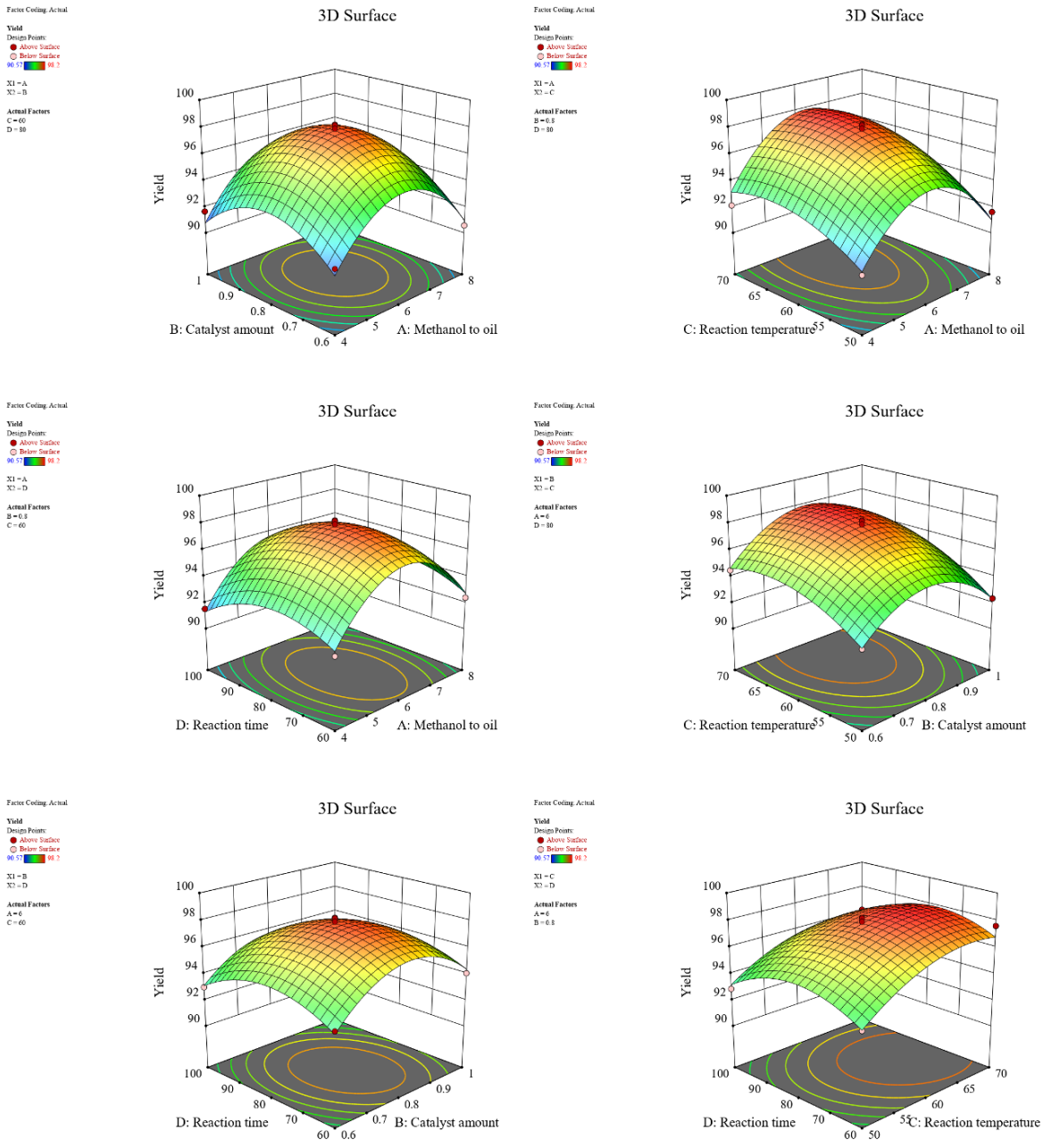


Figure 4. 3D RSM of biodiesel yield versus (a) AB, (b) AC, (c) AD, (d) BC, (e) BD, (f) CD.

Figure 4 shows that the effects of reaction factors on biodiesel productivity. The figures show 3D RSM demonstrating the correlation between biodiesel production and the combined effect of two factors variables.

Effects of factor A on biodiesel yield

The factor A of alcohol significantly impacts the biodiesel output [27]. Plots a–c shows how different catalyst quantities, reaction temperatures, and reaction times are affected by different molar ratios, which in turn affect biodiesel yield. How the catalyst concentration relates to the molar ratio. Biodiesel production rises as the alcohol quantity grows until it reaches its peak value. Excessive alcohol reduces biodiesel yield by increasing glycerol solubility in the biodiesel phase, making separation more challenging [28].

Effects of factor B on biodiesel yield

The amount of catalyst is a significant factor that affects biodiesel production by speeding up transesterification [29]. The greatest biodiesel production was achieved with a catalyst quantity of 0.8 weight percentage. The biodiesel yield reduced when the catalyst amount exceeded 0.8 wt%. Excessive catalyst will decrease biodiesel production due to saponification and hydrolysis issues.

Effects of factor C and factor D on the yield of biodiesel

This graph shows the impact of reaction temperature and duration on biodiesel production. An improved biodiesel production was seen in the alkali-catalyzed transesterification process when reaction temperatures were raised, as seen in the figure.

Optimizing and validating biodiesel yield

For each process variable, the ideal value was found using Regression Equation (3). Figure 5 shows the ideal parameters for making biodiesel. Based on the outcome of the RSM model, the optimal parameters are as follows: B of 0.811601 wt%, C of 75.8837°C, D of 98.2069 minutes, and A of 6.10935:1. The projected maximum biodiesel production under these ideal circumstances was 98.2069%. A yield of 97.762% was achieved in an experiment that used the optimum processing factors. The yield of Jatropha Oil methyl ester is 0.35% off from the ideal value, which is still within acceptable limits. The yield of Jatropha Oil methyl ester is 0.35% off from the ideal value, which is still within acceptable limits.

Engine performance analysis

Torque and Power

Fig 6 and 7 display the impact of engine functioning settings on braking torque and power. Figure 6 shows that at 2200 rpm, the braking power was maximal for all test fuels. The brake power ratings are negatively impacted by increasing concentrations of biodiesel blends. Torque readings taken at high engine speeds reveal a drop with increasing biodiesel blend percentage.

Exhaust emissions analysis

CO emission

Fig. 8 displays the effect of engine operating variables on CO emissions. The carbon monoxide emission value of fuel blends decreased as the biodiesel blend percentages increased. The oxygen concentration of biodiesel usually causes the decline since it makes combustion more difficult.

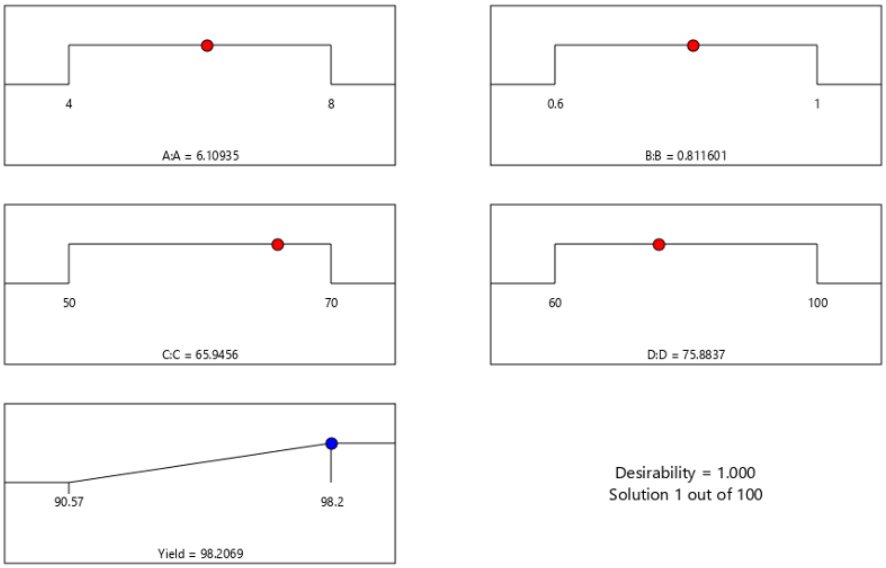


Figure 5. Optimized results of biodiesel yield

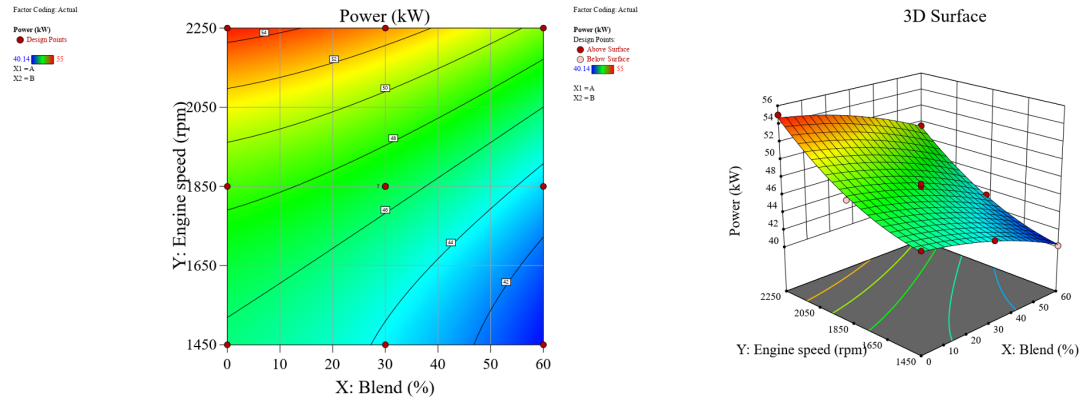


Figure 6. contour plot and 3 D RSM for power versus X and Y

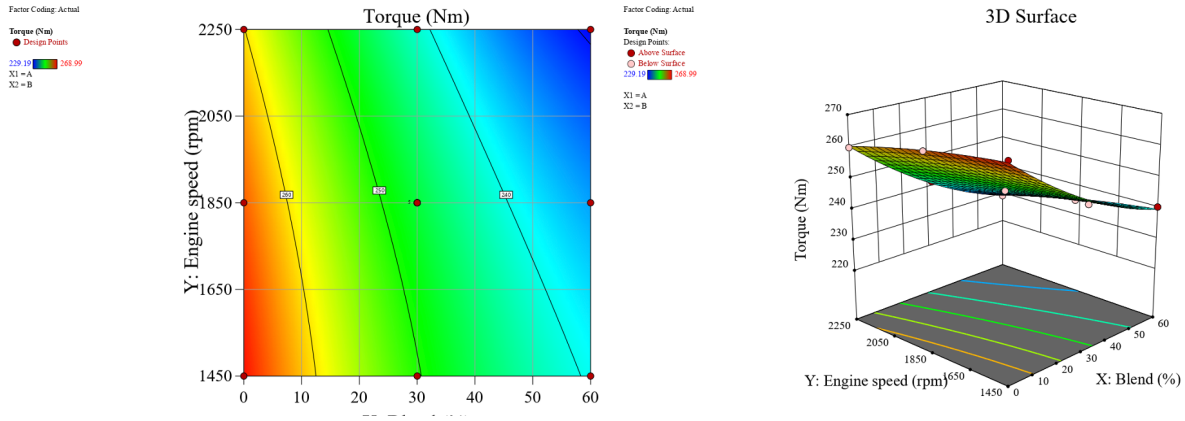


Figure 7. 2D and 3 D contour plot RSM for torque versus X and Y

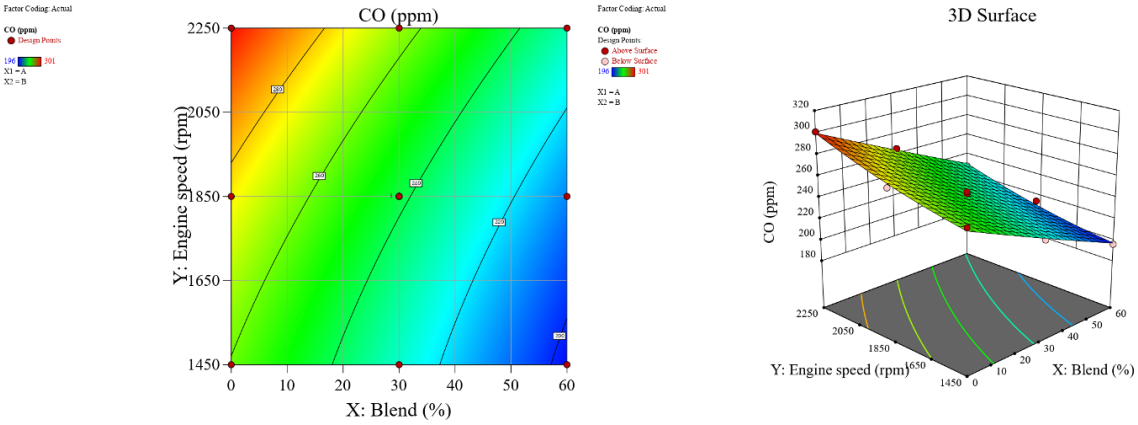


Figure 8. Contour plot and 3 D RSM for CO versus X and Y

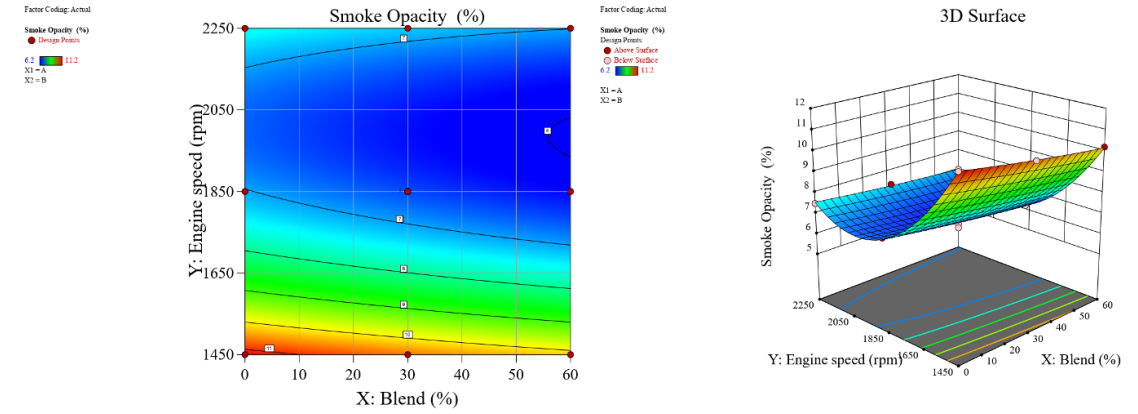


Figure 9. Contour plot and 3D RSM for smoke opacity versus X and Y

Smoke opacity

Fig. 9 displays a 2D contour plot and 3D RSM illustrating the changes in smoke opacity at various engine running settings. Biodiesel fuel mixtures have a lower smoke opacity value related to diesel fuel. This corresponds to the maximum oxygen content found in biodiesel, resulting in enhanced and complete fuel burning [30].

NOx emission

Figure 10 displays a 2D and 3D contour plot illustrating the combined effect of blending proportion and speed of engine on NOx releases. NOx emissions rise as the biodiesel blend ratios increased. NOx emissions are rising because biodiesel's higher oxygen content improves combustion, leading to increased combustion temperature and providing extra oxygen for NOx generation.

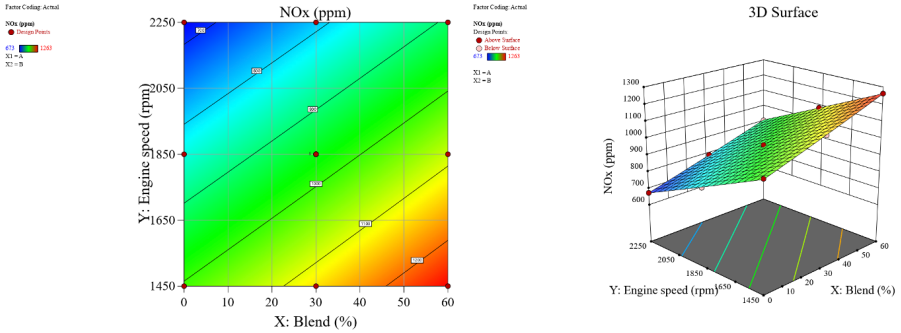


Figure 10. Contour plot and 3 D RSM for NOx versus X and Y.

Optimization and validation of engine results

The engine factors were optimized using Design Expert 13, and the outcomes are presented in Fig. 11. Reducing exhaust emissions while optimizing engine performance factors is the goal of this research. The findings indicate that the optimal anticipated values for torque, power, smoke opacity, NOx and CO are 254.757 Nm, 50.0817 kW, 6.48966%, 819.573 ppm and 270.009 ppm, respectively. These values are achieved with an engine speed of 2011.24 rpm and biodiesel blend of 12.5845%. Experimental testing was undertaken at the optimum input values to validate the optimized findings. Table 12 presents the test and predicted results. The validation findings indicate that the RSM model is highly effective for optimizing engine performance and emission values. Also Alcohols are promising alternative fuels to fossil-based gasoline. Ethanol and methanol are the alcohols that widely investigated for usability in internal combustion engines[31]. Moreover several opportunities exist for the future of fossil fuels, including technological advancements in CCS, the potential role of natural gas as a "bridge" fuel, and the use of fossil fuels in non-energy applications [32]. The engine performance of Jatropha biodiesel

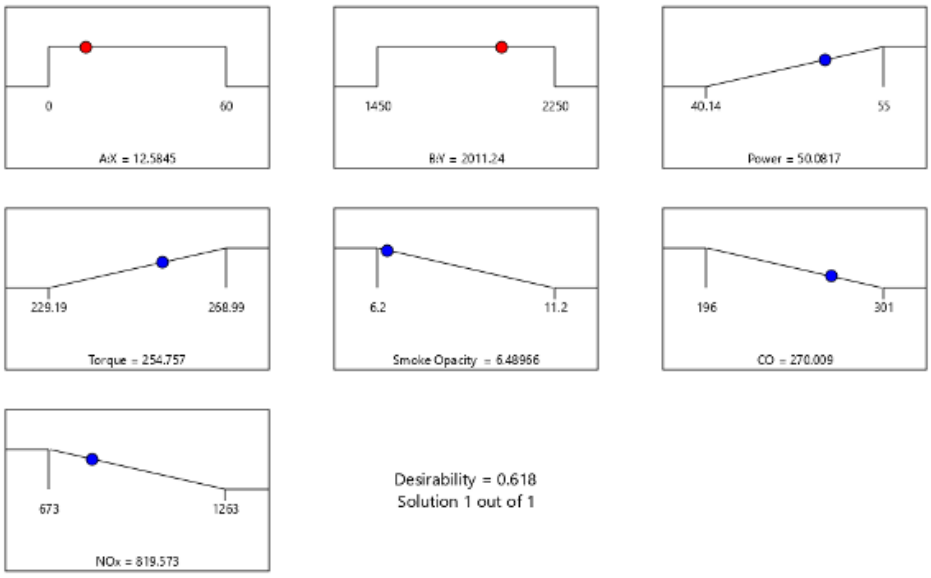


Figure 11. Optimization graph displaying torque, power, smoke opacity, NOx and CO

is equivalent to that of petroleum-based diesel [33].The oxygen content in biodiesel affects its combustion characteristics, often leading to a decrease in combustion efficiency due to incomplete combustion. 7:1 methanol/oil ratio and 0.9% catalyst when blended with petro-diesel (B20) gave the highest cetane number [34]. The analysis of variance showed that fuel type was the predominant operating factor influencing the grey relational grade which means fuel type was the most important parameter in the simultaneous optimization of exhaust emissions and engine performance higher output torque value, better thermal efficiency and durability [35,36].

Table 12. Checking for optimal performance and comparing emissions to prior studies

Factors	Predicted	Experimental	Error (%)
Blend (%)	12.5845	12.5845	–
Speed (rpm)	2011.24	2011.24	–
Load (%)	–	–	–
Injection pressure (bar)	–	–	–
Injection Timing bTDC	–	–	–
Torque (Nm)	254.757	253.59	0.46
Brake power (kW)	50.0817	49.13	1.92
BSFC (g/kWh)	–	–	–
BTE (%)	–	–	–
EGT (C)	–	–	–
NOx (ppm)	819.573	825.54	0.73
CO (ppm)	270.009	276	2.19
Smoke (%)	6.48966	6.71	3.34
UHC (ppm)	–	–	–

ECONOMIC ANALYSIS

The cost of Jatropha biodiesel production is influenced by factors such as seed procurement, oil extraction, transesterification, and purification processes. An economic analysis reveals that while initial setup and production costs can be high, optimizing these processes through methods like response surface methodology can enhance efficiency and reduce expenses. The parameters used to find economic costs for the design can be calculated mathematically energy sector could address the wastefulness associated with this particular waste stream [37,38].

CONCLUSIONS

➔This study used a transesterification procedure to create biodiesel from jatropha oil. To get the maximum biodiesel output, BBD was used. The adoption of CCD led to an increase in engine efficiency and a decrease in emissions. Here are the results:

➔The most important factors influencing biodiesel production, emission characteristics and engine performance can be identified with the use of statistical analysis. Its goal is to minimize the number of experiments needed to get the most reliable results.

➔The ideal settings for biodiesel generation were a 10935:1 molar ratio A, 0.811601 wt% B, 75.8837°C C, and 98.2069 min D. The projected maximum biodiesel production under these ideal conditions was 98.2069%. The experimental yield of 97.762% closely matches the projected yield of 98.2069% based on the results.

➔The optimization model for biodiesel had an R2 of 0.9596, whilst the corresponding values for torque, power, smoke opacity, NOx and CO were 99.63%, 99.35%, 99.54%, 99.96%, and 98.72% respectively.

➔With 50.0817 kW of power, 254.757 Nm of torque, 6.48966% of smoke opacity, 270.009 ppm of CO, and 819.573 ppm of NOx, respectively, these are the ideal values. These values are achieved with a biodiesel blend of 12.5845% at speed of engine of 2011.24 rpm.

➔Rendering to the validating test conducted under ideal conditions, the percentage of error between the optimal responses and the experimental results was less than 3%.

➔The results showed that the error rates for torque (0.46%), power (1.92%), smoke opacity (3.34%), NOx (0.73%), and

CO (2.19%).

➛The findings proved that RSM design is useful for optimizing biodiesel productivity processing variables and engine operating factors.

➛The successful application of RSM in this study suggests its potential for broader applications in optimizing other biofuel production processes, contributing to the development of more sustainable and efficient renewable energy sources.

NOMENCLATURE

ASTM	American Society for Testing and Materials
B20	20% Biodiesel Blend
B100	100% Biodiesel Blend
CN	Cetane Number
CO	Carbon Monoxide
CO_2	Carbon Dioxide
EGR	Exhaust Gas Recirculation
EPA	Environmental Protection Agency
BSFC	Brake Specific fuel consumption
BTE	Brake Thermal Efficiency
RSM	Response Surface Methodology

DATA AVAILABILITY STATEMENT

The author confirm that the data that supports the findings of this study are available within the article. Raw data that support the finding of this study are available from the corresponding author, upon reasonable request.

CONFLICT OF INTEREST

The author declared no potential conflicts of interest with respect to the research, authorship, and/or publication of this article.

USE OF AI FOR WRITING ASSISTANCE

Not declared.

ETHICS

There are no ethical issues with the publication of this manuscript.

REFERENCES

[1] V. Rajasekar, "Experimental investigations to study the effect of butanol and pentanol addition in a jatropha oil methyl ester fuelled compression ignition engine," Journal of Chemical and Pharmaceutical Sciences, vol. 9, no. 1, pp. 665–668, 2016.

[2] P. S. Yadav, Z. Said, R. Gautam, R. Raman, and H. Caliskan, "Novel investigation on atomization, performance, and emission characteristics of preheated jatropha oil methyl ester and ethyl ester," Energy, vol. 270, 2023.

[3] M. Subramaniam et al., "Performance Enhancement of Jatropha Methyl Ester by Utilizing Oxygen Enrichment in Diesel Engine," in Lecture Notes in Mechanical Engineering, 2022, pp. 261–271.

[4] V. Rajasekar, V. E. Geo, L. J. Martin, and B. Nagalingam, "The combined effect of low viscous biofuel and EGR on NO-smoke tradeoff in a biodiesel engine—an experimental study," Environmental Science and Pollution Research, vol. 27, no. 15, pp. 17468–17480, 2020.

[5] T. Bothiraj, K. Boopathi, K. Kalaiselvan, A. Benham, and S. Mayakannan, "Experimental investigations on mechanical and wear behavior of waste marble dust and coconut fiber reinforced hybrid bio composites," in Materials Today: Proceedings, 2022, pp. 2239–2242.

[6] N. R. Banapurmath and P. G. Tewari, "Performance, combustion, and emissions characteristics of a single-cylinder compression ignition engine operated on ethanol-biodiesel blended fuels," Proceedings of the Institution of Mechanical Engineers, Part A: Journal of Power and Energy, vol. 224, no. 4, pp. 533–543, 2010.

[7] B. N. Rao et al., "Utilization of additives in biodiesel blends for improving the diesel engine performance and minimizing emissions through a modified Taguchi approach," Heliyon, vol. 9, no. 6, 2023.

[8] R. Gautam, N. Kumar, and P. Sharma, "Experimental investigation on use of jatropha oil ethyl easter and diesel blends in small capacity diesel engine," in SAE Technical Papers, 2013.

[9] L. Karikalan and M. Chandrasekaran, "Effect of varying fuel injection pressure of selective vegetable oil biodiesel on C.I engine performance and pollutants," Int J Chemtech Res, vol. 8, no. 12, pp. 312–318, 2015.

[10] I. S. N. V. R. Prasanth et al., "Study of Friction and Wear Behavior of Graphene-Reinforced AA7075 Nanocomposites by Machine Learning," J Nanomater, vol. 2023, 2023.

[11] R. Gautam, N. Kumar, H. S. Pali, and P. Kumar, "Experimental studies on the use of methyl and ethyl esters as an extender in a small capacity diesel engine," Biofuels, vol. 7, no. 6, pp. 637–646, 2016.

[12] S. Yadav, M. Charniya, A. Biswal, P. Singh, S. Agrawal, and B. Nayak, "EXPERIMENTATION ON DIE-

SEL ENGINE IN DUAL FUEL MODE FUELED WITH JATROPHA OIL AND PRODUCER GAS," International Journal of Energy for a Clean Environment, vol. 23, no. 7, pp. 131–140, 2022.

[13] D. Balasubramanian, A. Rajarajan, R. Krishnamoorthy, and T. D. Quoc, "Experimental Investigation of Unmodified Diesel Engine on Performance, Combustion and Emission with Various Proportions of Jatropha Biofuel in Diesel," in Energy, Environment, and Sustainability, 2021, pp. 149–171.

[14] D. Dinesh Kumar et al., "Study of Microstructure and Wear Resistance of AA5052/B4C Nanocomposites as a Function of Volume Fraction Reinforcement to Particle Size Ratio by ANN," J Chem, vol. 2023, 2023.

[15] B. S. Chauhan, N. Kumar, and H. M. Cho, "A study on the performance and emission of a diesel engine fueled with Jatropha biodiesel oil and its blends," Energy, vol. 37, no. 1, pp. 616–622, 2012.

[16] M. S. Panithasan, D. Gopalakichenin, G. Venkadesan, and M. Malairajan, "Evaluating the working characters of a diesel engine fueled with biodiesel blends added with rice husk Nano particles," Energy Sources, Part A: Recovery, Utilization and Environmental Effects, 2020.

[17] B. Ramesh, S. Sathish Kumar, A. H. Elsheikh, S. Mayakannan, K. Sivakumar, and S. Duraithilagar, "Optimization and experimental analysis of drilling process parameters in radial drilling machine for glass fiber/nano granite particle reinforced epoxy composites," in Materials Today: Proceedings, 2022, pp. 835–840.

[18] R. Manikandan et al., "Optimization and experimental investigation on AA6082/WC metal matrix composites by abrasive flow machining process," Mater Today Proc, 2023.

[19] C. Sasikumar, K. Balamurugan, S. Jegadheeswaran, and R. Sathyamurthy, "Optimization of process parameter in the production of Jatropha Methyl Ester using response surface methodology," Biocatal Agric Biotechnol, vol. 27, 2020.

[20] A. Ashok, S. K. Gugulothu, R. V Reddy, A. E. Gurel, and B. Deepanraj, "Prediction-optimization of the influence of 1-pentanol/jatropha oil blends on RCCI engine characteristics using multi-objective response surface methodology," Renewable Energy Focus, vol. 42, pp. 8–23, 2022.

[21] R. Jayaraman, R. Girimurugan, V. Suresh, C. Shilaja, and S. Mayakannan, "Improvement on Tensile Properties of Epoxy Resin Matrix Sugarcane Fiber and Tamarind Seed Powder Reinforced Hybrid Bio-Composites," in ECS Transactions, 2022, pp. 7265–7272.

[22] A. Khalid et al., "Influences of Fuel Additive, Crude Palm and Waste Cooking Oil on Emission Characteristics of Small Diesel Engine," in IOP Conference Series: Materials Science and Engineering, 2017.

[23] L. Prasad, S. Pradhan, L. M. Das, and S. N. Naik, "Experimental assessment of toxic phorbol ester in oil, biodiesel and seed cake of Jatropha curcas and use of biodiesel in diesel engine," Appl Energy, vol. 93, pp. 245–250, 2012.

[24] R. Girimurugan, C. Shilaja, S. Mayakannan, S. Rajesh, and B. Aravinth, "Experimental investigations on flexural and compressive properties of epoxy resin matrix sugarcane fiber and tamarind seed powder reinforced bio-composites," in Materials Today: Proceedings, 2022, pp. 822–828.

[25] A. Ashok, S. K. Gugulothu, R. V Reddy, and H. Ravi, "Box-Behnken Response Surface Methodology Based Multi-Objective Optimization on Reactivity Controlled Compression Ignition Engine Characteristics Powered With Ternary Fuel," Journal of Energy Resources Technology, Transactions of the ASME, vol. 144, no. 12, 2022.

[26] H. Farouk, S. M. Zahraee, A. E. Atabani, M. N. Mohd Jaafar, and F. H. Alhassan, "Optimization of the esterification process of crude jatropha oil (CJO) containing high levels of free fatty acids: a Malaysian case study," Biofuels, vol. 11, no. 6, pp. 655–662, 2020.

[27] K.-T. Liu, S. Gao, T.-W. Chung, C.-M. Huang, and Y.-S. Lin, "Effect of process conditions on the removal of phospholipids from Jatropha curcas oil during the degumming process," Chemical Engineering Research and Design, vol. 90, no. 9, pp. 1381–1386, 2012.

[28] A. Singh, S. Sinha, and A. K. Choudhary, "Optimization of Operating Parameters of Diesel Engine Powered with Jatropha Oil Diesel Blend by Employing Response Surface Methodology," International Journal of Renewable Energy Research, vol. 11, no. 2, pp. 504–513, 2021.

[29] M. Athar et al., "Biodiesel production by single-step acid-catalysed transesterification of Jatropha oil under microwave heating with modelling and optimisation using response surface methodology," Fuel, vol. 322, 2022.

[30] E. Ramachandran, R. Krishnaiah, E. P. Venkatesan, S. Shaik, C. A. Saleel, and F. Hussain, "Investigation into the Ideal Concoction for Performance and Emissions Enhancement of Jatropha Biodiesel-Diesel with CuO Nanoparticles Using Response Surface Methodology," ACS Omega, vol. 8, no. 42, pp. 39067–39079, 2023.

[31] Solmaz H. A comparative study on the usage of fusel oil and reference fuels in an HCCI engine at different compression ratios. Fuel. 1;273:117775, 2020.

[32] Alagoz E, Alghawı Y. The Future of Fossil Fuels: Challenges and Opportunities in a Low-Carbon. IJESKA. December 2024;5(3):381-388.

[33] T. M. I. Riayatsyah, A. H. Sebayang, Current Progress of Jatropha Curcas Commoditisation as Biodiesel Feedstock: A Comprehensive Review, Frontiers in Energy Research, Volume 9 – 2022.

[34] Iqbal, N. & Ahiduzzaman, M. & Rahman, Md.

Hafizur & Ali, S.M.Y. & Onik, Jakaria. (2015). Extraction and Characteristics Analysis of Jatropha (Jatropha curcas) Seed Oil. International Journal of Business, social and scientific research. 4. 06-13.

[35] Çelik, M., Bayındırlı, C., & Mehregan, M. (2022). Multi-objective optimization of a diesel engine fueled with different fuel types containing additives using grey-based Taguchi approach. Environmental science and pollution research international, 29(20), 30277–30284. https://doi.org/10.1007/s11356-021-18012-1

[36] Çelik, M., Bayındırlı, C., & İlhak, M. İ. (2022). Investigation of the Performance and Emissions of an Engine Operated with CEO2 Nano Additive Doped Biodiesel. International Journal of Automotive Science And Technology, 6(2), 113-119. https://doi.org/10.30939/ijastech..1063986

[37] Hani Al-Rawashedh, Omar A, Laith M, (2023) Different Scenarios for Reducing Carbon Emissions, Optimal Sizing, and Design of a Stand-Alone Hybrid Renewable Energy System for Irrigation Purposes, International Journal of Energy research. https://doi.org/10.1155/2023/6338448

[38] Ala'a K. Al-Bawwat, Mohamed R. Gomaa, Antonio Cano, Francisco Jurado, Eid M. Alsbou,Extraction and characterization of Cucumis melon seeds (Muskmelon seed oil) biodiesel and studying its blends impact on performance, combustion, and emission characteristics in an internal combustion engine,Energy Conversion and Management: X, Volume 23,2024,100637,ISSN 2590-1745,https://doi.org/10.1016/j.ecmx.2024.100637.

Environ Res Tec, Vol. 8, Issue. 2, pp. 345-353, June 2025

Environmental Research and Technology
https://dergipark.org.tr/en/pub/ert
DOI: https://10.35208/ert.1499294

Research Article

From self-care to earth care: Uncovering the role of self-compassion in the link between environmental identity and pro-environmental behaviors in young men

Adem KANTAR*[1], Begum YILMAZCAN[2]

[1]Erzurum Technical University, Psychology Dept., Faculty of Letters, Erzurum, Türkiye,
[2]Cappadocia University, Psychology Department, Nevşehir, Türkiye

ARTICLE INFO

Article history
Received: 11 Jun 2024
Revised: 19 Aug 2024
Accepted: 04 Sep 2024

Key words:
Pro-environmental behaviors, environmental identity, self-compassion, men.

ABSTRACT

This study explores the role of self-compassion in promoting eco-friendly behaviors among young Turkish men, focusing on how it mediates the relationship between environmental identity and such behaviors. Involving 323 males aged 18 to 49 from Türkiye (M = 22.03, SD = 2.96), it employed self-report measures to assess environmental identity, self-compassion, and eco-friendly behaviors. The findings revealed positive correlations among these factors, highlighting that self-compassion significantly mediates the link between environmental identity and eco-friendly actions. This suggests that self-compassion might be critical in encouraging young males to engage in environmental conservation. The study underscores the potential of nurturing self-compassion as a strategy to promote eco-friendly behaviors in demographics traditionally less engaged in such practices. These findings can open avenues for environmental campaigns and education programs, focusing on psychological aspects to drive behavioral change.

Cite this article as: Kantar A, Yılmazcan B. From self-care to earth care: Uncovering the role of self-compassion in the link between environmental identity and pro-environmental behaviors in young men. Environ Res Tec 2025;8(2) 345-353.

INTRODUCTION

It is crucial to act ecologically friendly to address the current global environmental challenges that human activity has caused but which human action may also solve. Recognizing this, it has become imperative to adopt eco-friendly practices as a means to counter these global issues [1]. Thus, one must examine which factors influence an individual's pro-environmental behaviours [2].

Gender is a demographic factor that is often studied in the literature on environmentally friendly behaviors. Previous studies consistently found that females have stronger environmental protection attitudes and less favorable environmental utilization attitudes than males. Females are also more likely to engage in eco-friendly behaviors [3, 4, 5, 6]. Therefore, there is a need to investigate the factors that can encourage men's environmentally friendly behaviors.

Self-compassion may be one of these factors. More clearly, recent research [7, 8, 9, 10] has shown that a greater level of self-compassion is associated with higher levels of pro-environmental attitudes and behaviors. However, these results were only derived from the loose culture that Gelfand et al. [11] emphasized. Therefore, the role of self-compassion linked to eco-friendly behaviors in tight cultures, such as

***Corresponding author.**
*E-mail address: adem.kantar@erzurum.edu.tr

This is an open access article under the CC BY-NC license (http://creativecommons.org/licenses/by-nc/4.0/).

Türkiye, still needs to be studied. Furthermore, whether self-compassion for men promotes more environmentally friendly behavior has not yet been investigated.

As a result, this study aims to examine the mediating role of self-compassion in the link between environmental identity and pro-environmental behaviors in Turkish young men, controlling for socioeconomic level and age variables, in light of this gap in the literature.

LITERATURE REVIEW

The damage we do to nature is increasing daily due to industrialization, increasing consumption habits, and growing human populations. However, while there is still time, we can stop or reverse this damage [12]. With more clarity, reducing environmental problems may be possible if individuals internalize environmental problems and transform their daily behaviors [13]. For this reason, the researchers focus on individual factors linked to environmentally friendly behaviors [14, 15, 3, 4]. These factors can help reveal what motivates and hinders individuals from engaging in environmentally friendly behaviors. Gender is one of these factors [3, 4, 5, 6].

The literature defines gender differences as the environmental gender gap [15]. The environmental gender gap refers to the differences in attitudes, perceptions, and behaviors between women and men on environmental issues such as climate change, animal welfare, and plastic pollution [16]. Compared to men, women produce less waste, recycle more, and have a smaller carbon footprint [17]. Previous studies have shown that women are more aware of the climate crisis and support environmental regulations [3]. This difference between genders may be related to the socialization processes of men [18].

Indeed, as the specified Social Role Theory posits, people undergo a socialization process during early childhood, leading them to adopt gender-appropriate roles [19]. In the context of traditional gender roles, women are expected to be nurturing, caring, and empathetic, while men are expected to be independent, strong, emotionally detached, and assertive. In this respect, women's socialization into caregiving roles may make them more empathetic to environmental issues [14, 15, 20, 21]. In other words, green behaviors are associated with societal femininity [3].

Green behaviors such as caring for nature and choosing products with recycling options are associated with femininity in society [3]. Existing studies [22, 23] showed that men feel threatened when exposed to feminine roles and avoid behaviors that signalize femininity. As explained by Social Identity Theory [24], men who value masculine norms protect and enhance their in-group status by "avoiding feminine behaviors" [25]. That is why, for men who strongly conform to masculine norms, behaving in a feminine way means being perceived as unmanly [26]. For instance, men may perceive environmentally friendly behaviors such as recycling trash and using water and electricity sparingly as feminine. These behaviors can be perceived as a threat to their masculine identity [3, 22]. Therefore, there is a need to investigate the factors that can encourage environmentally friendly behaviors among young men. One of these factors may be self-compassion.

Self-compassion is treating oneself with kindness and understanding in the face of personal pain, perceived failure, or inadequacy [27]. Studies on self-compassion indicated that self-compassion is positively correlated with positive emotions (happiness, optimism, and life satisfaction) and negatively correlated with negative emotions (depression and anxiety symptoms). Additionally, meta-analytic studies on self-compassion [28, 29] consistently found that self-compassion positively correlates with psychological well-being.

According to recent research [30, 7, 31, 32], self-compassion affects not only one's own well-being but also contributes to caring for the well-being of others. From this perspective, it can be argued that self-compassionate individuals may be more sensitive to the pain of others. To put it more clearly, the degree to which a person recognises the suffering of nature or other people and the urge to act on it may be a factor in determining whether or not they intend to engage in environmentally conscious behaviour.

Indeed, previous studies [8, 9, 10] have found positive associations between self-compassion and pro-environmental behaviors. However, these relationships were obtained only in loose cultures. Therefore, the role of self-compassion in tight cultures such as Türkiye is not yet known. From this point, this research examines self-compassion linked to eco-friendly behaviors among young males in Türkiye, categorized as a norm-restrictive or "tight" culture, according to Gelfand et al. [11].

Gelfand et al. [11] classified cultures as either "loose" or "tight" according to how important societal norms and expectations are to each individual. According to Gelfand et al. [33], tight cultures place more value on conforming to social norms, which makes breaking from them more difficult. People in these cultures usually give the group's preferences precedence over their own.

As presented above, this study examines whether self-compassion encourages pro-environmental behaviors in tight cultures such as Türkiye, where social norms and group expectations are important. Previous studies have revealed that more self-compassionate people are less concerned with the opinions of others and exhibit more prosocial behaviors [34, 35, 36]. Based on this foreground, we predict that self-compassionate men will be more likely to engage in environmentally friendly behaviors. This is because we expect self-compassionate men to act in accordance with their own internal references rather than trying to conform to their in-group expectations or seek approval from others. Based on the current literature, we hypothesize that self-compassion may mediate the link between environmental identity and pro-environmental behaviors in Turkish young men, controlling for socioeconomic level and age variables. We tested the following hypotheses to examine our theoretical assumptions.

•Environmental identity and eco-friendly behaviors are pos-

itively correlated.

•Environmental identity and self-compassion are positively corelated.

•Self-compassion and eco-friendly behaviors are positively correlated.

•Self-compassion mediates the relationship between environmental identity and eco-friendly behaviors.

METHOD

Power Analysis

The number of participants in the study was decided using the Monte Carlo Power Analysis for Indirect Effects [37] as an a priori analysis. The R-based application facilitated the computation of the needed sample size for mediational analyses. The researchers defined the appropriate sample size for the study by considering a medium effect size (f 2 = 0.5), a desired power level of 0.85, and a significance level of 0.05. These specifications were chosen based on recommendations for conducting a mediational model, as highlighted by Cohen [38] and Schoemann et al. [39]. The target sample size of our study was calculated to be 320 participants based on the results of the power analysis. We aimed to recruit at least 330 participants to account for potential participant loss.

Participants and Procedure

323 male university students completed the web-based survey across Türkiye. The study included participants aged 18 to 49 (M = 22.03, SD = 2.96). 30% (n = 97) were from the Faculty of Letters, 21.4% (n = 69) of the participants were from the Faculty of Architecture and Engineering, 8.4% (n = 27) from the Faculty of Education, 8% (n = 26) were from the Faculty of Economics and Administrative Sciences, 5.3% (n = 17) from the Faculty of Medicine, 5% (n = 16) from the Faculty of Sport Sciences, 5.6% (n = 18) from the Faculty of Health Sciences and 16.3% (n=53) from the other faculties. Almost all participants were undergraduate students, comprising 89% of the total sample. Second-year students made up 89 (27.6%) of the participants, followed by first-year students, who made up 84 (%26). Students in their third and fourth years comprised the remaining group (46.4%).

Data were obtained from Turkish university students who self-identified as male. In the demographic section, they could describe their gender orientation in their own words. Almost all of them (98%) identified as heterosexual. Participants confirmed their voluntary attendance and consented to the study before the survey began. After the demographic questions, they filled out other instruments. The data were collected using an online survey platform, allowing them to leave the study anytime. The survey took almost 15 minutes to complete. The data collection session was initiated once the ethics committee, where the researchers were employed, was approved. The approval was documented under the number 04/26.

Measures

We collected research data via three scales. The details of the scales are presented below.

Pro-environmental Behaviour Scale (PEBS). Tanık Önal et al. [40] developed the PEBS to assess pro-environmental behaviors among university students. The scale is a 10-item Likert-type scale, with higher scores indicating a stronger positive attitude towards environmentally friendly behaviors. For example, one item is: "Talking to friends about environmental problems." Previous research has found that the PEBS has good internal consistency, with a Cronbach's alpha of 0.82 [40].

Self-Compassion Scale-Short Form (SCS-SF). The SCS-SF was developed by Raes et al. [41] to measure self-compassion. Kantaş [42] adapted the scale to Turkish culture. The scale is a 12-item Likert-type scale, with higher scores indicating higher levels of self-compassion. For example, one item is: "When I am going through a tough time, I give myself the caring and tenderness I need." Prior research has found that the SCS-SF has good internal consistency, with a Cronbach's alpha of 0.86 [41]

Environmental Identity Scale (EIS). The EIS was developed by Clayton [43] to measure environmental self-concept. Tanık et al. [40] adapted the scale to Turkish culture. The scale is a 14-item Likert-type scale, with higher scores indicating higher levels of environmental identity. For example, one item is: "The engagement in environmentally conscious behaviors holds significance in my personal values." Previous research has found that the EIS has good internal consistency, with a Cronbach's alpha of 0.88 [40]. The current study found a similar alpha of 0.85.

Data Set Preparation for Multivariate Statistical Analysis

Before we began the analyses, we checked to ensure that the data met the assumptions of multivariate statistics. According to George and Mallery [44], the distribution of the research variables was normal because both skewness and kurtosis values were within the acceptable range of ±2. All consistency metrics were greater than 0.70, indicating that the variables were internally consistent. The data did not contain any missing values. To identify outliers, we used the Mahalanobis Distance and Z scores methods. Seven people were removed from the dataset because they were identified as outliers using these methods [45]. We used the variance inflated factor (VIF), tolerance, and Durbin-Watson (DW) values to test for multicollinearity. All VIF values were less than 10, and all tolerance metrics were greater than 0.10. The DW value of 1.93 indicated that there were no meaningful correlations among the residuals, indicating that there was no problem with multicollinearity. As a result, a total of 323 people participated in the analyses.

Statistical Analyses

We conducted a series of analyses to investigate the relationship between environmental identity and pro-environmental behaviors. First, we calculated descriptive statistics and

bivariate correlations for the study variables. This allowed us to understand the basic characteristics of the data and the relationships between the variables. Second, we constructed a mediation model to test the mediating effect of self-compassion. A mediation model is a statistical model that examines how one variable (environmental identity) affects another variable (eco-friendly behaviors) indirectly through a third variable (self-compassion). Furthermore, the covariate variables were age and socioeconomic status [45].

We used the PROCESS macro for SPSS to analyze the mediation model. This macro uses a bootstrapping procedure to estimate the indirect effects. Bootstrapping is a statistical technique that randomly samples data from the original data set and re-estimates the model multiple times. This helps to reduce bias in the estimates of the indirect effects. We used 5,000 bootstrap samples to estimate the indirect effects. We considered an indirect effect to be statistically significant if its confidence interval did not include the zero value [45].

RESULTS

Descriptive Statistics

The bivariate correlations, mean values, and standard deviations for each variable are shown in Table 1. Additionally, it displays the variables' kurtosis and skewness values.

Table 1. Descriptive statistics of research variables and their correlations (n = 323).

Variable	Mean ± SD	Skewness	Kurtosis	1	2	3
Self-compassion (1)	70.50 ± 14.10	-,339	-,293	-	,278**	,262**
Eco-friendly behaviours (2)	38.59 ± 8.14	-,112	,060	-	-	,495**
Environmental identity (3)	35.53 ± 7.08	-,106	-,360	-	-	-

As shown in Table 1, self-compassion had positive and significant correlations with eco-friendly behaviors ($r = .278$, $p < .05$) and environmental identity ($r = .262$, $p < .05$). However, eco-friendly behaviors had positive and significant connection with environmental identity ($r = .495$, $p < .05$). Moreover, since the values for skewness and kurtosis are between +2 and -2 [44], the variables had a normal distribution.

Mediational Analysis

We conducted a mediation analysis after verifying that the assumptions were met. Figure 1 shows the model results for the mediating role of self-compassion in the link between environmental identity and eco-friendly behaviors, controlling for socioeconomic status and age.

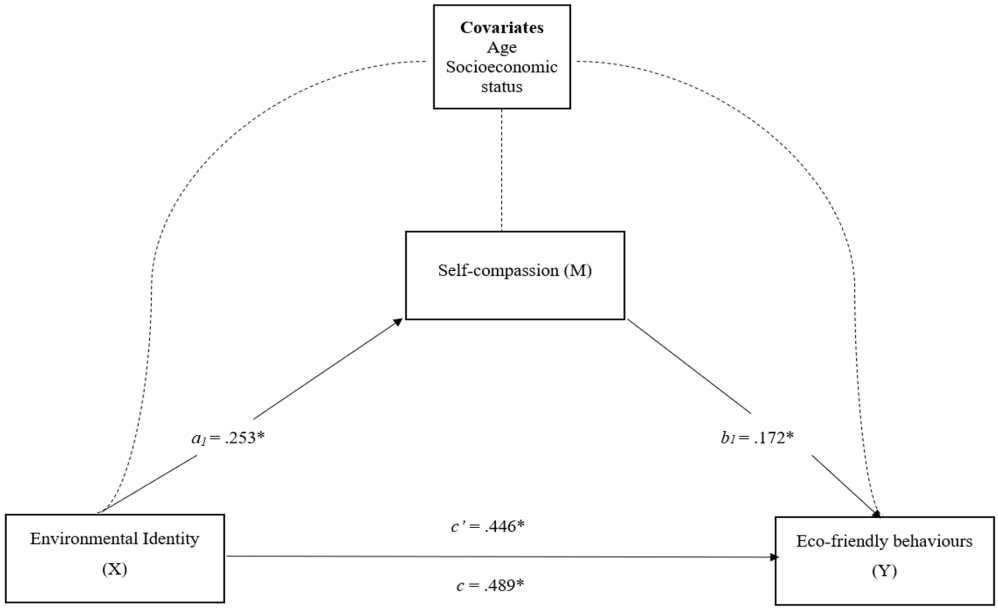


Figure 1. Mediational analysis results.

EI = Environmental identity, SC = Self-compassion, EFB = Eco-friendly behaviors. c = total effect, c' = direct effect. *p < .001. The coefficients displayed are standardized values.

Figure 1 and Table 2 show the results of the mediation analysis. The study found that there was a significant positive relationship between environmental identity and both self-compassion (β = 0.253, SE = 0.031, t = 4.64, p < 0.001) and eco-friendly behaviors (β = 0.446, SE = 0.024, t = 9.00, p < 0.001). This means that male university students with a strong sense of environmental identity are also more likely to be self-compassionate and engage in eco-friendly behaviors.

The study also found that self-compassion significantly predicted eco-friendly behaviors (β = 0.172, SE = 0.042, t = 3.50, p < 0.001). This means that self-compassion was associated with an increase in eco-friendly behaviors.

Table 2. The mediation model results in Fig 1

		Consequent						
		M1(SC)				*Y*(EFB)		
Antecedent		Coeff.	*SE*	*p*		Coeff.	*SE*	*p*
X (EI)	a_1	.253	.031	<.001	c'	.446	.024	<.001
M1 (SC)		-	-	-	b_1	.172	.042	<.001
Constant	i_{M1}	20.87	4.16	<.001	i_Y	20.79	3.31	<.001
		R^2 = .08 $F(3;319) = 9.30, p < .001$				R^2 = .29 $F(4;318) = 32.41, p < .001$		

Note. c' = direct effect. The coefficients displayed are standardized values.

The present study examined the potential role of self-compassion as a mediator in the relationship between environmental identity and eco-friendly behaviors. We used the Bootstrapping method to analyze the confidence intervals for the indirect effect coefficients (Hayes, 2022). Our findings suggest that self-compassion mediated the relationship between environmental identity and eco-friendly behaviors. This is because the confidence intervals for the indirect effect did not include zero (B = .0220, CI [.007, .040]). Additionally, the model was statistically significant, explaining 29% of the variance in eco-friendly behaviors (F(4;318) = 32.41, p < .001, R2 = .29).

DISCUSSION

This study aimed to examine the role of self-compassion in promoting environmentally friendly behaviors in young Turkish men. To this end, the study examined whether self-compassion mediates the relationship between environmental identity and eco-friendly behaviors. The findings supported the research hypotheses, which means that self-compassion mediates the relationship between environmental identity and eco-friendly behaviors. The independent variables explained 29% of the variation in eco-friendly behaviors.

No previous research has examined the relationship between self-compassion, environmental identity, and eco-friendly behaviors in male samples. However, previous studies [14, 8, 9, 10, 46] showed that empathy and compassion can promote eco-friendly behaviors in community or university samples. In this respect, the findings are consistent with previous findings in the literature.

First, an increased environmental identity was associated with increased eco-friendly behaviors. Similarly, a recent meta-analysis study [47] conducted with data from 188 studies found a positive relationship between environmental identity and pro-environmental behaviors. Second, an increased environmental identity was associated with increased self-compassion, which predicted higher levels of eco-friendly behaviors. In other words, self-compassion may make it easier for young men to self-identify as environmentalists and act accordingly. This study adds to previous research [8, 9, 10] by showing that self-compassion can increase environmental awareness. However, the current findings extend this line of research by demonstrating that compassion can increase environmental awareness not only when it is shown to others or nature, but also to oneself. This finding can emphasize how crucial self-compassion is for young men who are reluctant to be eco-friendly.

Self-compassion can be important for young men who avoid engaging in environmentally friendly behaviors. According to Neff and Vonk [35], more self-compassionate people are more aware of their own thoughts and feelings and less concerned with what others think of them. This means that they are less likely to internalize negative messages about themselves, such as the idea that they should be solid and challenging all the time. That is to say, increased levels of self-compassion can buffer against the internalization of external evaluations attributed to men, such as traditional masculine norms [48, 49]. This can help them to overcome the stigma associated with eco-friendly behaviors and engage in them more freely. Therefore, male university students might be more likely to engage in eco-friendly behaviors without being influenced by stereotypes attributed to men. Self-compassion can also motivate people to take action to protect the environment. When people are compassionate towards themselves, they are more likely to feel connected to others and to the world around them [9, 10, 50, 51]. This can lead to a sense of purpose and meaning, which can motivate people to take action to protect the environment. According to our research's findings, self-compassion could encourage males

who are reluctant to adopt eco-friendly behaviors.

There are some reasons why we conducted our study with this group. To put it more clearly, the reluctance of young men to adopt eco-friendly behaviors may result from certain sociocultural factors. In Türkiye, social expectations and norms significantly influence individual behaviors [11, 52]. To elaborate, achieving manhood is viewed as winning a societal status [23]. However, in Turkish traditions, indicators of manhood include rites such as circumcision, completing mandatory military service, securing employment, marrying, and fathering children [53]. Given this backdrop, societal standards might see them as unmanly since many male university students have not embarked on full-time jobs or fulfilled their military obligations. Therefore, these young men who are focused on asserting their manliness may avoid activities that diverge from conventional male standards, such as green behaviors.

The findings of this study contribute to understanding the environmental behaviors of young Turkish men through the lens of Social Identity Theory [63]. According to this theory, individuals define themselves through their group memberships, and these identities influence their behavior. Environmental identity refers to seeing oneself as an environmentalist, which can increase the likelihood of engaging in eco-friendly behaviors [43]. This study shows that self-compassion strengthens the link between environmental identity and eco-friendly behavior. Self-compassion may help men move beyond traditional masculine norms, making it easier for them to engage in eco-friendly behaviors. This findings, adds valuable insight into how social identity and self-compassion can shape environmental actions in young men.

The study's findings may also be related to traditional gender roles attributed to men in society. More clearly, previous studies showed that men are less likely to engage in environmentally friendly behaviors than women [54, 55, 56]. This is because the link between feminine and green behaviors makes men more concerned about their masculinity, which makes them less likely to engage in green behaviors [3, 57, 58, 18]. Men typically learn to behave in ways that are considered masculine, such as being assertive, competitive, and independent [59, 25]. People often expect women to be caregivers and cooperators, while men are expected to be more assertive. Therefore, men are generally less likely to engage in environmentally friendly behaviors than women because these behaviors are not seen as masculine [17]. In this respect, there is a necessity for studies to explore the underlying mechanisms behind men's reluctance to embrace environmental behaviors.

Conclusion, Implications and Mapping Future

Climate change can have a negative impact on people's mental health. Exposure to natural disasters such as flash floods, forest fires, heavy smoke, and living in areas with high air pollution or extreme temperatures can lead to increased stress, anxiety, depression, and post-traumatic stress disorder [60, 61, 62]. Therefore, the importance of promoting environmentally beneficial behaviors is growing.

Our study was conducted to gain insights into how to encourage men to engage in environmentally friendly behaviors. In this sense, we examined the mediating role of self-compassion in the link between environmental identity and environmentally friendly behaviors among young Turkish men. Based on our findings, it can be argued that self-compassion can motivate young men to engage in environmentally friendly behaviors.

The promoting role of self-compassion in encouraging environmentally friendly behaviors could be replicated in future studies with different variables such as various ethnic backgrounds, cultures, socioeconomic statuses, and sexual orientations. Additionally, experimental studies could be conducted to test the impact of self-compassion-based interventions on environmentally friendly behaviors. Moreover, focus group interviews using qualitative research methods could be conducted to understand better the role of traditional masculinity norms in displaying environmentally friendly behaviors.

ACKNOWLEDGEMENT

TUBITAK 2209 Project Acceptance No 1919B012222062

DATA AVAILABILITY STATEMENT

The author confirm that the data that supports the findings of this study are available within the article. Raw data that support the finding of this study are available from the corresponding author, upon reasonable request.

CONFLICT OF INTEREST

The author declared no potential conflicts of interest with respect to the research, authorship, and/or publication of this article.

USE OF AI FOR WRITING ASSISTANCE

Not declared.

ETHICS

The institutional ethics committee approved the research protocol under the 04/26 application number. consent was obtained from all individual participants included in the study.

REFERENCES

[1]. L. Steg, Ed., "Environmental Psychology," 2nd ed., Wiley-Blackwell, 2019.

[2]. S. B. Lezak and P. H. Thibodeau, "Systems thinking and environmental concern," Journal of Environmental Psychology, vol. 46, pp. 143–153, 2016, doi: 10.1016/j.jenvp.2016.04.005.

[3]. A. R. Brough, J. E. B. Wilkie, J. Ma, M. S. Isaac, and D. Gal, "Is Eco-Friendly Unmanly? The Green-Feminine stereotype and its effect on sustainable consumption," Journal of Consumer Research, vol. 43, no. 4, pp. 567–582, 2016, doi: 10.1093/jcr/ucw044.

[4]. P. J. Casey and K. Scott, "Environmental concern and behaviour in an Australian sample within an ecocentric – anthropocentric framework," Australian Journal of Psychology, vol. 58, no. 2, pp. 57–67, 2006, doi: 10.1080/00049530600730419.

[5]. A. Gökmen, "The effect of gender on environmental attitude: A meta-analysis study," Journal of Pedagogical Research, vol. 5, no. 1, pp. 243–257, 2021, doi: 10.33902/jpr.2021167799.

[6]. M. A. Vicente-Molina, A. Fernández-Sainz, and J. Izagirre-Olaizola, "Does gender make a difference in pro-environmental behavior? The case of the Basque Country University students," Journal of Cleaner Production, vol. 176, pp. 89–98, 2018, doi: 10.1016/j.jclepro.2017.12.079.

[7]. Z. Gerber, "Self-compassion as a tool for sustained and effective climate activism," Integrated Environmental Assessment and Management, vol. 19, no. 1, pp. 7–8, 2023, doi: 10.1002/ieam.4695.

[8]. L. S. Loy, A. Clemens, and G. Reese, "Mind–Body practice is related to pro-environmental engagement through self-compassion and global identity rather than to self-enhancement," Mindfulness, vol. 13, no. 3, pp. 660–673, 2022, doi: 10.1007/s12671-021-01823-1.

[9]. L. S. Loy and G. Reese, "Hype and hope? Mind-body practice predicts pro-environmental engagement through global identity," Journal of Environmental Psychology, vol. 66, p. 101340, 2019, doi: 10.1016/j.jenvp.2019.101340.

[10]. L. Ramstetter, S. Rupprecht, L. Mundaca, W. Osika, C. Stenfors, J. Klackl, and C. Wamsler, "Fostering collective climate action and leadership: Insights from a pilot experiment involving mindfulness and compassion," iScience, vol. 26, no. 3, p. 106191, 2023, doi: 10.1016/j.isci.2023.106191.

[11]. M. J. Gelfand, J. L. Raver, L. H. Nishii, L. A. Leslie, J. Lun, B. C. Lim, L. Duan, A. Almaliach, S. Ang, J. Arnadottir, Z. Aycan, K. Boehnke, R. Cabecinhas, D. K. Chan, J. S. Chhokar, A. D'Amato, M. a. B. Ferrer, I. C. Fischlmayr, and S. Yamaguchi, "Differences between tight and loose cultures: a 33-Nation study," Science, vol. 332, no. 6033, pp. 1100–1104, 2011, doi: 10.1126/science.1197754.

[12]. W. L. Milbrath. "Learning to think environmentally: While there is still time," Suny Press. 1996.

[13]. P. Subramanian, "Plastics recycling and waste management in the US," Resources Conservation and Recycling, vol. 28, no. 3–4, pp. 253–263, 2000, doi: 10.1016/s0921-3449(99)00049-x.

[14]. S. Arnocky and M. Stroink, "Gender differences in environmentalism: The mediating role of emotional empathy," Current Research in Social Psychology, vol. 16, no. 9, pp. 1-14, 2010.

[15]. R. J. Bord and R. E. O'Connor, "The gender gap in environmental attitudes: The case of perceived vulnerability to risk," Social Science Quarterly, vol. 78, pp. 830-840, 1997.

[16]. C. Jackson, "Gender Analysis and Environmentalisms," in Social Theory and the Global Environment, Routledge, 2013, doi: 10.4324/9780203427903-11.

[17]. Z. Zhao, Y. Gong, Y. Li, L. Zhang, and Y. Sun, "Gender-Related Beliefs, Norms, and the link with green consumption," Frontiers in Psychology, vol. 12, 2021, doi: 10.3389/fpsyg.2021.710239.

[18]. L. Zelezny, P. Chua, and C. Aldrich, "New Ways of Thinking about Environmentalism: Elaborating on Gender Differences in Environmentalism," Journal of Social Issues, vol. 56, no. 3, pp. 443–457, 2000, doi: 10.1111/0022-4537.00177.

[19]. A. H. Eagly, "Reporting sex differences," American Psychologist, vol. 42, no. 7, pp. 756–757, 1987, doi: 10.1037/0003-066x.42.7.755.

[20]. T. Dietz, L. Kalof, and P. C. Stern, "Gender, values, and environmentalism," Social Science Quarterly, vol. 83, no. 1, pp. 353–364, 2002, doi: 10.1111/1540-6237.00088.

[21]. J. Lee and S. Holden, "Understanding the determinants of environmentally conscious behavior," Psychology & Marketing, vol. 16, no. 5, pp. 373–392, 1999, doi: 10.1002/(sici)1520-6793(199908)16:5.

[22]. J. A. Vandello, J. K. Bosson, D. Cohen, R. M. Burnaford, and J. Weaver, "Precarious manhood," Journal of Personality and Social Psychology, vol. 95, no. 6, pp. 1325–1339, 2008, doi: 10.1037/a0012453.

[23]. J. A. Vandello and J. K. Bosson, "Hard won and easily lost: A review and synthesis of theory and research on precarious manhood," Psychology of Men and Masculinity, vol. 14, no. 2, pp. 101–113, 2013, doi: 10.1037/a0029826.

[24]. M. A. Hogg, "Social identity theory," in Understanding Peace and Conflict Through Social Identity Theory: Contemporary Global Perspectives, S. McKeown, R. Haji, and N. Ferguson, Eds. Springer International Publishing, 2016, pp. 3–17.

[25]. M. C. Parent and A. P. Smiler, "Metric invariance of the Conformity to Masculine Norms Inventory-46 among women and men," Psychology of Men and Masculinity, vol. 14, no. 3, pp. 324–328, 2013, doi: 10.1037/a0027642.

[26]. J. M. O'Neil, J. M, "Summarizing 25 years of research on men's gender role conflict using the gender role conflict scale," The Counseling Psychologist/ the Counseling Psychologist, vol. 36, no 3, pp. 358–445, 2008, doi: 10.1177/0011000008317057

[27]. K. D. Neff, "The development and validation of a scale to measure Self-Compassion," Self and Identity, vol. 2, no. 3, pp. 223–250, 2003, doi: 10.1080/15298860309027.

[28]. A. MacBeth and A. Gumley, "Exploring compassion: A meta-analysis of the association between

self-compassion and psychopathology," Clinical Psychology Review, vol. 32, no. 6, pp. 545–552, 2012, doi: 10.1016/j.cpr.2012.06.003.

[29]. U. Zessin, O. Dickhäuser, and S. F. Garbade, "The Relationship Between Self-Compassion and Well-Being: A Meta-Analysis," Applied Psychology: Health and Well-being, vol. 7, no. 3, pp. 340–364, 2015, doi: 10.1111/aphw.12051.

[30]. J. E. Cha, A. S. Serlachius, J.N. Kirby, N. S. Consedine, "What Do (and Don't) We Know About Self-Compassion? Trends and Issues in Theory, Mechanisms, and Outcomes," Mindfulness, vol. 14, pp. 2657–2669, 2023, doi: 10.1007/s12671-023-02222-4.

[31]. A. López, R. Sanderman, A. V. Ranchor, M. J. Schroevers, (2018). "Compassion for others and self-compassion: Levels, correlates, and relationship with psychological well-being" Mindfulness, vol. 9, no. 1, pp 325–331, 2018, doi: 10.1007/s12671-017-0777-z

[32]. B. K. Sahdra, J. Ciarrochi, M. I. Fraser, K. Yap, E. Haller, S. C. Hayes, S. Hofmann, and A. T. Gloster, "The Compassion Balance: Understanding the interrelation of self- and Other-Compassion for optimal well-being," Mindfulness, vol. 14, no. 8, pp. 1997–2013, 2023, doi: 10.1007/s12671-023-02187-4.

[33]. M. J. Gelfand, L. H. Nishii, J.L. Raver, "On the nature and importance of cultural tightness-looseness," Journal of Applied Psychology, vol. 91, no. 6, pp. 1225–1244, 2006, doi: 10.1037/0021-9010.91.6.1225

[34]. L. Barnard and J. F. Curry, "Self-Compassion: Conceptualizations, Correlates, & Interventions," Review of General Psychology, vol. 15, no. 4, pp. 289–303, 2011, doi: 10.1037/a0025754.

[35]. K. D. Neff and R. Vonk, "Self-Compassion versus global Self-Esteem: two different ways of relating to oneself," Journal of Personality, vol. 77, no. 1, pp. 23–50, 2009, doi: 10.1111/j.1467-6494.2008.00537.x.

[36]. F. M. Sirois, R. Kitner, and J. K. Hirsch, "Self-compassion, affect, and health-promoting behaviors," Health Psychology, vol. 34, no. 6, pp. 661–669, 2015, doi: 10.1037/hea0000158.

[37]. Z. Zhang, "Monte Carlo based statistical power analysis for mediation models: methods and software," Behavior Research Methods, vol. 46, no. 4, pp. 1184–1198, 2013, doi: 10.3758/s13428-013-0424-0.

[38]. J. Cohen, "Statistical Power Analysis for the Behavioral Sciences," 2nd ed., Hillsdale, NJ: Lawrence Erlbaum Associates, Publishers, 1988.

[39]. A. M. Schoemann, A. J. Boulton, and S. D. Short, "Determining power and sample size for simple and complex mediation models," Social Psychological and Personality Science, vol. 8, no. 4, pp. 379–386, 2017, doi: 10.1177/1948550617715068.

[40]. N. Tanık Önal, A. Kilinc, and S. Saraçoğlu, "Fen Bilgisi Öğretmen Adaylarının Çevre Kimliklerinin ve Çevre Dostu Davranışlarının İncelenmesi [Investigation of Prospective Science Teachers' Environmental Identities and Pro-Environmental Behaviors]," Uludağ Üniversitesi Eğitim Fakültesi Dergisi, 2020, doi: 10.19171/uefad.660668.

[41]. F. Raes, E. Pommier, K. D. Neff, and D. Van Gucht, "Construction and factorial validation of a short form of the Self-Compassion Scale," Clinical Psychology & Psychotherapy, vol. 18, no. 3, pp. 250–255, 2010, doi: 10.1002/cpp.702.

[42]. Ö. Kantaş, "Impact of Relational and Individuational Self-orientations on the Well-being of Academicians: the Roles of ego-or Eco-system Motivations, Self-transcendence, Self-compassion and Burnout," M.S. thesis, Middle East Technical University, 2013.

[43]. S. Clayton, "Enviromental identity: A conceptuaş and an operational definition," in Identity and the Natural Enviroment: The Psychological Significance of Nature, MIT Press, 2003, pp 45-65, doi: 10.7551/mitpress/3644.001.0001.

[44]. D. George and P. Mallery, "SPSS for Windows Step by Step: A Simple Guide and Reference 17.0 Update," 10th ed., Pearson, Boston, 2010.

[45]. A. F. Hayes, "Introduction to mediation, moderation, and conditional process analysis," 3rd ed., The Guilford Press, 2022.

[46]. L. Wang, G. Sheng, S. She, and J. Xu, "Impact of empathy with nature on pro-environmental behaviour," International Journal of Consumer Studies, vol. 47, no. 2, pp. 652–668, 2022, doi: 10.1111/ijcs.12856.

[47]. S. Vesely, T. Masson, P. Chokrai, A. M. Becker, I. Fritsche, C. A. Klöckner, and A. Panno, "Climate change action as a project of identity: Eight meta-analyses," Global Environmental Change, vol. 70, p. 102322, 2021, doi: 10.1016/j.gloenvcha.2021.102322.

[48]. P. J. Heath, R. E. Brenner, D. L. Vogel, D. G. Lannin, and H. A. Strass, "Masculinity and barriers to seeking counseling: The buffering role of self-compassion," Journal of Counseling Psychology, vol. 64, no. 1, pp. 94–103, 2017, doi: 10.1037/cou0000185.

[49]. P. J. Heath, R. E. Brenner, D. G. Lannin, and D. L. Vogel, "Self-compassion moderates the relationship of perceived public and anticipated self-stigma of seeking help," Stigma and Health, vol. 3, no. 1, pp. 65–68, 2018, doi: 10.1037/sah0000072.

[50]. M. R. Leary, E. B. Tate, C. Adams, A. B. Allen, and J. Hancock, "Self-compassion and reactions to unpleasant self-relevant events: The implications of treating oneself kindly," Journal of Personality and Social Psychology, vol. 92, no. 5, pp. 887–904, 2007, doi: 10.1037/0022-3514.92.5.887.

[51]. M. Terry and M. R. Leary, "Self-compassion, self-regulation, and health," Self and Identity, vol. 10, no. 3, pp. 352–362, 2011, doi: 10.1080/15298868.2011.558404.

[52]. Ç. Kağıtçıbaşı, "Özerk-ilişkisel benlik: Yeni bir sentez [Autonomous-relational self: A new synthesis]," Türk Psikoloji Dergisi, vol. 11, no. 37, pp. 36-43, 1996.

[53]. H. B. Boratav, G. O. Fişek, and H. Eslen-Ziya, "Erkekliğin Türkiye Halleri [The States of Masculinity in Turkey]," İstanbul: Bilgi Üniversitesi Yayınları,

2017.

[54]. R. E. Dunlap, K. D. Van Liere, A. G. Mertig, and R. E. Jones, "New Trends in Measuring Environmental Attitudes: Measuring endorsement of the new ecological paradigm: a revised NEP scale," Journal of Social Issues, vol. 56, no. 3, pp. 425–442, 2000, doi: 10.1111/0022-4537.00176.

[55]. B. Hampel, R. Holdsworth, and J. Boldero, "The Impact of Parental Work Experience and Education on Environmental Knowledge, Concern and Behaviour among Adolescents," Environmental Education Research, vol. 2, no. 3, pp. 287-300, 1996, doi: 10.1080/1350462960020303.

[56]. B. E. Rideout, K. Hushen, D. McGinty, S. D. Perkins, and J. A. Tate, "Endorsement of the new ecological paradigm in systematic and e-mail samples of college students," The Journal of Environmental Education, vol. 36, no. 2, pp. 15–23, 2005, doi: 10.3200/joee.36.2.15-23.

[57]. A. M. McCright and A. Sundström, "Examining gender differences in environmental concern in the Swedish general public, 1990-2011," International Journal of Sociology, vol. 43, no. 4, pp. 63–86, 2013, doi: 10.2753/ijs0020-7659430402.

[58]. J. K. Swim, A. J. Gillis, and K. J. Hamaty, "Gender Bending and Gender Conformity: The social consequences of engaging in feminine and masculine Pro-Environmental behaviors," Sex Roles, vol. 82, no. 5–6, pp. 363–385, 2019, doi: 10.1007/s11199-019-01061-9.

[59]. J. Feder, R. F. Levant, and J. C. Dean, "Boys and violence: A gender-informed analysis," Psychology of Violence, vol. 1, no. S, pp. 3–12, 2010, doi: 10.1037/2152-0828.1.s.3.

[60]. C. Campbell, D. Cotter, K. L. Bottenhorn, E. Burnor, H. Ahmadi, J. Gauderman, C. Cardenas-Iniguez, D. A. Hackman, R. McConnell, K. Berhane, J. Schwartz, J. Chen, and M. M. Herting, "Air pollution and emotional behavior in adolescents across the U.S.," medRxiv (Cold Spring Harbor Laboratory), 2023, doi: 10.1101/2023.04.19.23288834.

[61]. C. Stanke, V. Murray, R. Amlôt, J. Nurse, and R. Williams, "The effects of flooding on mental health: Outcomes and recommendations from a review of the literature," PLOS Currents, 2012, doi: 10.1371/4f9f-1fa9c3cae.

[62]. P. L. To, E. Eboreime, and V. I. O. Agyapong, "The Impact of wildfires on Mental Health: A scoping review," Behavioral Sciences, vol. 11, no. 9, p. 126, 2021, doi: 10.3390/bs11090126.J. Padhye, V. Firoiu, and D. Towsley, "A stochastic model of TCP Reno congestion avoidance and control," Univ. of Massachusetts, Amherst, MA, CMPSCI Tech. Rep. 99-02, 1999.

[63]. Tajfel, H., & Turner, J. C. (1979). An integrative theory of intergroup conflict. In W. G. Austin & S. Worchel (Eds.), The social psychology of intergroup relations (pp. 33-47). Brooks/Cole.

Environ Res Tec, Vol. 8, Issue. 2, pp. 354-371, June 2025

Environmental Research and Technology
https://dergipark.org.tr/en/pub/ert
DOI: https://10.35208/ert.1502586

Research Article

Spatio-temporal patterns of air quality on commuter lane of the sub-urban area of Yogyakarta, Indonesia

Arif Ashari*[1], Rizqya P.S. Nurussolikhin[1], Audyana Putri[1]
Muhamad Ervin[2], Muhammad A.I. Wardoyo[2]

[1]Department of Geography Education Universitas Negeri Yogyakarta, Indonesia, arif.ashari@uny.ac.id
[2]Geography Education Master Program, Universitas Negeri Yogyakarta, Indonesia

ARTICLE INFO

Article history
Received: 19 Jun 2024
Revised: 05 Sep 2024
Accepted: 10 Sep 2024

Key words:
Air quality, commuter lane, sub-urban, transportation geography

ABSTRACT

Yogyakarta, a city based on culture, education, and tourism, has different commuting activities from other industrialized cities in Indonesia. On the other hand, the city is also dominated by motorcycles, like most cities in Indonesia and Southeast Asia. The movement of commuters by motorcycle affects the instantaneous air quality. In this paper, the results of an investigation of the spatio-temporal pattern of air quality of commuter routes in the suburbs of Yogyakarta are presented. Data were collected through observation by measuring five air quality parameters and vehicle intensity in 10 commuter routes in Yogyakarta. Data were analyzed using GIS analysis using average nearest neighbour, statistical analysis using simple linear regression, and matching analysis referring to The World Air Quality Index and Vianney and Erfianto (2023), supported by descriptive analysis. There are three critical findings from this study. First, air quality varies spatially and temporally, with differences among commuter routes and travel times. Second, the relationship between passing vehicle intensity and air quality is unique. Some positively correlate with linear, exponential, logarithmic, or polynomial relationship properties. Third, poor air quality tends to be found on main routes with high vehicle intensity. In summary, this study provides new insights into air quality patterns concerning commuter traffic in motorcycle-dominated cities in Indonesia.

Cite this article as: Ashari A, Nurussolikhin RPS, Putri A, Ervin M, Wardoyo MAI. Spatio-temporal patterns of air quality on commuter lne of the sub-urban area of Yogyakarta, Indonesia. Environ Res Tec 2025;8(2) 354-371.

***Corresponding author.**
*E-mail address: arif.ashari@uny.ac.id

This is an open access article under the CC BY-NC license (http://creativecommons.org/licenses/by-nc/4.0/).

INTRODUCTION

Approaching a quarter of a century after the turn of the millennium, the world's population increasingly lives in urban areas. Data from the Population Reference Bureau shows that by 2023, 57% live in urban area [1]. With more and more people living in urban areas, urbanization has become a crucial contemporary issue in which urban transportation plays a fundamental role. The availability of good transportation facilities has proven to significantly impact the progress of cities and the welfare of residents of various cities in the world. However, urban transportation has also long been proven to be one of the factors responsible for degrading the environmental quality of urban areas, especially air pollution. This is a consequence of the increasing use of multi-modal transportation in terms of type and number [2], [3]. Studies conducted in China [4], [5] and Africa [6] prove that transportation activities impact urban air pollution. On the other hand, transportation improvements have been shown to reduce pollution levels in many cities of developed countries through innovations in green transportation modes [7] – [9] as well as mobility restrictions during the COVID-19 pandemic [10], [11].

There is a commuter zone in the city's spatial structure, especially in models that refer to the ecological approach. This zone is found in the suburbs or the outer part of the city as a link between where people live outside the city and their activities in the city [12], [13]. This area is crossed by many commuters from the hinterland and satellite areas to the inner city. In many Southeast Asian cities, this commuter zone is heavily populated by motorcycle users, as is the case in Indonesia [14], [15]; Vietnam [16], as well as Thailand [17]. High vehicle intensity in commuter zones has an impact on worsening air quality as a study conducted in Solo, Indonesia [18]; Hanoi, Vietnam [19], [20]; Bangkok, Thailand [21]; and Lagos, Nigeria [22]. Poor air quality is also detrimental to commuters' health. This issue has received much attention in previous studies in Vietnam [23] – [25], China [26]; India [27], [28]; and Taiwan [29], [30].

The problem is how much impact the flow of commuters has on the instantaneous air quality felt by commuters in these commuting zones has not been sufficiently addressed in previous literature. Previous studies in the past decade have mainly focused on the exposure to air pollutants among commuters and its impact on their health or the effect of private vehicle shifts to public transport and motorcycle to electric motorcycle conversions on air quality in urban areas [31] – [33]. Therefore, previous studies have not included analysis and discussion on the relationship between commuting activities in motorcycle-dominated cities. This indicates a scientific gap that needs to be addressed by further studies.

Yogyakarta is a city based on education, culture, and tourism. Like most cities in Indonesia, Yogyakarta also has commuter zones. However, the commuting pattern in this city is relatively different from those large industrial-based cities. For example, commuting patterns in Jakarta and Surabaya are based on BPS data [34], [36], [37] dominated by certain lines. Meanwhile, the condition in Bandung is relatively similar to Yogyakarta, where there is no dominance of certain commuter lines [35]. Besides being related to the activities of the population and the distribution of activity centers within the city, commuting patterns may also be associated with the geographical conditions of the city itself. The non-coastal morphology of Bandung and Yogyakarta allows for an even flow of commuters from all sides. In Yogyakarta, residents from the hinterland and satellite cities who commute to the city for education or employment in the public service sector come from all directions. This specific pattern also needs further evaluation to determine its influence on the instantaneous air quality pattern during commuter transportation activities.

In this paper, we describe the spatio-temporal air quality pattern in Yogyakarta's commuter zone. In this regard, there are three more specific objectives in this paper. First, to evaluate the variability of commuter characteristics in Yogyakarta commuter lines. Second, to assess the spatio-temporal pattern of air quality on the various commuter routes. Last, consider the influence of commuting activities on the instantaneous air quality in Yogyakarta's commuter routes. This study emphasizes the impact of commuting activities on instantaneous air quality, which has never been discussed before in various international publications. As such, this study offers new insights into the influence of commuting activities on instantaneous air quality. This study also provides alternative information on the air quality of suburban areas concerning commuter traffic using private vehicles.

MATERIALS AND METHODS

Research Methods

This study employs a geography approach, namely a spatial approach. This study also implements geography themes to analyze the problem, including location, place, human-environment interaction, movement, region, and landform. The subjects in this study are commuter routes in Yogyakarta City. The object of the research is the instantaneous air quality that occurs due to the influence of commuter activities.

The data in this study are primary data, collected through observation. Observations were conducted at ten points which are the main route of commuters in Yogyakarta City, including: Magelang Street, Palagan Street, Kaliurang Street, Solo Street, Wonosari Street, Imogiri Timur Street, Parangtritis Street, Bantul Street, Wates Street, and Godean Street. The intensity of vehicles passing every minute was measured at each location, consisting of motorcycles, cars, and total vehicles. Instantaneous air quality measurements were also taken, along with the vehicle intensity measurement. Air quality variables include PM2.5, PM10, CO_2, TVOC, and HCHO.

According to Zimakowska-Laskowska & Laskowski [80], CO_2 is one type of pollutant produced by transport. The Environmental Protection Agency of the United States (2024) also explains that burning fossil fuels like gasoline and diesel releases carbon dioxide, a greenhouse gas, into the atmo-

sphere. Meanwhile, the International Energy Agency [82] explains that motorised transport on land, sea and air remains dependent on internal combustion engines that generally run-on fossil fuels. Transport accounts for more than a third of CO_2 emissions from end-use sectors.

Observations at each location were conducted in the morning, afternoon, and evening to determine the temporal variation of air quality to commuting activities. Morning measurements were taken at 06:00-08:00, afternoon measurements at 12:00-14:00, and evening measurements at 16:00-18:00. The assumption made in this study is that the morning and evening are the peaks of commuting activity where in the morning there is a flow from the hinterland to the city and in the evening, there is a reverse flow. The midday measurement is intended as a comparison between the two busy times. Air quality and vehicle intensity were measured ten times at each measurement time. Thus, at each measurement location, there are 300 data points throughout the day, consisting of the results of morning, afternoon, and evening measurements. Air quality measurements were carried out with Particle Counter HTI HT 9600 instruments for PM2.5 and PM10 and a JLDG air quality tester for CO_2, TVOC, and HCHO measurements.

Data analysis was conducted using statistical analysis, matching analysis, and descriptive analysis. Statistical analysis was carried out using simple linear regression to see the effect of the number of vehicles passing through the commuter zone as an independent variable on instantaneous air quality as the dependent variable. Air quality consists of several parameters: PM 2.5, PM 10, CO_2, TVOC, and HCHO. The linear regression model used is formulated as follows.

$$Y = a + bX \quad \text{.....(1)}$$

X represents the number of vehicles travelling in each commuter zone in the measurement period, Y represents the air quality at the same time as the vehicle measurement, a is the intercept, and b is the regression coefficient that shows the impact of vehicles on air quality. The formula for a and b are as follows.

$$a = \frac{(\sum Y)(\sum X^2)-(\sum X)(\sum XY)}{n\sum X^2-(\sum X)^2} \text{ and } b = \frac{n\sum XY-(\sum X)(\sum Y)}{n\sum X^2-(\sum X)^2} \quad \text{.....(2)}$$

Descriptive analysis supported statistical analysis to clarify, sharpen, and provide additional descriptions of qualitative aspects. Data presentation with descriptive statistics using a summary statistics table and boxplot is used to support descriptive analysis. Furthermore, matching analysis was used for air quality categorization. PM parameters refer to The World Air Quality Index Project [38], using the Instant Air Quality Index (AQI converted directly from the 1-hour readings. Air quality categorization based on The World Air Quality Index Project [38], includes the categories of Good (0-50), Moderate (51-100), Unhealthy for Sensitive Groups (101-150), Unhealthy (151-200), Very Unhealthy (201-300), Hazardous (>300). Meanwhile, the parameters CO_2, TVOC and HCHO refer to the classification used by Vianney Augusta & Erfianto [39], which consists of five categories namely Excellent, Good Quality, Mild Pollution, Mediocre Pollution and Serious Pollution.

Research Area

This study was conducted in the commuter zone of Yogyakarta city. Referring to Rodrigue [12], based on The Burgess Urban Land Use Model and the Sector and Nuclei Urban Land Use Representations theory, commuter zones are located in suburban areas. Therefore, this study focused on these areas. Sample locations for measurements were purposively determined at points before entering the city center (Figure 1). There were 10 points used as observation locations, as shown in Table 1.

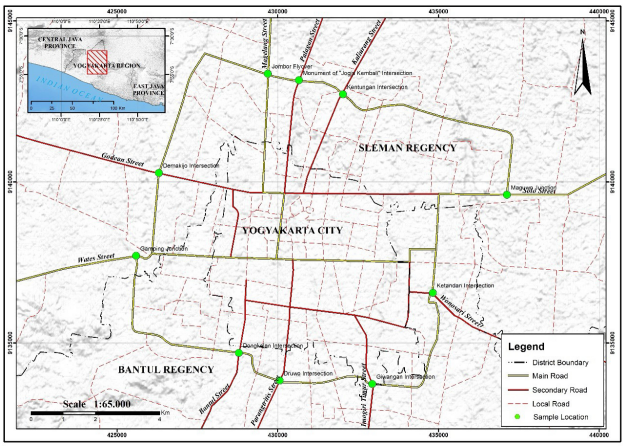


Figure 1. The Study Area

The research area is geomorphologically included in the landforms of the footplain to the fluviovolcanic plain of Merapi Volcano. The area is composed of the lithology of Young Merapi volcanic activity product with a high infiltration rate [40] – [42]. Yogyakarta City is the center of the Yogyakarta Special Region (locally known as Daerah Istimewa Yogyakarta or DIY), a relatively narrow area with complex landform characteristics [43].

RESULT AND DISCUSSION

The characteristics of commuting movement in the commuter lane of Yogyakarta

Commuting is the dominating transportation activity in the local scale spatial structure of the urban area. In terms of transportation modes, various road transportation modes tend to serve transportation at short distances in this local area [12]. Among the various modes of road transportation used in commuting activities in urban areas, motorcycles are the most widely used. Data from the Transportation Office of Yogyakarta Special Region [44] shows that in 2020, the total number of vehicles registered in DIY was 1,576,153 units. Of these, 86% were motorcycles. This high percentage of motorcycles is relatively stable in the five years between 2016-2020. Meanwhile, data from the Yogyakarta City Government [45] shows that in 2022, the number of motorcycles in Yogyakarta City reached 85% of all registered vehicles of 576,016 units.

By looking at the number of motorcycles in Yogyakarta City and other areas in Special Region of Yogyakarta as a hinterland, the typology of transportation modes and cities for the Yogyakarta region is motorcycle cities. Guerra & Duranton

Table 1. Location of the Measurement of Air Quality and Vehicle Intensity

No	Commuter lane	Location	Coordinate
1	Magelang Street	Jombor Flyover	429962, 9143359
2	Godean Street	Demakijo Intersection	426309, 9140276
3	Wates Street	Gamping Junction	425598, 9137705
4	Bantul Street	Dongkelan Intersection	428796, 9134692
5	Parangtritis Street	Druwo Intersection	430065, 9133831
6	Imogiri Timur Street	Giwangan Intersection	432947, 9133725
7	Wonosari Street	Ketandan Intersection	434832, 9136555
8	Solo Street	Maguwo Junction	437133, 9139599
9	Kaliurang Street	Kentungan Intersection	432035, 9142719
10	Palagan Street	Monument of "Jogja Kembali" Intersection	430664, 9143155

Source: Data analysis (2024)

[46] explain that motorcycle cities are dominated by motorcycles that sometimes uneasy and dangerous coexistence with other motorized vehicles. With three-quarters of the global two-wheeled vehicle fleet in Asia, Asian cities tiny to medium-sized cities, such as Taipei, Ho Chi Minh City, and Hanoi, are examples of this typology. In Indonesia, Surakarta is cited as a concrete example of this typology [18, 46]. Given the dominance of motorcycles in many Indonesian cities, motorcycle cities are a common typology for Indonesian cities, including Jakarta and Bandung [14], as well as Yogyakarta.

This study examines the movement of commuters during weekdays. Commuting activities in Yogyakarta during weekdays occur mainly in the morning and evening. This is related to the time of commuting to and from work, where commuters from various hinterland areas enter the sub-urban and CBD areas in the morning and then move back out of the city in the evening. In this study, we conducted 300 observations of commuter movements, with details in each of the 10 locations, we conducted three observations representing the morning, afternoon, and evening sessions, where ten observations were made in each session.

The study results show that the intensity of motorcycles passing within one minute is always more than cars. This was applicable at all points and all observation sessions. The highest average intensity of motorcycles in the morning was found on Parangtritis Street, while the lowest was on Godean Street. This is reasonable given that Parangtritis Street is an important route from the Bantul hinterland. At the same time, Godean Street comes from a less extensive hinterland, and there are many route options from the hinterland of Godean to the city. The highest maximum intensity in the morning session is found on Wonosari Street, while the lowest minimum intensity is again found on Godean Street.

In the Afternoon Session, the highest averages are found on Palagan Street and Kaliurang Street. Both roads are next to each other, which drain commuters from the same hinterland. The lowest average was found on Wates Street. This finding is interesting because Wates Street is a highway that connects Yogyakarta City to Yogyakarta International Airport and Central Java Province. Still, the intensity of motorcycles during the day is not high, whereas it is very high in the morning. This suggests that commuter activity on this road is relatively focused in the morning. Commuters come from relatively distant areas of Kulon Progo Regency.

The same condition as on Wates Street is also found on Magelang Street and Solo Street. These three roads connect Yogyakarta with other big cities and provinces. Magelang Street is a national road that connects Yogyakarta, the capital city of the Yogyakarta Special Region, with Semarang City, the capital city of Central Java Province. Meanwhile, Solo Street connects Yogyakarta with Surakarta City in Central Java Province. In the morning, the intensity of vehicles is very high, but in the afternoon, it drops drastically, which is related to the commuters' relatively distant areas of origin. The condition is very different from Palagan Street and Kaliurang Street, which are residential zones extend northward from Yogyakarta City.

Magelang Street, a national arterial road, tends to have a stable motorcycle intensity. The measurement results in the morning show a relatively stable intensity. In the morning when it is crowded, in the afternoon when it is quiet, and in the evening when it is crowded, the intensity is relatively stable from 10 observations made in one session. Different conditions were found at Palagan Street in the afternoon session and Imogiri Timur Street in the evening session, which showed high outliers. This means that among the ten observations in one session, there are very high motorcycle intensity events, while the other data is relatively stable (Figure 2). Overall, motorcycle movements in areas with many settlements show relatively stable conditions. This is demonstrated by the average intensity of motorcycles per minute in the morning, afternoon, and evening sessions, which are relatively not significantly different. Meanwhile, highways such as Magelang Street, Solo Street, and Wates Street, connecting routes to other cities, show significant average differences be-

tween the three sessions, with a decrease in intensity in the afternoon (Table 2).

Different findings were found for car traffic behaviour. In the morning, the highest average number of passing cars was found on Solo Street, while the lowest was on Godean Street and Wonosari Street. This is because Solo Street is the main road to Adisutjipto Airport in the east of Yogyakarta, and the main road connects Yogyakarta with Surakarta. Meanwhile, Godean Street is not a connecting road with other major cities, comes from a less extensive hinterland, and has many route options to avoid congestion in the morning. The highest maximum intensity of cars in one minute for the morning session is on Solo Street and Palagan Street. In contrast, the lowest minimum intensity occurs in Godean Street, Wonosari Street, and Imogiri Timur Street.

In the Afternoon Session, the highest averages are found on Palagan Street and Solo Street. Palagan Street is the route to the densely populated residential zone in the city's north. Meanwhile, Solo Street also still has the highest average car intensity during the day. Interestingly, the lowest average is found on Kaliurang Street. This finding is interesting because Kaliurang Street carries commuters from the same hinterland as Palagan Street. In the morning, the intensity of cars on these two roads is the same, but during the afternoon session, the intensity of cars on Kaliurang Street is relatively low, while Palagan Street remains high.

The change in car intensity between morning and afternoon is generally relatively small. In other words, the number of cars travelling in the morning and afternoon is relatively the same. This is the case in the majority of observation locations. However, there are anomalies at specific locations where car intensity drops or increases drastically. Although still showing the highest intensity in the afternoon, Solo Street experienced a significant decrease in intensity compared to the morning. Meanwhile, Godean Street, Bantul Street, and Imogiri Timur Street experienced a significant increase in the afternoon session (Table 2). Godean Street, Bantul Street, and Imogiri Timur Street are not connecting roads between cities but from densely populated hinterlands. The high intensity of cars in the afternoon session could be due to non-local traffic, or there is another possibility that car users tend to travel indifferent sessions to avoid congestion caused by the large number of motorcycles in the morning.

Compared to the average intensity of cars in the afternoon session, the average number of vehicles in the evening session increased at all observation points, except at Bantul Street, where it decreased. This decrease in the average intensity of cars on Bantul Street is still within reasonable limits because it does not show a significant difference. Compared to the morning session, the average intensity of vehicles in the evening shows an upward trend. Substantial increases are found in Kaliurang Street, Imogiri Timur Street, and Godean Street, all three routes to densely populated hinterlands, not inter-city roads. This indicates that the high intensity of cars in the evening comes from local commuters who share the road with motorcycle commuters.

The average intensity of passing cars is relatively same at eight observation points: Magelang Street, Kaliurang Street, Wonosari Street, Imogiri Timur Street, Parangtritis Street, Bantul Street, Wates Street, and Godean Street. This indicates that the commuters' return time is the same and spread evenly across the commuter routes in Yogyakarta City. Meanwhile, Palagan Street and Solo Street again show the highest average intensity of cars. The intensity of vehicles along the nine commuter routes in Yogyakarta City generally indicates a relatively stable condition. This can be seen through the average intensity of cars passing per minute in the morning, afternoon, and evening sessions, which is not significantly different. Only Solo Street, a national road and the route to the airport show a significant difference in average between the three sessions, with a decrease in intensity occurring in the afternoon. See Figure 2.

Spatio-temporal pattern of air quality on the commuter lanes of Yogyakarta

In this study, we measured ambient air quality at all observation sites and the intensity of vehicles passing by in one minute. Like the vehicle intensity measurements, air quality measurements were also taken at ten commuter lanes. Three measurement sessions were conducted at each location: morning, afternoon, and evening. In each session, ten measurements were taken. Thus, the total data collected from the study area was 300, with 100 data for the morning, afternoon, and evening sessions.

Five air quality parameters are measured in this study, namely PM2.5, PM 10, CO_2, TVOC, and HCHO. Particulate matter (PM) are particles consist of in the air, including dust, soot, dirt, smoke, and liquid droplets. PM2.5 is known to be the biggest threat from air pollution, among other types of pollutants. Li et al. [47] explained that PM2.5 is the most consistent and robust predictor of mortality based on long-term study findings. Huang et al. [48] also explained that PM is one of the most critical environmental problems in most world regions. One source of PM2.5 is transportation. The study conducted in China by Yu et al. [49] showed that transportation density and road network structure in urban transportation play an essential role in PM2.5 concentrations. A study conducted by C. Li & Managi[84] found that in the United States, 6.17 billion kilometres (km) per km2 on-road transportation increase is associated with a 1-μg/m3 county-level PM2.5 concentration increase. On this basis, they recommended county-level policies that consider the temporal and spatial variability of the relationship to mitigate PM2.5 from road transport.

In addition to PM2.5, PM10 is a pollutant source that has received much attention. PM10 has a diameter of 10 micrometers, making it coarser than PM2.5. Sloss & Smith [50] explain that PM10 and PM2.5 arise from natural and human sources. Potential sources of human activities include coal-fired power plants, industry, and road transportation. Given the crucial position of PM in air pollution, as well as the role of road transportation as one of the primary sources of PM, PM parameters, both PM2.5 and PM10, are used as the indicators of air quality in commuter routes in this study.

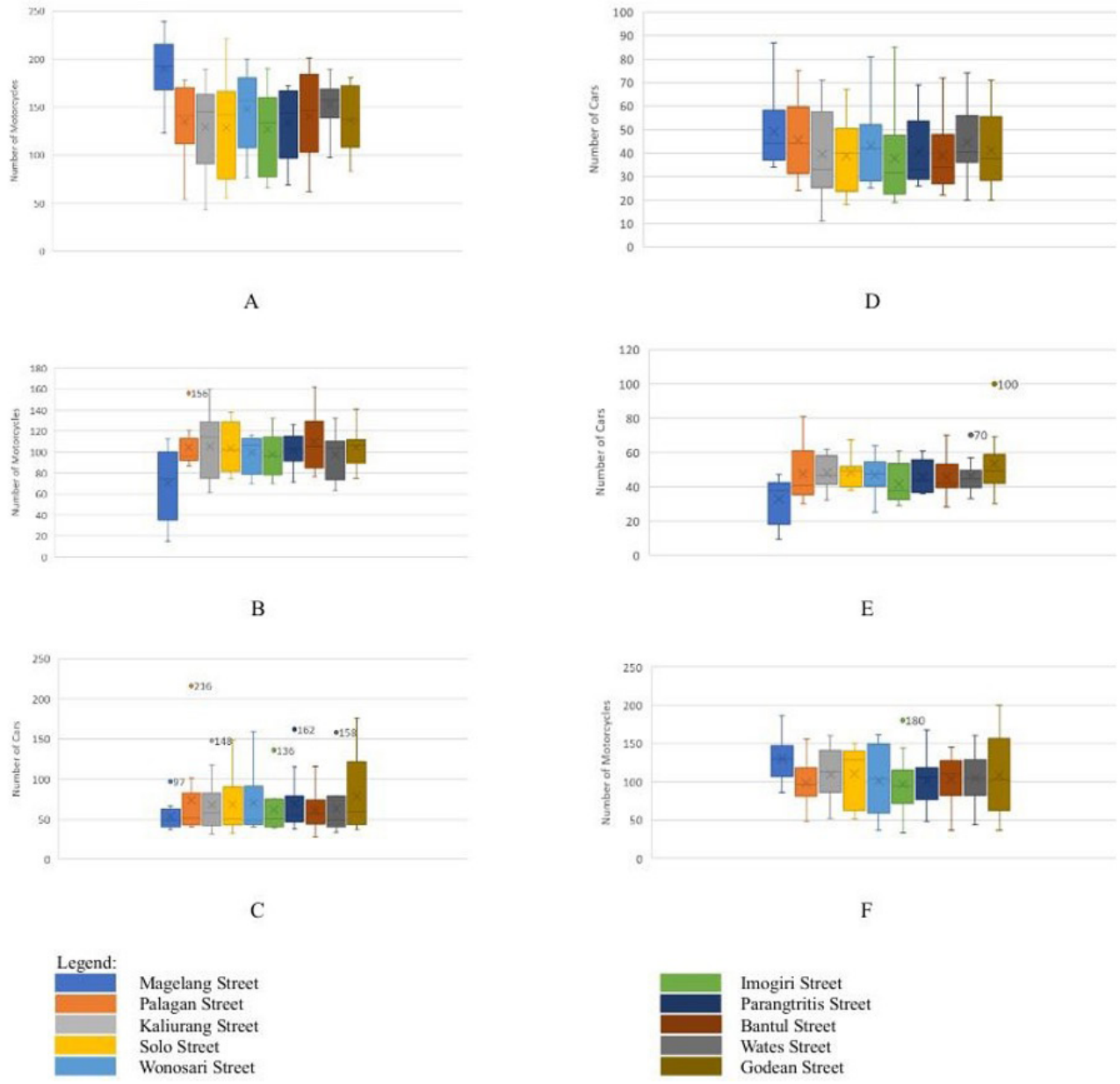


Figure 2. Boxplot for motorcycle and car intensity in the study area. (A) motorcycle in the morning, (B) motorcycle in the afternoon, (C) motorcycle in the evening, (D) car in the morning, (E) car in the afternoon, (F) car in the evening.

Other parameters used are CO_2, TVOC, and HCHO. After the COVID-19 pandemic, there was an increase in CO_2 from transportation, 72% of which was generated from road transportation [51]. He et al. [52] explained that volatile organic compounds, or VOCs, are commonly considered the major types of pollutants in urban air pollution. In road transportation, benzene is a source of VOCs from vehicles, including leaded gasoline, which still exists. Formaldehyde, or HCHO, is particularly influential in the troposphere, where traffic and transportation are essential anthropogenic sources [53].

The measurement results show that air quality conditions vary among locations and sessions. PM2.5 measurements show that PM2.5 concentrations tend to be higher in the morning and evening than the afternoon session. Measurements at 10 locations show that the average PM2.5 in the morning session is always higher than the afternoon session except at Kaliurang Street and Parangtritis Street. On Kaliurang Street, PM 2.5 in the afternoon is slightly higher than in the morning. Meanwhile, on Parangtritis Street, PM2.5 in the afternoon increased significantly compared to the morning. In the evening session, the average PM2.5 increased again compared to the afternoon, except on Palagan Street and Parangtritis Street. This pattern of increasing and decreasing PM2.5 concentrations between morning, afternoon and evening is thought to be related to commuter activities that are busier in the morning and evening than during the afternoon.

Maximum PM2.5 concentrations in the morning occur on Godean Street, which tends to be narrow and congested with motor vehicles. In the afternoon, the maximum con-

Table 2. Summary of statistical data on the intensity of motorcycles and cars in the study area in the morning, afternoon, and evening

Location	Parameters	Motorcycles			Cars		
		Morning	Afternoon	Evening	Morning	Afternoon	Evening
Magelang Street (Jombor Flyover)	N	10,0	10,0	10,0	10,0	10,0	10,0
	Mean	151,6	99,1	113,0	48,4	41,0	45,6
	Median	143,0	109,0	105,5	45,5	40,5	43,5
	Stdev	25,3	26,2	33,2	8,9	10,7	8,1
	Max	217,0	125,0	200,0	67,0	57,0	63,0
	Min	134,0	38,0	86,0	37,0	18,0	37,0
Palagan Street (Monument of Jogja Kembali Intersection)	N	10,0	10,0	10,0	10,0	10,0	10,0
	Mean	144,3	115,2	150,6	62,2	62,4	65,4
	Median	153,0	123,5	153,5	58,5	65,5	68,5
	Stdev	20,2	39,6	22,8	10,5	22,5	11,1
	Max	170,0	162,0	180,0	87,0	100,0	76,0
	Min	111,0	15,0	93,0	54,0	9,0	37,0
Kaliurang Street (Kentungan Intersection)	N	10,0	10,0	10,0	10,0	10,0	10,0
	Mean	164,9	115,4	133,5	38,7	31,1	44,1
	Median	173,0	114,0	133,0	38,5	30,5	40,5
	Stdev	22,0	37,2	19,0	6,9	7,9	19,4
	Max	189,0	160,0	162,0	47,0	48,0	97,0
	Min	135,0	25,0	108,0	30,0	17,0	28,0
	N	10,0	10,0	10,0	10,0	10,0	10,0
Solo Street (Maguwo Junction)	N	10,0	10,0	10,0	10,0	10,0	10,0
	Mean	174,1	89,9	95,0	70,1	58,3	73,4
	Median	168,5	92,5	96,5	71,0	57,5	65,5
	Stdev	19,0	17,2	29,5	10,4	11,8	37,9
	Max	215,0	120,0	135,0	85,0	81,0	176,0
	Min	156,0	63,0	50,0	46,0	37,0	41,0
Wonosari Street (Ketandan Intersection)	N	10,0	10,0	10,0	10,0	10,0	10,0
	Mean	96,5	103,2	54,1	26,5	40,1	128,0
	Median	81,5	107,5	46,0	26,5	39,5	136,5
	Stdev	53,8	17,3	31,6	5,6	6,5	46,4
	Max	239,0	129,0	140,0	34,0	49,0	216,0
	Min	54,0	71,0	33,0	18,0	32,0	55,0
Imogiri Timur Street (Giwangan Intersection)	N	10,0	10,0	10,0	10,0	10,0	10,0
	Mean	103,5	103,8	57,2	28,7	44,7	120,6
	Median	103,0	107,5	50,5	28,0	44,0	116,5
	Stdev	32,0	21,4	19,8	6,3	9,6	32,9
	Max	176,0	129,0	112,0	42,0	58,0	159,0
	Min	66,0	73,0	46,0	20,0	29,0	67,0

Parangtritis Street (Druwo Intersection)	N	10,0	10,0	10,0	10,0	10,0	10,0
	Mean	177,2	87,3	117,2	47,0	46,9	48,9
	Median	180,5	88,5	116,0	47,0	46,0	47,0
	Stdev	29,5	13,7	19,5	9,3	5,0	7,2
	Max	221,0	104,0	158,0	60,0	58,0	64,0
	Min	139,0	61,0	87,0	34,0	41,0	40,0
Bantul Street (Dongkelan Intersection)	N	10,0	10,0	10,0	10,0	10,0	10,0
	Mean	163,7	107,8	128,0	35,1	47,2	45,8
	Median	164,0	104,5	120,0	34,0	46,5	42,5
	Stdev	21,2	15,9	28,9	8,5	6,4	9,2
	Max	194,0	138,0	186,0	48,0	58,0	59,0
	Min	125,0	87,0	99,0	23,0	38,0	33,0
Wates Street (Gamping Junction)	N	10,0	10,0	10,0	10,0	10,0	10,0
	Mean	148,6	74,3	99,8	37,1	41,8	48,0
	Median	152,5	72,5	94,0	37,0	40,5	47,5
	Stdev	37,7	9,7	17,8	8,3	6,5	5,0
	Max	201,0	95,0	144,0	51,0	57,0	55,0
	Min	83,0	61,0	86,0	26,0	36,0	39,0
Street (Demakijo Intersection)	N	10,0	10,0	10,0	10,0	10,0	10,0
	Mean	95,4	98,4	114,5	25,0	42,3	49,8
	Median	99,5	101,0	110,5	24,0	41,5	46,0
	Stdev	37,3	12,7	17,7	8,8	5,8	9,8
	Max	160,0	120,0	150,0	42,0	53,0	71,0
	Min	43,0	75,0	89,0	11,0	34,0	41,0

Source: Data analysis (2024)

centration occurs on Parangtritis Street, which is the route to the beach, allowing local non-commuter transportation activities. In the evening, the maximum concentration occurs on Parangtritis Street. The maximum PM2.5 concentration is even higher than at other points and shows an extreme increase compared to the morning and afternoon. The minimum PM2.5 concentration in the morning occurred on Kaliurang Street, in the afternoon on Solo Street, and in the evening also on Solo Street. The minimum PM2.5 concentration in the evening at Wonosari Street is still the highest compared to the other nine measurement locations. The minimum measured number even has a significant difference compared to other locations. This shows that PM2.5 concentrations on Wonosari Street are high in the evening. According to C. Li & Managi [84], PM2.5 mainly comes from combustion emissions, although road transport is not a major source and contributes little to PM2.5. Meanwhile, Z. Li et al.[87] explained that heavy traffic activities are an important source of PM2.5, in addition to energy production and biomass burning. This answers why, during heavy traffic in the morning and evening, PM2.5 concentrations are higher than during the afternoon.

PM10 measurements show similar results to PM2.5. PM10 concentrations tended to be higher in the morning and evening than in the afternoon at almost all measurement points, except at Kaliurang Street and Parangtritis Street. In general, PM10 concentrations were high in the morning, then decreased in the afternoon and increased again in the evening. This can be seen from the average PM10 value, where there is a decrease in PM10 concentration during the afternoon, which then increases in the evening at eight observation points. Meanwhile, two other points, Kaliurang Street and Parangtritis Street, experienced an increase in PM10 concentrations during the afternoon and decreased in the evening. During the afternoon, the increase in PM10 concentration on Kaliurang Street was not much different from the morning and then it decreased again in the evening. While on Parangtritis Street, there was a significant increase in PM10 during the afternoon and then decreased significantly in the evening.

Maximum PM10 concentrations in the morning also occur on Godean Street, which is related to the characteristics of the street, which tends to be narrower and denser with vehicles. During the afternoon, the maximum PM10 concentration occurs on Parangtritis Street. These maximum concentrations significantly different from the other measurement locations and showed extreme increases and decreases between morning, afternoon, and evening. The

maximum PM10 concentration in the evening occurred on Wonosari Street, a route that connects the activity centre with the densely populated residential areas to the east of the city and the commuters' regions of origin further away in Gunungkidul Regency. The minimum PM10 concentration in the morning was found on Imogiri Timur Street, while in the afternoon and evening was found on Solo Street. Although the minimum PM10 concentration in the morning was found on Imogiri Timur Street, the average PM10 concentration from the point was the second highest. This shows that PM 10 concentration in Imogiri Timur Street does tend to be high.

PM10 concentrations are associated with exhaust gases from motorised vehicles, both cars and motorcycles. Harrison et al. [86] explains that vehicle exhaust emissions account for an average of 32% of PM10, especially during winter. Findings from a study in Jakarta, Indonesia, even show that PM 2.5 and PM 10 are mostly emitted from the road transport and industrial combustion sectors, each contributing around 43%-46%. Heavy vehicles are still the highest contributor to PM 2.5 emissions in the transport sector [90]. This validates the findings in our study that PM10 concentrations are higher in the morning and evening when more vehicles pass by. However, PM10, larger than 2.5 μm, does not stay in the air for long, and its spatial impact is usually limited because it tends to settle on the ground in the opposite direction of the emission source (EPA, 2018).

The CO_2 measurement results also show that this parameter tends to be higher in the morning and evening than in the afternoon, although the difference is insignificant. Measurements at 10 locations show that the average CO_2 in the morning is always higher than in the afternoon, except on Wonosari Street and Wates Street. On both streets, the CO_2 concentration in the afternoon was slightly higher than in the morning. In the evening, the average of CO_2 concentration increased again in almost all measurement locations except Bantul Street. Unlike the other measurement locations, in Bantul Street, the CO_2 concentration decreased in the evening. This condition shows the possibility that the pattern of increasing and decreasing CO_2 concentrations in the morning, afternoon, and evening are related to commuter activities, which tend to be busy in the morning and evening. This is related to the commuters' departure and return hours.

Maximum CO_2 concentrations in the morning session occurred on Kaliurang Street, which connects the CBD with residential areas in the north of Yogyakarta City. Traffic conditions in the morning on Kaliurang Street tend to be congested with motorized vehicles, so the CO_2 figures obtained are the highest compared to other places. Maximum CO_2 concentrations during the afternoon occurred on Wates Street and was the highest value compared to all measurement locations in the morning, afternoon, and evening. In the evening, maximum CO_2 concentrations occurred on Imogiri Timur Street. Minimum CO_2 concentrations in the morning were found on Wonosari Street and Bantul Street. During the afternoon, minimum CO_2 concentrations are relatively uniform in almost all measurement locations. Meanwhile, minimum CO_2 concentrations in the evening were found on Magelang Street and Parangtritis Street. However, there is no significant difference between the afternoon minimum CO_2 concentrations at all measurement locations.

Total Volatile Organic Compounds (TVOC) measurement results did not show significant differences in the morning, afternoon, and evening sessions. In the morning and evening, the average TVOC concentrations also tended to be higher than in the afternoon session, except on Wonosari Street, Bantul Street, and Parangtritis Street. On Wonosari Street, average TVOC concentration in the afternoon was higher than in the morning. Meanwhile, on Bantul Street and Parangtritis Street, average TVOC concentration in the afternoon was higher than in the evening. The highest average TVOC concentration in the morning was found on Kaliurang Street, in the afternoon on Wates Street and in the evening on Imogiri Timur Street. Maximum TVOC concentrations in the morning, afternoon, and evening were found on these three roads. Meanwhile, minimum TVOC concentration in the morning was found on Imogiri Timur Street, in the afternoon on Palagan Street, and in the evening on Parangtritis Street.

HCHO measurements at the 10 locations show highly variable conditions. As with other air quality parameters, HCHO concentrations tended to be high in the morning and evening. An exciting finding was found at Parangtritis Street and Bantul Street, where there was no significant difference in measurement results between the morning, afternoon, and evening sessions. HCHO concentrations tended to remain constant throughout the day. The highest average concentration of HCHO in the morning occurred on Kaliurang Street, which is congested with motorized vehicles; in the afternoon, it was on Wates Street; and in the evening, it was on Imogiri Timur Street. The highest maximum concentration in the morning was found on Kaliurang Street, in the afternoon on Bantul Street, and in the afternoon on Imogiri Timur Street. The minimum HCHO concentration in the morning was found in six locations: Magelang Street, Palagan Street, Wonosari Street, Imogiri Street, Parangtritis Street, and Bantul Street. While in the afternoon, it showed a minimum value in all measurement locations. In the evening, there are four locations: Magelang Street, Palagan Street, Parangtritis Street, and Bantul Street. Based on all measurements, it is concluded that there is minimal influence during the day, and even in some locations, there is no increase. A summary of the air quality measurement data in the study area is shown in Table 3.

Table 3. Summary of statistical data on the air quality measurement in the study area

Location	Parameters	PM2.5			PM10			CO_2			TVOC			HCHO		
		M	A	E	M	A	E	M	A	E	M	A	E	M	A	E
Magelang street	N	10,0	10,0	10,0	10,0	10,0	10,0	10,0	10,0	10,0	10,0	10,0	10,0	10,0	10,0	10,0
	Mean	35,2	19,0	30,8	48,7	24,7	44,1	685,2	409,1	485,9	0,3	0,0	0,1	0,1	0,0	0,0
	Median	35,5	19,5	30,5	49,5	24,0	44,0	710,5	391,0	409,5	0,3	0,0	0,0	0,1	0,0	0,0
	Stdev	7,6	4,1	8,3	10,5	5,8	11,8	107,9	42,3	118,5	0,1	0,0	0,1	0,0	0,0	0,0
	Max	50,0	24,0	44,0	69,0	31,0	62,0	766,0	520,0	664,0	0,4	0,1	0,3	0,1	0,0	0,1
	Min	20,0	9,0	12,0	29,0	11,0	17,0	400,0	385,0	385,0	0,0	0,0	0,0	0,0	0,0	0,0
Palagan Street	N	10,0	10,0	10,0	10,0	10,0	10,0	10,0	10,0	10,0	10,0	10,0	10,0	10,0	10,0	10,0
	Mean	30,1	22,5	21,9	42,1	29,7	33,6	731,1	410,6	643,6	0,4	0,0	0,3	0,1	0,0	0,0
	Median	30,0	24,0	14,5	41,0	32,5	19,5	775,5	392,0	661,5	0,4	0,0	0,3	0,1	0,0	0,0
	Stdev	3,0	6,9	11,6	4,8	9,4	23,4	127,7	47,3	181,7	0,1	0,0	0,2	0,0	0,0	0,0
	Max	35,0	30,0	41,0	49,0	38,0	85,0	833,0	541,0	861,0	0,5	0,2	0,6	0,1	0,0	0,1
	Min	26,0	7,0	13,0	36,0	9,0	17,0	387,0	385,0	386,0	0,0	0,0	0,0	0,0	0,0	0,0
Kaliurang Street	N	10,0	10,0	10,0	10,0	10,0	10,0	10,0	10,0	10,0	10,0	10,0	10,0	10,0	10,0	10,0
	Mean	16,3	17,8	20,2	22,1	25,5	22,2	833,6	445,7	646,0	0,5	0,1	0,2	0,1	0,0	0,0
	Median	16,0	14,0	20,5	21,0	19,0	22,5	905,0	407,5	611,0	0,6	0,0	0,2	0,1	0,0	0,0
	Stdev	2,9	8,9	4,9	3,8	14,1	4,4	162,2	68,6	133,2	0,2	0,1	0,2	0,1	0,0	0,0
	Max	22,0	33,0	29,0	30,0	48,0	28,0	922,0	541,0	822,0	0,7	0,2	0,5	0,3	0,0	0,1
	Min	12,0	8,0	10,0	16,0	9,0	15,0	412,0	385,0	454,0	0,0	0,0	0,0	0,0	0,0	0,0
Solo Street	N	10,0	10,0	10,0	10,0	10,0	10,0	10,0	10,0	10,0	10,0	10,0	10,0	10,0	10,0	10,0
	Mean	20,9	9,3	22,1	27,4	13,0	31,3	485,3	435,9	507,6	0,1	0,1	0,1	0,0	0,0	0,0
	Median	21,0	6,5	22,0	27,0	9,0	31,5	480,5	424,5	524,0	0,1	0,0	0,1	0,0	0,0	0,0
	Stdev	5,2	5,8	9,0	6,6	8,6	13,1	62,9	52,7	74,3	0,1	0,0	0,1	0,0	0,0	0,0
	Max	29,0	20,0	44,0	39,0	27,0	63,0	585,0	551,0	597,0	0,2	0,2	0,2	0,0	0,0	0,0
	Min	13,0	4,0	9,0	17,0	5,0	13,0	403,0	385,0	401,0	0,0	0,0	0,0	0,0	0,0	0,0
Wonosari Street	N	10,0	10,0	10,0	10,0	10,0	10,0	10,0	10,0	10,0	10,0	10,0	10,0	10,0	10,0	10,0
	Mean	44,2	9,3	64,6	62,0	12,6	95,9	404,7	433,0	635,6	0,0	0,1	0,3	0,0	0,0	0,0
	Median	43,0	9,5	53,0	58,5	12,0	75,5	399,5	414,0	610,0	0,0	0,0	0,2	0,0	0,0	0,0
	Stdev	6,1	1,6	56,9	8,6	2,4	87,5	19,7	56,3	115,5	0,0	0,2	0,1	0,0	0,0	0,0
	Max	60,0	12,0	222,0	81,0	16,0	338,0	441,0	539,0	760,0	0,1	0,6	0,4	0,0	0,0	0,1
	Min	39,0	7,0	28,0	54,0	9,0	41,0	385,0	385,0	461,0	0,0	0,0	0,1	0,0	0,0	0,0
Imogiri Timur Street	N	10,0	10,0	10,0	10,0	10,0	10,0	10,0	10,0	10,0	10,0	10,0	10,0	10,0	10,0	10,0
	Mean	50,0	11,2	17,3	64,4	21,0	25,2	461,6	420,1	957,9	0,1	0,0	0,8	0,0	0,0	0,1
	Median	50,0	8,0	15,0	69,5	13,0	22,0	470,5	403,5	952,5	0,1	0,0	0,7	0,0	0,0	0,2
	Stdev	16,7	7,1	6,1	29,1	16,7	9,2	56,4	44,7	216,2	0,1	0,0	0,4	0,0	0,0	0,1
	Max	75,0	30,0	27,0	103,0	57,0	41,0	538,0	524,0	1183,0	0,2	0,1	1,3	0,0	0,0	0,2
	Min	28,0	7,0	10,0	10,0	10,0	14,0	393,0	385,0	455,0	0,0	0,0	0,1	0,0	0,0	0,0
Parangtritis Street	N	10,0	10,0	10,0	10,0	10,0	10,0	10,0	10,0	10,0	10,0	10,0	10,0	10,0	10,0	10,0
	Mean	30,7	71,9	42,3	44,4	109,3	59,3	514,8	409,1	481,7	0,0	0,0	0,0	0,0	0,0	0,0
	Median	31,0	38,5	49,5	45,0	51,0	69,5	482,5	403,5	491,5	0,0	0,0	0,0	0,0	0,0	0,0
	Stdev	3,5	64,6	15,3	5,4	105,1	21,9	99,1	29,0	71,0	0,0	0,0	0,0	0,0	0,0	0,0
	Max	36,0	176,0	60,0	53,0	268,0	84,0	725,0	480,0	577,0	0,0	0,0	0,0	0,0	0,0	0,0
	Min	24,0	5,0	12,0	34,0	7,0	16,0	430,0	385,0	385,0	0,0	0,0	0,0	0,0	0,0	0,0

Bantul Street	N	10,0	10,0	10,0	10,0	10,0	10,0	10,0	10,0	10,0	10,0	10,0	10,0	10,0	10,0	10,0
	Mean	40,0	33,1	42,3	57,1	44,6	59,2	509,2	460,5	451,3	0,0	0,0	0,0	0,0	0,0	0,0
	Median	37,5	34,5	43,5	54,0	47,5	61,5	512,0	453,0	431,5	0,0	0,0	0,0	0,0	0,0	0,0
	Stdev	6,6	10,3	10,3	8,6	13,4	13,9	105,7	53,2	55,6	0,0	0,0	0,0	0,0	0,0	0,0
	Max	53,0	48,0	52,0	73,0	62,0	72,0	648,0	579,0	539,0	0,0	0,0	0,0	0,0	0,0	0,0
	Min	34,0	8,0	18,0	47,0	11,0	25,0	385,0	385,0	392,0	0,0	0,0	0,0	0,0	0,0	0,0
Wates Street	N	10,0	10,0	10,0	10,0	10,0	10,0	10,0	10,0	10,0	10,0	10,0	10,0	10,0	10,0	10,0
	Mean	45,0	21,2	42,5	61,9	29,1	61,9	617,1	687,6	644,4	0,2	0,4	0,2	0,0	0,1	0,0
	Median	38,5	18,0	45,0	56,0	24,0	65,5	582,0	602,0	617,5	0,2	0,2	0,2	0,0	0,0	0,0
	Stdev	17,4	14,0	13,3	18,4	20,0	19,8	93,1	321,5	91,9	0,1	0,6	0,1	0,0	0,1	0,0
	Max	92,0	58,0	57,0	112,0	83,0	83,0	796,0	1521,0	786,0	0,4	2,0	0,4	0,1	0,2	0,1
	Min	35,0	5,0	13,0	51,0	8,0	19,0	524,0	387,0	517,0	0,1	0,0	0,0	0,0	0,0	0,0
Go-dean Street	N	10,0	10,0	10,0	10,0	10,0	10,0	10,0	10,0	10,0	10,0	10,0	10,0	10,0	10,0	10,0
	Mean	57,3	19,6	31,3	78,7	27,1	45,8	515,2	570,3	610,6	0,1	0,2	0,2	0,0	0,0	0,0
	Median	47,0	19,0	29,0	66,0	25,5	39,5	523,0	572,5	560,0	0,1	0,2	0,2	0,0	0,0	0,0
	Stdev	37,1	8,5	14,3	46,8	11,5	25,1	83,5	158,2	153,3	0,1	0,2	0,2	0,0	0,0	0,0
	Max	162,0	39,0	68,0	211,0	54,0	113,0	669,0	833,0	900,0	0,3	0,5	0,6	0,1	0,1	0,1
	Min	38,0	5,0	12,0	55,0	8,0	17,0	405,0	386,0	409,0	0,0	0,0	0,0	0,0	0,0	0,0

Source: Field Measurements (2024)

The results of the matching analysis between the parameters PM2.5, PM10, CO_2, TVOC and HCHO with air quality categories referring to The World Air Quality Index Project [38] and Vianney Augusta & Erfianto [39] show a variety of air quality categories for each parameter in the morning, afternoon, and evening. The average PM2.5 is relatively uniform across all locations in the morning, afternoon, and evening, which is in the good category. However, several locations fall into the moderate category, including Godean Street in the morning, Parangtritis Street in the afternoon and Wonosari Street in the evening.

In the morning's PM10 parameter, five roads are included in the good category: Magelang Street, Palagan Street, Kaliurang Street, Solo Street, and Parangtritis Street. Five other locations in the moderate category include Wonosari Street, Imogiri Timur Street, Bantul Street, Wates Street, and Godean Street. PM10 conditions in the afternoon session fall into the good category in almost all locations. Still, an anomaly on Parangtritis Street shows that in 10 measurements, three reached >250 ppm and fell into the Unhealthy category for Sensitive Groups on average. Meanwhile, PM10 conditions in the evening session show that there are six locations that fall into the good category, including Magelang Street, Palagan Street, Kaliurang Street, Solo Street, Imogiri Timur Street, and Parangtritis Street; four locations with moderate categories, including Wonosari Street, Parangtritis Street, Bantul Street, and Wates Street.

CO_2 conditions in the morning and evening tend to be more diverse when it compared to the conditions in the afternoon. CO_2 conditions with the Excellent Quality category in the morning are found on Solo Street, Wonosari Street, Imogiri Timur Street, Parangtritis Street, Bantul Street, and Godean Street; Good Quality category is found on Magelang Street, Palagan Street, and Wates Street; while Mild Pollution category in the morning is found on Kaliurang Street. CO_2 conditions in the afternoon show a more uniform category with nine observation points included in the Excellent Quality category, except for Wates Street, which is included in the Good Quality category. Different conditions in each location are also shown in the CO_2 concentration in the evening. The Excellent Quality category is found in four locations: Magelang Street, Solo Street, Parangtritis Street, and Bantul Street. The Good Quality category is found on Palagan Street, Kaliurang Street, Wonosari Street, Wates Street, and Godean Street. In addition to these two categories, a Mild Pollution category is found on Imogiri Timur Street.

There is not too much significant variation in the TVOC parameter. Almost all locations have low TVOC concentrations and are included in the Excellent Quality category. Some locations that fall into the Good Quality category are Palagan Street in the morning and Wates Street in the afternoon. The TVOC concentrations in the Mild Pollution category were found at Kaliurang Street in the morning and Imogiri Timur Street in the evening. Meanwhile, the condition of HCHO in all locations is relatively the same, which is included in the Excellent Quality category.

Influence of commuting activities on the instantaneous air quality

In this section, we present the analysis results of the effect of

commuter transportation on instantaneous air quality. We conducted simple linear regression tests between the total number of vehicles and all air quality parameters used in this study, namely PM2.5, PM10, CO_2, HCHO, and TVOC. The test was conducted on all morning, afternoon, and evening data at ten observation locations, which are Yogyakarta commuter lanes.

The analysis shows that the relationship between the number of vehicles passing by in one minute and the instantaneous air quality at that time is entirely positive. Thus, it can be seen that an increase in the number of vehicles passing by affects the ambient air quality, which worsens during that period. Although this relationship is not always significant across all observation locations, this positive relationship shows a clear impact of additional vehicles on worsening air quality.

The relationship between the number of vehicles and various air quality parameters is generally polynomial. This relationship indicates that the impact on air quality is not always steady and linear. This is likely because the exhaust gases from motor vehicles are not the only source of pollutants in this study's air quality parameters. Querol et al. [88] explain that sources of coarse particles (PM2.5 to PM10) include re-suspension of loose soil or road dust, natural dust storms, and different industrial processes. Some minimal non-polynomial relationships were found for PM2.5, PM10, and TVOC. A logarithmic relationship between the number of vehicles and PM2.5 was found on Wates Street in the afternoon and Kaliurang Street in the evening. A linear relationship was found on Parangtritis Street in the evening. In the PM10 parameter, there is an exponential relationship, namely on Magelang Street in the morning. Meanwhile, in the TVOC parameter, there is a logarithmic relationship between Palagan Street and Solo Street in the morning and Wates Street and Bantul Street in the evening.

The most significant relationship between the number of vehicles and PM2.5 in the morning session occurred on Wonosari Street (r2 = 0.8223), the afternoon session on Magelang Street (r2 = 0.8365), the evening session on Wates Street (r2 = 0.5606). In the PM10 parameter, the most significant relationship in the morning session is on Wonosari Street (r2 = 0.7457), in the afternoon session on Magelang Street (r2 = 0.8664), and the evening session on Wates Street (r2 = 0.5443). The CO_2 parameter that has the most significant relationship is found on Magelang Street for the morning session (r2 = 0.8557), Wates Street for the afternoon session (r2 = 0.8105), and Solo Street for the evening session (r2 = 0.5566). For the TVOC parameter, the most significant relationships were found at Imogiri Timur Street (r2 = 0. 8432) for the morning session, Magelang Street (r2 = 0. 5382) for the afternoon session, and Solo Street (r2 = 0.7996) for the evening session. Finally, the most significant relationship on the HCHO parameter occurred on Imogiri Timur Street for the morning session (r2 = 0.8432), Magelang Street for the afternoon session (r2 = 0.5382), and Solo Street (r2 = 0.7996) for the evening session.

Two interesting findings regarding the relationship between the number of passing vehicles and instantaneous air quality exist. First, the nature of the relationship tends to be positive and significant in the morning and afternoon but weakens in the evening. This is likely because, in the evening, there has been an accumulation of pollutants in the atmosphere. Hence, the effect of an increase in the number of vehicles on changes in air quality at that time is only slight. Second, national roads connecting Yogyakarta with other major cities, namely Magelang Street, Wates Street, and Solo Street, appear most frequently as locations with the most significant relationships. This suggests that additional vehicle traffic strongly and positively affects instantaneous air quality on these roads. It seems that their function as national inter-city roads that not only channel commuters from the hinterland causes these roads to be traversed by a variety of vehicles, which in turn influences the worsening of air quality in some of the parameters measured in this study.

There are relationships between vehicle types and air quality parameters. Here, we compare streets with many motorcycles and few cars and streets with fewer motorcycles and more cars. In the study area, there are no motorcycle-only or car-only streets. All streets are dominated by motorcycles, while cars are less in number. With this in mind, we compared two types of streets: those with more motorcycles and fewer cars and those with fewer motorcycles and more cars. The first group of streets is represented by Kaliurang Street, which is passed by 78.4% motorcycles and 21.6% cars. The second group is represented by Wonosari Street, which is passed by 56.6% motorcycles and 43.4% cars.

The results of the T-test analysis show statistically significant differences between air quality parameters on Kaliurang Street and Wonosari Street. On PM2.5 and PM10 parameters, Wonosari Street, with more cars, has a worse air quality. Meanwhile, on CO_2, TVOC, and HCHO parameters, Kaliurang Street, dominated by motorcycles, has worse air quality. This shows a difference between streets that are heavily traveled by motorcycles and streets that are pretty heavily traveled by cars.

Discussion

One of the impacts of transportation activities on the environment is pollution caused by various transportation modes. Rodrigue [12] explains that the transportation sector accounts for about a quarter of global CO_2 emissions, of which 74% of CO_2 emissions come from land transportation. This condition shows that land transportation needs much attention as an essential source of atmospheric pollutants. In addition to CO_2, there are various other gases associated with engine combustion inland transportation modes, as well as particulate matter, which is an air pollutant comprising suspended particles in air, one of the primary sources of which is the activity of land transportation modes.

The issue of urban air quality and urban air pollution concerning commuting activities has received much attention from previous authors. Topics related to air pollution and its relationship with commuting activities that have become a trend of discussion in the last decade are commuter exposure to air pollution and its health risks, the effects of transporta-

tion on air quality in urban areas, and air quality improvement as a result of the COVID-19 pandemic. Commuter exposure to air pollution is the most discussed topic. This topic has been discussed since five decades ago [54] and continues to be a relevant topic of discussion in the following decades [55] – [58] and has been increasingly discussed in the last decade. Various studies have been conducted in this field, including in Taiwan [29], [30], China [59], U.K. [60], [61], India [61], Ethiopia [62], and Canada [63]. The topic of the effect of COVID-19 on improving air quality due to reduced transportation activity has been widely discussed, including in Russia [64], Canada [10], U.K. [65], France [66], China [67], India [68], and Italy [69].

Meanwhile, studies that address the causal relationship between transportation activities, especially commuting, and urban air quality are relatively undiscussed. Thus, our study provides additional information to fill the scientific gap in this area. In this study, we found that commuting activities affect the instantaneous air quality around commuter routes. By studying Yogyakarta City, which is dominated by the use of private vehicles, especially motorcycles, we found a positive relationship between the level of mobility represented by vehicle intensity and air quality. If the number of vehicles increases, the air quality tends to worsen. The results of 300 observations in 10 locations show that this relationship is not always significant, but all are positive with a polynomial trendline type.

There are several previous studies with topics that are relatively close to our study. Lim et al. [70] , in a study in Seoul, Korea, identified spatial and temporal variations in air quality along bicycle lanes. As expected, the study found that heavy traffic volume affected air pollution levels. This study has similar results in that the spatial and temporal analysis shows a positive influence of urban transportation activities on air pollution. However, this study does not explicitly mention commuting activities. Ferenczi et al. [71] in Budapest, Romania, found the influence of long-distance transportation on air quality, especially on SO2, NO2 and Particulate Matter parameters. Compared to our study, the Budapest study did not highlight commuting activities but long-distance transportation that causes regional-scale air pollution. Meanwhile, Sun et al. [72] also addressed urban air quality in their study of Chinese cities but linked it to public transit use. A comparative analysis with previous studies shows that increased transportation activity does affect worsening air quality. However, studies on the topic within the scope of commuting activities are relatively rare.

In Indonesia, several air quality studies in urban areas related to transportation activities have also been conducted, and they provide a foundation that supports the findings of this study. Several studies related to the influence of motorized vehicles on ambient air quality from [73] – [76], state that differences in time, direction, and volume of passing vehicles affect the concentration of air pollutants. In addition, weather conditions, such as temperature, humidity, and wind speed parameters, also influence the increase in pollutant concentrations. This weather factor is likely why the effect of increasing vehicle intensity on air pollution is not always significant.

Spatially, our findings also show that the correlation between vehicle intensity and air pollution also varies significantly from one location to another. This appears to be highly dependent on the type of vehicle passing through. Commuter lanes with motorcycles will tend to have a more significant relationship between vehicle intensity and air pollution than those with fewer motorcycles and more cars. This is because the type of vehicle passing by affects the emissions load that contributes to the atmosphere. Motorcycles are the most significant contributor to exhaust emissions on the highway compared to other types of vehicles because motorcycles fueled by gasoline have higher exhaust emissions than diesel-fueled vehicles [74], [77] – [79].

The findings of this study show that among the various commuter lanes in Yogyakarta, some routes are of poor quality in the morning and evening due to the large number of vehicles travelling on them. Some commuter routes that need attention include Parangtritis Street and Wonosari Street in the morning, Solo Street in the morning and evening, and Palagan Street and Kaliurang Street in the afternoon and evening. The heavy traffic on these commuter routes positively correlates with poorer air quality. Based on these findings, traffic management is recommended to reduce the amount of vehicle congestion on these routes so that it can impact better air quality. Concretely, the recommended traffic engineering is to divide the number of vehicles on Parangtritis Street by diverting the traffic flow through Bantul Street, which is adjacent to Parangtritis Street, in channelling commuters from the Bantul area. Meanwhile, traffic management on Solo Street and Kaliurang Street is recommended for adaptive traffic timing, which adapts traffic flow to the level of vehicle density during peak hours.

In the context of urban planning, several commuter routes that often experience congestion and high vehicle density are recommended to be built with adequate infrastructure. In concrete terms, Palagan Street has a narrow road section, so it is necessary to expand the road to increase the capacity of commuter vehicles. Wonosari Street, which has a wide road section but relatively high vehicle density intensity, is recommended to be built as a flyover on Magelang Street or an underpass built on Magelang Street and Kaliurang Street.

CONCLUSION

Transportation activities have long been known as one of the primary sources of pollutants in the atmosphere. Here, we have found spatio-temporal air quality patterns in Yogyakarta, Indonesia, whose transportation system is dominated by private vehicles, especially motorcycles. The spatio-temporal pattern of air quality in the commuter route of Yogyakarta city represents the influence of commuters' activities on air quality. There is a relationship between the mobility of commuters and the instantaneous air quality in the commuter routes. Measurements of five air quality parameters in 10 commuter routes show that air quality gets worse spatially

on busy roadways that drain many commuters from the hinterland. Temporally, air quality is worse in the morning and evening than the afternoon, which is related to higher mobility during these periods. The number of passing vehicles does have a positive relationship with the increase in pollutants, although it is not always significant.

For evaluation, this study still has limitations. In this study, instantaneous air quality monitoring results from sampling in the morning, afternoon, and evening sessions. Thus, temporally, this study can only compare conditions at these three times. Future studies are highly recommended to conduct measurements throughout the day systematically. This will not only compare conditions between sessions but also illustrate changes in commuter mobility and air quality throughout the day. Moreover, a concrete recommendation for policymakers based on the results of this study is to place ambient air quality monitoring devices on all commuter routes so that drivers can adjust to the pollution level. Also, traffic authorities must make engineering arrangements for traffic flow, especially on Kaliurang Street in the morning.

DATA AVAILABILITY STATEMENT

The author confirm that the data that supports the findings of this study are available within the article. Raw data that support the finding of this study are available from the corresponding author, upon reasonable request.

CONFLICT OF INTEREST

The author declared no potential conflicts of interest with respect to the research, authorship, and/or publication of this article.

USE OF AI FOR WRITING ASSISTANCE

Not declared.

ETHICS

There are no ethical issues with the publication of this manuscript.

REFERENCES

[1]. C. P. Kaneda, "World Population Data-Sheet-Boolet," Climate Vulnerability and Resilience (2nd ed.)," Katalog: 2301024, 2023.

[2]. J.P. Rodrigue, "The Geography of Transport Systems (3rd ed.)," In the Geography of Transport Systems, 2019.

[3]. A. Venkatram, and N. Schulte, "The Impact of Highways on Urban Air Quality," Urban Transportation and Air Pollution, pp. 77–104, 2018.

[4]. J. Li, P. Wang, and S. Ma, "The Impact of Different Transportation Infrastructures on Urban Carbon Emissions: Evidence from China", Energy, Article 131041, 2024.

[5]. B. Sun, C. Fang, X. Liao, X. Guo, and Z. Liu, "The Relationship Between Urbanization and Air Pollution Affected by Intercity Factor Mobility: A Case of the Yangtze River Delta Region," Environmental Impact Assessment Review, Article 107092, 2023.

[6]. O. Ghaffarpasand, D. Okure, P. Green, S. Sayyahi, P. Adong, R. Sserunjogi, E. Bainomugisha, and F. D. Pope, "The Impact of Urban Mobility on Air Pollution in Kampala, An Exemplar Sub-Saharan African City," Atmospheric Pollution Research, Vol. 15(4), Article 102057, 2024.

[7]. S. Bi, J. Hu, L. Shao, T. Feng, and A. Appolloni, "Can Public Transportation Development Improve Urban Air Quality? Evidence from China," Urban Climate, Vol. 54, Article 101825, 2024.

[8]. G. Cao, L. A. Zhou, C. Liu, and J. Zhou, "The Effects of The Entries by Bike-Sharing Platforms on Urban Air Quality," China Economic Quarterly International, Vol. 3(3), pp. 213–224, 2023.

[9]. D. Xie, Z. Gou, and X. Gui, "How Electric Vehicles Benefit Urban Air Quality Improvement: A Study in Wuhan," Science of the Total Environment, Article 167584, 2024.

[10]. X. Tian, C. An, Z. Chen, and Z. Tian, "Assessing the Impact of COVID-19 Pandemic on Urban Transportation and Air Quality in Canada," Science of the Total Environment, Article 144270, 2021.

[11]. Y. J. Wong, H. Y. Shiu, J. H. H. Chang, M. C. G. Ooi, H. H. Li, R. Homma, Y. Shimizu, P. T. Chiueh, L. Maneechot, and S. N. M. Nik, "Spatiotemporal Impact of COVID-19 on Taiwan Air Quality in the Absence of a Lockdown: Influence of Urban Public Transportation Use and Meteorological Conditions," Journal of Cleaner Production, Article 132893, 2022.

[12]. J. P. Rodrigue, "Case Study: Logistics Zones," In the Geography of Transport Systems, 2024.

[13]. H. S. Yunus, "Dinamika Wilayah Peri-Urban Determinan Masa Depan Kota," Pustaka Pelajar, 2008.

[14]. Aritenang, A. F, "The Crucial Role of Motorcycle-Based Ride-Hailing Among Commuters: The Case of Jakarta and Bandung in Metropolitan Areas," Journal of Public Transportation, Vol. 26, Article 100082, 2024.

[15]. T. Tjahjono, A. Kusuma, and A. Septiawan, "The Greater Jakarta Area Commuters Travelling Pattern," Transportation Research Procedia, Vol. 47, 2020.

[16]. T. H. Tran, S. Tanaka, and H. T. Nguyen, "The Heterogeneity in Commuters' Travel Behaviors Toward Different Types of Ride-Hailing Services: The Case of Hanoi, Vietnam," Asian Transport Studies, Vol. 10, Article 100126, 2024.

[17]. A. Ratanawaraha, and S. Chalermpong, "How the Poor Commute in Bangkok, Thailand," Transportation Research Record, pp. 83–89, Article 2568, 2016.

[18]. E. Guerra, "Electric Vehicles, Air Pollution, and

the Motorcycle City: A Stated Preference Survey of Consumers' Willingness to Adopt Electric Motorcycles in Solo, Indonesia," Transportation Research Part D: Transport and Environment, Vol. 68, pp. 52–64, 2019.

[19]. Y. Sakamoto, K. Shoji, M. T. Bui, T. H. Phạm, T. A. Vu, B. T. Ly, and Y. Kajii, "Air Quality Study in Hanoi, Vietnam in 2015–2016 Based on A One-Year Observation of NOx, O3, CO and A One-Week Observation of VOCs," Atmospheric Pollution Research, Vol. 9(3), pp. 544–551, 2018.

[20]. V. T. Tang, N. T. K. Oanh, E. R. Rene, and T. N. Binh, "Analysis of Roadside Air Pollutant Concentrations and Potential Health Risk of Exposure in Hanoi, Vietnam," Journal of Environmental Science and Health-Part A Toxic/Hazardous Substances and Environmental Engineering, Vol. 55(8), pp. 975–988, 2020.

[21]. S. T. Leong, S. Muttamara, and P. Laortanakul, "Influence of Benzene Emission from Motorcycle on Bangkok Air Quality," Atmospheric Environment, Vol. 36(4), pp. 651–661, 2002.

[22]. E. O. Okokon, P. Taimisto, A. W. Turunen, O. A. Amoda, A. E. Fasasi, L. G. Adeyemi, J. Juutilainen, and T. Lanki, "Particulate Air Pollution and Noise: Assessing Commuter Exposure in Africa's Most Populous City," Journal of Transport and Health, Vol. 9, pp. 150–160, 2018.

[23]. D. H. Huy, N. D. T. Chi, N. X. T. Nam, and T. T. Hien, "Commuter Exposures to In-Transit PM in An Urban City Dominated by Motorcycle: A Case Study in Vietnam," Atmospheric Pollution Research, Vol. 13(3), Article 101351, 2022.

[24]. T. N. Quang, N. T. Hue, M. V. Dat, L. K. Tran, T. H. Phi, L. Morawska, and P. K. Thai, "Motorcyclists have Much Higher Exposure to Black Carbon Compared to Other Commuters in Traffic of Hanoi, Vietnam," Atmospheric Environment, Article 118029, 2021.

[25]. S. Saksena, T. N. Quang, T. Nguyen, P. N. Dang, and P. Flachsbart, "Commuters' Exposure to Particulate Matter and Carbon Monoxide in Hanoi, Vietnam," Transportation Research Part D: Transport and Environment, Vol. 13(3), pp. 206–211, 2008.

[26]. P. deSouza, R. Lu, P. Kinney, and S. Zheng, "Exposures to Multiple Air Pollutants While Commuting: Evidence from Zhengzhou, China," Atmospheric Environment, Article 118168, 2021.

[27]. R. K. Ayyakkannu, J. Subbaian, M. Pandian, and D. L. Iruthayaraj, "Commuter Exposure to Fine Particulate Matter in Private Road Transport Modes in Salem, India," Thermal Science, Vol. 26(2), pp. 1695–1708, 2022.

[28]. P. Kumar, and N. C. Gupta, "Commuter Exposure to Inhalable, Thoracic and Alveolic Particles in Various Transportation Modes in Delhi," Science of the Total Environment, pp. 535–541, 2016.

[29]. K. J. Chuang, L. Y. Lin, K. F. Ho, and C. T. Su, "Traffic-Related PM2.5 Exposure and Its Cardiovascular Effects Among Healthy Commuters in Taipei, Taiwan," Atmospheric Environment: X, Vol. 7, Article 100084, 2020.

[30]. H. C. Li, P. T. Chiueh, S. P. Liu, and Y. Y. Huang, "Assessment of Different Route Choice on Commuters' Exposure to Air Pollution in Taipei, Taiwan," Environmental Science and Pollution Research, Vol. 24(3), pp. 3163–3171, 2017.

[31]. B. Y. Chiu, "Does the Bus Rapid Transit Reduce Motorcycle Use? Evidence from the Jakarta Metropolitan Area, Indonesia," Case Studies on Transport Policy, Vol. 10(3), pp. 1767–1774, 2022.

[32]. B. Y. Chiu, "Does Mass Rapid Transit Reduce Motorcycle Travel? Evidence from Taipei, Taiwan," Transportation Research Part D: Transport and Environment, Article 103844, 2023.

[33]. Y. H. Ho, T. C. Hsiao, and A. Y. Chen, "Emission Analysis of Electric Motorcycles and Assessment of Emission Reduction with Fleet Electrification," IEEE Transactions on Intelligent Transportation Systems, Vol. 24(12), pp. 15369–15378, 2023.

[34]. BPS, "Statistik Komuter DKI Jakarta Hasil Survei Komuter DKI Jakarta 2017," 2017.

[35]. BPS, "Statistik Komuter Bandung Raya Hasil Survei Komuter Bandung Raya dan Gerbangkertosusila 2017," 2017.

[36]. BPS, "Statistik Komuter Jabodetabek Hasil Survey Komuter Jabodetabek 2019," 2019.

[37]. BPS, "Statistik Komuter Jabodetabek Hasil Survey Komuter Jabodetabek 2023," 2023.

[38]. The World Air Quality Index Project, "2020 World Air Quality Report: Region & City PM2.5 Ranking," IQAir, pp. 1–41, 2020.

[39]. A. B. Vianney, and B. Erfianto, "Time Series On-Board Air Quality Index," pp. 23–36, 2023.

[40]. A. Ashari, and S. Purwantara, "Bentanglahan Vulkanik Indonesia (Issue April)," 2022.

[41]. A. Ashari, "Geomorphology of the Southern Flank of Merapi Volcano in Relation," pp. 183–192, 2017.

[42]. S. Purwantara, A. Ashari, and M. H. B. Ibrahim, "The Characteristics of Infiltration on The Southern Flank of Merapi Volcanic Plain, Yogyakarta, Indonesia," International Journal of GEOMATE, Vol. 19(74), pp. 201–209, 2020.

[43]. S. Purwantara, A. Ashari, and S. T. J. Putro, "The Relationship Between Landscape and Meteorological Parameters on COVID-19 Risk in A Small-Complex Region of Yogyakarta, Indonesia," Bulletin of Geography, Physical Geography Series, Vol. 21(1), pp. 27–43, 2021.

[44]. Special Region of Yogyakarta Transportation Service, "Transportasi Dalam Angka 2021," 2021.

[45]. Y. C. Government, "Jumlah Kendaraan Bermotor di Kota Yogyakarta Tahun 2022," 2023.

[46]. E. Guerra, and G. Duranton, "Transport Modes and Cities," In International Encyclopedia of Transportation: Volume 1-7, Vol. 5, 2021.

[47]. T. Li, Y. Guo, Y. Liu, J. Wang, Q. Wang, Z. Sun, M. Z. He, and X. Shi, "Estimating Mortality Burden Attributable to Short-Term PM2.5 Exposure: A National Observational Study in China," Environment International, pp. 245–251, 2019.

[48]. K. Huang, F. Liang, X. Yang, F. Liu, J. Li, Q. Xiao, J. Chen, X. Liu, J. Cao, C. Shen, L. Yu, F. Lu, X. Wu, L. Zhao, X. Wu, Y. Li, D. Hu, J. Huang, Y. Liu, and D. Gu, "Long Term Exposure to Ambient Fine Particulate Matter and Incidence of Stroke: Prospective Cohort Study from the China-PAR Project," The BMJ, pp. 1–9, 2019.

[49]. C. Yu, Y. Deng, Z. Qin, C. Yang, and Q. Yuan, "Traffic Volume and Road Network Structure: Revealing Transportation-Related Factors on PM2.5 Concentrations," Transportation Research Part D: Transport and Environment, Article 124, 2023.

[50]. L. L. Sloss, and I. M. Smith, "PM10 and PM2.5: An International Perspective," Fuel Processing Technology, pp. 127–141, 2000.

[51]. C. Fulton, "Urban Exploration: Traces of The Secretly Documented, Decayed, and Disused," Library Trends, Vol. 69(3), pp. 556 – 572, 2021.

[52]. L. He, Y. Duan, Y. Zhang, Q. Yu, J. Huo, J. Chen, H. Cui, Y. Li, and W. Ma, "Effects of VOC Emissions from Chemical Industrial Parks on Regional O3-PM2.5 Compound Pollution in the Yangtze River Delta," Science of the Total Environment, Article 906, 2024.

[53]. Y. Gao, H. Pan, L. Cao, C. Lu, Q. Yang, X. Lu, H. Ding, S. Li, and T. Zhao, "Effects of Anthropogenic Emissions and Meteorological Conditions on Diurnal Variation of Formaldehyde (HCHO) in the Yangtze River Delta, China," Atmospheric Pollution Research, Vol. 14(6), Article 101779, 2023.

[54]. V. J. Konopinski, and J. B. Upham, "Commuter Exposure to Atmospheric Lead," Archives of Environmental Health, Vol. 14(4), pp. 589–593, 1967.

[55]. C. C. Chan, J. D. Spengler, H. Ozkaynak, and M. Lefkopoulou, "Commuter Exposures to VOCs in Boston, Massachusetts," Journal of the Air and Waste Management Association, Vol. 41(12), pp. 1594–1600, 1991.

[56]. L. Y. Chan, and Y. M. Liu, "Carbon Monoxide Levels in Popular Passenger Commuting Modes Traversing Major Commuting Routes in Hong Kong," Atmospheric Environment, Vol. 35(15), pp. 2637–2646, 2001.

[57]. N. Shiohara, A. A. F. Bremauntz, S. B. Jimenez, and Y. Yanagisawa, "The Commuters' Exposure to Volatile Chemicals and Carcinogenic Risk in Mexico City," Atmospheric Environment, Vol. 39(19), pp. 3481–3489, 2005.

[58]. A. V. Vellopoulou, and M. R. Ashmore, "in the City of Athens," Vol. 24(7), pp. 713–720, 1998.

[59]. J. Zheng, Z. Qiu, H. O. Gao, and B. Li, "Commuter PM Exposure and Estimated Life-Expectancy Loss Across Multiple Transportation Modes in Xi'an, China," Ecotoxicology and Environmental Safety, Article 112117, 2021.

[60]. K. N. Dirks, J. Y. T. Wang, A. Khan, and C. Rushton, "Air Pollution Exposure in Relation to the Commute to School: A Bradford UK Case Study," International Journal of Environmental Research and Public Health, Vol. 13(11), pp. 1–10, 2016.

[61]. A. Namdeo, S. Ballare, H. Job, and D. Namdeo, "Commuter Exposure to Air Pollution in Newcastle, U.K., and Mumbai, India," Journal of Hazardous, Toxic, and Radioactive Waste, Vol. 20(4), pp. 1–15, 2016.

[62]. A. Embiale, F. Zewge, B. S. Chandravanshi, and E. S. Demessie, "Commuter Exposure to Particulate Matters and Total Volatile Organic Compounds at Roadsides in Addis Ababa, Ethiopia," International Journal of Environmental Science and Technology, Vol. 16(8), pp. 4761–4774, 2019.

[63]. Q. Miao, M. Bouchard, D. Chen, M. W. Rosenberg, and K. J. Aronson, "Commuting Behaviors and Exposure to Air Pollution in Montreal, Canada," Science of the Total Environment, pp. 193–198, Article 508, 2015.

[64]. A. S. Ginzburg, V. A. Semenov, E. G. Semutnikova, M. A. Aleshina, P. V. Zakharova, and E. A. Lezina, "Impact of COVID-19 Lockdown on Air Quality in Moscow," Doklady Earth Sciences, Vol. 495(1), pp. 862–866, 2020.

[65]. V. Kazakos, J. Taylor, and Z. Luo, "Impact of COVID-19 Lockdown on NO2 and PM2.5 Exposure Inequalities in London, UK," Environmental Research, Vol. 198(2), Article 111236, 2021.

[66]. S. Dahech, M. A. Abdmouleh, and S. Lagmiri, "Spatiotemporal Variation of Air Quality (PM and NO2) in Southern Paris during COVID-19 Lockdown Periods," Atmosphere, Vol. 13(2), 2022.

[67]. C. Liu, Z. Huang, J. Huang, C. Liang, L. Ding, X. Lian, X. Liu, L. Zhang, and D. Wang, "Comparison of PM2.5 and CO_2 Concentrations in Large Cities of China during the COVID-19 Lockdown," Advances in Atmospheric Sciences, Vol. 39(6), pp. 861–875, 2022.

[68]. G. Thomas, J. Thomas, R. S. Devika, A. Krishnan, A. V. Mathew, and A. J. Nair, "Impact of COVID-19 Lockdown on Ambient Air Quality in the Southwest Coastal Urban Regions of India," Aerosol Science and Engineering, Vol. 7(3), pp. 303–314, 2023.

[69]. M. Ravina, Z. S. Esfandabadi, D. Panepinto, and M. Zanetti, "Traffic-Induced Atmospheric Pollution during the COVID-19 Lockdown: Dispersion Modeling Based on Traffic Flow Monitoring in Turin, Italy," Journal of Cleaner Production, Article 128425, 2021.

[70]. C. C. Lim, H. Kim, M. J. R. Vilcassim, G. D. Thurston, T. Gordon, L. C. Chen, K. Lee, M. Heimbinder, and S. Y. Kim, "Mapping Urban Air Quality Using Mobile Sampling with Low-Cost Sensors and Machine Learning in Seoul, South Korea," Environment

International, Article 105022, 2019.
[71]. Z. Ferenczi, A. F. Sremac, and B. Szintai, "Understanding Air Quality under Different Weather and Climate Conditions in the Pannonian Basin," Background material for H2020-TWINN-2015: SERBian-Austrian-Italian (SAI) Partnership FORcing EXCELLence in Ecosystem Research View Project COST Action 734 (Issue January), 2017.
[72]. C. Sun, W. Zhang, X. Fang, X. Gao, and M. Xu, "Urban Public Transport and Air Quality: Empirical Study of China Cities," Energy Policy, Article 110998, 2019.
[73]. A. L. Ginting, dan M. Mirwan, "Analisis Kualitas Udara Berdasarkan Volume Lalu Lintas di Jalan Kedung Cowek Surabaya," INSOLOGI: Jurnal Sains Dan Teknologi, Vol. 1(5), pp. 603–613, 2022.
[74]. N. Kemala, A. Gani, dan Mahidin, "Jurnal Penelitian Transportasi Darat," Vol. 20(1), pp. 17–32, 2018.
[75]. D. R. Nurmaningsih, "Analisis Kualitas Udara Ambien Akibat Lalu Lintas Kendaraan Bermotor di Kawasan Coyudan, Surakarta," Al-Ard: Jurnal Teknik Lingkungan, Vol. 3(2), pp. 46–53, 2018.
[76]. R. Wirosoedarmo, B. Suharto, and D. E. Proborini, "Analyze the Effects of Wind Speed and Vehicles Number to Carbon Monoxide at Arjosari Terminal," Jurnal Sumberdaya Alam dan Lingkungan, Vol. 7(10), pp. 57–64, 2020.
[77]. D. R. Suhadi, dan A. S. Febrina, "Pedoman Teknis Penyusunan Inventarisasi Emisi Pencemar Udara di Perkotaan," Pedoman Teknis Penyusunan Inventarisasi Emisi Pencemar Udara di Perkotaan, 2013.
[78]. D. Y. Damara, I. W. Wardhana, dan E. Sutrisno, "Analisis Dampak Kualitas Udara Karbon Monoksida Akibat Kegiatan Car Free Day Menggunakan Program Caline4 dan Surfer," Jurnal Teknik Lingkungan, Vol. 6(1), pp. 1–14, 2017.
[79]. N. Hodijah, B. Amin, dan M. Mubarak, "Estimasi Beban Pencemar dari Emisi Kendaraan Bermotor di Ruas Jalan Kota Pekanbaru," Dinamika Lingkungan Indonesia, Vol. 1(2), Artikel 71, 2014.
[80]. M. Zimakowska-Laskowska, and P. Laskowski, "Comparison of Pollutant Emissions from Various Types of Vehicles," Combustion Engines, Vol. 197(2), pp. 139-145, 2024.
[81]. http://epa.gov/transportation-air-pollution-and-climate-change/carbon-pollution-transportation, The EPA website. [Online]. Available: (2024)
[82]. https://www.iea.org/energy-system/transport#tracking, The IEA website. [Online]. Available: (2024)
[83]. M. Leroutier, and P. Quirion, "Air Pollution and CO_2 from Daily Mobility: Who Emits and Why? Evidence from Paris," Energy Economics, Vol. 109, pp. 105941, 2022.
[84]. C. Li, and S. Managi, "Contribution of On-Road Transportation to PM2.5," Scientific Reports, Vol. 11(1), pp. 1–12, 2021.
[85]. https://www.gov.uk/government/statistics/emissions-of-air-pollutants/emissions-of-air-pollutants-in-the-uk-particulate-matter-pm10-and-pm25, The Department for Environtment Food & Rural Affairs website. [Online]. Available: (2024)
[86]. R. M. Harrison, R. A. Deacon, and M. R. Jones, "Sources and Process Affecting Concentration of PM10 and PM 2.5 Particulate Mater In Birmingham (U.K.)," Atmospheric Environtment, Vol. 31(24), pp. 4103-4117, 1997.
[87]. Z. Li, P. K. Hopke, L. Husain, S. Qureshi, V. A. Dutkiewicz, J. J. Schwab, F. Drewnick, and K. L. Demerjian, "Sources of Fine Particle Composition in New York City," Atmos. Environ, Vol. 38, pp. 6521-6529, 2004.
[88]. X. Querol, A. Alastuey, C. R. Ruiz, B. Artinano, H. C. Hansson, R. M. Harrison, E. Buringh, H. M. T. Brink, M. Lutz, P. Bruckmann, P. Straehl, and J. Schneider, "Speciation and Origin of PM10 and PM2.5 in Selected European Cities," Atmos. Environ, Vol. 38(6547), pp. 6555, 2004.
[89]. https://www.epa.gov/report-environtment, The EPA website. [Online]. Available: (2018)
[90]. P. Lestari, M. K. Arrohman, S. Damayanti, and Z. Klimont, "Emissions and Spatial Distribution of Air Pollutants from Anthropogenic Sources in Jakarta," Atmospheric Pollution Research, Vol. 13(9), pp. 1-15, 2022.

ABBREVIATIONS

BPS	Badan Pusat Statistik Republik Indonesia / Indonesian Statistical Agency
CBD	Central Business District
CO_2	Carbon Dioxide
DIY	Daerah Istimewa Yogyakarta / Yogyakarta Special Region
GIS	Geographic Information System
HCHO	Formaldehyde
NO2	Nitrogen Dioxide
PM2.5	Particulate Matter 2.5
PM10	Particulate Matter 10
SO2	Sulfur Dioxide
TVOC	Total Volatile Organic Compounds

Environ Res Tec, Vol. 8, Issue. 2, pp. 372-381, June 2025

Environmental Research and Technology
https://dergipark.org.tr/en/pub/ert
DOI: https://10.35208/ert.1493704

Research Article

Impact of additives on combustion behaviour and performance of a diesel engine powered by diesel-CIME blend: A comparative analysis

Anant G. NAGPURE*[1], Walmik S. RATHOD[2], Supriya B. CHAVAN[3]

[1]*Department of Mechanical Engineering, Konkan Gyanpeeth College of Engineering, Karjat, Maharashtra, India*
[2]*Department of Mechanical Engineering, Veermata Jijabai Technological Institute, Mumbai, Maharashtra, India*
[3]*Quality Control Department, Indian Biodiesel Corporation, Baramati, Maharashtra, India*

ARTICLE INFO

Article history
Received: 01 Jun 2024
Revised: 18 June 2024
Accepted: 11 Sep 2024

Key words:
Calophyllum inophyllum methyl ester, propanol, curcuma longa leaf oil, combustion, diesel engine, ANN.

ABSTRACT

This study evaluates the effects of blends containing diesel-Calophyllum Inophyllum Methyl Ester (CIME) with additives on the combustion and performance parameters of a diesel engine. In this investigation, the additives identified were propanol and Curcuma longa leaf oil. The engine characteristics were investigated by using 6%, 12%, and 18% (concentration by volume) of propanol and Curcuma longa leaf oil separately with a diesel-CIME blend (CI20). In comparison to diesel, propanol blends showed a lower heat release rate and a lower peak cylinder pressure. An increased proportion of propanol was found to cause significant engine knock at higher compression ratios, and the engine was unable to operate at higher loads while using CI20P18. The propanol blends reported comparable efficiencies compared to diesel. The average BTE of blend CI20P12 was 1.6% greater than that of diesel. The SFCs were seen to be higher for all blends when compared to diesel. 12.8% and 13.9% more average SFCs were recorded for the blends CI20P6 and CI20P12, respectively, than for diesel. In comparison to diesel and CI20, the Curcuma longa leaf oil blended modified blends had lower cylinder pressure, heat release rate, and mean gas temperature, while these modified blends had lower specific fuel consumption than the CI20 blend. The primary aim of this study is to investigate the potential for Calophyllum inophyllum oil, propanol and oil from the rising agricultural waste of Curcuma longa leaves. Experimental evaluation revealed that methyl ester, propanol, and Curcuma longa leaf oil could be effectively used as partial substitutes for diesel. The results of the artificial neural network (ANN) demonstrated a significant connection between the experimental and predicted values for the engine performance parameters.

Cite this article as: Nagpure, AG, Rathod WS, Supriya B. Chavan SB. Impact of additives on combustion behaviour and performance of a diesel engine powered by diesel-CIME blend: A comparative analysis. Environ Res Tec 2025;8(2) 372-381.

***Corresponding author.**
*E-mail address: nagpureag77@gmail.com

This is an open access article under the CC BY-NC license (http://creativecommons.org/licenses/by-nc/4.0/).

INTRODUCTION

Because of the global consumption of petroleum reserves, the importance of renewable alternative fuels in transportation, industry, electricity, and agriculture is steadily increasing [1]. Several researchers focused on producing unconventional fuels that are sustainable, economically viable, and simple to process due to the energy and environmental crises [2]. Biofuels are biodegradable, non-toxic, exhibit similar properties to petroleum fuels, and can be blended with petroleum fuels [3]. Adding biofuels to the fuel blend also has the significant advantage of reducing particulate matter emissions from diesel engines. [4]. Oil from several feedstocks has been used directly in diesel engines using techniques such as pyrolysis, dilution, and micro-emulsion. However, due to its highly viscous nature and low auto ignition quality, for short-term applications, these techniques work well as a partial substitute for diesel. The free fatty acid content can also cause numerous operational problems in diesel engines. These properties of oil can be improved by most commercial techniques of transesterification, converting it into biodiesel or methyl ester. The performance parameters of a diesel engine using methyl ester were examined in a number of studies. According to these studies, using straight methyl ester or diesel-methyl ester blends in diesel engines results in higher fuel usage. This is a result of methyl ester having higher densities and viscosities than regular diesel and having heating values that are relatively lower. Conversely, when methyl ester-diesel blends are used, diesel engine emissions usually become lower. Because methyl ester's inherent oxygen content improves combustion, resulting in lower emissions of CO, HC, and PM. Also, several studies have demonstrated that NOx emissions rise. The explanation for this rise is the inherent oxygen in methyl ester, which improves combustion and raises the temperature within the cylinder, allowing nitrogen to react with oxygen [5-6]. Research on methyl ester's impact on CO_2 emissions has yielded conflicting results. While some have concluded that methyl ester lowers emissions because of its low carbon-to-hydrogen ratio, others have concluded that because of its efficient combustion, emissions either increase or remain unchanged. However, taking into account the CO_2 life cycle circulation, methyl ester's CO_2 emissions are significantly lower [7]. Many studies have been conducted where the emphasis has been on diesel-methyl ester blends with specific additives. The various additives include lower-alcohol additives, higher-alcohol additives, and nanoadditives. Alcohol can potentially be combined with diesel and methyl ester more effectively as its carbon content rises [8]. Implementing alcohol as an additive to methyl ester blends is a promising process for increasing the use of both methyl ester and alcohol. However, many investigators found that low-carbon alcohols are not suitable due to their low heating value, poor antiknock qualities, and long ignition delay. H. Aydin et al. [9] studied the use of higher percentages of sunflower oil methyl ester with ethanol and reported higher torque at a lower average SFC with the methyl ester-ethanol blend. The CO_2 decrease with methyl ester-diesel was about 67%, while CO and SO2 were reduced with methyl ester-diesel and methyl ester-ethanol blends. This study also reported decreased NOx emissions with the methyl ester-diesel blend. B. Prabakaran et al. [10] investigated the engine characteristics with cottonseed oil methyl ester and anhydrous ethanol at 50%, 30%, and 10% (by volume). This study reported a thermal efficiency increase of about 8% with 50% ethanol. Also, the maximum pressure and heat release increased by 17% and 2.5 times with 50% ethanol. The HC, CO, and NOx emissions were 57%, 66%, and 29% less compared to diesel, respectively. L. Zhu et al. [11] investigated how diesel engine particulate emissions were affected by blends of methanol and methyl ester. The experimentation was carried out at different loads with diesel, methyl ester, and blends. Furthermore, increased mass fuel combustion was observed during the premixed combustion mode. The PM concentration decreased owing to the higher oxygen percent of the blends. N. Yilmaz et al. [12] studied the performance of the engine using 15% ethanol and 15% methanol separately with methyl ester. This study concluded that ethanol blending reduces the SFC as compared to methanol blending, as methanol has a greater heat of vaporization. Both the alcohols increased HC and CO emissions, but overall, methanol resulted in higher emissions. Lowered NOx emissions were reported with both alcohols, with no significant difference. Yilmaz N. et al. [13] used 5%, 10%, and 20% of pentanol in diesel-waste oil methyl ester. This study reported that pentanol can be safely used with diesel. With the use of pentanol, the SFC increased within the ranges of 5.27% and 8.61%, but the BTE decreased by a maximum of 5.33%. Also, the higher oxygen content showed higher exhaust temperatures. The latent heat of evaporation of pentanol caused a decrease in combustion efficiency as well as an increase in HC and CO. The maximum increase was 29.34% and 116.01% with 20% pentanol as compared to the diesel-methyl ester blend. The oxygen in pentanol increased NOx compared to diesel-methyl ester blends and regular diesel. While studying the emissions from n-pentanol/Fischer-Tropsch diesel fuelled diesel engine, with varying load and speed conditions, Ye L. et al. [14] reported lower HC, CO, NOX, and soot with this diesel than regular diesel. With n-pentanol, HC and CO increased, whereas NOX and soot decreased. Fischer–Tropsch diesel particles have a tighter arrangement than diesel particles. With the addition of n-pentanol, this effect becomes even more prominent. The maximum degree of graphitization is found in Fischer-Tropsch diesel, which decreases with the addition of n-pentanol. Rangabashiam D. et al. [15] looked into the effects of two oxygenated additives, dimethyl-carbonate and pentanol, on methyl ester/diesel blend ignition patterns in a diesel engine. At a 10% volume ratio, dimethyl-carbonate and pentanol were blended separately with blends of neem-methyl ester and diesel. Blending dimethyl carbonate and pentanol reduced SFC by 0.4 and 0.5 g/kW, respectively, while increasing BTE by 0.3 and 0.6%. At all loads, adding 10% volume of pentanol and dimethyl carbonate reduced CO emissions by 4.9% and 7.4%, respectively. HC emissions were also lowered by 3.1 and 4.7%, respectively. The peak pressure of the base fuel is enhanced by 2.3 and

3.1 bar, respectively, by adding dimethyl carbonate and pentanol. Due to its increased qualities, HRR was also improved. The effect of ethanol and isopropanol additions (15%) in diesel was investigated by Alptekin E. [16]. According to the findings, adding ethanol and isopropanol increased the SFC by 6.2% and 5.7%, respectively. Also, the cylinder pressure was higher with additives. The addition of alcohol increased both HC and CO emissions by 6% and 4.6%, respectively. Alcohol was also found to increase NOx levels by 7.1 and 9.4%, respectively. De Poures M.V. et al. [17] conducted a similar study using 1-hexanol at 10%, 20%, and 30% with diesel. Injection timings were set at 21o, 23o, and 25o CA bTDC, with EGR of 10%, 20%, and 30%, respectively. The results show that adding 1-hexanol improves premixed combustion and increases the ignition delay. It was the longest with the 30% 1-hexanol injection at 25o CA bTDC with 30% EGR. This condition also helped to lower smoke density by 35.9%; however, it also increased NOx and HC levels. S. Sivalakshmi et al. [18] used diethyl ether (5%, 10%, and 15% by volume) with methyl ester to investigate the effects on diesel engine characteristics. Better peak pressure with the improved BTE and SFC was noted with the 5% additive. With a reduction in CO, increased NOx was reported with a 5% additive. HC emissions were found to be increased for all blends compared to neat methyl ester. This study suggested a 5% addition of diethyl ether to methyl ester. With EGR (0%, 10%, and 20%) and ethyl hexyl nitrate additive (1% by volume) in diesel-methyl ester blends. Venkateswarlu K. et al. [19] worked on NOx reduction. The EGR increased BTE with a decrease in SFC and EGT. CO and HC emissions were found to be increased with EGR, with a decrease in NOx. This study reported that 20% EGR and methyl ester blend B40 with ethyl hexyl nitrate were the preferred combinations for a greater reduction in NOx. Imdadul H.K. et al. [20] worked with the 2-ethylhexyl nitrate additive in diesel-palm methyl ester-pentanol blends. The methyl ester was used in 10% and 20% concentrations, with 5% and 10% pentanol. The additive was used at a proportion of 1000 ppm and 2000 ppm. In addition to evaluating the thermal stability of the blends, performance and emission analyses were also carried out. As ethyl hexyl nitrate is a cetane improver, the blends resulted in an increased cetane number by 6.06% and 14.67% with 1000 ppm and 2000 ppm in the blends, respectively. The alcohol-methyl ester blends were found to be more thermally stable than methyl ester. With ethyl hexyl nitrate, the BTE and SFC were found to be improved. Also, the ternary blends resulted in improved NOx emissions with an increase in CO and HC emissions. A potentially helpful approach for enhancing engine characteristics is the use of nanoparticles in fuel blends. Different kinds of nanoparticles, which are added to fuel mixes, include metal-based, metal oxide-based, and carbonaceous-based particles. Adding metal oxide-based nanoparticles to methyl ester improves the properties of the fuel. There is only one drawback to adding nanoparticles to methyl ester: viscosity rises. Methyl ester burns cleaner when metal oxide nanoparticles are added because the metal oxides enrich the nanoparticles with oxygen atoms [21].

The literature stated mostly focuses on examining different methyl esters, either with or without additives, to observe how they affect the performance and emission characteristics of diesel engines. But investigating the impact on the combustion parameters is also essential. Therefore, this study compares the effects of diesel-methyl ester-additive blends mainly on the combustion behaviour and performance characteristics of a diesel engine. The additives selected for this investigation were comparatively less researched; the first additive was propanol, and the second additive was the oil derived from the increasing agricultural waste of Curcuma longa leaves. The primary goal of this investigation was to explore the potential for propanol, Calophyllum inophyllum oil, and oil derived from Curcuma longa leaves. This study has particular relevance to the region of India, where potential exists for both Calophyllum inophyllum oil and Curcuma longa leaf oil. Thus, this study investigates the suitability of Calophyllum inophyllum methyl ester and Curcuma longa leaf oil as renewable and green fuels for diesel engines in order to increase the variety of alternative fuels.

MATERIALS AND METHODS

Infrared (IR) Spectroscopy of Curcuma Longa Leaf Oil

The technique of infrared spectroscopy (IR) detects energy in the electromagnetic radiation spectrum at wavelengths shorter than radio waves but longer than visible light. Mid-IR contributes significantly to the structure information of functional groups [22].

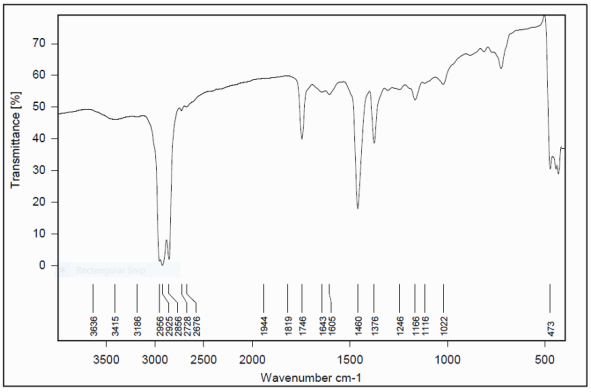


Figure 1. IR spectrum of Curcuma longa leaf oil

For the current study, the IR for Curcuma longa leaf oil was done. The graph of transmittance versus the wave number is presented in Fig. 1. It clearly shows the ester and carbonyl groups between wave numbers 1746 cm-1 and 1819 cm-1.

Fuel Sample Preparation and Characterization

The oil extracted from Calophyllum inophyllum was transesterified to yield methyl ester. To minimize the amount of free fatty acid in the raw oil, acid esterification was used in the first stage. The ideal reaction conditions were methanol (13 wt%), sulfuric acid (0.7 wt%), 90 minutes, 57 °C, and 650 rpm. This oil was used in a next stage base-catalyzed transesterification with ideal conditions of methanol (13 wt%), potassium hydroxide (0.7wt %), 90 min., 65 oC, and

500 rpm. After a 10-hour settling time, the impure methyl ester was collected and washed in hot distilled water before being dehydrated. The methyl ester was then mixed with diesel, propanol, and Curcuma longa leaf oil. The methyl ester percentage in the diesel was fixed with the Taguchi optimization and Taguchi-Grey relational optimization studies prior to this study. Also, as per ASTM D7467, methyl esters can be blended with diesel in amounts ranging from 6% to 20%, providing a good balance of cost, efficiency, and emissions [23]. The additive percentage was decided by studying the available literature. The concentration below 20% of the additives is recommended by most of the studies [24-25]. The blends were made by varying the volume proportions of propanol and Curcuma longa leaf oil (6%, 12%, and 18%) and methyl ester (20%) in diesel, designated as CI20P6, CI20P12, CI20P18, CI20CL6, CI20CL12, and CI20CL18.

Engine Tests

A single-cylinder, four-stroke diesel engine was used for the tests. The setup was equipped with an eddy current dynamometer. For the exhaust temperature measurement, K-type thermocouples were used. Table 1 shows engine specifications in detail, while Fig. 2 shows the schematic of the experimental set-up. Experiments were carried out at 1500 rpm, and the injection timing was 23 obTDC. The compression ratios were 14:1, 16:1, and 18:1, and the engine was loaded at intervals of 25%. In the initial testing, inophyllum methyl ester blends were used. CI05, CI10, CI15, CI20, CI25, and CI30 were the blends that were used. CI20 was shown to be the most feasible blend. Further research added 6%, 12%, and 18% (by volume) of propanol and Curcuma longa leaf oil to CI20, resulting in CI20P6, CI20P12, CI20P18, CI20CL6, CI-20CL12, and CI20CL18.

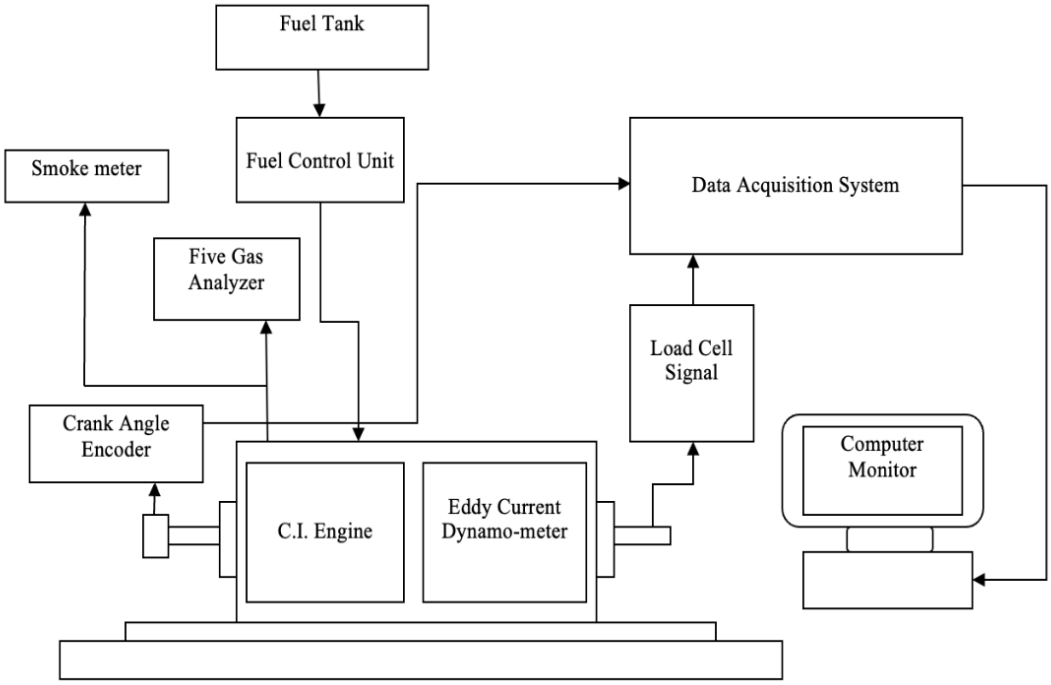


Figure 2. Schematic of experimental engine set up

Table 1. Engine specifications

Name of the Description	Details
Name	Kirloskar oil engine
Model	240PE, Single cylinder Four stroke Research Engine
Bore	87.5 mm
Stroke	110 mm
Swept Volume	661cm3
r/min	1500
Brake Horse Power	3.5 kW
Compression Ratio	12:1 – 18:1
Injection Variation	0-25 deg bTDC
Nozzle Operating Pressure	230 bar

Experiments were first performed with diesel to produce the baseline results. After recording these results, tests were carried out using CI20, CI20P6, CI20P12, CI20P18, CI20CL6, CI20CL12, and CI20CL18 blends. All the tests were conducted in steady-state settings to assure accuracy. Each test was done three times, and the average results at CR 18 and for the maximum loading condition are discussed for the combustion parameters, while the performance parameters are compared for the varying loading condition.

RESULTS AND DİSCUSSİON

Combustion Parameters

Cylinder Pressure: A clearer understanding of combustion activity is provided by the variation in gas pressure, which is dependent upon the fuel present during the uncontrolled combustion stage. [26-27]. The delayed combustion of diesel compared to methyl ester is due to the lower cetane number. The high cetane number of methyl ester accelerates the formation of ignition points [28]. From Fig. 3, it is noted that the cylinder pressure peaked between 6-9o aTDC for all test fuels. CI20 had the highest cylinder pressure of 62.50 bar at 7o aTDC, whereas diesel had 63.2 bar at 6o aTDC. In comparison to diesel, the high atomic weight species of CIME resulted in weak atomization, which reduced the mass of fuel combusted in the premixed combustion process and lower cylinder pressure. The pressure was reduced when propanol was added to CI20. At 8o aTDC, 6% propanol blending produced a peak pressure of 60.7 bar, whereas 12% blending produced a peak pressure of 57.7 bar. With the Curcuma longa leaf oil additive, it has been observed that premixed combustion takes most of the vaporized fuel.

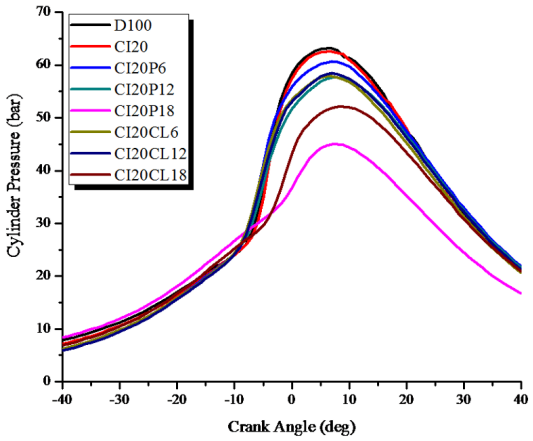


Figure 3. Cylinder pressure values related to crank angle

The variation in peak pressure was the same as diesel for all other blends, with an increasing additive percentage. 52.11 bar, 58.04 bar, and 57.92 bar were the pressures for CI20CL6, CI20CL12, and CI20CL18, respectively. Some studies reported higher in-cylinder pressures for methyl ester blends with high blending ratios owing to the higher cetane number of methyl ester, as the higher cetane number reduces ignition delay and gives an earlier start of combustion.

Heat Release Rate: The heat released in premixed combustion is determined by the heating value, ignition delay, and rate of air-fuel mixing [29]. The heat release analysis also reveals the design of the cylinder, fuel, injection system, and operating conditions, as well as their impact on combustion [30]. The experimentation was done with 23o bTDC injection timing. The heat release rate was negative past the commencement of premixed combustion in all of the samples, which followed the same pattern. This is the result of the absorption of latent heat from the surroundings. The spontaneous ignition of fuel increases the heat release rapidly. The change from a negative to a positive sign on the heat release rate occurs later in the case of diesel than in the case of methyl ester blend and additive blends. When compared to CI20 and other fuel samples, it has been observed from Fig. 4 that diesel combustion gives more heat release due to its higher heating value and longer ignition delay, which was found to be 56.66 J/deg. Due to its greater cetane number, CI20 began to burn slightly earlier. Because of the higher latent heat of vaporisation of propanol, the in-cylinder temperature was reduced during atomization, and combustion took place in a lower temperature environment. Therefore, the propanol-added blends had significantly lowered HRR.

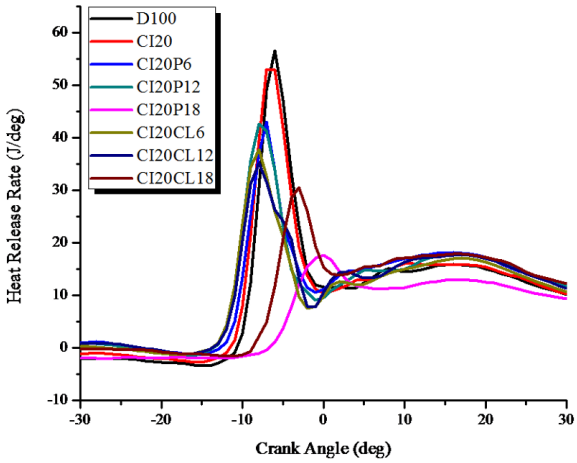


Figure 4. Heat release rate values related to crank angle

Owing to its good antiknock qualities, the methyl ester fuel starts combustion earlier than diesel. The addition of Curcuma longa leaf oil to diesel-methyl ester blends resulted in a comparatively lower heat release due to its lower heating value.

Cumulative Heat Release Rate and Mean Gas Temperature: It is the integration of the heat release rate that represents the total released combustion energy. Because of the higher heat of evaporation, the cumulative heat release rate of CI20 was more negative in stage one, as per Fig. 5. In the second and third stages, because of the higher burning rate aided by oxygen, CI20 surpasses D100. Even with the additives, the same trend has been observed. Since D100 has a higher heating value than all other blends, it has a higher total amount of released energy. The mean gas temperature shows the effectiveness of the combustion.

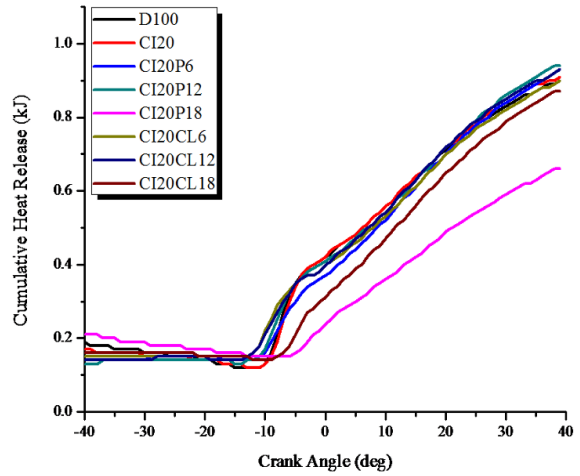


Figure 5. Ccumulative heat release values related to crank angle

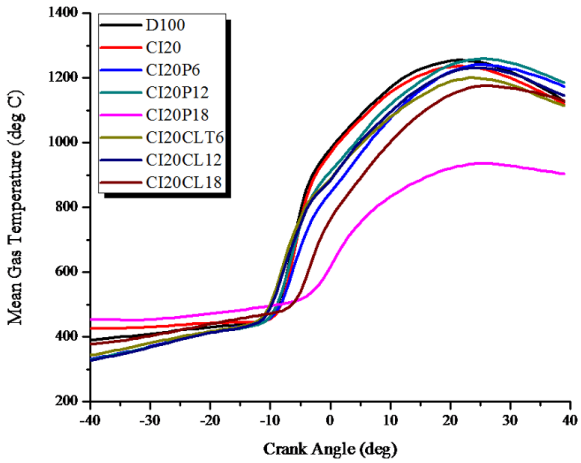


Figure 6. Mean gas temperature values related to crank angle

Cylinder temperatures against crank angle are depicted in Fig. 6. One can observe that for the CI20 and more so for the propanol and Curcuma longa leaf oil blends with respect to diesel, the temperatures were lower up to around their maximum values and appeared delayed, while later on during expansion, they seemed to recover. The maximum value of this temperature was achieved with methyl ester and additives at different crank angles. The highest temperature observed with D100 was 1254.5 oC at 22o aTDC, while with CI20 it was 1236 oC. The CI20P6 and CI20P12 blends reported 1241 oC and 1258 oC at 25o aTDC, respectively, but with 18% propanol, knocking was observed and the engine could not run at higher load conditions. The Curcuma longa leaf oil decreased this temperature, and the lowest temperature noted with an 18% addition was 1175 oC.

Mass Fraction Burned: How much energy is transformed throughout the combustion cycle at a certain crank angle is indicated by the mass fraction burnt. It is affected by the engine geometry, air-fuel ratio, ignition angle, residual mass, and so on. Also, the concentration of methyl ester affects the combustion rate and therefore the mean gas temperature, owing to poor atomization and poor spray characteristics. At a lower compression ratio, combustion began closer to the top dead centre. For higher compression ratios, it began a few degrees earlier. This could be due to an increased cylinder temperature.

From Fig. 7, it can be observed that the start of combustion for all blends was between 7o and 12o bTDC. For D100 and CI20, the maximum mass fraction burned was observed at 27o aTDC. With propanol addition, the maximum value of mass fraction burned was noted at 35o aTDC, particularly with the CI20P12 blend, while with CI20CL18 it was at 40 oaTDC. The combustion duration with additive blends was longer than diesel due to the higher volume of fuel supplied. Another factor is the decreased heating value and somewhat higher viscosity of the fuel, which could have resulted in poor mixture formation when compared to diesel.

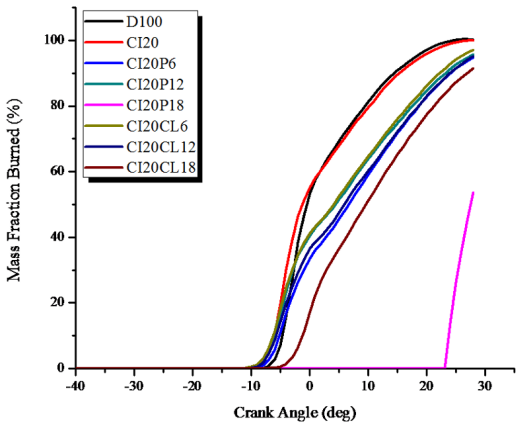


Figure 7. Mass fraction burned values related to crank angle

Performance Parameters

Brake Thermal Efficiency (BTE): BTE is affected by the viscosity, heating value, cetane number, and oxygen content of the fuel. It is the amount of energy recovered from burned fuel at the output [31]. Fig. 8 depicts the effect of various blends on BTE. Methyl ester in a higher percentage in the blends results in decreased efficiency as compared to diesel. It is due to poor volatility, poor atomization, and poor spray characteristics. The BTE of diesel was better compared with the CI20 blend.

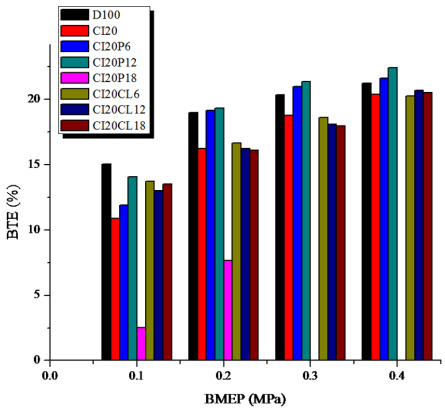


Figure 8. Brake thermal efficiency values related to BMEP

The modified blends with propanol resulted in lower BTE than base fuel at higher compression ratios and lower load conditions, but at higher loads, the CI20P6 and CI20P12 reported slightly higher BTE. At full load condition on the engine, D100 gave 21.5%, while CI20P12 reported 22.4% BTE. While analyzing engine characteristics with diesel-methyl ester-higher alcohol, Ramakrishnan et al. [32] reported a similar trend. Additionally, according to the research by S. Ravi et al. [33], the addition of propanol to waste plastic oil increased BTE because the fuel blend's density was reduced, which enhanced the fuel atomization properties. Among ternary blends of Curcuma longa leaf oil, the BTE values were very close to each other and lower than those of diesel. At full load, the blends CI20CL6, CI20CL12, and CI20CL18 had 20.24%, 20.7%, and 20.52% BTE, respectively.

Specific Fuel Consumption (SFC): The SFC results relative to engine loads are depicted in Fig. 9. At all CRs, SFC decreased with increasing load for all tested blends. One potential reason for this reduction is that brake power increases at a higher percentage with load than fuel consumption.

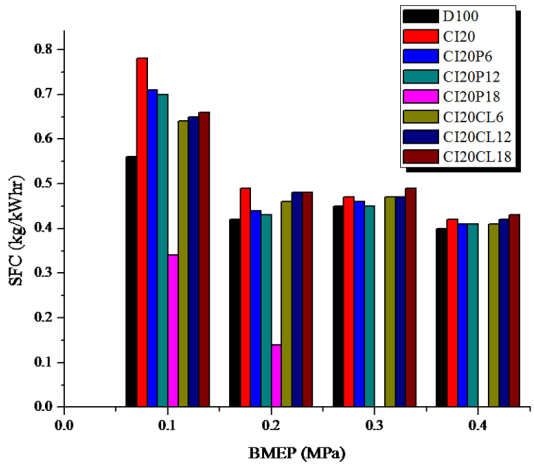


Figure 9. Sspecific fuel consumption values related to BMEP

As the percentage of additives in the blends was kept very close to each other, the variation in the specific fuel consumption has shown very little variation at all compression ratios. The CI20 blend has an average 17.27% higher SFC than diesel. The increase in SFC with CI20P6 and CI20P18 when compared to diesel was 12.8% and 13.9%, respectively. Since the blends have a lower heating value, their fuel consumption was higher than diesel. The Curcuma longa leaf oil also increased the SFC, and this increase in SFC of CI20CL6, CI20CL12, and CI20CL18 compared to diesel was 3% to 5% on average. The SFC may have increased compared to CI20 owing to a slight reduction in the calorific value of the modified blends, but the better atomization and improved density and viscosity helped to decrease it. Yoshimoto et al. [34] reported similar outcomes for butyl alcohol and biodiesel.

Artificial Neural Networks (ANN) Modeling for Performance Parameters

The data obtained from the investigation with the diesel-methyl ester-propanol and diesel-methyl ester-Curcuma longa leaf oil additives was used to create the neural network model for predicting only the performance parameters of the engine. Figs. 10 and 11 show the closeness between the input and target values using the regression coefficient metric of BTE and SFC.

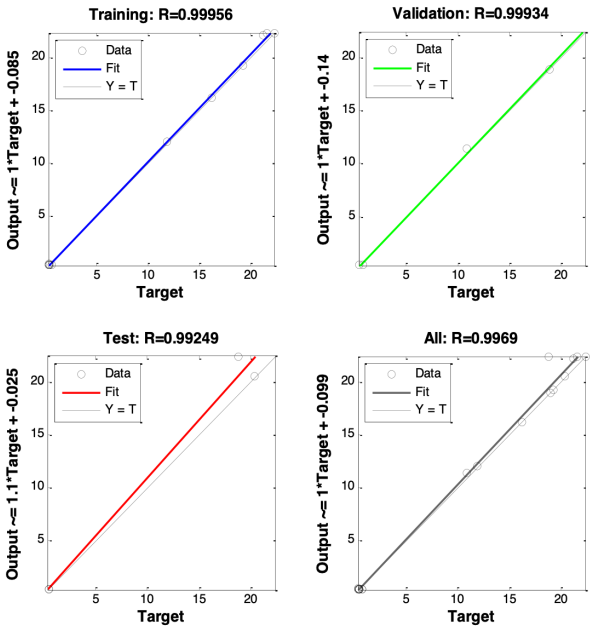


Figure 10. Closeness measure between the input and target values using the regression coefficient metric of BTE and SFC for the diesel-CIME-propanol blend

The ANN modeling was performed using the MATLAB environment. Out of many types, for creating the network, the feed-forward-back propagation method was selected. As per the literature survey, it produces better results. The training function used was TRAINGDM, i.e., gradient descent with momentum weight and biased function [35-36]. The performance function used was the mean squared error. The number of layers used was 2, with the number of neurons being 10. The transfer function used was a tangent sigmoidal function, which provides better results. While training the network, initially in the training parameters, the 1000 epochs were considered with a maximum failure of 6, and if the straight line is not fitted, the maximum failure is changed to value 1000. The learning rate and the momentum coefficient are taken as 0.01 and 0.9, respectively. It is understood from the figures that one can predict engine performance with correlation coefficients of 0.9969 for the propanol additive and 0.99042 for the Curcuma longa leaf oil additive, respectively. It is evident that the model was successful in predicting engine performance since there is a clear correlation between the measured values obtained from the experimental testing and the projected values made by the ANN model.

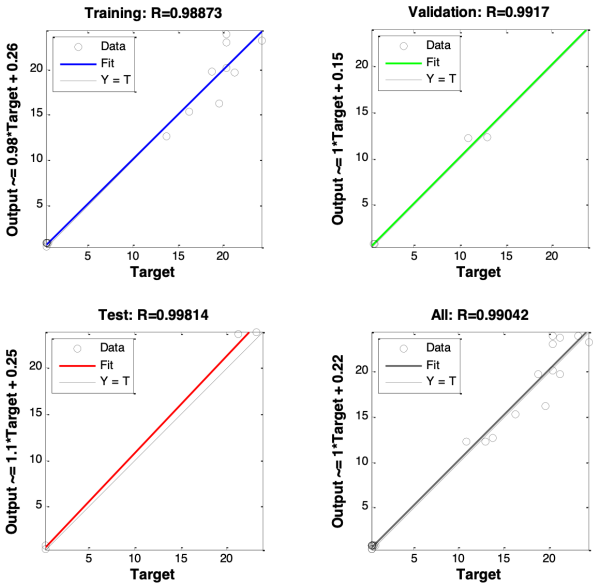


Figure 11. Closeness measure between the input and target values using the regression coefficient metric of BTE and SFC for the diesel-CIME-Curcuma longa leaf oil blend

The results of this investigation showed that while the lower calorific value of methyl ester and additives prevents improvement of the BSFC, it is possible to enhance the combustion characteristics. It is recommended to combine appropriate additives to improve the cetane number in order to optimize the overall engine performance. A few of the characteristics of Curcuma longa leaf oil, the second addition employed in this study, were examined. It is necessary to examine properties such as latent heat of vaporization, cetane number, cold filter plugging point, oxidation stability, and storage stability. The analysis of carbon deposits on pistons, valves, and injectors, as well as the examination of crankcase lubricating oil to determine any degradation or contamination brought on by blow-by leakage, can all be explored in future research.

CONCLUSION

The experimentation resulted in following conclusions.

1. Diesel had a maximum cylinder pressure of 63.2 bar, whereas diesel-methyl ester-propanol blends had a maximum cylinder pressure of 60.7 bar. With Curcuma longa leaf oil blended modified blends, there was a reduction in peak cylinder pressure. The cylinder pressure with diesel was the highest among all.

2. With diesel, the maximum heat release rate was 56.66 J/deg. All modified blends resulted in less heat release. The peak rates reported for CI20P6 and CI20P12 were 43.08 J/deg and 42.62 J/deg, respectively, while Curcuma longa leaf oil blends reported a peak heat release of 38 J/deg.

3. Modified blends with propanol provide higher combustion efficiency. The average BTE with the CI20P12 blend was the highest at CR 18, which was 1.6 % higher than diesel BTE. But with an increase in the percentage of Curcuma longa leaf oil in the diesel-methyl ester blend, BTE decreased.

4. With modified blends of propanol, SFC remained higher than diesel but decreased when compared to the CI20 blend. This increase was 12.8% and 13.9% with CI20P6 and CI20P18, respectively. With Curcuma longa leaf oil, there was a marginal increase in SFC. The SFC value of the modified fuel blends was lower than that of the CI20 fuel blend as well. Among the modified blends, the CI20CL6 blend reported the lowest SFC value.

5. The outcome demonstrated that the feed-forward-back propagation training method was appropriate for forecasting the brake thermal efficiency along with specific fuel consumption for various fuel blend ratios. Additionally, it was noted that for these parameters, R values were close to 1.

6. Analysis of the experimental data by the ANN showed that there was a good correlation between the measured data and the predicted data resulted from the ANN.

ACKNOWLEDGEMENT

The researchers are happy to express their gratitude to Indian Biodiesel Corporation, Baramati, and Apex Innovations Pvt. Ltd., Sangli, Maharashtra, India, for providing laboratory facilities to the experimental work.

DATA AVAILABILITY STATEMENT

The author confirm that the data that supports the findings of this study are available within the article. Raw data that support the finding of this study are available from the corresponding author, upon reasonable request.

CONFLICT OF INTEREST

The author declared no potential conflicts of interest with respect to the research, authorship, and/or publication of this article.

USE OF AI FOR WRITING ASSISTANCE

Not declared.

ETHICS

There are no ethical issues with the publication of this manuscript.

REFERENCES

[1] B.R. Kumar and S. Saravanan, "Effect of exhaust gas recirculation (EGR) on performance and emissions of a constant speed DI diesel engine fueled with pentanol/diesel blends," Fuel, Vol. 160, pp. 217–226, 2015.

[2] S.B. Chavan, M. Yadav, R. Singh, V. Singh, R.R. Kumbhar, and Y.C. Sharma, "Production of Biodiesel from Three Indigenous Feedstock: Optimization of Process Parameters and Assessment of Various

Fuel Properties," Environmental Progress and Sustainable Energy, 2017.

[3] M.H.M. Yasin, R. Mama, A.F Yusop, A. Aziz, and G.H. Najafi, "Comparative study on biodiesel-methanol-diesel low proportion blends operating with a diesel engine," Energy Procedia, Vol. 75, pp. 10-16, 2015.

[4] E. G., Giakoumis, C.D. Rakopoulos, A.M. Dimaratos, and D.C. Rakopoulos, "Exhaust emissions with ethanol or n-butanol diesel fuel blends during transient operation: A review," Renewable and Sustainable Energy Reviews, Vol. 17, pp.170-190, 2013.

[5] M. A. Asokan, S. S. Prabu, P. K. K. Bade, V. M. Nekkanti, and S. S. G. Gutta, "Performance, combustion and emission characteristics of juliflora biodiesel fuelled DI diesel engine," Energy, vol. 173, pp. 883–892, 2019.

[6] G. K. Mistri, S. K. Aggarwal, D. Longman, and A. K. Agarwal, "Performance and Emission Investigations of Jatropha and Karanja Biodiesels in a Single-Cylinder Compression-Ignition Engine Using Endoscopic Imaging," Journal of. Energy Resources Technology., Vol. 138(1), pp. 1–13, 2016.

[7] J. Xue, "Combustion characteristics, engine performances and emissions of waste edible oil biodiesel in diesel engine," Renewable and Sustainable Energy Reviews, Vol. 23, pp. 350-365, 2013.

[8] A. Atmanli, "Comparative analyses of diesel–waste oil biodiesel and propanol, n-butanol or 1-pentanol blends in a diesel engine," Fuel, Vol. 176, pp. 209–215, 2016.

[9] H. Aydin, and I. Cumali, "Effect of ethanol blending with biodiesel on engine performance and exhaust emissions in a CI engine," Applied Thermal Engineering, Vol. 30, pp. 1199–1204, 2010.

[10] B Prabakaran, and D. Viswanathan, "Experimental investigation of effects of addition of ethanol to bio-diesel on performance, combustion and emission characteristics in CI engine," Alexandrian Engineering Journal, Vol. 57, pp. 383-389, 2018.

[11] L. Zhu, C.S. Cheung, W.G. Zhang, and Z. Huang, "Influence of Methanol–Biodiesel Blends on the Particulate Emissions of a Direct Injection Diesel Engine," Aerosol Science and Technology, Vol. 44(5), pp. 362–369, 2010.

[12] N. Yilmaz, and T.M. Sanchez, "Analysis of operating a diesel engine on biodiesel-ethanol and biodiesel-methanol blends. Energy," Vol. 46(1), pp.126-129, 2012.

[13] N. Yilmaz, N. and A. Atmanli, "Experimental assessment of a diesel engine fueled with diesel-biodiesel-1-pentanol blends," Fuel, Vol. 191, pp. 190-197, 2017.

[14] L. Ye, Y. Shi, T. Liu, Q. Zheng, M. M. Ashfaq, C. Sun, A. Shi, and M. Ajmal, "Study on emission and particulate matter characteristics from diesel engine fueled with n pentanol/Fischer–Tropsch diesel," Energy Sources, Part A: Recovery, Utilization, and Environmental Effects. 2020.

[15] D. Rangabashiam, D.B. Munuswamy, D.S. Balasubramanian, and D. Christopher, "Performance, emission, and combustion analysis on diesel engine fueled with blends of neem biodiesel/diesel/ additives. Energy Sources," Part A: Recovery, Utilization, and Environmental Effects 2020.

[16] E. Alptekin, "Evaluation of ethanol and isopropanol as additives with diesel fuel in a CRDI diesel engine," Fuel. Vol. 205, pp. 161-172, 2017.

[17] M.V. De Poures, A.P. Sathiyagnam, D. Rana, R.B. Kumar, and S. Saravanan, "1-hexanol as a sustainable biofuel in DI engines and its effect on combustion and emissions under the influence of injection timimg and exhaust gas recirculation (EGR)," Applied Thermal Engineering. Vol. 113, pp. 1505-1513, 2017.

[18] S. Sivalakshmi, and T. Balusamy, "Effect of biodiesel and its blends with diethyl ether on the combustion, performance and emissions from a diesel engine," Fuel, Vol. 106, pp.106-110, 2013.

[19] K. Venkateswarlu, B.S.R. Murthy, V.V. Subbarao, and K. Vijaykumar, "Effect of gas recirculation and ethyl hexyl nitrate additive on biodiesel fuelled diesel engine for the reduction of NOx emissions," Frontier of Energy, Vol. 6(3), pp. 304-310,2012.

[20] H.K. Imdadul, H.H. Masjuki, M.A. Kalam, N.W.M. Zulkifli, A. Alabdulkarem, M.M. Rashed, and A.M. Ashraful, "Influences of ignition improver additive on ternary (diesel-biodiesel-higher alcohol) blend thermal stability and diesel engine performance," Energy Conversion and Management. Vol. 123, pp. 252-264, 2016.

[21] U. Agbulut M. Karagoz, S. Sarıdemir, and A. Ozturk, "Impact of various metal-oxide based nanoparticles and biodiesel blends on the combustion, performance, emission, vibration and noise characteristics of a CI engine," Fuel, Vol. 270, pp.117521, 2020.

[22] Wei-Bo Zhang, "Review on analysis of biodiesel with infrared spectroscopy," Renewable and Sustainable Energy Reviews, Vol. 16(8), pp. 6048-6058, 2012.

[23] M. Habibullah, "Biodiesel production and performance evaluation of coconut, palm and their combined blend with diesel in a single-cylinder diesel engine," Energy Conversion Management, Vol. 87, pp. 250-257, 2014.

[24] B. Rajesh Kumar, and B. Sarvanan, "Use of higher alcohol biofuels in diesel engines: a review," Renewable and Sustainable Energy Reviews. Vol. 60, pp. 84-115, 2016.

[25] A.G. Nagpure, W.S. Rathod, and S.B. Chavan, " Optimization of performance and emission characteristics of diesel engine fuelled with diesel-Alexandrian Laurel biodiesel blends using Taguchi approach," in AIP Conf. Proc. 2393, pp. 020113-1–020113-6, 2022.

[26] L. Wei, C.S. Cheung, and Z. Ning, "Effects of biodiesel-ethanol and biodiesel-butanol blends on the

combustion, performance and emissions of a diesel engine," Energy, Vol. 155, pp. 957-970, 2018.

[27] D. Barik, A.K. Satapathy, and S. Murugan, "Combustion analysis of the diesel–biogas dual fuel direct injection diesel engine – the gas diesel engine," International Journal of Ambient Energy. 38 (3), 259–266, 2017.

[28] A.G. Nagpure, S.B. Chavan, and W.S. Rathod, "Effects of diesel–Calophyllum inophyllum biodiesel–propyl alcohol blends on performance, emissions, and combustion of diesel engine," Environmental Progress and Sustainable Energy, Vol. 41(5), 2022.

[29] U. Rajak, P. Nashine, and T. Verma, "Assessment of diesel engine performance using spirulina microalgae biodiesel," Energy, Vol. 166, pp. 1025-1036, 2019.

[30] B. Ashok, K. Nanthagopal, A.K. Jeevanantham, P. Bhowmick, D. Malhotra, and P. Agarwal, "An assessment of calophyllum inophyllum biodiesel fuelled diesel engine characteristics using novel antioxidant additives," Energy Conversion Management, Vol. 148, pp. 935-943, 2017.

[31] K. Nanthagopal, B. Ashok, B. Sarvanan, D. Patel, B. Sudarshan, and R. Ramasamy, " An assessment on the effects of 1-pentanol and 1-butanol as additives with Calophyllum Inophyllum biodiesel," Energy Conversion and Management, Vol. 158, pp. 70-80, 2018.

[32] P. Ramakrishnan, R. Kasimani, M. S. Peer, and R. Sakthivel, "Assessment of n-pentanol/Calophyllum inophyllum/diesel blends on the performance, emission, and combustion characteristics of a constant-speed variable compression ratio direct injection diesel engine", Environmental Science and Pollution Research, Vol. 25, pp. 13731-13744, 2018.

[33] S. Ravi, and A. Karthikeyan, "Effect of propanol addition on the performance and emissions characteristics of a direct injection diesel engine fuelled with waste plastic oil", International Journal of Ambient Energy, Vol. 43, pp. 803–808, 2019.

[34] K. Yoshimoto, and O. Shanbu, "Influence of 1-butanol addition on diesel combustion with palm oil methyl ester/gas oil blends", Energy, Vol. 61, pp. 44-51, 2013.

[35] Shivakumar , P. Srinivasa Pai , B.R. Shrinivasa Rao, "Artificial Neural Network based prediction of performance and emission characteristics of a variable compression ratio CI engine using WCO as a biodiesel at different injection timings," Applied Energy, Vol. 88, pp. 2344-2354, 2011.

[36] A. Sharma, P. K. Sahoo, R. K. Tripathi and L. C. Meher, "ANN based prediction of performance and emission characteristics of CI engine using Polanga as a biodiesel," International Journal of Ambient Energy, Vol. 37 (6), pp. 559-570, 2015.

NOMENCLATURE

ANN	Artificial Neural Network	CO	Carbon Monoxıde
ASTM	American Society for Testing and Materials	CO_2	Carbon Dioxide
aTDC	After Top Dead Centre	CIME	Calophyllum Inophyllum Methyl Ester
bTDC	Before Top Dead Centre	CR	Compression Ratio
BTE	Brake Thermal Efficiency	D100	Diesel 100%
CA	Crank Angle	EGR	Exhaust Gas Recirculation
CI05	Diesel 95% + Calophyllum Inophyllum Methyl Ester 5%	EGT	Exhaust Gas Temperature
CI10	Diesel 90% + Calophyllum Inophyllum Methyl Ester 10%	HC	Hydrocarbons
CI15	Diesel 85% + Calophyllum Inophyllum Methyl Ester 15%	HRR	Heat Release Rate
CI20	Diesel 80% + Calophyllum Inophyllum Methyl Ester 20%	IR	Infrared Spectroscopy
CI25	Diesel 75% + Calophyllum Inophyllum Methyl Ester 25%	MATLAB	Matrix Laboratory
CI30	Diesel 70% + Calophyllum Inophyllum Methyl Ester 30%	NOx	Nitrogen Oxides
CI20P6	Diesel 74% + Calophyllum Inophyllum Methyl Ester 20% + Propanol 6%	NO	Nitric Oxide
CI20P12	Diesel 68% + Calophyllum Inophyllum Methyl Ester 20% + Propanol 12%	ppm	Parts Per Million
CI20P18	Diesel 62% + Calophyllum Inophyllum Methyl Ester 20% + Propanol 18%	PM	Partıculate Matter
CI20CL6	Diesel 74% + Calophyllum Inophyllum Methyl Ester 20% + Curcuma longa leaf oil 6%	rpm	Revolution per minute
CI20CL12	Diesel 68% + Calophyllum Inophyllum Methyl Ester 20% + Curcuma longa leaf oil 12%	SFC	Specific Fuel Consumption
CI20CL18	Diesel 62% + Calophyllum Inophyllum Methyl Ester 20% + Curcuma longa leaf oil 18%	SO2	Sulfur Dioxide

Environ Res Tec, Vol. 8, Issue. 2, pp. 382-398, June 2025

Environmental Research and Technology
https://dergipark.org.tr/en/pub/ert
DOI: https://10.35208/ert.1501290

Environmental Research & Technology

Research Article

Central composite experimental design for Indigo Carmine dye removal from solutions by applying electrocoagulation and electrooxidation processes

Mustafa KORKMAZ*

Balıkesir University, Engineering Faculty, Environmental Engineering Department, 10145 Çağış Campus, Balıkesir City, Türkiye

ARTICLE INFO

Article history
Received: 14 June 2024
Revised: 17 Sep 2024
Accepted: 19 Sep 2024

Key words:
Batch and continuous reactor, central composite design, electrocoagulation, electrooxidation, Indigo carmine dye removal

ABSTRACT

Indigo Carmine dye is a textile and food coloring dye reporting as toxic and harmfull for living creatures in the case of entrance to food chain above toxic levels. Sometimes textile and food industries produce toxic and harmfull dye-containing wastewaters that should be treated for safely discharge. The electrocoagulation (EC) and the electrooxidation (EO) methods for removal of dyes from wastewaters are being investigated for the last two decades. In this study, the Indigo Carmine dye removal was investigated by applying the EC and the EO methods. For this purpose, aluminum electrodes for EC and graphite plates for EO were used. The central composite experimental design was applied as the optimization method for the EC and the EO processes. The optimization parameters were selected as time (10-30 minutes), current density (0.4-2 Ampere/500 mL) and concentration (50-250 mg/L), natural pH (5.78-6.90) and room temperature (20-26.2 °C). The EO process was determined to be effective than the EC process. Statistically important parameters were concentration and time-current density interaction for the EC, but all the parameters were statistically unimportant for the EO. Dye removal percentages by the EC were calculated between 82.75% and 98.38%, and dye removal percentages by the EO were calculated between 46.88% and 100% for the experimental matrix. Electrical consumptions were a bit high for the EO than the EC. A column ion exchange process (Selion SBA 2000 resin) was applied to the dye residue after the EO treatment. From the oxidation reduction measurements, the treated solutions were determined as dischargeable.

Cite this article as: Korkmaz M. Central composite experimental design for Indigo Carmine dye removal from solutions by applying electrocoagulation and electrooxidation processes. Environ Res Tec 2025;8(2) 382-398.

INTRODUCTION

The dye pollution risk of the surface waters is a big concern throughout the world due to the textile and the food coloring industries. Dye usage in the food and the textile products causes to discharge dye-containing process waters. Dyes are visible even at 1 mg/L concentration in water body. The wastewaters of the textile and the food coloring industries contain color from the used dye [1]. Also, textile dye-containing wastewaters include heavy metals, high COD and BOI, suspended solid materials, and high salt concentration [1]. The textile dye types are reactive dyes, direct dyes, acid dyes, all-purpose dyes, nat-

***Corresponding author.**
*E-mail address: korkmazm@balikesir.edu.tr

This is an open access article under the CC BY-NC license (http://creativecommons.org/licenses/by-nc/4.0/).

ural dyes, VAT dyes, disperse dyes and azoic dyes [2]. The Indigo Carmine dye is an acid dye. This dye is reported as toxic for humans [3] and it is used as food and textile coloring agent. The Indigo Carmine dye may cause to skin and eye irritations, cancer, permanent damage to cornea and reproductive system [3]. The dyes that are mixed to the surface waters reduce the photosynthetic activity in the aqueous mediums by impeding the sun light penetration to the water [1,4,5]. Some of dyes and pigments cause to death of the soil microorganisms. Hence, toxic dye containing effluents are not appropriate for irrigation of soil [1]. There are several technologies for removal of dyes from wastewaters. Adsorption, coagulation, electrocoagulation, electrooxidation and biosorption methods are being applied for dye removal at laboratory scale nowadays [1, 6, 7, 8, 9]. The adsorption of dyes has been widely investigated by various materials [1, 4]. But, the more clean technologies are needed. The EC technology has advantages due to its low sludge production, low energy consuming, high removal performance for dyes and easy operation [10]. The EO technology has the same advantages for dye removal and also it does not produce sludge [11].

An EC process works by the electrical current that dissolves the metal electrode (anode) for coagulation and adsorption of dye molecules. In the EC process, the harmless electrodes like as iron and aluminum for removal of dyes can be used. In the EC treatment of anions, cations or organics, the sacrificed electrode (anode) cations play a neutralization role for the charged pollutants and the cations coagulates the pollutants. At the end, the filtration or sedimentation of sludge can be applied. Also, in the EC of organic matters like as dyes, the process oxidizes the organic matter to CO_2 and H2O, or the intermediate products at the anode side a bit degree and most of the removal occurs by coagulation and flotation [12]. The reactions in the EC process are as follows [13]: Firstly, the anode electrodes like as iron or aluminum are dissolved by the electrical current flow from a cathode to an anode. The electrons of the anode plate are transferred from the anode to the cathode. The organic matters are also destroyed at the anode surface by the direct oxidation or indirect oxidation in the reactor body. The reactions for aluminum electrode used in EC can be given as follows [14]:

In the EO, the electrons from the anode pass to the cathode and the electrical current moves to the anode from the cathode [13]. But, electrical dissolution of the anode plates like as graphite or boron doped diamonds do not realize strongly. There are four oxidation mechanisms of the organics in the EO like as anodic oxidation, active hydroxyl oxidation, chlorine based oxidant oxidation and hydrogen peroxide [15]. In this study, magnesium chloride hegza hydrate was used as electrolyte salt for adjustment of the current density or voltage and forms the source of the oxidizing chloride radicals. Its chloride content was the reason for selection of this salt. The oxidizing molecules like as chlorine (Cl2), hypochlorous acid (HOCl), hypochlorite (OCl-) are generated at reactor of the EC or EO in the presence of chloride anions and hydrogen peroxide is produced at cathode side. The EO and the EC chloride based oxidants are produced by the following reactions [15]:

Hypochlorous acid dissociates to produce the hypochlorite ions, which are generally present at higher pH (pH>6) [15]. These extremely vigorous oxidizing molecules (HOCl, OCl- and Cl2) can deteriorate the surface of the organic substance and can

$$\text{Anode: } Al \rightarrow Al^{3+} + 3e^- \quad \text{(Eq.1)}$$

$$\text{Cathode: } 3H_2O + 3e^- \rightarrow 3/2H_2 + 3OH^- \quad \text{(Eq.2)}$$

General reactions in the reactor body:

$$3Al^{+3} + 9H_2O + 3OH^- \rightarrow 3Al(OH)_4^- + 9/2H_2 \quad \text{(Eq.3)}$$

$$Al(OH)_3 + OH = Al(OH)_4^- \quad \text{(Eq.4)}$$

$$\text{Anode: } 2Cl^- \rightarrow Cl_2 + 2e^- \quad \text{(Eq.5)}$$

$$Cl_2 + H_2O \rightarrow H^+ + Cl^- + HOCl \quad \text{(Eq.6)}$$

$$HOCl \rightarrow OCl^- + H^+ \quad \text{(Eq.7)}$$

$$OCl^- + \text{Dye} \rightarrow H_2O + CO_2 + Cl^- \quad \text{(Eq.8)}$$

shred. An EO process works by passing electrons from cathode through anode The conversion of the organic molecules to CO_2, H2O or intermediate products realizes at the surface of an anode by electrons and by the indirect oxidizing molecules (HOCl, OCl, and Cl2) [15]. Also, the direct oxidation occurs by the produced active hydroxyl radicals at the anode. The EO technology is an ecofriendly method for treating dye wastewater, because of the following advantages [16]: (i) The absence of extra redox or oxidizing chemicals, (ii) close control of the desired reaction conditions like as reaction rate and oxidant source addition, and (iii) the increased possibility of on-site treatment. In this study, the EO technology was applied using an insoluble graphite plate and EC was applied using an aluminum electrode. The central composite experimental design was applied to data of the EC and the EO for comparison of removal percentage of the dye and the electrical consumption values.

In a study, the electrochemical treatment of Basic Blue 3 dye from the textile wastewaters was reported. It was achieved more than 97% color removal with pH (8) after 10 minutes. 92-95% and 72-60% dye removal efficiencies were obtained in 6 minutes for 50-400 mg/L and 500-600 mg/L initial dye concentrations, respectively [17].

It was reported that dye with larger molecular weights were more affected by the increase in pH for removal. In dye removal with pH increase, Reactive Black 39 (1021.16 g/mol) is affected by the pH increase by decreasing removal from 100% to 74.83. Remazol Red 3B (674.10 g/mol) is affected with pH increase with a removal decrease from 96.54% to 83.01 [18].

It was observed that the color removal and COD removal efficiencies increased with the increase of mixing speed. A significant value of 99.5% was reached for the removal efficiency of Acid Red 20 from aqueous solution. The results obtained showed that the EO method is an usable method for removing light azo dyes from water [19].

It was reported that within 20 min of electrochemical treatment, about 99.94% of the color was removed from the KCl and 39.90% from the Na2SO4 solutions. This degradation efficiency in the KCl solutions can be attributed to indirect electrochemical oxidation, where, in the presence of chlorides, the electrolyte generates strongly oxidizing species, which enhance the efficiency of the treatment at the Pt electrode [20].

In a study where the EC process equipped with iron and aluminum electrodes was used, the effects of initial pH, current density, conductivity and electrolysis time on the removal of Reactive Yellow 160 (RY160) dye were examined. High color removal efficiency was achieved in EC, regardless of the electrode material [21].

The central composite design tool of the response surface method in Minitab 16.0 software was used in data analysis. Firstly, Box and Wilson defined the response surface optimization (RSM) method [22]. They determined the experimental matrix giving the maximum output with the least number of runs. The model obtained from the central composite design method is formed with the help of regression analysis [22]. The importance of the main and their interactions in the model is determined by the regression coefficients and the confidence constants (p) [22]. The central composite design method is used in many areas of science and industry. In the central composite design method, the effects of two or more factors (up to ten factors) on output can be determined. The results obtained can be analyzed with three-dimensional and the counter graphics. The model obtained by the central composite design method is used to calculation of output of selected parameter levels for estimation of experimental data. The effectiveness of the model can be understood by the coefficient of determination values like as R-Sq, R-Sq(adj) and R-Sq(pred) [22].

In this study, the EO and the EC methods were compared in a batch reactor applying central composite design for Indigo Carmine dye removal. The reasons of selection of the EC and the EO processes were that these technologies are clean, rapid, effective and easily handable [10,11]. The Indigo Carmine dye was selected because this dye is toxic and widely used in the food and textile industries. Although Indigo Carmine dye is considered toxic and has many adverse effects, it is found in many foods, and the maximum permitted level is 500 mg/kg in foods [23]. The EC and EO methods removed the dye at high degree and these technologies were clean and very practical. The dye removal approaches by these technologies have been studied in litherature too, but every dye has own moleculer size, structure, structural bond and end by-products after treatment, therefore their behaviour under treatment give interesting and promising results, if the dye can be removed completely for high concentrations. Removal of dyes by EC occured by coagulation way as a result of coagulating aluminum cation and aluminum hydroxide and produced oxidizing chemicals like as chlorine gas, hypochlorous acid, reactive hydroxly ions and hydrogen peroxide [10,11]. The EO enables to remove dyes from waters without any sludge after treatment. On the other hand, EC sludge amount after treatment of dyes is very low. Similar to EC, EO runs by electron, chlorine gas, hypochlorous acid, reactive hydroxyl oxidations and hydrogen peroxide [20]. In addition to these, optimization of these technologies gives opportinuity for operation of real reactors by scale-up of miniaturized reactor to big reactor. The operation pHs, temperatures, the state of oxidizing species for dye removal and operability of these reactors is very important. In these respects, this study is important and complexity of the solution chemistries during removal is one of the important points that should be understand. Sometimes, coagulation, adsorption and especially ion exchange, biosorption materials can become ineffective for anionic dye removal from waters. For this purpose, EC and EO technologies show good performance for anionic dyes like Indigo Carmine [10,11].

In the literature, Huangfu et al. (2021) reported that the Indigo Carmine dye removal by graphite-graphite (C-C, anode-cathode), aluminum-graphite (Al-C, anode-cathode) and steinless steel-graphite (SS-C, anode-cathode) electrodes by the classical single parameter experiments [24]. In the present study, it was investigated the aluminum and graphite electrodes performances for Indigo Carmine dye removal in detail by investigating time, concentration and current density for central composite experimental design for upgrading the miniaturized reactor

to real big reactor. The energy consumptions were optimized for both the electrodes. Also, discharge potentiels of the treated solutions were evaluated by oxidation reduction potentiel analysises. Continuous reactor application for EO process were determined as the most effective than EC. Advanced treatment of dye residue after EO process treatment was done by anion exchange resin (Selion SBA 2000). Dye removal mechanisms, removal costs and literature comparision were described.

MATERIAL AND METHODS

Properties of Indigo Carmine Dye

The Indigo Carmine dye is an indigo-5,5'-disulfonic acid disodium salt and has formula of C16H8N2Na2O8S2. The dye solution has blue color at pHs up to 13 and above pHs 13, the dye solution has yellow color. It is a food and textile coloring agent. The stock dye solutions were prepared at per four days. During these four days, the color absorbance of the Indigo Carmine dye solution did not change.

EC and EO Experiments for Central Composite Experimental Design in a Batch Reactor

Two aluminum electrodes (anode and cathode) for EC and two graphite plates (anode and cathode) for EO were used for the Indigo Carmine dye removal from waters. The effective dimensions of one graphite plate had 50×70×10 mm (Width×Height×Thickness) and effective dimensions of one aluminum electrode had 50×70×2 mm (Width×Height×Thickness). The electrode total areas were 89 cm2 for EO and 73.8 cm2 for EC. The distance between the aluminum electrodes were 5.2 cm and the distance between the graphite plates were 4 cm in the batch reactors. One plate for anode and one plate for cathode were used for both of the EC and the EO processes. The low and high levels of the parameters in the EC and the EO for central composite design are given in Table 1. The stock dye solution was prepared as 2,000 mg/L concentration and the working solutions were prepared freshly from the stock solution. The central composite experimental design was studied for Indigo Carmine dye removal as a function of time (10-30 min), current density (0.4-2 A/500 mL) and concentration (50-250 mg/L) at natural pHs (5.78-6.9) and room temperature (20-26.2 °C). A batch reactor with 750 mL volume was filled with 500 mL dye solution and stirred at 1,000 rpm speed.

An amount of 3 or 6 g MgCl2.6H2O (Merck product) was added to the dye solution as supporting electrolyte. The 3 g salt was enough for all the experiments, but for only 2 ampere study, 3 gram salt did not provide 2 amper value, therefore 6 gram salt was added. Its chloride content was the reason for selection of this salt. The DC-power supply was switched on while the reactor content was being stirred. At the end of the reaction, 4 mL treated wastewater was pipetted and filtered with Whatman filter paper for the EC. The treated wastewater was taken directly for the EO. The spectrophotometers are very useable devices for color measurements and Indigo Carmine dye measurements were done after filtration of treated solution of EC by Whatman fitler paper which does not adsorb the Indigo Carmine dye. Measurement in spectrofotometer was done at 610 nm wavelengt by using one light road applying quartz cell. Measurements were done after dilution of supernatant solution. The calibraion curve was used for calculation of concentration and it was plotted between 0-10 mg/L concentration. After filtration of Whatman filter paper, there is any flock for EC and for bare dye solution, the filter paper was seen that it did not adsorb the dye.

$$\eta = \frac{(C_0 - C)\times 100}{C_0} \qquad \text{(Eq.9)}$$

The experiments were carried out according to the optimization experimental matrix established by Minitab 16.0 software. The reaction products and experimental setups are given in Figure 1, Figure 2 (EC) and Figure 3 (EO), respectively. The dye chemical structure is given in Figure 4. The initial solution temperatures were between 20 and 26.2 °C throughout the experiments at room conditions. The pure water was used in preparation of the working solutions. A vacuum filtration device was used for filtration of the treated dye solutions after the EC by using a special filtration tube. The Indigo Carmine dye has dense blue color. The dye removal percentage was calculated using the following equation.

Here, is the removal percentage (%). C0 and C are the initial and the treated water dye concentrations (mg/L).

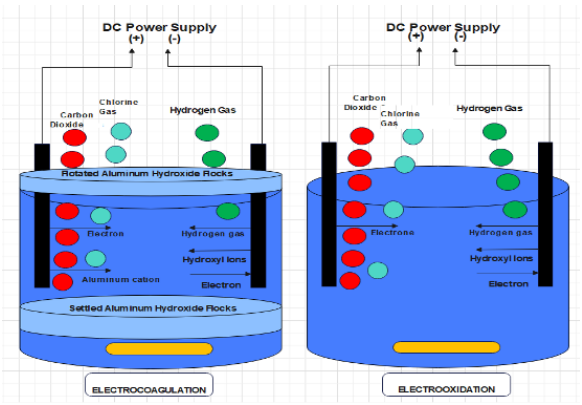


Figure 1. Reaction products in EC and EO processes

Ion Exchange Treatment of Persistent Dye Residue after EO by Selion SBA 2000 Resin

The dye residue after the EO treatment of the Indigo Carmine dye had yellow color. The dye residue after the EO process was treated with Selion SBA 2000 basic resin in a column reactor filled with 25 g resin. The resin was dried at ambient room temperature. The treatment parameters for the batch EO process was initial 100 mg/L Indigo Carmine dye concentration, current density 1.5 A, solution volume 500 mL, 2,500 rpm stirring speed, room temperature, and natural pH. Ion exchange treatment for the dye residue was applied after the batch EO process. Ion exchange column had 1.78 cm inner diameter and 25 cm height. The ion exchange experiments were carried out for only 100% removal (i.e. treated sample was taken for initial durations

Table 1. The low and high values of parameters for EC and EO processes

Parameter and levels	-2	-1	0	1	2
Time (min)	10	15	20	25	30
Current Density (A)	0.4	0.8	1.2	1.6	2
Concentration (mg/L)	50	100	150	200	250

of outlet solutions of column reactor) and these are not kinetic studies. The dye residue was the inert side of the dye after the EO treatment.

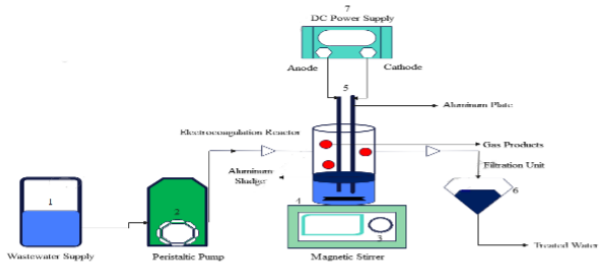


Figure 2. Experimental setup for EC process (The general experiments conducted in batch mode and continuous mode was applied only for comparision with EO, Data are not given for continuous reactor)

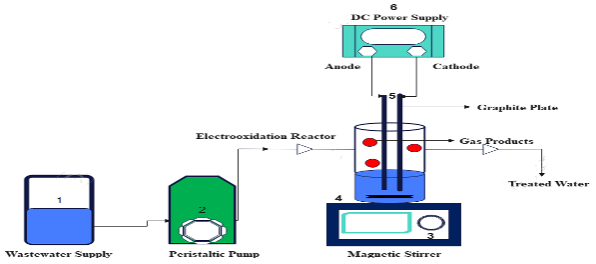


Figure 3. Experimental setup for EO process (The general experiments conducted in batch mode and continuous mode was applied only for comparision with EC)

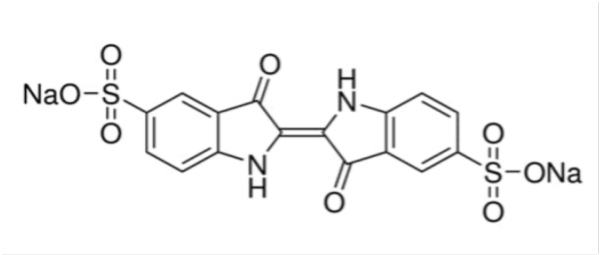


Figure 4. Open formula of Indigo Carmine dye

The central composite design is a tool in the response surface optimization method of Minitab 16.0 software. This optimization method is widely used for industry, science and other areas. It analyzes an experimental matrix determined by the software. The central composite experimental design is formed from an experimental matrix established by conducting the preliminary experiments for maximum concentration removal from wastewater. The central composite design may consist of a factorial or fractional factorial designs. The factorial design can be upgraded to the central composite design by adding the center and a group of axial points that allow estimation of optimum conditions [25]. Generally, the central composite design statistical analysis is formed from the following stages.

i-) Determination of the experimental matrix conditions from the preliminary studies conducting a series of the classical single parameter experiments for completely pollutant removal. Anova analysis of the parameters for whether one parameter is at statistically significant level or not, for instance 95% (i.e. $p<0.05$),

ii-) Development of the regression model such as linear, linear-square, linear-interaction or full quadratic,

iii-) Calculation of the model response by the regression model for true operation of the reactor and estimation of the experimental data by regression model. The regression model is useful to relate the factor and the response in a mathematical model by following equation.

$$\text{Dye removal (\%)} = b + b1X1 + b2X2 + b3X3 + b4X1X1 + b5X2X2 + b6X3X3 + b7X1X2 + b8X1X3 + b9X2X3 + \acute{\varepsilon} \quad \text{(Eq.10)}$$

Here, b, b1, b2, b3, b4, b5, b6, b7, b8, b9 are model constants and X1, X2, X3, X1X1, X2X2, X3X3, X1X2, X1X3, X2X3 are the coded factors and their interactions representing to time, current density, concentration and interactions of these parameters. $\acute{\varepsilon}$ is error. In this study, the uncoded values of the parameters were used for data analysis, that is, real values of the factors were used in the statistical analysis. Full quadratic model eqauation was used for model development.

RESULTS AND DISCUSSION

Central Composite Design of Removal of the Dye by EC and EO Processes

The parameters (current density, time and concentration) were studied for removal of the Indigo Carmine dye from water in a batch reactor. For this purpose, the EC and the EO processes were applied. The low and high level of parameters for the EC and the EO were time (10-30 min), current density (0.4-2 A), and concentration (50-250 mg/L). The experimental matrix for the EC and the EO is given in Table 2. The Anova analysis showing the statistically importance of the parameters is given in Table 3. The EC maximum dye removal percentage was obtained as 98.38% (10 minutes, 1.2 A, 150 mg/L) and the EO

maximum dye removal percentage was obtained as about 100% (20 minutes, 1.2 A, 50 mg/L). The confidence level of Anova analysis was selected as 95% ($p<0.05$) of which above the confidence constants show the statistically unimportance of the parameter. The statistically important parameters or interactions were model constant and time-current density interaction for the EC; however, all the parameters for the EO were determined as unimportant. In the optimization, currect density, concentration and time was studied. Natural pH, room temperature, current density, time and concentration are real operation parameters. Therefore, there is no necessitate for extending parameter number like as temperature and pH. The developed regression model could be estimate well the data. The estimation of the model to data is very meaningfull from statistically importance of parameter value change (p). R-Sq(adj) values show the enough number of parameters for modelling. R-Sq(pred) values show the low estimation of model the removal data. But, it was thought that the real estimated values of the removal percentages were enough for operation of reactors. The avarage error values between real and estimated data were around 6%. The full quadratic model was used in development of regression models. The regression models for the EC and the EO are obtained as follows:

EC Dye removal (%) = 76.8437 + 0.2136*T + 13.2956*CD + 0.0976*C + 0.0177*T*T + 0.3223*CD*CD – 0.0006*C*C – 1.2461*T*CD + 0.0027*T*C + 0.0531*CD*C (Eq.11)

EO Dye removal (%) = 66.5666 + 2.2818*T + 45.2960*CD – 0.4266*C – 0.0622*T*T – 30.1970*C*CD – 0.0003*C*C + 0.4756*T*CD + 0.0022*T*C + 0.2743*CD*C (Eq.12)

Here, T is time (min), CD is current density (A), C is concentration (mg/L).

The prediction of data by regression models is given in Table 2. The surface plots of the EC and the EO are given in Figure 5. The end point pHs and voltages are given in Table 2.

Time-Current Density Effect for the EC Process

Time effect on the Indigo Carmine dye removal from solution by the EC process was studied at time interval of 10 and 30 minutes. Results are given in Figure 5. From Figure 5, dye removal increased at high time-low current density interaction. Dye removal leaved as low at high current density studies. The increasing time and current density produced high amount of aluminum hydroxide and aluminum cation in the reactor and resulted in a high coagulant amount which was expected the more Indigo Carmine dye removal. But, high aluminum hydroxide and aluminum cations decreased the removal. It was thought that there was equilibrium between the dye and aluminum species interaction for high current density. For instance, boron adsorption on alunite [26], Dowex 2×8 ion exchange resin [27] and zinc hydroxide [28] remained as steady at high adsorbent amounts. Also, the removal percentage high from 95% in the Indigo Carmine dye removal can cause to this situation due to rapidly decreasing of concentration gradient at high current density. Because, as can be seen in Section 3.3 (concentration-time effect for the EC), dye removal increased at high concentrations. Removal percentages changed between 95-100%. Also, a desorption could be occurred at high current densities. Above pH 5.5, aluminum cations are at aluminum hydroxide form and at pHs (4-5.5), aluminum cations and aluminum hydroxides are present. High time and high current density cause to production of high aluminum species due to high electrolysis amount. In the reported studies, dye removal percentages in EC and EO processes were increased by current density increase for Basic Blue 3 and Acid Red 20 dyes, respectively [17,19]. In this study, the decreasing effect of high current can be related by solid-to-dye ratio relation, desorption and rapidly decrease in concentration of dye. Dye removal was determined as concentration dependent.

Concentration-Time Effect for the EC

The dye concentrations for the Indigo Carmine dye removal were studied at 50 and 250 mg/L concentration interval. Results are given in Figure 5. The figure indicates that the maximum dye removal was obtained at high concentration-stable time interaction. Time was ineffective at high concentrations. Due to driving force of high dye concentration [1], the dye removal increased at high concentrations. The ineffectiveness of time at high concentrations can be attributed to rapidly decrease of the dye concentration. Removal percentages were between 85 and 95%. On contrast to these results, Basic Blue 3 dye removal percentages decreased by concentration increase for EC process [17]. These results showed that the removal of the Indigo Carmine dye was concentration depended for aluminum electrodes.

Current Density-Concentration Effect for the EC Process

The current density is an important parameter in dissolution of metal electrodes for coagulation of dyes from waters. Also, high current density provides the high oxidation ratio of dye molecules due to raising electron transfer. Results are given in Figure 5. The current density raise generally increases the coagulant dosage and thus the removal yield is expected to increase. In the EC experiments, the dye concentration had raising effect on removal at high concentration-stable current density interaction conditions. The current density was ineffective at high concentrations. These results can be related with the solid-dye equilibrium conditions, because dye adsorption on low coagulant and high coagulant was same [29]. Removal percentages changed between 85-95%. Reactive Yellow 160 dye removal increased by current density increase and reached to steady at high current densities for aluminum and iron electrodes [21]. This situation in the present study can also be related by rapidly removal of dye because low concentrations decrease the removal (Figure 5).

Time-Current Density Effect for the EO Process

Time is a key parameter for dye removal from water by the EO process and operation time was studied at 10-30 time intervals by the central composite design. Results are given in Figure 5. The Figure 5 showed to increase of removal at high value of time and moderate current density. The effects of the parameters can be attributed the high interaction time and thus high

interaction opportunity of electrons with dye molecules [30]. Removal percentages changed between 40 and 95%. Moderate current density effect on removal may be due to operation solution temperature, pH and amounts of the produced oxidants like as active hydroxyl, hypochlorous acid, chlorine gas and hydrogen peroxide. The removal of Acid Red 20 dye by EO process increased with current density increase and moderate current provided enough removal percentage for about 100% extent [19].

Concentration-Time Effect for the EO Process

Results are given in Figure 5. High time and low concentration increased the removal yield. Removal percentages changed between 60 and 95%. High time increased the interaction opportunity of the dye and oxidants. Low concentration effect can be related with sufficient oxidant amounts like as electron, hypochlorous acid, hydrogen peroxide and active hydroxyl ions against low dye concentration. The removal of Reactive Blue 21 dye removal was reported to reach the maximum value at 10 minutes and high current by EO process [20].

Current Density-Concentration Effect for the EO Process

Current density controls the deterioration amount and rate of organics like as dyes by the EO process as the electron amount in the reactor body increases with the current density increase. The results are given in Figure 5. The Figure 5 indicated the increasing removal yield at high value of current density and low dye concentration. This increasing electron amount increased the removal. Removal percentages changed between 40 and 95%. The reason of low concentration can be attributed to high oxidizing opportunity between dye and chlorine gas, electron, hypochlorous acid, hydrogen peroxide and active hydroxyl ion amount. Manisha and coworkers reported to increase of Rhodamine B dye removal by current density and electrolyte concentration increase [31].

Comparison of the Batch and the Continuous Reactors for Dye Removal

Dye removal from wastewaters can be realized by batch and continuous reactors. For this purpose, this study provides two reactor types. EC and EO processes should be study for real operation conditions and their performances should be optimized for real operation of these two reactors. The batch reactor data comparison of yield of the EC and the EO processes are given in Figure 6. The most effective results were obtained for the EO process. The continuous reactor was, therefore, applied for the EO process. The experimental parameters for the EO process at the continuous mode were 100 mg/L dye concentration, 1,000 rpm stirring speed, 3 g/500 mL MgCl2.6H2O backround electrolyte amount, natural pH (6.85), initial temperature 26.2 °C, 1.6 Ampere, 500 mL reactor starting volume, 11.76 mL/min volumetric flow rate. The removal percentage change during the removal in the continuous process is given Figure 7. The dye could be treated as about 100% by continuous EO process although after passing 2.46 fold hydraulic retention time (HRT). The residence time was calculated as 42.5 minutes and it was measured that the reactor reached to steady state and removal percentage was about 100% during the removal in continuous reactor. The reactor was taken to continuous mode after operation of the batch reactor at 15 minutes for 500 mL dye solution. Although the dye removal was at about 100% extent, a bit yellow color as end residue was observed. The starting color of the dye was dense blue. Thus, dye removal extent was measured as a bit below 100% extent. Therefore, the dye residue from outlet water of the EO process should be removed. Therefore, an ion exchange process was applied to the persistent dye-containing solution after the batch EO process. The oxidation reduction potential (ORP) of aluminum coagulation for the dye was measured as - 448 mV after 4 g MgCl2.6H2O, 100 mg/L dye, 1.6 Ampere, 15 minute operation time, 500 mL. The oxidation reduction potential (ORP) of graphite treatment for the dye was measured as 670 mV after 3 g MgCl2.6H2O, 100 mg/L dye, 1.6 Ampere, 15 minute operation time, 500 mL. The oxidation reduction potential (ORP) of the used pure water was measured as 580 mV. As can be seen from these results, the treated solutions can be discharged directly. The negative value of aluminum coagulated solution shows the unoxidant property of the solution. The ORP values of some foods as examples are given in Figure 8 [32].

Persistent Dye Residue Treatment after the Batch EO by Applying Ion Exchange

The Indigo Carmine dye has dense blue color. The yellow dye residue after EO process treatment could be refined by ion exchange resin (Selion SBA 2000 basic resin) at 100% efficiency and photographs of dye residue and its refined outlet water from ion exchange column are given in Figure 9. It is clear from Figure 9 that dye residue could be treated at 100% extent. The used resin was an anionic material and removed completely dye residue. Dyes are generally visiable in the surface waters even at 1 mg/L concentration, therefore, a removal extent of 100% was selected as discharge standart. A neutralization operation can be proposed for discharge of acidic treated dye water after EO process and ion exchange process

Table 2. Experimental matrix for dye removal by EC and EO (20-26.2 oC, 1,000 rpm, 500 mL, Natural pH=5.78-6.90) (*6 g/500 mL MgCl2.6H2O was used and in other experiments 3 g/500 mL MgCl2.6H2O was used)

Parameters				Response (%)							
Run	T(min)	CD (A)	C (mg/L)	EC (%)	Predicted (%)	End pHs	Voltage (V)	EO (%)	Predicted (%)	End pHs	Voltage (V)
1	**15**	**0.8**	**200**	**92.88**	**98.04**	**4.40**	**13.1-12.5**	**71.48**	**62.58**	**2.98**	**17.4-14.7**
2	**30**	**1.2**	**150**	**94.63**	**89.09**	**4.21**	**20.5-17.2**	**99.21**	**95.57**	**2.63**	**20.4-15.1**
3	**25**	**0.8**	**200**	**96.81**	**102.68**	**4.34**	**12.4-11.5**	**69.92**	**68.73**	**2.69**	**15.9-13.4**
4	**20**	**1.2**	**150**	**95.25**	**98.01**	**4.24**	**19-14.3**	**89.58**	**94.84**	**2.61**	**23.7-15.8**
5	**25**	**0.8**	**100**	**95.56**	**93.92**	**4.24**	**13.2-12.3**	**98.50**	**92.94**	**2.60**	**16.2-12.8**
6	**15**	**0.8**	**100**	**92.81**	**85.98**	**4.35**	**11.7-11.1**	**99.41**	**89.00**	**2.52**	**16.5-13.4**
7	**15**	**1.6**	**200**	**95.78**	**102.83**	**4.16**	**24.6-20.9**	**90.63**	**90.44**	**2.77**	**25.1-23.7**
8	**20**	**0.4**	**150**	**96.08**	**96.02**	**4.54**	**7-7.1**	**46.88**	**56.73**	**2.68**	**8.9-8.6**
9	**10**	**1.2**	**150**	**98.38**	**101.46**	**4.34**	**17.3-16.1**	**72.92**	**81.68**	**2.32**	**23.2-18.4**
10*	**15***	**1.6***	**100***	**92.94**	**89.53**	**4.08**	**27.6-22.4**	**99.44**	**94.91**	**2.22**	**28.7-20.2**
11	**20**	**2**	**150**	**93.79**	**86.90**	**3.94**	**28.8-24.2**	**99.04**	**94.30**	**2.27**	**21.7-15.9**
12	**25**	**1.6**	**200**	**91.22**	**109.51**	**3.96**	**25.7-20.2**	**95.70**	**100.39**	**2.19**	**30.4-19.1**
13	**20**	**1.2**	**50**	**82.75**	**82.47**	**4.16**	**21-18**	**100.31**	**106.19**	**2.33**	**22.2-16.9**
14	**25**	**1.6**	**100**	**84.25**	**75.51**	**3.96**	**23.5-20.5**	**99.50**	**102.66**	**2.07**	**29.5-18.1**
15	**20**	**1.2**	**250**	**95.46**	**128.54**	**4.27**	**18-16.1**	**78.44**	**77.50**	**2.57**	**19.1-16.6**

Table 3. Anova analysis of dye removal by EC and EO processes

Parameters	EC R-Sq=90.91%, R-Sq(pred)=14.21%, R-Sq(adj)=74.54%		EO R-Sq=84.78%, R-Sq(pred)=0.00%, R-Sq(adj)=57.38%	
	Constant	p	Constant	p
Constant	**76.8437**	**0.023**	**66.5666**	**0.578**
T	**0.2136**	**0.871**	**2.2818**	**0.716**
CD	**13.2956**	**0.384**	**45.2960**	**0.524**
C	**0.0976**	**0.422**	**-0.4266**	**0.457**
T*T	**0.0177**	**0.533**	**-0.0622**	**0.641**
CD*CD	**0.3223**	**0.941**	**-30.1970**	**0.184**
C*C	**-0.0006**	**0.086**	**-0.0003**	**0.826**
T*CD	**-1.2461**	**0.024**	**0.4756**	**0.807**
T*C	**0.0027**	**0.432**	**0.0022**	**0.888**
CD*C	**0.0531**	**0.230**	**0.2743**	**0.197**

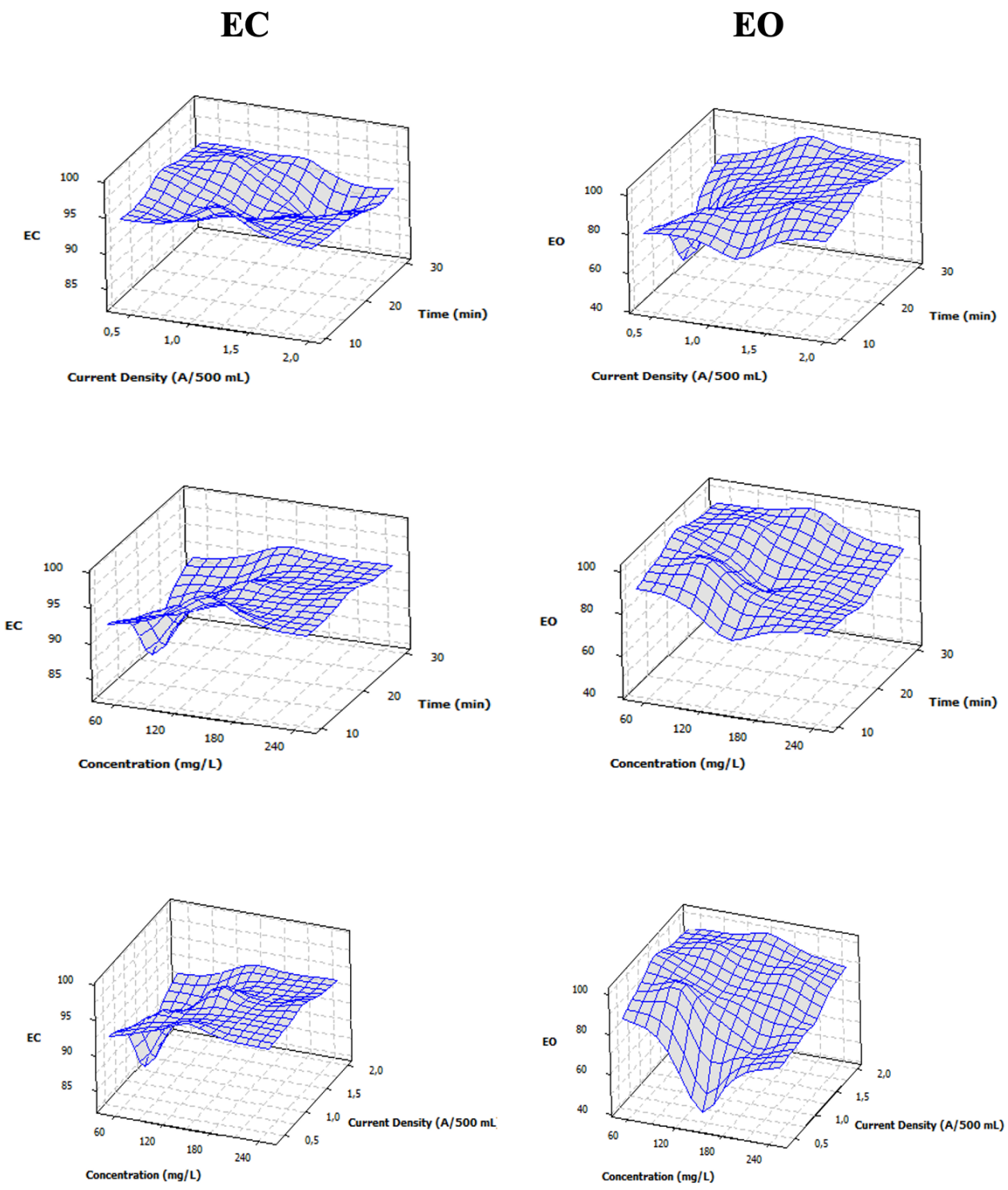
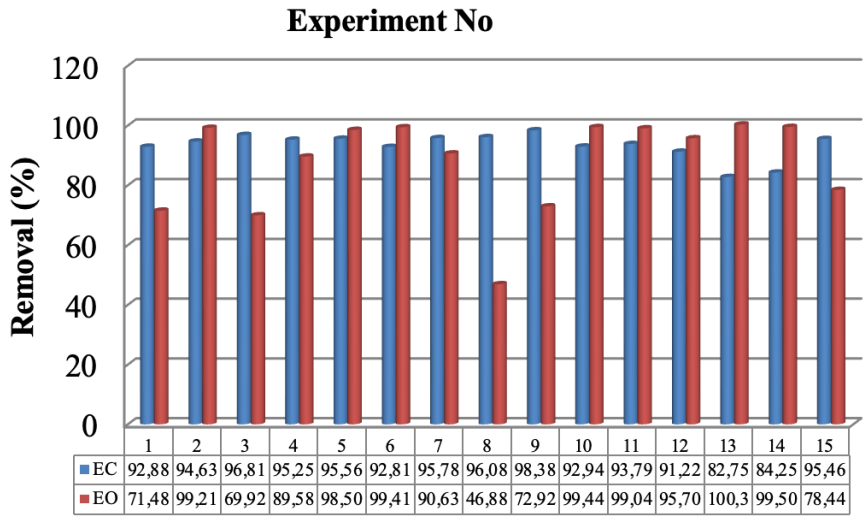
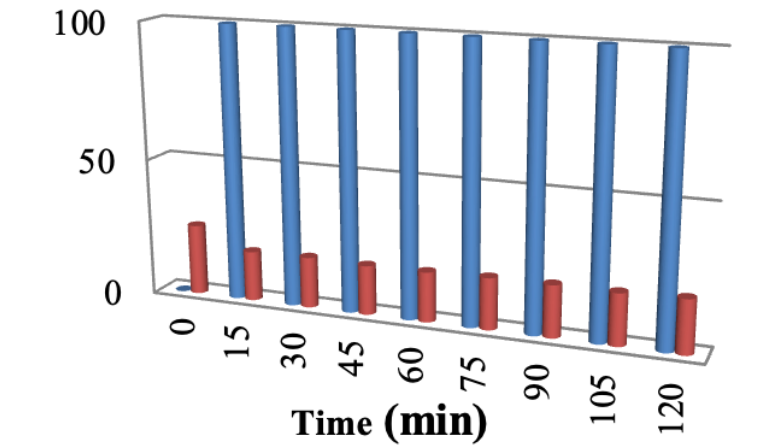


Figure 5. Removal percentage of dye as a function of parameters



	1	2	3	4	5	6	7	8	9	10	11	12	13	14	15
EC	92,88	94,63	96,81	95,25	95,56	92,81	95,78	96,08	98,38	92,94	93,79	91,22	82,75	84,25	95,46
EO	71,48	99,21	69,92	89,58	98,50	99,41	90,63	46,88	72,92	99,44	99,04	95,70	100,3	99,50	78,44

Figure 6. Removal percentage of dye for EC and EO processes



	0	15	30	45	60	75	90	105	120
Removal (%)	0	99,90	6100	100	100	100	100	100	100
Volt	25,6	18,1	18,4	17,9	18,1	18,7	18,8	18,7	19,4

Figure 7. Removal percentage of dye for EO in the continuous system

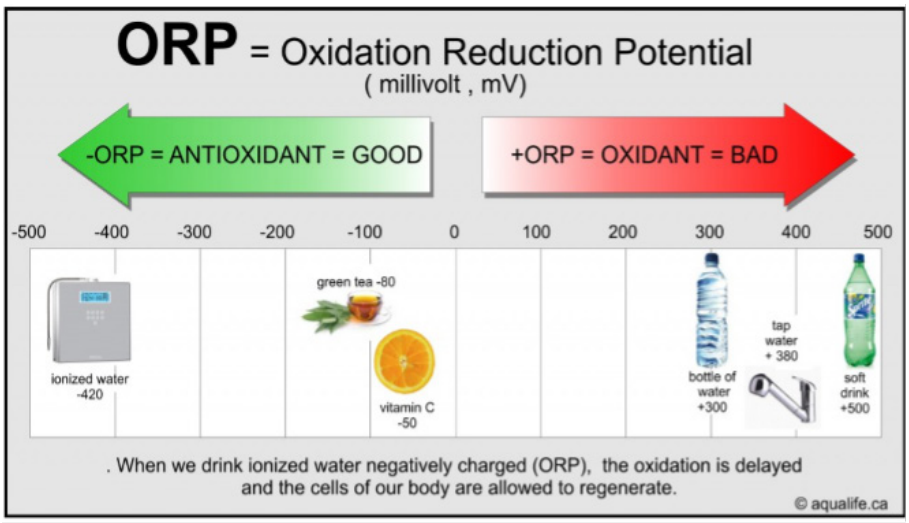


Figure 8. ORP values of some foods [32]

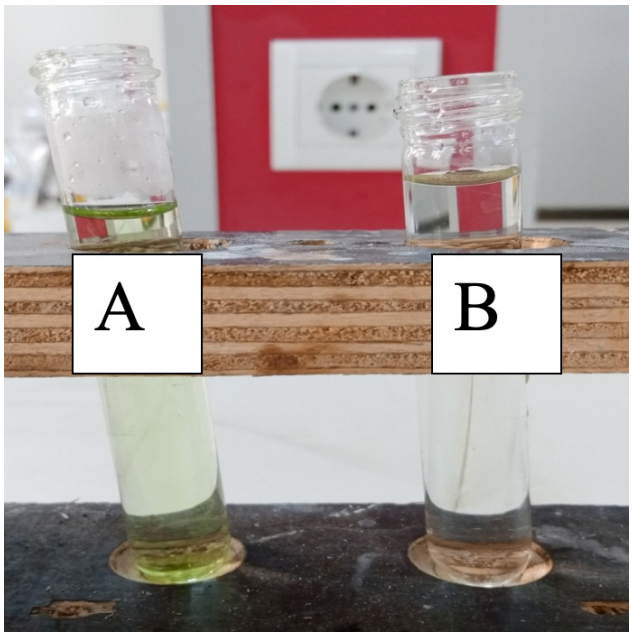


Figure 9. Treatment dye residue by Selion SBA 2000 anionic ion exchange resin after EO (A: Dye residue, B: Treated dye residue, 200 mg/L dye, constant 1.4 A, Natural pH, Room temperature (21.2 °C), 500 mL, 3 g MgCl.6H2O, 45 minutes oxidation time)

Energy consumption for the EC and the EO processes

The energy consumptions for the EC and the EO were calculated by the following equation [33].

Here, V, I and t are average voltage of the system (V), electrical current density (A) and reaction time (h), respectively.

The energy consumption in the EC and the EO processes is vital for applicability of the treatment to the dye-containing wastewaters. The energy consumption values are given in Figure 10. As can be seen in Figure 10, the energy consumption for the EC increased with high current-high time, constant concentration-high time and middle concentration-high current. The energy consumption for the EO increased with high current-high time, constant concentration-high time and middle concentration-high current. It is a general role for the electrochemical treatment processes that the energy consumption increases with time and current increase (Eq. 13 shows the evidence). The electrical consumption of the EO was generally a bit high from EC processes, and EO process is assumed as advantageous due to zero sludge production. The comparison of the EC and the EO processes was given in Figure 10 and 11.

Here, T is time (min), CD is current density (A), C is concentration (mg/L). WEC is energy consumption for electrocoagulation and WEO is energy consumption for electrooxidation.

The experimental matrix for the energy consumption by the EC and the EO processes is given in Table 4. The Anova analysis for the energy consumption by the EC and the EO processes is given in Table 5. The Anova analysis of the EC process showed that current density-current density interaction and time-current density interaction were statistically important, however, for the EO process, all the parameters were statistically unimportant. The uncoded factors were used in the development of regression models for the energy consumptions. As can be seen in Table 4, energy consumptions in EO process were a bit high from EC process but it was not so important. R-Sq(adj) values show the enough number of parameters for modelling. R-Sq(pred) values show the good estimation of model the energy consumptions.

$$W(\frac{kW \times h}{m^3}) = \frac{V \times I \times t}{Volume} \qquad \text{(Eq.13)}$$

$$WEC(\frac{kW \times h}{m^3}) = 12.6073 - 0.7623*T - 13.6215*CD - 0.0388*C + 0.0062*T*T + 7.1522*CD*CD + 0.0001*C*C + 0.9342*T*CD + 0.001*T*C - 0.0035*CD*C \qquad \text{(Eq.14)}$$

$$WEO(\frac{kW \times h}{m^3}) = -7.30407 + 0.04023*T + 5.87118*CD + 0.03770*C - 0.01940*T*T - 4.76620*C*CD - 0.00018*C*C + 1.16375*T*CD + 0.00048*T*C + 0.00429*CD*C \qquad \text{(Eq.15)}$$

Table 4. Experimental matrix for energy consumption by EC and EO (20 oC, 1000 rpm, 500 mL)

Parameters				Response			
Run	**T(min)**	**CD (A)**	**C (mg/L)**	**WEC**	**Predicted**	**WEO**	**Predicted**
1	15	0.8	200	5.12	6.14	6.42	7.01
2	30	1.2	150	22.62	23.20	21.30	23.06
3	25	0.8	200	7.97	10.47	9.77	9.92
4	20	1.2	150	14.00	15.02	15.80	17.67
5	25	0.8	100	8.50	9.13	9.67	10.01
6	15	0.8	100	4.56	5.80	5.98	7.58
7	15	1.6	200	18.20	19.62	19.52	17.21
8	20	0.4	150	1.88	2.23	2.33	-0.06
9	10	1.2	150	6.68	8.07	8.32	8.40
10	15	1.6	100	20.00	19.56	19.56	17.43
11	20	2	150	35.33	36.96	25.07	29.30
12	25	1.6	200	30.60	31.43	33.00	29.43
13	20	1.2	50	15.60	15.32	15.64	16.03
14	25	1.6	100	29.33	30.37	31.73	29.18
15	20	1.2	250	13.64	16.72	14.28	15.71

Table 5. Anova analysis of energy consumption by EC and EO

Parameters	**EC R-Sq=99.65%, R-Sq(pred)=97.07%, R-Sq(adj)=99.02%**		**EO R-Sq=94.58%, R-Sq(pred)=47.85%, R-Sq(adj)=84.82%**	
	Constant	**p**	**Constant**	**p**
Constant	12.6073	0.303	-7.30407	0.857
T	-0.7623	0.247	0.04023	0.985
CD	-13.6215	0.090	5.87118	0.807
C	-0.0388	0.488	0.03770	0.844
T*T	0.0062	0.635	-0.01940	0.672
CD*CD	7.1522	0.014	-4.76620	0.512
C*C	0.0001	0.651	-0.00018	0.696
T*CD	0.9342	0.004	1.16375	0.127
T*C	0.001	0.525	0.00048	0.928
CD*C	-0.0035	0.854	0.00429	0.949

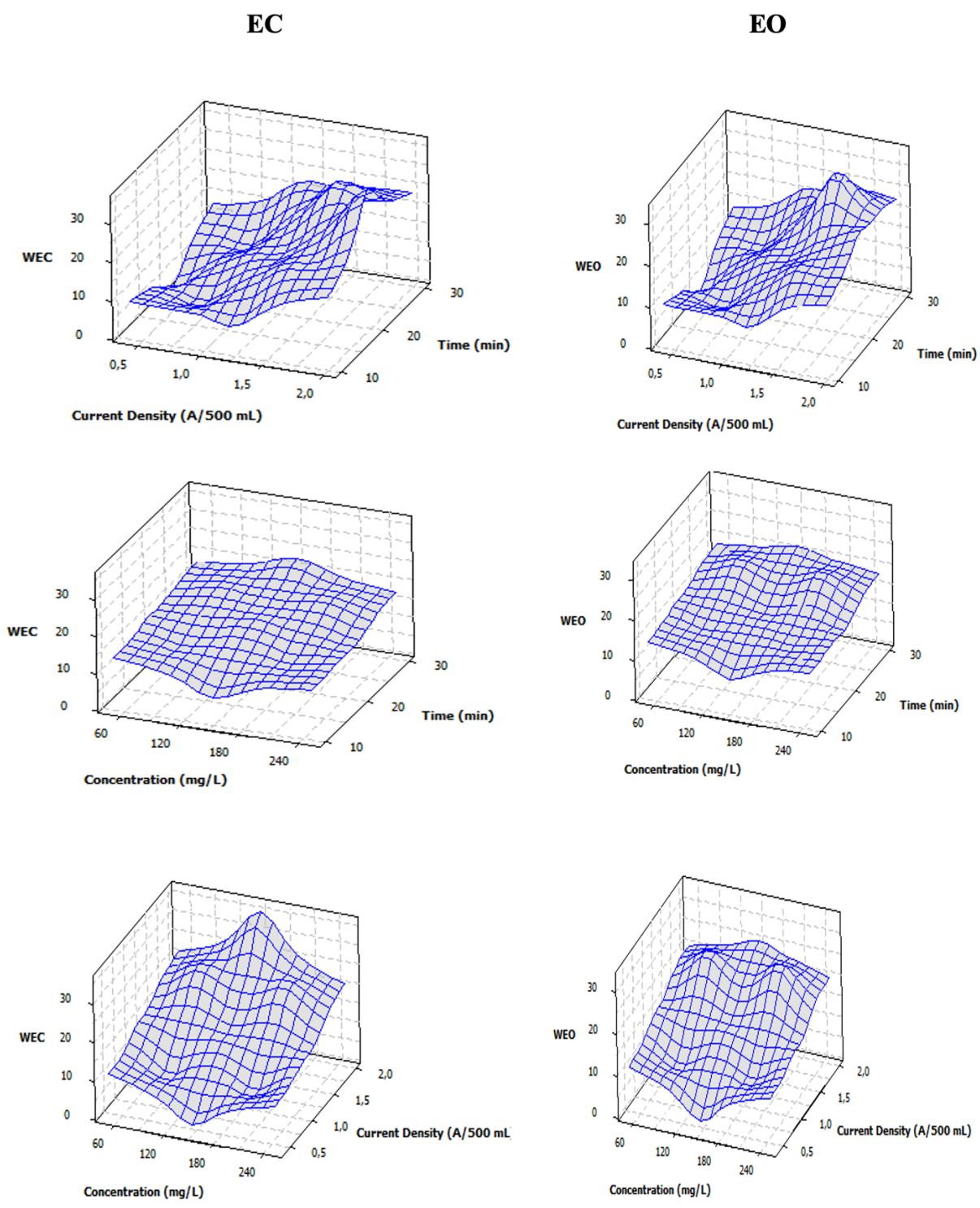
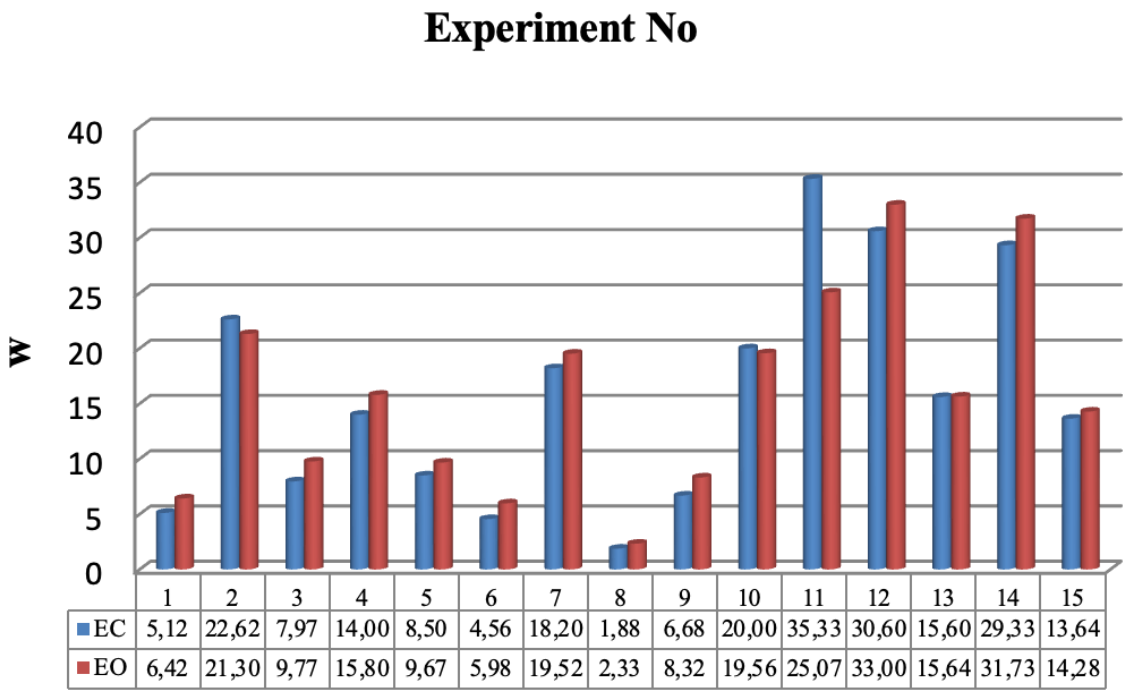


Figure 10. Energy consumption for EC and EO processes as a function of parameters



	1	2	3	4	5	6	7	8	9	10	11	12	13	14	15
EC	5,12	22,62	7,97	14,00	8,50	4,56	18,20	1,88	6,68	20,00	35,33	30,60	15,60	29,33	13,64
EO	6,42	21,30	9,77	15,80	9,67	5,98	19,52	2,33	8,32	19,56	25,07	33,00	15,64	31,73	14,28

Figure 11. Energy consumption for EC and EO processes as a function of experiment no

Dye Removal Mechanisms, Removal Costs and Literature Comparision

The amount of released aluminum cation from aluminum electrode (anode) was calculated using following equation and given in Table 6. The cost of energy consumption was given in Figure 12 per cubic meter treated wastewater. As can be seen in Figure 12, the cost of EO was found as a bit high from EC but EO process gave the best removal percentages for the dye. Also, graphite is not soluble in water and therefore, its cost is advantageous from soluble aluminum electrode. Salt cost for both the process is equal.

Here, I is current (A), t is time (second), M is molecular weight (g/mole), n is electron valence, F is Faraday constant (96,500 C/mole) [34].

Dye removal mechanisms for EO process was realized by direct oxidation with active hydroxyl radicals, indirect oxidation by hypochlorite anion, chlorine gas, hydrogen peroxide. The reactions for chlorine gas and hypochlorite anion were given in Eq (5-8). The generation of hydrogen peroxide at cathode is given in the following equations [35].

The active oxygens in the hydrogen peroxide is oxidized the organic matter or hydrogen peroxide is dissociated to active hydroxyl radicals to oxidize the organic matter like dyes. Similar to EO process, these oxidizing reactions occur in EC process but the general removal of dye occurs by coagulation and flotation.

$$Al^{3+}(g) = \frac{I \times t \times M}{n \times F} \qquad \text{(Eq. 16)}$$

$$Acidic - medium : O_2 + H_2 + 2e^- \rightarrow H_2O_2$$
$$Alkaline - medium : O_2 + H_2O + 2e^- \rightarrow HO_2^- + OH^- \qquad \text{(Eq. 17)}$$

$$OH^- + OH^- \rightarrow H_2O_2 \qquad \text{(Eq. 18)}$$

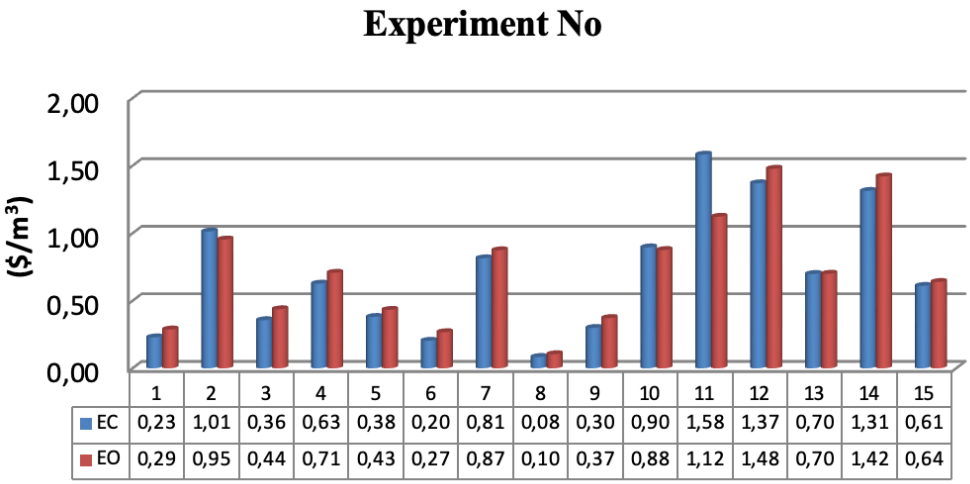


Figure 12. Energy consumption costs for EC and EO processes as a function of experiment no

Table 6. Al^{3+} amount release from anode to the solution phase for EC process

Experiment No	Amount (g)
1	0.067
2	0.201
3	0.112
4	0.134
5	0.112
6	0.067
7	0.134
8	0.045
9	0.067
10	0.134
11	0.224
12	0.224
13	0.134
14	0.224
15	0.134

In a reported study, energy consumption values were evaluated for textile dye decolorization (t=15 min) and COD removal (t=120 min) as 2.7-18.9 kWh/kg dye decolorization and 51.0-190.7 kWh/kg COD removal, respectively [36]. In an other study, for certain concentrations of 2.5 mM, 5.0 mM, 7.5 mM, and 10 mM NaCl, energy consumption values can be reported as follows: 4.21 kW-h/m3, 3.10 kW-h/m3, 2.96 kW-h/m3, and 2.60 kW-h/m3, respectively [37]. In this study, the energy consumptions showed to values of 1.88-35.33 kW-h/m3 for EC and 2.33-33.0 kW-h/m3 for EO. Dalvand and coworkers reported that electrode consumption, energy consumption and operating cost were 0.052kg/m3, 1.303kWh/m3 and 0.256US$/m3 for Reactive Red 198, respectively [38].

CONCLUSION

The Indigo Carmine dye removal from synthetically prepared solutions was investigated using the EC and the EO processes as a function of current density, concentration and time. The central composite design was applied for these two processes and the EO was found more effective than EC and 100% dye removal was achieved by the EO process followed the ion exchange. The batch and the continuous flow reactors were applied and the continuous flow reactor was determined as large time applicable for the EO method. Even after 2.46 fold hydraulic retention time, the dye removal performance of the continuous reactor was good. As a result, the removal of this dye could be achieved successfully in the batch and the continuous EO reactors for safely discharge. The electrical consumption of the EO was high a bit from the EC processes and due to sludge production of EC, EO process was determined to be advantageous. The persistent dye residue was removed at 100% yield from the outlet water of the batch EO reactor by ion exchange treatment. The experimental and the statistical analysis results of the dye removal can be summarized as follows. The statistically important parameters or interactions for dye removal were model constant and time-current density interaction for the EC; however, all the parameters for the EO were determined as unimportant. In the energy consumption analysis, the EC process showed that current density-current density interaction and time-current density interaction were statistically important, however, for the EO process, all the parameters were statistically unimportant.

•In the EC process: Dye removal increased at high time-low current density interaction. Dye removal increased at high concentration-stable time interaction. Dye concentration had raising effect on removal at high concentration-stable current density interaction conditions.

•In the EO process: The time-current density interaction effect showed to increase of removal at high value of time and moderate current density. High time and low concentration increased the removal yield. The concentration-current density interaction indicated the increasing removal yield at high value of current density and low dye concentration.

•In EC process, the sludge production was low and therefore, EO process was found as advantageous. pH change in EC for

0.8 A and 200 mg/L concentration at 0, 2, 5, 10 and 15 minutes were 5.60, 4.19, 3.92, 3.84 and 3.70 ± 0.1. pH change in EO for 0.8 A and 200 mg/L concentration at 0, 2, 5, 10 and 15 minutes were 5.60, 2.48, 2.32, 2.14 and 2.23 ± 0.1.

DATA AVAILABILITY STATEMENT

The author confirm that the data that supports the findings of this study are available within the article. Raw data that support the finding of this study are available from the cor responding author, upon reasonable request.

CONFLICT OF INTEREST

The author declared no potential conflicts of interest with respect to the research, authorship, and/or publication of this article.

USE OF AI FOR WRITING ASSISTANCE

Not declared.

ETHICS

There are no ethical issues with the publication of this manuscript.

REFERENCES

[1]. M. Korkmaz, C. Özmetin, BA. Fil, E. Özmetin, and Y. Yaşar, "Methyl violet dye adsorption onto clinoptilolite (Natural Zeolite): Isotherm and kinetic study," Fresenius Environmental Bulletin, Vol. 22(5), pp. 1523-1533, 2013.

[2]. https://textilelearner.net/different-types-of-dyes-with-chemical-structure/ [Online]. Available: (2024)

[3]. S.S. Bala, A.J. Alkhatib, S.S. Bashir, and M. Abdulhadi, "Photocatalytic degradation of Indigo Carmine in aqueous solutions by the antibacterial agent pefloxacin and UVA," Biomedical Journal of Scientific & Technical Research, Vol. 5, pp. 4903-4909, 2018.

[4]. B.L. Cíntia, Z.F.P. João, A.P. Julio, C. Polonio, "Effects of textile dyes on health and the environment and bioremediation potential of living organisms," Biotechnology Research & Innovation, Vol. 3(2), pp. 275-290, 2019.

[5]. M. Berradi, R. Hsissou, M. Khudhair, M. Assouag, O. Cherkaoui, A.E. Bachiri, and A.E. Harfi, "Textile finishing dyes and their impact on aquatic environs," Heliyon, Vol. 5(11), pp. 02711, 2019.

[6]. B. Shi, G. Li, D. Wang, C. Feng, H. Tang, "Removal of direct dyes by coagulation: the performance of preformed polymeric aluminum species," Journal of Hazardous Materials, Vol. 143(1-2), pp. 567-574, 2007.

[7]. F. Silva, L. Nascimento, M. Brito, K. Silva, W. Paschoal, and R. Fujiyama, "Biosorption of methylene blue dye using natural biosorbents made from weed," Materials (Basel), Vol. 12(15), pp. 2486, 2007.

[8]. N. Daneshvar, A. Oladegaragoze, N. Djafarzadeh, "Decolorization of basic dye solutions by electrocoagulation: an investigation of the effect of operational parameters," Journal of Hazardous Materials, Vol. 129(1-3), pp. 116-122, 2006.

[9]. A. Demir Delil, N. Gören, "Investigation of electrocoagulation and electrooxidation methods of real textile wastewater treatment," Eskişehir Techical University Journal of Science Techical Applied Science and Engineering, Vol. 20(1), pp. 80 – 91, 2019.

[10] Z. Yılmaz, M.B. Karagözoğlu, "Atıksuların arıtılmasında elektrokoagülasyon uygulamaları," BEÜ Fen Bilimleri Dergisi, Cilt 8 (1), s. 319-334, 2019.

[11] M.S. Najafinejad, S. Chianese, A. Fenti, P. Lovino, D. Musmarra, "Application of electrochemical oxidation for water and wastewater treatment: An overview," Molecules, Vol. 28, pp. 4208, 2023.

[12]. D.R. Ryan, "Electrocoagulation-electrooxidation for mitigating trace organic compounds in model source waters", Degree of Master of Science and Engineering, Marquette University, Milwaukee, Wisconsin 2019.

[13] T. Arslan, "Kompleks olarak bağlı ağır metal içerikli atık suların elektrokoagülasyon ile arıtımı," Yüksek Lisans Tezi, İstanbul Teknik Üniversitesi, İstanbul, Türkiye, 2008.

[14] M.A. Sadik, "Removal of reactive dye from textile mill wastewater by leading electrocoagulation process using aluminum as a sacrificial anode," Advances in Chemical Engineering and Science, Vol. 9, pp. 182-193, 2019.

[15] A.A. Beddai, B.A. Badday, A.M. Al-Yaqoobi, M.K. Mejbel, Z.S. Hachim, and M.K.A. Mohammed, "Color removal of textile wastewater using electrochemical batch recirculation tubular upflow cell," International Journal of Chemical Engineering, Vol. 2022, pp. 1-8, 2022.

[16] C. Wang, "Decolorization of congo red with three dimensional flow-by packed-bed electrodes," Journal of Environmental Science and Health Part A, Vol. 38(2), pp. 399–413, 2003.

[17] E. Bulut, "Tekstil atık sularından C.I. Bazik Mavi 3 boyarmaddesinin elektrokimyasal uygulama ile giderilmesi," SAÜ Fen Bilimleri Dergisi, Cilt. 20 (3), s. 521-531, 2016.

[18] L. Gazigil, O.T. Can, "Elektrokoagülasyon yöntemi ile sulardan boyarmadde gideriminde molekül büyüklüğü ve pH etkisi," APJES, Citt 5, s. 113-122, 2017.

[19] J. Erkmen, M. Adıgüzel, "Acid red-20 sentetik endüstriyel boyar maddenin elektro-oksidasyon yöntemi ile sulu çözeltiden uzaklaştırılması," NÖHÜ Mühendislik Bilimleri Dergisi, Cilt 11(2), s. 363-371, 2022.

[20] S.E. Aggadi, Z.E. Abbassi, A.E. Hourch, "Color removal from dye-containing aqueous solutions by electrooxidation," Desalination and Water Treatment, Vol. 215, pp. 232–236, 2021.

[21] A. Aygün, B. Eren, "Elektrokoagülayon yöntemiyle Reaktif Yellow 160 boyar maddesinin giderimi," APJES, Cit 5, s. 10-18, 2017.

[22] M. Korkmaz, E. Özmetin, Y. Süzen, E. Çalgan, C. Özmetin, "A new adsorbent (aluminum modified talc) for phosphate removal from alkaline solutions and optimization of data by central composite design," Desalination Water and Treatment, Vol. 245, pp. 178–190, 2022.

[23] M.E. Ristea, and O. Zarnescu, "Indigo Carmine: Between necessity and concern", Journal of Xenobiotics, Vol. 13(3), pp. 509–528, 2023.

[24] Z. Huangfu, and W. Zhang, S. Hao, M. Zhang, and J. Yao, "Construction of novel electrochemical treatment systems for indigo wastewaterand their performance," Pigment & Resin Technology, Vol. 50(3), pp. 264–270, 2021.

[25] Minitab 16.0 programme help tool description of central composite design

[26] D. Kavak, "Removal of boron from aqueous solutions by batch adsorption on calcined alunite using experimental design," Journal of Hazardous Materials, Vol. 163, pp. 308–314, 2009.

[27] N. Öztürk, and T.E. Köse, "Boron removal from aqueous solutions by ion-exchange resin: Batch studies," Desalination, Vol. 227, pp. 233–240, 2008.

[28] M. Korkmaz, C. Özmetin, E. Özmetin, E. Çalgan, Ö. Ziyanak, "Boron removal from colemanite mine wastewater by coagulation using zinc hydroxide—A factorial optimization study," Celal Bayar University Journal of Science, Vol. 18, pp. 77-83, 2022.

[29] Özmetin, C., Korkmaz, M., "Full factorial design of experiments for boron removal by iron hydroxide from colemanite mine wastewater", Journal of Balikesir University Institute of Science and Technology, 21(1):244-253, (2019).

[30] H.M.A. Asghar, T. Ahmad, S.N. Hussain, and H. Sattar, "Electrochemical oxidation of methylene blue in aqueous solution," International Journal of Chemical Engineering and Applications,Vol. 6(5), pp. 352-355, 2015.

[31] M.S. Kothari and K.A. Shah, "Electrochemical oxidation for decolorization of Rhodamine-B dye using mixed metal oxide electrode: modeling and optimization," Water Science & Technology, Vol. 81, pp. 720-731, 2020.

[32] https://aqualife.ca/orp-oxydation-reduction-potential/ [Online]. Available: (2024)

[33] A.E. Yilmaz, R. Boncukcuoglu, M.M. Kocakerim, M.T Yilmaz, C. Paluluoglu, "Boron removal from geothermal waters by electrocoagulation," Journal of Hazardous Materials, Vol. 153, pp. 146–151, 2008.

[34] A.E. Yılmaz, R. Boncukcuoğlu, M.M. Kocakerim, E. Kocadağistan, "An empirical model for kinetics of boron removal from boron containing wastewaters by the electrocoagulation method in a batch reactor," Desalination, Vol. 230, pp. 288–297, 2008.

[35] I. Dioufa, O. Diab, M.B. Diedhioua, P. Droguib, A.O. Tourea, S.M. Lo, M. Rumeaua, and C. Gueye Mar-Diop, "Electro-generation of hydrogen peroxide using a graphite cathode fromexhausted batteries: study of influential parameters on electro-Fenton process," Environmental Technology, Vol. 41, pp. 1434–1445, 2020.

[36] B.K. Körbahti and K. M. Turan, " Evaluation of energy consumption in electrochemical oxidation of Acid Violet 7 textile dye using Pt/Ir electrodes," JOTCSA, Vol. 3(3), pp. 75-92, 2016.

[37] O. Sözüdoğru, "Electrochemical oxidation of wastewater contaminated with Astrazon Red Violet 3RN Dye on $Ti/IrO_2/RuO_2$: Evaluation of process parameters, Kinetics, and energy consumption, Iranian Journal of Chemistry and Chemical Engineering, Vol. 42(11), pp. 3640-3658, 2023.

[38] A. Dalvand, M. Gholami, A. Joneidi, N. M. Mahmoodi, "Dye removal, energy consumption and operating cost of electrocoagulation of textile wastewater as a clean process," Clean– Soil, Air, Water, Vol. 39 (7), pp. 665–672, 2011.

Environ Res Tec, Vol. 8, Issue. 2, pp. 399-409, June 2025

Environmental Research and Technology
https://dergipark.org.tr/en/pub/ert
DOI: https://10.35208/ert.1472975

Environmental Research & Technology

Research Article

Assessing the carbon footprint of Gaziantep University's sporium building: A step towards environmental awareness and climate action in Türkiye

Serap ULUSAM SEÇKINER*[1], Belkıs Şevval ŞAHINALP[1]

[1]*Department of Industrial Engineering, Gaziantep University, 27310, Gaziantep, Türkiye*

ARTICLE INFO

Article history
Received: 25 Apr 2024
Revised: 18 Sep 2024
Accepted: 23 Sep 2024

Key words:
Carbon footprint calculation, sport center, emission, corporate carbon footprint, DEFRA.

ABSTRACT

There are many human activities in our developing, growing, and easier world. The priority in reducing the effects of human activities on the environment is awareness. It is important to measure the direct and indirect effects of humans on the environment to raise awareness and create behavioral change. One of the measurement methods that have been widely used is carbon footprint. The gas defined as carbon is a greenhouse gas. Many studies have been carried out to reduce greenhouse gases and raise awareness on this issue. Within the scope of these situations, it is aimed to calculate the carbon footprint measurement of the Gaziantep University Sporium Building according to the annual natural gas and air conditioning data in Scope 1, electricity and water data in Scope 2, and garbage data in Scope 3.

Cite this article as: Ulusam Seçkiner S, Şahinalp BŞ. Assessing the carbon footprint of Gaziantep University's sporium building: A step towards environmental awareness and climate action in Türkiye. Environ Res Tec 2025;8(2) 399-409.

INTRODUCTION

Today, increasing population, urbanization, economic activities, and variable consumption habits increase the impact on the environment and natural resources. The current problems related to environmental pollution, climate change, desertification, and destruction of forests; water scarcity and global warming maintain their place on the world agenda (The Intergovernmental Panel on Climate Change (IPCC) [1]. With the increase in the amount of greenhouse gases (GHG) in the atmosphere as a result of human activities, temperature of the world rises. Along with the visible rays from the sun, ultraviolet and infrared rays also hit the earth's surface; some of them are reflected from the surface, while some of them are trapped by greenhouse gases, preventing their exit from the atmosphere. This obstacle, on the other hand, ensures that the earth's surface remains at a certain temperature. Due to this condition of GHG, atmospheric temperature is about 15°C [1].

It is possible to say that the most important component of the ecological footprint in our country is the carbon footprint (CF) with a rate of 46%. This study on CF, known as a type of ecological footprint, draws attention to the dimensions of the CF caused by the energy, production, and import structure in our country in particular [2]. To prevent climate change (CC) on a global scale, several international policies have been planned the United Nations Framework Conven-

***Corresponding author.**
*E-mail address: seckiner@gantep.edu.tr

This is an open access article under the CC BY-NC license (http://creativecommons.org/licenses/by-nc/4.0/).

tion on Climate Change (UNFCCC) has been established and the Paris Agreement has put in force as of 2016. Within the scope of this agreement, the target of keeping the temperature increase at 1.5°C has been set, and it has been stated that this situation can greatly reduce the threat of CC. In this context, it is planned to provide technological, financial, and capacity-building support to developed countries to reduce the amount of GHG in these countries [3].

Since Türkiye is a party to the UNFCCC, it has also signed the Paris Agreement. For Türkiye certain responsibilities have been assigned like other countries, enabling it to make efforts to combat CC at a level that will not hinder sustainable development and economic developments worldwide. Following these studies, many protocols and agreements were signed, and participating countries made commitments by submitting national contribution declarations within their means to reduce and limit greenhouse gases. Türkiye prepared a National Contribution Declaration in 2015 and predicted that it would reduce greenhouse gas emissions by 30% by 2030. In this context, public institutions in Türkiye will need to analyze the current situation of their resources and activities within the scope of combating climate change.

In the light of these developments, as a case, the main purpose of this study is to calculate the CF of Gaziantep University Sporium Center, which many people visit and use daily, and to determine the carbon emission of this center.

LITERATURE REVIEW

GHG are gases present in the atmosphere that are part of a natural process called the greenhouse effect. Unlike other gases in the atmosphere GHG contribute to temperature regulation by affecting the total energy beneath the surface. However, in recent years, human activities have increased GHG, leading to global climate change [4]. Among the most common GHG are carbon dioxide (CO_2), methane (CH4), nitrogen oxides (NOx), chlorofluorocarbons (CFCs), and water vapor.

Increasing concentrations of GHG enhance their capacity to trap heat in the atmosphere, leading to global warming and CC. This situation can result in a range of adverse effects such as rising sea levels, extreme weather events, drought, and changes in ecosystems [5].

CF is a concept that measures the amount of GHG released into the atmosphere by an individual, organization, or product. It is typically expressed in terms of CO_2 equivalents, and is assessed at the personal, corporate, or product level. This monitoring process encompasses both direct and indirect GHG emissions, often involving various activities such as energy consumption, transportation, production, and consumption [6].

Personal CF is determined based on factors such as individuals' energy consumption habits, transportation preferences, and consumption patterns. At the corporate level, calculations consider companies' production processes, supply chains, and business operations. CF has gained significance as a concept supporting efforts to understand and reduce environmental impacts. In this context, it plays a fundamental role in the formulation and implementation of sustainability policies, serving as a cornerstone for informed and responsible environmental management. [7]. The issue of CF highlighted by the increase in carbon dioxide (CO_2) levels in the atmosphere due to industrialization and technological advancements is a prominent environmental concern worldwide. With the advent of the Industrial Revolution, the widespread use of fossil fuels and the growing energy demand have exacerbated the CF problem [8].

UNFCCC is an international agreement that was opened for signature in 1992, in Rio de Janeiro, to combat global climate change and mitigate its effects [3]. The main objectives of the convention are Combatting CC, Mitigating the Effects of Climate Change, Principle of Responsibility and Justice, and Alignment with Sustainable Development. The Kyoto Protocol has faced criticism, including challenges in certain countries meeting their commitments and the exclusion of developing countries from some obligations. In 2012, the Doha Amendment was adopted as a continuation of the Kyoto Protocol, but it also attracted criticism. The Paris Agreement establishes a framework for combating CC worldwide. It was adopted in 2015, during the 21st Conference of the Parties to the United Nations Framework Convention on Climate Change (COP21). The agreement came into effect in 2016 [9].

The primary objective of the Paris Agreement was Limiting GHG Emissions. It sets the goal of keeping global warming below 2°C and supports efforts to reduce it to 1.5°C if possible. Secondly, Enhancing Adaptation and Resilience Efforts is the agreement that supports efforts to help communities adapt to and build resilience against the impacts of CC. Thirdly, Providing Financial Support is the agreement that envisions providing financial resources to support the efforts of developing countries in combating climate change. Finally, Transparency and Accountability is the agreement that requires countries to transparently report their emission reduction commitments and undergo regular reviews. Unlike the Kyoto Protocol, the agreement has a more flexible structure and adopts a more inclusive approach by calling on both developed and developing countries to share common responsibilities [9].

Türkiye's CF is based on the country's GHG emissions. These emissions can originate from energy production, industrial processes, transportation, agriculture, and other activities [10]. The country's CF can vary depending on factors such as economic growth, energy usage, and other considerations. Factors such as carbon intensity in energy production, fossil fuel usage in the transportation sector, industrial processes, and agricultural practices play a significant role in determining the CF [10].

Steps of improving energy efficiency, transitioning to renewable energy sources, implementing sustainable agricultural practices, and other environmental policies can contribute to reducing Türkiye's CF. Policies and sanctions on CF reduction in Türkiye are based on Climate Action Plans, Re-

newable Energy Incentives, Energy Efficiency Policies, Carbon-Free Transportation Policies, Carbon-Free Industry Policies, Forest Management and Afforestation Projects, and Climate Change Adaptation Programs. Policies supporting the use of electric vehicles, incentives for public transportation, and measures such as developing carbon-free transportation infrastructure are aimed at reducing carbon emissions in the transportation sector. Various policies and technological supports are provided to reduce carbon emissions in the industry. Protecting forests, afforestation projects, and sustainable forestry practices contribute to reducing carbon emissions.

MATERIALS AND METHODS

There are gaps in our country regarding the measurement of CF. In this study, inspired by green transformation initiatives such as the Green Campus Project; we aim to address the measurement of CF in real environments. The Gaziantep University Sporium Center presents a valuable opportunity for considering CF measurements.

DEFRA methodology

The Department for Environment, Food and Rural Affairs (DEFRA) [11] is a government agency in United Kingdom (UK) responsible for environmental protection, food production and standards, agriculture, and fisheries. Annually, DEFRA releases emission factors for the sources of environmental pollution from industries, manufacturing, residences, and transportation to address global warming. In a study conducted using emission factors published by DEFRA in 2023, calculations were performed to determine CF arising from the consumption of water, electricity, natural gas, and air conditioning in a sample building. To measure and examine the CF, the following scopes have been established by considering the existing emissions either directly or indirectly:

•Scope 1: Directly measured GHG emissions from the operation of the assessed building or through its vehicles. Therefore, it is considered a direct CF.

•Scope 2: Includes indirect GHG emissions from electricity, water usage, heating, and cooling.

•Scope 3: Encompasses other indirect GHG emissions not accounted for in Scope 2. Emissions arising from personnel commuting and business travel are evaluated within this scope.

Establishment boundaries are initially determined. The institution's name, full address, and affiliated organizations are identified. Their affiliations must be found and proven. It is mandatory to identify all other units affiliated with the institution. The boundaries of the organization's activities and functions are defined. A commitment statement is prepared by addressing the principles under the title of principles in the ISO 14064 regulation, with relevance to compliance, accuracy, integrity, consistency, accuracy, and transparency. Thus, the foundation of calculations and the initial steps to guide their implementation are prepared.

GHG emissions inventory of the organization must be compiled. If there are consolidations that can be made in the institution's units, they are identified. The emission values resulting from all other activities related to Scope 1 (all combustion and incineration, bioenergy, refrigeration and cooling gases, fuels used for internal transportation and transmission), Scope 2 (Electricity, Heat, and Steam), and Scope 3 are classified and listed based on transportation-related activities. By also looking at sections 4, 5, and 6 related to Scope 3, the factors related to carbon emissions are identified. Thus, the emissions for purchased materials are determined in Category 4 (such as paper, food, workwear, glass, metal equipment, etc.), emissions rates related to the use of the product in Category 5, and emissions from natural disasters such as invasion, earthquake, fire, etc., in Category 6. Emission sources and scopes of the Sporium Center at Gaziantep University are presented in Table 1. Scopes 1 and 2 are mandatory because they are direct sources of GHGs. The inspection year is selected based on the data situation. Then access should be provided to a document containing GHG emission rates that contain the most current protocol, as it can be updated periodically. If any software is used, one must verify that the latest published emission rates for calculations and ensure that these rates are accurately incorporated into the software settings to meet the requirement. If the software is open source, this can be done. If not, calculating corporate CF with the DEFRA method is safer and more accurate. With the DEFRA method, the emission values of factors (sources) used in combustion and incineration works used for production or service are determined, and the cumulative value is obtained. It must be determined whether banned gases are used where factors such as air conditioning, refrigerators, and all climate control devices are used. Data about the number, quantity, and characteristics of the used sources is also collected. Only reliable data sources, where official evidence can be found, should be used in determining the data. Invoices, calibration reports, technical specifications, tickets for journeys, scale measurements, legal permits, and SCADA data are accepted as official proofs.

In addition, information is collected on the purposes of water use, water sources, and carbon emission sinks in recycling activities. Information is collected on many issues such as usage permits, licenses, network water meter information, and calibrations. Wastewater and waste disposal agreements should be questioned. Corporate reports should be accessed. Emission values resulting from electricity, heat, or steam sources in Scope 2 are determined. Here, especially which country's electricity emission need to be determined. Factors for electric vehicles are examined in detail under a separate heading, and emission values are determined according to vehicle types. Emission values resulting from out-of-business transportation in Scope 3 are searched. Domestic and international travels, accommodations, and vehicles used are all used as factors with their official evidence. Issues such as the fuel types of vehicles used are clarified. By examining sections 4, 5, and 6 related to Scope 3, factors related to

carbon emissions are determined. Thus, the values of GHGs from natural disasters such as invasions, earthquakes, and fire with all their official evidence are found.

After finding and calculating emissions in all scopes and categories, part of the report under reduction and improvement activities starts. Recommendations should be made under headings of energy demand and usage management, energy efficiency, technology or process improvements, GHG capture and storage, management of transportation and travel demands, fuel substitution or replacement, afforestation, waste reduction, alternative fuel, and raw material use to prevent waste disposal or burning, and refrigerant management. A report is further prepared for improvement activities, and in this report, the period covered by the target, including the target reference year and completion year, type of target, emission class, the amount and unit of reduction expressed according to the target type, climate science, reduction potential, international, national context, sectoral context considering criteria is determined. Sera gases management systems must be included in the organization's quality management systems in a manner consistent with the principles of this document. Consistency with the intended use of the GHG inventory is mandatory. Routine and consistent checks must be provided to ensure the accuracy and completeness of the GHG inventory. Errors and deficiencies should be identified and addressed; including documenting and archiving relevant GHG inventory records, including information management activities and key performance indicators. If the organization has a quality information management system, things become easier.

The responsibilities and authorities of those responsible for the development of the GHG inventory should be determined and reviewed. Appropriate training should be identified for members of the inventory development team. Establishment boundaries must be defined and reviewed. Review of GHG sources and sinks must be made. Selection of calculation approaches, including calculation and GHG calculation models used for data used in calculation approaches consistent with the intended use of the GHG inventory including data used for calculation and GHG calculation models, must be reviewed. Calculation approaches to ensure consistency between multiple facilities must be reviewed. A robust data collection system must be developed and maintained. Regular accuracy checks must be made. Periodic internal audits technical reviews and opportunities to improve information management processes must be periodically reviewed. GHG inventory must be documented and archived as required by quality management. Reasons for uncertainties should also be reported. Decisions taken under uncertainties are stated. Thus, the commitment statement is provided.

Table 1. Emission sources and scopes of Sporium Center at Gaziantep University

Scope	Emission Source	Units	Activity Data	Data Quality
Scope 1	Natural Gas	m^3	Monthly natural gas bills	Primary Data
	Air Conditioning	kWh	Monthly electricity bills	Primary Data
Scope 2	Electricity	kWh	Monthly electricity bills	Primary Data
	Water	m^3	Monthly water bills	Primary Data
Scope 3	Waste	Kg	Monthly amount of garbage thrown away	Primary Data

Computational analysis

Some methods such as IPCC [1], Environmental Protection Agency (EPA) [12], DEFRA [11], and ISO 14064 are used to calculate the amount of greenhouse gases. According to DEFRA (2023) [11], three different coverage approaches can be used in carbon footprint calculations in an excel sheet. In this study, within the scope of Gaziantep University Sporium Center, CF resulting from natural gas consumption and air conditioning use with the Scope 1 method, from electricity and water use with the Scope 2 method, and the amount of garbage with the Scope 3 method was calculated. In general, there are several formulas for calculating CF. These is;

•CF = Monthly Consumption x Emission Factor (1)

•Energy Consumption [TJ] = Fuel Consumption [t] × 10-3 × Conversion Factor [TJ/kt] (2)

•Carbon Content [Gg C] = Carbon Emission Factor [TC/TJ] × Energy Consumption [TJ] × 10-3 (3)

•Carbon Emission [Gg C] = Content of Carbon [Gg C] × Carbon Oxidation Ratio (4)

•Carbon Dioxide Emission [Gg CO_2] = Carbon emission [Gg C] × 44/12 (5)

Eq.1 is used directly when we multiply consumption data by carbon emissions. Eq.2-5 uses the formulas in the equations to transform consumption data.

CF due to natural gas consumption

Since natural gas is used only in the heating system in the sports center, natural gas consumption only occurs during the winter season and on certain dates of the year by Gaziantep Governorship. It is stated that the winter season is between 15 November and 15 April. For this reason, central heating systems are used only within the date ranges determined by the governorship. It provides service every day of the week, including weekdays and weekends. To determine the CF of the sports center resulting from natural gas con-

sumption, it is of great importance to make accurate calculations according to daily working hours of the sports center and the heating season, to observe the results well and interpret them correctly. Natural gas is consumed for an average of five months during the winter season. Since the natural gas in the sports center was allocated from the Gaziantep University heating center, monthly calculations could be made by converting the paid bills into m3. Calculation was made by the authorized personnel of the sports center using the records of natural gas bills and is presented in Table 2.

Table 2. Monthly natural gas consumption amounts the year 2023

Months	Natural Gas (m3)	CF (kg CO_2e)	Months	Natural Gas (m3)	CF (kg CO_2e)
January	29500	60180	July	14000	28560
February	30000	61200	August	14000	28560
March	22500	45900	September	19000	38760
April	15000	30600	October	22000	44880
May	14500	29580	November	28000	57120
June	14000	28560	December	29500	60180
				Total (Kg) (yearly)	514080

Table 3 shows the carbon emissions factor for natural gas consumption published by DEFRA in 2023. The equivalent emission factor in Table 3 is taken as the DEFRA natural gas emission factor. This emission factor used in CF calculations is multiplied by natural gas consumption values to calculate the equivalent carbon footprint using Equation 1;

Table 3. DEFRA 2023 natural gas emission factor

About Natural Gas Consumption Emission Factor	Equivalent Emission Factor $kgCO_2e$ 2.04
CF = Monthly Gas Consumption x Emission Factor	

Calculated CF are shown as monthly and one-year totals. The emission factor used in the calculations was taken as 2.04 $kgCO_2e$. According to calculations, CO_2 emission was determined as 514080 kg by multiplying the total amount of m3 natural gas consumed in a year with the carbon emission coefficient using Eq 1.

Since more natural gas is used in the winter months, more CO_2 is emitted compared to the summer months. It is calculated by considering that natural gas is used only in poolside showers and heating pool water during the summer months. Apart from these, another reason why natural gas carbon emission is low in the summer months is that the number of visitors to the sports center in the summer months is less than in the winter months.

CF from electricity consumption

The most used type of energy in sports center is electricity. This is because there are many activities in the sports center like pools, fitness, game rooms, astroturf pitches, basketball courts, etc. For these reasons, electricity is used in the sports center for twelve months of the year. Some machines operate twenty-four hours a day, and every day of the week. It has also been determined that electricity use varies according to months and seasons. Since there is no air conditioning in the winter months, it was determined that electricity usage was less than in the summer months. The number of visitors to the facility also made a difference in electricity usage. During calculation, monthly amount of electricity consumed was calculated based on the invoices determined by the Gaziantep University Administrative and Financial Affairs Department. It was converted into kilowatts according to the amount used by looking at the determined bills. The twelve-month electricity usage amount according to the electricity bills received is presented in Table 4.

Table 4. Monthly electricity consumption carbon emissions

Months	Monthly electricity consumption(kWh)	CF ($kgCO_2e$)	Months	Monthly electricity consumption amounts(kWh)	CF ($kgCO_2e$)
January	398452	82479.56	July	416556	86227.09
February	401865	83186.06	August	416865	86291.06
March	409563	84779.54	September	411976	85279.03
April	413048	85500.94	October	409368	84739.18
May	414535	85808.75	November	402192	83253.74
June	414898	85883.89	December	403767	83579.77
				TOTAL (kg) (yearly)	1017008,6

Table 5 shows the carbon emission factor for electricity consumption published by DEFRA in 2023. The equivalent emission factor in Table 5 is considered as the DEFRA electricity emission factor. This emission factor, used in carbon footprint calculations, is multiplied by electricity consumption values to calculate the equivalent carbon footprint. Using Equation 1;

In Table 4, the calculated CF are shown as monthly and 1-year total. The emission factor used in the calculations was taken as 0.207 $kgCO_2e$. In calculations, by multiplying the total kW value used for a year with the carbon emission coefficient, CO_2 emission was found to be 1017008.6 kg using Equation 1. Since more electricity is used in the summer months, slightly more CO_2 is emitted compared to the winter months. It was determined that the reason for this was the use of air conditioners (AC) in the sports center during the summer months. In addition, to determine the amount of carbon dioxide emissions resulting from electricity use in all sections of the sports center, CO_2 emissions of each section were calculated separately.

CF due to water consumption

There are many areas in the sports facility where water is used. The first of these areas is the pool. It is actively used twelve months of the year. Since pool maintenance is done once a week, all the water in the pool is renewed. General use of water is swimming pool, shower, WC, Canteen, Building cleaning, and irrigation in the garden. It is used in areas such as irrigation of basketball and football fields. An average of 200 people takes a shower per day at the facility. When calculating monthly water usage in the shower section, it is calculated based on the amount of water each person uses while taking a shower for an average of 5 minutes. Since there is active water use all throughout the year, not much difference was observed in monthly CO_2 emissions. Since there is no clear information on water use in each part of the facility, the amount of entire water used was calculated. In these calculations, the monthly water use was calculated based on the invoices determined by the Gaziantep University Administrative and Financial Affairs Department. It was converted to m3 according to the amount used by inspecting the determined invoices. The annual water use according to incoming water bills is presented in Table 6.

Table 5. DEFRA 2023 electricity emission factor

Pertaining Electricity Consumption Emission Factor	Equivalent Emission Factor $kgCO_2e$ 0.207
Carbon Footprint = Monthly Electricity Consumption x Emission Factor	

Table 6. Monthly water consumption amounts and carbon emissions

Months	Water (m^3)	CF ($kgCO_2e$)	Months	Water (m^3)	CF ($kgCO_2e$)
January	110000	19470	July	137000	24249
February	115000	20355	August	135000	23895
March	117500	20797.5	September	125000	22125
April	123000	21771	October	120000	21240
May	128000	22656	November	110000	19470
June	135000	23895	December	115000	20355
				Total (Kg) (yearly)	260278.5

Table 7 shows the carbon emission factor for water consumption published by DEFRA in 2023. The equivalent emission factor in Table 9 is taken as the DEFRA water emission factor. This emission factor, used in CF calculations, is multiplied by water consumption values to calculate the equivalent CF using Equation 1.

Table 7. DEFRA 2023 water emission factor

Water Consumption Emission Factor	**Equivalent Emission Factor** $kgCO_2e$
	0.177
CF = Water Consumption Data x Emission Factor	

In Table 6, the calculated CF amounts are shown as monthly and annually. The emission factor used in the calculations was taken as 0.177 $kgCO_2e$. According to calculations, when the annual total m3 value used is multiplied by the carbon emission coefficient, CO_2 emission is found to be 260278.5 kg using Equation 1. When an observational evaluation was made, it was seen that the most water usage areas were pools and showers. As a result of the calculations, it was seen that the amount of carbon emissions in the summer months was higher than in the winter months, depending on the amount of water used. Table 10 shows that carbon emissions in June, July, and August are slightly higher than the other months. The main reason for this fact is that the pool is used more in summer and therefore the showers are used more.

CF due to air conditioning use

During the winter months, natural gas is used for heating in the sports center. In summer, air conditioning is used for cooling purposes. Although using an AC may seem like consumption of electricity, air conditioners (ACs) contain gas. This gas affects carbon emissions. During the summer months, the sports center is open every weekday. During summer months, ACs operate between these hours. There is a total of 6 ACs in the facility. To determine the CF of the sports center resulting from the use of AC, it is of great importance to make accurate calculations according to the daily working hours of the sports center and the cooling season and to observe and interpret the results. The carbon emissions released from the effect of AC in the sports center on electricity consumption were calculated while calculating electricity consumption. In this section, only the carbon emissions resulting from the exhaustion time of the air conditioning gas are calculated. This calculation was done considering that the air conditioners used in the sports center are industrial ACs and contain R410A gas as presented in Table 9.

Table 8. Monthly air conditioning usage amounts and carbon emissions

Months	AC (kg)	CF ($kgCO_2e$)	Months	AC (kg)	CF ($kgCO_2e$)
January	11.3	21741.2	July	17.3	33285.2
February	11.4	21933.6	August	17.7	34054.8
March	10.6	20394.4	September	15.5	29822
April	14.6	28090.4	October	14.7	28282.8
May	15.3	29437.2	November	10.9	20971.6
June	17.4	33477.6	December	11.1	21356.4
				Total (Kg) (yearly)	322847.2

Table 9 shows the carbon emission factor for industrial air-conditioning gas use published by DEFRA in 2023. The equivalent emission factor in Table 12 is taken as the DEFRA industrial air conditioning gas use emission factor. This emission factor used in CF calculations is multiplied by industrial AC usages to calculate the equivalent CF using Equation 1.

Table 9. R410A gas emission factor

	Equivalent Emission Factor
Emission Factor Related to Industrial AC Gas Use	**$kgCO_2e$**
	1924
CF = R410A gas usage data x Emission Factor	

In Table 8, the calculated CF amounts are shown as monthly and annually. The emission factor used in the calculations was taken as 1924 $kgCO_2e$. According to calculations, when the annual total kg value of R410A air conditioning gas used is multiplied by the carbon emission coefficient, CO_2 emission is found to be 322847.2 kg using Equation 1.

There is a calculation on R410A gas used by the 6 air conditioners. An average AC consumes 13.6 kg of R410 gas after approximately 2 years (365x2x4=2920 hours) by operating 4 hours a day. According to this ratio, an AC that works 13 hours a day works 390 hours a month. Since there are six ACs in the facility, they operate for 2340 hours. Six ACs consume a total of 10.9 kg of R410 gas. The consumption amount in all months was calculated accordingly and multiplied by the carbon emission rate of R410A gas. As a result of these calculations, it was seen that less AC was used in the winter months than in the summer months (see Table 8).

CF from discarded garbage

There are many areas within the sports facility. In addition to the pool, fitness, and playgrounds, there is also a canteen where food and beverages are sold. It is provides service during the time the facility is open between 09.00 and 22.00 on weekdays and weekends. To determine the CF resulting from the amount of garbage in the sports center, it is of great importance to make accurate calculations, observe and interpret it according to the daily working hours of the sports center and the number of visitors in the canteen. The average amount of garbage using the canteen section on a monthly and annual basis is given by the personnel working at Gaziantep University Sporium Center. Monthly and annual amounts of garbage collected are presented in Table 10. Table 11 shows the carbon emission factor for the amount of litter published by DEFRA in 2023.

The calculated CF is shown monthly and annually. The emission factor used in the calculations was taken as 21.281 $kgCO_2e$. When the total annual kg used was multiplied by the carbon emission coefficient, CO_2 emission was found to be 925723.5kg. Since the total amount of garbage in the facility was calculated in general, it could not be determined in which areas more garbage was discarded.

It was seen that the amount of carbon emissions in the winter months was higher than in the summer months, depending on the amount of garbage. The main reason for this is that the number of people visiting the facility in the summer months varies between 1000-1500 people whereas this value in the winter months is between 3000-3500 people. It was observed that seasonal and monthly carbon emissions differ depending on the number of visitors.

CF of the facility due to the number of visitors

There are many activity areas in the sports facility. Use of

these activity areas varies depending on the number of visitors. These are the amount of garbage generated, and the amount of water used based on the number of visitors to the facility, use of game tables in playgrounds depending on the visitor density of the facility. Data provided by the personnel working at Gaziantep University Sporium Center, the number of visitors to the sports center could be calculated monthly. In Table 12, the monthly CF per person was calculated by adding up the CO_2 emissions of natural gas, air conditioning, electricity, water, and garbage used separately for each month and dividing by the number of visitors of that month. It was determined that the number of people visiting the facility was inversely proportional to the amount of CF per person. One of the most important reasons for this was the use of electricity and natural gas in the facility's operating areas, regardless of the number of visitors. CF data according to the number of visitors is given in Table 12. Using Equation 1;

January Carbon Footprint=268994 $kgCO_2e$/3200 visitors= 84 carbon footprint

April Carbon Footprint =239381 $kgCO_2e$ / 2150 visitors= 111 carbon footprint

Table 10. Monthly amounts of garbage and carbon emissions

Months	Garbage (kg)	CF ($kgCO_2e$)	Months	Garbage (kg)	CF ($kgCO_2e$)
January	4000	85124	July	3250	69163.25
February	4100	87252.1	August	3150	67035.15
March	3750	79803.75	September	3450	73419.45
April	3450	73419.45	October	3700	78739.7
May	3400	72355.4	November	3800	80867.8
June	3350	71291.35	December	4100	87252.1
				Total (Kg)(yearly)	925723.5

Table 11. DEFRA 2023 garbage emission factor

	Equivalent Emission Factor
Emission Factor for the Amount of Garbage	**$kgCO_2e$**
	21.281
CF = Garbage amount data x Emission Factor	

Annual CF calculations

Gaziantep University Sporium Center has been in service since 2014. Many activities are carried out in the sports center, whose number of visitors has been increasing day by day since the day it was opened. While performing these activities, some consumption and waste occur. There are consumption and wastes such as natural gas consumption, air conditioning consumption, electricity consumption, water consumption, and amount of garbage. It is open every day of the week, on weekdays and weekends, between 9 am and 10 pm. The carbon emissions of the sports center resulting from this consumption and waste were calculated separately according to the amount, type, and time of use. These calculations were calculated in line with the data by the staff of Gaziantep University Thermal Center and Sporium Center. Monthly carbon footprint calculations based on the monthly usage amounts of what is consumed in the facility and the numbers of visitors are given in Table 12. According to these data, annual average CO_2 emissions and monthly average CF per person were calculated. Finally, carbon emissions are presented in Table 13, showing the Monthly Average CO_2e and Average Monthly CF per person.

Table 12. Carbon footprint according to the number of monthly visitors

Months	Number of Visitors	CF ($kgCO_2e$)	Months	Number of Visitors	CF ($kgCO_2e$)
January (84.1)	3200	268994.8	July (161)	1500	241484.5
February (103.4)	2650	273926.8	August (184.5)	1300	239836
March (111.9)	2250	251675.2	September (110.8)	2250	249405.5
April (111.3)	2150	239381.8	October (105.3)	2450	257881.7
May (123	1950	239837.3	November (87.2)	3000	261683.1
June (124.7)	1950	243107.8	December (85.2)	3200	272723.3
				Total (Kg) (yearly)	3039937.8

Table 13. Annual CF of Gaziantep University Sporium Center

Monthly Average CO_2e	**253328.15 kg**
Average Monthly CF Amount per Person	**116 kg**

DISCUSSION

CF of the Gaziantep University Sporium Center was assessed by calculating the consumption of natural gas, water, air conditioning, electricity, and garbage. Equivalent emission coefficients published by DEFRA in 2023 were utilized in the calculations. Analysis of the calculated values reveals higher electricity carbon emissions in summer compared to winter. This is primarily attributed to increased air conditioning usage and more active utilization of the facilities during the summer months. It is observed that natural gas carbon emissions are higher in winter than in summer, primarily due to the facility's use of natural gas for heating during the colder months. There is minimal variation in water carbon emissions between winter and summer months, largely because the pool operates year-round, consuming water consistently. Higher AC R410A gas carbon emissions are observed in summer, reflecting the facility's use of natural gas for cooling during warmer months. Lower carbon emissions from garbage disposal are observed in summer compared to winter, primarily due to reduced visitor numbers during the summer months. It is noted that the average carbon footprint per person is inversely proportional to the number of facility visitors, as factors such as water usage in the pool and energy consumption remain relatively constant regardless of visitor numbers.

It is clear that sports competitions or the lives of athletes significantly impact carbon footprint. The average carbon emissions per person for a sports competition have been determined to be 100 kg in a sport activity [13]. Comparing our finding of 109 kg, we conclude that Gaziantep University Sporium Center is close to the average value.

CONCLUSION

CF calculation was made at the Gaziantep University Sporium Center for the year 2023. It has been calculated as kg equivalent CO_2;

•514080 $kgCO_2e$ emissions were calculated from the use of natural gas using the DEFRA Methodology Scope 1 approach of the facility's primary CF.

•322847.2 $kgCO_2e$ emissions were calculated from air conditioning by using the DEFRA Methodology Scope 1 approach of the facility's primary carbon footprint.

•1017008.6 $kgCO_2e$ emissions were calculated from electricity consumption using the DEFRA Methodology Scope 2 approach of the facility's primary carbon footprint.

•260278.5 $kgCO_2e$ emissions were calculated for plant's water use.

•925723.5 $kgCO_2e$ emissions were calculated for garbage disposal using the DEFRA Methodology Scope 3 approach.

The average monthly CO_2 emission of the facility has been calculated as 253328 tCO_2e. The average amount of CF per person per month was calculated as 116 kg.

According to the data, the largest share of CF belongs to electricity, natural gas, and air conditioning consumption, respectively. Since the largest share is electricity consumption, reducing emissions resulting from electricity consumption is an important step in reducing the CF. Our university needs to turn to renewable energy sources, and work on the effective use of energy in buildings should be accelerated. Electricity consumption mainly comes from lighting, heating/cooling, and air handling units, dressing rooms, game rooms, fitness centers, fields, and elevator use. Economical lamps are gen-

erally used in our university. Expanding the use of photocell lamps, replacing the equipment used in dressing rooms, game rooms, and fitness centers with energy-saving vehicles, and choosing stairs instead of elevators will reduce the carbon emissions caused by electricity for both the environment and our health.

DATA AVAILABILITY STATEMENT

The author confirm that the data that supports the findings of this study are available within the article. Raw data that support the finding of this study are available from the corresponding author, upon reasonable request.

CONFLICT OF INTEREST

The author declared no potential conflicts of interest with respect to the research, authorship, and/or publication of this article.

USE OF AI FOR WRITING ASSISTANCE

Not declared.

ETHICS

There are no ethical issues with the publication of this manuscript.

REFERENCES

[1] IPCC. (2006). National Greenhouse Gas Inventories Vol: 5 Waste, Intergovernmental. (Date of Access, December 2023).

[2] M., Batar, "Efficient Web-Based Application Development for Carbon Footprint Calculation: Example of Burdur Province", Celal Bayar University Journal of Science, Vol: 18, Issue: 1 pp: 33-39 2022. Doi: 10.18466/cbayarfbe.977279.

[3] United Nations Framework Convention on Climate Change; "The Paris Agreement" 1998, https://unfccc.int/sites/default/files/resource/parisagreement_publication.pdf (Date of Access, December 2023)

[4] IPCC, "AR4 Climate Change 2007: Synthesis Report". The Intergovernmental Panel on Climate Change, 2007. (Date of Access, December 2023)

[5] National Center for Biotechnology Information, 2019, (Date Of Access, December 2023) https://www.ncbi.nlm.nih.gov/.

[6] G. Binboğa, (2018) "A Research on the Calculation of the Carbon Footprint of Manisa Celal Bayar University on the Axis of Sustainability". International Journal of Economic and Administrative Studies, 2018 (21): 187-202 ISSN 1307-9832, 2018.

[7] Ministry of Environment and Forestry. "Kyoto Protocol Flexibility Mechanisms and Other International Emissions Trading Systems Specialized Commission Report" (Report No: B.18. ÇYG.0.02.00.04-020/8366). Ankara (2008). (Date Of Access, December 2023)

[8] M. M., Dam, "Sera Gazı Emisyonlarının Makroekonomik Değişkenlerle İlişkisi: Oecd Ülkeleri İçin Panel Veri Analizi". PhD. Thesis, 2014. http://adudspace.adu.edu.tr:8080/jspui/bitstream/11607/401/1/dr_tez-mdam.pdf.

[9] T.R. Ministry of Foreign Affairs, "Entrepreneurial and Humanitarian Foreign Policy Paris Anlaşması". T.C. Dışişleri Bakanlığı (mfa.gov.tr) 2022, (Date of Access, December 2023)

[10] Global Footprint Networking Türkiye's Ecological Footprint Report (2012) https://www.footprintnetwork.org/content/images/article_uploads/Türkiye_Ecological_Footprint_Report_Turkish.pdf (Date of Access, December 2023)

[11] DEFRA Methodology, 2023, https://www.gov.uk/government/publications/greenhouse-gas-reporting-conversion-factors-2021 (Date of Access, October 2023)

[12] Environmetal Protection Agency (EPA). 2021 "Sources of Greenhouse Gas Emissions" https://www.epa.gov/ghgemissions/sources-greenhouse-gas-emissions (Date of Access, December 2023)

[13] Ünal H., Bağcı E. 2017 Sports organizations in the light of environmental sustainability and ecologic footprint, Journal of Human Sciences, 14 (3), 3006-3021.

Environ Res Tec, Vol. 8, Issue. 2, pp. 410-424, June 2025

Environmental Research and Technology
https://dergipark.org.tr/en/pub/ert
DOI: https://10.35208/ert.1502424

Environmental Research & Technology

Research Article

Can renewable energy sources alleviate the pressure of military expenditures on the environment? Empirical evidence from Turkiye

Emre AKUSTA[1]

[1]*Kirklareli University, Department of Economics, Kofcaz, 39100 Kirklareli, Türkiye*

ARTICLE INFO

Article history
Received: 18 Jun 2024
Revised: 14 Aug 2024
Accepted: 24 Sep 2024

Key words:
Military expenditures, environmental impact, CO_2 emissions, renewable energy, ARDL.

ABSTRACT

This study analyzes the potential of renewable energy sources to reduce the environmental impact of military expenditures in Turkiye. ARDL method is preferred in the analysis using annual data for the period 1990-2021. In addition, an interaction term is added to the model to determine the effectiveness of renewable energy sources. The results show that military expenditures have a positive impact on CO_2 emissions in the short and long run with coefficients of 0.260 and 0.196, respectively. Moreover, renewable energy use has a statistically significant negative impact on CO_2 emissions in the short and long run with coefficients of -0.119 and -0.120, respectively. GDP has a positive impact on CO_2 emissions in the short and long run with coefficients of 0.162 and 0.193, respectively. Although population growth does not have a statistically significant impact in the short run, it is found to increase CO_2 emissions in the long run with a coefficient of 0.095. Moreover, the interaction term shows that renewable energy use reduces the environmental impact of military expenditures in Turkiye in the short and long run with coefficients of -0.130 and -0.140, respectively. The results indicate that renewable energy use can play an important role in mitigating the environmental impacts of military expenditures.

Cite this article as: Akusta E. Can renewable energy sources alleviate the pressure of military expenditures on the environment? Empirical evidence from Turkiye. Environ Res Tec 2025;8(2) 410-424.

INTRODUCTION

Security and defense have been one of the most important priorities of states throughout human history. This need is important for societies to sustain their existence, become a regional power and access new sources of wealth. This is described by [1] as states constantly strengthening their defense mechanisms in order to protect their economic welfare and ensure their security. However, in the modern world, this process is no longer limited to military capabilities. Economic dynamics, security challenges and environmental impacts determine defense strategies and policies.

The widespread use of oil after the industrial revolution increased the demand for energy and accelerated the industrialization and economic growth processes of countries. In this period, the results of wars were determined not by the number of soldiers but by technical weapons and logistical support. Therefore, having strong economies and industrialization became critical for defense [1], [2]. Stable economic growth requires industrialization and defense activities. Economic progress cannot be sustained without a developed industrial infrastructure and a strong defense mechanism. These three factors are closely integrated. Industrialization supports economic growth through its capacity to both create jobs and provide greater economic diversification. At the same time, advanced industrial production provides the infrastructure and technology needed to develop defense technologies. In addition to ensuring national security, a strong defense sector contributes to economic growth by stimulating high-tech research and innovation. This synergy

***Corresponding author.**
*E-mail address: emre.akusta@klu.edu.tr

This is an open access article under the CC BY-NC license (http://creativecommons.org/licenses/by-nc/4.0/).

is more apparent in developed countries. In underdeveloped countries, however, excessive military expenditures can have a negative impact on economic growth [3], [4]. However, these activities are not limited to military capacity, but are directly linked to the continuity of energy resources. Industrial activities, defense operations and economic growth cannot be sustained without energy resources. The importance of energy leads states to increase their defense expenditures in order to access or protect energy resources. This makes the interaction between energy and defense one of the most important economic and political issues for states. Therefore, there is a strong interaction between energy policies and defense expenditures. Military expenditure, which is intertwined with industrialization and economic growth, may also conflict with environmental sustainability goals. In this context, policies at the national and global level are central to the sustainability of economic activities, access to energy resources and defense strategies.

Interest in renewable energy sources has increased due to their potential to reduce environmental destruction and increase energy security. Therefore, global energy policies have been revised to reduce greenhouse gas emissions and increase the use of renewable energy sources. These steps have been supported by international agreements and protocols. For example, agreements such as the United Nations Framework Convention on Climate Change and the Kyoto Protocol have formalized countries' commitments to reduce greenhouse gas emissions. Renewable energy sources are also an important alternative for energy-dependent and resource-limited countries. By replacing limited fossil fuels, these resources can increase countries' energy security and improve their economic balance. Furthermore, the report by [5] estimates that renewable energy sources will account for two-thirds of the total energy supply by 2050. This plays a critical role in reducing energy-related CO_2 emissions and limiting global temperature rise.

Sustainable development can be defined as the process of meeting the needs of the present without compromising the ability of future generations to meet their needs. By supporting environmental sustainability in this process, renewable energy sources can provide many benefits such as increasing energy security and reducing environmental pollution. Moreover, energy R&D expenditures and innovative technologies can make significant contributions to increasing renewable energy production and reducing costs [6]. In this regard, integrating renewable energy policies with military strategies would be an important step in terms of both economic and environmental sustainability. However, the environmental impacts of military expenditures also pose a challenge for sustainable development. The environmental costs of military activities and the defense industry are one of the obstacles to sustainable growth. In this respect, a green growth approach can play a critical role in balancing both the economic and environmental impacts of military expenditures. Therefore, the impact of military expenditures on environmental quality should be reassessed and the use of renewable energy sources should be encouraged. This approach can both reduce environmental damage and support energy security and economic stability. To this end, this study investigates whether renewable energy sources can reduce the environmental impacts of military expenditures in Turkiye.

This study will contribute to the literature in at least three ways. Firstly, previous studies have generally investigated the impacts of military expenditures or renewable energy on the environment independently. However, there has been no analysis on the interactions between these two factors. To the best of our knowledge, this is the first study to investigate the potential of renewable energy sources to reduce the environmental impacts of military expenditures in Turkiye. Secondly, this study uses the interaction term methodology to analyze the interaction between military expenditures and renewable energy use in Turkiye. This methodology was chosen specifically to examine the interactive impacts of these two variables on the environment, an approach that is not often used in the Turkish context. Finally, this study is conducted using the most recent datasets available in Turkiye.

The rest of the paper is organized as follows: Section 2 presents military expenditures and CO_2 emissions in historical perspective, Section 3 presents the literature review, Section 4 presents the data and methodology, Section 5 presents the empirical findings and finally Section 6 presents the conclusions and policy implications.

MILITARY EXPENDITURES AND CO_2 EMISSIONS IN HISTORICAL PERSPECTIVE

Global warming and environmental pollution are one of the greatest challenges of today's world. The use of fossil fuels and industrial activities are often at the root of environmental problems, which can have serious consequences such as climate change and the degradation of ecosystems. However, another important but often overlooked source of environmental pollution is military expenditures and activities. Military expenditures are often associated with high energy consumption and fossil fuel use. This can trigger environmental pollution both directly and indirectly by increasing CO_2 emissions.

Military activities include a wide range of energy-intensive operations. These operations range from logistical support to the use of fighter aircraft, which consume high amounts of fossil fuels. Moreover, the construction and maintenance of military infrastructures also requires significant consumption of energy and resources. Obviously, understanding the impact of military expenditures on CO_2 emissions and their contribution to environmental pollution is an important area of research in line with sustainable development goals. Moreover, while many countries increase their defense budgets, they may ignore the environmental impacts of these expenditures. Increases in defense budgets are often in direct conflict with environmental policies [7]. Therefore, assessing the environmental impacts of military expenditures and developing strategies to minimize these impacts are of great importance for both national and global environmental poli-

cies. In this regard, the historical development of military expenditures in Turkiye and the world is presented in Figure 1.

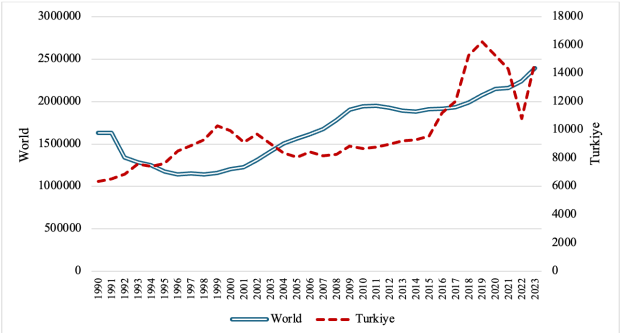


Figure 1. Evolution of military expenditures. Source: Constructed with data from [8].

Figure 1 shows military expenditures in Turkiye and the world in constant thousand dollars. Figure 1 shows that there was a general downward trend in military expenditures worldwide in the 1990-2000 period. Military expenditures decreased from approximately 1.6 trillion dollars in 1990 to approximately 1.2 trillion dollars in 2000. Factors such as the end of the Cold War and the dissolution of the Eastern Bloc were influential in the decline in expenditures during this period. These changes led many countries to cut their defense budgets and reduce their military expenditures. However, local conflicts and civil wars in some regions caused military expenditures to remain high on a local basis. Since 2001, military expenditures have started to increase again worldwide. While military expenditures were approximately 1.22 trillion dollars in 2001, they increased to approximately 1.94 trillion dollars in 2010. In this period, especially the counter-terrorism operations launched after the September 11 attacks and the conflicts in the Middle East were decisive in the increase in military expenditures. Many countries have sought to increase their defense capacities against security threats. The global war on terrorism led to significant increases in the defense budgets of the US and its allies [9], [10]. Military expenditures remained at high levels in the 2011-2023 period. Reaching 2.16 trillion dollars in 2021, expenditures increased to 2.39 trillion dollars in 2023. In this period, the increase in global security threats and the continuation of military conflicts in various regions caused expenditures to remain at high levels. During this period, China's efforts to increase its military power and events such as Russia's intervention in Ukraine were effective in increasing military expenditures [11]. At the same time, investments in new areas such as cyber security and space defense have also contributed to the increase in military budgets.

Figure 1 shows that Turkiye's military expenditures have generally fluctuated against the global trend. In the 1990-2000 period, Turkiye's military expenditures showed a general upward trend. From approximately 6.85 billion dollars in 1992, military expenditures reached 10.27 billion dollars in 1999. During this period, Turkiye's fight against terrorism was an important factor in the increase in military expenditures. Turkiye maintained a strong defense policy against internal security threats and accordingly increased its military expenditures [12], [13]. Turkiye's military expenditures fluctuated between 2001 and 2010. From 9.11 billion dollars in 2001, expenditures remained around 8.69 billion dollars in 2010. Economic crises and financial discipline were effective in the fluctuating course of expenditures in this period. In this period, Turkiye made adjustments in its defense budget in order to ensure economic stability. In the 2011-2023 period, a significant upward trend was observed in Turkiye's military expenditures. From USD 12.03 billion in 2017, expenditures reached USD 15.27 billion in 2018 and USD 14.32 billion in 2021. However, expenditures were recorded as USD 14.74 billion in 2023. Meanwhile, Turkiye's regional security policies, investments in the defense industry and operations in Syria played an important role in the increase in military expenditures. Turkiye took important steps to develop its own defense industry, which led to an increase in military expenditures. In particular, domestically produced weapons and equipment projects have played an important role in Turkiye's military budget. Moreover, Turkiye's efforts to protect its interests in the Eastern Mediterranean and disputes over energy resources in the region have also contributed to the increase in military expenditures.

After examining the historical evolution of military expenditures, it is important to review the historical evolution of CO_2 emissions in order to better understand the environmental impacts of these expenditures. Therefore, Figure 2 illustrates the historical development of CO_2 emissions for both Turkiye and the world.

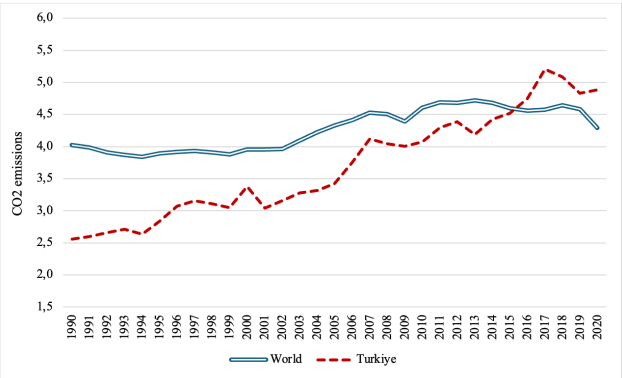


Figure 2. CO_2 emissions in Turkiye and the world. Source: Constructed with data from [14].

Figure 2 shows CO_2 emissions in Turkiye and the world in metric tons per capita. In the 1990-2000 period, CO_2 emissions per capita in the world generally followed a fluctuating trend. CO_2 emissions, which were about 4.02 metric tons in 1990, declined to about 3.95 metric tons in 2000. During this period, increased environmental awareness and straitening of environmental regulations in some industrialized countries were effective in reducing emissions. In particular, the signing of the Kyoto Protocol strengthened countries' commitments to reduce carbon emissions. However, increasing energy demand and intensive use of fossil fuels in developing countries limited the decline in global carbon emissions. The impact of global economic growth in this period should also be taken into account. Economic growth leads to an increase in energy consumption and thus higher carbon emissions.

However, the adoption of sustainable energy policies and investments in renewable energy sources can help offset this impact. Between 2001 and 2010, CO_2 emissions worldwide started to increase again. Emissions of about 3.96 metric tons in 2001 increased to about 4.60 metric tons in 2010. During this period, the increase in energy consumption and the widespread use of fossil fuels, especially in countries with rapid economic growth such as China and India, have been decisive in the increase in global CO_2 emissions [15]. In addition, high energy demand in developed countries such as the US has also contributed to the increase in global emissions. Some developed countries have continued their efforts to reduce carbon emissions through energy efficiency projects and renewable energy investments. However, the dominance of fossil fuels in energy production continued [16], [17]. On the other hand, CO_2 emissions worldwide followed a fluctuating pattern in the 2011-2020 period. Emissions, which were approximately 4.69 metric tons in 2011, decreased to approximately 4.29 metric tons in 2020. In this period, the increase in the use of renewable energy sources and energy efficiency measures were effective in reducing emissions. Moreover, with the signing of the Paris Agreement, many countries strengthened their commitments to reduce carbon emissions. However, the continued use of fossil fuels in some regions and the unabated industrialization caused global emissions to remain at high levels. The economic recession, especially during the COVID-19 pandemic, led to a decline in emissions in 2020, but this decline was not permanent [18].

In the 1990-2000 period, Turkiye's per capita CO_2 emissions showed a general upward trend. CO_2 emissions, which were about 2.56 metric tons in 1990, increased to about 3.37 metric tons in 2000. During this period, Turkiye's industrialization and urbanization processes accelerated and the increase in energy consumption and fossil fuel use played an important role in the increase in emissions. In particular, the widespread use of fossil fuels such as coal and natural gas in energy production contributed to the increase in Turkiye's carbon emissions. However, Turkiye's efforts to invest in renewable energy sources and implement energy efficiency projects can contribute to reducing carbon emissions in the long run [19]. Turkiye's CO_2 emissions followed a volatile trend in the period 2001-2010. Emissions increased from about 3.04 metric tons in 2001 to about 4.07 metric tons in 2010. In this period, Turkiye's economic growth and the increase in energy demand were the determinants of the increase in carbon emissions. The increased use of fossil fuels, especially in the industrial and transportation sectors, led to an increase in emissions. However, investments in renewable energy sources and energy efficiency projects have tried to limit the rate of increase in emissions. The widespread use of fossil fuels in the industrial and transportation sectors in Turkiye has been an important factor in the increase in carbon emissions [20]. During this period, shifting Turkiye's energy policies towards renewable resources and adopting environmental sustainability policies, expanding energy efficiency projects and reducing fossil fuel use can help reduce carbon emissions. In the period 2011-2020, Turkiye's CO_2 emissions showed a general upward trend. Emissions increased from about 4.29 metric tons in 2011 to about 4.88 metric tons in 2020. Throughout this period, Turkiye's efforts to transition to renewable sources in energy production increased, but fossil fuels continued to dominate. In particular, the high use of natural gas and coal led to an increase in carbon emissions. Turkiye's policies to comply with the Paris Agreement and its investments in renewable energy are considered as important steps towards reducing carbon emissions. Increasing the use of renewable energy sources and expanding energy efficiency projects can contribute to reducing Turkiye's carbon emissions. However, the dominance of fossil fuels in energy production and the continuation of the industrialization process will prevent the complete reduction of carbon emissions [21], [22]. In this regard, it is of great importance for Turkiye's energy policies to shift towards renewable energy sources and adopt environmental sustainability policies in line with sustainable development goals.

LITERATURE REVIEW

Studies investigating environmental degradation and its causes focus on factors such as urbanization and industrialization, as well as their links to variables such as energy consumption, globalization, military expenditures, financial development and economic growth. The environmental impacts of these factors vary according to the characteristics of the country, region or sample analyzed. The literature provides a wide range of findings to understand the impacts of these variables on environmental degradation, thus contributing to the shaping of environmental policies at the regional and global level.

It is widely recognized that the environmental impacts of military activities, the increasing need for energy and the fossil fuels used in this process cause environmental damage [23], [24]. Military operations consume large amounts of fossil fuels, leading to increased carbon dioxide emissions and environmental damage. In addition, equipment such as military vehicles, helicopters, tanks and ships also consume large amounts of fossil and nuclear fuels. Researchers such as [25] and [7] emphasize that this situation contributes to increasing environmental degradation. In particular, [26] point out that the environmental impacts of military activities are not limited to the period in which they are carried out and lead to long-term ecological destruction. Encouraging renewable energy sources can offer a solution to these problems. Renewable energy sources such as wind, solar and hydropower contribute to improving air quality and reducing environmental pollution [27]. Increasing renewable energy consumption can significantly reduce per capita carbon emissions, especially in low-income countries. This demonstrates the potential of renewable energy to alleviate environmental pressures [28]. Furthermore, renewable energy projects can address issues related to clean water and sanitation systems, such as sustainable water supplies, water reuse, recycling and providing treatment facilities [29]. Renewable

energy technologies are advantageous in terms of cost-effectiveness, safety and environmental sustainability and offer a more sustainable energy supply by reducing dependence on fossil fuels [30]. Therefore, the use of renewable energy to reduce the environmental impacts of military expenditures is of strategic importance for both national security and environmental sustainability.

Studies examining the relationship between energy consumption and environmental damage reveal the impacts of energy consumption on the environment. Kesbic and Bozduman [31] found that the increase in energy consumption in Turkiye increases CO_2 emissions and causes environmental pollution. Chontanawat [32] reported that there is a strong relationship between energy consumption and carbon emissions in ASEAN countries. Çetin and Yüksel [33] examined the relationship between energy consumption and carbon emissions in Turkiye within the framework of the Environmental Kuznets Curve (EKC) hypothesis and concluded that energy consumption increases carbon emissions. Al-Mulali and Sab [34] found a long-run relationship and bidirectional causality between electricity consumption and CO_2 emissions in Middle Eastern countries. Lee and Yoo [35], [36], in their separate studies for Mexico and Korea, observed bidirectional causality between energy consumption and CO_2 emissions. Doğan and Topallı [37] find bidirectional causality between energy consumption and CO_2 in Turkiye. Özkan and Erdemli [38], in their study on Turkiye and its border neighbors, showed that energy consumption has a positive relationship with CO_2 emissions in the long run.

The relationship between economic growth and environmental degradation has been analyzed in different aspects by various studies. The Environmental Kuznets Curve (EKC) hypothesis is a frequently used theory in these studies. Öztürk and Acaravcı [39] find that the EKC hypothesis is not valid for the period 1968-2005 in Turkiye. On the other hand, [40] find that the EKC hypothesis is valid for the period 1970-2010 in Algeria. Ahmad and Du [41], in their study for Iran, found that economic growth increases environmental pollution. Similarly, [42] showed that economic growth increases carbon emissions in Azerbaijan. Gökmenoğlu and Sadeghieh [43], in their long-run study on Turkiye, found that economic growth has a significant and negative impact on carbon emissions. The study by [44] in 12 MENA countries showed that economic growth causes environmental pollution. Chen et al. [45] found a unidirectional relationship between economic growth and carbon emissions in China and reported that economic growth continues to have negative impacts on the environment.

Studies investigating the impacts of financial development on environmental degradation reveal that financial development can have both positive and negative environmental consequences. Tamazian et al. [46] reports that high economic and financial development in BRIC economies improves environmental quality. Similarly, [47] finds that financial development in India reduces carbon emissions. Pata [48], in his analysis for Turkiye, showed that financial development increases carbon emissions along with energy consumption, urbanization and industrialization. Özkan and Erdemli [38] find a positive long-run relationship between energy consumption and environmental pollution in Turkiye and neighboring countries.

The environmental impacts of the globalization process vary between developed and developing economies. Shahbaz et al. [49] reported that globalization has negative impacts on environmental quality in developed economies. Apaydın [50] showed that globalization increased the ecological footprint of globalization in Turkiye but decreased the ecological footprint of exports. Wang et al. [51] reported that economic globalization increased environmental degradation in G7 countries, while the increase in the agricultural sector reduced carbon emissions. Karasoy [52] found that globalization, industrialization and urbanization have negative impacts on ecological footprint in Turkiye. Finally, [53] found that globalization reduces environmental damage in Turkiye, but urbanization increases environmental damage.

The rapid increase in urbanization leads to increased environmental damage, especially in developing countries. The impacts of urbanization on energy consumption, carbon emissions and ecological footprint are among the issues that have been researched. The environmental impacts of urbanization are intensively studied especially in developing countries. Yıldız and Göktürk [54] reported that urbanization creates a positive relationship between energy consumption and carbon dioxide emissions in Turkiye. Phong [55] showed that urbanization increases carbon dioxide emissions in ASEAN-5 countries and financial development supports this impact. Karasoy [52] found that urbanization, industrialization and energy consumption increase the ecological footprint in the short run in Turkiye. Apaydın [50] stated that the interactions between globalization and urbanization increase the ecological footprint, and this process triggers environmental degradation across Turkiye.

The literature on the environmental impacts of military expenditures generally analyzes the impacts of military expenditures on carbon emissions and environmental degradation. Ahmed et al. [56] examined the relationship between defense expenditures, energy consumption, carbon dioxide emissions and economic growth in Myanmar for the period 1975-2014. The results of the study show that defense expenditures have a negative impact on economic growth, while energy consumption supports growth. Ahmed et al. [57], in their study covering 22 OECD countries, found that defense expenditures increase carbon emissions. Similarly, [58] found a positive and significant relationship between military expenditures and CO_2 emissions in their study covering 120 countries. In a study conducted by [59] for 12 countries with the highest military expenditures, it was found that military expenditures have a positive impact on green growth in developed countries and a negative impact in less developed countries. A study by [25] on G7 countries finds a unidirectional causality between militarization and CO_2 emissions. In another study, [60] pointed out that militarization increases CO_2 emissions in the US. Erdoğan et al. [61], in their study for Greece, France, Italy and Spain, stated

that military expenditures have serious negative impacts on the environment.

Kwakwa [62] finds that military expenditures, along with industrialization and public expenditures, increase CO_2 emissions in Ghana. Similarly, [63] revealed the positive impacts of defense spending on CO_2, NO2 and methane emissions. Qayyum et al. [64] find that military expenditures and armed conflicts in South Asia led to ecological degradation. Zandi et al. [65] find that military expenditures increase CO_2 emissions in Far East Asian countries. On the other hand, there are few studies suggesting that military expenditures can improve environmental quality. For example, [66] argue that military R&D activities can reduce environmental degradation through technology innovation, while [67] argue that militarization in India can reduce carbon emissions.

The findings of studies conducted in Turkiye are similar to the general literature. Kurt and Kılıç [68] find that there is a long-run and bidirectional causality relationship between military expenditures and environmental damage. Gökmenoğlu et al. [6] found that military expenditures increase environmental degradation. Erdoğan [69], meanwhile, found no significant relationship between defense expenditures and carbon emissions in the long run, but showed that defense expenditures affect carbon emissions in the short run.

Contrary to the limited number of studies suggesting that military expenditures can improve environmental quality, it is generally found to cause environmental degradation and increase carbon emissions. However, how renewable energy sources can mitigate these negative impacts has not been examined in the literature. In this respect, this study investigates whether renewable energy sources can mitigate the environmental impacts of military expenditures in Turkiye.

DATA AND METHODOLOGY

Model Specification and Data

The empirical investigation of this study examines the potential role of renewable energy sources in reducing the environmental impacts of military expenditures in Turkiye. The study utilizes annual data for the period 1990-2021. This period was chosen based on the availability and suitability of the data for analysis. In our study, we used CO_2 emissions as the dependent variable and military expenditure, renewables energy, GDP per capita, population and interaction term as independent variables.

$$CO2_{(M-D)} = \alpha_0 + \beta_1 MILEX_t + \beta_2 RENEW_t + \beta_3 GDP_t + \beta_4 POP_t + \beta_5 INT_t + \mu_t \quad (1)$$

The model of our study can be expressed in the following functional form:

In Equation 1 α_0 is the constant term of the model. The coefficients β_1 to β_2 are slope coefficients that measure the impact of each independent variable on carbon dioxide emissions. μ_t is the error term of the model with zero mean and constant variance, where t denotes the time period.

Interaction term is a method used in statistical modeling to examine the combined impact of two or more independent variables on the dependent variable [70], [71]. Especially in multivariate regression analyses, it is used to indicate the interaction of independent variables with each other on the dependent variable beyond their direct impacts. In this study, the interaction term is used to analyze the potential role of renewable energy sources in reducing the environmental impacts of military expenditures in Turkiye. Thus, beyond the independent impacts of military expenditures and renewable energy use on carbon emissions, it measures the combined impact of these two factors. The indicators used in our study and their descriptive statistics are shown in Table 1.

Table 1. Descriptive statistics (1990-2021).

Variable	Notation	Description	Mean	Median	Min.	Max.	Std. Dev.	Source
CO_2 emissions	CO_2	metric tons per capita	0.562	0.554	0.409	0.716	0.097	WB
Military expenditure	MILEX	constant US$	3.968	3.951	3.802	4.210	0.102	SIPRI
Renewables energy	RENEW	% of primary energy	1.106	1.111	0.915	1.287	0.091	EIA
GDP per capita	GDP	constant US$	11.732	11.735	11.461	12.054	0.184	WB
Population	POP	total	0.147	0.143	-0.099	0.277	0.082	WB
Interaction term	INT	Military*Renewable	4.794	4.776	4.210	5.344	0.377	AUT

Note: (1) WB, SIPRI, EIA, AUT indicate World Bank-World Development Indicators, Stockholm International Peace Research Institute, U.S. Energy Information Administration, and Author's Calculated Data respectively. (2) All variables were logarithmized.

Table 1 shows that the average CO_2 emissions per capita is 0.562 metric tons. The median value is also close to the mean at 0.554, indicating a symmetrical distribution of the data. The standard deviation of 0.097 suggests that the data are closely clustered around the mean and hence show low variability. Military expenditures are calculated in constant US dollars, with a mean of $3,968. The median is $3,951, again indicating a symmetrical distribution of the data. The standard deviation is 0.102, which is a low value and indicates stability in military expenditures over the years.

The average share of renewable energy in primary energy is 1.106%. The median value of 1.111% is close to the average value and indicates a homogeneous distribution of renewable energy use in general. Renewable energy utilization rates range from a minimum of 0.915% to a maximum of 1.287%. These values show the diversity in renewable energy use across periods. The standard deviation of 0.091 indicates that these rates are generally similar and do not show large fluctuations. The average GDP per capita is 11,732 dollars. The median value is very close to the mean value at $11,735. This suggests that GDP values generally show a central trend. The standard deviation is 0.184, indicating a moderate level of variability, but there is still limited variability. Finally, the population size has a mean of 0.147. The median value of 0.143 is close to the mean value, indicating a symmetrical distribution of the data. The standard deviation of the population variable is 0.082, indicating low variability and a generally stable population size.

Unit Root Analysis

In time series analysis, it is important to determine whether the series are stationary in order to make robust estimates. Especially economic time series often exhibit non-stationary characteristics [72]. This leads to spurious regressions, causing biased and inconsistent estimates [73]. Therefore, Augmented Dickey-Fuller (ADF), Phillips-Perron (PP) and Kwiatkowski-Phillips-Schmidt-Shin (KPSS) unit root tests are used in this study. The application, rationale and explanation of the results of each of these tests are analyzed in the rest of the paper.

Augmented Dickey-Fuller (ADF) Unit Root Test: The ADF test developed by [74] is used to determine whether a time series is stationary. The ADF test accepts the null hypothesis that there is a unit root in the series. The alternative hypothesis is that the series is stationary. The test statistic measures the relationship between the previous and current values of the dependent variable in regression analysis. During the application of the test, the lag length is determined according to the model selection criteria (AIC, SIC, etc.). The general structure of the ADF test is shown in Equation 2 [74]:

$$\Delta y_t = \alpha + \beta_t + \gamma y_{t-1} + \sum_{i=1}^{p} \varphi i \Delta y_{t-1} + \varepsilon_t \quad (2)$$

In Equation 2 y_t is the series itself, Δy_t is the first difference of the series, y_{t-1} is the previous value of the series, α is the constant term, β_t is the trend term and ε_t is the error term. The null hypothesis of the ADF test is that the series has a unit root.

Phillips-Perron (PP) Unit Root Test: In contrast to the ADF test, the PP test developed by [75] makes additional corrections to model autoregressive and moving average structures in the series. The PP test uses nonparametric methods to correct for autocorrelation and heteroskedasticity in the series. This makes the test statistics more robust. The advantage of the PP test is that it eliminates the need to decide the lag structure of the model and is thus easier to use [75]. The formulation of the PP unit root test is shown in Equation 3:

$$y_t = \rho y_{t-1} + \varepsilon t \quad (3)$$

In Equation 3, the coefficient ρ is the correlation of the series with its previous values. εt is the error term and takes into account autocorrelation and heteroskedasticity. Both the ADF and PP tests suggest that the null hypothesis (the existence of a unit root in the series) should be rejected when the calculated test statistics are greater than the critical values.

Kwiatkowski-Phillips-Schmidt-Shin (KPSS) Test: The main difference of the test developed by [76] is that the null hypothesis assumes that the time series is stationary. The KPSS test tests stationarity by checking whether the series has a permanent trend. The test has the ability to test the level and trend stationarity of the series separately. In the application of the KPSS test, one of the trend or level stationarity options should be preferred in accordance with the structural characteristics of the series. The interpretation of the test results is that the series contains a unit root if the null hypothesis is rejected [76]. The regression model of the test is shown in Equation 4:

$$y_t = \mu + \tau_t + \varepsilon t \quad (4)$$

In Equation 4, μ is the constant term, τ_t is the deterministic trend and ε_t is the error term. The variance of the cumulative sum of the error terms is tested.

ARDL Cointegration Test

The Autoregressive Distributed Lag (ARDL) bounds testing method developed by [77] offers significant advantages over classical cointegration tests such as [72], [78], [79]. The ARDL approach allows the variables under study to be stationary at level or first differences, which means that the model can include both I(0) and I(1) series.

The ARDL model is more suitable for small sample sizes. It also allows the evaluation of short-run and long-run dynamics in the same model. This feature is ideal for investigating the existence of long-run relationships. The ARDL cointegration test is constructed to include past values of the dependent variable and both past and current values of the explanatory variables. The ARDL model is as in Equation 5 [77]. This equation represents the long-run cointegration relationship between short-run dynamics and the error correction term.

$$Y_t = a_0 + \sum_{i=1}^{p} a_i Y_{t-1} + \sum_{j=0}^{q} \beta_{j1} X_{1,t-j} + \cdots + \sum_{j=0}^{q} \beta_{jk} X_{k,t-j} + \epsilon_t \quad (5)$$

The optimal lag length in the model is determined using selection criteria such as Akaike Information Criterion (AIC) and Schwarz Information Criterion (SIC). The bounds determined by [77] are compared with the F-statistic to test for cointegration. If the F-statistic exceeds the upper critical value, cointegration between the variables is accepted. If the F-statistic is below the lower critical value, it is concluded that there is no cointegration. The robustness of the model is assessed by normal distribution, autocorrelation, variance and functional form tests. The stability of the long-run parameters is determined by the CUSUM and CUSUMQ tests developed by [80].

After cointegration is detected with the ARDL method, coefficients are estimated. In this process, long-run coefficients are calculated first. After the long-run coefficients, short-run coefficients are calculated. At this stage, a change is made in the configuration of the model and the error correction term is included in the model. This term is derived from one lagged value of the residuals of the model in which the long-run relationship was identified. The error correction term indicates how much of the short-run imbalance will be corrected in the long run. The general expectation is that this coefficient should be negative and significant. Because this indicates the capacity of the model to rapidly stabilize towards the long-run stability [81], [82].

EMPIRICAL FINDINGS

In this stage of our study, unit root tests, which is an important stage of the econometric modeling process, were applied. Unit root tests were applied for the six variables used in the study and their stationarity was analyzed. These variables were evaluated within the framework of both constant term and constant and trend term models. The results of these tests are shown in Table 2.

Table 2 shows that most of the variables are non-stationary in the ADF and PP tests, i.e. they contain unit roots. This implies that the original series do not have a constant mean and variance over time. However, when the first differences of the variables are taken, the obtained t-statistics are usually statistically significant. This indicates that taking the first differences makes the series stationary. Thus, the series are suitable for econometric modeling. The KPSS test works under the assumption that the series are stationary. The results of this test also confirm that most of the series are non-stationary at the first level but become stationary when first differences are taken. The results of the KPSS test support the findings of the ADF and PP tests. In the next stage of this study, ARDL bounds test is used to analyze the cointegration relationships between the series. The results of the ARDL bounds test are presented in Table 3.

Table 2. Unit root test results

Variable		ADF unit root test		PP unit root test		KPSS unit root test	
		t-statistic (level)	t-statistic (first difference)	t-statistic (level)	t-statistic (first difference)	t-statistic (level)	t-statistic (first difference)
CO_2	Constant	-0.866	-6.007***	-0.821	-8.439***	0.734	0.206***
MILEX		-0.630	-3.957***	-0.893	-3.939***	0.534	0.119***
RENEW		-2.088	-6.089***	-2.088	-6.584***	0.174***	0.176***
GDP		0.514	-5.509***	1.716	-6.344***	0.745	0.333***
POP		-2.050	-6.827***	-1.727	-10.519***	0.612*	0.500**
INT		-1.480	-6.117***	-1.388	-6.288***	0.493**	0.227***
CO_2	Constant and Trend	-3.163	-5.929***	-3.128	-7.855***	0.065	0.175**
MILEX		-1.263	-3.866**	-1.638	-3.845**	0.115*	0.112***
RENEW		-2.122	-3.411**	-2.122	-6.725***	0.160	0.131***
GDP		-2.582	-5.479***	-2.594	-7.065***	0.155*	0.206*
POP		-3.334*	-6.733***	-3.268*	-9.490***	0.127**	0.484**
INT		-1.498	-5.860***	-1.407	-6.204***	0.153*	0.083***

Note: The superscripts ***, **, and * denote the significance at a 1%, 5%, and 10% level, respectively.

Table 3. The results of ARDL cointegration test

Model	Optimal lag length	F-statistics	Critical values %5		Critical values %1	
			I(0)	I(I)	I(0)	I(I)
Model: F(CO_2| MILEX, RENEW, GDP, POP, INT)	(1, 1, 0, 0, 1)	6.694***	2.56	3.49	3.29	4.37

Note: The superscripts ***, **, and * denote the significance at a 1%, 5%, and 10% level, respectively.

Table 3 reveals that the structural formulation of the model and the optimal lag lengths are determined with the help of information criteria (AIC and SIC). The optimal lag length of the model is (1, 1, 1, 0, 0, 0, 1) and this structure is designed to capture the lagged impacts in the time series of the models in the best way. The F-statistic of the model is calculated as 6.694. The F-statistic exceeds the critical values at 5% and 1% significance levels. The results of the analysis indicate that there is a long-run and statistically significant relationship between the variables. This paved the way for estimating the long-run coefficients in the later stages of the study. Various specification tests were conducted to assess the econometric robustness of the model. These tests include the LM test for serial correlation, histogram-normality test, heteroskedasticity test and Ramsey RESET test. In addition, CUSUM and CUSUM of Squares tests were applied to detect structural breaks. The results of these tests reveal that there is no specification error in the model and the short and long-run estimations of the models are robust. The results of specification tests and long-run coefficient estimates are presented in Table 4, while the results of CUSUM and CUSUMSQ tests are presented in Figure 3.

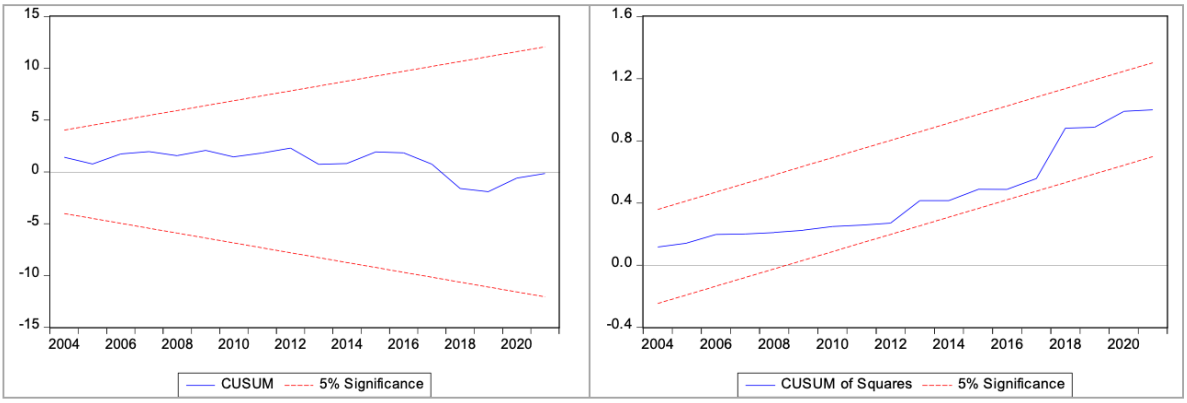


Figure 3. Plots of CUSUM and CUSUMSQ statistics.

Table 4. Short-run and long-run results

Dependent variable: CO_2(M-D)	Short-run coefficients	Long-run coefficients
Regressors		
MILEX	0.260***	0.196***
RENEW	-0.119**	-0.120***
GDP	0.162**	0.193***
POP	0.047	0.095***
INT	-0.130***	-0.140***
ECT(-1)	-0.445***	
C		-1.947**
Diagnostic tests		P value
x2 (Serial correlation)		0.58
x2 (Heteroskedasticity)		0.44
x2 (Normality)		0.55
x2 (Functional form)		0.73
CUSUM		Stable
CUSUMSQ		Stable

Note: The superscripts ***, **, and * denote the significance at a 1%, 5%, and 10% level, respectively.

Table 4 indicates that the error correction term (ECT) is negative and statistically significant. This result means that there is a long-run equilibrium relationship between the model variables and that short-run deviations will be eliminated in the long run. The value of the ECT coefficient (-0.445) indicates that approximately 45% of the short-run deviations will be corrected in the next period.

The results demonstrate that military expenditures have a positive impact (with coefficient of 0.260) on CO_2 emissions in the short run. Carbon emissions increase especially due to the use of fossil fuels by military vehicles and facilities. The impact of military expenditures on CO_2 emissions continues in the long run (with coefficient of 0.196). Military expenditures increase the defense capability of the country. However, the environmental impacts of this situation should also be taken into consideration. Therefore, it is very important to take steps towards the use of sustainable energy resources in military planning. On the other hand, the fact that the use of renewable energy reduces CO_2 emissions both in the short (with coefficient of -0.119) and long run (with coefficient of -0.120) proves that these energy sources are environmentally friendly. In addition to reducing carbon footprint, renewable energy offers a sustainable alternative to fossil fuels. From an economic perspective, investments in renewable energy technologies can provide economic benefits by reducing energy costs in the long run and have the potential to create jobs. On the other hand, the positive impact of GDP on CO_2 emissions (coefficients of 0.162 and 0.193 in the short and long run, respectively) suggests that economic growth is generally associated with increased energy consumption and industrial activity. This may increase the environmental pressure of the growth process. Adopting greener growth strategies, increasing energy efficiency and promoting sustainable industrial practices are needed to reduce the environmental impacts of economic growth. While the impact of population growth on CO_2 emissions is not statistically significant in the short run, it is positive in the long run (with coefficient of 0.095). Population growth leads to an increase in energy demand. As a result, environmental pressure increases and more CO_2 emissions are released. Therefore, economic and social policies should be sustainable in terms of population, urbanization and infrastructure. The results obtained in the study are consistent with studies such as [25], [57], [58], [60], [61].

Moreover, the interaction term is used to measure the combined impact of military expenditures and renewable energy use on CO_2 emissions in Turkiye. The results show that both the short-run (-0.130) and long-run (-0.140) coefficients of the interaction term are negative. These negative coefficients suggest that the use of renewable energy has the potential to reduce the negative impacts of military expenditures on the environment. It also indicates that this interaction offers an important opportunity for environmental sustainability. Military expenditures are generally energy-intensive activities and this energy use is usually based on fossil fuels. The combustion of fossil fuels releases gases such as CO_2 into the atmosphere. The findings of this study show that increasing renewable energy sources can reduce the environmental impact of military activities. The results imply a greater use of renewable energy sources, especially during military operations or in military installations. For example, solar panels could be installed on military bases or alternative energy sources could be developed for military vehicles. In the long run, the persistent negative impact of the interaction term highlights that such policies and technological integrations can increase their impact over time and underscores the importance of taking concrete steps towards sustainability goals in the military sector. Moreover, the positive consequences of this interaction will create a strategic synergy between national security and environmental policies. Considering environmental factors in military planning can strengthen Turkiye's environmentally friendly image in the international arena. Thereby, Turkiye's reputation for environmental sustainability could be enhanced and investments in green technologies could increase.

CONCLUSION

It is a widely accepted fact that military expenditures increase CO_2 emissions and environmental pressure. On the other hand, renewable energy sources are seen as sustainable and environmentally friendly alternatives and have the potential to reduce environmental pressures. Therefore, this study investigates whether renewable energy sources can reduce the environmental impact of military expenditures in Turkiye by using the ARDL method. To measure this impact, an interaction term is included in the ARDL model.

The findings of the study show that military expenditures in Turkiye have a significant impact on CO_2 emissions; military expenditures increase CO_2 emissions in both the short and long run. This is attributed to the high energy consumption of military activities and the fact that most of this energy is provided by fossil fuels. However, the use of renewable energy sources significantly reduces this negative impact. In both the short and long term, the use of renewable energy has been found to reduce CO_2 emissions. This suggests that renewable energy should be more widely adopted in the military sector. In addition, economic growth and population growth are also found to increase CO_2 emissions. These results reveal that Turkiye needs to make strategic moves to ensure environmental sustainability in its development process. In particular, it is important to implement policies that will balance the environmental impacts of economic growth and population growth. Finally, interaction term analysis reveals that the use of renewable energy has the potential to reduce CO_2 emissions from military expenditures. This potential will play a supportive role for the renewable energy sector while reducing the environmental impacts of military expenditures.

Based on the results, the use of renewable energy sources can alleviate the pressure of military expenditures on the environment. Therefore, a series of policy recommendations have been prepared to support the reduction of CO_2 emissions in Turkiye: (1) Turkiye should develop policies

to promote the use of renewable energy in its military and civilian infrastructure. The installation of solar panels and wind turbines on military installations should be supported and the use of electric or hybrid models for military vehicles should be encouraged. These steps would reduce the environmental impact of military expenditures and stimulate the renewable energy sector. (2) As part of efforts to reduce the environmental impact of military expenditures, mandatory environmental impact assessments should be conducted for military projects. These assessments will identify the potential impacts of projects on the environment and enable the development of strategies to minimize negative impacts. (3) Turkiye should align its economic growth strategies with the principles of environmental sustainability and encourage the use of environmentally friendly technologies in industrial production. In addition, the adoption of new energy efficient technologies and the promotion of environmentally friendly innovations should be a fundamental part of economic policies. (4) Urban planning and infrastructure projects should be designed in line with sustainable development objectives to manage the environmental impacts of population growth. Environmentally friendly practices such as energy-efficient buildings and waste management systems should be encouraged. (5) Increase cooperation between the military and civilian sectors on the use of renewable energy. These collaborations will accelerate the adoption of renewable energy technologies in both sectors and have the potential to have a widespread environmental impact.

Although this study provides important findings, it has some limitations. Future studies can address these limitations. Firstly, in this study, environmental pressure is measured by CO_2 emissions per capita. In future studies, other variables representing environmental pressure can be added to the model or an environmental pressure index can be constructed with these variables. Secondly, future studies can expand the sample to include both developed and developing countries. In this way, it can be compared whether the results differ in countries with different income levels. Thirdly, by using different econometric models, graphs reflecting the effectiveness of the use of renewable energy sources in reducing environmental impacts can be created. Finally, larger data sets and different analysis techniques can be used to test the consistency of the findings of this study.

DATA AVAILABILITY STATEMENT

The author declared that the data that supports the findings of this study are available within the article. Raw data that support the finding of this study are available from the corresponding author, upon reasonable request.

CONFLICT OF INTEREST

The author declared that there are no potential conflicts of interest with respect to the research, authorship, and publication of this article.

USE OF AI FOR WRITING ASSISTANCE

The author declared that AI was not used in writing or as a writing assistant in the manuscript.

ETHICS

The author declared that there are no ethical issues related to the publication of this article.

FUNDING STATEMENT

The author declared that the article has not received financial support.

REFERENCES

[1] F. Giray, "Savunma harcamalari ve ekonomik büyüme", Cumhuriyet Üniversitesi İktisadi ve İdari Bilimler Dergisi, vol. 5(1), pp. 181-199, 2004.

[2] V. Smil, "World History and Energy", in Encyclopedia of Energy, Elsevier, pp. 549-561, 2004. https://doi.org/10.1016/B0-12-176480-X/00025-5.

[3] A. Wijeweera and M. J. Webb, "Military spending and economic growth in south Asia: A panel data analysis", Defence and Peace Economics, vol. 22(5), pp. 545-554, 2011. https://doi.org/10.1080/10242694.2010.533905.

[4] S. Charles Shaaba and N. Ngepah, "Military expenditure, industrialisation, and economic growth in Africa : Evidence from a panel causality analysis", African Journal of Business & Economic Research, vol. 13(3), pp. 29-48, 2018. https://doi.org/10.31920/1750-4562/2018/V13n3a2.

[5] IRENA, "Global energy transformation: A roadmap to 2050", International Renewable Energy Agency, 2018. [Online]. Available: https://www.irena.org/-/media/Files/IRENA/Agency/Publication/2018/Apr/IRENA_Report_GET_2018.pdf (Accessed Feb 02, 2024)

[6] K. K. Gokmenoglu, N. Taspinar, and M. M. Rahman, "Military expenditure, financial development and environmental degradation in Turkey: A comparison of CO_2 emissions and ecological footprint", International Journal of Finance & Economics, vol. 26(1), pp. 986-997, 2021. https://doi.org/10.1002/ijfe.1831.

[7] D. N. Pellow, "Resisting global toxics: Transnational movements for environmental justice". MIT Press, Cambridge, MA, 2007. https://doi.org/10.7551/mitpress/7479.001.0001

[8] SIPRI military expenditure database. Stockholm International Peace Research Institute, Apr. 22, 2024.

[9] M. F. Dörtbudak, "Unmanned aerial vehicles (UAVs): A new tool in counterterrorism operations?", Sensors, and Command, Control, Communications, and Intelligence (C3I) Technologies for Homeland Security, Defense, and Law Enforcement XIV, SPIE, pp.

96-111, 2015. https://doi.org/10.1117/12.2085373
[10] T. Sandler and J. George, "Military expenditure trends for 1960-2014 and what they reveal", Global Policy, vol. 7(2), pp. 174-184, 2016. https://doi.org/10.1111/1758-5899.12328.
[11] N. Tian, D. Lopes Da Silva, L. Béraud-Sudreau, X. Liang, L. Scarazzato, and A. Assis, "Developments in military expenditure and the effects of the war in Ukraine", Defence and Peace Economics, vol. 34(5), pp. 547-562, 2023. https://doi.org/10.1080/10242694.2023.2221877.
[12] D. S. Kim and J.E. Lee, "Development of terrorism in Turkey: Focusing on the periodic features and key actors", Advanced Science Letters, vol. 22(11), pp. 3672-3675, 2016. https://doi.org/10.1166/asl.2016.7925.
[13] R. Erdağ, "Security environment and military spending of Turkey in the 2000s", Contemporary Review of the Middle East, vol. 8(1), pp. 120-139, 2021. https://doi.org/10.1177/2347798920976294.
[14] World Bank-World Development Indicators, World Bank, 2024. [Online]. Available: https://databank.worldbank.org/source/world-development-indicators (Accessed Jan 15, 2024)
[15] Q. Wang and Y. Zhou, "Evolution and drivers of production-based carbon emissions in China and India: Differences and similarities", Journal of Cleaner Production, vol. 277, Article 123958, 2020. https://doi.org/10.1016/j.jclepro.2020.123958.
[16] Md. S. K. Sarkar, R. A. Begum, S. Sadeka, and J. J. Pereira, "Current trends and policies of energy consumption and CO_2 emission from the largest Asian economies", International Journal of Global Warming, vol. 14(4), pp. 417-439, 2018. https://doi.org/10.1504/IJGW.2018.091530.
[17] Y. Li, D. Xu, J. Wang, Y. Zhang, and X. Yu, "Industrial path analysis for CO_2 transfers induced by final consumption: A comparison of the United States and China", Journal of Cleaner Production, vol. 251, Article 119604, 2020. https://doi.org/10.1016/j.jclepro.2019.119604.
[18] Z. S. Venter, K. Aunan, S. Chowdhury, and J. Lelieveld, "COVID-19 lockdowns cause global air pollution declines", Proceedings of the National Academy of Sciences, vol. 117(32), pp. 18984-18990, 2020. https://doi.org/10.1073/pnas.2006853117.
[19] F. Halicioglu, "An econometric study of CO_2 emissions, energy consumption, income and foreign trade in Turkey", Energy policy, vol. 37(3), pp. 1156-1164, 2009. https://doi.org/10.1016/j.enpol.2008.11.012
[20] H. Rüstemoğlu, "Environmental analysis of Turkey's aggregated and sector-level CO_2 emissions", Environmental Science and Pollution Researc, vol. 28(45), pp. 63933-63944, 2021. https://doi.org/10.1007/s11356-020-11895-6.
[21] I. Ari and R. F. Yikmaz, "The role of renewable energy in achieving Turkey's INDC", Renewable and Sustainable Energy Reviews, vol. 105, pp. 244-251, 2019. https://doi.org/10.1016/j.rser.2019.02.004
[22] S. Erat, A. Telli, O. M. Ozkendir, and B. Demir, "Turkey's energy transition from fossil-based to renewable up to 2030: Milestones, challenges and opportunities", Clean Technologies and Environmental Policy, vol. 23, pp. 401-412, 2021. https://doi.org/10.1007/s10098-020-01949-1
[23] A. K. Jorgenson, B. Clark, and J. Kentor, "Militarization and the environment: A panel study of carbon dioxide emissions and the ecological footprints of nations, 1970-2000", Global Environmental Politics, vol. 10(1), pp. 7-29, 2010. https://doi.org/10.1162/glep.2010.10.1.7
[24] A. Z. Isiksal, "Testing the effect of sustainable energy and military expenses on environmental degradation: evidence from the states with the highest military expenses", Environmental Science and Pollution Research, vol. 28(16), pp. 20487-20498, 2021. https://doi.org/10.1007/s11356-020-11735-7
[25] M. Bildirici, "CO_2 emissions and militarization in G7 countries: panel cointegration and trivariate causality approaches", Environment and Development Economics, vol. 22(6), pp. 771-791, 2017. https://doi.org/10.1017/S1355770X1700016X
[26] G. Hooks and C. L. Smith, "The treadmill of destruction: National sacrifice areas and native Americans", American Sociological Review, vol. 69(4), pp. 558-575, 2004. https://doi.org/10.1177/000312240406900405.
[27] L. Barroso, H. Rudrick, F. Sensfuss, and P. Linares, "The green effect", IEEE Power and Energy Magazine, vol. 8(5), pp. 22-35, 2010. https://doi.org/10.1109/MPE.2010.937595.
[28] R. Li, Q. Wang, and L. Li, "Does renewable energy reduce per capita carbon emissions and per capita ecological footprint? New evidence from 130 countries", Energy Strategy Reviews, vol. 49, 2023. https://doi.org/10.1016/j.esr.2023.101121.
[29] M. K. Shahid et al., "A review of membrane-based desalination systems powered by renewable energy sources", Water, vol. 15(3), Article 534, 2023. https://doi.org/10.3390/w15030534
[30] M. Suska-Szczerbicka, "Wind energy financing tools", Econ. Sociol, vol. 3, pp. 141-160, 2010.
[31] C. Kesbiç and E. T. Bozduman, "Türkiye'de sektör bazında enerji tüketiminin çevre kirliliği üzerine etkisi", Manisa Celal Bayar Üniversitesi Sosyal Bilimler Dergisi, vol. 19(2), pp. 289-299, 2021. https://doi.org/10.18026/cbayarsos.888607
[32] J. Chontanawat, "Relationship between energy consumption, CO_2 emission and economic growth in ASEAN: Cointegration and causality model", Energy Reports, vol. 6, pp. 660-665, 2020. https://doi.org/10.1016/j.egyr.2019.09.046
[33] M. Çetin and Ö. Yüksel, "Türkiye ekonomisinde enerji tüketiminin karbon emisyonu üzerindeki etkisi", Mehmet Akif Ersoy Üniversitesi İktisadi ve İdari

Bilimler Fakültesi Dergisi, vol. 5(2), pp. 169-186, 2018. https://doi.org/10.30798/makuiibf.409119

[34] U. Al-Mulali and C. N. B. Che Sab, "Electricity consumption, CO 2 emission, and economic growth in the Middle East", Energy Sources, Part B: Economics, Planning, and Policy, vol. 13(5), pp. 257-263, 2018, https://doi.org/10.1080/15567249.2012.658958.

[35] S.J. Lee and S.H. Yoo, "Energy consumption, CO 2 emission, and economic growth: Evidence from Mexico", Energy Sources, Part B: Economics, Planning, and Policy, vol. 11(8), pp. 711-717, 2016. https://doi.org/10.1080/15567249.2012.726695.

[36] S. R. Lee and S.H. Yoo, "Energy consumption, CO 2 emissions, and economic growth in Korea: A causality analysis", Energy Sources, Part B: Economics, Planning, and Policy, vol. 11(5), pp. 412-417, 2016. https://doi.org/10.1080/15567249.2011.635752.

[37] I. Dogan and N. Topalli, "Milli gelir, karbon emisyonu ve enerji tüketimi: Türkiye için dogrusal ve dogrusal olmayan nedensellik analizi", Business and Economics Research Journal, vol. 7(1), p. 107, 2016. https://doi.org/10.20409/berj.2016116807

[38] G. Sayar Özkan and M. Erdemli̇ , "Ekonomik büyüme ve enerji tüketiminin çevre kirliliğine etkisi: Panel veri analizi", Uluslararası Ticaret ve Ekonomi Araştırmaları Dergisi, vol. 1(2), pp. 19-37, 2017. https://doi.org/10.30711/utead.342589. https://doi.org/10.30711/utead.342589

[39] I. Ozturk and A. Acaravci, "CO_2 emissions, energy consumption and economic growth in Turkey", Renewable and Sustainable Energy Reviews, vol. 14(9), pp. 3220-3225, 2010. https://doi.org/10.1016/j.rser.2010.07.005.

[40] M. Bouznit and M. del P. Pablo-Romero, "CO_2 emission and economic growth in Algeria", Energy policy, vol. 96, pp. 93-104, 2016. https://doi.org/10.1016/j.enpol.2016.05.036

[41] N. Ahmad and L. Du, "Effects of energy production and CO_2 emissions on economic growth in Iran: ARDL approach", Energy, vol. 123, pp. 521-537, 2017. https://doi.org/10.1016/j.energy.2017.01.144

[42] J. I. Mikayilov, M. Galeotti, and F. J. Hasanov, "The impact of economic growth on CO_2 emissions in Azerbaijan", Journal of Cleaner Production, vol. 197, pp. 1558-1572, 2018. https://doi.org/10.1016/j.jclepro.2018.06.269.

[43] K. K. Gokmenoglu and M. Sadeghieh, "Financial development, CO_2 emissions, fossil fuel consumption and economic growth: The case of Turkey", Strategic Planning for Energy and the Environment, vol. 38(4), pp. 7-28, 2019. https://doi.org/10.1080/10485236.2019.12054409.

[44] M. Kahia, M. Ben Jebli, and M. Belloumi, "Analysis of the impact of renewable energy consumption and economic growth on carbon dioxide emissions in 12 MENA countries", Clean Technologies and Environmental Policy, vol. 21, pp. 871-885, 2019. https://doi.org/10.1007/s10098-019-01676-2

[45] Y. Chen, Z. Wang, and Z. Zhong, "CO_2 emissions, economic growth, renewable and non-renewable energy production and foreign trade in China", Renewable energy, vol. 131, pp. 208-216, 2019. https://doi.org/10.1016/j.renene.2018.07.047

[46] A. Tamazian, J. P. Chousa, and K. C. Vadlamannati, "Does higher economic and financial development lead to environmental degradation: Evidence from BRIC countries", Energy Policy, vol. 37(1), pp. 246-253, 2009. https://doi.org/10.1016/j.enpol.2008.08.025.

[47] M. A. Boutabba, "The impact of financial development, income, energy and trade on carbon emissions: Evidence from the Indian economy", Economic Modelling, vol. 40, pp. 33-41, 2014. https://doi.org/10.1016/j.econmod.2014.03.005

[48] U. K. Pata, "The effect of urbanization and industrialization on carbon emissions in Turkey: Evidence from ARDL bounds testing procedure", Environmental Science and Pollution Research, vol. 25(8), pp. 7740-7747, 2018. https://doi.org/10.1007/s11356-017-1088-6

[49] M. Shahbaz, S. J. H. Shahzad, M. K. Mahalik, and S. Hammoudeh, "Does globalisation worsen environmental quality in developed economies?", Environmental Modeling & Assessment, vol. 23(2), pp. 141-156, 2018. https://doi.org/10.1007/s10666-017-9574-2

[50] Ş. Apaydın, "Küreselleşmenin ekolojik ayakizi üzerindeki etkileri: Türkiye örneği", Ekonomi Politika ve Finans Araştırmaları Dergisi, vol. 5(1), pp. 23-42, 2020. https://doi.org/10.30784/epfad.695836

[51] L. Wang, X. V. Vo, M. Shahbaz, and A. Ak, "Globalization and carbon emissions: Is there any role of agriculture value-added, financial development, and natural resource rent in the aftermath of COP21?", Journal of Environmental Management, vol. 268, Article 110712, 2020. https://doi.org/10.1016/j.jenvman.2020.110712.

[52] A. Karasoy, "Küreselleşme, sanayileşme ve şehirleşmenin Türkiye'nin ekolojik ayak izine etkisinin genişletilmiş ARDL yöntemiyle incelenmesi", Hitit Sosyal Bilimler Dergisi, vol. 14(1), pp. 208-231, 2021. https://doi.org/10.17218/hititsbd.929092

[53] Ü. Kurt, G. Can, and F. Kiliç, "Türkiye'de küreselleşmenin çevresel tahribat üzerindeki etkisi", Çevre, Enerji ve Sürdürülebilirlik Ekonomik Bir Değerlendirme, pp.53-70, Gazi Kitabevi, 2022.

[54] T. Yildiz and T. B. Göktürk, "Sanayileşme, şehirleşme ve çevre kirliliği arasındaki ilişki: Türkiye için bir ARDL sınır testi yaklaşımı", Journal of Academic Value Studies, vol. 5(2), pp. 217-229, 2019. https://doi.org/10.13934/1999.393

[55] P. L.h, "Globalization, financial development, and environmental degradation in the presence of environmental Kuznets curve: Evidence from ASEAN-5 countries", 2019. https://doi.org/10.32479/

ijeep.7290.
[56] S. Ahmed, K. Alam, A. Rashid, and J. Gow, "Militarisation, energy consumption, CO_2 emissions and economic growth in Myanmar", Defence and Peace Economics, vol. 31(6), pp. 615-641, 2020. https://doi.org/10.1080/10242694.2018.1560566.
[57] Z. Ahmed, M. Ahmad, M. Murshed, A. I. Vaseer, and D. Kirikkaleli, "The trade-off between energy consumption, economic growth, militarization, and CO 2 emissions: Does the treadmill of destruction exist in the modern world?", Environmental Science and Pollution Research, vol. 29, pp. 18063-18076, 2022. https://doi.org/10.1007/s11356-021-17068-3
[58] N. B. Afia and S. Harbi, "The relationship between CO_2 emissions and military effort", Journal of Economics Studies and Research, vol. 2018, Article 342225, 2018. https://doi.org/10.5171/2018.342225
[59] F. Beşel, V. İnal, and M. Aydın, "Askeri harcamalar ve yeşil büyüme ilişkisi: Ampirik bir analiz", İktisadi İdari ve Siyasal Araştırmalar Dergisi, vol. 7(17), pp. 159-172, 2022. https://doi.org/10.25204/iktisad.970198
[60] M. E. Bildirici, "The effects of militarization on biofuel consumption and CO_2 emission", Journal of Cleaner Production, vol. 152, pp. 420-428, 2017. https://doi.org/10.1016/j.jclepro.2017.03.103
[61] S. Erdogan, A. Gedikli, E. İ. Çevik, and M. A. Öncü, "Does military expenditure impact environmental sustainability in developed Mediterranean countries?", Environmental Science and Pollution Research, vol. 29(21), pp. 31612-31630, 2022. https://doi.org/10.1007/s11356-021-18226-3
[62] P. A. Kwakwa, "The effect of industrialization, militarization, and government expenditure on carbon dioxide emissions in Ghana", Environmental Science and Pollution Research, vol. 29(56), pp. 85229-85242, 2022. https://doi.org/10.1007/s11356-022-21187-w
[63] B. A. Neila, "The relationship between military expenditure, military personnel, economic growth, and the environment", International Journal of Economics and Management Engineering, vol. 10(4), pp. 1059-1064, 2016.
[64] U. Qayyum, S. Anjum, and Samina Sabir, "Armed conflict, militarization and ecological footprint: Empirical evidence from South Asia", Journal of Cleaner Production, vol. 281, Article 125299, 2021. https://doi.org/10.1016/j.jclepro.2020.125299
[65] G. Zandi, M. Haseeb, and I. S. Z. Abidin, "The impact of democracy, corruption and military expenditure on environmental degradation: Evidence from top six ASEAN countries", Humanities & Social Sciences Reviews, vol. 7(4), pp. 333-340, 2019. https://doi.org/10.18510/hssr.2019.7443
[66] B. Ozcan and N. Apergis, "The impact of internet use on air pollution: Evidence from emerging countries", Environmental Science and Pollution Research, vol. 25(5), pp. 4174-4189, 2018. https://doi.org/10.1007/s11356-017-0825-1
[67] S. Ullah, Z. Andlib, M. T. Majeed, S. Sohail, and M. Z. Chishti, "Asymmetric effects of militarization on economic growth and environmental degradation: Fresh evidence from Pakistan and India", Environmental Science and Pollution Research, vol. 28(8), pp. 9484-9497, 2021. https://doi.org/10.1007/s11356-020-11142-y
[68] Ü. Kurt and C. Kılıç, "Küreselleşmenin savunma harcamalari üzerindeki etkisi: Türkiye için VAR analizi", Trakya Üniversitesi Sosyal Bilimler Dergisi, vol. 21(1), 2019. https://doi.org/10.26468/trakyasobed.471781
[69] F. Erdoğan, "Cumhuriyet döneminde savunma harcamaları ve çevre kirliliği ilişkisi üzerine bir inceleme", JOEEP: Journal of Emerging Economies and Policy, vol. 7(2), pp. 28-37, 2022.
[70] F. F. Adedoyin, I. Ozturk, F. V. Bekun, P. O. Agboola, and M. O. Agboola, "Renewable and non-renewable energy policy simulations for abating emissions in a complex economy: Evidence from the novel dynamic ARDL", Renewable Energy, vol. 177, pp. 1408-1420, 2021. https://doi.org/10.1016/j.renene.2021.06.018
[71] M. E. Hossain, S. Rej, S. M. Saha, J. C. Onwe, N. Nwulu, F. V. Bekun, and A. Taha, "Can energy efficiency help in achieving carbon-neutrality pledges? A developing country perspective using dynamic ARDL simulations", Sustainability, vol. 14(1)3, p. 7537, 2022. https://doi.org/10.3390/su14137537
[72] S. Johansen and K. Juselius, "Maximum likelihood estimation and inference on cointegration-with applications to the demand for money", Oxford Bulletin of Economics and Statistics, vol. 52(2), pp. 169-210, 1990. https://doi.org/10.1111/j.1468-0084.1990.mp52002003.x
[73] C. W. Granger and P. Newbold, 'Spurious regressions in econometrics', Journal of econometrics, vol. 2(2), pp. 111-120, 1974. https://doi.org/10.1016/0304-4076(74)90034-7
[74] D. A. Dickey and W. A. Fuller, "Distribution of the estimators for autoregressive time series with a unit root", Journal of the American Statistical Association, vol. 74(366a), pp. 427-431, 1979. https://doi.org/10.1080/01621459.1979.10482531
[75] P. C. B. Phillips and P. Perron, "Testing for a unit root in time series regression", Biometrika, vol. 75(2), pp. 335-346, 1988. https://doi.org/10.1093/biomet/75.2.335
[76] D. Kwiatkowski, P. C. B. Phillips, P. Schmidt, and Y. Shin, "Testing the null hypothesis of stationarity against the alternative of a unit root", Journal of Econometrics, vol. 54(1-3), pp. 159-178, 1992. https://doi.org/10.1016/0304-4076(92)90104-Y
[77] M. H. Pesaran, Y. Shin, and R. J. Smith, "Bounds testing approaches to the analysis of level relationships", Journal of applied econometrics, vol. 16(3), pp. 289-326, 2001. https://doi.org/10.1002/jae.616
[78] R. F. Engle and C. W. Granger, "Co-integration and

error correction: representation, estimation, and testing", Econometrica: Journal of the Econometric Society, Vol. 55(2), pp. 251-276, 1987. https://doi.org/10.2307/1913236

[79] P. C. B. Phillips and S. Ouliaris, "Asymptotic properties of residual based tests for cointegration", Econometrica, vol. 58(1), pp. 165-193, 1990. https://doi.org/10.2307/2938339

[80] R. L. Brown, J. Durbin, and J. M. Evans, "Techniques for testing the constancy of regression relationships over time", Journal of the Royal Statistical Society Series B: Statistical Methodology, vol. 37(2), pp. 149-163, 1975. https://doi.org/10.1111/j.2517-6161.1975.tb01532.x

[81] M. Şimşek and C. Kadılar, "Türkiye'nin ithalat talebi fonksiyonunun sinir testi yaklaşimi ile ebütünleme analizi", Doğuş Üniversitesi Dergisi, vol. 5(1), 2004.

[82] E. Esen, S. Yıldırım, and S. F. Kostakoğlu, "Feldstein-Horioka hipotezinin Türkiye ekonomisi için sınanması: ARDL modeli uygulaması", Eskişehir Osmangazi Üniversitesi İktisadi ve İdari Bilimler Dergisi, vol. 7(1), pp. 251-267, 2012.

Environ Res Tec, Vol. 8, Issue. 2, pp. 425-428, June 2025

Environmental Research and Technology
https://dergipark.org.tr/en/pub/ert
DOI: https://10.35208/ert.1485591

Environmental Research & Technology

Research Article

Carica papaya L. Latex mediated green synthesis of ZnO nanoparticles for its antimicrobial activity

Ananya MISHARA[1], Sagarika PARIDA[1]*

[1]*Department of Botany, School of Applied Sciences, Centurion University of Technology and Management, 752050, Bhubaneswar,Odisha, India*

ARTICLE INFO

Article history
Received: 17 May 2024
Revised: 10 Sep 2024
Accepted: 01 Oct 2024

Key words:
Antimicrobial activity, carica papaya, elemental composition, latex, ZnO NPs

ABSTRACT

Plant latex is a natural product produced by a number of plant species which are used by different tribal communities in India as a folk medicinal treatment on natural wounds or cuts. Plant latex has a huge demand as herbal products in an aspect of clinical, therapeutical and also in agricultural sectors. Natural latex is composed of different important biomolecules like, tannins, flavonoids, glycosides, sterols, saponins etc. These different active chemical constituents have versatile medicinal activities against different pathogens such as bacteria, fungi, viruses and protozoans etc. Therefore, development of novel biological techniques is significant for the biosynthesis of ZnO nanoparticles using the latex of Carica papaya L. This study reports on the biosynthesis of ZnO nanoparticles (Zn NPs) using latex of C. papaya as an effective reducing agent. Green synthesis of nanoparticles has advantageous over conventional methods because it does not require the use of toxic chemicals and therefore environmentally sustainable. Zinc oxide nanoparticles have gained potential recognition because of their distinctive characteristics and wide utilizatrion in various fields. Properties of synthesized ZnO NPs were characterized using various methods such as ultra violet visible spectrophotometer (UV-Vis), Scanning Electron Microscopy (SEM) and Fourier Transform İnfrared Spectroscopy (FT-IR). The elemental composition of C. papaya latex was also analysed using X-ray Fluorescence (XRF) technique. Green synthesized ZnO nanoparticles also assessed for its antimicrobial activity against selected bacterial species.

Cite this article as: Mishra A, Parida S. Carica papaya L. latex mediated green synthesis of ZnO nanoparticles for its antimicrobial activity. Environ Res Tec 2025;8(2) 425-428.

INTRODUCTION

Zinc oxide nanoparticles (ZnO NPs) are essential inorganic material with multiple applications and known for their bactericidal and fungicidal properties [1]. Green synthesis of nanoparticles is considered advantageous over conventional methods as it removes the utilization of toxic chemicals and reduces environmental impact.Among the biological sources, plant latex is one of the important resource for conversion of metal ions to nanoparticles because of potential reducing and stabilizing agents of bioactive compounds. Latex functions well as an antioxidant, anticoagulant, antitumor, and antimicrobial. Among the latex producing plants, Carica papaya L., belonging to the Caricaceae family, is most commonly found throughout Odisha. The plant has extensive biological utilizations, including antibacterial [2], anti-inflammatory, anti-cancer, anti-leprosy, wound-healing, and use against skin conditions. Unripe fruit latex is used in cosmetically for face-lifting operations, reduces blood pressure and whooping cough [2]. Papain has a number of industrial applications in textile, pharmacy, baking, brewing and wine producing industries [3, 4]. Unripe fruit latex contains various bioactive compounds viz., enzymes mostlypapain, cyclo-

***Corresponding author.**
*E-mail address: sagarika.parida@cutm.ac.in

This is an open access article under the CC BY-NC license (http://creativecommons.org/licenses/by-nc/4.0/).

transferase, lysozymes and chymopapain [2], polyphenols, alkaloids, tannins, terpens, sugars, gums [5] and secondary metabolites which contribute to the reduction and stabilization of nanoparticles. This work focuses on antimicrobial activity of crude latex of C. papaya L. and synthesis of ZnO nanoparticles using latex as an eco-friendly approach. Various characterization techniques are employed to analyse the nanoparticles, including UV-Vis spectroscopy, FT-IR and SEM. ZnO nanoparticles were evaluated for their potency against selected microorganisms. ZnO nanoparticles (ZnO NPs) were selected for this study because of its stability with a longer lifecycle than other organic-based compounds [6, 7, 8].

EXPERIMENTAL SECTION

Fruit Latex Collection

Latex was obtained in the month of Sepember, 2022, by making longitudinal incisions in the unripe fruit of healthy plant C. papaya L. early morning in a sterile container from the medicinal plant garden of Centurion University, Bhubaneswar campus with latitude of 20.1735040 and longitude of 85.7053790 for our study. The plant was identified and authenticated by Dr. Nabin Kumar Dhal, Chief Scientist, CSIR-IMMT, Bhubaneswar, Odisha, India.

ZnO Nanoparticles Synthesis Using Latex of C. papaya L.

Precursor zinc acetate (Zn(CH3COO)2) was taken as the precursor in synthesizing Zinc oxide nanoparticles (ZnO NPs) utilising the milky latex of C. papaya L. latex. Collected latex was dissolved in 30 ml distilled water and boiled for 15 minutes, then the solution was kept for cooling and filtered using Whatman No.-1 filter-paper. Two millilitre extracted latex was poured drop wise to 20 ml of 0.5 mM (ZCP1), 1 mM (ZCP2), and 2 mM (ZCP3) zinc acetate solution separately and continuously stirred for 4hr. The pH of the mixture was kept slightly acidic (6.5 to 6.7) and no precipitating agent like NaOH was added. A white coloured precipitate was formed, which was filtered, and kept for drying in an oven at 60-800C overnight. Three samples were calcinated separately at 4000C for 3 hrs to get ZnO nanopowder.

Characterisation of ZnO Nanoparticles

The absorbance of the prepared samples was carried out using UV-Visible light by Ei Make UV-Visible spectrophotometer, and FT-IR by Spectrum Two FT-IR spectrometer.

Morphological analyses of ZnO Nanoparticles

UV-Vis, FT-IR spectroscopy and SEM size and shape of ZnO NPs were characterized using a SEM (JEOL-JSM 6390, Japan).

Antimicrobial activity

Collection of microbial strains

Bacterial strains viz., Escherichia coli MTCC 614, Klebsiella pneumonia MTCC 109, Pseudomonas aeruginosa MTCC 741 and Proteus mirabilis MTCC 9242 741 and Proteus mirabilis MTCC 9242 were collected from Department of Botany, Utkal University, Bhubaneswar, Odisha and maintained on agar slants at 40C.

Antibacterial activity assay

Potato dextrose agar and Nutrient agar media are taken for culturing the collected fungal and bacterial samples respectively. Antibacterial and antifungal activity was evaluated by agar well diffusion method [9, 10, 11]. Two ml of crude latex was poured to the agar well and incubated at 370C for 24 hrs for bacterial strains. Sterile double distilled water was poured to the synthesized ZnO NPs and sonicated briefly to make uniform colloidal suspension to carry out antibacterial activity against the collected bacterial strains.

RESULTS AND DISCUSSION

Characterization of synthesized ZnO Nanoparticles

The optical absorption spectra were recorded in the range of 250-800 nm and depicted in Figure 1a. The spectra show a gradual blue shift of absorbance band with increasing the concentration of zinc percentage. As shown in the Figure 1a, the absorbance band for ZCP 1 appears at 360 nm but for ZCP2 and ZCP 3 it shifts to 356 and 346 nm respectively. The absorbance for ZCP2 and ZCP3 also increased with increasing concentration of zinc acetate solution. The blue shift of absorption band can be understood on the basis of quantum confinement effect of ZnO nanoparticles. The blue shift can be due to the smaller crystalline size resulting quantum confinement in the system [12]. Maximum absorption peak of ZnO nanoparticles in the range from 346 to 360 nm range is agreed with the previous findings [12].

FTIR spectra of all the three prepared samples were recorded in the range of 500-4000 cm-1 in transmittance mode and presented in Figure 1b.

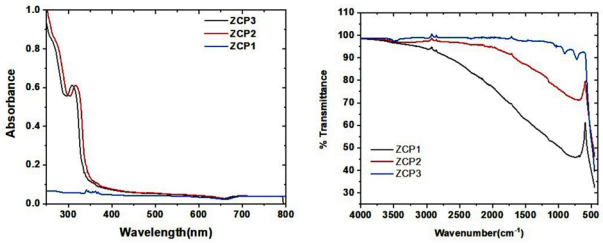
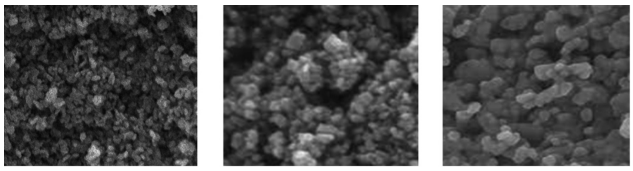


Figure 1.a UV absorption of ZCP1, ZCP2, and ZCP3; Figure 1b. FTIR spectral graph of ZCP1, ZCP2, and ZCP3

The spectra show a broad band at 680-720 cm-1 indicating the formation of Zn-O stretching vibration related to metal oxide stretching [13]. As the three samples were calcinated at 4000C, so no corresponding peaks related to OH or H2O groups were observed. Morphology of ZCP1, ZCP2 and ZCP3 was studied by SEM analyses which revealed the shapes are mostly spherical in shape and size varies in three different samples 25-36 nm,and to as observed in Figure 2a, Figure 2b, and Figure 2c.



(a) (b) (c)

Figure 2. SEM image: (a) ZCP1; (b) ZCP2; (c) ZCP3

The three distinct results (Figure 2a, Figure 2b; Figure 2c) correspond to the concentration ratios (latex : zinc acetate solution) of 2:0.5, 2:1, and 1:1 respectively. ZnO NPs in high latex concentration becomes spherical as observed in Figure 2a, which becomes clustered in increasing concentration of zinc acetate solution.

Antimicrobial activity

The anti-bacterial activity of the raw latex and ZnO NPs was quantitatively assessed against the collected bacteria strains.

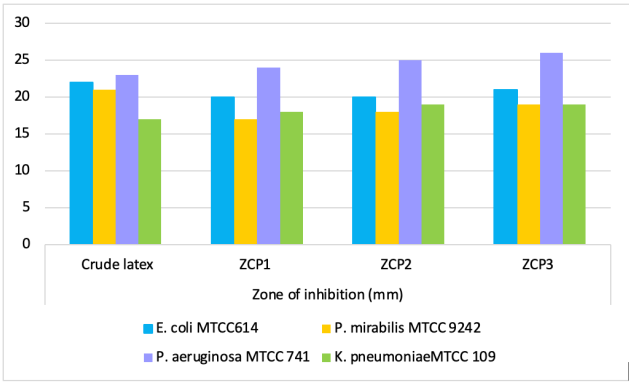


Figure 3. Antibacterial activity of crude latex and ZCP1, ZCP2, and ZCP3 nanoparticles

The antibacterial activity is classified [14] into sensitive, when zone of inhibition is greater than 21mm, intermediate (16-20 mm) and resistant (<15mm). P. aeuroginosa MTCC 741 showed highest antibacterial activity, followed by E. coli in both crude latex and ZnO NPs (Figure 3). Among these samples ZCP3 shows highest antibacterial activity.

C. papaya latex exhibited a zone of inhibition on Agrobacterium sp. (20.66 mm) and E. coli (16 mm) because of possessing antimicrobial constituents [15, 16]. The protein in the latex with a concentration of 138 mg/mL has been reported to show 100 per cent inhibiting activity against C. albicans [17]. Papaya fruit latex had shown to heal the wounds effectively than glycol, and gentamycin in diabetic Wister rats [18, 19]. According to the findings, C. papaya latex mediated green synthesised ZnO-NPs demonstrated good antibacterial activity against the tested bacteria. Among the three samples, ZCP3 possessed larger surface area with more numbers of zinc atom, which induce higher level of toxicity to the tested bacterial strains [20, 21, 22] might be because of adhesion of the nanoparticles with bacterial membrane which could be the underlying cause of inhibition of bacterial growth.

CONCLUSION

Plant latex contains different important biomolecules such as tannins, flavonoids, glycosides, sterols and saponins etc. and have versatile medicinal activities against different microorganisms. Phytochemicals are responsible for rapid reduction of zinc ion to metallic ZnO nanoparticles. In this study, latex of unripe fruit of healthy C. papaya L. was used as reducing agent to synthesize ZnO NPs, which is environmentally sustainable as it does not require the use of toxic chemicals. Synthesized ZnO NPs were characterized using UV-Vis, SEM and FT-IR. The spectra show a broad band at 680-720 cm-1 indicating the formation of Zn-O stretching vibration related to metal oxide stretching and these green synthesized ZnO nanoparticles were assessed for its antibacterial activity against selected bacterial strains viz., E. coli MTCC 614, K. pneumonia MTCC 109, P. aeruginosa MTCC 741 and Proteus mirabilis MTCC 9242. The results revealed that P. aeuroginosa MTCC 741 had the highest antibacterial activity, followed by E. coli in both crude latex and ZnO NPs. This results suggest that the ZnO NPs as the promising antibacterial agents which also depends upon the concentration ZnO nanoparticles .This study contributes to eco-friendly synthesis methods and the exploration of effective antimicrobial agents.

ACKNOWLEDGEMENT

Centurion University of Technology and Management and CSIR-IMMT, Bhubaneswar.

DATA AVAILABILITY STATEMENT

The author confirm that the data that supports the findings of this study are available within the article. Raw data that support the finding of this study are available from the corresponding author, upon reasonable request.

CONFLICT OF INTEREST

The author declared no potential conflicts of interest with respect to the research, authorship, and/or publication of this article.

USE OF AI FOR WRITING ASSISTANCE

Not declared.

ETHICS

There are no ethical issues with the publication of this manuscript.

REFERENCES

[1]. D. Sharma, J. Rajput, B.S. Kaith, M. Kaur, S. Sharma, "Synthesis of ZnO nano particles and study of their antibacterial and antifungal properties," Thin Solid Films, 519(3), pp. 1224–1229, 2010.

[2]. G. Aravind, D. Bhowmik, S. Duraivel, and G. Har-

ish, "Traditional and medicinal uses of Carica papaya. Journal of Medicinal Plants Studies," 1(1), pp. 7-15, 2013.

[3]. V. Yogiraj, P.K. Goyal, C.S. Chauhan, A. Goyal, and B. Vyas, "Carica papaya Linn: an overview. International Journal of Herbal Medicine," 2(5), pp. 01-8, 2014.

[4]. M. Chandrasekaran, S.M. Basheer, S. Chellappan, J.G. Krishna, P.S. Beena, "Enzymes in food and beverage production: an overview," Enzym Food Beverage Process CRC Press, 25, pp. 133-154, 2015.

[5]. S. Pandey, P.J. Cabot, P.N. Shaw, and A.K. Hewavitharana, "Anti-inflammatory and immunomodulatory properties of Carica papaya," Journal of İmmunotoxicology, 13(4):590-602, 2016.

[6]. C.J. Hewitt, S. R. Bellara, A. Andreani, G. Nebe-von-Caron, and C. M. McFarlane, "An evaluation of the anti-bacterial action of ceramic powder slurries using multi-parameter flow cytometry," Biotechnology Letters, 2001

[7]. S. Makhluf, R. Dror, Y. Nitzan, Y. Abramovich, R. Jelinek, and A. Gedanken, "Microwave-assisted synthesis of nanocrystalline MgO and its use as a bacteriocide," Advanced Functional Materials. 15(10), pp. 1708-1715, 2005.

[8]. R. Brayner, R. Ferrari-Iliou, N. Brivois, S. Djediat, M. F. Benedetti, and F. Fiévet, "Toxicological impact studies based on Escherichia coli bacteria in ultrafine ZnO nanoparticles colloidal medium," Nano Letters, 6(4), pp. 866-870, 2016.

[9]. N. G. Heatley, "A method for the assay of penicillin," Biochemical Journal. 1944;38(1):61.

[10]. Magaldi S, Mata-Essayag S, De Capriles CH, Pérez C, Colella MT, Olaizola C, and Ontiveros Y. , "Well diffusion for antifungal susceptibility testing," International Journal of İnfectious Diseases, 8(1), pp. 39-45, 2004.

[11]. C. Valgas, S. M. Souza, E.F. Smânia, and Jr. A. Smânia, "Screening methods to determine antibacterial activity of natural products," Brazilian Journal of Microbiology. 2007;38, pp. 369-380, 2007.

[12]. R. Sharma, R. Garg, and A. Kumari, "A review on biogenic synthesis, applications and toxicity aspects of zincoxide nanoparticles," EXCLI Journal, 19, pp. 1325, 2020.

[13]. K. Sowri Babu, A. Ramachandra Reddy, C. Sujatha, K. Venugopal Reddy, and A. N. Mallika, "Synthesis and optical characterization of porous ZnO," Journal of Advanced Ceramics, pp. 260-265, 2023.

[14]. K.Y. Ong, H.S. Chin, and K.C. Teo, "Biological screening of microbes isolated from soil of ex-tin mining land in Kampar Area," African Journal of Microbiology Research. 2011 Nov 23;5(27):4757-4763.

[15]. A. Islam, M.A. Al-Mamun, S. Parvin, M. Sarker, M.K. Zaman, P. Farhana, Z. Shahriar, and M. Salah Uddin, "Evaluation of antibacterial activities of latex of Caricaceae (Carica papaya L.)," Asian Journal of Pharmaceutical and Clinical Research, 8(1), pp. 308-311, 2015.

[16]. K. Maneesh, K. Vijayabhaskar, H. Firdouse, P.S. Rao, M. Prajwitha, and S. Swetha, "Evaluation of Antimicrobial of P. vesicularis, Streptococcus faecalis, Aeromonas hydrophilia, Salmonela typhae, Stphylococcus cohni, Serratia ficaria and E. coli. of crude and n-butanol fraction fruit latex of Carica papaya L.(Caricaceae),"Asian Journal of Pharmaceutical Research, 11(2), pp. 92-94, 2021.

[17]. T. Vij, and Y. Prashar, "A review on medicinal properties of Carica papaya Linn.," Asian Pacific Journal of Tropical Disease, 5(1), pp. 1-6, 2015.

[18]. R. Ajani, and K. Ogunbiyi, "Carica papaya latex accelerates wound healing in diabetic wistar rats," European Journal of Medicinal Plants, 9(3), pp. 1-2, 2015.

[19]. M. Ancheta, and L. Acero, "Wound healing property of Carica papaya stem in albino rats," International Jurnal of Bioscience, Biochemistry and Bioinfarmatics, 6(2), pp. 68-74, 2016.

[20]. K.R. Raghupathi, R. T. Koodali, and A. C. Manna, "Size-dependent bacterial growth inhibition and mechanism of antibacterial activity of zinc oxide nanoparticles," Langmuir. 5;27(7), pp. 4020-4028, 2011.

[21]. B. L. da Silva, B. L. Caetano BL, B.G. Chiari-Andréo, R. C. Pietro, and L.A. Chiavacci, "Increased antibacterial activity of ZnO nanoparticles: Influence of size and surface modification," Colloids and Surfaces B: Biointerfaces, 177, pp. 440-447, 2019.

[22]. Q. U. Naqvi, A. Kanwal, S. Qaseem, M. Naeem, S. R. Ali, M. Shaffique, and M. Maqbool, "Size-dependent inhibition of bacterial growth by chemically engineered spherical ZnO nanoparticles," Journal of Biological Physics, 45, pp. 147-159, 2019.

Environ Res Tec, Vol. 8, Issue. 2, pp. 429-446, June 2025

Environmental Research and Technology
https://dergipark.org.tr/en/pub/ert
DOI: https://10.35208/ert.1515094

Research Article

Predictive analysis of urban wastewater capacity using ANN and ODE model: A case study

Recep Sinan ARSLAN*[1], Murat TAŞYÜREK[1], Bahatdin DAŞBAŞI[2], Teslima DAŞBAŞI[1]

[1] *Kayseri University, Faculty of Engineering, Architecture and Design, Department of Computer Engineering, Kayseri, Türkiye*
[2] *Kayseri University, Faculty of Engineering, Architecture and Design, Department of Engineering Basic Sciences, Kayseri, Türkiye*
[3] *Kayseri University, Bünyan Vocational School, Kayseri, Türkiye*

ARTICLE INFO

Article history
Received: 12 Jul 2024
Revised: 24 Sep 2024
Accepted: 05 Oct 2024

Key words:
Wastewater quantity, ODE model, ANN activation function, parameter estimation, MSE

ABSTRACT

The discharge of urban wastewater represents a significant aspect to be considered in the development and design of water and wastewater treatment projects. In this study, the annual urban wastewater discharge was estimated using an artificial neural network (ANN) and differential equations. In order to achieve this, data pertaining to the recorded wastewater per capita amount for the Kayseri province (located in Turkey) over a 17-year period between 2003 and 2020, the city's population, capacity, number of WWTPs, the amount of daily wastewater discharged per person, and the wastewater treated in WWTPs (y(t)) were collated. As the initial data set was insufficient, it was augmented using the ARIMA model and then normalised. The augmented and normalised data was trained with ANN on two occasions, thus demonstrating the impact of other variables on the y(t) variable. Additionally, mathematical ANN activation functions in the form of a tangent hyperbolic function were proposed for this variable. Subsequently, the arbitrary parameters employed in a linear system comprising differential equations representing the aforementioned five variables were estimated utilising the normalised original data, thereby facilitating the formulation of an Ordinary Differential Equation (ODE) model. The performance of two ANN and ODE models was evaluated on normalized real data, and the results were compared. Consequently, the estimation of the quantity of wastewater with the lowest error rate of 0.00001 MSE among the models incorporating four time-dependent variables as inputs was conducted using the ODE model. The model exhibited an R^2 value of 0.9363 and a MAPE value of 0.0231. The promising estimation results obtained demonstrate the potential utility of this approach for the efficient management of wastewater demand and the protection of valuable water resources.

Cite this article as: Arslan RS, Taşyürek M, Daşbaşi B, Daşbaşi T. Predictive analysis of urban wastewater capacity using ANN and ODE model: A case study. Environ Res Tec 2025;8(2) 429-446.

***Corresponding author.**
*E-mail address: sinanarslanemail@gmail.com

This is an open access article under the CC BY-NC license (http://creativecommons.org/licenses/by-nc/4.0/).

INTRODUCTION

Rapid population growth, economic growth and urbanization have brought about serious problems in terms of environment and water [1]. One of the most important challenges in sustaining aquatic environments in the future is the issue of water pollution we face, both current and future, and its prediction. Along with population growth, domestic sewage and agricultural activities have caused pollution in water resources to increase and become a serious problem [2]. Especially in environments with industrial development, more industrial enterprises mean more wastewater generation. Water-related environmental issues are particularly challenging in Kayseri because Kayseri has a developed industry and dense population. Regarding wastewater, analysing and understanding the differences in terms of the daily amount of wastewater discharged per person, the amount of treated water, and the number of people is an important issue in terms of developing the integrated wastewater management plan in the country.

Wastewater management [3] is of significant importance in residential areas for several reasons, encompassing environmental [4], public health [5], and economic aspects [6]. Here are some key points highlighting the importance of wastewater management in residential areas: Public Health Protection, Environmental Protection, Resource Conservation, Water Conservation, Compliance with Regulations, Prevention of Soil and Groundwater Contamination, Infrastructure Maintenance, Quality of Life and Economic Considerations. Several factors can affect wastewater generation in residential areas. The amount and composition of wastewater produced can vary based on a range of factors related to population, lifestyle, infrastructure, and local practices [7, 8, 9]. Municipalities play an important role in managing wastewater to ensure public health, protect the environment and comply with regulatory standards. Some of the activities and responsibilities undertaken by municipalities for wastewater management are: Wastewater Collection [10], Treatment Plant Operation [11], Infrastructure Maintenance [12], Stormwater management [13], Wastewater Reuse Programs [14], etc. Therefore, effective wastewater management requires a comprehensive and integrated approach involving various departments in municipalities. Collaboration between local government, residents and businesses is essential to the success of wastewater management programs.

The main purpose of this study is to make Artificial Neural Network (ANN) and Ordinary Differential Equation (ODE) model predictions in the future analysis of the amount of wastewater to be treated data for the Kayseri province of Turkey, received from the Turkish Statistical Institute (TUIK), and to examine each input parameter comparatively. Thus, the purpose of using the relevant models for this estimation is to measure the error values and evaluate the input parameters in terms of their effect on the output. There are some studies in the literature regarding this evaluation, both ANN-based and ODE-based. However, the majority of these studies are concerned with estimating the chemical properties of treated wastewater rather than the amount of treated wastewater in any facility. Moreover, The comparison of the results obtained with the ANN and ODE models is presented as an innovation in the literature.Summary information regarding the studies in literature is as given below.

Nasr et al. [15], used an ANN with Feed Forward Back Propagation to estimate the performance of EL-AGAMY WWTP-Alexandria in terms of Chemical Oxygen Demand (COD), Biochemical Oxygen Demand (BOD) and Total Suspended Solids. They focused on the implementation of the approach. To do this, they used data collected during a study conducted over a 1-year period. They concluded that ANN provides an effective analysis and diagnostic tool for understanding and simulating nonlinear plant behaviour and is used as a valuable performance evaluation tool for plant operators and decision makers. Wongburi et al. [16] used ANN for predicting water quality in wastewater treatment plants (WWTP). The research evaluates ANNs and LSTM models on WWTP data, identifying optimal settings (epoch 50, batch size 100) for minimized training time and root mean square error (RMSE). The precise predictions of effluent parameters showcase the applicability of these models in detecting potential upsets in WWTP operations. Yang et al. [17] presented a resilient and adaptive dynamic neural network model designed to forecast effluent quality and facilitate potential real-time adjustments in wastewater treatment operations. They introduced in this investigation a dynamic nonlinear autoregressive network with an exogenous input (NARX) model to predict effluent quality, fine-tuning performance through varied time-delay parameters and training algorithms. Moreover, a PCA-NARX hybrid model was implemented, surpassing the performance of two stationary ANN models. Among the four training algorithms for the NARX model, they proposed that the BR algorithm stands out as the most efficient.

In recent years, a variety of modeling techniques, including ANN and ODE, have been employed to enhance the prediction accuracy and operational efficiency of wastewater treatment processes. These models offer valuable insights into the non-linear behaviors of such systems. Guo et al. [18] investigated the use of ANN models to forecast effluent quality parameters in municipal wastewater treatment plants. Their study emphasized the role of various input features and configurations in improving predictive performance. The results suggested that ANN models not only predicted effluent quality with a high degree of accuracy but also contributed to optimizing the operation costs of the plant without compromising the treatment efficacy. Waqas et al. [19] utilized ANN and SVM to optimize membrane permeability in a Membrane Rotating Biological Contactor (MRBC), focusing on operational parameters like disk rotational speed, hydraulic retention time (HRT), and sludge retention time (SRT). Their findings showed that ANN with 13 hidden layers achieved an R^2 value greater than 0.99, while SVM, using the Bayesian optimizer approach, also performed exceptionally well, indicating the effectiveness of machine learning in enhancing wastewater treatment. Godini et al. [20] modeled an industrial aerated lagoon system for waste-

water treatment, focusing on key operational parameters to predict system performance under various conditions. The primary objective was to identify potential bottlenecks and improvements in the system's operation. To achieve this, they used a neuro-evolutive approach that combined ANN with the Differential Evolution (DE) algorithm. Tarun et al. [21] explored the use of a Neural Networks-based Model Predictive Controller (MPC) for controlling Dissolved Oxygen (DO) in a wastewater treatment plant. The study addressed the complexity of wastewater treatment, which is influenced by biological, physical, and chemical factors. The regulation of DO is critical for maintaining the plant's efficiency. Zhao et al. [22] developed a parallel hybrid model combining ODE and ANN to simulate biological phosphorus removal (BPR) with greater accuracy and interpretability. The model incorporates the Activated Sludge Model No. 2d (ASM2d), a standard model in wastewater treatment, with an ANN to enhance the estimation of phosphate removal in anaerobic/aerobic sequencing batch reactors.

On the other hand, Differential Equation, is a mathematical tool used to model systems that involve rates of change with respect to a variable. Mathematical modeling using Differential Equations is prevalent in various fields, including Physics [23], Biology [24], Engineering [25], Medicine [26], Economics [27], Epidemic diseases [28, 29] and more. More complex systems involve systems of coupled ODEs, which might represent interactions between multiple variables. The specific form of the ODEs depending parameters depends varies according to the nature of the modelled system. Some studies in the literature on treated wastewater in WWTPs through differential equations are given below.

Diehl and Farås [30] modelled biological reactions in WWTP with two nonlinear ordinary differential equations and two hyperbolic partial differential equations (PDEs) with coefficients that are discontinuous functions in space due to the continuous sedimentation process, inputs, and outputs. They proved that the most desired steady-state solutions can be parameterized with a natural control variable. They supported their theoretical results with simulations. Zlateva and Dimitrova [31] defined a simplified mathematical model for the process of waste water treatment with active sludge in three nonlinear differential equation. They stated that their results may be useful in designing actual control strategies of active sludge waste water treatment processes.

The main contributions of this research study:

•The amount of wastewater treated through WWTP was estimated by modelling with ANN and ODE, based on real data.

•A comparative study on wastewater analysis was carried out in Turkey and an applicable simulation was provided for all regions in the world.

•With the ODE model, which can make predictions with a very low error rate (RMSE=0.0001), an analysis has been done that has the potential to contribute to future planning for sustainability in local government policies.

•The effects of four different input parameters on the amount of wastewater to be treated for the future were comparatively analyzed and the results were discussed.

The remainder of the article is organized in two sections broadly. One .section presents the proposed methodology and its details, and another section discusses the comparative analysis results and performance evaluations of both ANN and ODE models. In conclusion, a general evaluation of the study and suggestions for future studies is presented.

METHODOLOGY

The scope of this study includes analysis of wastewater data obtained from the Turkish Statistical institute (TUIK) of Kayseri province between 2003 and2020. For this analysis, mathematically presented and analyzed ANN activation functions and differential equation system were used. The process steps for the training, testing and analysis processes of the proposed models are as shown in Figure 1. The process starts with compiling the data from TUIK and augmenting the data with ARIMA modelling since 10 data from 18 years are not sufficient for ANN modelling. The augmented data was used only in the training processes of the ANN models, and only the original data obtained from TUIK was used in both the ODE model analysis and testing processes. In the next step, the data was normalized. The training processes of two different ANN models given as tangent hyperbolic (tanh) functions were carried out with the normalized data, and the parameters determination of the tanh activation function was carried out, as detailed in this section. After this process, the normalized original data was used to suggest two different ANN models and One (1) ODE model. With the data resulting from the estimation, MSE values were calculated separately for each model. Thus, the process of revealing the model was carried out with a comparative analysis, that predicts the amount of wastewater to be treated data with the lowest error rate.

Dataset

Kayseri (in Turkey) is a large city located in the central Anatolian region of Turkey. As of 2024, it is a crowded city with a population of approximately 1.5 million. There are more than 500 industrial establishments in the city and it is ranked 18th in Turkey according to industrial development. In Kayseri, which is a very large and developed city, it is very important to analyze both industrial and domestic wastewater production and the factors affecting it, and this study has addressed this issue.

Some of the factors affecting the amount of treated wastewater in a settlement can be given as a) population, b) capacity of WWTPs, c) number of WWTPs, and d) amount of daily wastewater discharged per person in municipalities. Therefore, the data obtained from TUIK for these five variables for Kayseri province, Turkey are given in Table 1 below.

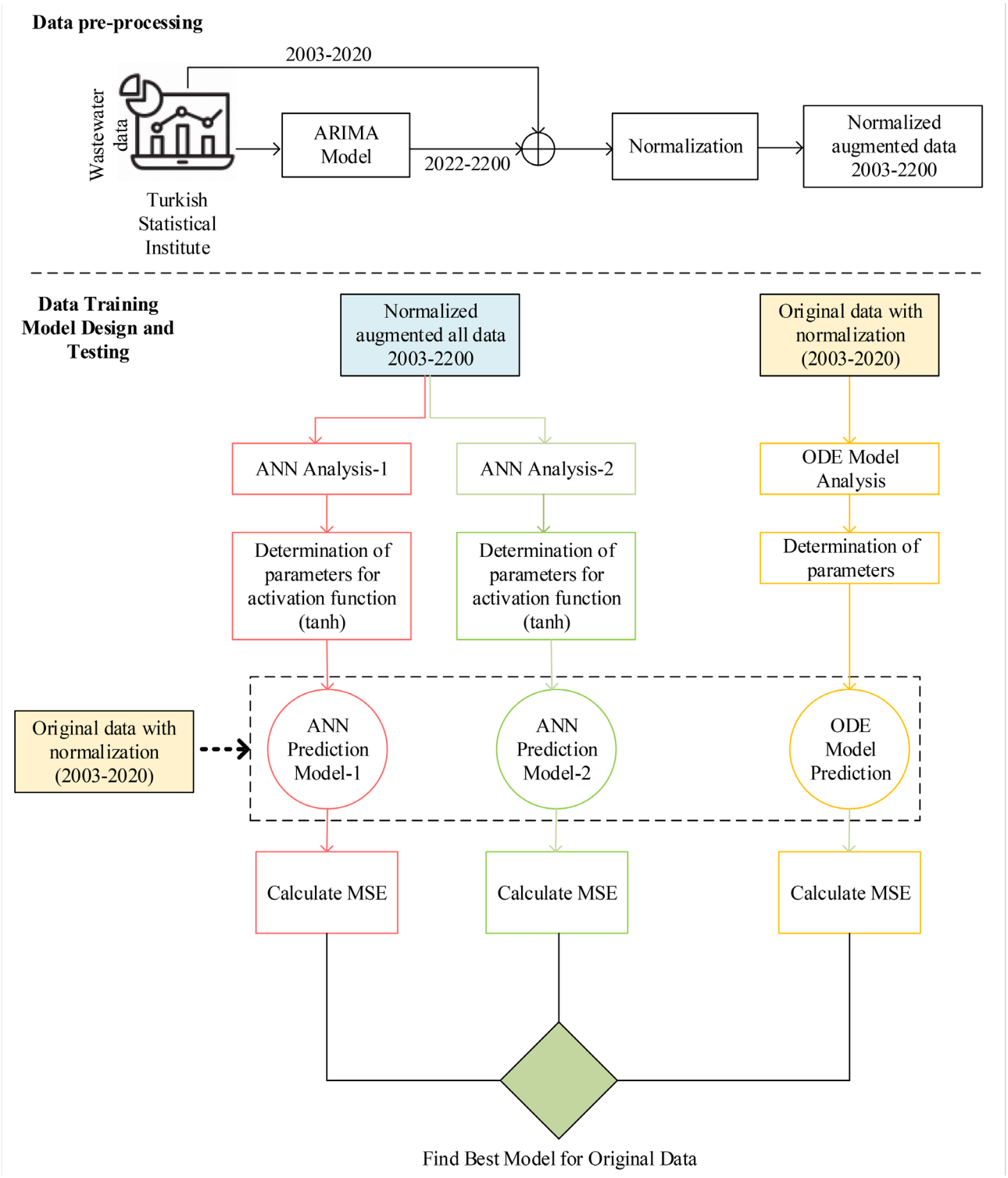


Figure 1. Methodology Diagram of Proposed Models through ANN activation functions and ODE

The analysis procedures in the remainder of the study were carried out based on the data in Table 1.

Data Augmentation with Autoregressive Integrated Moving Average (ARIMA)

ARIMA model is a traditional approach used for various time series forecasting and is used for applications such as economic forecasting and experimental parameter prediction [33]. However, ARIMA model is not suitable for non-stationary data [34]. For non-stationary data, model complexity increases and may lead to overfitting. Therefore, it is essential to investigate the stationarity of the data before using ARIMA model.

In order to test the stationarity of the data, the Augmented Dickey-Fuller (ADF) test table and p value calculation were performed within the scope of this study and it was investigated whether it was necessary to take a difference to make the series stationary. The test results were interpreted us-

ing the p value, ADF statistics and ADF critical values (1%, 5% or 10%). If the p value is typically lower than 0.05, the non-stationary null hypothesis is rejected and the stationarity of the series is proven [35] [36] In addition, if the ADF test statistics value is < ADF critical values, evidence for the stationarity of the series is obtained. A high p value is a situation that creates doubts about the stationarity of the series. In this case, the series should be made stationary by taking a derivative [37].

All these situations were evaluated together and the ADF test results performed on the original data were as shown in the Tablo-2. Accordingly, since the ADF_statistics value is lower than the ADF critical value, it shows that the original data is stationary. When the 1st degree derivative is taken, the p value also drops below 0.05 and supports stationarity.

Table 1. Some wastewater data for the years 2003-2020 obtained from TUIK for Kayseri province [32]

	Year	Population of the Municipality Served by the WWTP	WWTPs Capacity (Thousand M3/Year)	Number of WWTPs	Amount of aily Wastewater Discharged per Person in Municipalities (Litre per Person perDay)	Amount of Wastewater Treated in WWTPs (Thousand M3/ Year)
Order	**t**	**x(t)**	**k(t)**	**z(t)**	**h(t)**	**y(t)**
1	2003	576543	78475	1	172	42068
2	2004	595116	78475	1	195	50102
3	2006	872313	83835	2	165	51500
4	2008	861146	83835	2	161	51892
5	2010	986358	83835	2	160	58826
6	2012	1064662	87425	7	157	61416
7	2014	1164617	89836	10	155	65799
8	2016	1175068	89201	11	150	64349
9	2018	1321717	89603	14	126	60676
10	2020	1134304	51150	14	157	65008

Table 2. ADF Test Results

		ADF_statistic	ADF Critical Value (5%)	p-value	ADF_Result
Feature -1	Original	-1.64	-3.64	0.45	Stationary
	Diff_1	-4.22	-3.36	0.0	
	Diff_2	-3.48	-3.92	0.0	
Feature-2	Original	-0.74	-3.64	0.83	Stationary
	Diff_1	2.24	-3.64	0.99	
	Diff_2	-1.07	-3.47	0.72	
Feature-3	Original	0.1	-3.28	0.96	Stationary
	Diff_1	-2.46	-3.36	0.12	
	Diff_2	-3.14	-3.47	0.02	
Feature-4	Original	-1.13	-3.47	0.69	Stationary
	Diff_1	-5.23	-3.36	0.0	
	Diff_2	-4.04	-3.47	0.0	
Feature-5	Original	-2.14	-3.28	0.22	Stationary
	Diff_1	-3.07	-3.36	0.02	
	Diff_2	-2.81	-3.47	0.05	
Feature-4	Original	-1.13	-3.47	0.69	Stationary
	Diff_1	-5.23	-3.36	0.0	
	Diff_2	-4.04	-3.47	0.0	
Feature-5	Original	-2.14	-3.28	0.22	Stationary
	Diff_1	-3.07	-3.36	0.02	
	Diff_2	-2.81	-3.47	0.05	

The results prove that the original data is stationary in terms of time series and is suitable for ARIMA estimation. Data augmentation is a usable approach for problems where data is not sufficient [38], and in this study, data augmentation was performed with an ARIMA-based model.

Within the scope of this study, a time series forecasting based on Box-Jenkins models was carried out to augment the data taken from Turkish Statistical Institute (TUIK) to be used in the analysis and forecasting model of WWTP data. For this estimation, the ARIMA model structure was used within the designed algorithm as shown in Figure 2. The processing steps shown in Figure 1 were applied to select the p,d,q combination with the lowest RMSE value for each attribute. The p value indicates the number of autoregressive terms, the d value indicates the number of non-seasonal differences to maintain stationarity, and the q value indicates the number of lagged forecast errors in the forecast equation.

The general expression of the ARIMA (p,d,q) model can be shown as follows [39, 40]:

$$(w_t = \theta_1 w_{t-1} + \theta_2 w_{t-2} + \ldots + \theta_3 w_{t-p} + a_t - \theta_1 a_{t-1} - \theta_1 a_{t-2} - \ldots - \theta_q a_{t-q} \quad (1)$$

The moving average parameters (θ) are defined as negative in the equation following the Box-Jenkins convention. If the first differences make the series stationary, the d=1 difference equation will emerge, and, if the second differences make the series stationary, the d=2 difference equation will emerge, as shown in Eq.2 below:

$$\begin{aligned} w_t &= W_t \; for \; d = 0 \\ w_t &= W_t - W_{t-1} \; for \; d = 1 \\ w_t &= (W_t - W_{t-1}) - (W_{t-1} - W_{t-2}) \; for \; d = 2 \end{aligned} \quad (2)$$

Development of the model was implemented by Python version 3.10.6 and Matplotlib, Pandas, Seaborn, Numpy, Imblearn statsmodels. The performance evaluation criterion was taken into account with the calculation of Absolute Error ($\in_{AE}$) in Eq. 3. The original value and estimated value are symbolized as y_o and y_t, respectively.

$$\in_{AE} = |y_t - y_o \quad (3)$$

As stated in this section, it is important to select the p, d and q parameters in the ARIMA model structure, and the error values of the estimated values vary significantly depending on the selected values. Within the scope of this study, p,d,q parameters were selected separately for a total of 4 input and 1 output value within the flow diagram shown in Figure 1. For this selection, in the first stage, data was predicted for the years 2022-2200 using the original data (measured sensor data) containing records between 2003-2020 and the ARIMA model, which works with randomly selected p,d,q parameters. However, since there is no exact measurement value for the forecast period, it is not possible to measure the errors of the predicted values. For this reason, the same process was applied in reverse. Forecast data between 2022-2200 was fed to the same ARIMA model for training purposes, and data forecasting was performed for the years 2003-2020. We now have the ARIMA model forecast data and the original final data. Thus, the RMSE error value between both data was calculated. This process was repeated in 125 different combinations for all choices in the [0-5] range for p,d and q, and the ARIMA model parameter with the lowest RMSE value was selected. In this way, time-dependent data estimation was achieved with the lowest RMSE value and data that approximated the original data with the least error value was produced. The main purpose of the algorithm given in this section is to increase data with ARIMA and to ensure that these synthetic data are as close to the original data as possible. As a result, data augmentation was achieved with the ARIMA model, which uses the best p,d,q value for each attribute. The reason for this data increase is that it is not possible to train the ANN model with the smaller original data between 2003 and 2020, the details of which are explained in the next section,. This problem was intended to be overcome by using the ARIMA model structure to increase the data based on prediction.

Table 3 shows sample data regarding data predictions made within the flow chart given in Figure1. x(t),k(t),z(t),h(t) refer to the attributes given as input to the ANN and y(t) refers to the value received as output. The ARIMA model augmentation process was applied separately for each input and output value. This dataset, which includes original and predicted data, was used within the scope of this study to perform analysis with the model given in the form of ANN and differential equation system to estimate the amount of wastewater treated in WWTPs. In the last stage, the analysis results were compared with the original and real measurement data and the error values were compared.

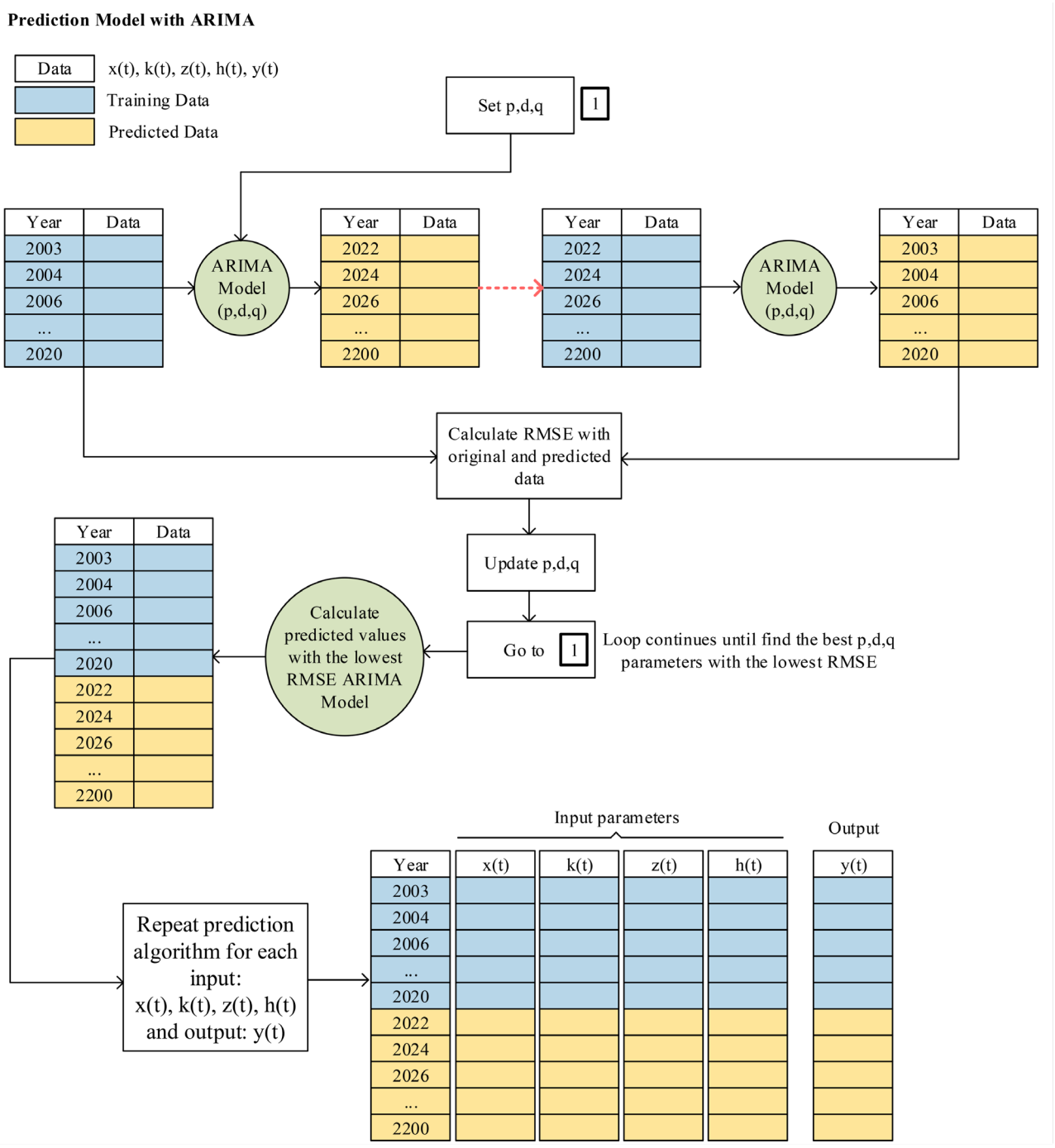


Figure 2. ARIMA data augmentation application flow diagram

Table 3. Increasing the Data in Table 1 to the Years 2022-2200 with ARIMA

Order	t	x(t)	k(t)	z(t)	h(t)	y(t)
11	2022	1227368	77580	15	155	67549
12	2024	1329078	76855	17	154	69309
…	…	…	…	…	…	…
26	2052	2756863	71279	37	130	91763
27	2054	2858848	70970	37	129	93311
…	…	…	…	…	…	…
41	2082	4286642	66640	58	106	114245
42	2084	4388627	66331	59	104	115687
…	…	…	…	…	…	…
56	2112	5816420	62001	79	81	135167
57	2114	5918405	61692	81	79	136509
…	…	…	…	…	…	…
71	2142	7346198	57363	101	56	154637
72	2144	7448184	57053	102	54	155885
…	…	…	…	…	…	…
86	2172	8875977	52724	122	31	172755
87	2174	8977963	52415	124	29	173917
…	…	…	…	…	…	…
100	2200	10303770	48394	142	8	188529

Normalization of Augmented Data

Here, the data in Table 2 are normalized with ARIMA sklearn.preprocessing.Normalizer (norm=l2). The purpose of doing this is to perform analysis with smaller error values. At the end of the analysis processes, normalized data will be denormalized and predictions will be made. The explanation is as follows:

Let $\omega=\omega_{orijinal}=(\omega_1,\omega_2,...,\omega_n)$, $n\in Z^+$ be elements of the data matrix. The normalized set of these data is given as $\omega_{normalized}=(\omega_1/\|\omega\|_2,\omega_2/\|\omega\|_2,...,\omega_n/\|\omega\|_2)$, where $\|\omega\|_2$ is the Euclidean norm in $\mathbb{R}^n$ such that $\|\omega\|_2=\sqrt{(\omega_1{}^2+\omega_2{}^2+\cdots+\omega_n{}^2)}$. Equation (4) is used to obtain original data from normalized data.

$$\blacksquare\omega_{orijinal}=(\|\omega\|_2)*(\omega_{normalized}) \quad (4)$$

For the data in Table 2, the norm of each variable is found to be

$$\blacksquare\|t\|_2\cong 21018,\ \|x\|_2\cong 60278211,\ \|k\|_2\cong 649511,\ \|z\|_2\cong 826,\ \|h\|_2\cong 1012,\ \|y\|_2\cong 1311678 \quad (5)$$

Therefore, the normalized set of values of the variables is given in Table 4.

ANN Analysis

The purpose of ANNs is essentially to enable machines to learn involve and acquire knowledge from data, discern and identify patterns, generate predictive insights, and perform tasks that traditionally required explicit programming [41, 42, 43, 44]. Their versatility and ability to handle complex relationships in data make them valuable tools across various domains. ANNs are a versatile technique used in many disciplines and industrial practice. Some branches and application areas where ANN is widely used are: Computer Science [45], Electrical and Electronics Engineering [46], Statistics [47] and Data Science [48], Chemistry and Biology [49], Medicine and Health Sciences [50], Finance [51], Transport and Logistics [52], Energy Systems [53], Agriculture and Environmental Sciences [54], Robotics and automation [55], and training and pedagogy [56]. ANNs have a wide range of applications in data analysis, modelling and predictability.

ANNs can be used for wastewater amount estimation by training the network on historical data that relates input features to the corresponding wastewater amounts. In an ANN, an activation function refers to a mathematical operation applied to the output of every neuron (or node) within a layer of the network. The activation function introduces non-linearity to the network, facilitating the acquisition of intricate patterns and relationships present in the data. The activation function determines whether a neuron should be activated (i.e., contribute to the network's output) based on its input.

There are several types of activation functions, each with its own characteristics. Here are some common activation functions used in ANNs [57, 58, 59, 60, 61, 62]:

- Sigmoid Activation Function,
- Hyperbolic Tangent (tanh) Activation Function,
- Rectified Linear Unit (ReLU) Activation Function,
- Leaky ReLU Activation Function,

Table 4. Increasing the Data in Table 1 to the Years 2022-2200 with ARIMA

Order	t	x(t)	k(t)	z(t)	h(t)	y(t)
1	**0.09530**	**0.009565**	**0.12082175**	**0.0012112**	**0.1700134**	**0.0320719**
2	**0.09535**	**0.009873**	**0.12082175**	**0.0012112**	**0.1927477**	**0.03819688**
3	**0.09544**	**0.014471**	**0.12907412**	**0.0024224**	**0.1630942**	**0.03926269**
4	**0.09554**	**0.014286**	**0.12907412**	**0.0024224**	**0.1591404**	**0.03956154**
5	**0.09563**	**0.016363**	**0.12907412**	**0.0024224**	**0.158152**	**0.0448479**
6	**0.09573**	**0.017662**	**0.13460135**	**0.0084782**	**0.1551866**	**0.04682247**
7	**0.09582**	**0.019321**	**0.13831338**	**0.0121118**	**0.1532097**	**0.05016399**
8	**0.09592**	**0.019494**	**0.13733572**	**0.0133229**	**0.1482675**	**0.04905854**
9	**0.09601**	**0.021927**	**0.13795465**	**0.0169564**	**0.1245447**	**0.04625831**
10	**0.09611**	**0.018818**	**0.07875161**	**0.0169564**	**0.1551866**	**0.04956095**
…	**…**	**…**	**…**	**…**	**…**	**…**
56	**0.10049**	**0.096493**	**0.09545876**	**0.0961713**	**0.0797777**	**0.10304878**
57	**0.10058**	**0.098185**	**0.09498262**	**0.0977679**	**0.0781384**	**0.10407191**
…	**…**	**…**	**…**	**…**	**…**	**…**
86	**0.10334**	**0.14725**	**0.08117461**	**0.1481703**	**0.030598**	**0.13170536**
87	**0.10344**	**0.148942**	**0.08069847**	**0.1498891**	**0.0289587**	**0.13259138**
…	**…**	**…**	**…**	**…**	**…**	**…**
100	**0.10467**	**0.170937**	**0.07450867**	**0.1724634**	**0.0076475**	**0.14373123**

•Parametric ReLU (PReLU) Activation Function,

•Exponential Linear Unit (ELU) Activation Function

The incorporation of these activation functions imparts non-linear characteristics to the network, facilitating its ability to learn and approximate intricate functions. The selection of an activation function is contingent upon the problem's inherent nature, the data's characteristics, and considerations for ensuring training stability. The Hyperbolic Tangent (tanh) activation function is a mathematical function commonly used in neural networks, especially in the hidden layers. The tanh activation function is often used in the hidden layers of neural networks, especially when the data is standardized or normalized. It is a common choice when the goal is to model relationships with complex and nonlinear patterns.

The structure used for ANN analysis of the data in Table 3 is given schematically in Figure 3.

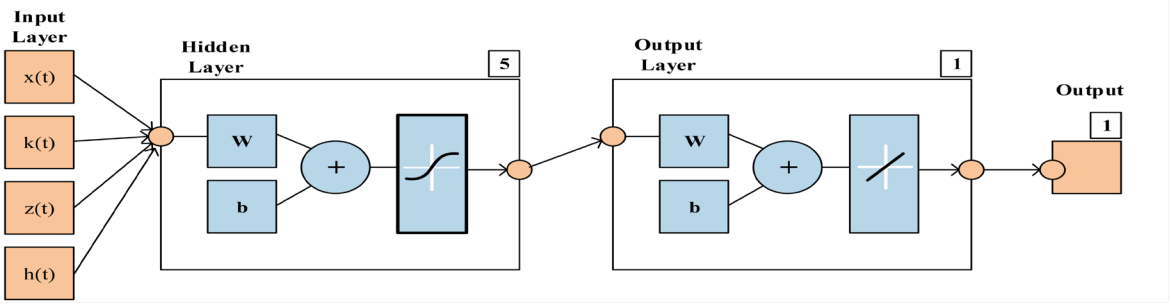


Figure 3. Structure of the used ANN Model

The ANN used in this study is a feedforward network with one hidden layer. The architecture of the ANN is designed to predict the y(t) variable using four input variables as described in Table 3. The details of the architecture and the hyperparameters selected for the ANN model are as follows:

Input Layer: The input layer consists of 4 neurons, each representing one of the input variables.

Hidden Layer: The hidden layer contains 5 neurons. The selection of 5 neurons was based on preliminary experiments aiming to balance model complexity and performance. Too many neurons could lead to overfitting, while too few neurons could lead to underfitting.

Output Layer: The output layer consists of 1 neuron, corresponding to the predicted y(t) variable.

Activation Function: In the hidden layer, the tanh activation function is used. The choice of the tanh function was made because it ensures non-linearity and better performance for normalized data by outputting values between -1 and 1.

Training Function: The Levenberg-Marquardt back-propagation algorithm (trainlm) was selected as the training function due to its efficiency in handling moderate-sized datasets and faster convergence compared to other methods like gradient descent.

Hyperparameters:

Number of epochs: 10,000 epochs were selected to ensure sufficient training time for convergence.

Learning rate: The learning rate is implicitly managed by the trainlm function, and no manual tuning of the learning rate was required.

Performance function: The mean squared error (MSE) was used as the performance function to measure the network's prediction error during training.

In this study, the y(t) variable was estimated by ANN with the help of other variables. In order to better demonstrate the performance of ANN, two different estimation processes were carried out.

ANALYSIS AND RESULTS

Within the scope of this study, three models based on ANN and ODE were proposed to perform wastewater analysis for Kayseri province and were analysed with data received from TUIK. Based on the result of the analysis, the aim was to find the best model for future prediction of the amount of wastewater to be treated and to present the estimate closest to the original data with the lowest MSE rate. In this section, the results and selected parameters for two (2) ANN models and one (1) ODE model are explained in detail.

Design of ANN Prediction Models and Results

With the two (2) ANN models proposed for this study, two (2) separate model designs were made. Training was carried out with different parameters, and they were tested with the normalized versions of the original data collected between 2003-2020.

Parameter selection of ANN

Different model parameters for the two (2) ANN analysis are shown in Table 5. Model parameter selections were determined by considering the situations in which the best results were obtained.

When Eq. 5 and the coefficients in Table 5 are considered together, two different ANN mathematical models are given below. Therefore, we have

$$yANN\ Prediction_1(t) = (0.3924) - 0.0767\cdot\tanh(2.8205 - 9.5779\cdot x(t) + 18.4063\cdot k(t) + 1.1281\cdot z(t) - 20.0762\cdot h(t)) + 0.0698\cdot\tanh(-0.3346 - 15.4020\cdot x(t) + 4.3192\cdot k(t) + 19.2210\cdot z(t) - 3.4523\cdot h(t)) + 0.0224\cdot\tanh(-2.1522 + 21.5775\cdot x(t) + 17.3640\cdot k(t) - 11.9887\cdot z(t) - 2.5399\cdot h(t)) - 0.2423\cdot\tanh(3.9206 + 8.7037\cdot x(t) + 6.6566\cdot k(t) - 21.5598\cdot z(t) - 6.7050\cdot h(t)) - 0.0089\cdot\tanh(-4.6525 - 0.9762\cdot x(t) + 27.8592\cdot k(t) - 18.2762\cdot z(t) + 11.3490\cdot h(t))$$ and

$$yANN\ Prediction_2(t) = (0.0396) + 0.0086\cdot\tanh(2.1338 + 10.7134\cdot x(t) - 38.3338\cdot k(t) + 1.9339\cdot z(t) - 15.7047\cdot h(t)) - 0.0817\cdot\tanh(-8.4515 + 5.3516\cdot x(t) + 60.4351\cdot k(t) + 8.0447\cdot z(t) - 0.5551\cdot h(t)) - 0.0240\cdot\tanh(1.2683 + 15.7308\cdot x(t) - 1.4211\cdot k(t) - 16.2572\cdot z(t) - 9.8105\cdot h(t)) + 0.0674\cdot\tanh(-3.2027 + 3.9454\cdot x(t) + 42.6491\cdot k(t) + 5.3263\cdot z(t) - 16.1992\cdot h(t)) + 0.0248\cdot\tanh(4.1221 - 19.2592\cdot x(t) - 29.3135\cdot k(t) - 5.1683\cdot z(t) - 10.2564\cdot h(t))$$

Activation function of ANN

The resulting model with activation function (tanh) of ANN is shown in Eq. 5.

$$■(y(t)=b_2+LW\ \tanh(b_1+IWx)\&(5)\ )$$

Thus, the obtained coefficients of Eq. 5 are given in Table 6.

For ANN analysis, 15 of the 100 Normalized Data for the years 2003-2200 were used for testing and 15 for verification. Regarding the results obtained, the training, validation and test graphics of the 1st and 2nd ANN models are shown in Figure 4 and Figure 5, respectively. As seen in Figure 4 and Figure 5, the lowest training R value was 0.99 for ANN training and 0.98 for validation. High R values obtained during the training process generally indicate how well the model has learned the relationship between input data and target output. As the R value approaches 1, it is stated that the variations in the model's training data are more strongly associated with the variations in the target output. This indicates that the models are well adapted to the training data. A high R value on the training set (0.99) generally indicates that the model has learned the patterns in the training data very well. However, a validation set is often used to evaluate the model's ability to apply the same success to new, unseen data. The R value (0.98) obtained in the validation set shows that the model can be successfully generalized to data outside the training set. This shows that the models do not have overfitting problems and have a good performance in general.

Table 5. Training Progress for ANN

	ANN Prediction_1			ANN Prediction_2		
	Initial Value	Stopped Value	Target Value	Initial Value	Stopped Value	Target Value
Epoch	**0**	**18**	**10000**	**0**	**12**	**10000**
Elapsed Time	-	**00:00:03**	-	-	**00:00:03**	-
Performance	**0.773**	**3.53e-07**	**0**	**2.31**	**1.64e-06**	**0**
Gradient	**3.52**	**0.000171**	**1e-07**	**5.44**	**7.6e-05**	**1e-07**
Mu	**0.001**	**1e-07**	**1e+10**	**0.001**	**1e-06**	**1e+10**
Validation Checks	**0**	**6**	**6**	**0**	**6**	**6**

Table 6. Table coefficient of tangent hyperbolic model in Equation (2).

	ANN Prediction_1	ANN Prediction_2
b_1	$\begin{pmatrix} 2.8205 \\ -0.3346 \\ -2.1522 \\ 3.9206 \\ -4.6525 \end{pmatrix}_{5x1}$	$\begin{pmatrix} 2.1338 \\ -8.4515 \\ 1.2683 \\ -3.2027 \\ 4.1221 \end{pmatrix}_{5x1}$
b_2	$(0.3924)_{1x1}$	$(0.0396)_{1x1}$
IW	$\begin{pmatrix} -9.5779 & 18.4063 & 1.1281 & -20.0762 \\ -15.4020 & 4.3192 & 19.2210 & -3.4523 \\ 21.5775 & 17.3640 & -11.9887 & -2.5399 \\ 8.7037 & 6.6566 & -21.5598 & -6.7050 \\ -0.9762 & 27.8592 & -18.2762 & 11.3490 \end{pmatrix}_{5x4}$	$\begin{pmatrix} 10.7134 & -38.3338 & 1.9339 & -15.7047 \\ 5.3516 & 60.4351 & 8.0447 & -0.5551 \\ 15.7308 & -1.4211 & -16.2572 & -9.8105 \\ 3.9454 & 42.6491 & 5.3263 & -16.1992 \\ -19.2592 & -29.3135 & -5.1683 & -10.2564 \end{pmatrix}_{5x4}$
LW	$(-0.0767 \quad 0.0698 \quad 0.0224 \quad -0.2423 \quad -0.0089)_{1x5}$	$(0.0086 \quad -0.0817 \quad -0.0240 \quad 0.0674 \quad 0.0248)_{1x5}$

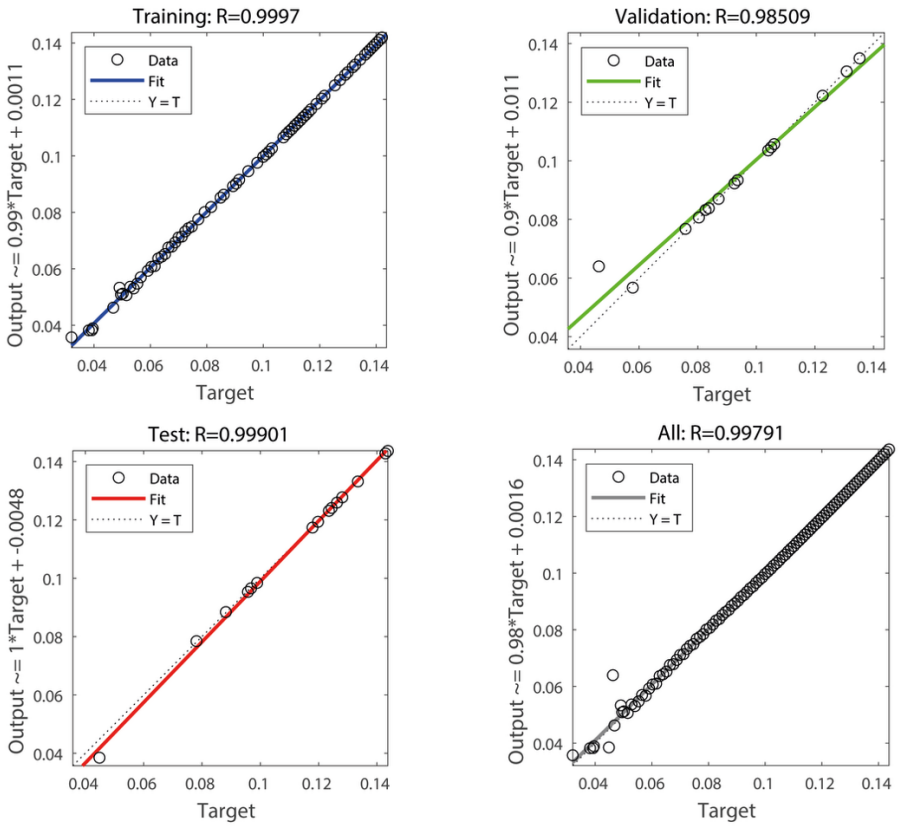


Figure 4. Graphical Representation of Analysis Results for ANN Prediction_1

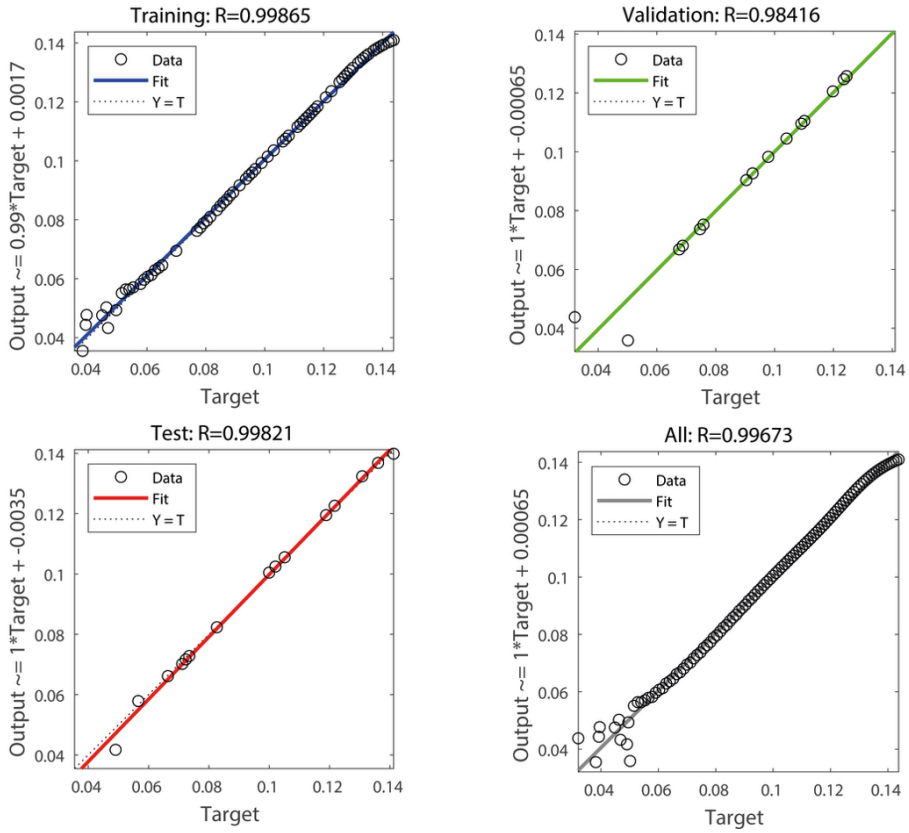


Figure 5. Graphical Representation of Analysis Results for ANN Prediction_2

Determining the ODE Model and Its Parameters

Let t denote the time parameter and the independent variable. The proposed general linear ODE mathematical model is as shown below.

$$\begin{aligned}
\frac{dx}{dt} &= \theta_1 x + \theta_2 k + \theta_3 z + \theta_4 h + \theta_5 y + \theta_6 \\
\frac{dk}{dt} &= \theta_7 x + \theta_8 k + \theta_9 z + \theta_{10} h + \theta_{11} y + \theta_{12} \\
\frac{dz}{dt} &= \theta_{13} x + \theta_{14} k + \theta_{15} z + \theta_{16} h + \theta_{17} y + \theta_{18} \\
\frac{dh}{dt} &= \theta_{19} x + \theta_{20} k + \theta_{21} z + \theta_{22} h + \theta_{23} y + \theta_{24} \\
\frac{dy}{dt} &= \theta_{25}\square\square + \theta_{26} k + \theta_{27} z + \theta_{28} h + \theta_{29} y + \theta_{30}
\end{aligned} \qquad (6)$$

where x ≡ x(t), k ≡ k(t), z ≡ z(t), h ≡ h(t) and y ≡ y(t) and the system (6) has to be finished with positive initial conditions $x(t_0) = x_0$, $k(t_0) = k_0$, $z(t_0) = z_0$, $h(t_0) = h_0$ and $y(t_0) = y_0$ for $t \geq t_0$. The dependent variables and their definitions used in the system in (6) are shown in Table 7 below.

The ODE model in (6) was solved with the Matlab R2023a program rungekutta45, and then the parameter values closest to the values in Table 1 (giving the minimum error) were found by using the lsqcurvefit function. The function lsqcurvefit, which is used as a tool in Matlab, is used to find the coefficients that will best fit a nonlinear function (with the logic of least squares). Find coefficients x that solve the problem minx $||F(x, x_{data}) - y_{data}||^2 2$ = minx $\sum i(F(x, x_{datai}) - y_{datai})^2$, given input data x_{data}, and the observed output y_{data}, where x_{data} and y_data are matrices or vectors, and $F(x,x_{data})$ is a matrix-valued or vector-valued function of the same size as y_{data}. lsqcurvefit simply provides a convenient interface for data-fitting problems. Rather than compute the sum of squares, lsqcurvefit requires the user-defined function to compute the vector-valued function. Additionally, x = lsqcurvefit(fun, x_0, x_{data}, y_{data}) starts at x_0 and finds coefficients x to best fit the nonlinear function fun(x,x_{data}) to the data y_{data} (in the least-squares sense). y_{data} must be the same size as the vector (or matrix) F returned by fun [63] [64] . In differential equation systems, the parameter values used in the system are calculated with this function. In this context, the parameters used in the system can be found with the coefficients of the nonlinear curve that produces the closest results to the real values of the solution of the system based on the initial values of the variables [65] [66].

In this context, the approach in [67] was used. Thus, the parameters θ_i for i=1,2,...,30 obtained are given in Table 8.

Comparison of ANN and ODE Models and Discussion

In this section, the estimation results of two (2) ANN and one (1) ODE models for normalized original data and the effects of the input parameters on the result are analysed and discussed. In Table 9, ANN and ODE model prediction re-

sults for quantity of wastewater (y(t)) are presented for 10 original normalized data. When the results were examined, it was understood that both ANN models and ODE model could predict the original data with low MSE values. According to the comparative results, the lowest MSE value among the three models was with the ODE model.

If the parameter values obtained by the least squares method is rewritten in the suggested ODE model in (6), then we have the Eqs (7) as shown below.

When the normalized values of Table 1 are compared with Eqs. (7), the results obtained is shown in Figure 6 below.

$$\begin{aligned}
\frac{dx}{dt} &= 0.26850x + 1.94674k + 0.14510z + 2.63931h + 0.62586y + 15.33129 \\
\frac{dk}{dt} &= 0.12103x + 0.57664k + 0.08480z + 0.81543h + 0.19972y + 4.08364 \\
\frac{dz}{dt} &= 0.30291x + 2.26687k + 0.15939z + 3.06476h + 0.72651y + 17.96241 \\
\frac{dh}{dt} &= -0.29066x - 4.12683k - 0.00916z - 5.69884h - 1.11164y - 34.75096 \\
\frac{dy}{dt} &= 0.37755x + 3.15511k + 0.17317z + 4.30412h + 0.96812y + 25.30082.
\end{aligned} \tag{7}$$

Table 7. State Variables

Variable	Definition
x(t)	**Population of the Municipality Served by the WWTP at time t**
k(t)	**WWTPs Capacity at time t**
z(t)	**Number of WWTPs at time t**
h(t)	**Amount of Daily Wastewater Discharged per Person in Municipalities at time t**
y(t)	**Amount of Wastewater Treated in WWTPs at time t**

Table 8. Rate Constants of Equations in (6)

θ_1=0.26850	**θ_7=0.12103**	**θ_13=0.30291**	**θ_19=-0.29066**	**θ_25=0.37755**
θ_2=1.94674	**θ_8=0.57664**	**θ_14=2.26687**	**θ_20=-4.12683**	**θ_26=3.15511**
θ_3=0.14510	**θ_9=0.08480**	**θ_15=0.15939**	**θ_21=-0.00916**	**θ_27=0.17317**
θ_4=2.63931	**θ_10=0.81543**	**θ_16=3.06476**	**θ_22=-5.69884**	**θ_28=4.30412**
θ_5=0.62586	**θ_11=0.19972**	**θ_17=0.72651**	**θ_23=-1.11164**	**θ_29=0.96812**
θ_6=15.33129	**θ_12=4.08364**	**θ_18=17.96241**	**θ_24=-34.75096**	**θ_30=25.30082**

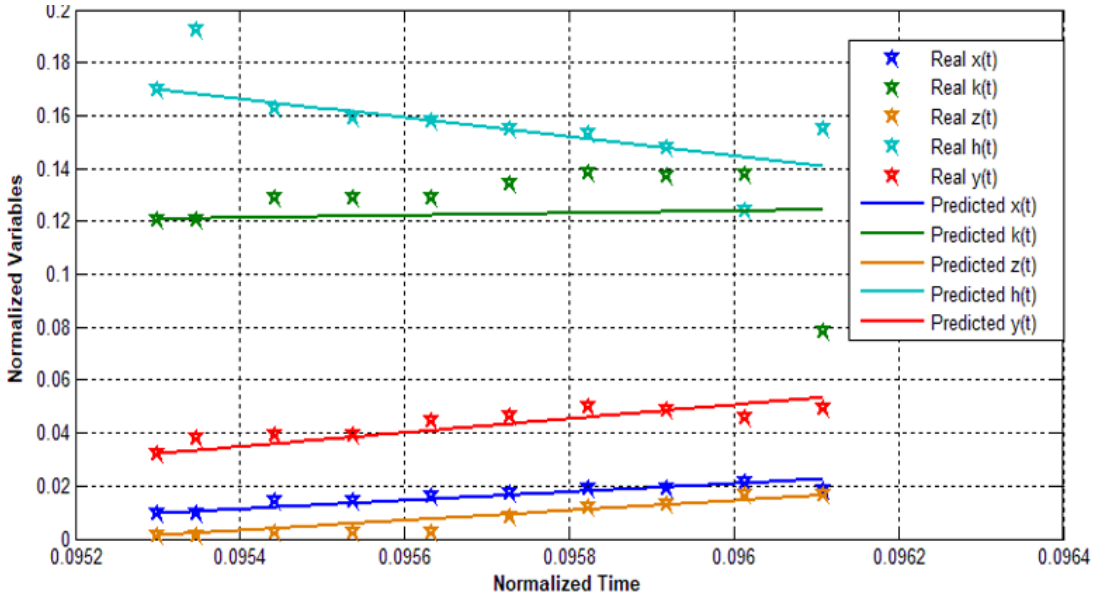


Figure 6. Graphical representation of the proposed ODE system

Table 9. The prediction performances of the proposed models according to the normalized values of Table 1

Order	Original Data y(t)	y(t) according to ANN Prediction_1	y(t) according to ANN Prediction_2	y(t) according to ODE Model
1	**0.0320719**	**0.0357**	**0.0438**	**0.03207**
2	**0.03819688**	**0.0382**	**0.0355**	**0.03337**
3	**0.03926269**	**0.0382**	**0.0443**	**0.03574**
4	**0.03956154**	**0.0389**	**0.0477**	**0.03855**
5	**0.0448479**	**0.0385**	**0.0476**	**0.04071**
6	**0.04682247**	**0.0462**	**0.0433**	**0.04351**
7	**0.05016399**	**0.0512**	**0.0359**	**0.04589**
8	**0.04905854**	**0.0533**	**0.0417**	**0.04847**
9	**0.04625831**	**0.0640**	**0.0503**	**0.05084**
10	**0.04956095**	**0.0509**	**0.0493**	**0.05343**
	ERROR VALUE (MSE)	**0.00004**	**0.00005**	**0.00001**
	R2	**0.7475**	**0.6251**	**0.9363**
	MAPE	**0.0724 (or 7.24%)**	**0.1105 (or 11.05%)**	**0.0231 (or 2.31%)**

As shown in Table 8, the results obtained show the success of the ODE model in predicting the original data. In real world, the selected variables may not always be in sufficient number to mathematically analyse the relationship between them and make predictions. Making predictions about variables, even with little data, can be vital. In this way, precautions can be taken by developing various control strategies. Especially in ANN analysis, it is important to increase the data sufficiently in such cases. One of the first methods that comes to mind for this is ARIMA. According to the working principle of ARIMA, in order to increase the data, it increases the data according to at least two previous values of the relevant prediction. In ANN analysis using data augmented in this way, the output tends to be a linear function of the inputs. However, in most real-world problems these relationships are non-linear. The activation function chosen for ANN in this study is non-linear tangent hyperbolic. In this sense, the ODE model in this study, whose solutions are nonlinear, was found to be quite successful in predicting the original data compared to the ANN activation function.

On the other hand, one of the aims of this study is to make predictions for the future and analyse the results of these predictions after determining the best model based on the original data. Therefore, for the period until 2100 (approximately 80 years later)

The projections are regarding the following as illustrated in Figure 7 below::

a) The change graph of Quantity of wastewater to be treated over the years, and

b) The change graph of the ratio of the Quantity of wastewater to be treated value to population size over the years

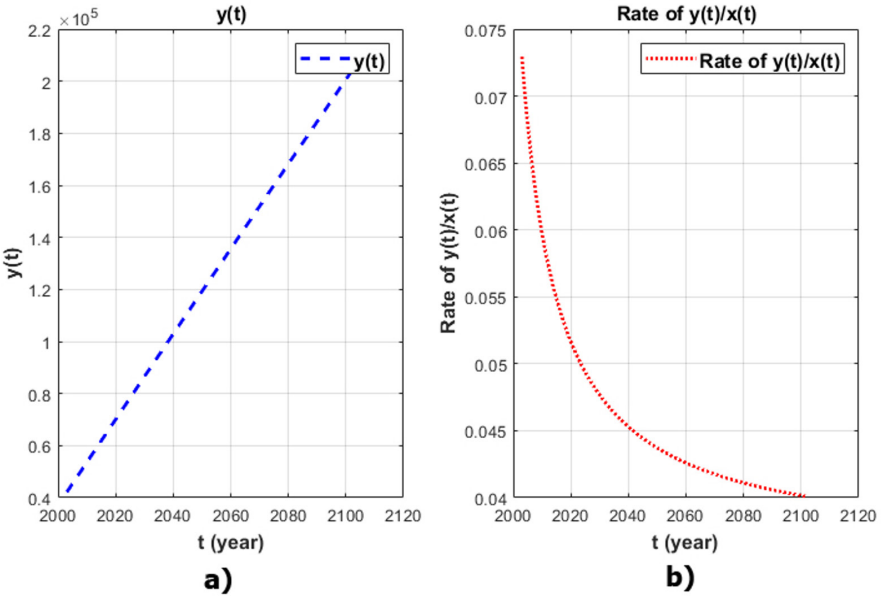


Figure 7. Analysis graph of wastewater amount according to various inputs

The results of the ODE model in Eqs. (7) are given in Table 10 and predictions have been made for the quantity of treated wastewater in WWTPs and population of the Municipality.

Table 10. The forecast results of the ODE model for the years 2020-2100

t	x(t)	y(t)	t	x(t)	y(t)	t	x(t)	y(t)
2003.015	**576561.1**	**42068.01**	**2009.756**	**886398.4**	**53186.52**	**2060.693**	**3215076**	**136740.4**
2003.083	**579692.7**	**42180.39**	**2011.458**	**964577.8**	**55991.93**	**2065.616**	**3438977**	**144773**
2003.152	**582824.3**	**42292.77**	**2016.381**	**1190571**	**64101.43**	**2070.54**	**3662669**	**152798**
2003.22	**585955.9**	**42405.14**	**2021.305**	**1416354**	**72203.21**	**2075.463**	**3886154**	**160815.4**
2003.288	**589087.4**	**42517.52**	**2026.228**	**1641927**	**80297.27**	**2080.387**	**4109431**	**168825.1**
2003.628	**604744.4**	**43079.38**	**2031.152**	**1867291**	**88383.63**	**2085.31**	**4332500**	**176827.2**
2003.969	**620400.4**	**43641.2**	**2036.075**	**2092444**	**96462.29**	**2090.233**	**4555363**	**184821.7**
2004.309	**636055.4**	**44202.99**	**2040.999**	**2317389**	**104533.3**	**2095.157**	**4778018**	**192808.6**
2004.649	**651709.4**	**44764.73**	**2045.922**	**2542124**	**112596.6**	**2100.08**	**5000466**	**200787.9**
2006.352	**729964.3**	**47572.92**	**2050.846**	**2766650**	**120652.2**			
2008.054	**808193.9**	**50380.18**	**2055.769**	**2990967**	**128700.1**			

When Figure 7 is considered, the decrease in the average amount of wastewater treatment per capita may result from a combination of factors. These factors may include technological advances, water management policies, community awareness and administrative support. This situation can be considered as a positive development in terms of environmental sustainability and water resources management.

The ANN and ODE based wastewater forecasting model developed in this study offers municipalities and wastewater treatment plants a practical tool with which to make informed decisions. The model facilitates the optimisation of wastewater treatment plant capacity, thereby preventing plants from becoming inadequate or over-utilising capacity in response to future demands. Furthermore, the model facilitates strategic planning by aiding infrastructure maintenance and expansion decisions based on wastewater production trends. The integration of the model into smart city infrastructure will enable real-time monitoring and long-term planning for sustainable wastewater management. With regard to policy recommendations, it would be prudent for governments to consider investing in AI-enabled smart infrastructure, introducing regulations mandating infrastructure upgrades in line with predictive models, and promoting water reuse and recycling practices. Such measures will contribute to the more efficient management of future wastewater demand and the protection of precious water resources.

CONCLUSION

In this study, two distinct ANN and one ODE model were employed to forecast the time series of annual total wastewater volume in Kayseri province, Turkey. The models identify the impact factors of wastewater discharge, predict the amount of urban wastewater in the coming years, and analyse the impact degree of all factors. Upon evaluation of the ODE model exhibiting the highest performance among the three models, the following results were obtained in the test phase: R^2 = 0.9363, MSE = 0.00001, and MAPE = 0.0231. These results demonstrate that the model exhibits an acceptable degree of accuracy in predicting the volume of wastewater in the Kayseri province. It is important to note that future predictions for the quantity of wastewater using the model proposed in this study should not be considered as a replacement for direct measurements. Nevertheless, the method may result in a discrepancy in grid data for modelling and urban water management, particularly for research purposes, in instances where measured data are unavailable (such as for the year 2100) or legally restricted. By evaluating discharged waters in conjunction with land use plans and modelling various future scenarios by analysing agricultural productivity factors, it is possible to simulate changes in land use habits.

ACKNOWLEDGEMENT

We would like to thank TUIK for providing information about wastewater data and the factors affecting this data.

DATA AVAILABILITY STATEMENT

The author confirm that the data that supports the findings of this study are available within the article. Raw data that support the finding of this study are available from the corresponding author, upon reasonable request.

CONFLICT OF INTEREST

The author declared no potential conflicts of interest with respect to the research, authorship, and/or publication of this article.

USE OF AI FOR WRITING ASSISTANCE

Not declared.

ETHICS

There are no ethical issues with the publication of this manuscript.

REFERENCES

[1] C. Vörösmarty ve J. S. R. L. P. Green, "Global water resources: Vulnerability from climate change and population growth," Science, vol. 289, no. 5477, 284-288, 2000.

[2] V. Novotny, "Diffuse pollution from agriculture — A worldwide outlook," Water Science and Technology, vol. 39, no. 3, 1-13, 1999.

[3] J. McLean, S. B. Cleveland, M. D. II, M. P. Lucas, R. J. Longman, T. W. Giambelluca ve G. A. Jacobs, "Building a portal for climate data—Mapping automation, visualization, and dissemination," Concurrency and Computation: Practice and Experience, p. e6727, 2023.

[4] M. Ahmadi, M. E. Lotfy, R. Shigenobu, A. M. Howlader ve T. Senjyu, "Optimal Sizing of Multiple Renewable Energy Resources and PV Inverter Reactive Power Control Encompassing Environmental, Technical, and Economic Issues," IEEE Systems Journal, 3026--3037, 2019.

[5] S. S. Biswas, "Role of chat gpt in public health," Annals of biomedical engineering, 868-869, 2023.

[6] G. Zhang, Y. Ge, Z. Ye ve M. Al-Bahrani, "Multi-objective planning of energy hub on economic aspects and resources with heat and power sources, energizable, electric vehicle and hydrogen storage system due to uncertainties and demand response," Journal of Energy Storage, p. 106160, 2023.

[7] M. Carrascal, E. Sánchez-Jiménez, J. Fang, C. Pérez-López, A. Ginebreda, D. Barceló ve J. Abian, "Sewage protein information mining: discovery of large biomolecules as biomarkers of population and industrial activities," Environmental science & technology, 10929--10939, 2023.

[8] C. Johnson ve S. J. Bell, "Linking emerging contaminants to production and consumption practices," Wiley Interdisciplinary Reviews: Water, p. e1615, 2023.

[9] J. Li, X. Li, H. Liu, L. Gao, W. Wang, Z. Wang, T. Zhou ve Q. Wang, "Climate change impacts on wastewater infrastructure: A systematic review and typological adaptation strategy," Water Research, 120282, 2023.

[10] C. Song, J.-J. Zhu, J. L. Willis, D. P. Moore, M. A. Zondlo ve Z. J. Ren, "Methane Emissions from Municipal Wastewater Collection and Treatment Systems," Environmental Science & Technology, 2248--2261, 2023.

[11] R. Herrera-Navarrete, A. Colı´n-Cruz, H. J. Arellano-Wences, M. L. Sampedro-Rosas, J. L. Rosas-Acevedo ve A. L. Rodrı´guez-Herrera, "Municipal wastewater treatment plants: Gap, challenges, and opportunities in environmental management," Environmental Management, 75--88, 2022.

[12] M. M. Emily ve G. Muyengwa, "Maintenance of municipality infrastructure: a case study on service delivery in Limpopo Province at South Africa," American Journal of Operations Research, 309--323, 2021.

[13] S. Geyler, N. Bedtke ve E. Gawel, "Sustainable stormwater management in existing settlements—Municipal strategies and current governance trends in Germany," Sustainability, p. 5510, 2019.

[14] C. T. Finnerty, A. E. Childress, K. M. Hardy, E. M. Hoek, M. S. Mauter, M. H. Plumlee, J. B. Rose, M. D. Sobsey, P. Westerhoff, P. J. Alvarez ve others, "The Future of Municipal Wastewater Reuse Concentrate Management: Drivers, Challenges, and Opportunities," Environmental Science & Technology, 2023.

[15] M. Nasr, M. Moustafa, H. Seif ve G. E. Kobrosy, "Application of Artificial Neural Network (ANN) for the prediction of EL-AGAMY wastewater treatment plant performance-EGYPT," Alexandria engineering journal, vol. 51, no. 1, 37-43, 2012.

[16] P. Wongburi ve J. K. Park, "Prediction of Wastewater Treatment Plant Effluent Water Quality Using Recurrent Neural Network (RNN) Models," Water, p. 3325, 2023.

[17] Y. Yang, K.-R. Kim, R. Kou, Y. Li, J. Fu, L. Zhao ve H. Liu, "Prediction of effluent quality in a wastewater treatment plant by dynamic neural network modeling," Process Safety and Environmental Protection, 515-524, 2022.

[18] H. Guo, K. Jeong, J. Lim, J. Jo, Y. M. Kim, J.-p. Park, J. H. Kim ve K. H. Cho, "Prediction of effluent concentration in a wastewater treatment plant using machine learning models", Journal of Environmental Sciences, no. 32, 90-101, 2015.

[19] S. Waqas, N. Y. Harun, N. S. Sambudi, U. Arshan, N. A. H. M. Nordin, M. R. Bilad, A. A. H. Saeed ve A. A. Malik, "SVM and ANN Modelling Approach for the Optimization of Membrane Permeability of a Membrane Rotating Biological Contactor for Wastewater Treatment", Membranes, vol. 12, no. 9, 821, 2022.

[20] K. Godini, G. Azarlan, A. Kimiaei, E. N. Dragoi ve S. Curteanu, "Modeling of a real industrial wastewater treatment plant based on aerated lagoon using a neuro-evolutive technique", Process Safety and Environmental Protection, vol. 148, 114-124, 2021.

[21] A. Tarun ve G. P. Reddy, "Artificial Neural Networks for Waste-water Treatment Plant Control", Proceedings of International Conference on Industrial Instrumentation and Control , vol. 815, 409-419, 2022.

[22] G. y. Zhao, H. Furumai ve M. Fujita, "Supporting data–enhanced hybrid ordinary differential equation model for phosphate dynamics in municipal wastewater treatment", Bioresource Technology, vol. 409, 131217, 2024.

[23] P. Veeresha, M. Yavuz ve C. Baishya, "A computa-

tional approach for shallow water forced Korteweg–De Vries equation on critical flow over a hole with three fractional operators," An International Journal of Optimization and Control: Theories & Applications, vol. 11, no. 3, 52-67, 2021.

[24] P. A. Naik, Z. Eskandari, H. E. Shahkari ve K. M. Owolabi, "Bifurcation analysis of a discrete-time prey-predator model," Bulletin of Biomathematics, vol. 1, no. 2, 111-123, 2023.

[25] B. Ersoy, B. Daşbaşı ve E. Aslan, "Mathematical modelling of fiber optic cable with an electro-opticalcladding by incommensurate fractional-order differential equations," An International Journal of Optimization and Control: Theories & Applications, vol. 14, no. 1, 50-61, 2024.

[26] B. Daşbaşı, "Fractional order bacterial infection model with effects of anti-virulence drug and antibiotic," Chaos, Solitons & Fractals, vol. 170, no. 113331, 1-17, 2023.

[27] E. K. Akgül, A. Akgül ve M. Yavuz, "New illustrative applications of integral transforms to financial models with different fractional derivatives," Chaos, Solitons & Fractals, vol. 146, no. 110877, 2021.

[28] L. Boulaasair, "Threshold properties of a stochastic epidemic model with a variable vaccination rate," Bulletin of Biomathematics, vol. 1, no. 2, 177-191, 2023.

[29] U. T. Mustapha, Y. U. Ahmad, A. Yusuf, S. Qureshi ve S. S. Musa, "Transmission dynamics of an age-structured Hepatitis-B infection with differential infectivity," Bulletin of Biomathematics, vol. 1, no. 2, 124-152, 2023.

[30] S. Diehl ve S. Farås, "Control of an ideal activated sludge process in wastewater treatment via an ODE–PDE model," Journal of Process Control, vol. 23, no. 3, 359-381, 2013.

[31] P. Zlateva ve N. Dimitrova, "Analysis of Some Properties of an Activated Sludge Wastewater Treatment Model," %1 içinde The 6th International Conference on Energy and Environmental Science, 2022.

[32] TUIK, "Merkezi Dağıtım Sistemi," 15 December 2023. [Online]. Available: https://biruni.tuik.gov.tr/medas/?locale=tr.

[33] A. Dishan, M. Barel, S. Hizlisoy, R. S. Arslan, H. Hizlisoy, D. A. Gundog, S. Al ve Z. Gonulalan, "The ARIMA model approach for the biofilm-forming capacity prediction of Listeria monocytogenes recovered from carcasses", BMC Veterinary Research, vol. 20, no. 123, 1-13, 2024.

[34] N. Minhaj, R. Ahmed, I. A. Khalique ve M. Imran, "A Comparative Research of Stock Price Prediction of Selected Stock Indexes and the Stock Market by Using Arima Model", Global Economics Science, vol. 4, no. 1, 1-19, 2022.

[35] S. Majumder, "Time Series Analysis — Stationarity Check using Statistical Test", Analytics Vidhya, 02 05 2020. [Online]. Available: https://medium.com/analytics-vidhya/time-series-analysis-stationarity-check-using-statistical-test-f106e9045370#:~:text=If%20p%20%3E%200.05%2C%20then%20the,present%20data%20and%20past%20data.. [Access: 23 09 2024].

[36] "Stationarity and detrending (ADF/KPSS)", statsmodels, 16 09 2024. [Online]. Available: https://www.statsmodels.org/dev/examples/notebooks/generated/stationarity_detrending_adf_kpss.html#Stationarity-and-detrending-(ADF/KPSS). [Access: 23 09 2024].

[37] "Interpret all statistics and graphs for Augmented Dickey-Fuller Test,» Minitab, 01 01 2024. [Online]. Available: https://support.minitab.com/en-us/minitab/help-and-how-to/statistical-modeling/time-series/how-to/augmented-dickey-fuller-test/interpret-the-results/all-statistics-and-graphs/#:~:text=The%20p%2Dvalue%20is%20a,value%20to%20your%20significance%20level.). [Access: 23 09 2024].

[38] S. Hizlisoy, R. S. Arslan ve E. Çolakoğlu, "Singer identification model using data augmentation and enhanced feature conversion with hybrid feature vector and machine learning", EURASIP Journal on Audio, Speech, and Music Processing, vol. 2024, no. 14, 1-14, 2024.

[39] R. Nau, "The mathematical structure of arima models," Duke University Online Article, vol. 1, no. 1, 1-8, 2014.

[40] R. Nau, ARIMA models for time series forecasting. Statistical Forecasting: Notes on Regression and Time Series Analysis, Durham: Duke University, 2017.

[41] R. S. Arslan ve M. Tasyurek, "AMD-CNN: Android malware detection via feature graph and convolutional neural networks," Concurrency and Computation: Practice and Experience, p. e7180, 2022.

[42] M. Taşyürek, "Odrp: a new approach for spatial street sign detection from exif using deep learning-based object detection, distance estimation, rotation and projection system," The Visual Computer, 2023.

[43] M. Tasyurek ve R. S. Arslan, "RT-Droid: a novel approach for real-time android application analysis with transfer learning-based CNN models," Journal of Real-Time Image Processing, 1-17, 2023.

[44] Y.-c. Wu ve J.-w. Feng, "Development and application of artificial neural network," Wireless Personal Communications, p. 1645–1656, 2018.

[45] A. Baliyan, K. Gaurav ve S. K. Mishra, "A review of short term load forecasting using artificial neural network models," Procedia Computer Science , p. 121–125, 2015.

[46] F. Zakaria, S. A. C. Kar, R. Abdullah, S. I. Ismail ve N. I. M. Enzai, " A Study on Correlation of Subjects on Electrical Engineering Course Using Artificial Neural Network (ANN)," Asian Journal of University Education, p. 144–155, 2021.

[47] B. M. Al-Maqaleh, A. A. Al-Mansoub ve F. N. Al-

Badani, " Forecasting using artificial neural network and statistics models," International Journal Education and Management Engineering, p. 20–32, 2016.

[48] M. M. Saritas ve A. Yasar, "Performance analysis of ANN and Naive Bayes classification algorithm for data classification," International journal of intelligent systems and applications in engineering, p. 88–91, 2019.

[49] S. Agatonovic-Kustrin ve R. Beresford, "Basic concepts of artificial neural network (ANN) modeling and its application in pharmaceutical research," Journal of pharmaceutical and biomedical analysis, p. 717–727, 2000.

[50] F. Amato, A. López, E. M. Peña-Méndez, P. Vanhara, A. Hampl ve J. Havel, "Artificial neural networks in medical diagnosis," Journal of applied biomedicine, 47-58, 2013.

[51] E. Sariev ve G. Germano, "Bayesian regularized artificial neural networks for the estimation of the probability of default," Quantitative Finance, p. 311–328, 2020.

[52] J. Gao, "Performance evaluation of manufacturing collaborative logistics based on BP neural network and rough set," Neural Computing and Applications, p. 739–754, 2021.

[53] P. Jiang, Z. Liu, X. Niu ve L. Zhang, "A combined forecasting system based on statistical method, artificial neural networks, and deep learning methods for short-term wind speed forecasting," Energy, p. 119361, 2021.

[54] A. Escamilla-Garcı´a, G. M. Soto-Zarazúa, M. Toledano-Ayala, E. Rivas-Araiza ve a. A. Gastélum-Barrios, "Applications of artificial neural networks in greenhouse technology and overview for smart agriculture development," Applied Sciences, p. 3835, 2020.

[55] H. Su, W. Qi, C. Yang, J. Sandoval, G. Ferrigno ve E. D. Momi, "Deep neural network approach in robot tool dynamics identification for bilateral teleoperation," IEEE Robotics and Automation Letters, p. 2943–2949, 2020.

[56] R. Shaw ve B. K. Patra, "Classifying students based on cognitive state in flipped learning pedagogy," Future Generation Computer Systems, p. 305–317, 2022.

[57] Q. Cheng, H. Li, Q. Wu, L. Ma ve K. N. Ngan, "Parametric deformable exponential linear units for deep neural networks," Neural Networks, p. 281–289, 2020.

[58] D. Kim, J. Kim ve J. Kim, "Elastic exponential linear units for convolutional neural networks," Neurocomputing , p. 253–266, 2020.

[59] Y. Koçak ve G. Ü. Şiray, "New activation functions for single layer feedforward neural network," Expert systems with applications, p. 113977, 2021.

[60] A. Maniatopoulos ve N. Mitianoudis, "Learnable leaky relu (LeLeLU): An alternative accuracy-optimized activation function," Information , p. 513, 2021.

[61] B. Olimov, S. Karshiev, E. Jang, S. Din, A. Paul ve J. Kim, "Weight initialization based-rectified linear unit activation function to improve the performance of a convolutional neural network model," Concurrency and Computation: Practice and Experience, p. e6143, 2021.

[62] H. Pratiwi, A. P. Windarto, S. Susliansyah, R. R. Aria, S. Susilowati, L. K. Rahayu, Y. Fitriani, A. Merdekawati ve I. R. Rahadjeng, "Sigmoid activation function in selecting the best model of artificial neural networks," Journal of Physics: Conference Series, p. 012010, 2020.

[63] MathWorks. [Online]. Available: https://www.mathworks.com/help/optim/ug/lsqcurvefit.html. [Access: 15 September 2024].

[64] O. Toolbox, "Isqcurvefit", [Online]. Available: http://www.ece.northwestern.edu/local-apps/matlabhelp/toolbox/optim/lsqcurvefit.html. [Access: 15 September 2024].

[65] MathWorks, "Isqcurvefit fitting kinetic model to estimate kinetic parameter.", [Online]. Available: https://www.mathworks.com/matlabcentral/answers/1990058-lsqcurvefit-fitting-kinetic-model-to-estimate-kinetic-parameter. [Access: 15 September 2024].

[66] MathWorks, "Fitting two differential equations simultaneously using Isqcurvefit", [Online]. Available: https://www.mathworks.com/matlabcentral/answers/1657480-fitting-of-two-differential-equations-simultaneously-using-lsqcurvefit. [Access: 15 September 2024].

[67] H. Pratiwi, A. P. Windarto, S. Susliansyah, R. R. Aria, S. Susilowati, L. K. Rahayu, Y. Fitriani, A. Merdekawati ve I. R. Rahadjeng, "Sigmoid activation function in selecting the best model of artificial neural networks," Journal of Physics: Conference Series, p. 012010, 2020.

Environmental Research and Technology
https://dergipark.org.tr/en/pub/ert
DOI: https://10.35208/ert.1520902

Research Article

Exploring the relationship between rainfall and crop yield and best practices adoption using participatory approach

Arunya KALAIYARASI GANESAPANDIAN*[1] Krishnaveni MUTHIAH[2]

[1]*Centre for Water Resources, Anna University, Guindy, Chennai, India*
[2]*Institute for Ocean Management, Anna University, Guindy, Chennai, India*

ARTICLE INFO

Article history
Received: 31 Jul 2024
Accepted: 05 Oct 2024

Key words:
Precipitation, ground truthing, participatory approach, İmplementation of results.

ABSTRACT

Crop yield is a standard measurement for the amount of agricultural production. Sustainable agriculture demands an increase in crop yield. This study deals with rainfed agriculture; hence, precipitation becomes the driving factor for crop yield. Heat maps are used to examine the rainfall and crop yield correlations. ML is an essential tool in decision-making, and many ML algorithms are available for prediction. This study uses the ML algorithms to predict whether the crop yield will increase with increased rainfall. Logistic regression, Decision tree classifier, Random Forest classifier, and XGBoost classifier are the algorithms chosen for analysis. Altogether this region consists of forty crops but focuses on five predominant annual crops. Implementation-based results are the universal goal of every research which society needs. The chances of implementation are associated with two major components: the reliability of the results and society's willingness. Analysis of these components needs ground truthing and Participatory Rural Appraisal, respectively. Farmers and villagers filled out a questionnaire about the details required for this study. The survey was an active approach to collecting necessary information from the participants. The survey showed positive results among one hundred and fifty samples from six blocks. Finally, cashew nut, sugarcane, and turmeric showed good dependency on the precipitation, and around 88% of villagers are ready to implement the results derived from ML algorithms.

Cite this article as: Arunya KG, Krishnaveni M. Exploring the relationship between rainfall and crop yield and best practices adoption using participatory approach. Environ Res Tec 2025;8(2) 447-455.

INTRODUCTION

Many models have evolved and validated for crop yield predictions, which is one of the significant issues in agriculture, as [1] found. Though crop yield depends on many factors [2], such as climate, seed variety, irrigation, soil fertility, and fertilizer, this study tests the dependency of crop yield on rainfall. Many statistical methods are available for yield loss using all the above parameters [3]. Rainfall is a predominant factor that affects agricultural production [4]. Since rainfall is a complex atmospheric process, it takes work to predict. Difficulty in predicting rainfall affects people in many different ways, such as tourism, pilgrimage, and many other factors [5], including agriculture.

Yield prediction has greater significance in terms of yield measuring, yield evaluation, and coordinating harvest supply. [6]. Many studies have analyzed various techniques used for crop yield prediction and concluded that the data mining techniques are the best [7]. Computational models such as deep learning can predict by adequately adjusting the input parameters. However, sometimes, the output may fit the data well during the training but will provide poor results due to overfitting or overtraining [8]. Machine Learning algorithms are less computationally expensive than these computational models. Researchers used algorithms such as Neural Net-

***Corresponding author.**
*E-mail address: arunya0517@gmail.com

This is an open access article under the CC BY-NC license (http://creativecommons.org/licenses/by-nc/4.0/).

works, Linear Regression, Support Vector Machines, Random Forest, and Gradient Boosting Trees to predict crop yields [1].

Participation and empowerment are new words in the field [9]. To achieve sustainable adaptation, we need to enhance the site-specific knowledge of the locals. The traditional research method focuses little on community capacity building; however, disseminating predicted results is more critical [10]. It is essential to increase sensitivity in the minds of the locals towards their responsibility to society's social and physical conditions. Participatory Rural Appraisal (PRA) makes the local's joint action increase awareness and responsibility [11]. PRA's main aim is to develop context-based solutions with the combined effort of professionals, universities, state agency officials, and local communities [12]. Hence using PRA, this study analyses the possibilities for implementation with the help of the locals.

MATERIALS AND METHODS

Study Area

Paravanar basin is one of the minor River basins in Neyveli, Cuddalore District of Tamil Nadu. The latitude and longitudinal extent of Paravanar River Basin are 11°18" to 11°45" North latitude and 79°18" to 79°45" East longitude which is shown in figure 1. The Penniyar River basin bounds the Paravanar River basin in the North, the Vellar River basin in the South and West, and the Bay of Bengal in the East.

The word "Paravanar" in Tamil means spreading River. Numerous small streams are spreading over this basin area, forming the River Paravanar. The sedimentary rock type covers the Paravanar River Basin, occurring from tertiary to recent age. The Basin receives a high amount of rainfall during North – East Monsoon. In this basin, district, taluk headquarters, and major towns are well connected with Road and Rail networks. The average annual rainfall of this basin is 1197.70mm.

Two sub-basins cover the Paravanar River basin. The upper part of the Paravanar River is called the Paravanar sub-basin, and the lower part of the Paravanar River is called the Uppanar sub-basin. The areas covered by these two sub-basins are Paravanar Sub Basin (435.016 Sq. Km) and Uppanar Basin (437.325 Sq. Km), which covers a total area of 872.34Sq.Km.

The "Neyveli Lignite Corporation" is located within this basin. Mine 1, Mine 1A & Mine 2 are the three opencast mines operated in this area. The Perumal Tank utilizes the groundwater pumped from the mines via the Walajah tank for irrigation.

Test taken on the command area of the Perumal Tank indicates that the water used for irrigation from both Perumal Tank and Walajah Tank has no adverse effect on the soils to hinder crop growth.

The topographic trend is falling towards the south and southeast direction. Paravanar is a plain and upland terrain basin devoid of hills and related morphologies. Geologically the basin is covered with sedimentary formation. About 70% of the basin area covered Cuddalore sandstone of the Tertiary Age, which consists of laterite, sandstone, clay, silt, and sand. River alluvium and coastal alluvium of recent age cover 30% of the basin area.

The Paravanar River has yet to fully develop and is only present during certain seasons. It comes from various streams in the highlands northwest of the Neyveli lignite corporation area, specifically from the Semmakottai Reserve forest near Raghavankuppam and Kovilankuppam villages, at an elevation of approximately 100 meters above MSL. The River Paravanar is joined by several small streams in its upper reaches, which flow eastward and eventually drain into the Walajah Tank. The Sengal Odai and the Kanniyakovil odai are two streams originating in Mulaikuppam village and Southeast Neyveli Township, respectively. These two streams merge in Ellaikudi village, where the River Middle Paravanar begins and flows into the Perumal tank. Some streams that flow eastward from the Walajah tank eventually reach the Satapadi tank, and the excess water from this tank forms the

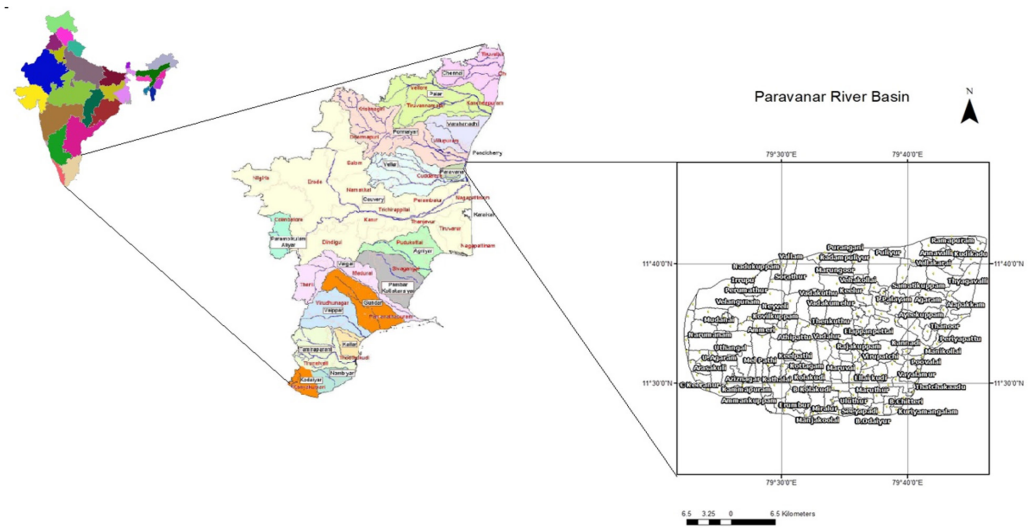


Figure 1. Paravanar River Basin

Uppanar River. As it flows northeast, the Uppanar River is fed by excess water from the Perumal tank near Periyapakkam, Anniyampettai, and Pundiyankuppam. Eventually, the river merges with the Bay of Bengal to the north of Semabadakuppam and south of Cuddalore O.T. The Uppanar River spans roughly 24 kilometers and has 37 tanks within its basin, overseen by WRD/PWD, with 16 of these tanks having an ayacut of over 100 hectares. The main tanks responsible for receiving and distributing water for irrigation are the Perumal Tank and Walajah Tanks.

The crops chosen for this study are the crops that are cultivated throughout the year and depend majorly on rainfall. Hence the yearly rainfall chose for this analysis. They follow crop rotation also, which depends on the rain and the crop harvested during the previous year. This basin cultivates the following crops which are areca nut, arhar, bajra, banana, black pepper, cashew nut, castor seeds, coconut, coriander, cotton, cowpea, dry chilly, garlic, gram, ground nut, guar seed, horse gram, jowar, maize, masoor, moong, onion, potato, ragi, mustard, rice, sannhamp, sesamum, minor millets, sugarcane, sunflower, sweet potato, tapioca, tobacco, turmeric, urad and other cereals, kharif, and rabi pulses. Farmers cultivate these crops in six seasons: autumn, kharif, rabi, summer, winter, and yearly. The data is collected from 1998 to 2020. As the data quantity increases, ML accuracy also increases, so it is advisable to use a considerable amount of data.

Data Collection

The data used for rainfall is the Precipitation Estimation from Remotely Sensed Information using Artificial Neural Networks – Climate Data Record (PERSIANN CDR) from National Centres for Environmental Information – National Oceanic and Atmospheric Administration for the location 11°18" to 11°45" North latitude and 79°18" to 79°45" East longitude. The PERSIANN algorithm on Gridsat - B1 Infrared satellite data produces the data from 1983 with 0.25° resolution, including data from most geostationary satellites. Validation of satellite rainfall data is mandatory for any analysis [13]. Therefore, the data is validated using the rain gauge station data, and the correlation is 0.76.

India's Agriculture and farmers welfare ministry contains the agriculture crop production data. The data consists of 1998-present data with more than 40 crops cultivated in that region. The primary five annual crops are the main focus of this study. They are Cashew nut, Coriander, Sugarcane, Sweet Potato, and Turmeric. Cashewnut, Sugarcane and Turmeric are annual crops whereas Coriander and Sweet Potato are seasonal crops (June to September). Hence the correlation study for the annual crops are analysed with the annual rainfall and the seasonal crops are analysed with the southwest monsoon rainfall. The data validation uses ground truthing with the farmers through a questionnaire survey conducted during Rapid Rural Appraisal.

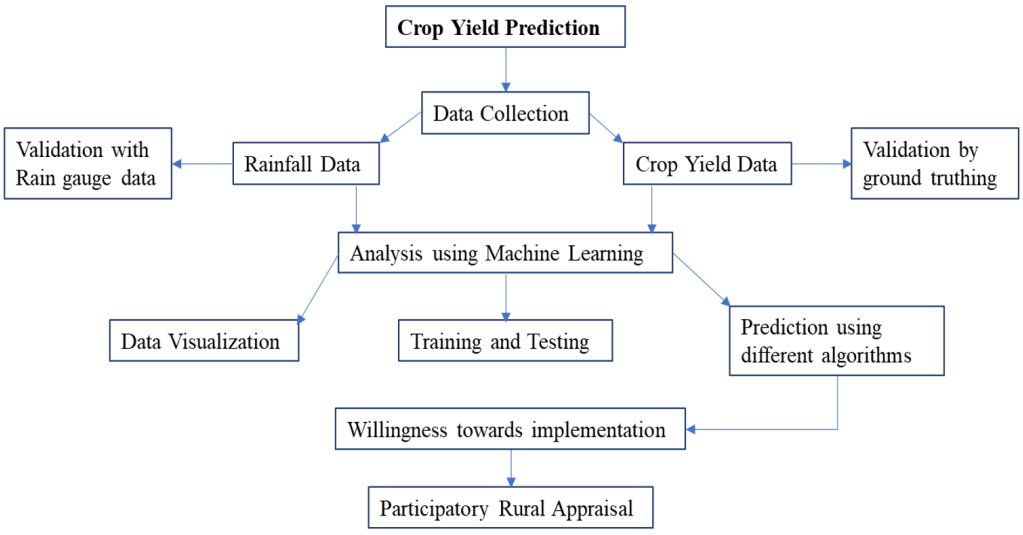


Figure 2. Methodology Flow Chart

ML Analysis

The overall methodology is explained in a flow chart denoted as figure 2. The field of machine learning falls under the umbrella of artificial intelligence and involves training machines to learn independently without external assistance. Through machine learning, machines can analyze past data to improve their future decision-making processes. This practice uses various tools, techniques, and algorithms to achieve better results and explore new knowledge from existing data sets. The choice of machine learning algorithms depends on the type of prediction needed, whether it is an estimate or classification [4]. Supervised learning is often chosen for prediction as it provides labels for data division and desired output, offering insights into fields such as health and education [14]. To learn, the algorithm compares its work with the trained output, identifies mistakes, and makes necessary adjustments. The present research employs multiple classifiers such as Logistic Regression, Decision Tree Classifier, Random Forest Classifier, and XGBoost Classifier to examine whether increased rainfall positively affects crop yield.

Logistic regression

Logistic regression is a frequently used ML technique that follows the supervised learning technique. It predicts the categorical dependent variable from the independent variables. It is similar to linear regression, but it fits the data with an S-curve which predicts two extreme values. Logistic regression is a good predictor with low incidences and simple predictors [15]. Hence it is chosen for our prediction.

Decision tree classifier
The decision tree is also a supervised technique similar to logistic regression. A decision tree predicts basic tests efficiently and works under the principle of Boolean logic [16]. Each tree comprises nodes and branches. This study concentrates on only a fundamental analysis of this classifier chosen for prediction.

Random forest classifier
Random forest classifier comprises many simple decision tree classifiers. [17] Researchers found that this classifier is an ensemble learning technique, and the individual trees follow the same technique as the decision tree in the ensemble. According to the pseudo-code, every tree in the forest contributes to a voting system to determine the classification, with the tree that receives the most votes being chosenjij overcomes the problem of overfitting data in the decision tree classifier. It takes the average of various subsets of the decision tree, which improves the accuracy of random forest classifier prediction.

XGBoost classifier
It is also called the eXtreme Gradient Boosting algorithm, created to decrease the time of model prediction for large datasets. Researchers developed this for highly accurate predicting [18]. Researchers in this study found that this classifier dominates the structured datasets on predictive modeling [19].

Village Cluster based Participatory Rural Appraisal (PRA)
Understanding the crop species is vital for its improvement [20]. Collaborative analysis can identify the needs and strengths of the local people and provide a wide range of information [21]. The study will be explained to the local farmers in detail before the survey, and then the questionnaire will be given to the farmers. We divided the study area into 6 clusters and the farmer groups into small and large-scale farmers from all six blocks of the study basin. The main aim is to make the locals to adopt the best-practice, The best-practice in the study make the locals represent and analyze the study results about their crop production and make their plans accordingly. Also, ground truthing helps in validating the predicted results. Ground truthing means validating the predicted results by doing a questionnaire survey from the local farmers. Also, the farmers helped to identify their willingness to implement the predicted results through a questionnaire survey.

RESULTS AND DISCUSSION

The results were showed as maps and tables. ML predicts the crop yield for the selected crops with the accuracy scores and are shown in table 1. The heat maps were generated for all the five crops to test the dependency of different factors which were shown in figures 3-7.

And the preliminary survey details from the participatory approach with the gender, age group and the type of farmer is showed in table 2. Ground truthing results and the willingness for implementation from the survey has been displayed in table 3 and figure 8 respectively.

Table 1. Accuracy scores for different algorithms

S.No	Crop	ML Algorithms	Accuracy Scores
1	Cashewnut	Logistic Regression	0.82
		Decision Tree	0.91
		Random Forest	0.91
		XGBoost Classifier	0.86
2	Coriander	Logistic Regression	0.71
		Decision Tree	1.0
		Random Forest	0.9
		XGBoost Classifier	0.66
3	Sugarcane	Logistic Regression	0.88
		Decision Tree	0.85
		Random Forest	0.85
		XGBoost Classifier	0.88
4	Sweet Potato	Logistic Regression	1.0
		Decision Tree	0.62
		Random Forest	0.81
		XGBoost Classifier	0.9
5	Turmeric	Logistic Regression	0.91
		Decision Tree	0.91
		Random Forest	0.91
		XGBoost Classifier	0.66

Table 2. Primary details from a questionnaire survey

S.No	Description	Percentage
1	Gender	
	Male	58
	Female	42
2	Age group	
	21-45	28
	45-60	57
	>60	15
3	Type of Farmers	
	Small Scale (<5 acres)	32.5
	Large Scale (>5acres)	67.5

Table 3. Ground truthing on the dependency of crop yield over rainfall

S.No	Crops	Results
1.	Cashewnut	Increase
2.	Coriander	Increase
3.	Sugarcane	No notable changes
4.	Sweet Potato	Increase
5.	Turmeric	Increase

ML Predictions

ML models can make two kinds of decisions which can be descriptive and predictive. Descriptive models help to gain knowledge about the data, whereas predictive models help to make predictions from the data [22]. Descriptive and predictive analysis are both essential for this study. The descriptive analysis uses heat maps to learn about the data and its dependency on rainfall. The following Figures represent the heat maps for all the crops, in the following Figures. Four algorithms, such as Logistic Regression, Decision Tree, Random Forest, and XGBoost, help in predictive analysis. This study identifies which of the four algorithms can accurately predict this region and data. Hence, this study chose the accuracy scores as the evaluating factor.

A heat map is a graphical representation of data in a two-dimensional color matrix with columns and rows. It is used to visualize the strength of correlation among the variables. In this study, the heat map contains the factors of the year of rainfall and yield, area of crop cultivated, production in tonnes, crop yield, rainfall in millimeters (mm), and rainfall in meters (m). It has a scale that ranges from -1 to +1. This scale represents the values of correlation coefficients. The major concentration is identifying the correlation between crop yield and rainfall.

Figure 3 shows the heat map of cashew nuts. The cashew nut shows good dependency on rainfall with yield and also, and it states that the area is also a contributing factor to the yield. The heat map contains a scale with a range of -1 to +1. The value falls between 0.4 to 0.6 for the dependency of rainfall over the yield.

The coriander shows less dependency on all the terms in the heat map than the cashew nut except the rainfall with yield, as shown in Figure 4. The value of dependency falls somewhere between 0.25 to 0.5 on the scale.

Also, from Figure 5, the heat map of sugarcane needs to show a better dependency on all of the factors. It is evident from the scale, too, that yield dependency over rainfall is -0.25 from the heat map.

Figure 6 shows that the Sweet potato also show good relationships with the factors in the heatmap, and the value from the heat map is 0.4 to 0.6 for the dependency of yield over rainfall.

Inference from Figure 7 shows a good relationship between turmeric yield and rainfall with a value that falls between 0.4 to 0.6 from a scale of -1 to +1. Hence, the descriptive modeling shows that cashew nuts and turmeric yield depends on rainfall.

Four ML algorithms show their accuracy scores for all five crops. The algorithm with the highest accuracy score best predicts crop yield with increased rainfall. The bifurcation of the data is as follows: 80% of the data is for training, and the remaining 20% is for testing. The algorithm predicts whether the yield will increase if rainfall increases. Since this study has yet to accurately predict future rainfall, we have identified the best algorithm for it. We will estimate the amount of rainfall in the future by conducting further studies.

The Cashewnut accuracy scores are 0.82, 0.91, 0.91, and 0.86 for logistic regression, decision tree classifier, random forest classifier, and the XGBoost classifier, respectively. Hence it is identified that the production of cashew nuts in the study region depends on the rainfall.

The accuracy scores for coriander are 0.71, 1.0, 0.9, and 0.66, respectively. The accuracy score of 1 denotes an error value due to the low amount of dataset for training and testing. Hence, the coriander production depend on the annual rainfall in the study region.

The accuracy scores for sugarcane are 0.88, 0.85, 0.85, and

0.88, respectively. However, since the current yield does not correlate with the rainfall, increasing the dataset record length needs further analysis.

The accuracy scores are estimated as 1.0, 0.62, 0.81, and 0.9, respectively, for sweet potatoes. The random forest and XG Boost predict pretty accurately, and the heat map shows that the sweet potato yield directly depend on rainfall.

Moreover, the accuracy scores are 0.91 for the first three algorithms and 0.66 for the XGBoost classifier in turmeric. Therefore, logistic regression, decision tree, and random forest classifiers can predict the turmeric yield for this study region. The heat map estimates the yield of turmeric depending on the annual rainfall.

Village Cluster based PRA for Best-Practices Adoption

Even with crop yield prediction, the implementation could only be possible with the help of the end users or the farmers. Here comes the role of Participatory Rural Appraisal (PRA). The PRA method asses the willingness for best-practices adoption. The assessment includes a site visit, direct farmer interaction, and a questionnaire survey. Among the interactions made with more than 150 farmers, this study identifies that around 85% are eagerly willing to adopt if the prediction accuracy is about 85-90%. Successful implementation of these predicted results will increase crop yield, thereby improving the chances of other farmers for adopting the best-practices.

The PRA employs a method of sampling known as cluster sampling or 'two-stage sampling.' The first stage involves selecting a sample of geographical areas, while the second involves selecting a sample of respondents within those areas. This method divides the population into clusters of similar units based on geographical proximity. Totally six blocks in this study region with more than 50 villages, including the mine sites, are covered during this study. They blocks are Cuddalore, Panruti, Kurinjipadi, Kammapettai, Mel Bhuvanagiri and Parangipettai. More than 50% of farmers are male, with an age group of 45-60. This region contains many large-scale farmers compared to small-scale farmers.

Table 3 explains the ground truthing of the predicted results; it matches precisely with cashew nut, coriander, and turmeric. The main question they asked for ground truthing is, "Whether the yield of the particular crop will increase if there is an increase in rainfall?". Cashewnut yield is increasing, whereas coriander yield has no notable change, even if there is an increase in rainfall. Moreover, they said the sugarcane yield would also increase, but it does not match the ML prediction. Sweet potato yield will increase with rainfall during the early cropping period. Furthermore, the ML prediction also does not show the dependency of Sweet Potato yield over rainfall. Finally, the turmeric yield also increases with an increase in rainfall.

A questionnaire survey helps this study to calculate their willingness towards implementation based on the predicted results by the ML by explaining the findings to them. We identified that 78% could readily accept and cultivate crops based on predictions. 18% of people are willing to accept only after successful implementation results, and 4% are unwilling to implement based on rainfall dependency since they are unsure about their cropping pattern. The following pie chart shows the results in Figure 8.

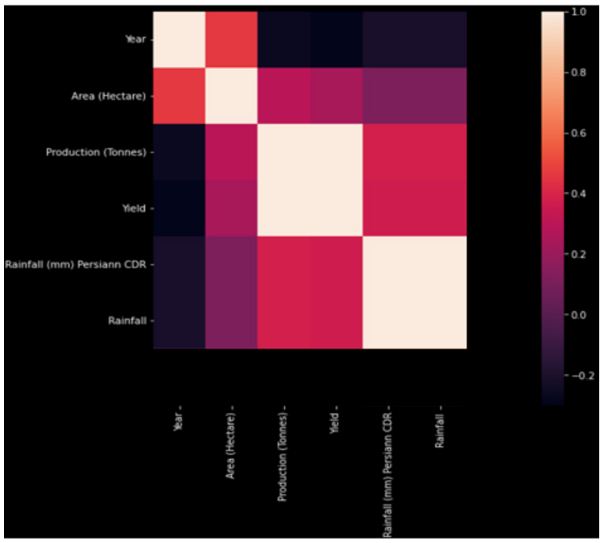


Figure 3. Heat map of Cashew Nut

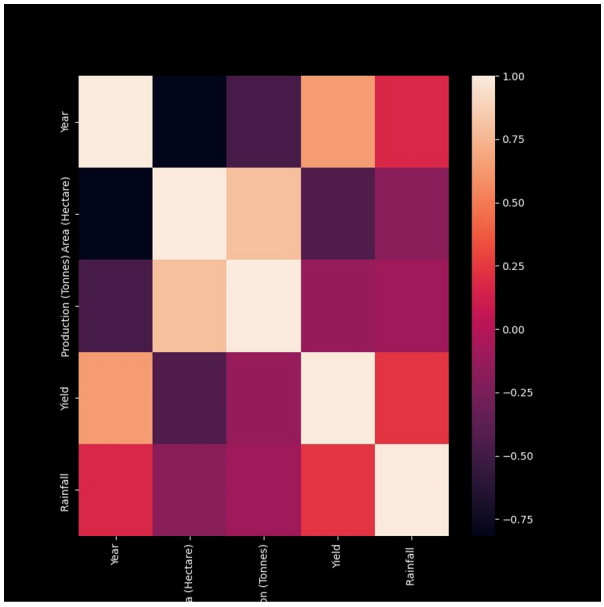


Figure 4. Heat map of Coriander

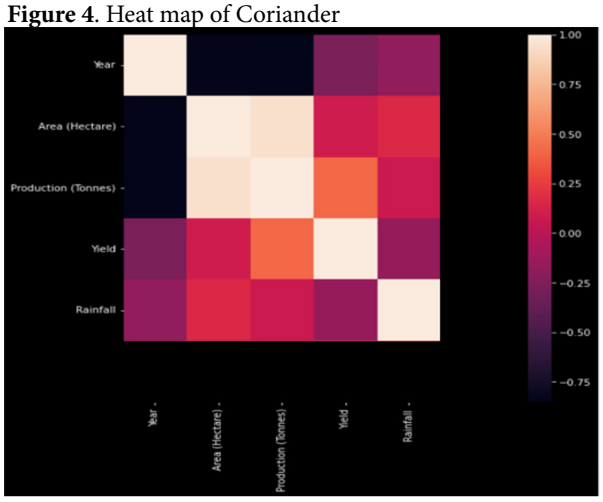


Figure 5. Heat map of Sugarcane

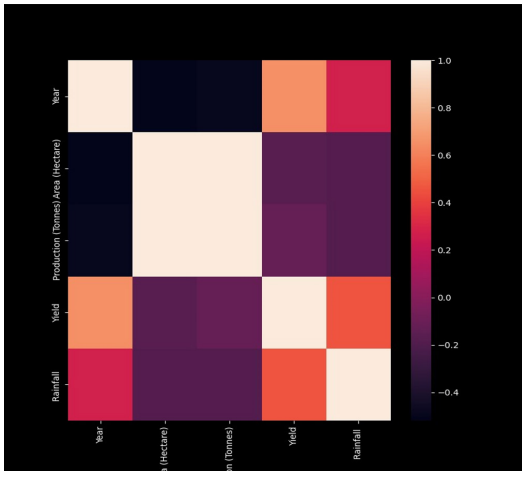


Figure 6. Heat map of Sweet Potato

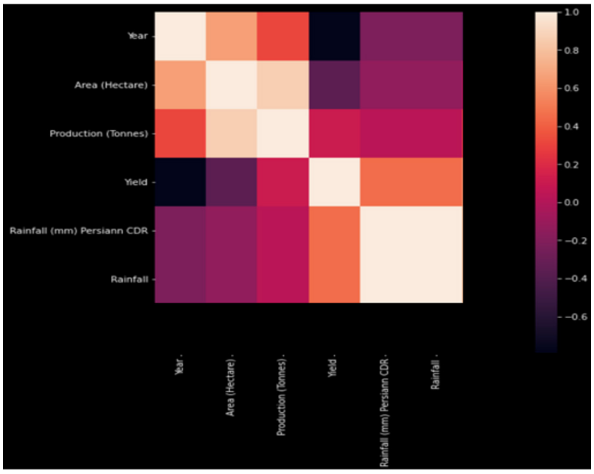


Figure 7. Heat map of Turmeric

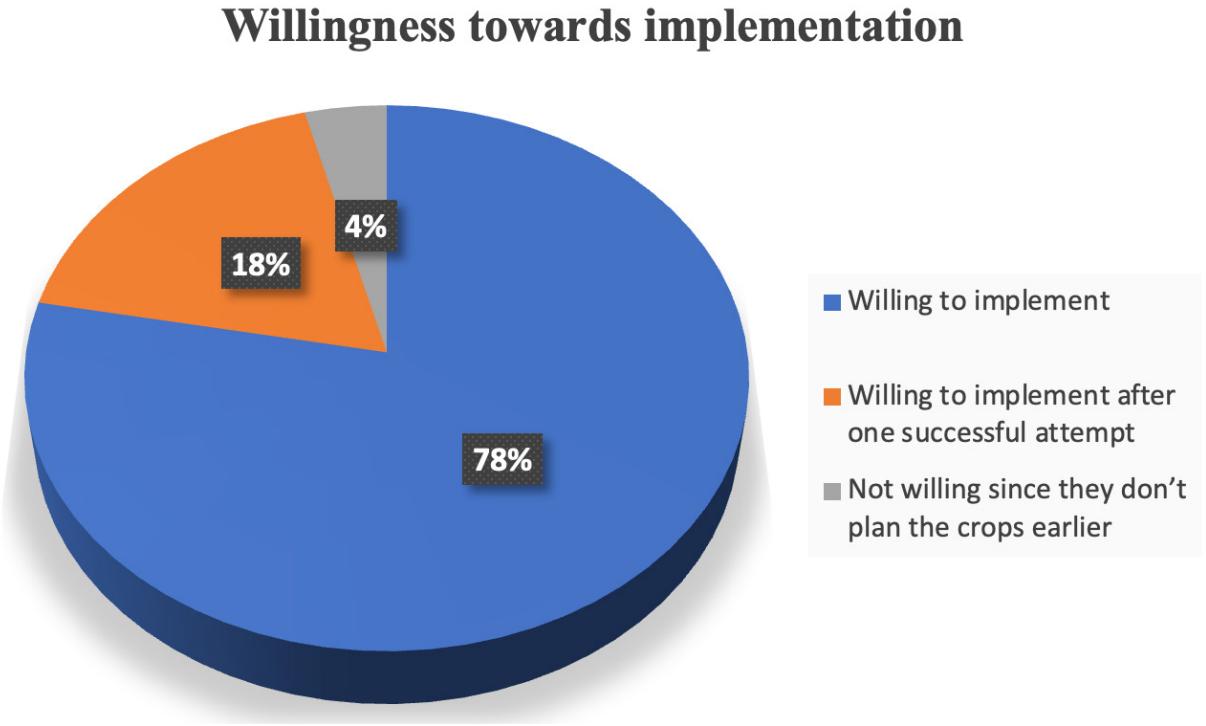


Figure 8. Willingness to implementation of results

CONCLUSION

On the whole, this study tests the dependency of crop yield in the Paravanar River basin on the annual rainfall using logistic regression, decision tree, random forest, and XG-Boost classifiers of ML algorithms. The results are validated using field observations called the participatory rural appraisal technique, and also the results are correlated well. Hence the ML predictions are found to be similar to the ground results. The drawback felt in this study is the data record length; still, these predictions require vast datasets. That will increase the accuracy of the predictions. Hence, using more than 50 years of data for these predictions is recommended. ML predictions based on the heat maps and accuracy scores are best interpreted and identified. Ground truthing with the farmers enhances the reliability of this study with the help of a questionnaire survey, and all the ML predictions match the field data, except for sugarcane and sweet potato. Sugarcane has an increase in yield if there is an increase in rainfall. The above statement is a fact inferred from the farmer's survey, but in ML, it does not show any increase in yield. Increasing the length of the data can rectify the error. Sweet potato shows no increase in ML prediction, whereas, from the survey, this study identifies that the yield will increase if rainfall increases during the sowing season. Otherwise, the rainfall does not impact the yield of sweet potatoes. Hence, crops such as cashew nut, sugarcane, and turmeric depend on annual rainfall in this region.

Moreover, the best algorithm for cashew nuts is a decision tree and random forest with an accuracy score of 0.91. The sugarcane prediction's best algorithm is logistic regression

and XGBoost, with an accuracy score of 0.88. The best algorithm for turmeric prediction is logistic regression, decision tree, and random forest, with an accuracy score of 0.91. The participatory rural appraisal identifies whether the farmers and the villagers are eager to implement the results of ML predictions. This analysis shows positive results, with 88% of the people ready to cultivate crops based on this prediction. Further extension of this study involves predicting the rainfall so that the results can help in decision-making and successful implementation based on the dependency of predicted rainfall.

Data Availability Statement
It is stated that the published publication includes all data collected or developed during the study. The data sources are mentioned for the secondary data used in this study.

ACKNOWLEDGEMENT

Anna University, Department of Science and Technology, Chennai, India.

DATA AVAILABILITY STATEMENT

The author confirm that the data that supports the findings of this study are available within the article. Raw data that support the finding of this study are available from the corresponding author, upon reasonable request.

CONFLICT OF INTEREST

The author declared no potential conflicts of interest with respect to the research, authorship, and/or publication of this article.

USE OF AI FOR WRITING ASSISTANCE

Not declared.

ETHICS

There are no ethical issues with the publication of this manuscript.

REFERENCES

[1] Klompenburga TV, Kassahuna A, and Catalb C, "Crop yield prediction using machine learning: A systematic literature review," Computers and Electronics in Agriculture, vol. 177, 2020.

[2] Xu X et al., "Design of an integrated climatic assessment indicator (ICAI) for wheat production: a case study in Jiangsu Province, China," Ecological Indicators, vol. 101, pp. 943–953, 2019.

[3] Pradyumn Kumar et al., "Assessment of crop loss caused by Chilo partellus in maize," Indian Journal of Agricultural Sciences, vol. 91, no. 2, pp. 218–221, 2023.

[4] Steve Oberlin, "Machine Learning, Cognition and Big Data," CA Technology Exchange, United States., 2012.

[5] Niveditha Nath, "From Pilgrim Landscape to Pilgrim Road: Tracing the transformation of the Char Dham Yatra in Colonial Garhwal," Journal for the study of religion, nature and culture, pp. 419–437, 2018.

[6] Ramos PJ, Prieto FA, Montoya EC, and Oliveros CE, "Automatic fruit count on coffee branches using computer vision," Computer Electronics and Agriculture, vol. 137, pp. 9–22, 2017.

[7] Beulah R, "A survey on different data mining techniques for crop yield prediction," International Journal of Computer Science Engineering, vol. 7, no. 1, pp. 738–744, 2019.

[8] Weigend A, "An overfitting and the effective number of hidden units. Lawrence Erlbaum Associates," Hillsdale, pp. 335–342, 1993.

[9] Chandra G, "PARTICIPATORY RURAL APPRAISAL Issues and Tools for Social Science Research in Inland Fisheries," Central Inland Fisheries Research Institute. Bulletin, vol. 163, pp. 286–302, 2010.

[10] Lilian A Omondi, "Learning together: Participatory rural appraisal for coproduction of climate change knowledge," Action Research, vol. 21, no. 2, 2020.

[11] Rudi Saprudin Darwis, Risna Resnawaty, and Eva Nuriyah, "Increasing the Sensitivity of Local Leadership in Citarum River Management through Participatory Rural Appraisal (PRA) techniques in Rancamanyar Village," Kumawula Journal of Community Service, vol. 3, no. 1, pp. 48–59, 2020.

[12] Pankaj Kumar, Dheeraj Kumar, Sachin Kumar, Jitendra Kumar, Kiran Pal, and Nikhil Jadhav, "Historical Perspective of Watershed Management in India: A Participatory Rural Appraisal (PRA) based Assessment," Asian Journal of Agricultural Extension, Economics & Sociology, vol. 40, no. 10, pp. 406–418, 2022.

[13] Alejo LA and Alejandro AS, "Validating CHIRPS ability to estimate rainfall amount and detect rainfall occurrences in the Philippines.," Theoritical Applications of Climatology, vol. 145, pp. 967–997, 2021.

[14] Jainendra Singh, "Big Data Analytic abd Mining with Machine Learning Algorithm," International Journal of Information and Computation Technology, vol. 4, no. 1, pp. 33–40, 2014.

[15] Nusinovici S et al., "Logistic regression was as good as machine learning for predicting major chronic diseases," Journal of Clinical Epidemiology, vol. 122, pp. 56–69, 2020.

[16] Jijo BT and Abdulazeez AM, "Classification Based on Decision Tree Algorithm for Machine Learning," Journal of Applied Science and Technology Trends, vol. 2, no. 1, pp. 20–28, 2021.

[17] Peter DC and Arandejelovic O, "Precision medicine

in digital pathology via image analysis and machine learning," Artificial Intelligence and Deep Learning in Pathology, pp. 149–173, 2021.

[18] Jerome H Friedman, "Greedy Function Approximation: A Gradient Boosting Machine," Annals of statistics, pp. 1189–1232, 2001.

[19] Ramraj S, Nishant U, Sunil R, and Shatadeep B, "Experimenting XGBoost algorithm for prediction and classification of different datasets," International journal of control theory and applications, vol. 9, pp. 615–662, 2016.

[20] Muralidhara MB et al., "Survey, collection and characterization of Indian Avocado (Persea Americana) germplasm for morphological characters," Indian Journal of Agricultural Sciences, vol. 93, no. 2, pp. 139–144, 2023.

[21] Katiha P, Vass KK, Sharma AP, and Bhaumik U, "Issues and Tools for Social Science Research in Inland Fisheries," Central Inland Fisheries Research Institute. Bulletin, vol. 163, 2010.

[22] Alpaydin E, Introduction to Machine Learning, 2nd Edition. MIT Press, Cambridge, MA, 2010.

Environmental Research and Technology
https://dergipark.org.tr/en/pub/ert
DOI: https://10.35208/ert.1501449

Review Article

A decade of eco-friendly active and intelligent food packaging research: A quantitative review

Supratim SUIN

Department of Chemistry, Ramakrishna Mission Vivekananda Centenary College, Rahara Kolkata, 700118, India

ARTICLE INFO

Article history
Received: 14 Jun 2024
Revised: 05 Aug 2024
Accepted: 28 Aug 2024

Key words:
Biodegradable, active packaging, smart packaging, antioxidant, bibliometric analysis.

ABSTRACT

The thrust for active and intelligent food packaging systems utilizing sustainable biopolymer resources has gained significant momentum in recent years as the global food industry seeks innovative solutions to enhance product freshness and safety while reducing environmental impact. Active packaging aims to extend the shelf life of packaged foods through the incorporation of substances. Intelligent packaging, on the other hand, is intended to offer up-to-date data on the quality, freshness, or safety of packaged foods by integrating various indicators into the packaging film that displays variations in storage conditions, gas levels, pH, and other factors. The present quantitative review is targeted to investigate quantitatively the research activity in the biodegradable multifunctional packaging utilizing the Web of Science database data. The top ten authors, countries, and journals associated with the present topic have been analyzed using the Bibliometrix-Biblioshiny package of R. This software package also utilizes the thematic evolution in terms of trend topic analysis. In addition, the VOS viewer software package has been used to predict inter-country collaboration, as well as, collaboration between authors. This software package also predicts co-occurrences and the evolution of keywords. Such an extensive computational approach thus expected to predict the grey areas in eco-friendly active and smart food packaging research both in terms of synthesis and properties.

Cite this article as: Suin S. A decade of eco-friendly active and intelligent food packaging research: A quantitative review. Environ Res Tec 2025;8(2) 456-470.

INTRODUCTION

Packaging is an inevitable part of the modern food industry as it plays important role in maintaining food freshness, food safety and extending the shelf life of the food [1-4]. As per the Food and Agriculture Organization, about 1.3 billion tons of food materials are wasted globally in a year, which accounts for one-third of the worldwide production of food [5]. This deterioration is caused by several detrimental factors, such as, mechanical deterioration, environmental factors, oxidation, growth of unwanted microbes, difficulty in transportation etc. [6, 7] Packaging protects food from external factors by providing a boundary between food and the environment and thus facilitates food containment, preservation, and protection. Traditional food packaging materials utilizes synthetic polymers, such as, polystyrene (PS), polyethylene (PE), polypropylene (PP), polyvinylchloride (PVC), ethylene vinyl alcohol (EVA), polyethylene terephthalate (PET) [8-10]. For instance, the packaging of meat nowadays is done by utilizing low-density polyethylene (LDPE), high-density polyethylene (HDPE), polypropylene (PP), polyesters, polystyrene, and polyamide [11]. In addition, LDPE, LLDPE (linear low-density polyethylene) or their blend (LDPE-LLDPE) is generally utilized in packaging milk and other dairy products such as curd, butter milk etc. [12] These synthetic polymers are very much attractive from a consumer viewpoint, owing to its good processibility, mechanical robustness, optical clarity, and barrier properties

*Corresponding author.
*E-mail address: supratim1988@rkmvccrahara.org

This is an open access article under the CC BY-NC license (http://creativecommons.org/licenses/by-nc/4.0/).

[13]. It has raised the demand of such synthetic polymers in the last few decades reaching 320 million global productions in the current years [13, 14]. However, the unlimited use of these synthetic plastics have threated lives on earth associated with the persistency of the plastics in the environment for years and contamination of soils and water with the micro-plastics or nano- plastics generated from these materials [13, 14]. Additionally, significant research focus has been put by the worldwide research communities towards the development of new packaging materials utilizing renewable resources as an alternative to the conventional non-renewable petroleum based synthetic polymers [15, 16].

Biopolymers, such as, proteins, polysaccharides, and lipids from different biological resources are well established renewable raw materials owing to their high abundance in nature, non-toxicity and inherent biodegradability. Machado et al. [17] defined biodegradable polymers as materials that can degrade and allow anaerobic digestion forming carbon dioxide, methane, and water in an open atmosphere in the presence of microorganisms. To get rid of environmental issues the use of biodegradable polymers should be maximized in the packaging era for the sustainable development of the environment. The most widely investigated bio-polymeric materials for polysaccharide-based films are starch, cellulose and their derivatives, chitosan and starch, while casein, whey, and gelatin are the protein based matrix materials. There are several literatures considering protein gelatin derived from skin and bones of animals [18, 19]. However, these protein and polysaccharide based materials suffer from inherent brittleness and extreme mechanical weakness limiting their utilization in commercial packaging. This problem can be partially solved by crosslinking the biopolymer matrix using citric acid [20] gluteraldehyde [21], ascorbic acid [22] etc. Enhancing the chemical and structural properties of biopolymers can also be achieved by incorporating reinforcing agents, which make them suitable for commercial applications. In recent years, there has been a growing interest in utilizing nanotechnology in packaging [23]. Nanofillers are employed to improve the properties of polymeric materials in composites for specific applications [24].

Nowadays, consumers have become health conscious and thus ready to bear extra pennies to have healthier, fresh food [25, 26]. This necessitates the development of new generation active and smart food packaging systems which not only ensure the preservation of the food for a longer time by shielding or controlled release, but also display the spoiling of food by visual change [27]. As a consequence, the food packaging sector witnessed a paradigm shift towards the development of biodegradable, non-toxic, safe biopolymer based active, smart films [28]. Active packaging enhances the shelf life of the food by interacting with the packaged food [29]. The packaging materials help to retain the quality of food by releasing preservative substances or absorbing undesirable substances coming out of the packaged food. The active ingredient in the packaging may exist in the form of sachet and labels, coatings or may be in the matrix phase of the packaging [30]. The active packaging can either be absorbers of oxygen, ethylene, and moisture or emitters of carbon dioxide, antimicrobial agents, antioxidants, preservatives, and flavors [31]. On the contrary, intelligent packaging enables consumer real–time evaluation of the quality and freshness of the packaged food [1, 32, 33]. The indicator present in the packaging material ensure the food quality from visual color change during storage [34, 35]. During microbial growth in the packaged food, the metabolite of microbes and indicator reacts, resulting chromatic changes of the indicator through change in pH. The indicator present in the packaging thus results in visual change originating from the change in pH with the growth of microorganisms in the packaged food. Thus, the consumer can detect the food freshness and quality status from the color of indicator in the packaging film [33]. Numerous synthetic dyes, such as, bromocresol green, bromocresol purple, xylenol, chlorophenol, cresol red have been used by different scientific communities to serve the purpose [36, 37]. However, the toxicity, even carcinogenicity, associated to these dyes has limited their application in food packaging owing to the sustainability of the life and the environment [38, 39]. Renewable and nontoxic natural pigments can preserve food safety and fulfill consumer expectation hygienic safe food. Natural pigments, such as, anthocyanin [40, 41], curcumin [42, 43], alizarin [44], betalain [45], shikoin [46], green tea extract [47], chlorophyll [48], carotenoids [33], tannins [49] etc. have proved themselves as efficient indicator in the pH responsive films. These natural indicators, being incorporated during the fabrication of biopolymer films, restrict the microbial growth in the packaged food, leading to good antibacterial activity [50]. Additionally, the interaction of the packaged food with the natural pigments present in the packaging material can inhibit oxidation of the oxygen-sensitive food by scavenging free radicals, leading to impressive antioxidant activity, enhancing the stability of the food and favoring its preservation for a longer period [51].

In the era of eco-friendly packaging systems, significant research focus has been put in the development of active packaging, which by virtue of its release into the food restricts the spoilage of food items packed and smart or intelligent packaging, which can detect the spoilage of food by the visual alternation of color. Several active or smart ingredients are strategically introduced into the biodegradable packaging systems for specific purposes. In the present investigation, bibliometric parameters, viz. the year-wise growth, country-wise distribution, journal wise distribution in the biodegradable active and smart packaging research have been discussed thoroughly. The collaboration between authors, as well as, countries can also be found in the present manuscript. The evolution of keywords and their inter-links are very much important to find the eligible materials for active and intelligent food packaging systems. Thus, this bibliometric study is expected to be helpful to new researchers in selecting processes and materials for biodegradable next generation packaging systems.

METHODOLOGY

Publication Data Retrieval

This review considers the data published on biodegradable smart or active packaging materials utilizing a unique search string related to the present topic in the Web of Science (WoS) database, presently maintained by Clarivate Analytics (previously by Thomson Reuters). This database extensively covers the present research field and has proved itself to be a widely accepted tool for systematic bibliometric investigations. The search string in the present bibliometric investigations was "TS=(((biodegrad* OR sustain* OR (eco friend*)) AND packag* AND (smart OR active OR intelligen*))" in the 'Advance search' of WoS database limiting the period of analysis to 01-01-2014 to 31-12-2023 i.e., last ten years. A total number of 1891 publications were resulted on limiting our study only to the articles. All the articles thus obtained were manually scrutinized to verify their acceptability in the present study. After meticulous analysis, 1399 number of articles displayed their suitability in the present consideration. The present review article is confined into these 1399 articles.

Bibliometric Parameters Analysis

Here, the Bibiometrix-Biblishiny package of R was utilized for analyzing different bibliometric parameters associated with the quantitative analysis in the said topic [52]. The year-wise growth of publication along with mean total citations per article (MTCPA), and mean total citations per year (MTCPY) have been plotted in the same plot to explore the year wise growth of publications with related citation parameters. The most involved authors worldwide were analyzed along with average citations per publication (ACPP), and h-index to explore the most active author in the said research avenue. The most productive countries around the globe and related citation parameter were also investigated. The year wise growth of top five countries in the present topic was also evaluated. This software package was also utilized to predict the most related keywords in terms of a number of mention in the articles under consideration. The growth of the top ten most significant keywords was also analyzed. This software package also facilitates to analyze the number of articles, ACPP, and h-index of articles published in different journals. The Biblioshiny package was also utilized for trend topic analysis.

Analysis of Collaborative Networks Between Countries, Authors

The interconnecting networks between different countries, as well as, authors were studied in terms of bibliometric parameters, such as, co-authorship, and utilizing VOS viewer, a java based software tool for creating network clusters. This tool has proved itself very promising for overall analysis of the entire subject area and cluster analysis [53]. This software package utilizes bibliometric data from Scopus or Web of Science database. Here, the Web of Science database has been utilized for the present investigation.

Analysis of Interconnection between Journals

The interconnections between journals were studied in terms of citations utilizing the same VOS viewer software package. In this analysis, the optimizations of the related parameters are required. In the present study, the number of publications, as well as, citations was optimized at 20 to have visually detectable connections between the journals.

Analysis of Co-Occurrence of Keywords

The correlation between different keywords mentioned in different publications considered during this period can also be predicted by utilizing this VOS viewer. This software package also enables visualization of the co-occurrence of keywords. During this analysis the minimum number of occurrences of keywords was optimized at 100, as it resulted in visually fair networks.

RESULTS

Analysis of the Key Bibliometric Parameters

The key bibliometric parameters related to biodegradable smart and active packaging have been summarized in Table 1. The present systematic review considers the 1399 articles published during the last decade, i.e. 2014-2023 from the Web of Science database after manual investigation. The articles has been found to be published in 242 sources, which includes both journals and books with an annual growth of 9.11 %, suggesting the present research field to be flourishing in the last decade. Moreover, the articles received an appreciably good number of average citations 24.51. It is worth mentioning that, the complete collection of the publications has generated 2173 keywords in keywords plus, while 3121 keywords in the author's keywords. Moreover, all the publications are co-authored by 5148 authors worldwide, of which 16 documents are single authored. The co-authorship per document 5.2 and international co-authorship to be 28.68 %

WOS Categories

Fig 1 depicts the top ten most relevant categories in which the articles on the present topics were published in our considered time frame. As evident from the figure, the highest numbers of articles on biodegradable multifunctional packaging belongs to "Food Science and Technology" followed by "Polymer Science", "Chemistry Applied", "Biochemistry Molecular Biology" and "Materials Science Multidiscipline". Thus, the present bibliometric analysis data suggests the close interrelation of the present field with food science, polymer science, applied chemistry, biochemistry, and materials science discipline. The abovementioned wings has been analyzed to produce highest number of articles on biodegradable multifunctional packaging in the last decade.

Table 1. Summary of the key bibliometric data associated with biodegradable smart and active packaging research in the last decade

Description	Results
MAIN INFORMATION ABOUT DATA	
Timespan	2014:2024
Sources (Journals, Books, etc)	242
Documents	1399
Annual Growth Rate %	9.11
Document Average Age	3.15
Average citations per doc	24.51
References	48635
DOCUMENT CONTENTS	
Keywords Plus (ID)	2173
Author's Keywords (DE)	3121
AUTHORS	
Authors	5148
Authors of single-authored docs	13
AUTHORS COLLABORATION	
Single-authored docs	16
Co-Authors per Doc	5.2
International co-authorships %	28.68
DOCUMENT TYPES	
article	742
article; early access	635
article; proceedings paper	22

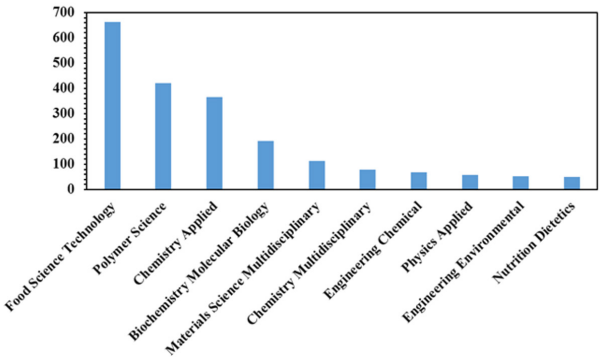


Figure 1. Top ten WOS categories publishing articles on biodegradable multifunctional packaging

Year-wise Growth of Publication and Citation Parameters

Fig 2 depicts the year wise growth of publications, as well as, mean total citations per year (MTCPY) and mean total citations per author (MTCPA) during the last ten years (2014-2023). As evident from the data plot, the biodegradable active or smart packaging research is found to be on the inclining trend, proving itself as a field of growing interest for the worldwide scientific community. It is worthy to mention that, the first five years of research produced 236 numbers of articles, while the last five years of research produced 1163 articles in the field under consideration. Moreover, the citation parameters (MTCPA, MTCPY) can be found in an appreciably good value in the given data plot.

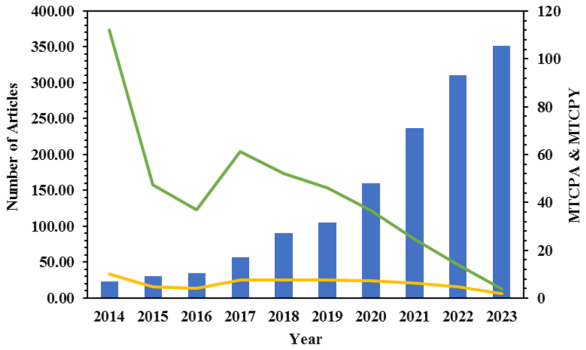


Figure 2. Year wise growth of number of publications, mean total citations per article (MTCPA) and mean total citations per year (MTCPY) in the period 2014-2023

Most Productive Countries and Their Citation Impact

Fig 3A depicts the total number of publications (as bar), as well as, average citations per publications (ACPP). China, Brazil, Iran, India, and Spain are found to publish in high frequency in the said field. However, the articles published by Portugal, USA, Spain, Iran, and Thailand received the most ACPP i.e. average citations per publication, an important parameter to reveal good acceptability of the article towards the worldwide scientific community. Good ACPP is directly related to the quality of investigation. The countries with fairly good ACPP reflect their quality, as well as, acceptability of their investigation towards the scientists involving in biodegradable packaging research around the globe.

The most relevant countries (top ten) by corresponding author publishing articles on biodegradable multifunctional food packaging during the period under consideration has been plotted in Fig 3B. The publication by each country includes both the single country publication (SCP) and multiple country publication (MCP). As can be seen, China published the highest number of publications in terms of affiliation of the corresponding author, followed by Brazil, Iran, India, and Spain. It is worthy to note that, the MCP of China is significantly greater than that of Brazil, signifying greater inter-country coauthored articles. Moreover, the inter-country collaborating articles were found to be significantly high in the articles originated from Spain. However, to obtain the inter-country collaboration extent more sophisticated analysis will be required.

Fig 3C represents the growth of the biodegradable multifunctional food packaging research done by the most active five countries in the last ten years. According to the Web of Science database, these five countries include Brazil, China, India, Iran, and Spain. It is well evident from the data plot that the said field flourished more specifically after 2018, i.e. in the 5-6 years. Although, all five countries are found to give almost linear stagnant numbers in the first five years, Brazil is found to lead the field during the early period of research in biodegradable multifunctional food packaging research. It is very interesting to find that, China led the area after 2022

followed by Brazil and Iran. Very surprisingly, the articles published by India increased significantly in the recent year, although the number of articles published by India was below the rest four countries in the entire period under consideration. The acceptability of the present field in recent years is well evident from this outcome.

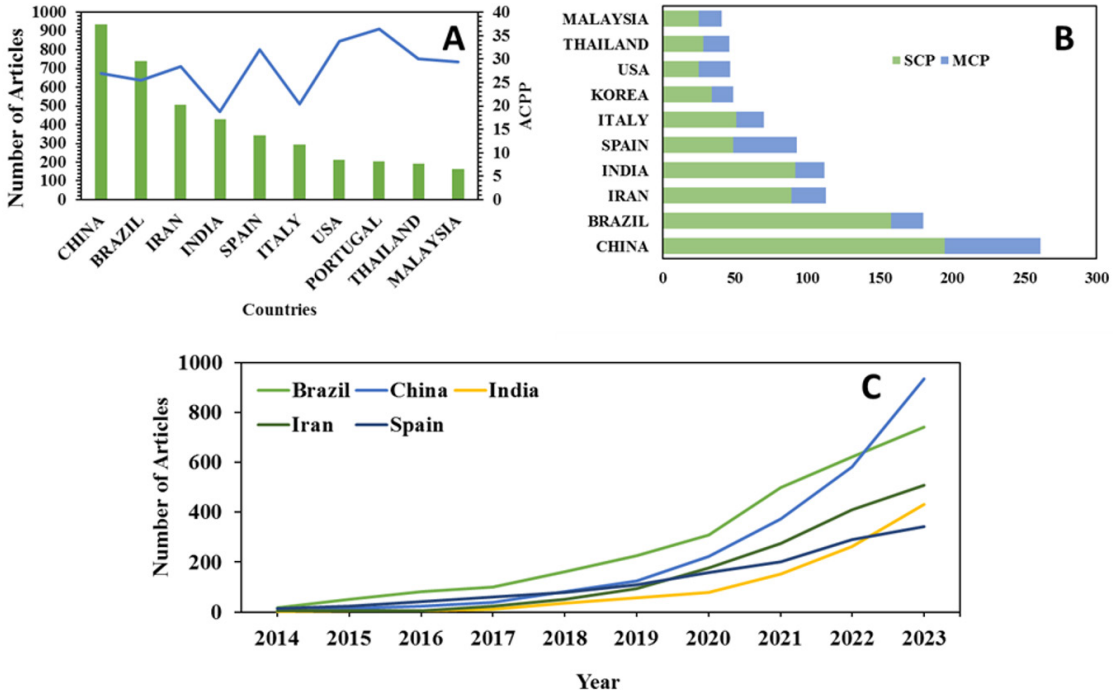


Figure 3. (A) Country wise distribution of number of publications, average citation per publication (ACPP) (B) Most relevant countries by corresponding author doing research on biodegradable smart or active packaging (C) Growth of biodegradable active or smart packaging research executed by top five countries in the period 2014-2023.

Most Active Authors: Number of Publications and Citation Parameters

Fig 4 depicts the top ten most relevant authors in terms of number of publications, ACPP, and h-index. As can be seen, Wang Y (29) published the highest number of articles on the said topic followed by Liu Y (21), Wang X (16), Li J (15), and Song KB (14). In terms of h-index Liu Y, Wang Y, Li X and Song KB have the highest h-index on the articles published on biodegradable smart or active packaging during the ten years. It is noteworthy that, the ACPP of the articles published by Flores SH is highest, followed by Haas Costa TM, Raos AO, and Mcclements DJ.

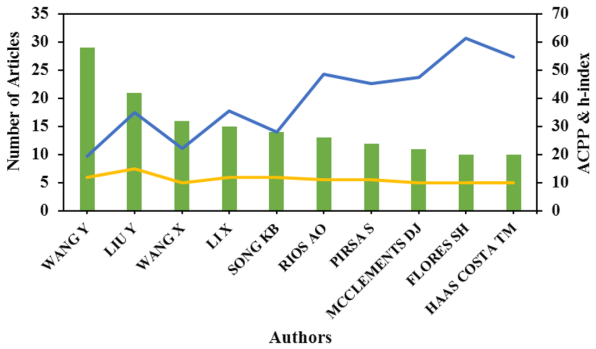


Figure 4. Number of articles, ACPP, and h-index of most active authors (top ten) publishing articles on biodegradable multifunctional food packaging in the period 2014-2023

Most Frequent Journals and Citation Parameters

The distribution of articles in different journals, ACPP, and h-index has been summarized in Fig 5. As can be found, the highest number of articles was published in the esteemed journal International journal of biological macromolecules (135). Food packaging and shelf life, a very good journal of international repute, published appreciably good number of articles (122) in the field under consideration. This trend was followed by highly reputed journals like, Food hydrocolloids (70), Polymers (62), LWT-Food Science and Technology (40), Carbohydrate polymers (40) etc. It is worthy to mention that, the citation related parameters, such as, ACPP, h-index was found to be highest in Food hydrocolloids.

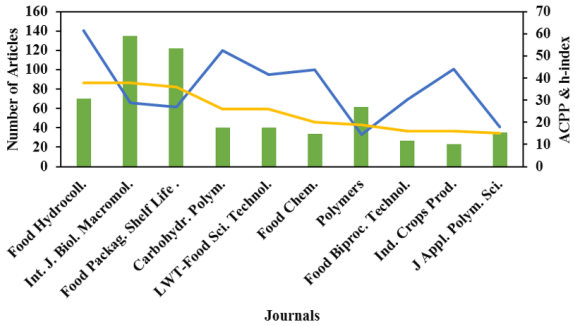


Figure 5. Total number of publications, h-index, and average citations per publication (ACPP) in the top ten journals

Most Frequent Keywords and Keywords Growth

Fig 6A and Fig 6B represent the most widely used keywords

on biodegradable multifunctional food packaging in the period 2014-2023. Both the bar plot and word cloud format has been introduced in the same figure for quantification, as well as, easy visual recognition. As can be seen, antioxidant, chitosan, films, edible films, and mechanical properties received the most attention in the said period under consideration. These keywords are directly related to biodegradable active packaging materials. The antioxidant property has proved itself to be very important active food packaging for the preservation of food for a longer time [54]. Chitosan, an important biopolymer, has been used for several years for inhibiting microbial growth in the packed food [55]. Edible films and films appeared in the keywords list due to the investigations on the biodegradable materials for packaging were mostly based on biopolymer matrices and thus the resulting films are expected to be edible in nature [56]. As biopolymer films suffer from severe mechanical weakness, mechanical properties needs to be improved for making them suitable for food packaging [57]. The next five keywords in the list are, nanoparticles, shelf-life, antimicrobial activity, barrier properties, and starch. Nanoparticles have been used for several years for improving properties of the films, as well as, introducing active agent for preserving food for longer time [58]. The shelf-life appeared in the important keywords list associated with its strong connection with the said topic. Foods generally get spoiled from the growth of microbes inside them. The antimicrobial films thus play a vital role in active packaging. The antimicrobial, as well as, antibacterial property thus plays important role in the fabrication of biodegradable films for active food packaging. For preserving food for longer period another parameter viz. barrier properties appears to be very much relevant. Biopolymers have received immense attention in food packaging research in the last decades owing to their easy availability from renewable resources and ease of processing [59]. Starch, a well accepted biopolymer, has been investigated thoroughly in the considered time frame resulting in its appearance in the list of mostly used keywords. The essential oils from different natural resources are introduced into the biopolymer matrices to make the film active. The spoiled food releases different acidic or alkaline chemicals leading to the alternation of pH of the film. Anthocyanin and other phenolic compounds are introduced into the film to monitor the spoiling of food resulting from the pH change [60-62]. The spoilage of beef and fish results in an increase in pH associated with the liberation of ammonia vapour [63]. The color of the film thus changes from colorless to yellow at pH 6 and orange-red at pH 11[64]. On the other hand, the pH of cow milk decreases (starting from 6.8) on spoiling due to the increase in acidic content in the spoiled milk [65]

The growth of the most important keywords related to our investigation has been plotted in Fig 6C. As evident from the plot, all the keywords lie in an almost linear zone till 2017. After 2017, growth of all the keywords begins, suggesting the growth of the current study in the last 6-7 years. Antioxidant and Chitosan have become increasingly important and become most important in the last couple of years. After 2017, the most important growth was displayed by Edible films, Mechanical properties, and Films. It is worthy to mention that, they are still important in the last couple of years after Antioxidant and Chitosan. In summary, all the related keywords have become increasingly important in the last five years suggesting enhanced interest of the worldwide scientific community in the biodegradable next generation packaging research.

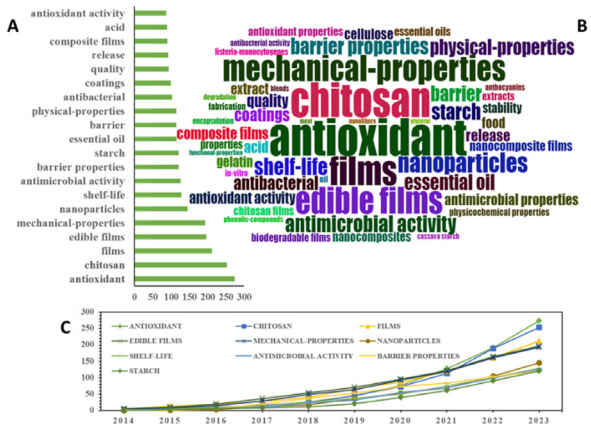


Figure 6. (A) Mostly used keywords on biodegradable smart or active packaging as bar plot and (B) keywords cloud of the most mentioned keywords; (C) Growth of the most active keywords in the considered time frame

Trend Topics Analysis

Fig 7 depicts the evolving trends in the top twenty keywords related to biodegradable multifunctional food packaging during the period 2014-2023. The horizontal line is indicative of the coverage year in the use of keywords and the position of the bubble indicates the year in which the use of the keyword was maximized. Additionally, the size of the bubble is directly related to the frequency of the term mentioned in the publications retrieved from the database. As evident from the figure, the size of the bubbles was maximized in the period 2021-2023, supporting greater number of publications in this period. The most widely used keywords are, 'antioxidant', 'chitosan', and 'nanoparticles' covering the years 2020-2023, maximized at 2022. Another three keywords, viz. 'films', 'edible films', and 'mechanical properties' are found to dominate in the period 2018-2022, being maximized in 2021. So, the trend topic analysis represents six keywords related to multifunctional food packaging in the recent years of investigation. Chitosan has proved itself as an attractive biopolymer for active packaging. As biopolymers are primarily utilized in the fabrication of packaging films, the films appeared as edible. It is worthy to mention that, the biopolymer films suffer from severe mechanical weakness. Thus, the mechanical properties of the composite films appeared as important in the articles retrieved. In the period, 2018-2022, another three keywords, 'barrier properties', 'nanocomposites', 'essential oil' appears to be dominates, maximizing in 2020. Essential oils have been used for the past years for the preservation of food for longer periods. The naturally extracted essential oils are thus utilized in the fabrication of active food packaging materials. Moreover, the barrier properties appear as important when it comes to food packaging.

The incorporation of different nanofillers (nanoparticles, nanosheets, nanoflakes) leads to the improvement in several properties in the nanocomposites. However, the early period of research on multifunctional food packaging was found to be very much chaotic and no inference can be done at the initial phase of any research area. As the development of biodegradable multifunctional food packaging materials was initiated during 2013-2016, there was lack of consistency in the use of keywords and thus a chaotic nature in trend topics analysis plot is evident.

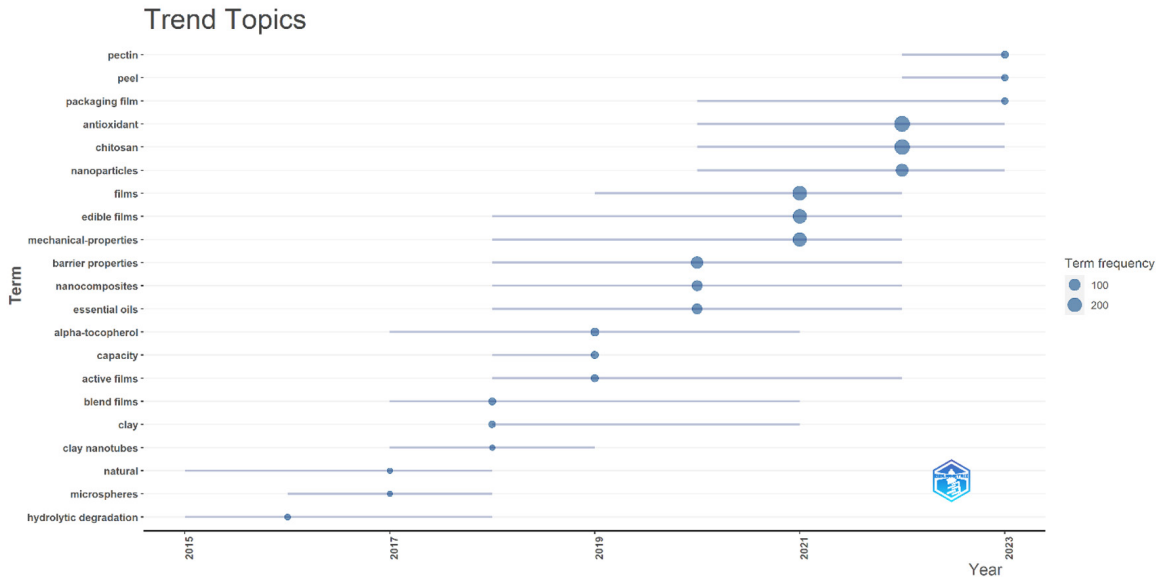


Figure 7. Trend topics analysis for the period 2014-2023

Sustainable Development Goals

Fig 8 predicts the suitable sustainable development goals (SDGs) mentioned in different literatures considered in our study. Sustainable development goals are set by United Nation, targeted to be fulfilled by a certain period. In 2015, seventeen such goals were fixed to be achieved by 2030. These SDGs are also called global goals, focusing mainly on zero poverty, protection of earth and ensuring peace and prosperity of people. The literatures on biodegradable multifunctional food packaging materials predict five major SDGs (SDG 3, 6, 11, 12, and 13) to be associated with this topic. The SDG 3 i.e. "Good Health and Well Being" achieved the maximum mention associated with its close association with the biodegradable smart or active packaging. It was followed by SDG 12 i.e. "Responsible Consumption and Production", SDG 13 i.e. "Climate Action". All the SDGs achieved are closely related with the eco-friendly packaging systems as considered in our present investigation which speaks about sustainability of environment and health of lives on earth.

Analysis of Collaborative Networks between Countries and Authors

Fig 9 represents the network linkages between different countries in terms of co-authorship. The consideration of minimum 10 publications in each author along with 10 minimum citations results in 36 countries which have connections. As evident from the data, China had published highest number of documents (296) followed by Brazil (204), India (141), Iran (133), and Spain (131). Although, the number of documents produced by Spain is less among the five, the link strength is found to be highest in Spain (104). China followed Spain in terms of link strength, and had link strength of 97 during the period considered in the present investigation. USA is found to possess fair link strength (96) after China and Spain. Brazil, with a fairly good number of documents (204) had the least collaborative network strength (41). India with 140 published articles are found to possess mention worthy linkage strength (59). In summing up the results of collaboration between countries, Spain is found to possess highest number of collaboration, while least number of collaborations in Brazil among the five most publishing countries.

The collaboration between different authors in terms of co-authorship has been depicted in Fig 10. The optimization of related parameters (minimum publication = 05; minimum citation per article = 05) results in 110 authors, of which 18 are found to be connected. As evident from the figure, both Mcclements DJ and Ehsani Ali have the same number of documents (12), although Ehsani Ali have more impressive collaborative networks. The link strength of Ehsani Ali (30) is greater than Mcclements DJ (20). This was followed by Hamishehkar H (11 documents and 16 link strength) Sani MA (10 documents 24 link strength). The other authors with appreciably good collaborations are, Tavassoli M, Alizadeh-Sani M with 26 and 12 link strength, respectively.

Analysis Connecting Networks between Journals

The connective links between different journals was studied by studying citations of the published articles in different journals and plotted in Fig 11. In this analysis, the minimum number of publications and minimum number of citations were fixed at 20. Out of the total 242 sources (journals), 15 sources are found to meet the threshold and possesses active connections. The number of documents is found to be highest (154) in 'International Journal of Biological Macro-

molecules' followed by 'Food Packaging and Shelf Life' (122), 'Food Hydrocolloids' (76), and Polymers (62). The link strength was also found to be maximized in 'International Journal of Biological Macromolecules' displaying a total link strength of 586. This was followed by sources like 'Food Hydrocolloids' (461), 'Food Packaging and Shelf Life' (457), and 'Carbohydrate Polymers'. The other mention-worthy sources with fairly good link strengths are, 'LWT Food Science and Technology' (176), 'Food Chemistry' (161) and 'Polymers' (146).

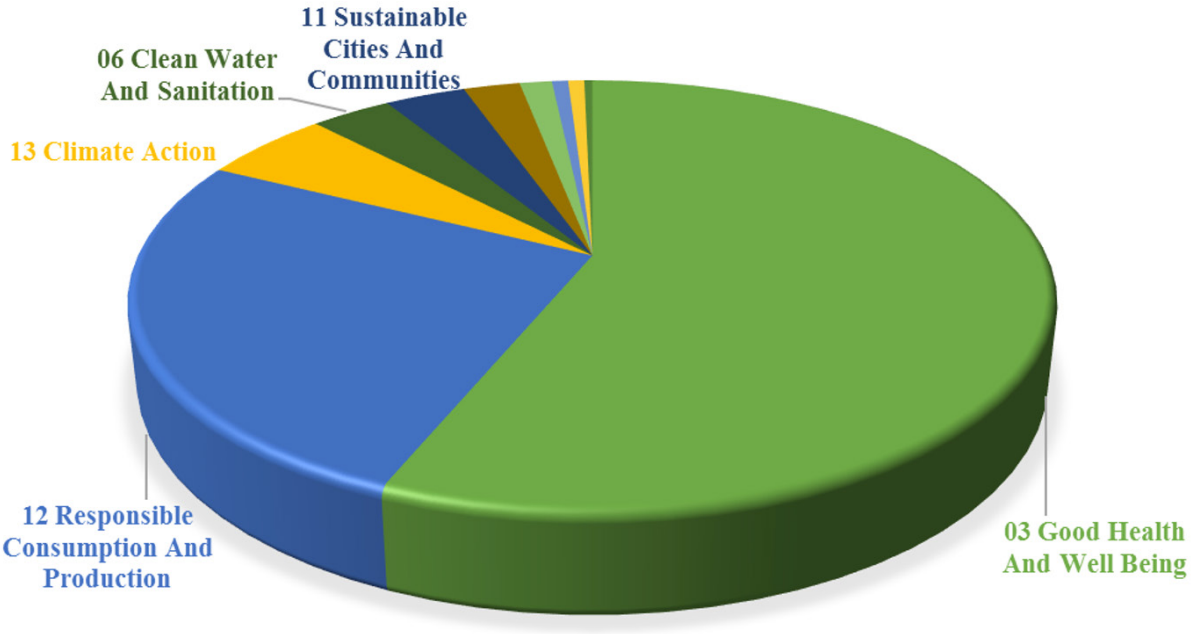


Figure 8. Sustainable development goals mentioned in different articles in the period 2014-2023

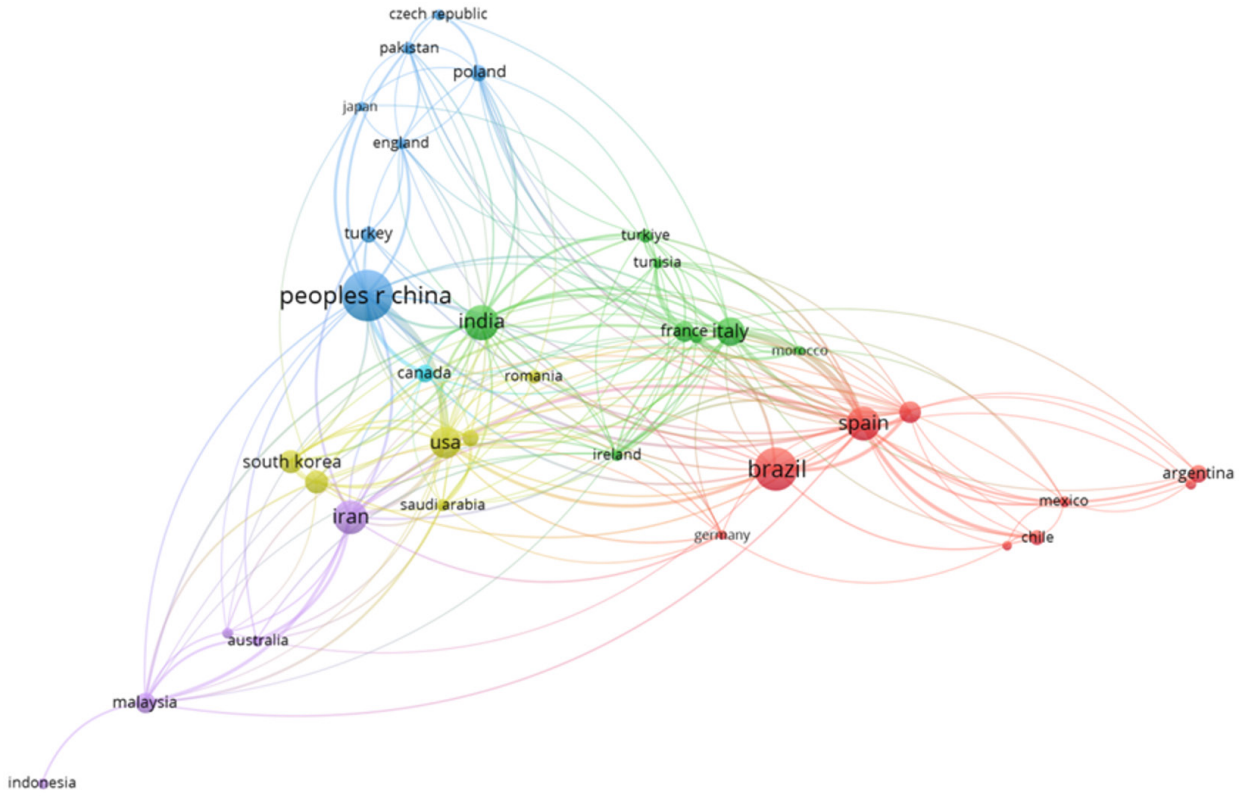


Figure 9. Collaborative networks between different countries in biodegradable smart and active packaging research during 2014-2023

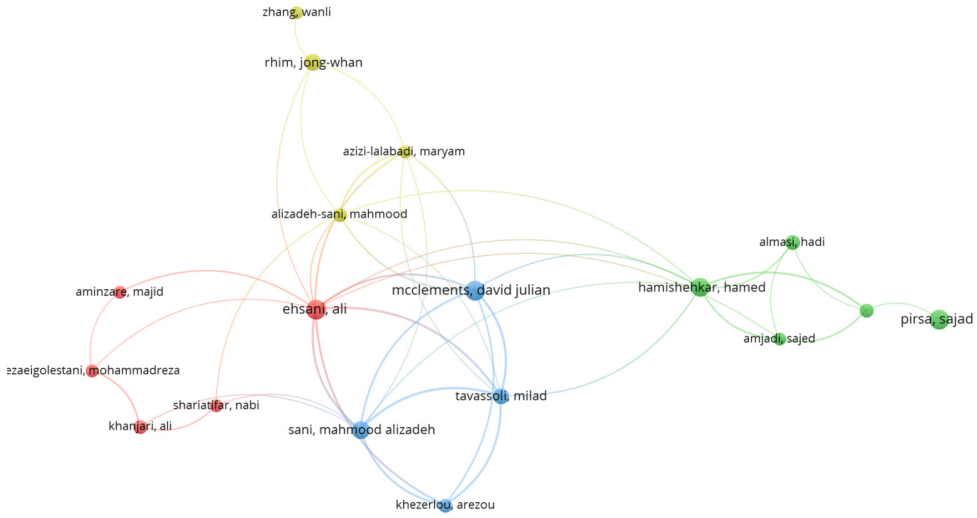


Figure 10. Collaborative networks between different authors in biodegradable smart and active packaging research during 2018-2022

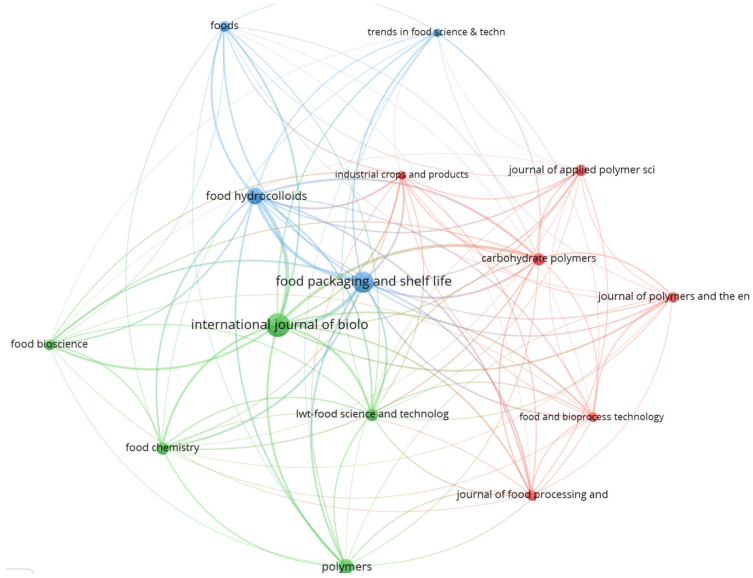


Figure 11. Interconnecting networks between sources publishing articles in biodegradable smart and active packaging during 2018-2022

Analysis of Co-occurrence of Keywords

Fig 12 depicts the co-occurrences of most relevant keywords during the period 2018-2022. To obtain this representation the minimum number of occurrences of the keywords was optimized to 100. This results in 24 interconnected keywords. As evident from the figure, 'Chitosan' had the highest number of mention (364) along with highest link strength (1047). This was followed by 'active packaging' and 'antioxidant' with occurrences 353 and 342, respectively. Although, the link strength of 'antioxidant' (982) is slightly greater than that of 'active packaging' (949). The other keywords with mention worthy occurrences and link strengths are, 'Edible Films' (231, 802), 'mechanical properties' (200, 642), 'antimicrobial activity' (191, 563) and 'Barrier Properties' (160, 552).

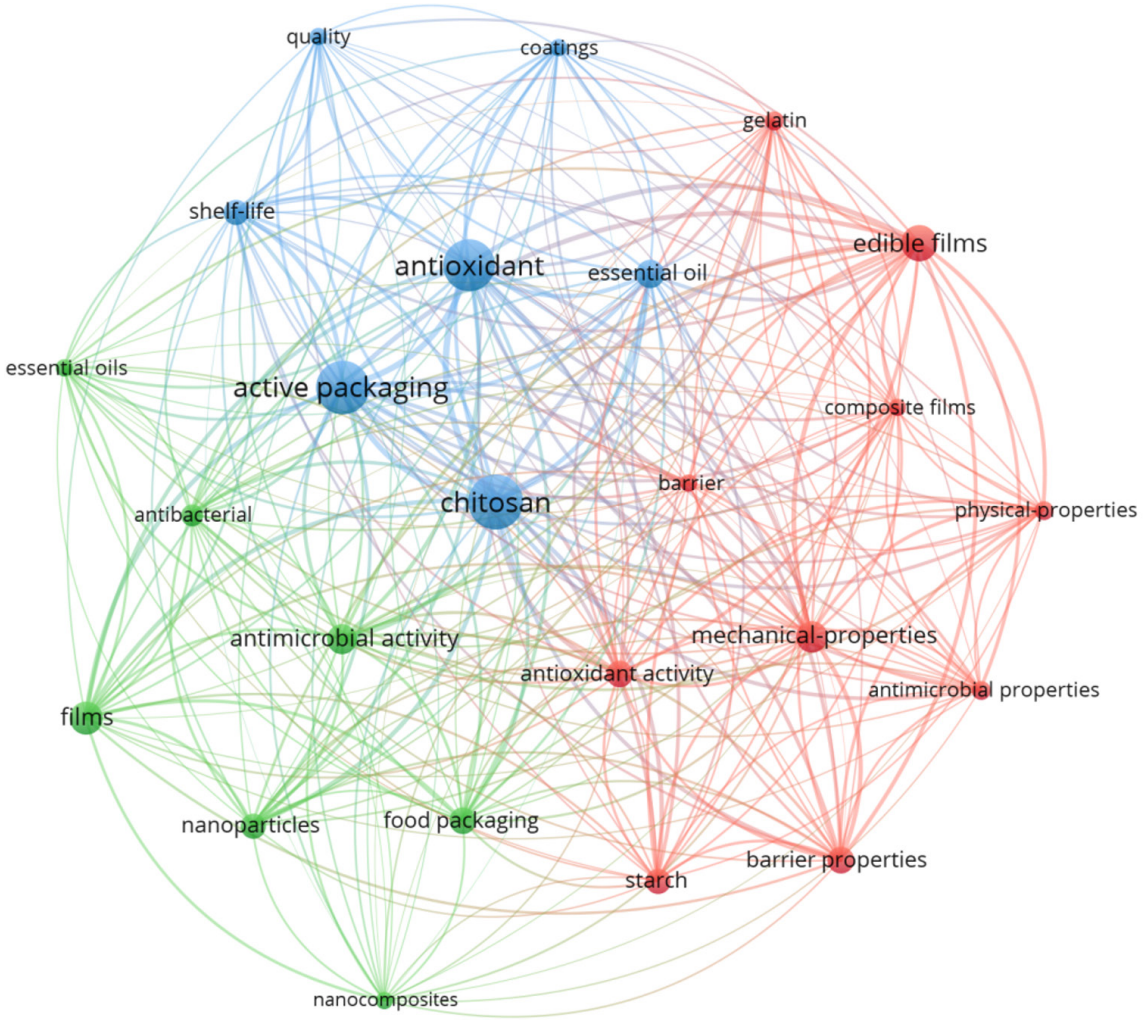


Figure 12. Co-occurrence of most relevant keywords and evolution in biodegradable smart and active packaging research during 2018-2022

DISCUSSION

The present review considers the advancement in the active and smart food packaging systems in the last ten years. The bibliometric parameters related to the present investigation were retrieved from the Web of Science database. The raw data were analyzed by software packages like the Bibliometrix-Biblioshiny package of R, and VOS viewer. As observed, a total 1891 articles were published during 2014-2023, of which 1399 articles were found to be most correlated with the present review.

The global participation in the advanced packaging research finds that the majority of research articles are from China, Brazil, Iran, India, and Spain (in sequence). Although, the ACPP results predict the sequence as, USA, Portugal, Thailand, and Spain, signifying more globally acceptable results from articles produced by these countries. Moreover, the year-wise growth of the present research topic by the top five countries predicts Brazil as the leader in smart and active food packaging research till 2022. However, in the later period, China exceeded Brazil in the number of articles produced. Although the SCP of China and Brazil were equal, the MCP of China was significantly greater than that of Brazil. The greater collaborative links of China as compared to that of Brazil are also evident from the co-authorship analysis via VOS viewer. Very surprisingly, Spain possess the highest inter connecting collaboration links and thus the MCP and SCP of Spain was found to be equal.

The top five producing authors on the present topic are, Wang Y, Liu Y, Wang X, Li J, and Song KB. The highest number of collaborating networks was found to be produced by Mcclements DJ and Ehsani Ali. Thus, the co-authorship analysis predicts Mcclements DJ and Ehsani Ali to be the most competent in global collaboration relating to smart and active food packaging research.

The analysis of the sources of the articles finds 'International Journal of Biological Macromolecules' as the most producing journal in the said topic during 2014-2023, followed by 'Food Packaging and Shelf Life', 'Food Hydrocolloids', 'Polymer', and 'LWT-Science and Technology'. On investigating the citation parameters, the highest ACPP and h-index is found to be highest in 'Food Hydrocolloids'. However, the interconnecting networks between journals in terms of citation predict the 'International Journal of Biological Macromolecules' as the most connected in terms of citations, followed

by 'Food Hydrocolloids' and 'Food Packaging and Shelf life'. In summarizing the sources of the articles produced during 2014-2023, it can be concluded that, all the articles were published in food chemistry and polymer chemistry related, highly reputed journals of international repute. .

The analysis of the most frequent keywords related to this topic predict 'antioxidant' as the mostly used author keyword during the said period, followed by 'chitosan', 'films', 'edible-films' and 'mechanical properties'. The growth of the related keywords in the last 5-7 years is indicative of the growing interest in active and smart food packaging systems in the recent years. The analysis of the trending topic predicts, terms like 'antioxidant', 'chitosan', and 'nanoparticles' covering the years 2020-2023, maximized in 2022. Another three keywords, viz. 'films', 'edible films', and 'mechanical properties' are found to dominate in the period 2018-2022, being maximized in 2021. The trend topics data are thus indicative of the motivation of the worldwide scientific community towards sustainable advanced packaging systems utilizing naturally occurring biopolymer resources, resulting the films to be edible. In addition biopolymer films usually suffer from mechanical weakness, thus the enhancement in mechanical properties is very important to make the films eligible for packaging applications; thus, the investigation of mechanical properties has appeared as trending in the recent years. Nanomaterials, such as, zinc oxide, titanium dioxide [66], silver [67], gold [68] etc. are used in the packaging systems in order to make the film eligible for active packaging, restricting the growth of microbes in the packaged food. Chitosan has proved itself as very promising in the active food packaging very recently. The antioxidant property, appearing in the trend topics list (centered at 2021), is a very much important parameter in the active food packaging [69]. Thus, the trend topic data is indicative of a clear switch towards nanopackaging and active packaging.in the most recent years. However, the smart/intelligent packaging systems have still not been explored much and thus have created a lacuna in the advanced packaging systems. The interconnection of keywords was obtained from the VOS viewer network structure. The greater frequency of keywords is associated with their greater number of mentions in the articles considered in our analysis and the number of links signifies their connection with other keyword. The highest mentioned keyword, 'Chitosan' was found to possess the highest link strength signifying its strong correlation with other keywords. The other keywords with the greater number of mentions and link strengths are, 'active packaging', 'antioxidant', 'edible films' 'mechanical properties', 'antimicrobial activity' etc. All these keywords are strongly associated with active packaging systems. However, a lesser connection and appearances has been found with the keywords related to smart packaging systems. Thus, the fabrication of eco-friendly composites for intelligent food packaging has not yet been explored much and has remained as a field of extensive investigation for worldwide scientific community doing research in biodegradable food packaging materials.

FUTURE SCOPE

In investigating the articles related to biodegradable smart packaging, it was found that natural resources, such as, starch, cellulose, and chitosan were used primarily as the matrix polymer. Very few non-renewable polymers, viz. poly(-lactic acid) [70], poly(vinyl alcohol) [71] were also found to be utilized as biodegradable matrix polymers. The main demerits of naturally occurring biopolymers are their severe mechanical weakness, along with their high hygroscopic nature. Several nanomaterials, such as, zinc oxide [72], titanium oxide [66], and graphene oxide [73] were used to overcome the shortcomings associated with these pristine polymers. The incorporated nanoparticles were also reported to preserve the freshness of food for a longer time and inhibit its spoiling. However, the water repellency of the composite films were not well been explored. Wet foods liberate water vapor present in them, and thus the packaging films may get destroyed if not significantly robust enough to restrict water. The chemical structure of the biopolymers suggest enormous hydroxyl groups in the biopolymer surfaces, making them hygroscopic. Crosslinking with suitable molecules thus appeared as a more convenient method to restrict water and make the films robust. Thus, more research focus should be put on generating hydrophobicity of the composite films by considering chemical forces and interaction.

In addition, fabrication of active packaging systems were explored much utilizing renewable biopolymer resources, inorganic nanomaterials, and natural plant extracts. The sustained release from the packaging films restricts the microbial growth and helps in the preservation of food for a longer period. On the other hand, the intelligent films offers the spoilage of food from the color change of the indicator film. Several, natural extracts were incorporated into the biopolymer matrix to track the food spoilage from the change in color of the packaging films. The spoilage of food generates volatile chemicals leading to changes in the pH of the films. Naturally occurring indicators are introduced into the matrix to make the pH change visible. Although, active packaging systems were widely explored in the last decade, very little work has been done on the smart packaging utilizing natural extracts and thus has created a lacuna in the biodegradable advanced packaging systems. Moreover, there is a significant scarcity of investigation in the complete advanced packaging systems, which not only restricts food spoilage, but also indicates the spoilage of food from the visual change of packaging systems.

CONCLUSIONS

The progression in the biodegradable active and smart packaging research in the last decade has been quantitatively reviewed in the present manuscript. The Web of Science database was utilized in the present topic as it gives more relevant articles compared to the other existing databases. As evident from the data, the number of publications was in an inclining trend, suggesting the growing interest of the research community towards biodegradable active and smart packaging

research. Moreover, the last five years of research on biodegradable smart packaging systems produced more articles compared to the earlier five years, signifying the enhanced research interest of the scientific community in recent years. The participation of the countries around the globe predicted, countries like China, Brazil, Iran, India, and Spain are major contributors to this research. However, articles from the USA, Portugal, Thailand, and Spain received more citations, indicating their wider acceptance in the global scientific community. China had the highest number of collaborative networks, while Brazil had the fewest. Spain, despite fewer publications, had a significant number of collaborations. From 2014 to 2023, leading journals publishing on this topic included 'International Journal of Biological Macromolecules', 'Food Packaging and Shelf Life', 'Food Hydrocolloids', 'Polymer', and 'LWT-Science and Technology'. The most frequent keywords in this research were 'antioxidant', 'chitosan', 'edible films', 'films', and 'mechanical properties'. Most studies used biopolymers, which are edible but have mechanical weaknesses, making the study of their mechanical properties crucial. Chitosan is widely used due to its effectiveness in active packaging systems, and antioxidants are commonly mentioned due to their relevance in active packaging. The analysis of the trend topics also suggests properties, such as mechanical properties and antioxidants, matrix materials, such as chitosan, and nanomaterials as reinforcements as the prime topics in the recent years of biodegradable active and smart food packaging research. The analysis also highlighted gaps in research. For instance, water resistivity and chemical interactions between components, crucial for wet food packaging, are not well-explored. Smart packaging systems using natural extracts and the dual use of packaging for both smart and active functions also remain challenging areas.

ACKNOWLEDGEMENT

The author is very much thankful to Swami Kamalasthananda, principal of RKMVCC, Rahara, for providing required facilities associated with this review.

DATA AVAILABILITY STATEMENT

No data was used for the research described in the article.

CONFLICT OF INTEREST

The author declared no potential conflicts of interest with respect to the research, authorship, and/or publication of this article.

USE OF AI FOR WRITING ASSISTANCE

Not declared.

ETHICS

There are no ethical issues with the publication of this manuscript.

REFERENCES

[1]. E. Balbinot-Alfaro, D. V. Craveiro, K. O. Lima, H. L. G. Costa, D. R. Lopes, and C. Prentice, "Intelligent packaging with pH indicator potential," Food Engineering Reviews, vol. 11, pp. 235-244, 2019.

[2]. H. Yousefi, H. M. Su, S. M. Imani, K. Alkhaldi, C. M. Filipe, and T. F. Didar, "Intelligent food packaging: A review of smart sensing technologies for monitoring food quality," ACS Sensors, vol. 4, no. 4, pp. 808-821, 2019.

[3]. S. Y. Sung, L. T. Sin, T. T. Tee, S. T. Bee, A. R. Rahmat, W. A. W. A. Rahman, and M. Vikhraman, "Antimicrobial agents for food packaging applications," Trends in Food Science and Technology, vol. 33, no. 2, pp. 110-123, 2013.

[4]. V. Siracusa, P. Rocculi, S. Romani, and M. Dalla Rosa, "Biodegradable polymers for food packaging: a review," Trends in Food Science and Technology, vol. 19, no. 12, pp. 634-643, 2008.

[5]. J. Tkaczewska, "Peptides and protein hydrolysates as food preservatives and bioactive components of edible films and coatings - A review," Trends in Food Science and Technology, vol. 106, pp. 298-311, 2020.

[6]. M. Hoseinnejad, S. M. Jafari, and I. Katouzian, "Inorganic and metal nanoparticles and their antimicrobial activity in food packaging applications," Critical Reviews in Microbiology, vol. 44, no. 2, pp. 161-181, 2018.

[7]. A. M. Youssef and S. M. El-Sayed, "Bionanocomposite materials for food packaging applications: Concepts and future outlook," Carbohydrate Polymers, vol. 193, pp. 19-27, 2018.

[8]. N. Peelman, P. Ragaert, B. De Meulenaer, D. Adons, R. Peeters, L. Cardon, and F. Devlieghere, "Application of bioplastics for food packaging," Trends in Food Science and Technology, vol. 32, no. 2, pp. 128-141, 2013.

[9]. T. N. Tran, A. Athanassiou, A. Basit, and I. S. Bayer, "Starch-based bio-elastomers functionalized with red beetroot natural antioxidant," Food Chemistry, vol. 216, pp. 324-333, 2017.

[10]. R. Muthuraj and T. Mekonnen, "Recent progress in carbon dioxide (CO2) as feedstock for sustainable materials development: Co-polymers and polymer blends," Polymer, vol. 145, pp. 348-373, 2018.

[11]. K. W. McMillin, "Advancements in meat packaging," Meat Science, vol. 132, pp. 153-162, 2017.

[12]. F. Tornuk, M. Hancer, O. Sagdic, and H. Yetim, "LLDPE based food packaging incorporated with nanoclays grafted with bioactive compounds to extend shelf life of some meat products," LWT-Food Science and Technology, vol. 64, no. 2, pp. 540-546, 2015.

[13]. K. J. Groh, T. Backhaus, B. Carney-Almroth, B. Geueke, P. A. Inostroza, A. Lennquist, and J. Muncke, "Overview of known plastic packaging-associated chemicals and their hazards," Science of the

Total Environment, vol. 651, pp. 3253-3268, 2019.
[14]. M. I. Din, T. Ghaffar, J. Najeeb, Z. Hussain, R. Khalid, and H. Zahid, "Potential perspectives of biodegradable plastics for food packaging application - review of properties and recent developments," Food Additives & Contaminants: Part A, vol. 37, no. 4, pp. 665-680, 2020.
[15]. S. Sid, R. S. Mor, A. Kishore, and V. S. Sharanagat, "Bio-sourced polymers as alternatives to conventional food packaging materials: A review," Trends in Food Science and Technology, vol. 115, pp. 87-104, 2021.
[16]. S. Shankar, L. Jaiswal, and J. W. Rhim, "Gelatin-based nanocomposite films: Potential use in antimicrobial active packaging," in Antimicrobial Food Packaging, Academic Press, 2016, pp. 339-348.
[17]. A. V. Machado, A. I. S. Araújo, and M. Oliveira, "Assessment of polymer-based nanocomposites biodegradability," 2015.
[18]. T. de Moraes Crizel, A. de Oliveira Rios, V. D. Alves, N. Bandarra, M. Moldão-Martins, and S. Hickmann Flôres, "Biodegradable films based on gelatin and papaya peel microparticles with antioxidant properties," Food and Bioprocess Technology, vol. 11, pp. 536-550, 2018.
[19]. N. S. Said, N. K. Howell, and N. M. Sarbon, "A review on potential use of gelatin-based film as active and smart biodegradable films for food packaging application," Food Reviews International, vol. 39, no. 2, pp. 1063-1085, 2023.
[20]. N. Reddy and Y. Yang, "Citric acid cross-linking of starch films," Food Chemistry, vol. 118, no. 3, pp. 702-711, 2010.
[21]. E. Franco, R. Dussán, D. P. Navia, and M. Amú, "Study of the annealing effect of starch/polyvinyl alcohol films crosslinked with glutaraldehyde," Gels, vol. 7, no. 4, p. 249, 2021.
[22]. S. D. Yoon, "Cross-linked potato starch-based blend films using ascorbic acid as a plasticizer," Journal of Agricultural and Food Chemistry, vol. 62, no. 8, pp. 1755-1764, 2014.
[23]. J. Y. Huang, X. Li, and W. Zhou, "Safety assessment of nanocomposite for food packaging application," Trends in Food Science & Technology, vol. 45, no. 2, pp. 187-199, 2015.
[24]. R. Sharma, K. S. Sharma, and D. Kumar, "Introduction to nanotechnology," Nanomaterials in Clinical Therapeutics: Synthesis and Applications, pp. 1-31, 2022.
[25]. S. Singh, K. K. Gaikwad, M. Lee, and Y. S. Lee, "Thermally buffered corrugated packaging for preserving the postharvest freshness of mushrooms (Agaricus bisporus)," Journal of Food Engineering, vol. 216, pp. 11-19, 2018.
[26]. R. Irkin and O. K. Esmer, "Novel food packaging systems with natural antimicrobial agents," Journal of Food Science and Technology, vol. 52, pp. 6095-6111, 2015.
[27]. S. D. F. Mihindukulasuriya and L. T. Lim, "Nanotechnology development in food packaging: A review," Trends in Food Science and Technology, vol. 40, no. 2, pp. 149-167, 2014.
[28]. M. Imran, A. M. Revol-Junelles, A. Martyn, E. A. Tehrany, M. Jacquot, M. Linder, and S. Desobry, "Active food packaging evolution: Transformation from micro- to nanotechnology," Critical Reviews in Food Science and Nutrition, vol. 50, no. 9, pp. 799-821, 2010.
[29]. E. da Costa Monção, C. V. B. Grisi, J. de Moura Fernandes, P. S. Souza, and A. L. de Souza, "Active packaging for lipid foods and development challenges for marketing," Food Bioscience, vol. 45, p. 101370, 2022.
[30]. R. Ribeiro-Santos, M. Andrade, N. R. de Melo, and A. Sanches-Silva, "Use of essential oils in active food packaging: Recent advances and future trends," Trends in Food Science and Technology, vol. 61, pp. 132-140, 2017.
[31]. A. Dey and S. Neogi, "Oxygen scavengers for food packaging applications: A review," Trends in Food Science and Technology, vol. 90, pp. 26-34, 2019.
[32]. P. Müller and M. Schmid, "Intelligent packaging in the food sector: A brief overview," Foods, vol. 8, no. 1, p. 16, 2019.
[33]. M. Sohail, D. W. Sun, and Z. Zhu, "Recent developments in intelligent packaging for enhancing food quality and safety," Critical Reviews in Food Science and Nutrition, vol. 58, no. 15, pp. 2650-2662, 2018.
[34]. B. Kuswandi, Y. Wicaksono, Jayus, A. Abdullah, L. Y. Heng, and M. Ahmad, "Smart packaging: Sensors for monitoring of food quality and safety," Sensing and Instrumentation for Food Quality and Safety, vol. 5, pp. 137-146, 2011.
[35]. S. Y. Lee, S. J. Lee, D. S. Choi, and S. J. Hur, "Current topics in active and intelligent food packaging for preservation of fresh foods," Journal of the Science of Food and Agriculture, vol. 95, no. 14, pp. 2799-2810, 2015.
[36]. A. Dirpan, R. Latief, A. Syarifuddin, A. N. F. Rahman, R. P. Putra, and S. H. Hidayat, "The use of color indicator as a smart packaging system for evaluating mangoes Arummanis (Mangifera indica L. var. Arummanisa) freshness," IOP Conference Series: Earth and Environmental Science, vol. 157, p. 012031, 2018.
[37]. Y. S. Musso, P. R. Salgado, and A. N. Mauri, "Gelatin-based films capable of modifying its color against environmental pH changes," Food Hydrocolloids, vol. 61, pp. 523-530, 2016.
[38]. H. M. F. A. El-Wahab and G. S. E. D. Moram, "Toxic effects of some synthetic food colorants and/or flavor additives on male rats," Toxicology and Industrial Health, vol. 29, no. 2, pp. 224-232, 2013.
[39]. S. Kobylewski and M. F. Jacobson, "Toxicology of food dyes," International Journal of Occupational and Environmental Health, vol. 18, no. 3, pp. 220-

246, 2012.
[40]. R. Andretta, C. L. Luchese, I. C. Tessaro, and J. C. Spada, "Development and characterization of pH-indicator films based on cassava starch and blueberry residue by thermocompression," Food Hydrocolloids, vol. 93, pp. 317-324, 2019.
[41]. M. Koosha and S. Hamedi, "Intelligent Chitosan/PVA nanocomposite films containing black carrot anthocyanin and bentonite nanoclays with improved mechanical, thermal and antibacterial properties," Progress in Organic Coatings, vol. 127, pp. 338-347, 2019.
[42]. S. Roy and J. W. Rhim, "Carboxymethyl cellulose-based antioxidant and antimicrobial active packaging film incorporated with curcumin and zinc oxide," International Journal of Biological Macromolecules, vol. 148, pp. 666-676, 2020.
[43]. M. Vadivel, M. Sankarganesh, J. D. Raja, J. Rajesh, D. Mohanasundaram, and M. Alagar, "Bioactive constituents and bio-waste derived chitosan/xylan based biodegradable hybrid nanocomposite for sensitive detection of fish freshness," Food Packaging and Shelf Life, vol. 22, p. 100384, 2019.
[44]. P. Ezati, H. Tajik, M. Moradi, and R. Molaei, "Intelligent pH-sensitive indicator based on starch-cellulose and alizarin dye to track freshness of rainbow trout fillet," International Journal of Biological Macromolecules, vol. 132, pp. 157-165, 2019.
[45]. S. R. Kanatt, "Development of active/intelligent food packaging film containing Amaranthus leaf extract for shelf life extension of chicken/fish during chilled storage," Food Packaging and Shelf Life, vol. 24, p. 100506, 2020.
[46]. H. Dong, Z. Ling, X. Zhang, X. Zhang, S. Ramaswamy, and F. Xu, "Smart colorimetric sensing films with high mechanical strength and hydrophobic properties for visual monitoring of shrimp and pork freshness," Sensors and Actuators B: Chemical, vol. 309, p. 127752, 2020.
[47]. H. Wen, Y. I. Hsu, T. A. Asoh, and H. Uyama, "Antioxidant activity and physical properties of pH-sensitive biocomposite using poly(vinyl alcohol) incorporated with green tea extract," Polymer Degradation and Stability, vol. 178, p. 109215, 2020.
[48]. M. Vadivel, M. Sankarganesh, J. D. Raja, J. Rajesh, D. Mohanasundaram, and M. Alagar, "Bioactive constituents and bio-waste derived chitosan/xylan based biodegradable hybrid nanocomposite for sensitive detection of fish freshness," Food Packaging and Shelf Life, vol. 22, p. 100384, 2019.
[49]. F. H. Santos, D. C. Ferreira, J. R. Matheus, A. E. Fai, and F. M. Pelissari, "Antioxidant Activity Assays for Food Packaging Materials," in Food Packaging Materials: Current Protocols, New York, NY: Springer US, pp. 293-309, 2024.
[50]. S. Chavoshizadeh, S. Pirsa, and F. Mohtarami, "Sesame oil oxidation control by active and smart packaging system using wheat gluten/chlorophyll film to increase shelf life and detecting expiration date," European Journal of Lipid Science and Technology, vol. 122, no. 3, p. 1900385, 2020.
[51]. J. J. L. Lee, X. Cui, K. F. Chai, G. Zhao, and W. N. Chen, "Interfacial assembly of a cashew nut (Anacardium occidentale) testa extract onto a cellulose-based film from sugarcane bagasse to produce an active packaging film with pH-triggered release mechanism," Food and Bioprocess Technology, vol. 13, pp. 501-510, 2020.
[52]. M. Aria and C. Cuccurullo, "bibliometrix: An R-tool for comprehensive science mapping analysis," Journal of Informetrics, vol. 11, no. 4, pp. 959-975, 2017.
[53]. N. Van Eck and L. Waltman, "Software survey: VOSviewer, a computer program for bibliometric mapping," Scientometrics, vol. 84, no. 2, pp. 523-538, 2010.
[54]. S. C. Lourenço, M. Moldão-Martins, and V. D. Alves, "Antioxidants of natural plant origins: From sources to food industry applications," Molecules, vol. 24, no. 22, p. 4132, 2019.
[55]. S. Kumar, A. Mukherjee, and J. Dutta, "Chitosan-based nanocomposite films and coatings: Emerging antimicrobial food packaging alternatives," Trends in Food Science and Technology, vol. 97, pp. 196-209, 2020.
[56]. A. Kumar, M. Hasan, S. Mangaraj, M. Pravitha, D. K. Verma, and P. P. Srivastav, "Trends in edible packaging films and its prospective future in food: a review," Applied Food Research, vol. 2, no. 1, p. 100118, 2022.
[57]. J. Pires, C. D. D. Paula, V. G. L. Souza, A. L. Fernando, and I. Coelhoso, "Understanding the barrier and mechanical behavior of different nanofillers in chitosan films for food packaging," Polymers, vol. 13, no. 5, p. 721, 2021.
[58]. A. Ashfaq, N. Khursheed, S. Fatima, Z. Anjum, and K. Younis, "Application of nanotechnology in food packaging: Pros and Cons," Journal of Agriculture and Food Research, vol. 7, p. 100270, 2022.
[59]. J. R. Westlake, M. W. Tran, Y. Jiang, X. Zhang, A. D. Burrows, and M. Xie, "Biodegradable biopolymers for active packaging: demand, development and directions," Sustainable Food Technology, vol. 1, no. 1, pp. 50-72, 2023.
[60]. M. Duan, S. Yu, J. Sun, H. Jiang, J. Zhao, C. Tong, et al., "Development and characterization of electrospun nanofibers based on pullulan/chitin nanofibers containing curcumin and anthocyanins for active-intelligent food packaging," International Journal of Biological Macromolecules, vol. 187, pp. 332-340, 2021.
[61]. Y. Qin, Y. Liu, H. Yong, J. Liu, X. Zhang, and J. Liu, "Preparation and characterization of active and intelligent packaging films based on cassava starch and anthocyanins from Lycium ruthenicum Murr," International Journal of Biological Macromolecules, vol. 134, pp. 80-90, 2019.

[62]. F. Wang, C. Xie, H. Tang, W. Hao, J. Wu, Y. Sun, et al., "Development, characterization and application of intelligent/active packaging of chitosan/chitin nanofibers films containing eggplant anthocyanins," Food Hydrocolloids, vol. 139, p. 108496, 2023.

[63]. A. Sobhan, K. Muthukumarappan, and L. Wei, "A biopolymer-based pH indicator film for visually monitoring beef and fish spoilage," Food Bioscience, vol. 46, p. 101523, 2022.

[64]. N. S. Said, N. K. Howell, and N. M. Sarbon, "A review on potential use of gelatin-based film as active and smart biodegradable films for food packaging application," Food Reviews International, vol. 39, no. 2, pp. 1063-1085, 2023.

[65]. R. Eshaghi, E. K. Sadrabad, A. Jebali, S. Hekmatimoghaddam, and F. A. Mohajeri, "Application of pH indicator label based on beetroot color for determination of milk freshness," Journal of Environmental Health and Sustainable Development, 2020.

[66]. W. Zhang and J. W. Rhim, "Titanium dioxide (TiO2) for the manufacture of multifunctional active food packaging films," Food Packaging and Shelf Life, vol. 31, p. 100806, 2022.

[67]. L. Kuuliala, T. Pippuri, J. Hultman, S. M. Auvinen, K. Kolppo, T. Nieminen, et al., "Preparation and antimicrobial characterization of silver-containing packaging materials for meat," Food Packaging and Shelf Life, vol. 6, pp. 53-60, 2015.

[68]. S. Chowdhury, Y. L. Teoh, K. M. Ong, N. S. R. Zaidi, and S. K. Mah, "Poly(vinyl) alcohol crosslinked composite packaging film containing gold nanoparticles on shelf life extension of banana," Food Packaging and Shelf Life, vol. 24, p. 100463, 2020.

[69]. N. Oladzadabbasabadi, A. M. Nafchi, F. Ariffin, M. J. O. Wijekoon, A. A. Al-Hassan, M. A. Dheyab, and M. Ghasemlou, "Recent advances in extraction, modification, and application of chitosan in the packaging industry," Carbohydrate Polymers, vol. 277, p. 118876, 2022.

[70]. I. Armentano, N. Bitinis, E. Fortunati, S. Mattioli, N. Rescignano, R. Verdejo, et al., "Multifunctional nanostructured PLA materials for packaging and tissue engineering," Progress in Polymer Science, vol. 38, no. 10-11, pp. 1720-1747, 2013.

[71]. F. Parvin, M. A. Rahman, J. M. Islam, M. A. Khan, and A. H. M. Saadat, "Preparation and characterization of starch/PVA blend for biodegradable packaging material," Advanced Materials Research, vol. 123, pp. 351-354, 2010.

[72]. I. Kim, K. Viswanathan, G. Kasi, S. Thanakkasaranee, K. Sadeghi, and J. Seo, "ZnO nanostructures in active antibacterial food packaging: Preparation methods, antimicrobial mechanisms, safety issues, future prospects, and challenges," Food Reviews International, vol. 38, no. 4, pp. 537-565, 2022.

[73]. Y. A. Arfat, J. Ahmed, M. Ejaz, and M. Mullah, "Polylactide/graphene oxide nanosheets/clove essential oil composite films for potential food packaging applications," International Journal of Biological Macromolecules, vol. 107, pp. 194-203, 2018.

Environ Res Tec, Vol. 8, Issue. 2, pp. 471-486, June 2025

Environmental Research and Technology
https://dergipark.org.tr/en/pub/ert
DOI: https://10.35208/ert.1511775

Environmental Research & Technology

Review Article

Examining the use of marble waste as a substitute of conventional materials in concrete: A brief review

Mustapha Nuhu GARKO[1*], Shashivendra DULAWAT[1], Esar AHMAD[1]
Salihu Sarki UBAYI[1], Ibrahim Abdullahi IBRAHIM[1]

[1] *Department of Civil Engineering Mewar University Rajasthan, India*

ARTICLE INFO

Article history
Received: 06 Jul 2024
Revised: 19 Aug 2024
Accepted: 10 Sep 2024

Key words:
Concrete, marble waste, sustainability.

ABSTRACT

The use of waste marble in concrete as a substitute for conventional materials is gaining attention due to its potential environmental and economic benefits. This review comprehensively examines the feasibility of utilizing marble waste in concrete, focusing on three primary replacement levels: cement, fine aggregate, and coarse aggregate. The study synthesizes recent research on substituting marble waste for cement, fine aggregates, and coarse aggregates, focusing on performance metrics such as workability, strength, and durability. Findings reveal that waste marble can effectively replace up to 10% of cement in concrete mixtures. For fine aggregates, optimal replacement levels range between 20-30%, When used as a coarse aggregate substitute, marble waste can be replaced up to 50%, balancing improved resource efficiency with maintained strength and durability. The review highlights that incorporating waste marble into concrete not only reduces the reliance on natural resources but also minimizes landfill waste and lowers the carbon footprint. Recommendations for future research include standardizing marble waste particle sizes, evaluating long-term durability, and assessing environmental impacts through comprehensive life cycle analyses. This study aims to influence industry stakeholders and policymakers to consider waste marble as a viable and eco-friendly alternative in sustainable construction practices.

Cite this article as: Garko, MN, Dulawat S, Ahmad E, Ubayi SS, Ibrahim IA. Examining the use of marble waste as a substitute of conventional materials in concrete: A brief review. Environ Res Tec 2025;8(2) 471-486.

INTRODUCTION

Concrete is among the most widely used construction materials across the globe because of its appropriate mechanical qualities, longevity, and ease of access. The world concrete consumption is estimated to about 25 billion tons per year [1]. Essentially, concrete is a composite material made up of four primary components: cement, fine aggregates, coarse aggregates, and water, the continuous utilization of this ingredients leads to the reduction of available natural materials. Approximately 70% of the concrete volume is composed of aggregates [2], These aggregates are obtained naturally from quarries and rivers [3]. The rise in concrete production leads to the depletion of natural resources and triggers environmental issues like soil erosion and habitat destruction. In order to eliminate this problem, numerous research initiatives have been undertaken to explore the substitution of aggregates with waste materials [4]. Numerous solid waste materials have the capacity to serve as substitutes for fine and coarse aggregates. These materials originate from agro-industrial processes and are often discarded in landfills, contributing to health and environmental concerns [5]. Marble

***Corresponding author.**
*E-mail address: nuhugarkomustapha@gmail.com

This is an open access article under the CC BY-NC license (http://creativecommons.org/licenses/by-nc/4.0/).

dust is one of these waste materials.

Marble dust is a fine particle result from cutting process or polishing of marble. It does not possess pozzolanic properties, but it does produce more void-free concrete by filling in concrete mixtures [6]. It is usually produced in large amount during the mining and processing phases by Marble industry. This waste is dumped on open land, leading to various environmental hazards [7]. Also, these waste cause waterlogging, sterility to the land, and also causes harm to the ecosystem in the neighboring areas [8]. To curtail these environmental challenges, it is crucial to adopt sustainable approaches like proper waste management, recycling efforts, and the integration of eco-friendly technologies in the marble industry.

The sustainable utilization of marble waste in both concrete and sculptures is gaining attention as a means to moderate environmental concerns related to the construction industry. Marble waste, consisting mainly of marble fines and slurry, can be utilized effectively in various applications, thereby reducing waste disposal issues and promoting circular economy principles. In general, the distribution of marble waste generation by country is not readily available as a specific statistic. However, it is possible to approximate based on general knowledge of marble production, as waste generation is typically proportional to the amount of marble quarried and processed. The pie chart in Figure 1 illustrates the global distribution of marble waste generation, with a clear emphasis on the dominance of certain countries. Most notably, China emerges as the largest contributor to marble waste, emphasizing its significant role in the global marble industry. This substantial waste generation can be attributed to China's massive marble extraction and processing activities, which are driven by its extensive infrastructure development and construction projects [9]. Following China, other countries such as India, Turkey, and Italy also contribute considerably to global marble waste. These countries are well-known for their rich marble reserves and longstanding tradition in marble production. The distribution pattern observed in the pie chart highlights the geographical concentration of marble production and waste generation in specific regions. This distribution is influenced by factors such as the availability of marble reserves, the level of industrialization, and the demand for marble in domestic and international markets.

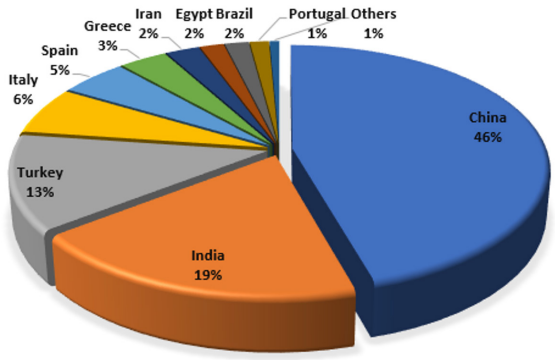


Figure 1. Global marble production by country (2023 estimates)[10]

In concrete production, marble waste serves as a partial replacement for natural aggregates like sand and gravel. This practice reduces the consumption of virgin raw materials, conserves natural resources, and lowers the overall cost of construction projects [11], [12], [13]. Studies indicate that incorporating marble waste into concrete can improve its mechanical and durability characteristics, such as enhanced compressive strength, split tensile strength, and resistance to acid attack [14].

Marble waste can also be employed in sculpture making, providing a unique and eco-friendly alternative to traditional carving materials. For instance, marble slurry can be molded into decorative elements, such as wall panels, floor tiles, and architectural details [13]. This approach allows for the repurposing of waste materials while offering innovative design solutions. Figure 2. (a) shows the dumped marble waste whereas figure 2 (b) displays the marble mining quarry.



Figure 2. (a) marble wastes (fine sized dust, middle and large sized marble pieces) [15]



Figure 2. (b) marble mining quarry [15]

SIGNIFICANCE OF THE REVIEW

This review primarily explores the potential of marble waste as a sustainable alternative in concrete production, addressing the dual challenges of waste management and resource depletion. By investigating the use of marble waste as a substitution for conventional materials such as cement, coarse

aggregates, and fine aggregates, the review contributes to reducing the environmental impact of the construction industry. It critically assesses the technical feasibility and performance of marble waste in concrete applications, providing insights into its mechanical properties, durability, and overall effectiveness. Additionally, the review identifies challenges and research gaps, offering a roadmap for future studies by highlighting areas that require further investigation, such as long-term durability, environmental impact assessments, and the development of standardized guidelines. Ultimately, this study seeks to promote sustainable practices in the construction industry by demonstrating the positive environmental contributions and potential benefits of using marble waste in concrete, aiming to influence industry stakeholders, policymakers, and researchers to consider marble waste as a viable and eco-friendly alternative in the pursuit of sustainable development.

STUDIES INCLUDED IN THE SCOPE OF THE REVIEW

In this section, the utilization and recycling options for marble waste were thoroughly assessed through a comprehensive literature review, focusing on studies published after 2014. The review provides a detailed and concise summary of research conducted across various fields where waste marble dust has been applied.

Use of Marble Waste as a Partial Substitute for Traditional Coarse Aggregate

Numerous experimental studies have been conducted to assess the feasibility of using marble waste aggregate as a potential substitute for conventional natural coarse aggregate in concrete. The study conducted by [16], Marble waste aggregate was used in varying percentages from 0% to 100% by weight. The concrete mixtures were prepared with a constant water-cement ratio of 0.60. The result demonstrated a substantial improvement in the workability of concrete mixes that included marble aggregate of 11% more than that of control concrete. Similarly, all of the concrete mixtures with marble aggregate showed an average increase in compressive strength of 56% and 35% after 7 and 28 days, respectively.

In a similar study, Basaran et al. [17] examined the impact of substituting standard coarse aggregate with coarse marble aggregate in various proportions on the compressive strength of concrete. They analyzed a total of 93 compressive strength tests sourced from existing literature and conducted multivariate regression analyses on these results. Their findings revealed that replacing coarse aggregates with coarse marble aggregates can have both positive effects (increasing strength by up to 75%) and negative effects (decreasing strength by up to 32%) on concrete compressive strength. They also concluded that coarse marble aggregates can be used in substantial amounts, up to 50%, to achieve either a maximum increase or decrease in compressive strength.

However, Sowjanya et al. [18] studied the performance of concrete made with replacement of natural aggregate with black marble stone waste aggregates in proportion of (0%, 20%, 40%, 60%, 80%, and 100%). The results indicated a significant decline in workability and water absorption to about 42.85% and 91.46% respectively. Nevertheless, the compressive strength at 28-days curing age decreased to about 15.45% at 40% replacement level.

Saloni et al. [19] in their study discovers the using waste marble aggregates (WMA) as a substitute for natural aggregates (NA) in the production of sustainable alkali activated concrete (AAC). The research found that replacing up to 50% of NA with WMA led to an increase in the mechanical properties and elastic modulus of the AAC. However, the results indicates that higher replacement levels resulted in a non-homogeneous mixture and lower strength. Durability tests showed satisfactory gas permeation and resistivity up to 50% replacement, but water penetration resistance, density and slump decreased with the addition of WMA respectively. The study concludes that WMA can replace up to 50% of NA in AAC production, potentially leading to significant energy and cost savings and reducing environmental impacts from marble industries. Table 1 summarizes the experimental results of various tests conducted by different authors, comparing the use of marble-based aggregate with natural aggregate in the studies reviewed. Generally, the replacement of natural aggregates with marble waste led to notable improvements in the mechanical properties of concrete, as evidenced by the percentage increases in compressive, flexural, and splitting tensile strengths. These enhancements suggest that marble waste can contribute to a denser microstructure, which likely reduces the permeability of the concrete, as indicated by the reduced water penetration values. The variation in optimum replacement levels reported by different authors emphasizes the need for further research to determine the most effective replacement percentage, which may depend on factors such as the specific characteristics of the marble waste and the intended application of the concrete.

Use of Marble Waste as a Partial Substitute for Natural Sand

Marble Dust as a Fine Aggregate in Concrete Production

Marble dust has been extensively studied for its potential to replace fine aggregate in concrete mixes, specifically with water-cement ratios ranging from 0.4 to 0.6. The majority of investigations have employed marble dust with a calcite basis for their research [21]. Here, Demir [22] was conducting research in this field. Demir and Alyamac [22] used marble powder of different particle sizes to replace fine aggregate, in proportions of 0%, 8%, 16% and 24%. The results indicate that incorporating marble powder enhanced the compressive strength of the concrete mixes by 4.2% at an 8% substitution level, while workability diminished with incremental increases in marble powder replacement. The decrease in workability is associated with high water absorption characteristic by the marble powder which lead to a drier mixture as more water might be needed to achieve the desired consistency. Hence a high ranged water reducers admixture had to be used to improve the workability. Alyamac and Aydin [23] investigated the use of marble powder at 10%, 20%, 30%, 40%, 50%, and 90% by volume as a replacement for sand and examined compressive strength values at 7, 28,

and 90 days. Their study found that marble powder is effective as a sand replacement material up to a 40% substitution level. Unconventionally, Ghani et al. [24] used waste marble powder (fineness modulus 0.99) as a partial replacement of sand (fineness modulus 3.00) they achieved a better performance in terms of compressive strength (an improvement up to 38.55% at 40%, and 28-days curing age) and splitting tensile strength at 20% replacement level. At 80% replacement level, these parameters were lower than those of the control concrete. The addition of waste marble dust to concrete in place of fine aggregate increases the material's tensile, flexural, and compressive strengths [25]. However, According to Memon et al. [5], Marble Powder (MP) may be able to partially substitute sand without sacrificing strength. Also, it was observed that the finest results were obtained when 50% of the sand was replaced with MP, which resulted in increases in compressive and flexural strength of 13.52% and 35.54%, respectively, above the control sample.

Varadharajan et al. [26] aimed to explores the substitution of cement with rice husk ash (RHA) and fine aggregate with marble waste powder (MWP) in concrete, along with the addition of 1.5% steel fibers. The study found that the optimal mix was 15% RHA, 30% MWP, and 1.5% steel fibers, which resulted in a 44.4%, 60%, and 46.13% increase in compressive strength, tensile strength, and flexural strength respectively. The combination also reduced porosity and water absorption. Despite a 6.3% cost increase, the improved mechanical properties and environmental benefits justified the cost. The environmental assessment showed significant reductions in CO2 emissions and particulate matter, contributing to a more sustainable and cleaner environment. The proposed equations from the regression analysis to determine the mechanical properties showed a high correlation with the experimental results.

Anitha et al. [27] investigated the use of marble Powder (MP) as a substitute for fine aggregates in concrete, aiming to reduce environmental degradation and material scarcity. The research involved replacing fine aggregate with MP in increments of 10%, up to 50%, in concrete specimens. These specimens were then cured for 7, 14, and 28 days. The results indicated that increasing marble powder (MP) ratios improved the mechanical properties of the concrete. However, the optimal mix was found to be with 10% MP, which demonstrated superior characteristics compared to control mixes. This suggests that MP can replace fine aggregate in concrete, enhancing efficiency and being cost-effective due to its availability and production. The study concludes that MP can replace up to 10% of fine aggregate in concrete, contributing to environmental and economic sustainability. The study also suggested that future work should investigate the durability characteristics of MP in concrete. The results summarized in the Table 2 provide a clear overview of the impact of using waste marble as a substitute for conventional fine aggregate in concrete mixes. Generally, the data reveals a consistent trend of enhanced mechanical properties, such as compressive, flexural, and splitting tensile strengths, across various replacement levels when compared to the control mix. The table also gave an insight on optimal replacement value at which the positive effects are maximized before a decline is observed.

Table 1. Results Summary: Marble Waste Replacing Conventional Coarse Aggregate in Concrete Mixes

References	Replacement Ratios	Slump (mm)	Compressive Strengthchange	Flexural Strength change	Split tensile strength change	Water penetration	Optimum replacement value
[16]	(0%, 20%, 40%, 60%, 80% and 100%)	Inc.	Inc. by 35% at 80% and 28-days curing age	-	-	Inc. by 83% at 80% replacement level	80%
[18]	(0%, 20%, 40%, 60%, 80% and 100%)	Inc.	Inc. by 15.45% at 40% and 28-days curing age	-	-	Dec. by 91.46% at 100% replacement level	40%
[20]	0-50% at 5% increment	-	Dec. by 4.49% at 30% and 28-days curing age	-	-	-	30%
[19]	(0%, 25%, 50%, 75% and 100%)	Dec.	Inc. by 25.11% at 50% and 28-days curing age	Inc. by 16.63% at 50% and 28-days curing age	Inc. by 11.92% at 50% and 28-days curing age	Dec. by 7% at 50% replacement level	50%

Table 2. Results Summary: Marble Waste Replacing Fine Aggregate in Concrete Mixes

References	Replacement Ratios	Slump (mm)	Compressive Strengthchange	Flexural Strength change	Split tensile strength change	Water absorption	Optimum replacement value
[22]	(0%, 8%, 16% and 24%)	Dec	Inc. by 4.2% at 8%	-	-	-	8%
[24]	(0%, 20%, 40% 60% and 80%)	Dec	Inc. by 38.55% at 40%	-	Inc. by 6.87% at 20%	Dec	40%
[25]	(0%, 25%, 50%, and 100%)	-	Inc. by 28% at 50%- and 28-days curing age	Inc. by 13.28% at 50%- and 28-days curing age	Dec. by 66% at 100% Replacement level	-	50%
[5]	(0%, 25%, 50%, 75%, and 100%)	-	Inc. by 13.52% at 50%- and 28-days curing age	Inc. by 35.54% at 50%- and 28-days curing age	-	-	50%
[28]	(0%, 5%, 10%, 15%, and 20%)	Inc	Inc. by 54.5% at 15%- and 28-days curing age	Inc. by 24.30% at 15%- and 28-days curing age	Inc. by 12.14% at 15%- and 28-days curing age	-	15%
[26]	(10%, 20% and 30%)	Dec	Inc. by 27% at 30%- and 28-days curing age	Inc. by 15.23% at 30%- and 28-days curing age	Inc. by 23.11% at 30%- and 28-days curing age	Reduced by 16.3% at 30%- and 28-days curing age	30%
[27]	(10%, 20%, 30%, 40%, and 50%)	Inc. by 14.28%	Inc. by 61.02% at 10%- and 28-days curing age	Inc. by 36.42% at 10%- and 28-days curing age	Inc. by 48.41% at 10%- and 28-days curing age	-	10%

Marble Dust as a Substitute of Fine Aggregate in Mortars

Kabeer and Vyas [29] evaluates the use of waste marble powder as a replacement for river sand in cement mortars. The research tested various mortar mix proportions and found that replacing 20% of river sand with marble powder enhances the workability, compressive strength, bond, and adhesive strengths of the mortar, while maintaining similar drying shrinkage, water absorption, and porosity to conventional mortars. This improvement is attributed to the thixotropic property of marble powder, which reduces water requirements and promotes the formation of a denser microstructure with superior hydration products. The findings suggest that incorporating marble powder in construction materials can significantly reduce the dependency on natural river sand and water, and provide a sustainable solution for marble waste management, contributing to a cleaner production process in the marble industry.

Bentlemsan et al. [30] explores the potential of recycling marble waste into self-compacting mortar (SCM) by substituting natural sand with various proportions of marble waste (MW). The findings indicate that substituting up to 50% of natural sand with MW enhances the workability and flow time of the mortar in its fresh state. Particularly at 30% substitution, both compressive and flexural strengths improved significantly at 90 days, with an 8% and 17% increase, respectively. Additionally, the porosity decreased by 27% at this substitution rate, indicating better durability. Marble-based mortars had enhanced strength after 180 days of immersion, demonstrating superior durability against sulfate attack. These results suggest that using marble waste as a substitute for natural sand not only enhances the mechanical properties and durability of SCM but also contributes to environmental sustainability by reducing quarry exploitation and waste disposal. Future research should investigate the leaching behavior, aging, and techno-economic feasibility of marble waste recycling.

Chahour and Safi [31] investigated the use of marble sand as a substitute for natural sand in mortar, examining its effects on properties like mechanical strength, rheology, and durability over curing periods up to 56 days. Mortars were prepared with varying marble sand content (0%, 30%, 50%, 70%, and 100%). Findings indicate that replacing natural

sand with marble sand enhances compactness, compressive, flexural, and punching strength, particularly at a 50% substitution rate. Panels with 70% marble sand showed similar punching strength to control panels, and slabs with 100% marble sand displayed improved mechanical behavior. Durability tests revealed decreased weight loss due to acid attack with higher marble sand content, but water permeability increased beyond a 50% substitution rate. Overall, marble sand improves mechanical properties and conserves natural resources, although further research on durability is necessary.

Khyaliya et al. [32] used marble waste as a fine aggregate in lean mortar mixes, replacing river sand with marble waste in proportions ranging from 0% to 100% by volume. The best results were achieved with a 25% to 50% substitution, where water demand decreased by 6% and compressive strength significantly improved from 2.84 MPa to 7.04 MPa. The durability tests showed that mortars having 25% marble waste performed similarly to the control mix in aggressive environments. The study concluded that marble waste is suitable for both aggressive and non-aggressive environments, with 25% substitution recommended for aggressive conditions and up to 50% for non-aggressive conditions. Future research should include X-ray diffraction analysis to understand the mineralogical changes contributing to the improved performance of the mortar mixes.

Maza et al. [33] explores the recycling of marble waste in the form of powder and crushed aggregates as additions to cementitious building materials, aiming to enhance environmental protection. By incorporating marble powder into natural dune sand mortars and mixed sand mortars, the research achieved a notable decrease in porosity and significant improvements in mechanical properties. Specifically, a 15% marble powder addition, with or without admixture, improved compressive and flexural strengths. The use of crushed marble sand further optimized the granularity and cohesion of the mortar. Results showed that combining 15% marble powder with 20% crushed marble sand and a superplasticizer reduced water absorption and enhanced mechanical strengths, achieving compressive and flexural peaks of over 74 MPa and 12 MPa, respectively. The study concludes that recycling 35% of marble waste into the cement matrix effectively improves mortar properties and contributes to environmental conservation, recommending further research on substituting crushed marble with glass sand and marble powder with fine dune sand.

Marble Dust Used as a Fine Aggregate or Filler in Self-Compacting Concrete

Arun Kumar et al. [34] investigated the use of waste marble as a substitute for fine aggregate in self-compacting concrete (SCC), and polypropylene fiber as an additive to enhance flexural and tensile strength. Three replacement levels of 20%, 30%, and 40% were tested, with a fixed polypropylene fiber ratio of 0.4%. The results disclosed that up to 20% marble waste replacement improved compressive strength, while up to 40% replacement yielded acceptable fresh concrete results. The inclusion of fibers generally increased flexural and tensile strength. All fresh concrete properties were within acceptable values specified in European Federation of National Associations Representing producers and applicators of specialist building products for Concrete (EFNARC) guidelines, although the passing and filling capability reduced due to friction between powder particles and fiber surface area. Similarly, Vaidevi et al. [35] Investigates the application of marble waste as a fine aggregate in self-compacting concrete (SCC) for M60 grade, aiming to improve sustainability and workability. Various tests were conducted on fresh and hardened SCC, including slump flow, L-box, V-funnel, U-box, compressive strength, tensile strength, and flexure strength tests. The SCC specimens were cured for 14, 28, and 56 days with waste marble dust replacements of 0%, 25%, 50%, and 100%. Durability tests such as Rapid Chloride Penetration Test (RCPT), Water Penetration Test (WPT), and chemical attack tests were also conducted. The results showed that up to 25% replacement of fine aggregate with marble waste yielded satisfactory results in terms of workability, strength, and durability. Ahmadi et al. [36] aimed to investigates the potential of using waste from marble mining as a substitute for fine aggregates in the production of sustainable self-compacting concrete (SCC). According to the study, the compressive strength and flexural strength of the concrete were enhanced by adding 0.5% steel fiber by weight of cement and substituting up to 20% of the sand with marble waste. The presence of steel fibers was found to significantly improve the impact resistance of the specimens, more so than the recycled components. The study also revealed that fiber bridging greatly influences the final strength of specimens containing fibers. Furthermore, increasing the replacement percentage of recycled aggregates in the specimens enhances their resistance to impact loads. The water absorption rate showed no specific trend with the replacement of marble aggregates. Overall, the study concluded that SCC with recycled marble aggregate performed satisfactorily, demonstrating that the incorporation of recycled marble aggregate and steel fibers into self-compacting concrete can increase its mechanical properties and impact resistance.

Amit Kumar Tomar and Ankit Kumar [37] aimed to explores the properties of self-compacting concrete (SCC) when fine aggregate is replaced with waste marble powder at varying percentages (0%, 10%, 20%, 30%, 40%, and 50%). The research found that as the dose of waste marble powder increased, so did the workability of SCC. The most optimal results were observed at a 30% replacement level, where the fresh properties and compressive strength of the SCC outperformed other mixes at both 7 and 28 days. This suggests that waste marble powder could be a viable and effective substitute for fine aggregate in SCC, enhancing its performance and sustainability.

Karakurt and Dumangöz [38] investigated the use of waste marble dust (MD) and granulated blast furnace slag (GBFS) in the production of self-compacting concrete (SCC). The results revealed that the use of MD and GBFS improves the fresh and hardened properties of SCC. However, MD above a

10% ratio and GBFS above 30% negatively affect workability. GBFS contributes more to compressive strength compared to MD, with the maximum strength attained by the GBFS30 specimen due to its pozzolanic property. Both MD and GBFS improve the durability of SCC and contribute to pore filling. The use of these industrial wastes in SCC production not only increases concrete performance but also provides a solution for waste utilization. However, the transportation and screening of these wastes may raise the cost of SCC. Future research could investigate the compatibility of mineral additives and powder materials that enhance viscosity, as well as the use of binary and ternary combinations of MD and GBFS with other waste materials.

Singh et al. [39] studied the use of marble dust as a substitute for fine aggregates in concrete production. Experimental results showed that replacing up to 30% of sand with marble dust had slight effect on the compressive or flexural strength of the concrete. Specifically, the compressive strength increased by 4.9% with 15% marble dust, and by 12% with 30% marble dust. However, further increases in marble dust content (45% and 60%) resulted in smaller increases in compressive strength (3% and 2.1% respectively). Similar trends were observed for split tensile strength and flexural strength. The workability of the concrete was optimal at 30% marble dust replacement. However, workability and strength decreased as the concentration of marble dust increased beyond this point.

Use of Marble Dust as a Substitute for Cement in Concrete

Marble Dust as an Additional Cementitious Material for Concrete Production

The following research papers were identified that discuss the effects of marble dust as an additional cementitious material in concrete production.

Quanth and Kalra [40] carried out an experimental study on the use of marble dust powder as a partial replacement for cement and fine aggregates in concrete. In their research, natural fine aggregates were substituted with marble dust powder at replacement levels of 0%, 25%, 50%, and 100%, while cement was replaced by marble dust at 0%, 5%, and 10% replacement ratios. The results indicate that using marble powder up to 10% replacement by weight cement and 25% replacement by weight of fine aggregate can be effectively utilized without sacrificing concrete quality. Similarly, Gupta et al. [41] performed an experimental study on utilization of marble powder for sustainable construction, the results show that When marble dust powder containing less than or equal to 10% by replacement of cement slightly increases the compressive strength of the concrete and enhances the fresh properties of concrete such as workability and setting time. Raghunath et al. [42] conducted an experimental investigation into mechanical and durability properties of marble-powder-based high-strength concrete. It was observed that when cement is substituted with marble powder up to 10% the compressive strength, flexural strength and modulus of elasticity increases by 9.23%, 19.29% and 21.51% respectively. compared to the control specimen. Additionally, the test specimens showed minimal chloride ion penetration. However, both the marble powder concrete and conventional concrete displayed similar water absorption capacities. Rehan Ali [43] studied the influence of marble dust as a substitute of cement in concrete for environmental sustainability. The results indicated that replacing cement with marble dust at 5% and 10% has minimal impact on the strength of normal concrete at 7 and 28 days. Therefore, substituting up to 10% of cement with marble dust can be done without compromising the strength or workability of the concrete mix.

Yunusa et al. [44] Investigated the use of waste marble dust (WMD) as a partial replacement for cement in concrete. Concrete samples with 0%, 10%, 20%, and 30% WMD were tested for strength after 28 days of curing. The results showed that incorporating WMD significantly affected the compressive, split-tensile, and flexural strengths of the concrete, with the best performance at 20% replacement. This suggests that WMD can be effectively used in concrete production, helping to reduce environmental pollution, utilize waste profitably, and potentially lower construction costs since WMD is free. Therefore, a 20% replacement of cement with WMD is suggested for producing structural concrete. Chirumamilla et al. [45] in their study examines the use of marble powder as a cement substitute in M40 grade concrete to manage waste from the marble industry, which produces a large amount of dust. Cement was replaced with marble powder at 5%, 10%, 15%, 20%, and 25% by weight, and tests were carried out to measure compressive, split tensile, and flexural strength at 7, 28, 56, and 90 days. The findings revealed that replacing up to 20% of cement with marble powder enhances all three strength parameters, with the best results observed at 20% replacement. Beyond this point, strength started to decrease.

Kanhar et al. [46] examines the use of marble powder (MP) as a substitute for cement in M30 grade concrete to address environmental and waste management issues in Pakistan, where the marble industry contributes significantly to Gross Domestic Product (GDP) but also generates considerable waste. By substituting 5% and 10% of cement with MP, the research investigates the effects on workability, compressive strength, and flexural strength over time. Results showed that MP increases workability and, although initial compressive strength is lower, it improves significantly by 90 days, along with flexural strength. The summary of results in Table 3 emphasizes the considerable potential of using waste marble as a cement substitute in concrete mixes, demonstrating improvements in various mechanical and durability properties. The data shows that incorporating marble waste enhances compressive strength, flexural strength, and splitting tensile strength, frequently exceeding the performance of conventional mixes, especially at optimal replacement levels.

Table 3. Results Summary: Marble Waste Replacing Cement in Concrete Mixes

References	Replacement Ratios	Grade of concrete	Slump (mm)	Compressive Strengthchange	Flexural Strength change	Split tensile strength change	Water absorption (%)	Optimum replacement value
[41]	(0%, 5%, 10%, 20%, 30%, and 40%)		Dec	Inc. by 14.23% at 10%- and 28-days curing age	-	-	-	10%
[42]	(0%, 5%, 10%, 15%, and 20%)		-	Inc. by 19.23% at 10%- and 28-days curing age	Inc. by 19.29% at 10%- and 28-days curing age	-	Inc	10%
[43]	(0%, 5%, 10%, and 15%,)		Inc	Dec. by 16.7% at 15%- and 28-days curing age	-	-	-	10%
[44]	(0%, 10%, 20%, and 30%,)	M30	Inc	Inc. by 7.73% at 20%- and 28-days curing age	Inc. by 11.48% at 20%- and 28-days curing age	Inc. by 12.32% at 20%- and 28-days curing age	-	20%
[45]	(5%, 10%, 15%, 20% and 25%,)	M40	-	Inc. by 16.01% at 20%- and 28-days curing age	Inc. by 13.59% at 20%- and 28-days curing age	Inc. by 19.71% at 20%- and 28-days curing age	-	20%
[46]	(0%, 5%, and 10%,)	M30	Inc	Inc. by 17.27% at 10%- and 90-days curing age	Inc. by 12.54% at 5%- and 90-days curing age	-	-	10%

Table 4 presents a comprehensive summary of the physical characteristics of marble waste as reported by various authors, offering valuable insights into its potential as a substitute for conventional materials in concrete. The specific gravity which varies slightly across different studies, suggests that marble waste contributes to a denser concrete mix, which directly influences the weight and strength of the resulting concrete mix. Bulk density reflects the compactness of the waste, affecting the overall mass and porosity of the concrete. The maximum nominal size of the particles provides an indication of the aggregate's grading, which can impact the workability and compaction of the mix. Water absorption and fineness modulus are critical factors affecting the water-cement ratio and the fineness of the aggregate. Overall, these variations in physical characteristics highlight the importance of standardizing preparation and testing methods to ensure consistent and reliable results when incorporating marble waste into concrete.

Table 5 summarizes the oxide compositions of marble waste as reported by different authors, revealing a consistent trend across different studies. calcium oxide (CaO) emerges as the predominant component. The high CaO content emphasizes the potential of marble waste to act as a viable substitute for conventional cementitious materials. Calcium oxide is a primary ingredient in cement clinker, and its presence in marble waste suggests that this material could contribute to the strength and durability of concrete when used as a partial replacement for cement [48]. The reactivity of CaO in hydration reactions could enhance the overall performance of concrete, especially in terms of early strength development. However, the dominance of CaO in marble waste reflects its origin from calcite-rich marble, which is primarily composed of calcium carbonate ($CaCO_3$). During the processing of marble, $CaCO_3$ is converted into CaO, retaining its chemical identity. This consistent chemical profile across different sources of marble waste suggests a level of predictability in its behavior when used in concrete, which is advantageous for both researchers and practitioners.

Table 4. The physical characteristics of marble waste utilized by different authors

References	Marble wasteemployed as	Process for formation of aggregate	Specific Gravity	Water absorption (%)	Fineness Modulus	Maximum nominal size of Particle	Bulk Density (kg/m^3)	Specific surface area (cm^2/g)
[40]	cement and Fine aggregate	Crushing	2.60	0.80	2.03	-	1118	-
[22]	Fine aggregate	Crushing	2.71	-	-	2-4mm	-	3920
[24]	Fine aggregate	Crushing	2.41	0.34	0.99	0-1mm	8475	-
[47]	Cement	Marble dust obtained from	Inc	Inc. by 7.73% at 20%- and 28-days curing age	Inc. by 11.48% at 20%- and 28-days curing age	Inc. by 12.32% at 20%- and 28-days curing age	-	20%
[25]	Fine aggregate	Marble dust obtained from	-	2.50	< 300 microns	-	-	20%
[42]	Cement	Collected from local market	2.40	-	-	< 300 microns	-	-
[16]	Coarse aggregate	crushing	2.70	0.5	-	20mm	-	-
[18]	Coarse aggregate	crushing	2.77	0.6	3.49	20mm	-	-
[20]	Coarse aggregate	Broken marble tiles	2.10	0.1	-	20mm	-	-
[19]	Coarse aggregate	crushing	2.64	1.3	5.21	10-20mm	1383	-
[39]	Fine aggregate	crushing	3.02	-	3.79	-	690	-
[26]	Fine aggregate	crushing	2.64	1.83	2.45	-	-	-
[27]	Fine aggregate	crushing	2.445	-	8		2800	-
[29]	Fine aggregate in mortars	powder	2.70	-	-		1380	3500
[30]	Fine aggregate in mortars	crushing	2.556	0.5	2.7	Sieved through 5mm sieve	-	-
[31]	Fine aggregate in mortars	crushing	2.73	0.39	2.2	-	-	-
[32]	Fine aggregate in mortars	crushing	2.56	8.23	1.45	-	1670	-
[33]	Fine aggregate in mortars	crushing	2.63	-	2.98	Sieved through 5mm sieve	1780	-

Table 5. Oxides composition of marble waste utilized by different authors

References	SiO_2 (%)	CaO (%)	Al_2O_3 (%)	Fe_2O_3 (%)	MgO (%)	Na_2O (%)	K_2O (%)	SO_3(%)	Loss of Ignition (%)
[22]	28.35	40.45	0.17	9.70	16.25	0.05	0.01	0.02	4.84
[24]	-	55.45	-	0.678	-	-	-	-	43.58
[47]	3.86	28.63	4.62	0.78	16.9	-	-	-	43.3
[41]	26.35	42.45	0.52	9.40	1.52	-	-	-	19.76
[16]	3.75	33.12	-	0.13	17.91	-	-	-	45.07
[42]	1.28	50.10	1.38	0.54	1.72	0.29	-	0.21	44.48
[19]	3.70	35.12	Traces	0.12	18.12	-	-	-	42.94
[36]	0.46	53.49	0.05	0.32	0.12	0.01	-	0.015	43.26
[38]	0.61	53.35	0.23	0.13	0.79	0.69	0.03	0.54	43.07
[26]	5.87	41.54	0.56	0.8	15.55	0.07	0.073	0.11	-
[27]	28.35	40.45	0.42	9.70	16.25	-	-	-	-
[29]	1.57	32.19	0.18	1.18	19.85	-	-	-	-
[30]	0.15	63.75	0.058	0.029	-	-	-	0.012	-
[31]	0.15	54.86	0.08	0.04	1.03	-	-	-	-
[32]	3.75	33.12	traces	0.13	17.91	-	-	-	45.07
[33]	-	55.78	0.09	0.01	0.47	-	-	0.05	-

COMPARISION AND DISCUSSION OF RESEARCH FINDINGS

In this section the comparative analysis and discussion were made for all the recycling options when waste marble based is used as a substitute for conventional materials in concrete.

Comparative Analysis of Waste Marble Dust as a Cement Substitute

Figure 4. (a) vividly illustrates the relationship between slump values and water-cement ratios when waste marble dust replaces cement in concrete. Remarkably, studies [22], [49] found that high slump values were achieved even with a low water-cement ratio. This suggests that marble dust may enhance workability due to its particle size and smooth texture, which could act as a lubricant within the mix. In contrast, studies [43] [46] [44] reported moderate slump values at higher water-cement ratios, indicating that increased water content was necessary to achieve workability. This likely stems from the marble dust's finer particles, which increase water demand due to a larger surface area for hydration. These findings highlight the variability in how marble dust affects concrete properties. While low water-cement ratios usually reduce workability, marble dust can mitigate this effect under certain conditions. Conversely, higher water-cement ratios needed for moderate slump values suggest that more water is required for mixes with higher replacement levels or different aggregate combinations. Overall, the results underscore the need for careful mix design adjustments to optimize performance when using waste marble dust as a cement substitute

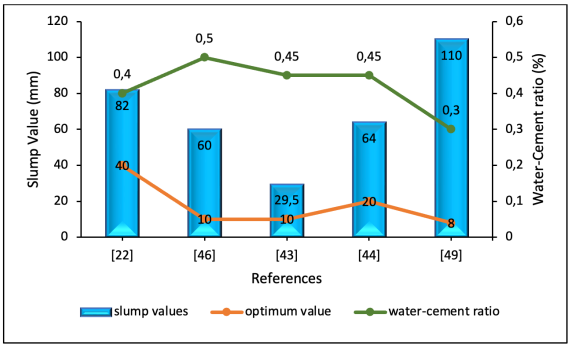


Figure 4. (a) Comparison of Slump, Water-cement Ratio, and Optimum Replacement level for cement substituted with waste marble dust

Comparative Analysis of Waste Marble Dust as a Fine Aggregate Substitute

Figure 4. (b) presents a comparison of slump values, water-cement ratios, and optimum replacement levels when substituting fine aggregate with waste marble dust. Studies [23],[24],[25] observed that higher replacement levels of marble dust led to lower slump values. This can be attributed to the dust's fine particle size, which increases the surface area and thus the water demand, resulting in reduced workability. As the replacement level rises, the mixture becomes denser and more cohesive, leading to lower slump values despite variations in the water-cement ratio. In contrast, studies [6],[27],[28] reported very high slump values at lower replacement levels, irrespective of the water-cement ratio. This indicates that when marble dust is used in smaller quantities, its impact on workability is less significant. The enhanced

fluidity at low replacement levels is likely due to the dust's ability to fill voids between aggregate particles, thereby improving workability without substantially increasing the water demand. Overall, these findings highlight that while waste marble dust can serve effectively as a fine aggregate replacement, its impact on slump values is highly dependent on the replacement level. Higher replacement levels generally reduce workability, necessitating adjustments in the mix design to achieve the desired balance between cohesion and flow properties. Conversely, at lower replacement levels, marble dust contributes positively to workability, offering potential benefits for improving concrete fluidity in specific applications.

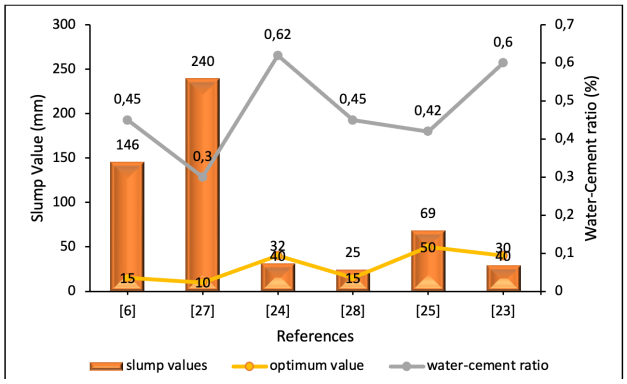


Figure 4. (b) Comparison of Slump, Water-cement Ratio, and Optimum Replacement level for fine aggregate substituted with waste marble dust

Comparative Analysis of Waste Marble Aggregate as Natural Coarse Aggregate Substitute

Figure 4. (c) compares slump, water-cement ratio, and optimum replacement level when substituting coarse aggregate with waste marble aggregate. The data shows that all reviewed studies report consistently high slump values at elevated replacement levels, regardless of the water-cement ratio. This consistent trend suggests that substituting marble aggregate for coarse aggregate significantly enhances workability. The high slump values observed can be attributed to the smooth texture and angular shape of marble aggregates, which reduce internal friction within the mix and facilitate better flow. Notably, the high slump remains stable across varying water-cement ratios, indicating that at high replacement levels, the characteristics of the marble aggregate dominate over traditional factors influencing workability. This is particularly advantageous in applications requiring high workability, such as complex formwork or densely reinforced sections. However, while the increased slump is beneficial, it is crucial to consider potential impacts on strength, durability, and overall mix stability. Excessive slump can sometimes lead to issues such as segregation or reduced structural integrity.

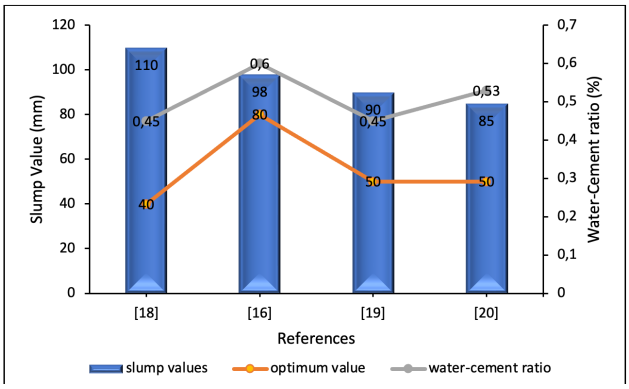


Figure 4. (c) Comparison of Slump, Water-cement Ratio, and Optimum Replacement level for coarse aggregate substituted with waste marble dust

CHALLENGES FOR FEATURE RESEARCH

Utilizing marble waste as a substitute for traditional materials in concrete presents both opportunities and challenges that require further research to optimize its application. One of the primary challenges is the heterogeneity of marble waste, which leads to variability in its properties and, consequently, the performance of the concrete. This variability makes it difficult to predict how marble waste will behave in concrete mixtures, necessitating more systematic studies to better understand its effects [50].

Another significant issue is the particle size distribution of marble waste, which can greatly influence the workability and strength of the concrete. Improperly sized particles can lead to problems such as poor workability and reduced strength, highlighting the need for standardized methods to achieve optimal particle sizes [51]. The chemical interactions between marble waste and cementitious materials also pose a challenge. Marble waste, particularly its calcium carbonate content, can influence the hydration process of cement, affecting the early strength and overall performance of the concrete. More detailed studies are needed to understand these interactions and optimize mix designs [52]. Optimizing these mix designs to balance strength, durability, and workability is another critical area of research. Finding the right proportion of marble waste as a substitute for conventional materials is complex and requires advanced modeling and experimentation [53].

Moreover, the lack of universally accepted standards and guidelines for the use of marble waste in concrete is a barrier to widespread adoption. Developing these standards, supported by robust research data, is essential for broader industry acceptance [52]. Finally, scaling up from laboratory research to real-world applications presents its own set of challenges. Transitioning to large-scale use requires adjustments in mix design, consistency in material properties, and thorough testing under varied conditions. Large-scale pilot projects and field studies are necessary to validate laboratory findings and ensure successful implementation [54].

ENVIRONMENTAL BENEFITS AND POSITIVE IMPACTS OF USING MARBLE WASTE IN CONCRETE

It has been testified from the previous researches that the use of marble waste especially in the production concrete offers numerous benefits ranging from environmental sustainability, economic efficiency, health and safety, innovation and research as well as performance related benefits.

By incorporating marble waste into concrete mixtures, their negative impact on environments is decreased. An example of this is the successful use of marble slurry in concrete pavements in Rajasthan, India, which not only utilized waste material but also led to improved pavement performance [55].

Integrating marble waste into concrete production can significantly boost job creation in both the recycling and manufacturing sectors [56]. This process involves collecting, processing, and repurposing marble waste, which requires a dedicated workforce for waste management, material handling, and quality control. For example, a company specializing in sustainable construction materials could establish a facility that employs local workers to crush and prepare marble waste for use in concrete mixtures. This not only diverts waste from landfills but also creates new employment opportunities across various stages of the supply chain, from waste collection to the final production of eco-friendly concrete products.

By incorporating marble waste into concrete production, companies not only reduce disposal costs but also create a market for eco-friendly building materials. For instance, marble dust can substitute part of the cement in concrete mixtures, enhancing the material's strength and durability. This innovative approach not only diminishes the environmental footprint of marble mining by repurposing waste but also addresses the construction industry's demand for sustainable materials. This symbiotic relationship between waste management and construction opens up new avenues for revenue while promoting environmental stewardship.

Utilizing marble waste in concrete production presents a significant environmental and health benefit by mitigating the rampant uncontrolled disposal of marble dust and fragments along roadsides, marble quarries, and in nearby environments (in some countries). This practice not only alleviates the unpleasant accumulation of waste but also importantly reduces air pollution associated with airborne marble dust particles. Such particles, when inhaled, can penetrate deep into the lungs, potentially leading to respiratory diseases. For instance, a study conducted in areas with high marble waste showed a marked decrease in local air quality, correlating with increased incidences of lung-related health issues among residents [26]. By incorporating marble waste into concrete, the generation of harmful dust is minimized, fostering a cleaner environment and promoting public health. Additionally, this practice exemplifies sustainable waste management and contributes to the circular economy by transforming a pollutant into a valuable construction resource.

Using marble waste in concrete production can significantly lower the overall carbon footprint of industries by reducing the need for energy-intensive quarrying and processing of new marble. Instead of discarding marble waste, it can be repurposed as a substitute for traditional concrete components. For instance, in the construction industry, incorporating marble waste into concrete mixtures can decrease the demand for freshly mined aggregates, which are typically extracted through environmentally damaging methods. This practice not only conserves natural resources but also cuts down on the emissions associated with mining and transporting new materials.

GAP IN RESEARCH

The majority of studies conducted in the recent literature focused on concrete grades of low to medium strength, ranging from M20 to M35. very rare studies were carried out on higher-grade concrete such as high strength concrete and high-performance concrete incorporating waste marble dust. However, with the limited data available from the research being conducted so far, concrete incorporating marble waste was found to be effective for the use in the construction of residential building and other structures that does not support heavy or dynamic loads. To enhance the application and utilization of marble waste in specific concrete types capable of supporting heavy and dynamic loads, such as in industrial buildings or railway sleepers, it is essential to conduct a comprehensive strength and durability analysis of high-grade concrete incorporating marble waste as a substitute for conventional materials. This would determine whether marble dust is suitable for use in high-strength concrete applications.

The compatibility of marble waste with various admixtures and additives in concrete is a critical yet often overlooked research gap in the field of sustainable construction materials. Marble waste, increasingly used as a partial replacement for conventional aggregates in concrete, interacts differently with chemical admixtures and additives such as superplasticizers, accelerators, retarders, and mineral admixtures like fly ash and silica fume. These interactions can significantly influence concrete properties including workability, early and long-term strength development, and durability. Understanding the specific effects of these additives on concrete containing marble waste is crucial for optimizing mixture proportions and achieving desired performance characteristics. Research addressing this gap would contribute significantly to advancing the sustainable use of marble waste in concrete, ensuring that its incorporation not only utilizes waste effectively but also enhances concrete performance in real-world applications.

The utilization of marble waste in concrete presents a promising avenue for sustainable construction practices. However, a significant research gap exists concerning the regional variations in marble waste characteristics and their direct impact on concrete properties. Most current studies are conducted in specific regions with access to particular types of marble waste, leading to findings that may not gen-

eralize across different geographical areas. Factors such as marble waste composition, waste particles' size distribution, and chemical properties can vary widely depending on the source location, affecting concrete's mechanical, durability, and aesthetic properties differently. Addressing these regional variations is crucial for developing concrete formulations that optimize the use of locally available marble waste while ensuring consistent and predictable performance across diverse environmental conditions and construction practices. Future research should focus on systematically exploring these variations to establish robust guidelines and standards for the effective integration of marble waste in concrete on a global scale.

The lack of standardized guidelines for incorporating marble waste in concrete presents a critical research gap that hinders its widespread adoption in construction practices. Currently, there is a notable absence of universally accepted procedures, comprehensive testing methods, and clear guidelines tailored for engineers and construction practitioners interested in utilizing marble waste as a supplementary material in concrete. This gap leads to inconsistencies in material properties, performance variations, and uncertainties regarding the long-term durability and structural integrity of concrete containing marble waste. Addressing this gap requires focused research efforts aimed at developing standardized protocols for the selection, processing, and incorporation of marble waste, as well as robust testing methodologies to ensure the reliability and predictability of concrete properties when incorporating these waste materials. Such guidelines are essential to foster confidence among stakeholders and encourage the broader adoption of sustainable construction practices leveraging marble waste.

Research in the field of utilizing marble waste in concrete predominantly centers on its compatibility with Portland cement, with significant strides made in understanding its effects on mechanical and durability properties. However, there remains a notable gap in investigating its compatibility with other types of cement, such as blended cements and sulfate-resistant cements. Blended cements, for instance, incorporate supplementary cementitious materials that could interact differently with marble waste compared to Portland cement, potentially altering concrete properties. Similarly, sulfate-resistant cements are designed for environments with high sulfate concentrations, presenting a distinct chemical environment that may affect the reactivity and performance of marble waste as a cementitious additive. Understanding these interactions is crucial for expanding the applicability of marble waste in various concrete applications, ensuring both sustainability and enhanced performance across different environmental conditions. Further research addressing these gaps could provide valuable insights into optimizing the use of marble waste in concrete beyond conventional Portland cement applications.

CONCLUSIONS

Based on the various studies accessed within the scope of the review the following conclusions can be drawn:

1.The use of waste marble in concrete production offers a dual benefit: it reduces costs while enhancing durability and addresses environmental challenges. Recycling waste marble not only supports the marble industry but also contributes significantly to the national economy. Efforts should be directed towards advancing recycling applications to maximize these benefits. This approach aligns with promoting environmental sustainability and safeguarding human health. Moreover, the findings from reviewed studies consistently highlight the potential of waste marble to improve concrete performance, making it a promising material for future sustainable construction practices.

2.The impact of incorporating waste marble in concrete on its strength has been extensively studied, revealing that substituting conventional materials with waste marble whether as coarse or fine aggregate, cement can increase the overall strength of the concrete. The strength gains are primarily attributed to better particle packing, reduced void content, and the pozzolanic reactivity of marble waste when used as a partial replacement for production of sustainable concrete.

3.The findings revealed that the optimal replacement level for waste marble powder as a cement substitute in concrete was 10%. At this replacement rate, the concrete exhibited its highest strength performance, indicating that incorporating 10% waste marble powder as a cement replacement produces the most favorable concrete strength.

4.The results demonstrated that substituting aggregate with waste marble in concrete proved to be more effective compared to using waste marble as a cement replacement.

5.The efficiency of replacing ordinary Portland cement (OPC) with marble waste can be improved when combined with other industrial by-products like ground granulated blast furnace slag (GGBS), silica fume, rice husk ash, and fly ash. The combined use results in a significant performance improvement that cannot be achieved when marble waste and these other materials are used individually.

6.The addition of marble powder generally requires water reducers like superplasticizers to maintain workability due to its high-water absorption. Moreover, innovative combinations, such as the incorporation of rice husk ash and steel fibers, have shown remarkable improvements in mechanical characteristics and environmental benefits, despite a slight cost increase.

ACKNOWLEDGEMENT

The successful completion of this article is due to the unwavering commitment and valuable input from all the authors. Their varied insights and expertise have significantly strengthened its content and overall quality.

DATA AVAILABILITY STATEMENT

No data was used for the research described in the article.

CONFLICT OF INTEREST

The author declared no potential conflicts of interest with respect to the research, authorship, and/or publication of this article.

USE OF AI FOR WRITING ASSISTANCE

Not declared.

ETHICS

There are no ethical issues with the publication of this manuscript.

REFERENCES

[1] S. A. Zareei, F. Ameri, N. Bahrami, P. Shoaei, H. R. Moosaei, and N. Salemi, "Performance of sustainable high strength concrete with basic oxygen steel-making (BOS) slag and nano-silica," Journal of Building Engineering, vol. 25, p. 100791, Sep. 2019, doi: 10.1016/j.jobe.2019.100791.

[2] R. B. Ardalan, Z. N. Emamzadeh, H. Rasekh, A. Joshaghani, and B. Samali, "Physical and mechanical properties of polymer modified self-compacting concrete (SCC) using natural and recycled aggregates," Journal of Sustainable Cement-Based Materials, vol. 9, no. 1, pp. 1–16, Jan. 2020, doi: 10.1080/21650373.2019.1666060.

[3] N. Tošić, S. Marinković, T. Dašić, and M. Stanić, "Multicriteria optimization of natural and recycled aggregate concrete for structural use," Journal of Cleaner Production, vol. 87, pp. 766–776, Jan. 2015, doi: 10.1016/j.jclepro.2014.10.070.

[4] M. Sandanayake, Y. Bouras, R. Haigh, and Z. Vrcelj, "Current Sustainable Trends of Using Waste Materials in Concrete—A Decade Review," Sustainability, vol. 12, no. 22, p. 9622, Nov. 2020, doi: 10.3390/su12229622.

[5] M. J. Memon, A. A. Jhatial, Z. A. Rid, T. A. Rind, and A. R. Sandhu, "Marble Powder as Fine Aggregates in Concrete," Engineering, Technology & Applied Science Research, vol. 9, no. 3, pp. 4105–4107, Jun. 2019, doi: 10.48084/etasr.2698.

[6] D. K. Ashish, "Concrete made with waste marble powder and supplementary cementitious material for sustainable development," Journal of Cleaner Production, vol. 211, pp. 716–729, Feb. 2019, doi: 10.1016/j.jclepro.2018.11.245.

[7] S. D. Kore and A. K. Vyas, "Impact of marble waste as coarse aggregate on properties of lean cement concrete," Case Studies in Construction Materials, vol. 4, pp. 85–92, Jun. 2016, doi: 10.1016/j.cscm.2016.01.002.

[8] S. Parmar and S. K. Das, "Effect of marble slurry as a partial substitution of ordinary Portland cement in lean concrete mixes," Structural Concrete, vol. 22, no. S1, Jan. 2021, doi: 10.1002/suco.202000059.

[9] X. C. Meng, C. Li, Z. H. Wang, X. Z. Gong, Y. Liu, and B. X. Sun, "A Life Cycle Inventory Case Study for Marble Mining in China," Materials Science Forum, vol. 787, pp. 171–175, Apr. 2014, doi: 10.4028/www.scientific.net/MSF.787.171.

[10] MarketWatch, Stock Market News. Accessed: Jun. 06, 2024. [Online]. Available: www.marketwatch.com.

[11] S. D. Kore, A. K. Vyas, and S. A. Kabeer K.I., "A brief review on sustainable utilisation of marble waste in concrete," International Journal of Sustainable Engineering, vol. 13, no. 4, pp. 264–279, Jul. 2020, doi: 10.1080/19397038.2019.1703151.

[12] O. Gencel, M. Nodehi, O. B. Yavuz, G. Kaplan, and A. Benli, "The use of waste marble for cleaner production of structural concrete: A comprehensive experimental study," Construction and Building Materials, vol. 361, p. 129612, Dec. 2022, doi: 10.1016/j.conbuildmat.2022.129612.

[13] K. Khan, W. Ahmad, M. N. Amin, A. Ahmad, S. Nazar, A. A. Abdullah, and A. M. Arab, "Exploring the Use of Waste Marble Powder in Concrete and Predicting Its Strength with Different Advanced Algorithms," Materials, vol. 15, no. 12, p. 4108, Jun. 2022, doi: 10.3390/ma15124108.

[14] J. Ahmad, F. Aslam, R. Martinez-Garcia, J. de-Prado-Gil, S. M. A. Qaidi, and A. Brahmia, "Effects of waste glass and waste marble on mechanical and durability performance of concrete," Scientific Reports, vol. 11, no. 1, p. 21525, Nov. 2021, doi: 10.1038/s41598-021-00994-0.

[15] H. A. El-Sayed, A. B. Farag, A. M. Kandeel, A. A. Younes, and M. M. Yousef, "Characteristics of the marble processing powder waste at Shaq El-Thoaban industrial area, Egypt, and its suitability for cement manufacture," HBRC Journal, vol. 14, no. 2, pp. 171–179, Aug. 2018, doi: 10.1016/j.hbrcj.2016.06.002.

[16] S. D. Kore and A. K. Vyas, "Impact of marble waste as coarse aggregate on properties of lean cement concrete," Case Studies in Construction Materials, vol. 4, pp. 85–92, Jun. 2016, doi: 10.1016/j.cscm.2016.01.002.

[17] B. Basaran, I. Kalkan, C. Aksoylu, Y. O. Özkılıç, and M. M. S. Sabri, "Effects of Waste Powder, Fine and Coarse Marble Aggregates on Concrete Compressive Strength," Sustainability, vol. 14, no. 21, p. 14388, Nov. 2022, doi: 10.3390/su142114388.

[18] M. Sowjanya, N. Raju, L. Bhavananda, O. V. Vardhan, and S. S. Lokesh, "Behaviour of Previous Concrete Using Marble Waste as Coarse Aggregate," Journal of Engineering Sciences, vol. 14, no. 02, 2023.

[19] Saloni, Parveen, Y. Y. Lim, T. M. Pham, Jatin, and J. Kumar, "Sustainable alkali activated concrete with fly ash and waste marble aggregates: Strength and Durability studies," Construction and Building Materials, vol. 283, p. 122795, May 2021, doi: 10.1016/j.

conbuildmat.2021.122795.

[20] A. Sugathan, "Investigation on compressive strength of concrete utilizing broken marble tiles as coarse aggregate," International Journal of Engineering Sciences & Research Technology vol. 03, no. 05. May 2016. e-ISSN: 2395 -0056.

[21] S. D. Kore, A. K. Vyas, and S. A. Kabeer K.I., "A brief review on sustainable utilisation of marble waste in concrete," International Journal of Sustainable Engineering, vol. 13, no. 4, pp. 264–279, Jul. 2020, doi: 10.1080/19397038.2019.1703151.

[22] T. DemiR and K. E. Alyamaç, "Investigation of the Use of Marble Powder in Production of High Strength Concretes," Open Journal of Nano, vol. 7, no. 1, pp. 18–25, Jun. 2022, doi: 10.56171/ojn.1034691.

[23] K. E. Alyamaç and A. B. Aydin, "Concrete properties containing fine aggregate marble powder," KSCE Journal of Civil Engineering, vol. 19, no. 7, pp. 2208–2216, Nov. 2015, doi: 10.1007/s12205-015-0327-y.

[24] A. Ghani, Z. Ali, F. A. Khan, S. R. Shah, S. W. Khan, and M. Rashid, "Experimental study on the behavior of waste marble powder as partial replacement of sand in concrete," SN Applied Sciences, vol. 2, no. 9, p. 1554, Sep. 2020, doi: 10.1007/s42452-020-03349-y.

[25] G. V. Vigneshpandian, E. A. Shruthi, C. Venkatasubramanian, and D. Muthu, "Utilisation of Waste Marble Dust as Fine Aggregate in Concrete," IOP Conference Series: Earth and Environmental Science, vol. 80, p. 012007, Jul. 2017, doi: 10.1088/1755-1315/80/1/012007.

[26] S. Varadharajan, A. Jaiswal, and S. Verma, "Assessment of mechanical properties and environmental benefits of using rice husk ash and marble dust in concrete," Structures, vol. 28, pp. 389–406, Dec. 2020, doi: 10.1016/j.istruc.2020.09.005.

[27] A. S. S.D., D. A., and S. B. V., "Investigation of waste marble powder in the development of sustainable concrete," Materials Today: Proceedings, vol. 44, pp. 4223–4226, 2021, doi: 10.1016/j.matpr.2020.10.536.

[28] A. Dhanalakshmi and M. Shahul Hameed, "Strength Properties of Concrete Using Marble Dust Powder," East Asian Journal of Multidisciplinary Research, vol. 1, no. 11, pp. 2521–2530, Dec. 2022, doi: 10.55927/eajmr.v1i11.1785.

[29] K. I. S. A. Kabeer and A. K. Vyas, "Utilization of marble powder as fine aggregate in mortar mixes," Construction and Building Materials, vol. 165, pp. 321–332, Mar. 2018, doi: 10.1016/j.conbuildmat.2018.01.061.

[30] N. Bentlemsan, W. Yahiaoui, and S. Kenai, "Strength and durability of self-compacting mortar with waste marble as sand substitution," Case Studies in Construction Materials, vol. 19, p. e02331, Dec. 2023, doi: 10.1016/j.cscm.2023.e02331.

[31] K. Chahour and B. Safi, "Mechanical behavior and chemical durability of marble-based mortar: Application to panels subjected to punching," Construction and Building Materials, vol. 232, p. 117245, Jan. 2020, doi: 10.1016/j.conbuildmat.2019.117245.

[32] R. K. Khyaliya, K. I. S. A. Kabeer, and A. K. Vyas, "Evaluation of strength and durability of lean mortar mixes containing marble waste," Construction and Building Materials, vol. 147, pp. 598–607, Aug. 2017, doi: 10.1016/j.conbuildmat.2017.04.199.

[33] M. Maza, N. Tebbal, S. Zitouni, and Z. E. A. Rahmouni, "Combined Effect of Marble Waste as Powder and Aggregate Form on the Proprieties of the Mortar," Annales de Chimie - Science des Matériaux, vol. 45, no. 6, pp. 467–476, Dec. 2021, doi: 10.18280/acsm.450605.

[34] M. Arun Kumar, S. Balaji, S. Selvapraveen, and P. Kulanthaivel, "Laboratory study on mechanical properties of self compacting concrete using marble waste and polypropylene fiber," Cleaner Materials, vol. 6, p. 100156, Dec. 2022, doi: 10.1016/j.clema.2022.100156.

[35] C. Vaidevi, T. F. Kala, and A. R. R. Kalaiyarrasi, "Mechanical and durability properties of self-compacting concrete with marble fine aggregate," Materials Today: Proceedings, vol. 22, pp. 829–835, 2020, doi: 10.1016/j.matpr.2019.11.019.

[36] M. Ahmadi, E. Abdollahzadeh, and M. Kioumarsi, "Using marble waste as a partial aggregate replacement in the development of sustainable self-compacting concrete," Materials Today: Proceedings, p. S2214785323019739, Apr. 2023, doi: 10.1016/j.matpr.2023.04.103.

[37] A. K. T. Amit Kumar Tomar and A. K. Ankit Kumar, "Strength Chracteristics of Self-Compacting Concrete Partially Replaced with Waste Marble Powder," Journal of Environmental Nanotechnology, vol. 7, no. 4, pp. 46–50, 2018, doi: 10.13074/jent.2018.12.184332.

[38] C. Karakurt and M. Dumangöz, "Rheological and Durability Properties of Self-Compacting Concrete Produced Using Marble Dust and Blast Furnace Slag," Materials, vol. 15, no. 5, p. 1795, Feb. 2022, doi: 10.3390/ma15051795.

[39] H. Singh, C. V. Teja, V. Kumar, H. Singh, and A. Sharma, "Properties of self-compacting concrete developed using marble dust as a partial replacement of fine aggregates," IOP Conference Series: Earth and Environmental Science, vol. 1327, no. 1, p. 012013, Apr. 2024, doi: 10.1088/1755-1315/1327/1/012013.

[40] K. K. Quanth and T. Kalra, "Experimental Utilization of Marble Dust Powder as Partial Replacement of Cement and Fine Aggregates in Concrete," International Journal of Engineering, vol. 3, no. 2456.

[41] S. Gupta, S. Srivastva, N. Kumar, A. Tripathi, and S. Jaiswal, "An Experimental Study on Utilization of Marble Powder for Sustainable Construction," International Research Journal of Engineering and Technology (IRJET), April 2022 vol. 09, no. 04, e-ISSN:

2395-0056.

[42] P.N. Raghunath, K. Suguna, J. Karthick, and B. Sarathkumar, "Mechanical and Durability Characteristics of Marble Powder Based High Strength Concrete," Scientia Iranica, vol. 26, no. 6, pp. 3159–3164, Dec. 2018, doi: 10.24200/sci.2018.4953.1005.

[43] S Rehan Ali and J. Abhi, "Partial Replacement of Cement by Marble Dust in Concrete for Environmental Sustainability," International Journal of Engineering Sciences & Research Technology, Jun. 2022, doi: 10.5281/ZENODO.6623536.

[44] A. Yunusa, M. A. Onugba, A. O. Austyns, C. U. Ojih, and A. E. Oni, "The use of Waste Marble Dust as Partial Replacement for Cement in Concrete," Current Journal of Applied Science and Technology, pp. 39–46, Apr. 2022, doi: 10.9734/cjast/2022/v41i831684.

[45] Chirumamilla. M. C. Shaik abdul hafeez Siva Kishore. Ikkurthi, "Investigation On Mechanical Properties of Concrete by Partial replacement of Cement with Marble Dust in M40 grade concrete (M40)," vol. Volume 21, no. Issue 6, p. Page 224-236, 2023, doi: doi: 10.48047/nq.2023.21.6.NQ23027.

[46] R. A. Kanhar, M. J. Memon, A. R. Sandhu, A. A. Jhatial, and A. K. Mastoi, "Mechanical Properties of Concrete Incorporating Marble Powder as Partial Cement Replacement," Quaid-e-Awam University Research Journal of Engineering Science & Technology, vol. 19, no. 1, pp. 59–64, Jun. 2021, doi: 10.52584/QRJ.1901.08.

[47] M. Singh, A. Srivastava, and D. Bhunia, "Analytical and Experimental Investigations on Using Waste Marble Powder in Concrete," Journal of Materials in Civil Engineering, vol. 31, no. 4, p. 04019011, Apr. 2019, doi: 10.1061/(ASCE)MT.1943-5533.0002631.

[48] S. Ali, S. Ahmad, and I. Ullah, "Utilization of waste marble dust as cement and sand replacement in concrete," Discover Civil Engineering, vol. 1, no. 1, p. 15, May 2024, doi: 10.1007/s44290-024-00014-w.

[49] S. Parmar and S. K. Das, "Effect of marble slurry as a partial substitution of ordinary Portland cement in lean concrete mixes," Structural Concrete, vol. 22, no. S1, Jan. 2021, doi: 10.1002/suco.202000059.

[50] M. Meera and S. Gupta, "Performance evaluation of marble powder and fly ash concrete for non-structural applications," Journal of Building Engineering, vol. 84, p. 108499, May 2024, doi: 10.1016/j.jobe.2024.108499.

[51] E. Kuoribo and H. Mahmoud, "Utilisation of waste marble dust in concrete production: A scientometric review and future research directions," Journal of Cleaner Production, vol. 374, p. 133872, Nov. 2022, doi: 10.1016/j.jclepro.2022.133872.

[52] A. Sahoo and P. K. Parhi, "Experimental Investigation of Mechanical and Durability Properties of Recycled Aggregate Concrete Added with Marble Powder, Copper Slag, and Polypropylene Fibre," AMC Indian Journal of Civil Engineering, vol. 6, no. 2, p. 7, Dec. 2023, doi: 10.17010/ijce/2023/v6i2/173475.

[53] K. Thangamani, N. N. Kumar, and T. S. R. Babu, "Experimental study on partial replacement of cement with using marble powder and coarse aggregate with demolished waste," presented at the 8th Annual International Seminar On Trends in Science and Science Education (AISTSSE), Medan, Indonesia, 2022, p. 020032. doi: 10.1063/5.0114525.

[54] A. F. Omran, E. D.-Morin, D. Harbec, and A. Tagnit-Hamou, "Long-term performance of glass-powder concrete in large-scale field applications," Construction and Building Materials, vol. 135, pp. 43–58, Mar. 2017, doi: 10.1016/j.conbuildmat.2016.12.218.

[55] Y. Abbas, R. Djebien, and N. T. Seghir, "Utilization of marble waste as fine aggregate in the composition of high performance concrete containing mineral additions," Canadian Journal of Civil Engineering, p. cjce-2024-0113, Jul. 2024, doi: 10.1139/cjce-2024-0113.

[56] O. Benjeddou, R. Alyousef, C. Soussi, M. Khadimallah, H. Alabduljabbar and M. Tahir "Utilisation of waste marble powder as low-cost cementing materials in the production of mortar," Journal of Building Engineering, vol. 32, p. 101642, Nov. 2020, doi: 10.1016/j.jobe.2020.101642.

Environ Res Tec, Vol. 8, Issue. 2, pp. 487-498, June 2025

Environmental Research and Technology
https://dergipark.org.tr/en/pub/ert
DOI: https://10.35208/ert.1521758

Review Article

Enhancement of biogas production by means of ultrasonic pre-treatment: State of art and review

Rana KIDAK[1]*

[1]*Cyprus International University, Faculty of Engineering, Department of Environmental Engineering, Mersin 10, Turkiye*

ARTICLE INFO

Article history
Received: 25 Jul 2024
Revised: 09 Sep 2024
Accepted: 24 Sep 2024

Key words:
Biogas; ultrasound pretreatment; substrates

ABSTRACT

Currently, fossil fuels are being used in an aberrant manner and greenhouse gases are negatively impacting the environment, causing research into renewable energy sources to be pioneered. As highlighted by the International Treaty called the UN Framework Convention on Climate Change during the Conference of Parties (COP) meetings every year, the international community is striving to expedite worldwide climate action by reducing emissions, intensifying adaptation initiatives, and increasing the availability of suitable financial resources. Production of biogas is a way to help overcome these challenges by reducing wastage and preventing environmental damage. The anaerobic digestion technique faces some barriers like elongated reaction times, cost of heating or low biogas yields. Several techniques have been used to enhance the biogas yield. Among these techniques the use of ultrasound technology as a pretreatment in biogas production revolutionized the process with its widespread application, providing an environmentally friendly and low-cost alternative. This paper reviews research studies on ultrasonic pretreatment of several substrates categorized according to different sources, for biogas production and puts an effort to compare and advise various operation parameters. Low frequency ultrasound (10-50kHz) results in an increase between 15-800 % biogas production from several substrates, at varying operation periods of 2-300 minutes. The operators are advised to test different operation conditions to obtain the best yield in real case applications.

Cite this article as: Kıdak R. Enhancement of biogas production by means of ultrasonic pre-treatment: state of art and review. Environ Res Tec 2025;8(2) 487-498.

INTRODUCTION

Biogas is a mixture of gases, primarily consisting of CH_4 (50-60%), CO_2, (40-50%), and the trace of other gases such as H_2S_2, O_2, and H_2 [1,2]. It is produced from materials such as livestock/agricultural waste, industrial, institutional and commercial waste, waste-activated sludge from wastewater treatment plants, landfill leachate and algae. It is a renewable energy source because the "production- and- use cycle is continuous". From a carbon standpoint, the growth of the primary bio-resource absorbs an equal amount of carbon dioxide from the atmosphere as it emits when it is eventually transformed into energy.

Typically, biogas is generated by the anaerobic digestion of biodegradable organic waste either at landfill sites or in specially-designed reactors [2]. In an anaerobic digestion process, microbial fermentation of the organic residual occurs in the absence of oxygen, as a result the mixture of gases is produced [1]. This process is a complex biological process that includes many consecutive steps of conversion and biodegradation of the organic waste namely hydrolysis, acidogenesis, acetogenesis and methanogenesis [3]. If we analyze each stage, hydrolysis emerges as the initial step in which extracellular enzymes facilitate the conversion of complex organic polymers and lipids into essential building blocks such as fatty acids, monosaccharides, amino acids,

***Corresponding author.**
*E-mail address: rkidak@ciu.edu.tr

This is an open access article under the CC BY-NC license (http://creativecommons.org/licenses/by-nc/4.0/).

and other related compounds. These transformed substances serve as a valuable energy source and contribute to the formation of cellular tissues [4]. During acidogenesis, fermentative bacteria break down soluble organic monomers of sugars and amino acids, resulting in the production of volatile fatty acids such as propionic, butyric, and valeric acids. Additionally, acetate (CH_3COO^-), H_2, and CO_2 are generated. The degradation of amino acids in this process also leads to the production of ammonia (NH3) [5]. In the acetogenesis step, both long-chain fatty acids and volatile fatty acids are destroyed, resulting in the production of acetate, carbon dioxide, and water [6]. Methanogenesis is the last step, and it involves bacteria breaking down the hydrogen and acetic acid to methane gas and carbon dioxide. The bacteria that cause this conversion are called methanogenic because they are strict anaerobes [7].

The hydrolysis step serves as the rate-limiting step, wherein hydrolytic enzymes secreted by specific groups of bacteria break down complex organic compounds (such as carbohydrates, proteins, and fats) into their respective constituent monomers. These monomers are molecules that are more soluble and can be easily transported through the cell membrane. There are several methods to enhance the rate of hydrolysis and ultrasonic pre-treatment has become one of the most popular methods among them.

The principle behind sonication of heterogeneous reactions lies in the disruption of the solids, caused by the jetting phenomenon resulting from the collapse of cavitation bubbles. It is worth mentioning that numerous similar effects can be observed when the heterogeneous medium is exposed to low frequency or power ultrasound (US) within the 20–100 kHz range. [8]. The impact of ultrasonic phenomenon on the fluid can be expressed as follows:

• Compounds are physically destroyed due to the presence of very high hydrodynamic shear stress [9].

• Chemical reactions are advanced as a result of high stress and extremely high local heating, reaching temperatures of nearly 5000 °C [10].

In particular, when low frequency ultrasound is applied to organic-rich samples, it enhances the ratio of Soluble COD/Total COD (SCOD/TCOD) by converting particulate matter into soluble COD. Another phenomenon that occurs during ultrasonic irradiation is the formation of acoustic flow. This acoustic flow is generated at the interface between a solid and a liquid when the solid interface vibrates with regular oscillations. The main advantage of acoustic flow is its ability to effectively mix substances in an aquatic environment, ensuring that ultrasonic energy is evenly distributed throughout the entire volume of a heterogeneous medium. Additionally, it facilitates the rapid distribution of heat. [11].

Ultrasound helps to break the large compounds into more biodegradable forms via the physical effects mentioned above. In this way, both the particle sizes and the biodegradability properties of the substrate are changed and the time for hydrolysis is reduced. Therefore, this review paper aims to recover a broad range of scientific enhanced work on the production of biogas through ultrasound pretreatment. Many researchers working on this subject, have created a rich content for the scientific literature by using different measurement parameters and examining different environmental factors. A large number of studies were examined in order to see the similarities and differences by bringing these studies together.

For ease of assessment, the research has been categorized according to the raw material (substrate) content as below:

1.Livestock/agriculture waste

2.Activated sludge from wastewater treatment plants

3.Industrial, institutional and commercial waste (including food waste)

4.Algae

5.Landfill leachate

Each category has unique specifications and the concluded enhancements will be considered specifically for each of them, as well as the final conclusion of comparison among all raw materials. Some studies fall into mixed categories of substrate, however they are mentioned when evaluated in the text when considering them. Several other environmental factors effecting the biogas production such as temperature, reaction retention time, concentration of initial substrate etc. have been referred to, while perusing the ultrasonic contribution to the process. The energy balance of ultrasonic pretreatment is determined by the surplus energy generated after pretreatment, subtracted by the energy consumed during the pretreatment process. This balance is greatly influenced by the concentration of Total Solids (TS) in the substrate. Too high concentrations can produce adverse effects on sludge rheology and transportability as well as on possible inhibitor concentrations, while too dilute substrates can absorb the energy in the liquid portion of the liquor. It is obvious that for each substrate, the optimum conditions must be examined with great care, to produce highest possible energy potential.

This paper reviews research studies on ultrasonic pretreatment of several substrates categorized according to different sources, for biogas production and puts an effort to compare and advise various operation parameters for the enhancement of biogas production.

REVIEWED PAPERS ACCORDING TO SUBSTRATE CATEGORIES

Livestock/agriculture waste

This category defines the wastes produced in the farm/agricultural facilities (i.e., manure, crop residues, husks, agricultural production residues etc.). Improperly managed livestock wastes can lead to fecal contamination of waters receiving agricultural runoff. Livestock waste poses a significant threat as it emits noxious gases, harmful pathogens, and unpleasant odors. Consequently, it raises concerns for both public health and the environment. Therefore, it is crucial to

effectively manage livestock waste to reduce the production of these pollutants and safeguard the environment. One effective approach is to properly utilize livestock waste in the production of biogas and compost, which can greatly enhance crop yield and promote sustainability.

Castrillón et al. [12] studied the influences of fragmentation of substrate on biogas production in the presence of ultrasound waves as a pretreatment method under mesophilic and thermophilic conditions using the batch reactor. The cattle manure was either screened or ground. Several experimental parameters were investigated. The results showed limited effect of sonication time, however, the higher solubilization ratios were obtained using higher ultrasonic energy. Regarding the biogas production and methane content, the best result was obtained at 35^0C for the sonicated mixture of screened manure with "365.4 L biogas/kg COD" with a methane content of around 60% (v/v). However, high temperature of 55^0C produced a high percentage of gases of 581.6 L biogas/kg COD from a mixture of sonicated grounded manure with the same methane content.

Braeutigam et al. [13] reported the impact of sonication time (1-2 min), amplitude (63, 94, and 125 ⊔m) and consumed energy on biogas yield from biological waste material (5% chicken manure), at room temperature of 25^0C using frequency at 24kHz with 200W. The better outcomes were obtained at 2 min of reaction time with an amplitude of 94 ^{0}m leading to an increase in biogas yield to 41% with respect to the non-sonicated sample. However, an intensive energy input could result in acidification, which causes less methane production. Therefore, low amplitudes and high reaction times, or vice versa, could yield the best outcomes. Moreover, the generated energy was higher than the consumed energy for disintegration by 36.6% per kg of chicken manure (2.72 kWh/kg substrate). The correlation of the biogas yield with soluble chemical oxygen demand (SCOD) and particle size was also investigated and the results showed that a linear relationship was observed for both SCOD increase and particle size reduction. The biogas yield was measured as 393 L/kg VS.

Zieliński et al. [14] carried out an experiment on ultrasonic pretreatment and hydrodynamic cavitation pretreatment to improve the production of biogas from dairy cattle manure mixed with wheat straw residues in a small-scale agricultural biogas plant. The energy balance with or without substrate pretreatment was analyzed. The small-scale plant was designed to include a special cavitation chamber and contained 60 transducers each with 10 kW power. Ultrasonic pretreatment and hydrodynamic cavitation pretreatment were found to significantly improve the production of biogas to 430 and 460L/kg VS, with a value greater than the other researchers working on agricultural substrates. Therefore, this study implies that cavitational operations were efficient for agriculture residues pretreatment.

You, Z. et al. [15] carried an experiment for the production of biogas through the enhancement of the fermentation of corn stover using pretreatment of sodium hydroxide in the company of additive calcium oxide together with 40 kHz US (150 W). Sodium hydroxide is a costly technique applied at high temperature and long retention time (a few days) for lignin dissolution. Addition of calcium oxide along with US method decreased the cost of pretreatment of sodium hydroxide on corn stover at low temperature considering low time treatment (30 min). The result implies that the process of the pretreatment was able to intensify the transformation of lignin to about 60%, promoting production of biogas to 500 mL/g TS. Benefit to cost ratio was determined through a method related to the process and the pretreatment came about an increase in the ratio from 1.40 to 1.65, indicating a cost effective technique.

Similar to You, Z et al. [16], Dong et al. [17], also carried out a research about improvement of the production of biogas from the corn stalk by dual US frequency (20 kHz and 57 kHz) in the company of alkaline pretreatment. However, the study documented the procedure and highlighted that the stimulation program demonstrated the superiority of energy over frequency. The corn stalk underwent anaerobic fermentation for a duration of 53 days after being pretreated with dual-frequency US and alkali. The findings revealed that the dual frequency process resulted in a cumulative biogas yield that was respectively 11.1%, 28.2%, and 56.6% higher than that of single-frequency US combined with alkali pretreatment, alkali pretreatment alone, and no pretreatment. The simulation program also attributed this outcome to the larger radius of the cavitation bubble in the case of dual frequency.

Zou, S. et al. [18] carried out research in anaerobic co-digestion of dairy manure and maize straw for biogas production at various ratios, through ultrasonic pretreatment. 50 kHz, 250 W US was applied on the dairy manure and maize straw separately and in combination at certain time intervals and power intensities. The authors have implied that ultrasonic pretreatment improved biogas production via changes in surface structures before and during anaerobic digestion process. Scanning electron microscope was used to detect the surface structure changes. The highest biogas produced of co digestion obtained was (240.32mL/gVS) when the dairy manure was pretreated for 30 min. However, the operation was affected by some other factors such as pH, reducing sugar, cellulosic activity at numerous stages digestion, as well.

Amirante, R. et al. [19] studied the biogas production from a 3-phase of olive pomace with and without ultrasonic pretreatment. The olive pomace produced in an olive oil mill in the southern regions of Italy was observed during anaerobic digestion for 43 days. During the pre-treatment, a frequency of 37 kHz and an installed power of 256 W were utilized to apply low-frequency and high-power US. The duration of this application was 1.88 minutes, aiming to achieve a specific energy range of 15-18 kJ/kg. It was crucial to prevent the destruction of bacterial flora. Consequently, the thermal conditions of the ultrasonic process were continuously monitored using an infrared thermometer throughout the experiments. The observations have proved an increase of 45% in biogas volume caused by the ultrasonic addition. In the same paper effect of nanoparticles, the addition was also investi-

gated and the authors found that nanoparticles showed positive effects for the first week of the process but after 23 days the effect was negligible.

The research conducted by Azman S. et al. [20] focused on exploring the potential of using US disintegration as a strategy for treating manure digestate. Digestate treatment involves the application of physical, chemical, or biological methods to treat and recycle the effluents in anaerobic digesters. This process aims to enhance the utilization potential of the digester by providing supplementary feed for energy conversion. The study found that applying 20 kHz US with a specific energy input of 1500 kJ/kg TS for a duration of 30 days significantly improved the efficiency of biogas production compared to the system without US assistance. On the other hand, the continuous process set-up had a negative energy balance due to the high energy requirements of the US digester, so the operation was not sustainable at all.

A recent study by Bianco F.et al. [21] showed that biogas production from Hazelnut Shells was improved by 2.3 folds after pretreatment by 20 kHz, 200 W ultrasound system for 10 minutes in combination with hydrothermal treatment (HT). The optimum solid to liquid ratio was 1:10 (w:w), resulting in the highest COD solubilization (9526 mg/L) at 100oC at the end of 16 days of anaerobic digestion (AD). Authors have declared production of 137 mL CH_4 per g VS under the optimized US+HT+AD conditions, which is a high value for a waste of high cellulose and lignin content.

Industrial, institutional and commercial waste

This category includes organic wastes that can be used for biogas production from households, institutions and industries. In this category food wastes, municipal solid wastes, and residues of institutional and production activities can be considered.

In the research conducted by Cesaro et al. [22], the effects of sonication were investigated on both municipal solid wastes and a combination of solid waste and sewage sludge. The experiments were conducted using different sonication durations (30 and 60 minutes) and various ultrasonic densities (0.1, 0.2, and 0.4 W/mL). To ensure comparability, the total solid percentage was maintained below 10% for all tests. Notably, a significant improvement of 60% in SCOD (Soluble Chemical Oxygen Demand) was observed when sonication was performed for 60 minutes with an ultrasonic density of 0.4 W/mL. Additionally, after a period of 32 days, the biogas production from the sonicated mixture was found to be 24% higher compared to the untreated mixture. Furthermore, comprehensive analysis of full-scale studies revealed that utilizing 1 kW of ultrasonic energy for sludge pretreatment resulted in the generation of approximately 7 kW of electrical energy after accounting for losses. The system was highly energy efficient.

Joshi & Gogate [23] examined the use of the 20 kHz US for the pretreatment of food waste from a university canteen. The results showed that biogas production increased twice as much in the US-supported system as without it. After 15 days 80% COD removal was recorded at the optimum conditions of 200W and 10 min, while the anaerobic digestion process without the US obtained 10% COD removal at the same conditions. As the applied power increased, biogas production increased and reached its highest point at 14800 mg/L at 0.04 W/mL power density. The authors have suggested that, due to an increase in the cell wall porosity by the US irritation, more amount of nutrients can be transferred from fermentation media to microbial cells, promoting the production of biogas.

In their research, Zeynali et al. [24] investigated the effectiveness of ultrasonic pre-treatment in improving the production of biogas from waste generated by the fruits and vegetable wholesale market. The substrate was subjected to three different sonication times (9, 18, 27 min) at a frequency of 20 kHz and an amplitude of 80 μm. The results showed that the highest methane yield was achieved with 18 minutes of sonication, while longer exposure to sonication resulted in a decrease in methane yield. This biogas production was achieved within a batch time of 12 days. Furthermore, the energy content of the biogas obtained from this reactor was twice the amount of energy input required for sonication.

Martinez-Jimenez et al. [25] conducted a study to assess the effectiveness of ultrasonic (US) treatment on the anaerobic co-digestion of sugarcane straw and vinasse substrates under thermophilic conditions (55°C) in a semi-continuous process. Vinasse is a residual liquid that remains after the fermentation and distillation of alcoholic liquors, while biohythane is a mixture of H2 (5–20%) and CH4 (80–95%). The researchers evaluated two different US pretreatments: one with 180 W of ultrasonic power irradiated at 37 kHz for 30 minutes, and the other with 800 W of ultrasonic power irradiated at 19 kHz for 15 minutes. They observed significant differences in the composition of biogas produced by the two pretreatments. Over a period of 42 days of hydraulic retention time, the methane concentration in the biohythane consistently increased in the first setup.

Rasapoor et al. [26] performed a study focusing on the on the solid concentration of organic fraction of municipal solid waste (4–10 %), different ultrasonic power intensities and time intervals. The outcome insinuated (p less than 0.01) strong effects sonication of time and power density on the final production of biogas after seventy-two hours' digestion. The applied US was 20 kHz and 400W. In conclusion the study implies that the specific input energy between 5000 and 10,000 kJ/kg TS, the optimum power intensity of 52 W/mL will effectively increase the production of biogas for 6% in 30 min. The final biogas production after US pretreatment reached as high as 440 mL/g VS after 25 days of digestion, which was 24% higher than plain operation.

In some studies, hydrogen gas production was observed instead of biogas or methane. Gadhe et al. [27] examined biohydrogen production from food waste. The substrate of organic complex was characterized by TCOD, SCOD, TS, and VS equivalent to 98600, 52900, 72500 and 51106 mg/L, respectively, while the US power and frequency for this study were equivalent to 1200W, 20 kHz. The ultrasonic pretreatment efficiency was evaluated in terms of improvement in

rate and hydrogen yield. The response surface methodology results demonstrated that when TS content and ultrasonic time were increased, so did the hydrogen yield. The ideal conditions were as follows: with TS 8% and sonication time 12 min., the best hydrogen yield was 149mL/g VS (corresponding to 1500 mL biogas/g VS approximately) and the rate was 5.23mL/h, with 104% increase compared to initial conditions.

The effectiveness of US (in combination with other pretreatment methods) on food residues, such as hazelnut skin, almond shell, and spent coffee grounds, was investigated by Oliva et al. [28] to determine their potential in terms of methane production and polyphenol and sugar solubilization using 35 kHz, 200W, at ambient temperature and 80 ^{0}C, in aqueous and methlyalcohol medium. The authors did not observe the COD or TS variations during the process, but the structural sugars and the lignins were recorded throughout the study. The results showed that the water-based liquors exhibited a higher methane potential than the MeOH-based liquors, achieving maximal 255.4 (±7.4) and 366.2 (±4.2) mL CH4/g VS, respectively. Although, the highest polyphenols and sugar solubilization were obtained in the MeOH-based medium, due to the inhibition effect of MeOH in anaerobic digestion process, it resulted in low methane potential.

In India, Deepanraj et al. [29] examined the effect of three pretreatment methods (autoclave, microwave and ultrasonication) on the food waste and poultry manure. The results revealed that, better degradation efficiency (of VS and COD) and biogas yield were achieved by ultrasonication compared to others. So, the highest total biogas yield was obtained with the ultrasonication technique of 9926 mL using 20 kHz and 130 W power for 30 min. The initial VS was 41.96 mg/L. Biogas produced from ultrasonically-treated samples contained 62.47% methane and 35.07 % carbon dioxide. The ratio is an indication of high quality biogas production.

Buller et al. [30] investigated the ultrasonication of brewer's spent grains as a pretreatment prior to anaerobic digestion using 19 kHz, 800W US. The results revealed that the US pretreatment increased the production of biomethane from 29% to 56% compared to the unpretreated condition. Also, the pre-treated system showed higher potential in energy recovery pathways, including electrical energy and thermal energy, with 0.23 MWh/t and 1200 MJ/t, respectively, whereas system without pretreatment generating 0.15 MWh /t electrical energy and 790 MJ/t thermal energy. Further, pre-treatment with US reduces Green House Gas (GHG) emissions by up to 80% compared to anaerobic digestion alone.

Waste Sludge

Waste activated sludge (WAS) is a polluting waste that has significant negative impacts on the environment and must be managed in a manner that prevents pollution and health problems. To treat this waste, the sludge obtained from primary and secondary water treatment is collected and subjected to anaerobic digestion. Prior to being introduced into the digesters, the sludge is occasionally screened and then concentrated to achieve a dry solids content of up to 7%. This is done to prevent excessive energy consumption for heating, which would occur if the sludge had a high water content. Additionally, this sludge has the potential to produce biogas and can also be utilized as a soil stabilizer through compost generation.

Elalami et al. [31] carried out a review on a number of studies about the production of biogas through pretreatment and co-digestion of wastewater sludge. They indicated that while co-digestion aims at enhancing methane production by adjusting several factors such as pH, moisture, the C/N ratio and nutrient availability, the efficiency is not guaranteed. The feasibility should be managed in detail about the techno-economic, out turn of the pretreatment on the sludge properties in the physical, chemical together with the digestant standard. Hence, it is very vital to make sure that the process is sustainable in fields of the legislatives as well socio environmental.

In one of the earliest studies, Tiehm et al. [32] used ultrasonic disintegration as a pretreatment for waste activated sludge with SCOD of 240 -622mg/L. The range of the ultrasonic frequency was 41-3217 kHz, with 30 – 150min application of 45 W power. Large cavitation bubbles are produced by low frequency US and when they collapse, they start strong jet streams that impose substantial shear stresses in the liquid while the smaller cavitation which prevents the beginning of strong shear forces, is thought to be the cause of the declining sludge disintegration efficiency seen at higher frequencies. Sludge floc deagglomeration was achieved with short sonication times without destruction of bacteria cells. The waste activated sludge's anaerobic digestion was substantially improved. Along with a rise in the breakdown of volatile solids (VS degraded 27.3 – 33.7%), a rise in biogas generation was observed, but the authors did not focus on this theme.

Lizama et al. [33] studied the biochemical methane potential of WAS through co-operation of US and anaerobic digestion with specific energy input, frequency and supplied US power, 5000- 35000 kJ/kg TS, 20kHz and 750 W, respectively. The authors found that the solubilization of SCOD increased from 888 to 12970 mg/L, when the energy applied changed from 15000 to 35000 kJ/kg TS. Consequently, the accumulative biogas production raised up from 501mL/gVS to 658 mL/gVS at the same level of applied energy. This corresponded to 31.43% increment in biogas yield.

Gallipoli et al. [34] carried out an experiment on the 200 kHz sonochemical breakdown of organic pollutants in secondary sludge sampled from the recycle stream before secondary clarifier in a domestic wastewater treatment plant. The sludge was gravity thickened for 24 h at 4 °C up to a total solids concentration of 21–24 g/L. The corresponding VS was about 12-14 g/L. The 90-100 W US application provided more readily biodegradable COD to the system while extra inoculum was added to the system to enhance the anaerobic digestion for biogas production. Authors have concluded that the sonication indicated better performance for VS removal at higher Substrate/Inoculum ratios, with an optimum of 0.9.

Riau et al. [35] carried out an experiment on biochemical methane potential in order to determine how ultrasonic pretreatment would affect the Temperature Phased Anaerobic Digestion of waste activated sludge. The initial characteristics of sludge were as flows: COD= 19.0 g/L, TS= 47.8 g/kg, VS= 41.0 g/kg. The ultrasonic parameters were as follows: Frequency= 24kHz, Power=400W, time= 5–30 min. The WAS was subjected to US before or after the thermophilic stage (specific energy 3380kj/ kg TS). The results revealed that US application before the thermophilic stage was more effective where total production of methane improved by more than 50% and the elimination VS increased by 13%.

Martin et al. [36] also studied waste sludge with an initial COD of 160 g/L, TS of 132 g/L with 88 g/L of VS. The researchers sonicated the raw sludge in an ultrasonic bath at 150W for 0-15-30-45 and 60 min. The sludge digestion system had its optimum organic loading rate values of up to 4.1 kg VS/m3·d providing an increase in methane yield coefficient from 88 to 172 mL /g VS (STP, 0 °C, 1 atm) after the ultrasonic pre-treatment, in 110 h hydraulic retention time.

Algae

Biogas can be produced from sustainable biomass, especially materials that are locally available. Several substrates are considered in this category including plants and algae, which is a quickly reproducing specie in natural environments. Plant cells are completely enclosed in cell membranes and one or two cell walls which depend on the plant type. The cell wall should be broken down to obtain a source for biogas production potential. There are various types of algae species present in the nature but their common property is that they are in vast amounts especially in polluted surface waters, due to eutrophication.

In a reviewed study carried out by Rodriguez et al. [37] algae were investigated. Different pretreatment methods were taken into consideration to disrupt the structure of algae, categorizing them into mechanical, microwave and US, biological, chemical, thermal, and combined groups. Pretreatment with low energy input had a low impact on the production of biogas and methane compared to pretreatments with high energy demand. This study implied that the main technique applicable to macroalgae was mechanical pretreatment because it causes the size of the particles to be reduced from the feedstock which enhances the availability of the substrate from the lignocellulose materials, while thermal pretreatment was for microalgae which had the highest production for methane increasing with lower energy required. Almost all the pretreatment methods had the disadvantage of high energy requirements (except for biological and chemical). In another study by Rodriguez et al. [1] grassland has been investigated because it received considerable attention in recent years as a source of bioenergy due to its less need for irrigation. For instance, in the United Kingdom, there are 55 biogas plants working with grass as feedstock from a total of 913. The grass contains different amounts of sugar and fiber depending on when it is harvested. As a result, biogas production from grass can be improved by 50% or more with most pretreatment techniques. Mechanical methods increase the improvement to about 60%. In regards to biological and chemical treatments, there is a need for new compounds and enzymes to be studied in order to increase the efficiency as well as toxicity reduction and pretreatment time shortening. Hence it is proposed that parameters for pretreatment should be taken into consideration, in order to obtain high production of biogas alongside a positive energy balance.

Microbial biomass, Scenedesmus, was subjected to US and thermal pretreatment methods using a batch system to improve its ability for biogas production as reported by González-Fernández et al. [38]. The US pretreatment experiment was operated at 20kHz with different energy levels at 35^0C for more than 30d. While thermal pretreatment experiments were carried out by pumping hot water into the reactor. Higher energy level values had a high impact on cell wall disruption. The thermally pretreated samples at 80^0C exhibited higher particle diameter (9.8 ⊔m) compared to the untreated sample (7.4 ⊔m). Additionally, SCOD increased 2.2- to 3.1-fold with increasing energy level. The methane production was much higher in sonicated samples (153 mL CH_4/g COD) than in the untreated sample of (81.8 mL CH_4/g COD) at 129 MJ/kg of specific energy level, but thermally treated biomass at 80 °C produced a lower amount.

Park et al. [39] carried out an investigation of the disruption and digestion of the single-cell microalgae (chlorella vulgaris) that grows in swine wastewater. The unicellular microalgae were cultivated following the disintegration of the cell wall of the chlorella vulgaris through the use of an ultrasonic homogenizer ranging from 5-200 J/mL. In a series of biochemical methane potential assays, it was found that the production of methane was limited from the batch anaerobic process due to the fact that the microalgae cell wall is very hard thereby causing high resistance to chemicals and enzymes. 20 kHz, 750 W US application showed higher soluble COD with higher energy applied. The cell disruption due to the application of US during batch digestion increased when compared to the untreated sample by 90% at 200J/ml of the energy. Addition of sludge increased the biogas production.

Lee et al. [40] did an experiment on the biomass of the filamentous algae through US pretreatment ranging from 10 – 5000J/mL (around 150W) for the enhancement production of biogas. When higher energy was applied, disruption of the cells increased, while the SCOD rose from 250 to 1000mg/L at 2500J/ml. The methane formation efficiency was improved by up to 2.3 times when the US changed the chemical composition and enhanced the substrate solubility.

El Nemr et al. [41] conducted a study in which they added sonication-modified sawdust-derived biochar into the biogas production system from the green algae Cheatomorpha Linum (C. Linum), either alone or in combination with another potential co-substrate. They discovered that the addition of biochar significantly increased biogas production. According to the results of the experiments, the best amount of biochar addition was 50.0 mg/L and increasing the amount resulted in a decrease in biogas production. With biochar, the biogas yield increased compared to the control sample which did not include the biochar, yielding 1059 and

629 mg/L VS, respectively.

Passos et al. [42] investigated the effect of US irradiation on algal solubilization, biodegradability, and methane output. US irradiation was used before the microalgae anaerobic digestion process to enhance the methane output at the specific energy range of 16-67 MJ/kg TS. A positive linear association was discovered between the applied specific energy and the methane output of microalgal biomass. The more the applied specific energy, the greater the methane output. Application of 20kHz, 70 W US increased the methane by 101%.

Cesaro et al. [43] carried out a research to evaluate how well solid organic substrates treated with US can improve anaerobic digestion yields for energy production. The substrate had TS 3.1% with VS 62.1%TS. US was applied at 20Khz, 1KW for 5-15 min, and it gave rise to the increment of production of biogas by 71% with ultrasonic energy inputs in the range of 31-93W h/L. For protein rich substrate, a smaller biogas increase in the range of 3-23% was discovered. The findings showed that the link between solubilization and anaerobic biodegradability varied greatly depending on the combination of US / anaerobic digestion process.

Alzate et al. [44] conducted research on the methane produced by microalgae, regarding the effects of biomass concentration, a substrate to inoculum ratio, and pretreatment (one being US). The authors did not give any detailed information about the frequency of the ultrasound but regardless of the microalgae studied, Substrate/Inoculum ratios between 0.5 and the microalgae concentration of 10 g TS/kg led to the highest ultimate methane productions ranging from 188 – 395mLCH4/gVS. The ultrasound pretreatment increased CH4 productivity by 6% - 24%, but no additional increases were seen at higher energy inputs. The outcomes obtained proved that thermal pretreatment is a better promising method than ultrasonic pretreatment for the generation of renewable energy.

A recent study by Roshni et al. [45] provided another point of view for anaerobic digestion of 2 species of algae. As SCOD efficiency it was observed that the two species had higher soluble COD at two different applied energies, where T. suecica had a SCOD efficiency of 5% at a specific energy of 10 MJ/kgTS, while N. oceanica had a SCOD efficiency of 18% at a specific energy of 27 MJ/kgTS. This could mean that with the increased SCOD efficiency, the cell wall was ruptured, and cellular material was released. However, from an AD perspective, for our study results, it could also mean that ultrasound energy was insufficient to achieve adequate cell disruption for increased specific methane production or that it resulted in the release of material that are inhibitive for AD. Therefore, additional pre-treatment could be needed to allow better digestion of the cell wall residues.

Landfill Leachate

When the organic portion of domestic wastes are stored in the landfill, leachate occurs over time. It is a high organic matter and ammonium nitrogen strength wastewater formed as a result of percolation of rain water through landfills. It is possible to obtain biogas from leachate with high organic content. Landfills are generally designed with biogas facilities. If the landfill contains the organic part of the separated household waste, only, the organic load of the resulting leachate will be quite high and will have favorable conditions for biogas production.

A set of experiments were conducted in Burkina Faso by Nikiema et al. [46] to improve the production of biogas by combining bovine dung and leachate from municipal organic waste. The contents of VS in cow dung and leachate were 72.41 and 70.48%, respectively. The volatile Fatty Acids (VFA) to alkalinity ratio in the leachate from organic waste was high (>3600). Increase in the organic matter level, improved microbial development, and increased stability of anaerobic biomass. The biogas yield of 152mL/g VS was obtained in the combined system. Since leachate contains high organic load in liquid form, it provides great benefit in increasing the efficiency of the existing systems by enriching the content of the substrates used for biogas production.

In cases when the waste separation is not effective and the leachate has high particulate matter and non-biodegradable organics, further improvements may necessitate. Oz & Yarimtepe [47] reported that the ratio of SCOD/TCOD increased from 47% to 63% when the landfill leachate was sonicated at 600 W/L for 45 min., whereas the biogas production in the ultrasonically pretreated reactor increased by 40% (the contribution of methane production was about 60% of the total increase). The particulate COD was successfully transferred into soluble COD and the optimum conditions were as follows: reactor temperature 35 oC, the pH 7. Authors have concluded that integration of ultrasound pretreatment with anaerobic processes can be suitable to enhance anaerobic treatability of other complex industrial waste waters, as well as leachate.

Scientists investigate various analytical parameters such as COD or BOD5 to express the organic strength of the feedstocks. Effects of 20 kHz and 12 ⊔m ultrasonic waves were also investigated by Grosser, et al. [48], to find the optimum conditions for the improvement of biological landfill leachate treatment. Reaction time varied between 0.5 to 15 min., with an optimum of 3 min. The BOD5/COD ratio increased 2.7 times compared to that without ultrasound application. The practice of releasing landfill leachate into wastewater treatment plants (WWTP) is widely used in numerous countries as a means of managing leachate. According to the research conducted, subjecting landfill leachates to sonication resulted in a significant increase in leachate biodegradability (up to 270%—from 0.1 to 0.3) and a decrease in toxicity towards microorganisms present in the activated sludge. As a result, the initial conditioning of leachate not only improved the quality of sewage sludge but also enhanced the overall effectiveness of its treatment process.

Nazimudheen et al. [49] have found the following findings about ultrasonic pretreatment of leachate: Leachate properties are influenced by both physical and chemical effects of sonication. Pretreatment with low power US was more suitable for anaerobic digestion. Oxidizing radicals generated in high power US treatment degrade organic matter.

Kwarciak-Kozłowska et al. [50] conducted a study on the ultrasonic disintegration of leachate using a low-frequency ultrasonic field ranging from 10 to 50 kHz and an intensity exceeding 1 W/cm2. Following a 300-second ultrasonic pretreatment at an amplitude of 14 μm, an anaerobic granular sludge bed reactor was operated. The application of this pretreatment resulted in a 7% increase in COD removal efficiency compared to the fermentation of nonconditioned wastewater. Consequently, the COD removal efficiency reached 88.0%. Additionally, on the 8th day of the process, there was a 2.6% increase in biogas production, with the specific methane yield in sonicated leachate being 22% higher than that in non-conditioned leachate. Therefore, this study provided that ultrasonic irradiation has a positive effect on the hydrolysis phase of refractory compounds in leachate. Hence, in 8 days of digestion time, the efficiency of SCOD removal in the sonicated leachate increased to 88% from 81.1% in the non-sonicated leachate. This was accomplished at 14 μm with 22 kHz frequency and in 300 seconds.

RESULTS

It had been concluded that the anaerobic digestion of the substrates with high organic content is a complex process which may be challenging to obtain high biogas yields. The researchers have added auxiliary techniques to their set-ups in order to find optimal solutions to overcome the challenges. Ultrasonic irradiation technique seems to be the most promising among the others. When the operational parameters in various papers were investigated, the organic contents of the substrates were expressed with various assay parameters such as COD, SCOD, TOC, TS, or VS. The summarized table below reveals the selected common operational parameters for biogas production set-ups. The papers reviewed here have investigated the topics from different aspects. In order to increase the comprehensibility of the table, the operating parameters given with different units have been converted into common units using the data in the papers. The most important operating parameters were categorized as those related to US and those to biogas production. The substrate with the lowest initial organic content was the algae with 55-250 mg/L COD. The authors have preferred to use this bio-source together with WAS because the two substrates supported the enrichment of the nutrient content for microorganisms with high Carbon from the sludge and high Nitrogen and Phosphorus from the algae. The biogas formation was limited to 326 L/kg VS (with 230 % increase by US irradiation). On the other hand, the complex food waste had reached 1500 L of biogas production per kg of VS, with 75% increase by US irradiation. The initial COD was around 100000 mg/L. Regarding the research papers, the indicated process parameters and the resultant finding were in diverse units and it was quite difficult to compare the various techniques with each other. Table 1 shows the gathered data together and the unit conversions to bring them at a base of common understanding.

The researchers had different set-ups for anaerobic digestion and the hydraulic retention time changed between 4 to 50 days. US practice mostly induces positive improvements in biogas production. Regarding diverse applications, the main findings were summarized below:

1-Increase in the applied US energy causes high COD solubilization.

2-Sonication time is effective in a limited way.

3-Probe type of sonicators are much more efficient in shorter time (30 sec. – 5min.) than ultrasonic baths (1 h.) and the provided energy is comparatively lower for the first one.

4-US creates changes in the rheology of the particulate portion of the substrates while solubilizing most of the substrates and leading to further biodegradation by anaerobic bacteria

5-The particle size of substrate is an important parameter; such that the screened substrate produces less biogas compared to ground substrate.

6-When the digestion temperature increases the biogas production efficiency is positively affected.

7-The pretreatment is preferable if the applied energy is not more than the potential energy of the biogas produced in the system.

Table 1. Summary of operational parameters from selected articles

	US Related Parameters				Substrate Related Parameters			Biogas Related Parameters			
Reference Paper	**Reaction Time (min)**	**Amplitude (μm)**	**Power (W)**	**Frequency (kHz)**	**TS mg/l**	**VS mg/L**	**COD mg/L**	**Retention Time (d)**	**Biogas Yield (l/kg VS)**	**Energy Content (kWh/kg VS)**	**% Increase before and after US**
Industrial, institutional and commercial waste (Food waste in this categories)											
Buller et al. [30]	15	_	800	19	41000	30170	_	50	48,9	0,31	27
Joshi & Gogate [23]	5	_	200	20	43000	27500	11500	15	_	_	100
Rasapoor et al. [26]	30	_	400	20	6000	5340	_	25	441	6000kJ/kg TS	24
Zeynali et al.[24]	18	80	100	20	18700*	14025*	_	12	396	_	80
Gadhe et al.[27]	30	_	1200	20	72500	51106	98600		1500	_	75
Deepanraj et al.[29]	30	_	130	20	75000	71340	69920	30	140*	_	15*
Landfill Leachate											
Oz & Yarimtepe[47]	45	_	600	20	2300	_	28500	4	477	_	40
Kwarciak-Kozłowska, et al (2005) [50]	300	14	1W/cm2	10-50	_	_	_	8	_	_	22
Algae											
Lee et al.[40]	30	_	150	20	10000	87000	250	10	326,2	50J/mL	230
Park et al.[39]		_	150	20	_	49,1	55	25	366	_	65,1
Activated Sludge from wastewater treatment plant											
Lizama et al.[33]	33	_	750	20	_	_	46433	50	658	35000 kJ/kg TS	31.4
Gallipoli [34]	40	_	100	200	21300	12500	_	20	140	_	40
Livestock/Agricultural waste											
Braeutigam [13]	**2**	**125**	**200**	**24**	_	_	**14550**	_	**393**	_	**41**
Dong [17]	**30**	_	**150**	**40**	**49500***	**46150***		**53**	**1000**	_	**56,6**
(Castrillón et al.[12] for Screened manure	**4**	_	**100**	**20**	_	**35000**	**45000**	_	**298.7**	_	**121**
(Castrillón et al.[12] for ground manure	**4**	_	**100**	**20**	_	**35000**	**45000**	_	**291.6**	_	**800 (w/glyc)**

*The numbers are re-calculated using the data given in the text in order to have comparable values with the rest of the table

CONCLUSION

The increasing concern for the environment has led to the widespread adoption of biogas as an alternative energy source. Biogas, being renewable and clean, offers an effective solution to combat global warming. By reducing reliance on fossil fuels like oil and coal, it helps in mitigating the negative impact on the environment. The production process of biogas involves converting waste into valuable resources, namely biogas and organic fertilizers. These fertilizers are the solid byproduct obtained after the anaerobic digestion process.

The technology used to produce biogas is categorized as part of the circular economic system, which emphasizes the reuse and regeneration of materials or products. This approach ensures sustainable and environmentally friendly production methods.

Biogas plants can be utilized even in small-scale settings, such as farms, where the waste produced by livestock can be converted into biogas. Remarkably, the waste from a single cow can generate enough energy to power a lightbulb for an entire day. In larger plants, biogas can be compressed to match the quality of natural gas and used as a fuel for automobiles.

The improvement of biogas systems is archived by various pretreatment techniques and Power ultrasound (20-100kHz) is the best alternative because it is easy to use and energy efficient. Operators can produce up to 1500 L of biogas per kg of VS in the substrate if the digesters are operated efficiently with help of US pretreatment.

DATA AVAILABILITY STATEMENT

No data was used for the research described in the article.

CONFLICT OF INTEREST

The author declared no potential conflicts of interest with respect to the research, authorship, and/or publication of this article.

USE OF AI FOR WRITING ASSISTANCE

Not declared.

ETHICS

There are no ethical issues with the publication of this manuscript.

REFERENCES

[1] C. Rodriguez, A. Alaswad, K.Y. Benyounis, and A.G. Olabi, "Pretreatment techniques used in biogas production from grass," Renewable and Sustainable Energy Reviews, Vol. 68, pp. 1193–1204, 2017.

[2] L. Lombardi, E. Carnevale, R. Baciocchi, and G. Costa, "Biogas Upgrading by a Combination of Innovative Treatments Based on Carbonation of Waste Incineration Residues," Waste and Biomass Valorization, Vol. 6, pp. 791–803, 2015.

[3] R. Chandra, H. Takeuchi, and T. Hasegawa, "Methane production from lignocellulosic agricultural crop wastes: A review in context to second generation of biofuel production," Renewable and Sustainable Energy Reviews, Vol. 16, pp. 1462–1476, 2012.

[4] W. Yan, L. Zhang, S.M. Wijaya, and Y. Zhou, "Unveiling the role of activated carbon on hydrolysis process in anaerobic digestion," Bioresource Technology, Vol. 296, pp. 1223-1266, 2020.

[5] M. Zhou, B. Yan, J.W.C. Wong, and Y. Zhang, "Enhanced Volatile fatty acids production from anaerobic fermentation of food waste: A mini-review focusing on acidogenic metabolic pathways," Bioresource Technology, Vo 248, pp. 68–78, 2018.

[6] H.N. Gavala, I. Angelidaki, and B.K. Ahring, "Kinetics and modeling of anaerobic digestion process," Advances in Biochemical Engineering / Biotechnologies, Vol. 81, pp. 57–93, 2003.

[7] Y. Li, Y. Chen, and J. Wu, "Enhancement of methane production in anaerobic digestion process: A review," Applied Energy, Vol. 240, pp. 120–137, 2019.

[8] B.G. Pollet. "Does power ultrasound affect heterogeneous electron transfer kinetics?," Ultrasonics Sonochemistry, Vol. 52, pp. 6–12, 2019.

[9] Z. Guo, R. Feng, Y. Zheng, and X. Fu, "Improvement in properties of coal water slurry by combined use of new additive and ultrasonic irradiation," Ultrasonics Sonochemistry, Vol. 14, pp. 583–588, 2007.

[10] N. Pokhrel, P.K. Vabbina, and N. Pala, "Sonochemistry: Science and Engineering," Ultrasonics Sonochemistry, Vol. 29, pp. 104–128, 2016.

[11] A. Ghadyani, M. Noaparast, and S.Z. Shafaei Tonkaboni, "A Study on the Effects of Ultrasonic Irradiation as Pretreatment Method on High-Ash Coal Flotation and Kinetics," International Journal of Coal Preparation and Utilization, Vol. 38, pp. 374–391, 2018.

[12] L. Castrillón, Y. Fernández-Nava, P. Ormaechea, and E. Marañón, "Optimization of biogas production from cattle manure by pre-treatment with ultrasound and co-digestion with crude glycerin," Bioresource Technology, Vol. 102, pp. 7845–7849, 2011.

[13] P. Braeutigam, M. Franke, and B. Ondruschka, "Effect of ultrasound amplitude and reaction time on the anaerobic fermentation of chicken manure for biogas production," Biomass & Bioenergy, Vol. 63, pp. 109–132014.

[14] M. Zieliński, M. Dębowski, M. Kisielewska, A. Nowicka, M. Rokicka, and K. Szwarc, "Cavitation-based pretreatment strategies to enhance biogas production in a small-scale agricultural biogas plant," Energy for Sustainable Development, Vol. 49, pp. 21–26, 2019.

[15] Z. You, S.Y. Pan, N. Sun, H. Kim, and P.C. Chiang,

"Enhanced corn-stover fermentation for biogas production by NaOH pretreatment with CaO additive and ultrasound," Journal of Clean. Production, Vol. 238, p. 117813, 2019.

[16] S. Hashemi, L.Solli, , K. M. Lien, J.J. Lamb, and S.J. Horn, "Culture adaptation for enhanced biogas production from birch wood applying stable carbon isotope analysis to monitor changes in the microbial community," Biotechnology for Biofuels and Bioproducts, Vol. 16, p. 77, 2023.

[17] C. Dong, J. Chen, R. Guan, X. Li, and Y. Xin, "Dual-frequency ultrasound combined with alkali pretreatment of corn stalk for enhanced biogas production," Renewable Energy, Vol. 127. Pp. 444–451, 2018.

[18] S. Zou, X. Wang, Y. Chen, H. Wan, and Y. Feng, "Enhancement of biogas production in anaerobic co-digestion by ultrasonic pretreatment," Energy Conversion and Management, Vol. 112, pp. 226–235, 2016.

[19] R. Amirante, G. Demastro, E. Distaso, M.A. Hassaan, A. Mormando, and A.M. Pantale, "Effects of Ultrasound and Green Synthesis ZnO Nanoparticles on Biogas Production from Olive Pomace," Energy Procedia, Vol. 148, pp. 940–947, 2018.

[20] S. Azman, H. Milh, M.H. Somers, H. Zhang, I. Huybrechts, and E. Meers, "Ultrasound-assisted digestate treatment of manure digestate for increased biogas production in small pilot scale anaerobic digesters," Renewable Energy, Vol. 152, pp. 664–673, 2020.

[21] F. Bianco, H. Senol, S. Papirio, H. Zenk, A. Kara, and S. Atasoy, "Combined ultrasonic–hydrothermal pretreatment to improve the biomethane potential of hazelnut shell," Biomass and Bioenergy, Vol. 165, p.106554, 2022.

[22] A. Cesaro, V. Naddeo, V. Amodio, and V. Belgiorno, "Enhanced biogas production from anaerobic codigestion of solid waste by sonolysis," Ultrasonics Sonochemistry, Vol. 19, pp. 596–600, 2012.

[23] S.M. Joshi, and P.R. Gogate, "Intensifying the biogas production from food waste using ultrasound: Understanding into effect of operating parameters," Ultrasonics Sonochemistry, Vol. 59, p. 104755, 2019.

[24] R. Zeynali, M. Khojastehpour, and M. Ebrahimi-Nik, "Effect of ultrasonic pre-treatment on biogas yield and specific energy in anaerobic digestion of fruit and vegetable wholesale market wastes," Sustainable Environment Research, Vol. 27, pp. 259–264, 2017.

[25] F.D. Martinez-Jimenez, M.P. Macie Pinto, A. Mudhoo, T. de Alencar Neves, M.A. Rostagno, and T. Forster-Carneiro, "Influence of ultrasound irradiation pre-treatment in biohythane generation from the thermophilic anaerobic co-digestion of sugar production residues," Journal of Environmental Chemical Engineering, Vol. 5, pp. 3749–58, 2017.

[26] M. Rasapoor, Y. Ajabshirchi, M. Adl, R. Abdi, and A. Gharibi, "The effect of ultrasonic pretreatment on biogas generation yield from organic fraction of municipal solid waste under medium solids concentration circumstance," Energy Conversion Management, Vol. 119, pp. 444–452, 2016.

[27] A. Gadhe, S.S. Sonawane, and M.N. Varma, "Ultrasonic pretreatment for an enhancement of biohydrogen production from complex food waste," International Journal of Hydrogen Energy, Vol. 39, pp. 7721–7729, 2014.

[28] A. Oliva, S. Papirio, G. Esposito, and P.N.L. Lens, "Ultrasounds application for nut and coffee wastes valorisation via biomolecules solubilisation and methane production," Waste Management, Vol. 150, pp. 373–382, 2022.

[29] B. Deepanraj, V. Sivasubramanian, and S. Jayaraj, "Effect of substrate pretreatment on biogas production through anaerobic digestion of food waste," International Journal of Hydrogen Energy, Vol. 42, pp. 26522–26528, 2017.

[30] L.S. Buller, W.G. Sganzerla, M.N. Lima, K.E. Muenchow, M.T. Timko, and T. Forster-Carneiro, "Ultrasonic pretreatment of brewers' spent grains for anaerobic digestion: Biogas production for a sustainable industrial development," Journal of Cleaner Production, Vol. 355, p. 131802, 2022.

[31] D. Elalami, H. Carrere, F. Monlau, K. Abdelouahdi, A. Oukarroum, and A. Barakat, "Pretreatment and co-digestion of wastewater sludge for biogas production: Recent research advances and trends," Renewable and Sustainable Energy Reviews, Vol. 114, p. 109287, 2019.

[32] A. Tiehm, K. Nickel, M. Zellhorn, U. Neis, and A. Tiehm, "Ultrasonic waste activated sludge disintegration for improving anaerobic stabilization," Water Resources, Vol. 35, pp. 2003–2009, 2001.

[33] A.C. Lizama, C.C. Figueiras, R.R. Herrera, A.Z. Pedreguera, and J.E. Ruiz Espinoza, "Effects of ultrasonic pretreatment on the solubilization and kinetic study of biogas production from anaerobic digestion of waste activated sludge," International Biodeterioration & Biodegradation, Vol. 123, 1–9, 2017.

[34] A Gallipoli, A Gianico, MC Gagliano, and CM Braguglia, "Potential of high-frequency ultrasounds to improve sludge anaerobic conversion and surfactants removal at different food/inoculum ratio," Bioresource Technology, Vol. 159, pp. 207–14, 2014.

[35] V. Riau, M.A. de la Rubia, and M. Pérez, "Upgrading the temperature-phased anaerobic digestion of waste activated sludge by ultrasonic pretreatment," Chemical Engineering Journal, Vol. 259, pp. 672–681, 2015.

[36] M.Á. Martín, I. González, A. Serrano, and J.Á. Siles, "Evaluation of the improvement of sonication pre-treatment in the anaerobic digestion of sewage sludge," Journal of Environmental Management, Vol. 147, pp. 330–337, 2015.

[37] C. Rodriguez, A. Alaswad, J. Mooney, T. Prescott, and A.G. Olabi, "Pre-treatment techniques used for anaerobic digestion of algae," Fuel Processing Tech-

nology, Vol. 138, pp. 765–779, 2015.

[38] C. González-Fernández, B. Sialve, N. Bernet, and J.P. Steyer, "Comparison of ultrasound and thermal pretreatment of Scenedesmus biomass on methane production," Bioresource Technology, Vol. 110, pp. 610–616, 2012.

[39] K.Y. Park, J. Kweon, P. Chantrasakdakul, K. Lee, and H.Y. Cha, "Anaerobic digestion of microalgal biomass with ultrasonic disintegration," International Biodeterioration & Biodegradation, Vol. 85, pp. 598–602, 2013.

[40] K. Lee, P. Chantrasakdakul, D. Kim, M. Kong, and K.Y. Park, "Ultrasound pretreatment of filamentous algal biomass for enhanced biogas production," Waste Management, Vol. 34, pp. 1035–40, 2014.

[41] A. el Nemr, M.A. Hassaan, M.R. Elkatory, S. Ragab, M.A. El-Nemr, and L.Tedone L, "Enhancement of biogas production from individually or co-digested green algae Cheatomorpha linum using ultrasound and ozonation treated biochar," Ultrasonics Sonochemistry, Vol. 90, p. 106197, 2022.

[42] F. Passos, S. Astals, and I. Ferrer, "Anaerobic digestion of microalgal biomass after ultrasound pretreatment," Waste Management, Vol. 34, pp. 2098–2103, 2014.

[43] A. Cesaro, S. Velten, V. Belgiorno, and K. Kuchta, "Enhanced anaerobic digestion by ultrasonic pretreatment of organic residues for energy production," Journal of Cleaner Production, Vol. 74, pp. 119–24, 2014.

[44] M.E. Alzate, R. Muñoz, F. Rogalla, F. Fdz-Polanco, and S.I. Pérez-Elvira, "Biochemical methane potential of microalgae: Influence of substrate to inoculum ratio, biomass concentration and pretreatment," Bioresource Technology, Vol. 123, pp. 488–494, 2012.

[45] R. Paul, A. Silkina , L. Melville, S. Suhartini, and M. Sulu, "Optimisation of Ultrasound Pretreatment of Microalgal Biomass for Effective Biogas Production through Anaerobic Digestion Process," Energies, Vol. 16, p. 553, 2023.

[46] M. Nikiema, N. Barsan, Y. Maiga, M.K. Somda, E. Mosnegutu, and C.A.T. Ouattara, "Optimization of Biogas Production from Sewage Sludge: Impact of Combination with Bovine Dung and Leachate from Municipal Organic Waste," Sustainability. Vol. 14, p.4380, 2022.

[47] N.A. Oz, and C.C. Yarimtepe, "Ultrasound assisted biogas production from landfill leachate," Waste Management, Vol. 34, pp. 1165–1170, 2014.

[48] A. Grosser, E. Neczaj, M. Madela, and P. Celary, "Ultrasound-assisted treatment of landfill leachate in a sequencing batch reactor," Water, Vol. 11(3), p.516, 2019.

[49] G. Nazimudheen, K. Roy, T. Sivasankar, and V.S. Moholkar, "Mechanistic investigations in ultrasonic pretreatment and anaerobic digestion of landfill leachates," Journal of Environmental Chemical Engineering, Vol.6, pp. 1690–1701, 2018.

[50] A. Kwarciak-Kozłowska, J. Bohdziewicz, E. Neczaj, and A. Kwarciak, "Influence of ultrasound field on landfill leachate treatment by means of anaerobic process," Environmetal. Protection Engineering, Vol. 31, pp. 61-71, 2005.

Environ Res Tec, Vol. 8, Issue. 2, pp. 499-522, June 2025

Environmental Research and Technology
https://dergipark.org.tr/en/pub/ert
DOI: https://10.35208/ert.1499952

Environmental Research & Technology

Review Article

Study of microplastic accumulation in halophyte plants and macroalgae: A critical review

Meita Eka FARA*[1,3], Muslim MUSLIM[2], Miftakul MUNIR[3]

[1]Diponegoro University, Marine Science Department, Semarang, Central Java 50275, Indonesia
[2]Diponegoro Üniversitesi, Oşinografi Bölümü, Semarang, Orta Java 50275, ENDONEZYA, muslim@lecturer.undip.ac.id
[3]Research Center for Radioisotope, Radiopharmaceutical, and Biodosimetry Technology, National Research and Innovation Agency, KST BJ Habibie, South Tangerang, Banten 15314, Indonesia

ARTICLE INFO

Article history
Received: 13 Jun 2024
Revised: 17 Sep 2024
Accepted: 25 Sep 2024

Key words:
Microplastic, salt-tolerant plant, accumulation

ABSTRACT

Marine litter and microplastic contamination are severe dangers to aquatic ecosystems. The interaction between halophyte plants and micro/nanoplastics has recently gained attention. Halophyte plants and maritime macroalgae are capable of trapping substantial volumes of marine debris, leading to areas of buildup, known as 'sinks', of anthropogenic particles. The review of existing studies exposes that halophyte plants can serve as sinks for micro-nano plastics by absorbing them on their surface. Moreover, these plastics can be absorbed by plants. Plastic on the surfaces and within plant tissue can cause various harmful effects. The present review highlights an understanding of microplastic abundance, bioavailability, influencing factors, technological detection, and potential salt-tolerant plants for bioremediation. According to these findings, we advocate the addition of microplastic on halophyte plants and algae in prospective monitoring studies, describe acceptable methodologies, and advise doing exposure studies alongside risk assessments, strategies for preventing and controlling policies of these underestimated pollutants in vegetated coastal ecosystems and establishes a basis for future research.

Cite this article as: Fara ME, Muslim M, Munir M. Study of microplastic accumulation in halophyte plants and macroalgae: A critical review. Environ Res Tec 2025;8(2) 499-522.

INTRODUCTION

Microplastic (MP) and nanoplastic (NP) are distributed in the environments worldwide. Plastics disintegrate slowly in natural ecosystems, therefore the accumulation of plastic contaminants has eventually become a concern [1]. Understanding the accumulation of plastic and its life cycle in the environment is crucial and requires frequent sampling over a long period [2]. Seeruttun et al. (2023) [3] estimated that the number of microplastics worldwide produced 350 tonnes in 2017, and approximately 4.8 to 12.7 million tonnes of various sizes entered the world's oceans and aquatic basins. Microplastics are numerous and likely irreversible repercussions of plastic pollution, including habitat disruption, harm to biota, and others [4]. Microplastic contaminant spans a family of contaminants, as plastic particles vary in chemical element, color, shape, size, and others [5]. The physicochemical characteristics of each plastic particle can be modified in various ways, driven by abiotic influences such as water salinity or UV light and biotic ones such as surface changes by microbes [6]. This weathering process might release plastic monomers and additives [6, 7]. Therefore, it is difficult to estimate the worldwide toxicity of microplastics and their compounds released into the environment [8].

Coastal ecosystems are unique and vital areas at the inter-

***Corresponding author.**
*E-mail address: meitafara.edu@gmail.com

This is an open access article under the CC BY-NC license (http://creativecommons.org/licenses/by-nc/4.0/).

section of marine and terrestrial processes [9], commonly known as mangroves, seagrasses, saltbush, saltmarsh, and macroalgae. Plants and algae represent 80% of Earth's total biomass, serving as a fundamental component in all ecosystems [10]. The accumulation of MPs can generate several complex harmful effects on plants, with the highest deposition in plant roots and germinating seed surfaces rather than being absorbed into the plants [11]. Plastic can accumulate in the environment for a long period, depending on its stability. Halophytes are plants that can survive and complete their biological cycles at salt concentrations above 100-200 mM NaCl without suffering significant negative impacts on their growth or development [12, 13, 14]. They could be a significant food source, particularly in coastal regions and areas with unfavorable environmental conditions [15]. Zhang et al. (2023) [16] demonstrated that halophytes accumulate sulfur, sodium, and chlorine during their growth period, indicating their ability to absorb various mineral nutrients selectively. Kiliç and Yücel (2024) [17] research has shown that MPs and macro-size plastics can be easily captured in invasive aquatic plants (Pontederia crassipes) due to their root structure. This may also contribute to their accumulation in halophyte tissues and trapping in algae.

Halophyte plants have shown potential as vegetation due to their ability to accumulate salts in their tissues, making them valuable plants for environmental management [18]. Such plants serve crucial functions in the carbon and oxygen cycles. They are essential pillars of the ecological balance, including climate regulation, preventing wind and sand erosion, soil and water conservation, and provisioning for biological habitats [1, 19]. The survival and vitality of halophyte plants serve as crucial bioindicators for assessing the overall health of aquatic ecosystems worldwide [20, 21]. Extensive MP research has been conducted in both marine and terrestrial environments. In recent years, the focus has mainly been on water, soil, air, animal, and terrestrial plants [22, 23, 24]. However, there needs to be more reviews on saltwater plants, making it essential to conduct a review on research concerning these plants. A review of the field's current situation is required. This paper analyzes relevant studies to discuss the following two aspects: the effects of MPs and NPs on halophyte plants and macroalgae and technologies for MPs detection in plants and algae. Furthermore, prospects for future study on this issue are presented for developing strategies to effectively manage and mitigate its effects and preserve these vital coastal ecosystems.

MATERIALS AND METHODS

The preliminary review of salt-tolerant plants and macroalgae included analyzing MPs articles published from 2014 to 2024 (Fig. 1a). Sixty-eight published articles on MP worldwide (Fig. 1b) were initially screened. All of the materials utilized here are from Internet databases. Multiple databases were used to discover relevant studies, examine data collected over a long period, and ensure that this evaluation appropriately reflects the most current advances in the field. Studies were found in the ScienceDirect, Scopus, PubMed, Springer, Nature, and MDPI databases. The keywords "microplastic", "plastic pollution", "marine litter", "accumulation", "microplastic analysis", "halophyte plant", and "algae" were used in the literature search. However, we independently screened microplastic-related research to ensure a complete literature collection because not all relevant literature can be retrieved using these words.

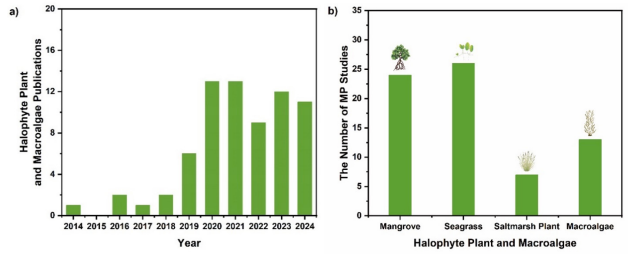


Figure 1. a) Publication trend on MP studies around 10 years; b) reviewed number of MP studies in saltwater plants and algae (retrieved on May 27th, 2024)

POTENTIAL SOURCE AND EXPOSURE ROUTES

Microplastic Distribution in Halophyte Plants and Macroalgae

Oceans are the ultimate sink for MPs, especially in the coastal environment, a habitat of salt-tolerant plants and macroalgae. In addition, the terrestrial ecosystem is a crucial recipient of plastics of any size. Due to the massive volume of anthropogenic waste [25], the terrestrial ecosystem is responsible for 80-90% of MPs in aquatic environments [26], maritime activities (marine aquaculture and ocean navigation) [27], tidal or wave action [28], airborne settlement [29, 30], and other sources such as atmospheric particulate deposition [31]. As mentioned earlier, salt-tolerant plants such as mangrove swamps, marshes, sloughs, and seashores are generally characterized by high biological productivity and organic matter levels. Therefore, MPs can be transported to these plants from multiple and complex sources. Compared to marine sources, terrestrial sources are estimated to contribute more significantly to the pollution of saltwater plants [32]. Generally, there are many sources of MPs. Fig. 2 mainly classified MP contamination pathways from land-into ocean-based sources in salt-tolerant plants.

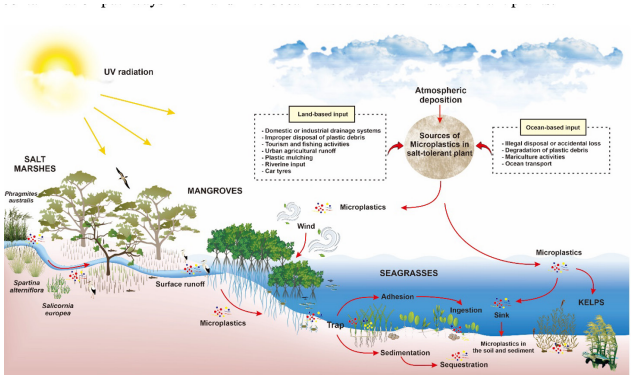


Figure 2. MPs contamination distribution pathway in the salt-tolerant plants and macroalgae

MPs enter the oceans through the breakdown of plastics, landfill leachates, illegal disposal or accidental loss, wastewater, sewage discharged into the atmosphere, agricultural runoff, tourism, fishing activity along the coast, and other sources propelled from beaches by winds and currents. As shown in Fig. 2, MPs are present in salt marshes, mangroves, seagrasses, and algae. They are also found in seawater, sediment, and land (including ice and freshwater) and are associated with various organisms. Several factors, including mechanical stress, washing, microbiological deterioration, and UV radiation damage, can produce microplastics [33]. Plastic debris is transported by rivers and lakes from far inland to the ocean, significantly contributing to ocean pollution. [34] calculated that between 0.8 to 2.7 million tons of riverine plastic are released into the ocean per year worldwide, with 1000 rivers being responsible for about 80% of these emissions. MPs in saltwater tend to collect slowly, primarily on coastlines with high human population density [35]. Ocean currents are essential for plastic waste's movement, dispersion, and accumulation [36]. Hydrodynamic parameters influencing MP transportation and sedimentation include turbulence, turbidity, current velocity, and residual circulation [37]. The distribution of MPs is also affected by their features, including particle size, surface alteration, and environmental circumstances such as pH, DOM, and light. However, quantifying these effects still needs to be expanded [38].

Uptake of Microplastics by Halophyte Plants

Bioaccumulation is the progressive increase in the concentration of a contaminant (compound) within an organism due to the uptake rate of the contaminant being more significant than its release [39]. The pattern of microplastic bioaccumulation is extensively studied across various trophic-level pyramids, especially in coastal and marine ecosystems [40]. Plastics form plastispheres that look similar to food sources for marine organisms. These plastisphere or aggregates form through microbial attachment, acting as a vector for the transportation of harmful bacterial species and phytoplankton on the plastic surface [41].

Plants primarily absorb both MPs and non-plastics through root hairs [42, 43]. In addition, some seedlings typically exhibit strong cell division and rapid nutrient translocation, enhancing the potential for nutrient and contaminant absorption. Due to their hydrophobic, dense, and high specific surface area properties, MPs easily adhere to root surfaces, subsequently absorbed and accumulated within plants, thereby affecting root metabolism [44]. Most studies on the impact of MPs on plants are conducted during the seedling stage with test particles on a submicron scale (<1 μm). Seedling roots can absorb small MPs (80 nm) and significantly inhibit plant growth and development [45, 46]. Larger particles can also accumulate in plant tissues, as demonstrated by [40]. The data summarized about methodology, study area, and MP features in Table 1 indicate MP contamination in 16 species of mangrove, 30 species of seagrass, five species of saltmarsh plant, and 25 species of macroalgae.

Particulate matter, including MP, must pass through various chemical and physiological barriers that determine the size exclusion limits (SELs) during plant absorption and translocation. The thickness and construction of these barriers vary depending on the species, growth stage, and environmental circumstances. Despite the modest SELs (<20 nm) of plant roots, it is widely acknowledged that plants can absorb very big nanoparticles (above 100 nm) [40]. MPs can penetrate the stele through epidermal gaps and then move to the plant's aboveground parts via the xylem through transpiration. During this process, the plant's transpiration force is critical to the absorption and transportation of microplastics. Another entry pathway is through the mode of crack entry, where the emergence of lateral roots on the primary root creates crack areas, and particles enter the circulation system through cellular gaps produced by the lateral root bulge area. Once entered into the vascular bundle, plants can absorb plastic particles from roots to stems through the vascular system and transpiration flow. Illustrations of the MPs entry process in plants are presented in Fig. 3.

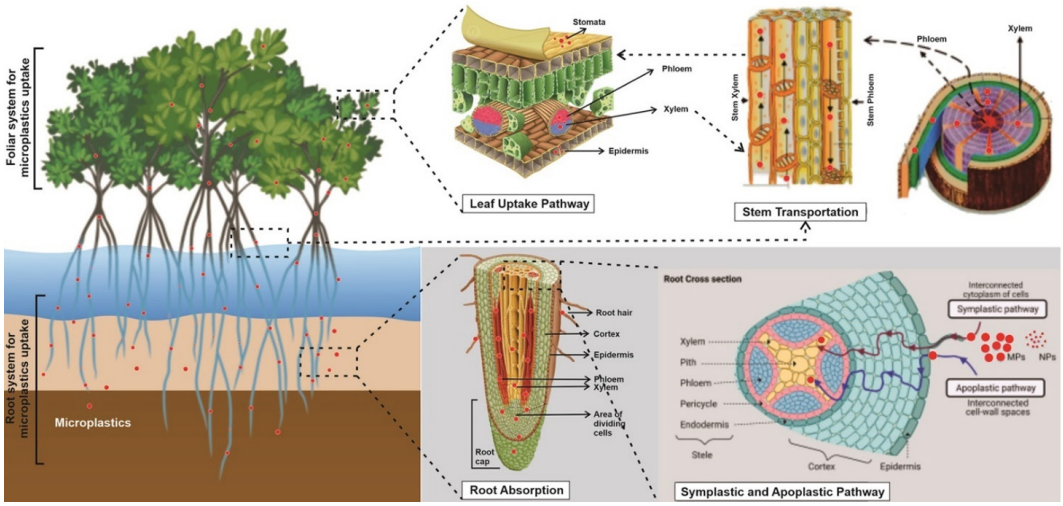


Figure 3. The uptake and movement of MPs in mangrove rhizospheres and non-rhizospheres underroot absorption pressure (Modified from [43, 47])

Table 1. Summary of MP contamination reported in salt-tolerant plants and macroalgae

Type of samples	Study location	Abundance	Types of MPs	Shape of MPs	Absorption	Ref.
Mangrove						
Mangrove and saltmarsh sediment	Singapore	36.8 ± 23.6 items.g-1 dry sediment	PE, PP, Nylon, PVC	FB, FL, GN	aerial root	[48]
Mangrove	Qinzhou Bay, China	15 to 12.852 items.kg-1	PS, PP, PE	FG, FB, Sphere	none	[49]
Mangrove	Colombia	31 and 2863 items.kg-1	PE, PS, Nylon	FG, FIL, PL, GN, FL, FO	pneumatophore	[32]
K. obovata	Saudi Arabia	9.3% ± 1.8% of all items, N = 1018	PS, PET	FG	pneumatophore	[50]
K. obovata, R. stylosa, B. gymnorhiza	Persian Gulf, Iran	19.5-34.5 items.kg-1	PE, PA	FB, FG	none	[51]
K. obovata	Beibu Gulf, China	Sediment & root hair zone: 70 ± 8 to 3967 ± 252 items.kg-1; rhizosphere: 127 ± 12 to 2607 ± 123 items.kg-1	PP, PET, PE	FB	root hair, rhizosphere	[63]
Mangrove	Mauritius	Ferney: 107.4 ± 76.42 items.kg-1 and Mahebourg: 140.2 ± 85.38 items.kg-1	PVC	FG, FB, PL, FL, FO	none	[3]
A. marina sediment	Sea of Oman	147.88 ± 99.24 items.kg-1	PE, HDPE, PS, PP, LDPE	FG, PL, FB	root	[64]
S. caseolaris, S. apetala, Aegiceras corniculatum, Acanthus ilicifolius, K. obovata	Seagull Island, China	1223 items.m-2.day-1 dry sediment	CA, Rayon	FB, FG, PL, FL	leaf	[65]
A. corniculatum	Nansha, Guangzhou, China	NA	PS, PMMA	NA	leaves of seedlings	[66]
Mangrove	The eastern coast of Thailand	2213.33 ± 1787.74 items.kg-1 dry sediment	PP, PE,	FB, FG	root	[67]
Rhizophora candle, A. marina, Excoecaria agallocha, A. corniculatum	Qinzhou Bay, China	1.76 n.g-1 to 15.45 n.g-1 and 0.74 n.g-1 to 3.28 n.g-1	PS, PP, PET, PC, Nylon	FB, FL, FG, BD, FO	leaf	[68]
Seagrass						
	Tyrrhenian Sea, Italy	NA	PS, PP, PE, PES, PVC, PU, ABS, PET, PA, PEST, Nylon, CA	FB	egagropiles	[69]

Type of samples	Study location	Abundance	Types of MPs	Shape of MPs	Absorption	Ref.
Thalassia testudinum	Turneffe Atoll, North America	NA	NA	FB, MBD	seagrass blades	[70]
Cymodocea rotundata	Barrang Caddi Island, South Sulawesi	NA	PE, PS, PP, Nylon	MFB, MFG	leaf tips, leaf base	[71]
Endocladia muricata, Pelvetiopsis limitata	Sonoma County, California	E. muricata: 2.5 to 24.3 items.g-1, P. limitata: 0.58 to 8.0 items.g-1	NA	NA	none	[72]
Zostera noltii, Zostera marina, Cymodocea nodosa, Caulerpa prolifera, saltmarsh Sporobolus maritimus	Ria Formosa lagoon, Portugal	1.3-17.3 macroplastics 100 m-2, 18.2-35.2 items.kg-1	NA	FB, FL, FO, FG, MBD	shoot	[73]
Enhalus acoroides	Xincun Bay and Li'an Bay, China	Xincun bay: 93.3 ± 15.3 items.kg-1 dry sediment, 196.7 ± 16.1 items.kg-1; Li'an bay: 267.1 ± 60.5 items.kg-1 dry sediment, >780.2 ± 147.0 items.kg-1 dry sediment	PE, PP, PA, PS	FB, FG, PL, FL, FO	leaf, root, rhizome	[74]
Seagrass	Rameswaram island, India	Water: 24 ± 9 to 96 ± 57 items.L-1; sediment: 55 ± 21 to 259 ± 88 items.kg-1	PS, PA, PE, PET, PVC, PP, CP, PU, PEST, PVA	FB, FL, FG, FO	blades, root	[75]
Z. marina L.	Orkney, Scotland	4.25 kg-1 ± 0.59 SE	PE, PP, PA, PS, PU, PTT	FB, FG, Flake	blades	[76]
E. acoroides, Thalassia hemprichii	Barrang Lompo island, Makassar	E. acoroides: 0.10 ± 0.02 items.cm-2; T. hemprichii: 0.24 ± 0.05 items.cm-2	NA	LN	leaf	[77]
C. serrulata, C. rotundata, Sargassum ilicifolium, T. hemprichii, Padina sp.	Singapore	0.051 items.cm-2, 0.060 items.cm-2, 0.036 items.cm-2, 0.012 items.cm-2, 0.007 items.cm-2, 0.029 items.cm-2	NA	MFB, MFG	blades	[78]
P. oceanica	NW Mediterranean	Sediment: 79.61 ± 1.99 items.g-1; pseudofeces: 52.59 ± 1.22 items.g-1	PET, Nylon, PE, PVC	FB, FG	none	[79]
P. oceanica	Spanish Mediterranian coast	3819 items.kg-1, 2173 items.kg-1, 68-362 items.kg-1	PVC, PU, PS, VC, PE, PTFE, EVA, HDPE, LDPE	FB, FL	root, rhizome	[80]

Type of samples	Study location	Abundance	Types of MPs	Shape of MPs	Absorption	Ref.
Zostera japonica, Halophila beccarii, Halophila ovalis, A. corniculatum, A. marina	Guangxi, China	17.68 ± 8.10 to 611.75 ± 81.52 items.kg-1 dry sediment	PE, PP, PS, PVS, EPDM, PA	FB, FG, PL, FL, FO	shoots, branches, trunks, aerial roots	[81]
Z. marina	Baltic Sea, Estonia	72,1 ± 9,1 g per 50 mL	PVC	FB, FL, Angular, other (incl. round, oval, etc.)	none	[82]
Cladophora	Laurentian Great Lakes	32 ± 10 items.g-1, 34 ± 22 items.g-1	PE, PET, PAN, CA	MFB	none	[83]
Z. marina, Ulvaceae, Gracilariaceae	Northern Adriatic Sea	0.16 to 330 items.g-1	PS	FB	none	[84]
Z. marina, Zostera noltii	Southern England and Wales	215 ± 163 items.kg-1 dry sediment, 221 ± 236 items.kg-1 dry sediment	NA	FB, FG, FL, Fiber bundles	shoot to the tip, leaf	[85]
C. nodosa, Caulerpa cylindracea	Ligurian Sea, Italy	NA	HDPE	FG	root, rhizome, internodes, shoot, apical meristem	[86]
C. nodosa	Italy	68 μg.L-1 (4.5 × 1012 items.L-1 and 9.8 × 108 items.L-1)	PS	FG	root, rhizome, shoot, leaf	[87]
Zostera capensis	South African Estuary	91 (SD = 85) items.kg-1, 99 (SD = 102) items.kg-1, 83 (SD = 63) items.kg-1, 89 (SD = 58) items.kg-1, 94 (SD = 106) items.kg-1 dry sediment	NA	FB	leaf	[88]
Z. noltii, C. nodosa, Sporobolus maritimus	Cádiz Bay, Sothern Spain	Spring: 14.8 ± 2 items 1000.m-2; summer & winter: 12 ± 1.6 and 11.1 ± 1.3 items 1000.m-2; autumn: 8.7 ± 1,3 items 1000.m-2	NA	FB	none	[89]
Halophila ovalis	Swan-Canning Estuary, Perth, Western Australia	1000 ± 100,37 items.kg-1, 972 ± 92,19 items.kg-1	PE, PP	FG, FB	blades	[90]
P. oceanica	Germany	NA	NA	NA	canopy, shoot	[91]
H. ovalis, Halophila spinulosa, Halophila decipiens, Halodule uninervis	North-eastern shores of Singapore	12.65 ± 0.04 items.g-1 dry sediment, 69.65 ± 0.189 items.g-1 dry sediment	PET, PA	FB, FL, FO, FG, PL, Fiber bundle	canopy	[92]

Type of samples	Study location	Abundance	Types of MPs	Shape of MPs	Absorption	Ref.
Seagrasses, saltmarshes	United Kingdom	300 items.L-1	PVC, PET, PA	FB, FG, Flake	stem, blades, branches, leaves	[93]
Saltmarsh Plants						
Spartina alterniflora	Southeast Zhejiang, China	9600-130725 and 200-4350 n.m-2	PS, PE, PP, PU, PA, PC, PET, PVA, PVC, ABS	FG, FB, PL, FO	none	[94]
S. alterniflora, Phragmites australis	Dafeng Elk National Nature Reserve, China	2.97 ± 2.73 items.g-1; 5.39 ± 6.58 items.g-1	PET, CP, PE, PP, PA, PAN	FB, FG, FO	none	[95]
S. alterniflora	Bahía Blanca Estuary, Argentina	> 20,060 items.m-2	HDPE, LDPE, PP, PS	FG, FL, FB, PL, FO	none	[96]
Salicornia europaea	Shawan County, China	28.00 ± 5.29 item.kg-1 to 1426.67 ± 136.49 items.kg-1	PE, PP	FB, FL	Root	[97]
P. australis	Lima Estuary, Portugal	NA	PE	FG, FB	root, rhizome	[98]
Macroalgae						
Fucus vesiculosus	Helgoland, North Sea	NA	PS, PA	MBD, FG, FB	thalli	[99]
Kelp	Southern California, USA	NA	NA	NA	none	[100]
Ulva prolifera	Yellow Sea, China	4603.3 ± 1167.2 items.kg-1 dry sediment	PS, PET	FO, FL	branches	[101]
U. prolifera	Yellow Sea, China	NA	PE, PET, PS, PA, PP, rayon, PVC, PEU, (PE-PP)	MBD, FL, FG, FO, FB	thalli	[102]
Pyropia yezoensis, U. prolifera, Ulva pertusa, Sargassum homeri, Cladophora sp., Undaria pinnatifida	Haizhou Bay, China	Culture periods: 0.17 ± 0.08 items.kg-1 fresh weight, non-culture periods: 1.04 ± 0.32 and 1.86 ± 0.49 items.L-1	PR, Rayon, PP, PS, CP, PE-PP, PET, PAN, Nylon, PS&PAN&PMMA, PMMA	FB, FO, FL	branches, thalli	[103]
Furcellaria lumbricalis, Cocctylus truncatus, Polysiphonia fucoides, Cladophora rupestris, Cladophora glomerata	Russian sector	2.6 ± 1.0 items.individual-1, 5.2 ± 1.8 items.individual-1	PP, PVC, PE, PES/PET, CE	FG, FL, FB	blades, thalli	[104]

Type of samples	Study location	Abundance	Types of MPs	Shape of MPs	Absorption	Ref.
Rhodophyta	Spain	NA	NA	NA	thalli	[105]
Ulva sp., Ulva lactuca, Ulva flexuosa, Ulva intestinalis, Gelidium pusillum, Colpomenia sinuosa, Phycoclidia acanthophora,	Hongkong	3.15 ± 6.82 fibers.g-1 dry sediment, 1.74 ± 3.79 fragment.g-1 dry sediment	PE, PP, PA, PS, PET, PVC, PE/PP	FB, FG, PL, FO, FL	thallus	[106]
U. prolifera, U. lactuca, Gracilaria lemaneiformis, Chondrus ocellatus, Saccharina japonica	The eastern coast of China	Macroplastics: 0 to 201.5 items.kg-1 dry sediment; mesoplastics: 0 to 1178.0 items.kg-1 dry sediment; MPs: 0 to 355.6 items.kg-1 dry sediment	PS, PE, PET, Rayon	FB, FO, FL	branches	[107]
Gelidium corneum	San Lorenzo Beach (Gijón, Asturias)	NA	PET, PEI, PES, PA	GN, FB	none	[108]
Caulerpa lentilifera, Gracilaria tenuistipitata	Qiuhai Lake, China	100 mg.L-1	PA, PS	Microspheres	none	[109]
Polysiphonia morrowii, Blidingia Minima, Ceramium rubrum, Ulva spp.	Argentina coastal area	38.20 ± 53.74 items.L-1, 7 ± 2.44 items.L-1	CE, PTFE, PP, PET, PE, PA, PES, PAN	FB, FG, FL, PL	thalli	[110]
U. lactuca	Southwest England	7.5 items.g-1 to 110 items.g-1	Rayon, Cotton Acrylic, PET, PE, PA, PP, PU, Nylon	FB, BD, FG	none	[111]

PS: Polystyrene, PP: Polypropylene, PE: Polyethylene, PU: Polyurethane, PA: Polyamide, PC: Polycarbonate, CA: Cellulose Acetate, CP: Cellulose Propionate, CE: Cellulose Ether, VC: Vinyl Chloride, BR: Polybutadiene/Butadiene Rubber, PET: Polyethylene Terephthalate, PES: Polyethersulfone, PVC: Polyvinyl Chloride, PVA: Polyvinyl Acetate, PTT: Polytrimethylene Terephthalate, PVS: Polyvinyl Sulfide, PAN: Polyacrylonitrile, PEU: Polyether Urethane, EVA: Ethylene Vinyl Acetate, PLA: Polyactic Acid, PBS: Polybutylene Succinate, PEI: Polyetherimide, ABS: Acrylonitrile Butadiene Styrene, PEST: Polyester, LDPE: Low-Density Polyethylene, PTFE: Polytetrafluoroethylene, EPDM: Ethylene Propylene Diene Monomer, PES/PET: Polyester (Polyethylene Terephthalate), PMMA: Polymethyl Methacrylate, HDPE: High-Density Polyethylene, PP-PE: Polypropylene-Polyethylene (blend), FB: Fiber, MFB: Microfiber, FG: Fragment, MFG: Microfragment, FO: Foam; PL: Pellet, GN: Granule, BD: Bead, MBD: Microbead, FIL: Filament, LN: Line, NA: Not Available.

Mangrove

The mangrove ecosystem is one of the world's most valuable marine habitats, both economically and ecologically. Indonesia's mangrove forests currently cover 3,364,076 hectares, contributing about 23% of the global mangrove forest area and serving as home to 45 out of 75 valid mangrove species worldwide [112]. Mangroves effectively store long-term carbon inside their sediments, with an estimated global storage of 12 billion metric tons. Mangrove ecosystems are crucial for mitigating climate change and carbon sequestration. Coastal wetlands such as mangrove forests can absorb carbon 4-5 times more effectively than tropical terrestrial forests. This ecosystem provides various services such as coastal protection, pollution control, and habitat for a large number

of fauna, which are essential components of the food chain [113]. The trapped MPs by mangroves hinder the tree and neighboring animals by impeding gas exchange and emitting toxic compounds [50, 114]. Many benthic organisms live within the mangrove forest, such as crustaceans and clams, which have deposit-feeding capabilities, thus increasing the chances of these organisms ingesting MPs that settle in the mangrove sediment [114].

Seagrass

Seagrass meadows and beds offer valuable ecological services such as nitrogen cycling [115], and carbon sequestration [116], and support commercial fisheries [41]. These grazing grounds provide habitat, food, and shelter to a variety of related herbivores such as fish, gastropods, dugongs, and turtles [117]. Seagrass meadows also serve as a significant trap of particulate matter like MPs due to their particle-trapping abilities [88]. Recently, MP presence has been reported in environmental samples of Padina sp., T. hemprichii, T. testudinum, S. ilicifolium, E. acoroides, C. rotundata, and C. serrulate [22, 78]. [82] investigated surface water in seagrass beds containing 0.04 to 1.2 MP/L, and the sediments of the seagrass beds had 0 to 131 MP/50 mL sediment-water suspension. [70] and [90] found microfibers and microbeads encrusted on epibiont communities on T. testudinum and H. ovalis seagrasses. Marine herbivores can easily consume MPs in the ecosystem by preying on seagrasses [41], which MPs enter the lower trophic levels of coastal food chains. This accumulation of MPs may expose the seagrass flora and fauna to anthropogenic pollutants. Furthermore, MPs may leach toxins from the environment, including PAHs, PCBs, and DDTs, contaminating benthic organisms in seagrass beds. MPs collected in the seagrass beds could also potentially harm humans through the food chain [118].

Saltmarsh plant

Salt marsh plants, such as S. alterniflora, S. europea, and P. australis are known for their capability to trap suspended particles from water and appear to enhance salt marshes' ability to capture plastic materials [94]. [95] found that the abundance of MPs in P. australis reeds (5.39 ± 6.58 items.g-1) was higher than in cord grass S. alterniflora (2.97 ± 2.73 items.g-1). Reeds may have broader leaves and longer fibrous stalks, making it more straightforward for plants to absorb and hold MPs in the environment. Furthermore, there is S. europea which has diverse ecological values, including fresh consumption, fodder source to feed cattle, production of edible oil and salt, as well as applications in industry, biofuel, and the press cake [15, 119]. This plant has phytoremediation and biofiltration capabilities for pollutants from industrial or aquaculture systems in coastal or inland areas [120, 121, 122]. Genus Salicornia can be categorized into three main groups: phytoextractors, phytostabilizers, and phytodegraders. The pythoextractors absorb and transport pollutants to the shoot for accumulation, excretion, or exudation, while the phytostabilizers stabilize pollutants within the root system or rhizosphere. Phytodegraders break down pollutants into insoluble or nontoxic compounds [123, 124].

Macroalgae

Macroalgae are primarily linked to rocks or other substrates and play an essential ecological role in coastal environments [35], such as sediment stabilization and offering habitat for epifauna and infauna [100, 125]. They are also used as animal feed and human nourishment [125, 126], suggesting that MPs in macroalgae can be transferred to animals and humans through the food system. Four plastic-trapping mechanisms (wrapping, twining, embedding, and attachment) on or in macroalgae were revealed, explaining why the plant has such a strong potential to trap MPs. Twinning and attachment are the two main ways U. prolifera catches polymers. It is easier to separate from the thalli than embedded and wrapped ones; therefore, the plastic trapping changes with the migration path [102]. [110] found macroalgae acquire a more significant proportion of high-density polymers (PAN, PMMA, CE, PES, and PE) detected in six species such as U. intestinalis, U. rigida, U. flexuosa, C. rubrum, P. morrowii, B. minima. [99] investigated that the F. vesiculosus retains suspended MPs on the surface and proved that seaweeds are an efficient pathway for MPs to reach marine benthic herbivores like common periwinkle L. littorea. [108] identified PEI and PE from G. corneum collected near sandy substrates. [104] also identified microfibers on filamentous algae like C. rupestris, C. glomerata, and P. fucoides. The report values for MP concentration in macroalgae differ between the algae species shown in Table 1 due to their varying ability to hold plastic particles. Coastal macroalgae are successfully employed as the most effective biomonitors of MP fiber contaminants in the coastal zone [111]. Macroalgae tend to accumulate MPs, resulting in biomagnification, making them sensitive biomarkers of environmental conditions.

Types of Microplastics

Several researchers have studied the type of MPs in various halophyte plants and algae, and these review studies may provide valuable insights into the distribution of MPs in these ecosystems. [126] indicated a high tolerance plants to MPs, which can be a potential bio-trapper for MPs. Fig. 4a represents the primary forms of MP contamination in salt-tolerant plants and maritime macroalgae identified in the reference studies. MPs were quantified and categorized by type (fibers, fragments, films, foams, beads). Fibers (29%) were the dominant type of MP in field investigations, followed by fragments (24%) and films (14.2%) due to terrestrial material transport. Water currents and tide patterns contribute to dispersing fibers in salt-tolerant plant habitats. Fibers frequently released from textiles have unique environmental impacts [127]. These fibers can configure marine species, causing physical injury and potentially affecting ecosystems if consumed [128]. Fragments from the mechanical deterioration of more significant plastic items contribute to extensive contamination and constitute a direct physical hazard to marine life [64]; their accumulation in sediments and coastal regions may have distinct biological implications in those areas [129]. Other forms such as pellets, foams, granules, microbeads, and filaments almost equally follow films. The majority of these fibers were identified in seagrass (37.2%)

(Fig. 5). Plastics are made of synthetic materials, including polyethylene, polystyrene, polyethylene terephthalate, polypropylene, polyamide, polyvinyl chloride, and nylon. Plastics are also made from semi-synthetic polymers, such as cellulose derivatives [35]. The percentage of different types of MP polymers during the recent year has been described in Fig. 5. Due to its commercial worth and availability, PE (15.8%) is commonly used as MPs in experimental studies. Compared to other MPs like PA, PE, and PP harmed archaeal communities in the sediment of mangrove ecosystems [130, 131]. PS harmed macroalgal physiology [40]. Natural environment contamination studies have revealed that macroalgae are simultaneously exposed to various MPs. [104, 106] and [108] identified a combination of PE, PET, PS, and PP, with PE and PS being the most prominent.

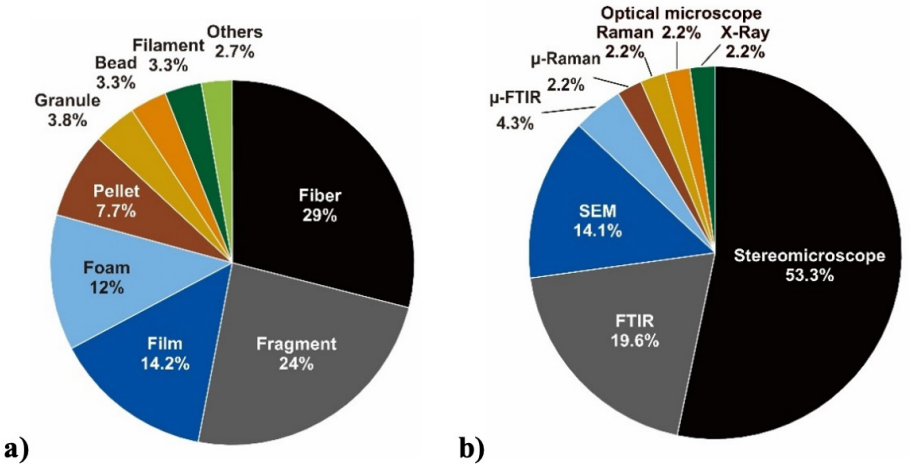


Figure 4. a) The shape of MP contaminations; b) Technological for MP detection in salt-tolerant plants and macroalgae

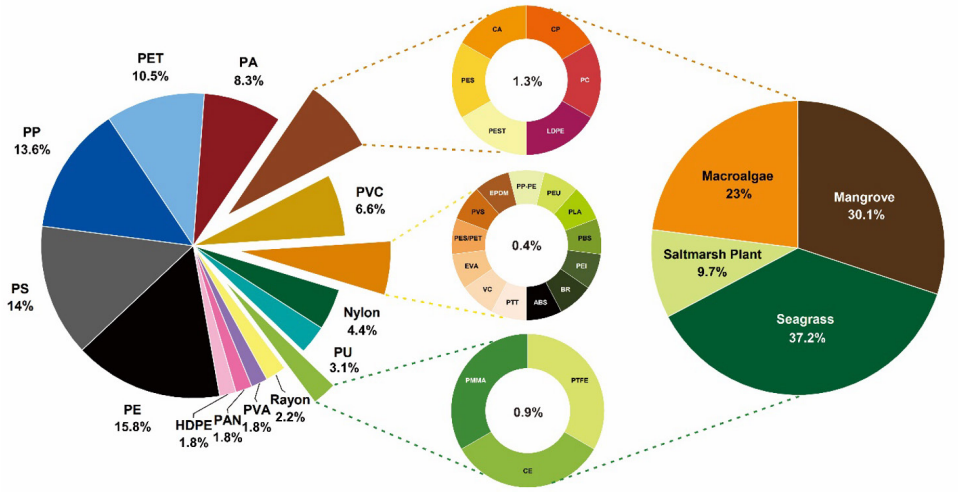


Figure 5. Percentage of MPs polymer type in salt-tolerant plant and macroalgae

Environmental Factors Influencing MPs' Bioavailability

Environmental factors are crucial for plant growth and survival, especially halophyte plants. Environmental factors encompass external elements that influence adsorption by altering the properties of MPs and organic pollutants or indirectly alter heavy metal chemical speciation, transport, and the fate of MPs [132, 133].

Salinity

Salinity is an important factor influencing the bioavailability of MPs in the marine environment. Salinity can influence the adsorption mechanism by altering the potential of electrostatic contact and the ion exchange capacity of MPs and organic pollutants. A greater quantity of Na+ may severely compete against cation exchange sites on the surface of MPs, leading to diminished organic pollutant adsorption [134]. [135] examined the adsorption of sulfamethoxazole by various types of MPs such as (PP, PA, PET, PVC) and observed that Na+ adhered more easily to negatively charged MPs via electrostatic interaction, displacing hydrogen ions from acidic groups with Na+, blocking hydrogen bond formation and decreasing the uptake capacity. [136] and [137] indicated that excessive salinity could have a salting-out impact on organic pollutants in solution, lowering their solubility and enhancing their adsorption onto MPs.

Temperature

The temperature significantly influences the abiotic and

biotic ageing processes of MPs. Temperature can influence the kinetic energy of polymer molecule chains, affecting the dynamics of numerous physical processes and chemical reactions in abiotic processes. Temperature influences catalase, neutral phosphatase activities [138], and the adsorption process primarily by altering the composition of MPs [139]. In general, an optimal temperature exists for the adsorption mechanism. When ambient temperatures are below this optimum, raising the temperature increases the fluidity and solubility of organic pollutants. It decreases the adsorption energy of the endothermic process, therefore improving the adsorption [140]. [141] showed that 25^{0}C was the ideal temperature for adsorbing three synthetic musks on polypropylene. Warmer temperatures exacerbated MP toxicity, and although this effect was observed only at concentrations not currently found in nature, these concentrations are feasible in pollution hotspots due to pulse pollution events or deteriorating environmental contamination in the future [142].

pH and ion strength

The pH primarily influences the adsorption by affecting the electrical characteristics of MPs, i.e. zeta potential [143]. pH can change MP's zeta potential and heavy metal precipitation. The MP zeta potentials decrease with rising pH value. At the same time, some metals' precipitation occurs in environments with pH > 7 [133]. The increase in pH value enhanced the adsorption quantities of Ni, Co, Zn, Cd, Pb, and Cu onto MPs [144]. Conversely, the adsorption of Cr6+ onto MPs was observed to reduce the positive charge on their surface [145]. Ionic strength can be modified with the surface charge, MP aggregation, sorption site, and heavy metal activity. MPs are inhibited by increasing ionic strength [144, 146]. High ionic strength can enhance heavy metal competition for sorption sites on MPs, decreasing heavy metal solution activity concurrently [147].

Dissolved Organic Matter (DOM)

DOM is a naturally occurring organic compound capable of enhancing the stability of MPs, modifying their surface characteristics, altering desorption capacities, and significantly affecting the adsorption of organic contaminants on MPs [132, 148]. For example, the absorption of Cu, Pb, Ag, and Cr on MPs was increased by organic matter [149, 150]. This occurs because the organic matter that exists naturally adhering to the surface of MPs can enhance the binding with heavy metals. These enhancements could also be attributed to more adsorption sites and functional groupings on the MP surfaces [133]. Furthermore, the enhancement of DOM was observed to mitigate the toxicity of Ag+ and plastic nanoparticles to D. magna [150]. These findings suggested that organic matter modulated the desorption/adsorption, accumulation, and toxicity dynamics of pollutants associated with MPs.

Surfactants

Surfactants are molecules possessing both lipophilic and hydrophilic structures, typically engaging with different phases with diverse chemical dissolution properties [151]. As a hydrophobic substance, MPs are easily combined with the hydrophobic end of surfactants, altering their physical and chemical properties, consequently changing MPs' migratory and adsorption properties and potentially raising ecological and environmental concerns [152], [153]. The combination of surfactants with MPs is posed to aid the separation of MPs from water utilizing biodegradable organic reagents in flotation processes. The adsorption of biodegradable organic pollutants on MPs by flotation emerges as a highly effective approach for MPs removal from aquatic environments. Additionally, multiple studies have highlighted surfactants' ability to accelerate the desorption rate of organic contaminants from MPs [154]. [155] observed significant enhancements in the desorption rate of chemical compounds from PE and PVC facilitated by surfactants during the desorption process.

TECHNOLOGICAL TECHNIQUES FOR DETECTING MPS AND NPS

No standard method exists for identifying and measuring the MPs [156]. Due to scientific limits, there are considerable discrepancies between the data discovered for the levels of MPs or NPs in various samples (Fig. 4b). The biggest impediment is the need for an established methodology for MPs or NPs characterization, detection processes, and preparation of samples [157]. Researchers have studied numerous methods, including microscopy, py-GC/MS, spectroscopy, nuclear techniques, and flow cytometry. The MP analysis consists of several phases: sampling, processing, and analysis (identification, characterization, and quantification).

Microscopic Examination

Fluorescent Microscopy

A fluorescent microscope integrates the ability of a light microscope to magnify objects with the ability of chemicals to emit fluorescence. This approach has a 78% accuracy rate when analyzing the samples for MPs [158]. For staining MPs, various dyes (rose bengal, acridine orange, neutral red, rhodamine B, trypan blue, and Nile Red (NR)) have been investigated [159]. Fluorescence tracking of particles could be a better method. Still, it is one of the best currently accessible technologies for tracking non-metallic nanoparticles, such as protein interaction, cell signaling events, or distinguishing spectrally overlapped fluorophores [160]. The chemical incorporation of fluorescence dyes into the polymer network reduces the risk of dye leaching [31]. Due to its strong affinity, higher fluorescent intensity, and quicker processing time, NR is the dye that is better suited for MP staining among the ones that have been researched. The environment's hydrophobicity affects the fluorescence of NR, which is hydrophobic by nature [161]. Other drawbacks of the NR staining method include its propensity to co-stain lipids in MP samples tainted with organic debris [162].

Scanning Electron Microscopy (SEM)

SEM examination was most helpful in obtaining high-resolution particle surface structure properties of the material and

elemental composition signatures. This technique utilized a picture by scanning the material's surface with a relatively short electron beam [163]. Furthermore, Energy-dispersive X-ray spectroscopy (EDS) can be combined with this method to evaluate the composition of MPs. Combining SEM with EDS can be determined by size, shape, and morphology of MPs. Furthermore, SEM-EDS can eliminate non-plastic particles and analyze prepared samples to identify potential MPs based on their elemental signatures and surface properties. SEM images revealed typical cracks associated with environmental exposure and pigment particles consistent with manufacturer materials [163]. [31] identifies the presence of plastic beads in the plant tissues based on size and morphology. However, this method cannot fully determine whether the observed particles are PE, PP, or others.

Spectroscopy

FTIR Spectroscopy

These are the spectroscopic methods that are most frequently applied to MP analysis. The measurement of the infrared radiation that MPs absorb forms the basis of the FTIR analysis. The infrared spectrum serves as a sample's fingerprint and aids in identifying functional groups because various compounds are composed of distinct atoms. This method works with liquid, solid samples, and gaseous materials [164]. A microscope is necessary for the localization of smaller particles, but FTIR can identify MPs. Progression of FTIR research, such as μ-FTIR could rapidly identify the morphological and chemical properties of MPs without harm (not appropriate for detecting particle sizes <10 μm) [165]. The method's accuracy and efficiency have grown with machine learning and automated spectra evaluation [166]. The asymmetric vibrations of polar groups are best studied by FTIR spectroscopy, whereas the symmetric vibrations of non-polar groups are better studied by Raman spectroscopy [167, 168].

Raman Spectroscopy

Raman imaging is an analytical technique utilized to determine molecular structure by investigating the vibrational frequencies of molecular bonds present in the sample [169]. This technique is particularly suitable for analyzing MPs at the micron-sized size with improved sensitivity to non-polar functional groups and reduced water interference with a resolution of 1 μm [165, 168]. The ability to identify MPs without modification is lowered in conventional Raman spectroscopy. Custom-designed μ-Raman spectroscopy allows for imaging, size quantification, and characterization of MPs [169]. By employing spherical gold nanoparticles (14 to 46 nm) to boost the scattered signal, [170] could detect plastic particles at concentrations below 10 μg/mL utilizing surface-enhanced Raman scattering techniques [171] classified MPs based on their size (<100 μm, 100 to 500 μm, 500 to 1000 μm, and >1000 μm), colour, shape, and type using 3D Raman spectroscopy without consideration of composite fractions in mangrove sediment.

X-ray Photoelectron Spectroscopy (XPS)

XPS is a susceptible and particular technology that evaluates the elements present on the surface of a sample, not only general chemical information but also on the surface, tiny areas, and depth distribution when examining electronic materials and detecting MPs [172, 173]. This method can identify and detect components and their binding condition in the material based on the photoelectric effect. Samples are exposed to X-ray radiation, which causes the sample surface to emit photoelectrons [162]. XPS can only analyze the top few nanometers of a surface that demands a high vacuum [174]. MP oxidation can improve organic contaminant adsorption and increase MPs' function as contaminant vectors in the aquatic food chain. They did this by using XPS and other techniques to determine the adsorption characteristics of PP and HDPE for different pollutants.

Gas Chromatography and Mass Spectrometry (GC-MS)

GC-MS simultaneously monitored and quantified the mixed films [156]. The pyrolysis technique was paired with gas chromatography and mass spectrometry as a thermoanalytical approach to predict the chemical structure of MPs, concentration, and quality of the particles. However, the quantity and particle size of the MPs are inadequate [175, 176, 177]. This combination cannot count or provide size and shape information since MPs are thermally destroyed throughout the process. In another study, [178] developed ten plastic polymers: PS, PVC, nylon-6,6, PE, PP, PMMA, NBR, PET, ABS, and PC using this method as a new technology that allows the low-level and exact identification of MPs in environmental samples [179] successfully identified and quantified PE, PS, PP, PVC, and PMMA in seafood using Py-GC/MS analysis.

Flow Cytometry

Flow cytometry is a well-known technology for quickly and automatically examining cells and particulate compounds in aqueous samples [180, 181]. Detection of MPs using flow cytometry was pioneered in 2016 [182], with the advantage that it can discriminate MPs from false positives (e.g. bacteria) and detects particle size ranges from 0.2 to 100 μm using fluorescence straining, thus covering the low range of MPs (< 1 μm) [183, 184]. This approach is primarily used with liquid samples, where MPs are passed under a light beam one at a time, and the scattering and fluorescent intensity of the particles are identified by an accurate photomultiplier tube. Flow cytometry assessed and classified the samples depending on their size. In another study, it can also quantify plastic particles between 0.6-15 μm [162]. [185] showed this approach to identify polyethylene MPs with 70% efficiency, PS and PVC with 96% efficiency with 90s time analysis, which is significantly faster than spectroscopy.

Nuclear Technique

Radiotracer methodologies are extensively utilized for troubleshooting due to their advantages over conventional tracking methods [186]. While the conventional technique needs intricate processes and a large number of animal subjects, the nuclear method provides an accurate, sensitive, and real-time technique using radiolabeled micro-nanoplastics as a tracer [187]. The presence of radionuclide activity can fa-

cilitate the monitoring of specific components of MPs that can harm the environment [188, 189], thereby assisting in assessing plant responses, investigating mechanisms, and understanding the subtle interactions between plants, MPs, and other pollutants at a sub-microscopic level. Detecting MPs within plants presents a technical challenge due to their diminutive size and resemblance to biomass constituents.

The radiotracer should have the least or zero radiochemical toxicity to avoid any radiological threat to the operator, public, and environment [186]. [190] discovered a production method for Iodine-131 radiolabeled polyvinyl chloride (PVC) as a possible radiotracer of MPs bioaccumulation and biodistribution studies in organisms due to their stability radiochemical purity assessment [191] investigated the uptake of 137Cs on milkfish (C. chanos) from aquaculture farms in Jakarta Bay via seawater pathways experiment. Bioaccumulation studies of 65Zn and 137Cs in M. micropterus from Jakarta Bay were also investigated via the water pathways. A high-resolution gamma spectrometer equipped with a high-purity germanium (HPGe) detector was utilized to determine the radioactivity concentrations of these tracers [192], and a gamma spectrometer with NaI(Tl) detector to analyze Cd accumulation in P. viridis through food pathways [193]. [194] exposed 14C-radiolabeled 24 nm and 250 nm polystyrene NPs in mollusk (P. maximus) using autoradiography, which analyzed conduct 6 hours later, revealed that 250 nm NPs accumulated in the intestine, whereas 24 nm particles were disseminated throughout the body.

POTENTIAL EFFECT OF MPS ON HALOPHYTE PLANT

The toxicity of MPs was investigated using a variety of marine organism models, including oysters, nematodes, and zebrafish. Early research on MPs' toxicity concentrated mainly on marine organisms including, vertebrates and invertebrates [195, 196]. The impact on halophyte plants is predominantly unexplored, as most research focuses on terrestrial plants. MPs toxicity factors can be classified as physical, chemical, and biological components [194]. Because of the chemical and physical characteristics of salt-tolerant plants, the impact of plastics could damage their residents through enhanced bioavailability and have the potential to alter the functioning of the ecosystem. Coastal wetlands plants not only capture and confine MPs but can also constrain plant growth by influencing soil composition, nitrogen transport, pollutant adsorption and transport, hazardous release, and microbial populations [197]. Plastics, the majority of which are inert, are not easily degraded in coastal wetlands and can be exploited as a carbon source. Despite that, as plastic debris gradually degrades into tiny plastic pieces, plant-interrooted microorganisms can exploit these MPs as a carbon source, changing the functional features of plants [198].

Bioaccumulation of MPs and NPs affects various marine organisms by changing activities such as reproduction, growth, feeding, and survival, as well as the behavior of fish and filter-feeding organisms [118]. Several studies indicate that MPs can potentially influence phytotoxic effects on the structure and function of salt-tolerant plants [199, 200]. Interaction between mangrove roots and polystyrene (PS) polymers may restrict the transfer of energy and substances, leading to decreased nutrient uptake and light penetration [201, 202]. This interaction can cause damage to the cellular structure through puncturing, as well as morphological alterations such as the thickening of cell walls and deformation of thylakoids. Moreover, it disrupts nutrient cycles by inhibiting nitrogen fixation by diazotrophs, elevates toxin levels that interfere with metabolic processes, and inhibits microbial activities [203]. Fig. 6 summarizes microplastic effects on halophyte plants and maritime macroalgae observed in review studies.

MPs significantly increased the dry weight of the root and shoots, the relative growth rate, and the decrease in the main shoot length in M. spicatum (1753) and Elodea sp. [204]. Recent studies also indicate adverse effects on the growth of microalgae and terrestrial plants; tiny microplastics (200 nm) and nanoplastics adsorbed on roots compile in plant tissues and eventually translocate to shoots [40], causing toxicity, increased oxidative stress, obstruction of light and nutrient entry, turbidity of the water, DNA damage, changes in gene expression, reduced photosynthesis, inhibition of seed germination, and affecting the shape and thickness of root and leaf cell membranes [87]. [103] showed that the floating macroalgae can spatially and temporally influence plastic dispersion via their trap and release. The impact of MPs on plants, including halophytes, gets more problematic in saline conditions. Salinity and MP pollution stress damage numerous essential plant activities like respiration, photosynthesis, antioxidant defence mechanisms, nutrient absorption, and transfer. The most prominent consequences found in published research [1, 123]. The risk-level criteria for MP pollution are showed in Table 2.

Table 2. The risk-level threshold for microplastic contamination [205]

Risk category	I	II	III	IV
Polymer index values	< 10	10 to 100	101 to 1000	> 1000
Pollution load index values	< 10	10 to 20	20 to 30	> 30

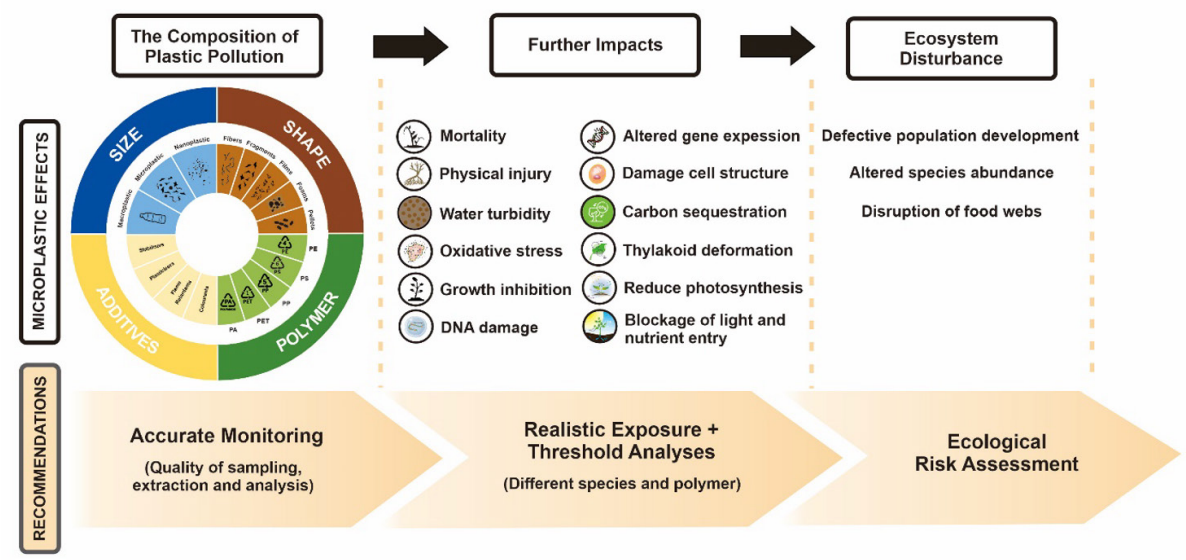


Figure 6. Summary of microplastic effects on halophyte plants and maritime macroalgae observed in review studies

POTENTIALS OF HALOPHYTE PLANTS AND MACROALGAE: BIOREMEDIATION OF MPS

Multiple plants with various taxonomic characteristics can be utilized for successful phytoremediation of MP [206]. Seaweeds (F. vesiculosus) can retain suspended MPs on their surfaces. Aquatic plants are unaffected ecologically by nano- and microplastics at environmentally realistic concentrations. These plant systems could be explored further for MPs bioremediation potential [84, 99]. Seagrasses, aquatic macrophytes, and their accompanying bacteria may be promising candidates for MPs bioremediation in marine and brackish environments [206]. MPs are further fragmented into nanoplastics, which are even more challenging to detect and remove. Advances in modeling and monitoring tools are critical for tracking MP migration, accumulation, and hotspots. These tools enable focused cleanup activities and guide future mitigation approaches.

CONCLUSIONS AND PERSPECTIVES

The current review emphasized microplastic pollution, its degradation, technological approaches, and the interaction mechanism for negatively impacting the halophytic plant and macroalgae. The constant accumulation of MPs in the environment inevitably causes environmental issues and health emergencies. Currently, the study of MP contamination is restricted not only to rivers, oceans, and other water-based ecosystems but also to coastal environments and various other ecosystems. There has also been an increase in the depth of study. Considering the study of MPs on salt-tolerant plants, dissimilar investigations admitted numerous gaps, including the incidence of MPs on wild mangroves and mechanisms of MPs on plant tissue for reducing theirs. At the same time, other research emphasized the distribution, quantity, characteristics, and consequences of MPs on plants and algae. This review summarizes a new tool for investigating MP toxicology that is predicted to address the difficulty of accurately quantifying MPs in plants and algae, hence providing a basis for understanding and evaluating the MPs' toxicity in the body.

Research on MP contamination in coastal environments, especially salt-tolerant plants and macroalgae, still needs to be improved. According to this, the subsequent research directions should be taken to create comprehensive pollution assessment methods and integrate them into routine monitoring of the environmental schemes. The ecological risk assessment framework for MP pollution in the coastal environment needs to be clarified. The United Nations Environment Programme has linked the magnitude and seriousness of MP contamination to climate change. However, concerning the coastal environment as a risk evaluation is still needed to build a comprehensive MPs contamination assessment system and environmental monitoring protocols. The majority of research on MPs and their impact on ecosystem services takes place in laboratory settings, where the ecological conditions significantly diverge from the genuine environment. MPs have nanometer-sized particles, making measuring nanoplastic concentrations in the actual environment challenging. Consequently, additional research is needed to ascertain the effects of MPs on ecosystem functions in the field environment. Creating strategies for preventing and controlling policies for MP pollution in coastal environments to identify the primary sources of contamination, reduce MP emissions and pollution from the root, eliminate the source of MP deterioration, and investigate factors for aggravating MP pollution in coastal environments based on the current research.

ACKNOWLEDGMENT

The authors would like to thank UPT Library & UNDIP Press and the ELSA system for helping with communication related to the support of manuscript checking services.

DATA AVAILABILITY STATEMENT

The authors affirm that the data supporting the study's conclusions may be found within the article. Upon a reasonable

request, the corresponding author can provide raw data that supports this study's findings.

AUTHOR'S CONTRIBUTIONS

Meita Eka Fara: Writing – original draft, Writing – Review & editing, Methodology, Conceptualization, Visualisation, Validation. Muslim Muslim: Writing – review & editing, Validation, Supervision. Miftakul Munir: Writing – review & editing, Conceptualization, Validation, Supervision.

CONFLICT OF INTEREST

The authors state that there are no known conflicts of interest or personal relationships that could have influenced the work presented in this study.

ETHICS

There are no ethical concerns about publishing this manuscript.

REFERENCES

[1] L. Yin, X. Wen, D. Huang, C. Du, R. Deng, Z. Zhou, J. Tao, R. Li, W. Zhou, Z. Wang, and H. Chen, "Interactions Between Microplastics/Nanoplastics and Vascular Plants," Environmental Pollution, Vol. 290, pp. 1–11, 2021. [CrossRef]

[2] S. DuBay, B. Weeks, P. Davis-Kean, C. Fuldner, N. Harris, S. Hughes, B. O'Brien, M. Perkins, and C. Weyant, "Measuring Historical Pollution: Natural History Collections as Tools for Public Health and Environmental Justice Research," Ecology and Evolution, pp. 1–23, 2023. [CrossRef]

[3] L. D. Seeruttun, P. Raghbor, and C. Appadoo, "Mangrove and Microplastic Pollution: A Case Study from a Small Island (Mauritius)," Regional Studies in Marine Science, Vol. 62, pp. 1–10, 2023. [CrossRef]

[4] M. MacLeod, H. P. H. Arp, M. B. Tekman, and A. Jahnke, "The Global Threat from Plastic Pollution," Science, Vol. 373, pp. 61–65, 2021. [CrossRef]

[5] A. A. Koelmans, P. E. Redondo-Hasselerharm, N. H. M. Nor, V. N. de Ruijter, S. M. Mintenig, and M. Kooi, "Risk Assessment of Microplastic Particles," Nature Review Materials, Vol. 7(2), pp. 138–152, 2022. [CrossRef]

[6] H. P. H. Arp, D. Kühnel, C. Rummel, M. MacLeod, A. Potthoff, S. Reichelt, E. Rojo-Nieto, M. Schmitt-Jansen, J. Sonnenberg, E. Toorman, and A. Jahnke, "Weathering Plastics as a Planetary Boundary Threat: Exposure, Fate, and Hazards," Environmental Science & Technology, Vol. 55(11), pp. 7246–7255, 2021. [CrossRef]

[7] V. Dettling, S. Samadi, C. Ratti, J.-B. Fini, and C. Laguionie, "Can Natural History Collection Specimens be Used as Aquatic Microplastic Pollution Bioindicators?," Ecological Indicators, Vol. 160, pp. 1–12, 2024. [CrossRef]

[8] K. Bucci and C. M. Rochman, "Microplastics: a Multidimensional Contaminant Requires a Multidimensional Framework for Assessing Risk," Microplastics and Nanoplastics, Vol. 2(1), pp. 1–9, 2022. [CrossRef]

[9] B. B. Hughes, R. Beas-Luna, A. K. Barner, K. Brewitt, D. R. Brumbaugh, E. B. Cerny-Chipman, S. L. Close, K. E. Coblentz, K. L. De Nesnera, S. T. Drobnitch, J. D Figurski, B. Focht, M. Friedman, J. Freiwald, K. K. Heady, W. N. Heady, A. Hettinger, A. Johnson, K. A. Karr, B. Mahoney, M. M. Moritsch, A. M. K. Osterback, J. Reimer, J. Robinson, T. Rohrer, J. M. Rose, M. Sabal, L. M. Segui, C. Shen, J. Sullivan, R. Zuercher, P. T. Raimondi, B. A. Menge, K. Grorud-Colvert, M. Novak, and M. H. Carr, "Long-Term Studies Contribute Disproportionately to Ecology and Policy," Bioscience, Vol. 67(3), pp. 271–278, 2017. [CrossRef]

[10] Y. M. Bar-On, R. Phillips, and R. Milo, "The Biomass Distribution on Earth," Proceedings of the National Academy of Sciences of the United States of America, Vol. 115(25), pp. 6506–6511, 2018. [CrossRef]

[11] T. Roy, T. K. Dey, and M. Jamal, "Microplastic/Nanoplastic Toxicity in Plants: An Imminent Concern," Environmental Monitoring and Assessment, Vol. 195(27), pp. 1–35, 2023. [CrossRef]

[12] L. Li, Y. Zhao, G. Han, J. Guo, Z. Meng, and M. Chen, "Progress in the Study and Use of Seawater Vegetables," Journal of Agricultural and Food Chemistry, Vol. 68(22), pp. 5998–6006, 2020. [CrossRef]

[13] J. M. Oliveira, M. A. Pardal, L. Pereira, A. M. Matos, and E. T. Rodrigues, "Portuguese Macroalgae and Halophytes for Human Consumption: Minimal Risk of Norovirus and Salmonella Infection," Food Control, pp. 1–21, 2024. [CrossRef]

[14] Md. M. Rahman, M. G. Mostofa, S. S. Keya, Md. N. Siddiqui, Md. M. U. Ansary, A. K. Das, Md. A. Rahman, and L. S. Tran, "Adaptive Mechanisms of Halophytes and Their Potential in Improving Salinity Tolerance in Plants," International Journal of Molecular Sciences, Vol. 22(19), pp. 1–28, 2021. [CrossRef]

[15] S. Cárdenas-Pérez, A. Piernik, J. J. Chanona-Pérez, M. N. Grigore, and M. J. Perea-Flores, "An Overview of the Emerging Trends of the Salicornia L. Genus as a Sustainable Crop," Environmental and Experimental Botany, Vol. 191, pp. 1–15, 2021. [CrossRef]

[16] K. Zhang, N. Gao, Y. Li, S. Dou, Z. Liu, Y. Chen, C. Ma, and H. Zhang, "Responses of Maize (Zea mays L.) Seedlings Growth and Physiological Traits Triggered by Polyvinyl Chloride Microplastics is Dominated by Soil Available Nitrogen," Ecotoxicology and Environmental Safety, Vol. 252, pp. 1–10, 2023. [CrossRef]

[17] E. Kılıç and N. Yücel, "Proposal of Invader Pontederia crassipes as a Savior of Micro and Macro Size Plastic Pollution," Marine Science and Technology

Bulletin, Vol. 13(2), pp. 135–141, 2024. [CrossRef]
[18] M. S. Fountoulakis, G. Sabathianakis, I. Kritsotakis, E. M. Kabourakis, and T. Manios, "Halophytes as Vertical-flow Constructed Wetland Vegetation for Domestic Wastewater Treatment," Science of the Total Environment, Vol. 583, pp. 432–439, 2017. [CrossRef]
[19] Y. Chae and Y. J. An, "Nanoplastic Ingestion Induces Behavioral Disorders in Terrestrial Snails: Trophic Transfer Effects: Via Vascular Plants," Environmental Science: Nano, Vol. 7(3), pp. 975–983, 2020. [CrossRef]
[20] M. E. Conti, M. Mecozzi, and M. G. Finoia, "Determination of Trace Metal Baseline Values in Posidonia oceanica, Cystoseira sp., and Other Marine Environmental Biomonitors: a Quality Control Method for a Study in South Tyrrhenian Coastal Areas," Environmental Science and Pollution Research, Vol. 22(5), pp. 3640–3651, 2015. [CrossRef]
[21] S. Huang, R. Jiang, N. J. Craig, H. Deng, W. He, J.-Y Li, and L. Su, "Accumulation and Re-Distribution of Microplastics via Aquatic Plants and Macroalgae - A Review of Field Studies," Marine Environmental Research, Vol. 187, pp. 1–10, 2023. [CrossRef]
[22] Y. Huang, X. Qing, W. Wang, G. Han, and J. Wang, "Mini-Review on Current Studies of Airborne Microplastics: Analytical Methods, Occurrence, Sources, Fate and Potential Risk to Human Beings," TrAC - Trends in Analytical Chemistry, Vol. 125, pp. 1–8, 2020. [CrossRef]
[23] M. Kumar, X. Xiong, M. He, D. C. W. Tsang, J. Gupta, E. Khan, S. Harrad, D. Hou, Y. S. Ok, and N. S. Bolan, "Microplastics as Pollutants in Agricultural Soils," Environmental Pollution, Vol. 265, pp. 1–11, 2020. [CrossRef]
[24] S. Xu, J. Ma, R. Ji, K. Pan, and A.-J. Miao, "Microplastics in Aquatic Environments: Occurrence, Accumulation, and Biological Effects," Science of the Total Environment, Vol. 703, pp. 1–14, 2020. [CrossRef]
[25] S. Karbalaei, A. Golieskardi, H. Hamzah, S. Abdulwahid, P. Hanachi, T. R. Walker, and A. Karami, "Abundance and Characteristics of Microplastics in Commercial Marine Fish from Malaysia," Marine Pollution Bulletin, Vol. 148, pp. 5–15, 2019. [CrossRef]
[26] K. Duis and A. Coors, "Microplastics in the Aquatic and Terrestrial Environment: Sources (With a Specific Focus on Personal Care Products), Fate and Effects," Environmental Science Europe, Vol. 28(2), pp. 1–25, 2016. [CrossRef]
[27] C. Alomar, M. Sanz-Martín, M. Compa, B. Rios-Fuster, E. Álvarez, V. Ripolles, J. M. Valencia, and Deudero, "Microplastic Ingestion in Reared Aquaculture Fish: Biological Responses to Low-Density Polyethylene Controlled Diets in Sparus aurata," Environmental Pollution, Vol. 280, pp. 1–12, 2021. [CrossRef]
[28] Y. Zhang, S. Kang, S. Allen, D. Allen, T. Gao, and M. Sillanpää, "Atmospheric Microplastics: A Review on Current Status and Perspectives," Earth Science Reviews, Vol. 203, pp. 1–15, 2020. [CrossRef]
[29] H. Deng, J. He, D. Feng, Y. Zhao, W. Sun, H. Yu, and C. Ge, "Microplastics Pollution in Mangrove Ecosystems: A Critical Review of Current Knowledge and Future Directions," Science of the Total Environment, Vol. 753, pp. 1–16, 2021, [CrossRef]
[30] A. I. Osman, M. Hosny, A. S. Eltaweil, S. Omar, A. M. Elgarahy, M. Farghali, P. S. Yap, Y. S. Wu, S. Nagandran, K. Batumalaie, S. C. B Gopinath, O. D. John, M. Sekar, T. Saikia, P. Karunanithi, M. H. M. Hatta, and K. A. Akinyede, "Microplastic Sources, Formation, Toxicity and Remediation: A Review," Environmental Chemistry Letters, vol. 21(4), pp. 2129–2169, 2023. [CrossRef]
[31] L. Li, Y. Luo, R. Li, Q. Zhou, W. J. G. M. Peijnenburg, N. Yin, J. Yang, C. Tu, and Y. Zhang, "Effective Uptake of Submicrometre Plastics by Crop Plants Via a Crack-Entry Mode," Nature Sustainability, Vol. 3(11), pp. 929–937, 2020. [CrossRef]
[32] O. Garcés-Ordóñez, V. A. Castillo-Olaya, A. F. Granados-Briceño, L. M. B. García, and L. F. E. Díaz, "Marine Litter and Microplastic Pollution on Mangrove Soils of the Ciénaga Grande de Santa Marta, Colombian Caribbean," Marine Pollution Bulletin, Vol. 145, pp. 455–462, 2019. [CrossRef]
[33] K. Min, J. D. Cuiffi, and R. T. Mathers, "Ranking Environmental Degradation Trends of Plastic Marine Debris Based on Physical Properties and Molecular Structure," Nature Communication, Vol. 11(727), pp. 1–11, 2020. [CrossRef]
[34] L. J. J. Meijer, T. Van Emmerik, R. Van Der Ent, C. Schmidt, and L. Lebreton, "More than 1000 Rivers Account for 80% of Global Riverine Plastic Emissions into the Ocean," Science Advances, Vol. 7, pp. 1–13, 2021. [CrossRef]
[35] V. N. Salomone, V. Passucci, and M. M. Areco, "Microplastic Pollution in Marine Environments: Exploring Sources, Sinks, and Consequences with a Focus on Algal Interactions," Regional Studies Marine Science, Vol. 68, pp. 1–12, 2023. [CrossRef]
[36] A. Alfaro-Núñez, D. Astorga, L. Cáceres-Farías, L. Bastidas, C. S. Villegas, K. Macay, and J. H. Christensen, "Microplastic Pollution in Seawater and Marine Organisms Across the Tropical Eastern Pacific and Galápagos," Scientific Reports, Vol. 11(6424), pp. 1–8, 2021. [CrossRef]
[37] D. Liu, Z.-F. Ghuo, Y.-Y. Xu, F. K. S. Chan, Y.-Y Xu, M. Johnson, and Y.-G. Zhu, "Widespread Occurrence of Microplastics in Marine Bays with Diverse Drivers and Environmental Risk," Environment International, Vol. 168, pp. 1–10, 2022. [CrossRef]
[38] D. W. Skaf, V. L. Punzi, J. T. Rolle, and K. A. Kleinberg, "Removal of Micron-Sized Microplastic Particles from Simulated Drinking Water via Alum Coagulation," Chemical Engineering Journal, Vol. 386,

pp. 1–8, 2020. [CrossRef]
[39] C. M. Lanctôt, M. Al-Sid-Cheikh, A. I. Catarino, T. Cresswell, B. Danis, H. K. Karapanagioti, T. Mincer, F. Oberhänsli, P. Swarzenski, I. Tolosa, and M. Metian, "Application of nuclear techniques to environmental plastics research," Journal of Environmental Radioactivity, Vol. 192, pp. 368–375, 2018. [CrossRef]
[40] R. Li, C. Tu, L. Li, X, Wang, J. Yang, Y. Feng, X. Zhu, Q. Fan, and Y. Luo, "Visual Tracking of Label-Free Microplastics in Wheat Seedlings and Their Effects on Crop Growth and Physiology," Journal of Hazardous Materials, Vol. 456, pp. 1–9, 2023. [CrossRef]
[41] E. M. Tuuri and S. C. Leterme, "How Plastic Debris and Associated Chemicals Impact the Marine Food Web: A Review," Environmental Pollution, Vol. 321, pp. 1–12, 2023. [CrossRef]
[42] T. Bosker, L. J. Bouwman, N. R. Brun, P. Behrens, and M. G. Vijver, "Microplastics Accumulate on Pores in Seed Capsule and Delay Germination and Root Growth of the Terrestrial Vascular Plant Lepidium sativum," Chemosphere, Vol. 226, pp. 774–781, 2019. [CrossRef]
[43] I. Azeem, M. Adeel, M. A. Ahmad, N. Shakoor, G. D. Jiangcuo, K. Azeem, M. Ishfaq, A. Shakoor, M. Ayaz, M. Xu, and Y. Rui, "Uptake and Accumulation of Nano/microplastics in Plants: A Critical Review," Nanomaterials, Vol. 11(11), pp. 1–22, 2021. [CrossRef]
[44] S. Rong, S. Wang, H. Liu, Y. Li, J. Huang, W. Wang, B. Han, S. Su, and W. Liu, "Evidence for the Transportation of Aggregated Microplastics in the Symplast Pathway of Oilseed Rape Roots and their Impact on Plant Growth," Science of The Total Environment, Vol. 912, pp. 1–11, 2024. [CrossRef]
[45] Y. Liu, R. Guo, S. Zhang, Y. Sun, and F. Wang, "Uptake and Translocation of Nano/microplastics by Rice Seedlings: Evidence from a Hydroponic Experiment," Journal of Hazardous Materials, Vol. 421, pp. 1–8, 2022. [CrossRef]
[46] H. Sun, C. Lei, J. Xu, and R. Li, "Foliar Uptake and Leaf-to-Root Translocation of Nanoplastics with Different Coating Charge in Maize Plants," Journal of Hazardous Materials, Vol. 416, pp. 1–10, 2021. [CrossRef]
[47] Z. Dehghanian, K. Habibi, M. Dehghanian, S. Aliyar, B. A. Lajayer, T. Astatkie, T. Minkina, and C. Keswani, "Micro (Nano) Plastics Uptake, Toxicity and Detoxification in Plants: Challenges and Prospects," Heliyon, Vol. 8, pp. 1–12, 2023. [CrossRef]
[48] N. H. M. Nor and J. P. Obbard, "Microplastics in Singapore's Coastal Mangrove Ecosystems," Marine Pollution Bulletin, Vol. 79, pp. 278–283, 2014. [CrossRef]
[49] J. Li, H. Zhang, K. Zhang, R. Yang, R. Li, and Y. Li, "Characterization, Source, and Retention of Microplastic in Sandy Beaches and Mangrove Wetlands of the Qinzhou Bay, China," Marine Pollution Bulletin, Vol. 136, pp. 401–406, 2018. [CrossRef]
[50] C. Martin, H. Almahasheer, and C. M. Duarte, "Mangrove Forests as Traps for Marine Litter," Environmental Pollution, Vol. 247, pp. 499–508, 2019. [CrossRef]
[51] A. Naji, M. Nuri, P. Amiri, and S. Niyogi, "Small Microplastic Particles (S-MPPs) in Sediments of Mangrove Ecosystem on the Northern Coast of the Persian Gulf," Marine Pollution Bulletin, Vol. 146, pp. 305–311, 2019. [CrossRef]
[52] R. Li, L. Yu, M. Chai, H. Wu, and X. Zhu, "The Distribution, Characteristics and Ecological Risks of Microplastics in the Mangroves of Southern China," Science of the Total Environment, Vol. 708, pp. 1–11, 2020. [CrossRef]
[53] L. Zuo, Y. Sun, H. Li, Y. Hu, L. Lin, J. Peng, and X. Xu, "Microplastics in Mangrove Sediments of the Pearl River Estuary, South China: Correlation with Halogenated Flame Retardants' Levels," Science of the Total Environment, Vol. 725, pp. 1–7, 2020. [CrossRef]
[54] M. R. Cordova, Y. I. Ulumuddin, T. Purbonegoro, and A. Shiomoto, "Characterization of Microplastics in Mangrove Sediment of Muara Angke Wildlife Reserve, Indonesia," Marine Pollution Bulletin, Vol. 163, pp. 1–9, 2021. [CrossRef]
[55] J. Duan, J. Han, S. G. Cheung, R. K. Y. Chong, C.-M. Lo, F. W.-F. Lee, S. J.-L. Xu, Y. Yang, N. F.-Y. Tam, and H.-C. Zhou, "How Mangrove Plants Affect Microplastic Distribution in Sediments of Coastal Wetlands: Case Study in Shenzhen Bay, South China," Science of the Total Environment, Vol. 767, pp. 1–10, 2021. [CrossRef]
[56] G. C. Zamprogno, F. B. Caniçali, C. dos R. Cozer, M. B. P. Otegui, J. B. Graceli, and M. B. da Costa, "Spatial Distribution of Microplastics in the Superficial Sediment of a Mangrove in Southeast Brazil: A Comparison Between Fringe and Basin," Science of the Total Environment, Vol. 784, pp. 1–10, 2021. [CrossRef]
[57] M. Jiao, L. Ren, Y. Wang, C. Ding, T. Li, S. Cao, R. Li, and Y. Wang, "Mangrove Forest: An Important Coastal Ecosystem to Intercept River Microplastics," Environmental Research, Vol. 210, pp. 1–8, 2022. [CrossRef]
[58] Y. Li, R. Huang, L. Hu, C. Zhang, X. Xu, L. Song, Z. Wang, X. Pan, G. Christakos, and J. Wu, "Microplastics Distribution in Different Habitats of Ximen Island and the Trapping Effect of Blue Carbon Habitats on Microplastics," Marine Pollution Bulletin, Vol. 181, pp. 1–9, 2022. [CrossRef]
[59] E. da S. Paes, T. V. Gloaguen, H. dos A. da C. Silva, T. S. Duarte, M. da C. de Almeida, O. D. A. V. Costa, M. R. Bomfim, and J. A. G. Santos, "Widespread Microplastic Pollution in Mangrove Soils of Todos os Santos Bay, Northern Brazil," Environmental Research, Vol. 210, pp. 1–10, 2022. [CrossRef]
[60] B. Tan, Y. Li, H. Xie, Z. Dai, C. Zhou, Z.-J. Qian, P.

Hong, Y. Liang, L. Ren, S. Sun, and C. Li, "Microplastics Accumulation in Mangroves Increasing the Resistance of its Colonization Vibrio and Shewanella," Chemosphere, Vol. 295, pp. 1–9, 2022. [CrossRef]

[61] M. Chai, R. Li, B. Li, H. Wu, and L. Yu, "Responses of Mangrove (Kandelia obovata) Growth, Photosynthesis, and Rhizosphere Soil Properties to Microplastic Pollution," Marine Pollution Bulletin, Vol. 189, pp. 1–11, 2023. [CrossRef]

[62] B. Hu, J. Lin, J. He, M. Zheng, J. Wang, Y. Nan, and Y Wu, "Sediment and Interstitial Water Heavy Metals in Mangrove Restoration Wetland and Preliminary Exploration of Microplastics in Interstitial Water," Catena, Vol. 221, pp. 1–10, 2023. [CrossRef]

[63] T. Li, Y. Wang, M. Jiao, Z. Zhao, R. Li, and C. Qin, "Distinct Microplastics Abundance Variation in Root-Associated Sediments Revealed the Underestimation of Mangrove Microplastics Pollution," Science of the Total Environment, Vol. 899, pp. 1–9, 2023. [CrossRef]

[64] M. Al-Tarshi, S. Dobretsov, and W. Gallardo, "Marine Litter and Microplastic Pollution in Mangrove Sediments in the Sea of Oman," Marine Pollution Bulletin, Vol. 201, pp. 1–10, 2024. [CrossRef]

[65] Y. Huang, Z. Zhu, T. Li, M. Li, Z. Cai, X. Wang, H. Gong, and M. Yan, "Mangrove Plants are Promising Bioindicator of Coastal Atmospheric Microplastics Pollution," Journal of Hazardous Materials, Vol. 465, pp. 1–9, 2024. [CrossRef]

[66] J.-W. Huang, Y.-Y. Sun, Q.-S. Li, H.-Z. Zhou, Y.-H. Li, X.-X. Fan, and J.-F. Wang, "Increased Risk of Heavy Metal Accumulation in Mangrove Seedlings in Coastal Wetland Environments due to Microplastic Inflow," Environmental Pollution, Vol. 349, pp. 1–11, 2024. [CrossRef]

[67] P. Prarat, P. Hongsawat, and B. Chouychai, "Microplastic Occurrence in Surface Sediments from Coastal Mangroves in Eastern Thailand: Abundance, Characteristics, and Ecological Risk Implications," Regional Studies Marine Science, Vol. 71, pp. 1–12, 2024. [CrossRef]

[68] Y. Wei, M. Jiao, Z. Zhao, L. Tang, Y. Wang, J. Deng, G. Peng, R. Li, and Y. Wang, "Secreted Salt and Hydrodynamic Factors Combine to Affect Dynamic Fluctuations of Microplastics on Mangrove Leaves," Journal of Hazardous Materials, Vol. 467, pp. 1–11, 2024. [CrossRef]

[69] L. Pietrelli, A. D. Gennaro, P. Menegoni, F. Lecce, G. Poeta, A. T. R. Acosta, C. Battisti, and V. Iannilli, "Pervasive Plastisphere: First Record of Plastics in Egagropiles (Posidonia spheroids)," Environmental Pollution, Vol. 229, pp. 1032–1036, 2017. [CrossRef]

[70] H. Goss, J. Jaskiel, and R. Rotjan, "Thalassia testudinum as a Potential Vector for Incorporating Microplastics into Benthic Marine Food Webs," Marine Pollution Bulletin, Vol. 135, pp. 1085–1089, 2018. [CrossRef]

[71] S. S. Datu, S. Supriadi, and A. Tahir, "Microplastic in Cymodocea rotundata Seagrass Blades," International Journal of Environment, Agriculture and Biotechnology, Vol. 4(6), pp. 1758–1761, 2019. [CrossRef]

[72] A. M. Saley, A. C. Smart, M. F. Bazerra, T. L. U. Burnham, L. R. Capece, L. F. O. Lima, A. C. Carsh, S. L. Williams, and S. G. Morgan, "Microplastic Accumulation and Biomagnification in a Coastal Marine Reserve Situated in a Sparsely Populated Area," Mar Pollut Bull, Vol. 146, pp. 54–59, 2019. [CrossRef]

[73] L. Cozzolino, K. R. Nicastro, G. I. Zardi, and C. B. de los Santos, "Species-Specific Plastic Accumulation in the Sediment and Canopy of Coastal Vegetated Habitats," Science of the Total Environment, Vol. 723, pp. 1–10, 2020. [CrossRef]

[74] Y. Huang, X. Xiao, C. Xu, Y. D. Perianen, J. Hu, and M. Holmer, "Secreted Salt and Hydrodynamic Factors Combine to Affect Dynamic Fluctuations of Microplastics on Mangrove ?," Environmental Pollution, Vol. 257, pp. 1–9, 2020. [CrossRef]

[75] K. I. Jeyasanta, J. Patterson, G. Grimsditch, and J. K. P. Edward, "Occurrence and Characteristics of Microplastics in the Coral Reef, Sea Grass and Near Shore Habitats of Rameswaram Island, India," Marine Pollution Bulletin, Vol. 160, pp. 1–16, 2020. [CrossRef]

[76] K. L. Jones, M. G. J. Hartl, M. C. Bell, and A. Capper, "Microplastic Accumulation in a Zostera marina L. Bed at Deerness Sound, Orkney, Scotland," Marine Pollution Bulletin, Vol. 152, pp. 1–10, 2020. [CrossRef]

[77] R. Sawalman, S. Werorilangi, M. Ukkas, S. Mashoreng, I. Yasir, and A. Tahir, (2021). Microplastic Abundance in Sea Urchins (Diadema setosum) from Seagrass Beds of Barranglompo Island, Makassar, Indonesia. in IOP Conference Series: Earth and Environmental Science, IOP Publishing Ltd (pp. 1–9). [CrossRef]

[78] N. Seng, S. Lai, J. Fong, M. F. Saleh, C. Cheng, Z. Y. Cheok, and P. A. Todd, "Early Evidence of Microplastics on Seagrass and Macroalgae," Marine and Freshwater Research, Vol. 71(8), pp. 922–928, 2020. [CrossRef]

[79] F. Bulleri, C. Ravaglioli, S. Anselmi, and M. Renzi, "The Sea Cucumber Holothuria tubulosa Does Not Reduce the Size of Microplastics but Enhances Their Resuspension in the Water Column," Science of the Total Environment, Vol. 781, pp. 1–8, 2021. [CrossRef]

[80] M. Dahl, S. Bergman, M. Björk, E. Diaz-Almela, M. Granberg, M. Gullström, C. Leiva-Dueñas, K. Magnusson, C. Marcon-Méndez, N. Piñeiro-Juncal, and M. Á. Mateo, "A Temporal Record of Microplastic Pollution in Mediterranean Seagrass Soils," Environmental Pollution, Vol. 273, pp. 1–13, 2021. [CrossRef]

[81] Y. Huang, X. Xiao, K. Effiong, C. Xu, Z. Su, J. Hu, S.

Jiao, and M. Holmer, "New Insights into the Microplastic Enrichment in the Blue Carbon Ecosystem: Evidence from Seagrass Meadows and Mangrove Forests in Coastal South China Sea," Environmental Science & Technology, Vol. 55(8), pp. 4804–4812, 2021. [CrossRef]

[82] R. Kreitsberg, M. Raudna-Kristoffersen, M. Heinlaan, R. Ward, M. Visnapuu, V. Kisand, R. Meitern, J. Kotta, and A. Tuvikene "Seagrass Beds Reveal High Abundance of Microplastic in Sediments: A Case Study in the Baltic Sea," Marine Pollution Bulletin, Vol. 168, pp. 1–7, 2021. [CrossRef]

[83] J. Peller, M. B. Nevers, M. Byappanahalli, C. Nelson, B. G. Babu, M. A. Evans, E. Kostelnik, M. Koller, J. Johnston, and S. Shidler, "Sequestration of Microfibers and Other Microplastics by Green Algae, Cladophora, in the US Great Lakes," Environmental Pollution, Vol. 276, pp. 1–11, 2021. [CrossRef]

[84] A. A. Sfriso, Y. Tomio, A. S. Juhmani, A. Sfriso, C. Munari, and M. Mistri, "Macrophytes: A Temporary Sink for Microplastics in Transitional Water Systems," Water, Vol. 13(21), pp. 1–12, 2021. [CrossRef]

[85] R. K. F. Unsworth, A. Higgs, B. Walter, L. C. Cullen-Unsworth, I. Inman, and B. L. Jones, "Canopy Accumulation: Are Seagrass Meadows a Sink of Microplastics?," Oceans, Vol. 2(1), pp. 162–178, 2021. [CrossRef]

[86] V. Menicagli, E. Balestri, F. Vallerini, D. De Battisti, and C. Lardicci, "Plastics and Sedimentation Foster the Spread of a Non-Native Macroalga in Seagrass Meadows," Science of the Total Environment, Vol. 757, pp. 1–12, 2021. [CrossRef]

[87] V. Menicagli, M. R. Castiglione, E. Balestri, L. Giorgetti, S. Bottega, C. Sorce, C. Spanò, and C. Lardicci, "Early Evidence of the Impacts of Microplastic and Nanoplastic Pollution on the Growth and Physiology of the Seagrass Cymodocea nodosa," Science of the Total Environment, Vol. 838, pp. 1–, 2022. [CrossRef]

[88] B. J. Boshoff, T. B. Robinson, and S. von der Heyden, "The Role of Seagrass Meadows in the Accumulation of Microplastics: Insights from a South African Estuary," Marine Pollution Bulletin, Vol. 186, pp. 1–7, 2023. [CrossRef]

[89] L. G. Egea, J. Cavijoli-Bosch, I. Casal-Porras, A. Yamuza-Magdaleno, F. G. Brun, and R. Jiménez-Ramos, "Comparison of Macroplastics Dynamic Across a Tidal-Dominated Coastal Habitat Seascape Including Seagrasses, Salt Marshes, Rocky Bottoms and Soft Sediments," Marine Pollution Bulletin, Vol. 196, pp. 1–10, 2023. [CrossRef]

[90] J. Wright, R. K. Hovey, H. Paterson, J. Stead, and A. Cundy, "Microplastic Accumulation in Halophila ovalis Beds in the Swan-Canning Estuary, Western Australia," Marine Pollution Bulletin, Vol. 187, pp. 1–10, 2023. [CrossRef]

[91] N. B. Kerpen, B. E. Larsen, T. Schlurmann, M. Paul, H. G. Guler, K. D. Goral, S. Carstensen, E. D. Christensen, and D. R. Fuhrman, "Microplastic Retention in Marine Vegetation Canopies under Breaking Irregular Waves," Science of the Total Environment, Vol. 912, pp. 1–14, 2024. [CrossRef]

[92] J. Ledet, C. Tan, X. H. Guan, C. L. X. Yong, L. Ying, and P. Todd, "Trapping of Microplastics and Other Anthropogenic Particles in Seagrass Beds: Ubiquity Across a Vertical and Horizontal Sampling Gradient," Marine Environmental Research, Vol. 197, pp. 1–11, 2024. [CrossRef]

[93] H. K. McIlwraith, P. K. Lindeque, A. Miliou, T. J. Tolhurst, and M. Cole, "Microplastic Shape Influences Fate in Vegetated Wetlands," Environmental Pollution, Vol. 345, pp. 1–9, 2024. [CrossRef]

[94] W. Yao, D. Di, Z. Wang, Z. Liao, H. Huang, K. Mei, R. A. Dahlgren, M. Zhang, and X. Shang, "Micro- and Macroplastic Accumulation in a Newly Formed Spartina alterniflora Colonized Estuarine Saltmarsh in Southeast China," Marine Pollution Bulletin, Vol. 149, pp. 1–9, 2019. [CrossRef]

[95] T. Zhang, Z. Sun, Y. Liu, K. Song, and Z. Feng, "Occurrence of Microplastic Pollution in Coastal Wetlands-A Typical Rare Wildlife Sanctuary in China," Regional Studies in Marine Science, Vol. 67, pp. 1–9, 2023. [CrossRef]

[96] L. Girones, M. E. Adaro, K. Pozo, M. Baini, C. Panti, M. C. Fossi, J. E. Marcovecchio, A. C. Ronda, and A. H. Arias, "Spatial Distribution and Characteristics of Plastic Pollution in the Salt Marshes of Bahía Blanca Estuary, Argentina," Science of the Total Environment, Vol. 912, pp. 1–10, 2024. [CrossRef]

[97] B. Liu, W. Li, X. Pan, and D. Zhang, "The Persistently Breaking Trade-Offs of Three-Decade Plastic Film Mulching: Microplastic Pollution, Soil Degradation and Reduced Cotton Yield," Journal of Hazardous Materials, Vol. 439, pp. 1–8, 2022. [CrossRef]

[98] E. Manjate, S. Ramos, and C. M. R. Almeida, "Potential Interferences of Microplastics in the Phytoremediation of Cd and Cu by the Salt Marsh Plant Phragmites australis," Journal of Environmental Chemical Engineering, Vol. 8(2), pp. 1–8, 2020. [CrossRef]

[99] L. Gutow, A. Eckerlebe, L. Giménez, and R. Saborowski, "Experimental Evaluation of Seaweeds as a Vector for Microplastics into Marine Food Webs," Environmental Science & Technology, Vol. 50(2), pp. 915–923, 2016. [CrossRef].

[100] D. Reed, L. Washburn, A. Rassweiler, R. Miller, T. Bell, and S. Harrer, "Extreme Warming Challenges Sentinel Status of Kelp Forests as Indicators of Climate Change," Nature Communications, Vol. 7, pp. 1–7, 2016. [CrossRef]

[101] F. Gao, J. Li, J. Hu, X. Li, and C. Sun, "Occurrence of Microplastics Carried on Ulva prolifera from the Yellow Sea, China," Case Studies in Chemical and Environmental Engineering, Vol. 2, pp. 1–6, 2020. [CrossRef]

[102] Z. Feng, T. Zhang, H. Shi, K. Gao, W. Huang, J. Xu, J. Wang, R. Wang, J. Li, and G. Gao, "Microplastics in

Bloom-Forming Macroalgae: Distribution, Characteristics and Impacts," Journal of Hazardous Materials, Vol. 397, pp. 1–12, 2020. [CrossRef]
[103] Z. Feng, T. Zhang, J. Wang, W. Huang, R. Wang, J. Xu, G. Fu, and G. Gao, "Spatio-Temporal Features of Microplastics Pollution in Macroalgae Growing in an Important Mariculture Area, China," Science of the Total Environment, Vol. 719, pp. 1–11, 2020. [CrossRef]
[104] E. E. Esiukova, O. I. Lobchuk, A. A. Volodina, and I. P. Chubarenko, "Marine Macrophytes Retain Microplastics," Marine Pollution Bulletin, Vol. 171, pp. 1–12, 2021. [CrossRef]
[105] D. Menendez, A. Alvarez, P. Peon, A. Ardura, and E. Garcia-Vazquez, "From the Ocean to Jellies Forth and Back? Microplastics Along the Commercial Life Cycle of Red Algae," Marine Pollution Bulletin, Vol. 168, pp. 1–5, 2021. [CrossRef]
[106] K. L. Ng, K. F. Suk, K. W. Cheung, R. H. T. Shek, S. M. N. Chan, N. F. Y. Tam, S. G. Cheung, J. K.-H. Fang, and H. S. Lo, "Macroalgal Morphology Mediates Microplastic Accumulation on Thallus and in Sediments," Science of the Total Environment, Vol. 825, pp. 1–8, 2022. [CrossRef]
[107] Q. Li, L. Su, C. Ma, Z. Feng, and H. Shi, "Plastic Debris in Coastal Macroalgae," Environmental Research, Vol. 205, pp. 1–9, 2022. [CrossRef]
[108] A. Bilbao-Kareaga, D. Menendez, P. Peón, A. Ardura, and E. Garcia-Vazquez, "Microplastics in Jellifying Algae in the Bay of Biscay. Implications for Consumers' Health," Algal Research, Vol. 72, pp. 1–9, 2023. [CrossRef]
[109] Z. Li, D. Fu, S. Lü, and Z. Liu, "Interaction Between Macroalgae and Microplastics: Caulerpa lentillifera and Gracilaria tenuistipitata as Microplastic Bio-Elimination Vectors," Journal of Oceanology and Limnology, Vol. 41(6), pp. 2249–2261, 2023. [CrossRef]
[110] A. D. Forero-López, G. N. Rimondino, D. M. Truchet, C. V. Colombo, N. S. Buzzi, F. E. Malanca, C.V. Spetter, and M. D. Fernández-Severini, "Chemical Analysis of Marine Microdebris Pollution in Macroalgae from the Coastal Areas of Argentina," Science of the Total Environment, Vol. 923, pp. 1–13, 2024. [CrossRef]
[111] C. Rimmer, J. Fisher, and A. Turner, "Biomonitoring of Microplastics, Anthropogenic Microfibres and Glass Retroreflective Beads by Marine Macroalgae," Environmental Pollution, Vol. 348, pp. 1–10, 2024. [CrossRef]
[112] E. Efriyeldi, S. Syahrial, I. Effendi, I. P. Almanar, and A. D. Syakti, "The Mangrove Ecosystem in a Harbor-Impacted City in Dumai, Indonesia: A Conservation Status," Regional Studies in Marine Science, Vol. 65, pp. 1–9, 2023. [CrossRef]
[113] P. L. Biswas and S. R. Biswas, "Mangrove Forests: Ecology, Management, and Threats," Springer Nature Switzerland, pp. 1–14. 2019. [CrossRef]
[114] J. John, A. R. Nandhini, P. V. Chellam, and M. Sillanpää, "Microplastics in Mangroves and Coral Reef Ecosystems: a Review," Environmental Chemistry Letters, Vol. 20(1), pp. 397–416, 2022. [CrossRef]
[115] O. Serrano, A. Arias-Ortiz, C. M. Duarte, G. A. Kendrick, and P. S. Lavery, "Impact of Marine Heatwaves on Seagrass Ecosystems," Ecological Studies, Vol. 241, pp. 345–364, 2021, [CrossRef]
[116] D. Krause-Jensen and C. M. Duarte, "Substantial Role of Macroalgae in Marine Carbon Sequestration," Nature Geoscience, Vol. 9(10), pp. 737–742, 2016. [CrossRef]
[117] J. M. Fong, S. Lai, S. M. Yaakub, Y. X. Ow, and P. A. Todd, "The Diet and Feeding Rates of Gastropod Grazers in Singapore's Seagrass Meadows," Botanica Marina, Vol. 61(3), pp. 181–192, 2018. [CrossRef]
[118] L. G. A. Barboza, A. Dick Vethaak, B. R. B. O. Lavorante, A. K. Lundebye, and L. Guilhermino, "Marine Microplastic Debris: An Emerging Issue for Food Security, Food Safety and Human Health," Marine Pollution Bulletin, Vol. 133, pp. 336–348, 2018. [CrossRef]
[119] G. Ranjbar, H. Pirasteh-Anosheh, F. Dehghanie, S. Keshtkar, and M. Race, "Feasibility of Growing Salicornia Species in a Coastal Environment Through Planting Date and Density Management in a Direct Seawater Irrigation System," Environmental Science and Pollution Research, Vol. 29(31), pp. 47800–47809, 2022. [CrossRef]
[120] R. Garza-Torres, E. Troyo-Diéguez, A. Nieto-Garibay, G. Lucero-Vega, F. J. Magallón-Barajas, E. García-Galindo, Y. Fimbres-Acedo, and B. Murillo-Amador, "Environmental and Management Considerations for Adopting the Halophyte Salicornia bigelovii torr. as a Sustainable Seawater-Irrigated Crop.," Sustainability, Vol. 12(2), pp. 1–14, 2020. [CrossRef]
[121] T. Lou, S. Lü, and Y. Li, "Application Potential of Salicornia europaea in Remediation of Cd, Pb and Li Contaminated Saline Soil," Chinese Journal of Biotechnology, Vol. 36(3), pp. 481–492, 2020. [CrossRef]
[122] R. Khalilzadeh, A. Pirzad, E. Sepehr, S. Khan, and S. Anwar, "The Salicornia europaea Potential for Phytoremediation of Heavy Metals in the Soils Under Different Times of Wastewater Irrigation in Northwestern Iran," Environmental Science and Pollution Research, Vol. 28, pp. 47605–47618, 2021. [CrossRef]
[123] P. G. Caparrós, M. Ozturk, A. Gul, T. S. Batool, H. Pirasteh-Anosheh, B. T. Unal, V. Altay, and K. N. Toderich, "Halophytes Have Potential as Heavy Metal Phytoremediators: A Comprehensive Review," Environmental and Experimental Botany, Vol. 193, pp. 1–15, 2022. [CrossRef]
[124] K. Usman, M. H. Abu-Dieyeh, and M. A. Al-Ghouti, "Evaluating the Invasive Plant, Prosopis juliflora in the Two Initial Growth Stages as a Potential Candi-

date for Heavy Metal Phytostabilization in Metalliferous Soil," Environmental Pollutants and Bioavailability, Vol. 31(1), pp. 145–155, 2019. [CrossRef]

[125] G. Gao, A. S. Clare, C. Rose, and G. S. Caldwell, "Ulva rigida in the Future Ocean: Potential for Carbon Capture, Bioremediation and Biomethane Production," GCB Bioenergy, Vol. 10(1), pp. 39–51, 2018. [CrossRef]

[126] N. C. Purayil, B. Thomas, and R. T. Tom, "Microplastics – A Major Contaminant in Marine Macro Algal Population: Review," Marine Environmental Research, Vol. 193, pp. 1–8, 2024. [CrossRef]

[127] B. M. C. Almroth, L. Åström, S. Roslund, H. Petersson, M. Johansson, and N. K. Persson, "Quantifying Shedding of Synthetic Fibers from Textiles; a Source of Microplastics Released into the Environment," Environmental Science and Pollution Research, Vol. 25(2), pp. 1191–1199, 2018. [CrossRef]

[128] A. Rebelein, I. Int-Veen, U. Kammann, and J. P. Scharsack, "Microplastic Fibers — Underestimated Threat to Aquatic Organisms?," Science of the Total Environment, Vol. 777, pp. 1–16, 2021. [CrossRef]

[129] A. B. Castillo, M. El-Azhary, C. Sorino, and L. Le-Vay, "Potential Ecological Risk Assessment of Microplastics in Coastal Sediments: Their Metal Accumulation and Interaction with Sedimentary Metal Concentration," Science of the Total Environment, Vol. 906, pp. 1–15, 2024. [CrossRef]

[130] Q. Wang, G. Zheng, L. Ni, H. Wang, W. Li, P. Guo, Y. Wang, D. Zheng, J. Wu, and D. Zhang, "Colonization Characteristics and Dynamic Transition of Archaea Communities on Polyethylene and Polypropylene Microplastics in the Sediments of Mangrove Ecosystems," Journal of Hazardous Materials, Vol. 471, pp. 1–10, 2024. [CrossRef]

[131] J. Li, X. Li, J. Luo, P. Huang, C. Ge, X. Yang, and H. Wang, "Effects of Polypropylene Films and Leached Dissolved Organic Matters on Bacterial Community Structure in Mangrove Sediments," Science of the Total Environment, Vol. 939, pp. 1–13, 2024. [CrossRef]

[132] Y. Xia, S. Niu, and J. Yu, "Microplastics as Vectors of Organic Pollutants in Aquatic Environment: A Review on Mechanisms, Numerical Models, and Influencing Factors," Science of the Total Environment, Vol. 887, pp. 1–15, 2023. [CrossRef]

[133] G. Liu, P. H. Dave, R. W. M. Kwong, M. Wu, and H. Zhong, "Influence of Microplastics on the Mobility, Bioavailability, and Toxicity of Heavy Metals: A Review," Bulletin of Environmental Contamination and Toxicology, Vol. 107(4), pp. 710–721, 2021. [CrossRef]

[134] G. Liu, Z. Zhu, Y. Yang, Y. Sun, F. Yu, and J. Ma, "Sorption Behavior and Mechanism of Hydrophilic Organic Chemicals to Virgin and Aged Microplastics in Freshwater and Seawater," Environmental Pollution, Vol. 246, pp. 26–33, 2019. [CrossRef]

[135] X. Guo, C. Chen, and J. Wang, "Sorption of Sulfamethoxazole onto Six Types of Microplastics," Chemosphere, Vol. 228, pp. 300–308, 2019. [CrossRef]

[136] L.-Z. Zuo, H.-X. Li, L. Lin, Y.-X. Sun, Z.-H. Diao, S. Liu, Z.-Y. Zhang, and X.-R. Xu, "Sorption and Desorption of Phenanthrene on Biodegradable Poly(butylene adipate co-terephtalate) Microplastics," Chemosphere, Vol. 215, pp. 25–32, 2019. [CrossRef]

[137] M. Llorca, G. Schirinzi, M. Martínez, D. Barceló, and M. Farré, "Adsorption of Perfluoroalkyl Substances on Microplastics under Environmental Conditions," Environmental Pollution, Vol. 235, pp. 680–691, 2018. [CrossRef]

[138] F. Guo, B. Liu, J. Zhao, Y. Hou, J. Wu, H. Hu. C. Zhou, H. Hu, T. Zhang, and Z. Yang, "Temperature-Dependent Effects of Microplastics on Sediment Bacteriome and Metabolome," Chemosphere, Vol. 350, pp. 1–12, 2024. [CrossRef]

[139] H. Du, Y. Zhang, H. Jiang, and H. Wang, "Adsorption of Rhodamine B on Polyvinyl Chloride, Polystyrene, and Polyethylene Terephthalate Microplastics in Aqueous Environments," Environmental Technology & Innovation, Vol. 27, pp. 1–11, 2022. [CrossRef]

[140] A. Müller, R. Becker, U. Dorgerloh, F. G. Simon, and U. Braun, "The Effect of Polymer Aging on the Uptake of Fuel Aromatics and Ethers by Microplastics," Environmental Pollution, Vol. 240, pp. 639–646, 2018. [CrossRef]

[141] X. Zhang, M. Zheng, L. Wang, Y. Lou, L. Shi, and S. Jiang, "Sorption of Three Synthetic Musks by Microplastics," Marine Pollution Bulletin, Vol. 126, pp. 606–609, 2018. [CrossRef]

[142] N. Klasios, A. Birch, A. M. Murillo, and M. Tseng, "Warming Temperatures Exacerbate Effects of Microplastics in a Widespread Zooplankton Species," Environmental Pollution, Vol. 349, pp. 1–10, 2024. [CrossRef]

[143] Y. Qiu, M. Zheng, L. Wang, Q. Zhao, Y. Lou, and L. Shi, "Sorption of Polyhalogenated Carbazoles (PHCs) to Microplastics," Marine Pollution Bulletin, Vol. 146, pp. 718–728, 2019. [CrossRef]

[144] Z. Lin, Y. Hu, Y. Yuan, B. Hu, and B. Wang, "Comparative Analysis of Kinetics and Mechanisms for Pb(II) Sorption onto Three Kinds of Microplastics," Ecotoxicology and Environmental Safety, Vol. 208, pp. 1–8, 2021. [CrossRef]

[145] L. A. Holmes, A. Turner, and R. C. Thompson, "Interactions Between Trace Metals and Plastic Production Pellets under Estuarine Conditions," Marine Chemistry, Vol. 167, pp. 25–32, 2014. [CrossRef]

[146] L. Lin, S. Tang, X. Wang, X. Sun, and A. Yu, "Hexabromocyclododecane Alters Malachite Green and Lead(II) Adsorption Behaviors onto Polystyrene Microplastics: Interaction Mechanism and Competitive Effect," Chemosphere, Vol. 265, pp. 1–11, 2021. [CrossRef]

[147] J. Zou, X. Liu, D. Zhang, and X. Yuan, "Adsorption of Three Bivalent Metals by Four Chemical Distinct

Microplastics," Chemosphere, Vol. 248, pp. 1–12, 2020. [CrossRef]

[148] W. Chen, Z.-Y. Ouyang, C. Qian, and H.-Q. Yu, "Induced Structural Changes of Humic Acid by Exposure of Polystyrene Microplastics: A Spectroscopic Insight," Environmental Pollution, Vol. 233, pp. 1–7, 2018. [CrossRef]

[149] V. Godoy, G. Blázquez, M. Calero, L. Quesada, and M. A. Martín-Lara, "The Potential of Microplastics as Carriers of Metals," Environmental Pollution, Vol. 255, pp. 1–12, 2019. [CrossRef]

[150] F. A. Monikh, M. G. Vijver, Z. Guo, P. Zhang, G. K. Darbha, and W. J. G. M. Peijnenburg, "Metal Sorption onto Nanoscale Plastic Debris and Trojan Horse Effects in Daphnia magna: Role of Dissolved Organic Matter," Water Research, Vol. 186, pp. 1–10, 2020. [CrossRef]

[151] P. Heinrich and T. Braunbeck, "Bioavailability of Microplastic-Bound Pollutants in Vitro: The Role of Adsorbate Lipophilicity and Surfactants," Comparative Biochemistry and Physiology Part - C: Toxicology and Pharmacology, Vol. 221, pp. 59–67, 2019. [CrossRef]

[152] Y. Xia, J.-J. Zhou, Y.-Y. Gong, Z.-J. Li, and E. Y. Zeng, "Strong Influence of Surfactants on Virgin Hydrophobic Microplastics Adsorbing Ionic Organic Pollutants," Environmental Pollution, Vol. 265, pp. 1–9, 2020. [CrossRef]

[153] Y. Jiang, X. Yin, X. Xi, D. Guan, H. Sun, and N. Wang, "Effect of Surfactants on the Transport of Polyethylene and Polypropylene Microplastics in Porous Media," Water Research, Vol. 196, pp. 1–11, 2021. [CrossRef]

[154] Z. Zhang, X. Wu, H. Liu, X. Huang, Q. Chen, X. Guo, and J. Zhang, "A Systematic Review of Microplastics in the Environment: Sampling, Separation, Characterization and Coexistence Mechanisms with Pollutants," Science of the Total Environment, Vol. 859, pp. 1–17, 2023. [CrossRef]

[155] A. Bakir, S. J. Rowland, and R. C. Thompson, "Enhanced Desorption of Persistent Organic Pollutants from Microplastics under Simulated Physiological Conditions," Environmental Pollution, Vol. 185, pp. 16–23, 2014. [CrossRef]

[156] J. Y. Cho, S. H. Kim, D. H. Cho, H. J. Jung, B. C. Kim, S. K. Bhatia, R. Gurav, J. Lee, S.-H. Park, K. Park, H.-S. Joo, and Y.-H. Yang, "Simultaneous Monitoring of Each Component on Degradation of Blended Bioplastic using Gas Chromatography-Mass Spectrometry," Analytical Biochemistry, Vol. 655, pp. 1–10, 2022. [CrossRef]

[157] S. Mustapha, J. O. Tijani, R. Elabor, R. B. Salau, T. C. Egbosiuba, A. T. Amigun, D. T. Shuaib, A. Sumaila, T. Fiola, Y. K. Abubakar, H. I. Abubakar, I. F. Ossamulu, A. S. Abdulkareem, M. M. Ndamitso, S. Sagadevan, and A. K. Mohammed, "Technological Approaches for Removal of Microplastics and Nanoplastics in the Environment," Journal of Environmental Chemical Engineering, Vol. 12(2), pp. 1–24, 2024. [CrossRef]

[158] H. Kang, S. Park, B. Lee, J. Ahn, and S. Kim, "Modification of a Nile Red Staining Method for Microplastics Analysis: A Nile Red Plate Method," Water, Vol. 12(11), pp. 1–12, 2020. [CrossRef]

[159] H. Tong, Q. Jiang, X. Zhong, and X. Hu, "Rhodamine B dye staining for visualizing microplastics in laboratory-based studies," Environmental Science and Pollution Research, Vol. 28, pp. 4209–4215, 2021. [CrossRef]

[160] A. Monteleone, W. Schary, F. Wenzel, H. Langhals, and D. R. Dietrich, "Label-Free Identification and Differentiation of Different Microplastics using Phasor Analysis of Fluorescence Lifetime Imaging Microscopy (FLIM)-Generated Data," Chemico-Biological Interactions, Vol. 342, pp. 1–9, 2021. [CrossRef]

[161] V. C. Shruti, F. Pérez-Guevara, P. D. Roy, and G. Kutralam-Muniasamy, "Analyzing Microplastics with Nile Red: Emerging Trends, Challenges, and Prospects," Journal of Hazardous Materials, Vol. 423, pp. 1–19, 2022. [CrossRef]

[162] S. K. Bhatia, G. Kumar, and Y.-H. Yang, "Understanding Microplastic Pollution: Tracing the Footprints and Eco-Friendly Solutions," Science of the Total Environment, Vol. 914, pp. 1–17, 2024. [CrossRef]

[163] Z. M. Wang, J. Wagner, S. Ghosal, G. Bedi, and S. Wall, "SEM/EDS and Optical Microscopy Analyses of Microplastics in Ocean Trawl and Fish Guts," Science of the Total Environment, Vol. 603–604, pp. 616–626, 2017. [CrossRef]

[164] S. Veerasingam, M. Ranjani, R. Venkatachalapathy, A. Bagaev, V. Mukhanov, D. Litvinyuk, M. Mugilarasan, K. Gurumoorthi, L. Guganathan, V. M. Aboobacker, and P. Vethamony, "Contributions of Fourier Transform Infrared Spectroscopy in Microplastic Pollution Research: A Review," Critical Reviews in Environmental Science Technology, Vol. 51(22), pp. 2681–2743, 2021. [CrossRef]

[165] C. F. Araujo, M. M. Nolasco, A. M. P. Ribeiro, and P. J. A. Ribeiro-Claro, "Identification of Microplastics using Raman Spectroscopy: Latest Developments and Future Prospects," Water Research, Vol. 142, pp. 426–440, 2018. [CrossRef]

[166] Y. Chen, D. Wen, J. Pei, Y. Fei, D. Ouyang, H. Zhang, and Y. Luo, "Identification and Quantification of Microplastics using Fourier-Transform Infrared Spectroscopy: Current Status and Future Prospects," Environmental Science & Health, Vol. 18, pp. 14–19, 2020. [CrossRef]

[167] P. J. Larkin, Infrared and Raman Spectroscopy: Principles and Spectral Interpretation, Second Edition. Cambridge: John Fedor, 2018.

[168] Z. Yang, M. Çelik, and H. Arakawa, "Challenges of Raman Spectra to Estimate Carbonyl Index of Microplastics: A Case Study with Environmental Sam-

ples from Sea Surface," Marine Pollution Bulletin, Vol. 194, pp. 1–11, 2023. [CrossRef]

[169] M. Sunil, M. N, M. Charles, S. Chidangil, S. Kumar, and J. Lukose, "Visualization and Characterisation of Microplastics in Aquatic Environment using a Home-Built Micro-Raman Spectroscopic Set Up," Journal of Environmental Management, Vol. 354, pp. 1–15, 2024. [CrossRef]

[170] J. Caldwell, P. Taladriz-Blanco, B. Rothen-Rutishauser, and A. Petri-Fink, "Detection of Sub-Micro- and Nanoplastic Particles on Gold Nanoparticle-Based Substrates Through Surface-Enhanced Raman Scattering (SERS) Spectroscopy," Nanomaterials, Vol. 11(5), pp. 1–18, 2021. [CrossRef]

[171] M. Jiao, S. Cao, L. Ren, and R. Li, "Analysis of Composite Microplastics in Sediment using 3D Raman Spectroscopy and Imaging Method," Journal of Hazardous Materials Advances, Vol. 3, pp. 1–9, 2021. [CrossRef]

[172] Y. Ye, K. Yu, and Y. Zhao, "The Development and Application of Advanced Analytical Methods in Microplastics Contamination Detection: A Critical Review," Science of the Total Environment, Vol. 818, pp. 1–15, 2022. [CrossRef]

[173] C. Fang, Z. Sobhani, D. Zhang, X. Zhang, C. T. Gibson, Y. Tang, Y. Luo, M. Megharaj, and R. Naidu, "Capture and Characterisation of Microplastics Printed on Paper Via Laser Printer's Toners," Chemosphere, Vol. 281, pp. 1–9, 2021. [CrossRef]

[174] K. Bhagat et al., "Aging of Microplastics Increases Their Adsorption Affinity Towards Organic Contaminants," Chemosphere, Vol. 298, pp. 1–9, 2022. [CrossRef]

[175] Z. Zhang, Y. Geng, W. Zhou, X. Shao, H. Lin, and Y. Zhou, "Development of a Multi-Spectroscopy Method Coupling μ-FTIR and μ-Raman Analysis for One-Stop Detection of Microplastics in Environmental and Biological Samples," Science of the Total Environment, Vol. 917, pp. 1–12, 2024. [CrossRef]

[176] R. Nakano, R. K. Gürses, Y. Tanaka, Y. Ishida, T. Kimoto, S. Kitagawa, Y. Iiguni, and H. Ohtani, "Pyrolysis-GC–MS Analysis of Ingested Polystyrene Microsphere Content in Individual Daphnia magna," Science of the Total Environment, Vol. 817, pp. 1–7, 2022. [CrossRef]

[177] A. E. Christian and I. Köper, "Microplastics in Biosolids: A Review of Ecological Implications and Methods for Identification, Enumeration, and Characterization," Science of the Total Environment, Vol. 864, pp. 1–11, 2023. [CrossRef]

[178] A. Torres-Agullo, G. Zuri, and S. Lacorte, "Pyr-GC-Orbitrap-MS Method for the Target/Untargeted Analysis of Microplastics in Air," Journal of Hazardous Materials, Vol. 469, pp. 1–10, 2024. [CrossRef]

[179] F. Ribeiro, E. D. Okoffo, J. W. O'Brien, S. Fraissinet-Tachet, S. O'Brien, M. Gallen, S. Samanipour, S. Kaserzon, J. F. Mueller, T. Galloway, and K. V. Thomas, "Quantitative Analysis of Selected Plastics in High-Commercial-Value Australian Seafood by Pyrolysis Gas Chromatography Mass Spectrometry," Environmental Science & Technology, Vol. 54(15), pp. 9408–9417, 2020. [CrossRef]

[180] K. Gao, H. Lian, C. Xue, J. Zhou, and X. Yan, "High-Throughput Counting and Sizing of Therapeutic Protein Aggregates in the Nanometer Size Range by Nano-Flow Cytometry," Analytical Chemistry, Vol. 94(50), pp. 17634–17644, Dec. 2022. [CrossRef]

[181] C. Li, L. C. Campos, and R. Busquets, "A Novel High-Throughput Analytical Method to Quantify Microplastics in Water by Flow Cytometry," Green Analytical Chemistry, Vol. 5, pp. 1–9, 2023. [CrossRef]

[182] L. Sgier, R. Freimann, A. Zupanic, and A. Kroll, "Flow Cytometry Combined with viSNE for the Analysis of Microbial Biofilms and Detection of Microplastics," Nature Communications, Vol. 7, pp. 1–10, 2016. [CrossRef]

[183] N. Kaile, M. Lindivat, J. Elio, G. Thuestad, Q. G. Crowley, and I. A. Hoell, "Preliminary Results From Detection of Microplastics in Liquid Samples Using Flow Cytometry," Frontiers in Marine Science, Vol. 7, pp. 1–12, 2020. [CrossRef]

[184] J. P. G. L. Frias and R. Nash, "Microplastics: Finding a Consensus on the Definition," Marine Pollution Bulletin, Vol. 138, pp. 145–147, 2019. [CrossRef]

[185] A. Bianco, L. Carena, N. Peitsaro, F. Sordello, D. Vione, and M. Passananti, "Rapid Detection of Nanoplastics and Small Microplastics by Nile-Red Staining and Flow Cytometry," Environmental Chemistry Letters, Vol. 21(2), pp. 647–653, 2022. [CrossRef]

[186] H. J. Pant, "Applications of the Radiotracers in the Industry: A Review," Applied Radiation and Isotopes, Vol. 182, pp. 1–35, 2022. [CrossRef]

[187] M. Munir et al., "Development of a Polystyrene-Based Microplastic Model for Bioaccumulation and Biodistribution Study using Radiotracing and Nuclear Analysis Method," Marine Pollution Bulletin, Vol. 201, pp. 1–, 2024. [CrossRef]

[188] C. Bedia, "Metabolomics in environmental toxicology: Applications and challenges," Trends in Environmental Analytical Chemistry, Vol. 34, pp. 1–13, 2022. [CrossRef]

[189] J. Portugal, S. Mansilla, and B. Piña, "Perspectives on the Use of Toxicogenomics to Assess Environmental Risk," Bioscience Research Institute. 2022. [CrossRef]

[190] M. Munir, M. Subechi, A. Nurmanjaya, K. E. Prasetya, F. Rindiyantono, Chairuman, C. Pratama, Yanto, A. Pujiyanto, H. Setiawan, D. A. Sarwono, E. Sarmini, M. E. Fara, and H. Suseno, "Iodine-131 Radiolabeled Polyvinylchloride: A Potential Radiotracer for Micro and Nanoplastics Bioaccu-

mulation and Biodistribution Study in Organisms," Marine Pollution Bulletin, Vol. 188, pp. 1–8, 2023. [CrossRef]

[191] W. R. Prihatiningsih, H. Suseno, N. P. Zamani, and D. Soedharma, "Bioaccumulation and Retention Kinetics of Cesium in the Milkfish Chanos chanos from Jakarta Bay," Marine Pollution Bulletin, Vol. 110(2), pp. 647–653, 2016. [CrossRef]

[192] B. Budiawan, H. Suseno, F. Afriani, and W. R. Prihatiningsih, "Bioaccumulation and Retention Kinetics of Trace Elements in the Horse Mussels Modiolus micropterus Exposed to Different Environmental Conditions," Environmental Toxicology and Pharmacology, Vol. 87, pp. 1–7, 2021. [CrossRef]

[193] O. Exaudina, W. R. Prihatiningsih, H. Suseno, and B. Budiawan, "Study of Cadmium Bioaccumulation in Perna viridis through Food Pathway and Its Decontamination," Walisongo Journal of Chemistry, Vol. 4(1), pp. 17–22, 2021. [CrossRef]

[194] J. Wu, H. Chen, J. Xu, M. S. U. Rahman, S. Li, J. Wang, S. Huang, C. C. Han, S. Xu, and Y. Liu, "The Lull Before Microplastics Pollution Outbreaks: Some Implications for Human Health and Control Strategies," Nano Today, Vol. 54, pp. 1–23, 2024. [CrossRef]

[195] L. Guilhermino, L. R. Vieira, D. Ribeiro, A. S. Tavares, V. Cardoso, A. Alves, and J. M. Almeida, "Uptake and Effects of the Antimicrobial Florfenicol, Microplastics and Their Mixtures on Freshwater Exotic Invasive Bivalve Corbicula fluminea," Science of the Total Environment, Vol. 622–623, pp. 1131–1142, 2018. [CrossRef]

[196] M. Al-Sid-Cheikh, S. J. Rowland, K. Stevenson, C. Rouleau, T. B. Henry, and R. C. Thompson, "Uptake, Whole-Body Distribution, and Depuration of Nanoplastics by the Scallop Pecten maximus at Environmentally Realistic Concentrations," Environmental Science & Technology, Vol. 52(24), pp. 14480–14486, 2018. [CrossRef]

[197] N. Li, M. Wu, Y. Zhang, W. Yuan, J. Wu, and X. Shao, "A Review on Microplastics Pollution in Coastal Wetlands," Watershed Ecology and the Environment, Vol. 5, pp. 24–37, 2023. [CrossRef]

[198] M. C. Rillig, R. Ingraffia, and A. A. De Souza Machado, "Microplastic Incorporation Into Soil in Agroecosystems," Frontiers in Plant Science, Vol. 8, pp. 1–4, 2017. [CrossRef]

[199] C. M. Gerstenbacher, A. C. Finzi, R. D. Rotjan, and A. B. Novak, "A Review of Microplastic Impacts on Seagrasses, Epiphytes, and Associated Sediment Communities," Environmental Pollution, Vol. 303, pp. 1–7, 2022. [CrossRef]

[200] D. Medina-Contreras and F. Arenas, "Are Stable Isotopes an Efficient Tool for Tracking the Effect of Anthropogenic Activities on Mangrove Food Web Structure and Function?," Hydrobiologia, Vol. 850(6), pp. 1237–1249, 2023. [CrossRef]

[201] V. Thiagarajan, S. A. Alex, R. Seenivasan, N. Chandrasekaran, and A. Mukherjee, "Toxicity evaluation of nano-TiO2 in the presence of functionalized microplastics at two trophic levels: Algae and crustaceans," Science of The Total Environment, Vol. 784, pp. 1–11, 2021. [CrossRef]

[202] X. Zheng, W. Zhang, Y. Yuan, Y. Li, X. Liu, and X. Wang, "Growth Inhibition, Toxin Production and Oxidative Stress Caused by Three Microplastics in Microcystis aeruginosa," Ecotoxicology and Environmental Safety, Vol. 208, pp. 1–9, 2021. [CrossRef]

[203] Y. Mao, H. Ai, Y. Chen, Z. Zhang, P. Zeng, L. Kang, W. Li, W. Gu, Q. He, and H. Li, "Phytoplankton Response to Polystyrene Microplastics: Perspective from an Entire Growth Period," Chemosphere, Vol. 208, pp. 59–68, 2018. [CrossRef]

[204] S. van Weert, P. E. Redondo-Hasselerharm, N. J. Diepens, and A. A. Koelmans, "Effects of Nanoplastics and Microplastics on the Growth of Sediment-Rooted Macrophytes," Science of the Total Environment, Vol. 654, pp. 1040–1047, 2019. [CrossRef]

[205] P. Xu, G. Peng, L. Su, Y. Gao, L. Gao, and D. Li, "Microplastic Risk Assessment in Surface Waters: A Case Study in the Changjiang Estuary, China," Marine Pollution Bulletin, Vol. 133, pp. 647–654, 2018. [CrossRef]

[206] A. Talukdar, P. Kundu, S. Bhattacharya, and N. Dutta, "Microplastic Contamination in Wastewater: Sources, Distribution, Detection and Remediation Through Physical and Chemical-Biological Methods," Science of the Total Environment, Vol. 916, pp. 1–18, 2024. [CrossRef]